SPECIAL PUBLICATION SJ2005-SP15

DEVELOPMENT OF AN INTEGRATED SURFACE WATER/GROUND WATER MODEL (ISGM) IN WESTERN ORANGE AND SEMINOLE COUNTIES, FLORIDA

FINAL REPORT

DEVELOPMENT OF AN INTEGRATED SURFACE WATER/GROUND WATER MODEL (ISGM) IN WESTERN ORANGE AND SEMINOLE COUNTIES, FLORIDA

FINAL REPORT

Prepared for

St. Johns River Water Management District
Highway 100 West
Palatka, FL 32178

Prepared by

HydroGeologic, Inc.

January 2005

TABLE OF CONTENTS

Page

LIST OF TABLES

LIST OF FIGURES

DEVELOPMENT OF AN INTEGRATED SURFACE WATER/ GROUND WATER MODEL (ISGM) IN WESTERN ORANGE AND SEMINOLE COUNTIES, FLORIDA

1.0 BACKGROUND AND OBJECTIVES

The St. Johns River Water Management District (SJRWMD) is responsible for managing the water resources within its jurisdiction including water supply, water quality, and the protection of natural systems related to water resources. Physically based numerical models have been used in resource assessment and management, and have helped delineate Water Resource Caution Areas which include most of the central Florida portion of the SJRWMD. The most recent and updated modeling effort in east-central Florida (ECF) was conducted by McGurk and Presley (2002), to determine the steady-state changes in the groundwater flow system in ECF due to projected 2020 withdrawals. The groundwater flow model was calibrated to average 1995 conditions, and verified against predevelopment conditions. The model was developed using the entire hydrologic budget to determine groundwater recharge, by accounting for runoff and evapotranspiration losses from precipitation. In spite of that, its ability to adequately address the effects of pumping of the Floridan Aquifer on water levels in the Surficial Aquifer System, or on the numerous lakes and wetlands in the region is of concern. The District therefore wishes to determine the accuracy of the ECF groundwater model in addressing these issues, by developing an Integrated Surface water/Groundwater Model (ISGM) that rigorously models the unsaturated zone and surficial processes and has a better characterization of the Surficial Aquifer within the region.

The purpose of this project was to develop an Integrated Surface-water/Groundwater Model of Western Orange and Seminole County (WOSC-ISGM). The regional groundwater flow model (McGurk and Presley, 2002) entirely encompasses the current area of interest, however, the interactions between pumping of the Floridan Aquifer and water levels in the Surficial Aquifer System, or the numerous lakes and wetlands in the region were not rigorously considered therein. The primary focus of the current modeling effort was to address these interactions with a physically-based model of the entire hydrologic cycle, to further quantify the deficiencies (or validity) of a groundwater model alone. The objectives of this work are summarized as follows:

1. Simulate the surface and groundwater flow systems within the areas of interest.

2. Characterize trends in stage of groundwater and surface water monitoring stations (i.e., calibrate the model to emulate the available surface and subsurface flow data).

3. Predict the effects of projected future Floridan Aquifer withdrawals on water-table elevations and on connected lakes and wetlands.

Other issues that are addressed as part of this work include:

4. Addressing/quantifying the grid-scale errors of the regional groundwater flow model (i.e., examining if finer grids can produce more accurate results).

5. Addressing/quantifying the conceptual errors and limitations of the regional groundwater flow model in terms of the approximations used for handling surface water features (i.e., examining if more refined modeling of the unsaturated zone and surface water physics can produce more accurate results).

6. Examining the long-term transient effects of increased Floridan Aquifer pumping upon the water table and on connected lakes and wetlands.

1.1 MODEL DOMAIN

The area selected for the WOSC-ISGM is delineated in Figure 1.1. This area has been selected in consultation with District staff to include two regions of interest - one in Seminole County which contains several conjunctive-water features such as springs, streams, lakes and wetlands and the other in Orange County which is sparse of such features and is internally drained. The sub-basins in this study include the Wekiva River basin, Little Wekiva River basin, Soldier Creek Reach, Gee Creek, Island Lake, Cranes Roost Outlet, Mirror Lake Outlet, Long Lake basin, Lake Lovely Outlet, Trout Lake Outlet, Lake Apopka Outlet, and Unnamed Lake District. Some of these basins are internally drained while others have some form of surface outlet. Since both types of basins occur within the ECF model area, the understanding gained from this study may also quantify the deviation of ECF model results in other similar basins, resulting from use of larger grids, and from use of a groundwater flow model alone. The selected domain boundary lies along basin or sub-basin boundaries to adequately accommodate boundary conditions for the surficial domain, as a no-flow condition across the basin divide along the boundary. This area was selected for discretizing the surface as well as subsurface domains, with use of telescopic refinement from the District's ECF model to provide the lateral boundary conditions in the underlying aquifers, for all the simulated scenarios.

1.2 DATA REVIEW

Availability of pertinent data for this study was facilitated by B. McGurk of the SJRWMD (personal communication). This data was reviewed and assimilated with a view towards developing conceptual and subsequent numerical models of surface and subsurface flow within the WOSC area. It is grouped into four broad classifications for conceptualization of the flow system, as follows:

- **Hydrogeologic data** defines the subsurface conceptualization including aquifer confinement and stratification, aquifer/aquitard hydraulic properties, and potentiometric surfaces and water levels in wells. Interpretations of the local hydrogeology contained in the ECF model (McGurk and Presley, 2002) were taken as the starting point for model development in the current study, unless updated by more recent data or interpretations as noted in the subsequent sections.

- **Water balance data** defines the various inflow and outflow components of water to the system including precipitation, runoff, evapotranspiration, withdrawals, flow to springs and applied water. Note that some of these components were external to the ECF groundwater model but are internal flux components to the ISGM.

- **Topographic and surface flow characteristics** define the surface flow conceptualization including runoff and drainage patterns (natural or altered), streams, rivers and other conveyance or control structures, lakes and wetlands.

- **Unsaturated zone flow data** necessary to quantify unsaturated soil characteristics and evapotranspiration characteristics.

In the following four sections, available data and associated model conceptualization for the study area are presented according to the broad classifications provided above, with application towards systematically developing, parameterizing and calibrating a numerical model of conjunctive surface/subsurface flow over the region of interest. Data shortfalls are also identified and replaced by literature values or estimated within a reasonable range of values through the model calibration process.

1.3 MODELING CODE

The MODHMS integrated surface/subsurface flow modeling code was selected for this study. The following features of MODHMS make it the appropriate tool for this study:

- MODHMS is built on the USGS groundwater modeling code MODFLOW which was used for the ECF study. Therefore, expanding the ECF groundwater flow model to include unsaturated zone and surface water dynamics is accomplished in a straightforward manner while maintaining consistency with the ECF groundwater model.

- MODHMS contains all the features required for this modeling study including the unsaturated zone, comprehensive evapotranspiration calculations, the overland flow surface, and complex surface-water hydraulics.

- MODHMS contains state-of-the-art numerical schemes for robust and efficient solutions to non-linear equations involved with the integrated model. In addition, it solves all flow domains simultaneously thus avoiding errors and inefficiencies of linked approaches.

- MODHMS includes pre- and post-processing and visualization tools that assist in model development and analysis of results. The ViewHMS system that drives MODHMS includes interfaces to complex hydraulic databases to allow for easy and automated input of detailed hydraulics.

1.4 ORGANIZATION OF THIS REPORT

This report is organized as follows:

- Chapter 1 introduces the background and objectives of this study;
- Chapter 2 describes the hydrogeologic data and groundwater flow conceptualization;
- Chapter 3 discusses the water balance data and conceptualization;
- Chapter 4 gives an account of surface water flow data and conceptualization;
- Chapter 5 defines the unsaturated flow data and conceptualization;
- Chapter 6 presents the model development methodology;
- Chapter 7 addresses the calibrated steady-state model representing average 1995 conditions;
- Chapter 8 reports the sensitivity study for the steady-state model;
- Chapter 9 provides the transient simulation from June 1995 through September 1999;
- Chapter 10 details transient sensitivity analysis;
- Chapter 11 puts forth a discussion on the predictive simulation from 1999 through 2025;
- Chapter 12 is a description of the predictive sensitivity simulation; and
- Chapter 13 summarizes the results of the project.

2.0 HYDROGEOLOGIC DATA AND GROUNDWATER FLOW CONCEPTUALIZATION

2.1 GENERAL

The District's ECF groundwater flow model was the basis for initial conceptualization and parameterization of the aquifers within the current study area. McGurk and Presley (2002) provide a detailed discussion of the hydrogeology and hydrostratigraphy of the study region and the model thereof provides a good understanding of the simulated subsurface flow dynamics. The WOSC-ISGM of the current study builds upon this understanding in a systematic manner to effectively use previous work, and to note the cause of differences encountered between the groundwater model and the ISGM, as it was being developed. Thus, the current report defers to the ECF model report for details except where the groundwater flow conceptualization is different (or updated) from the ECF model study of McGurk and Presley (2002).

2.2 HYDROSTRATIGRAPHY

The various aquifers of interest for this study are shown in Figure 2.1 and include the Surficial Aquifer System (SAS), the Intermediate Confining Unit (ICU), and the Floridan Aquifer System comprised of the Upper Floridan Aquifer (UFA) and the Lower Floridan Aquifer (LFA). The UFA was further subdivided into a more productive Upper Zone (UFA-UZ), and a lower Dolostone Zone (UFA-DZ). As conceptualized by the District's ECF model, the saltwater interface (or 5000 ppm isochlor) acts as a bottom no-flow boundary to the freshwater flow model. Therefore the 5000 ppm isochlor was used for the elevation of the bottom of a model layer if this was higher than the respective aquifer's bottom elevation. Within the current study domain, only the LFA's bottom elevation was adjusted due to the saltwater interface, the other hydrostratigraphic units being above the 5000 ppm isochlor's depth. Figure 2.2 shows the bottom elevation of the conceptualized freshwater model domain, which has been raised from the LFA bottom elevation as a result of the salt water interface. Note that the above figures (and subsequent ones in this report) are displayed at the finest grid resolution of the WOSC-ISGM modeling effort, to provide the information (and Figures) at the resolution at which it was ultimately used in the model study.

The top-most ISGM model layer represents the overland flow surface (surficial layer) or the surface water features (lakes, ponds, streams, rivers, channels and other conveyance structures) within the domain. This layer is discussed later, in terms of its mechanisms for surface water flow and characteristics for infiltration. The top-most **subsurface** model layer represents the topsoil, including about a couple of feet of material beneath the land surface. This layer is significant in its role in generating runoff. Underneath the topsoil lies the SAS which is represented in this study by two hydrogeologic units – an upper higher conductivity unit representing the upper sands, and a lower unit of lesser conductivity representing the silty-sands and clays, separated by the first clay units encountered within the SAS. The upper SAS unit was further subdivided in two layers - an upper layer which is unsaturated or contains the water table, and a lower layer (the third subsurface model layer) which is typically saturated or contains the water-table. The fourth model layer represents the lower sandy-silts of the SAS. This is an extension to the District's ECF model, wherein the SAS was modeled as one hydrogeologic unit represented by one model layer. In the Lake Marden Basin area (delineated on Figure 2.2), it was noted (P. B. Water, Inc, 2000) that approximately the upper third of the SAS was more conductive (averaging 50 ft/d) than the lower portions (averaging about 2 ft/d), so it was decided to explore this (or similar segregation of the SAS based upon available data) further, on a model-wide basis in the WOSC-ISGM. The fifth subsurface model layer of the ISGM represents the UFA-UZ. The ICU was represented in a quasi-three dimensional manner, linking the SAS to the underlying UFA-UZ. For this study, a quasi-three dimensional concept was applied for groundwater flow through aquitard layers. This conceptualization neglects storage in aquitard units for transient simulations, but saves on a layer of nodes for the aquitard units by directly providing a leakance term through the confining material. The sixth subsurface model layer is the UFA-DZ modeled explicitly as per the District's ECF model, though there is little difference in observed heads between the UFA-UZ and the UFA-DZ. The seventh subsurface model layer represents the freshwater portions of the LFA, with leakance between the UFA-DZ and the LFA provided in a quasi-three-dimensional manner, across the MSCU. Figure 2.1 shows the subsurface model conceptualization and the vertical numerical discretization.

Parameterization of the subsurface aquifer/aquitard units for the WOSC-ISGM is also an extension of the District's ECF regional model including relevant tops and bottoms of aquifer units (specifically, the SAS as a single hydrogeologic unit, the UFA-UZ, the UFA-DZ, and the LFA), horizontal hydraulic conductivities of these aquifer units, and vertical leakances through the aquitard units (specifically, the ICU and the MSCU). The ISGM's subsurface stratigraphy is as follows:

1. The SAS was considered as two units in the WOSC-ISGM study, with a sandy unit overlying a silty-sand unit. This is an extension to the District's ECF model conceptualization. The land surface elevation represents the top of the SAS system (including the unsaturated zone), which was derived from 1 ft contours obtained from the District, merged with 5 ft contours in locations where the finer resolution was not available. The land surface elevation was then averaged onto the model's finite difference mesh in an area-weighted manner to provide the top of the SAS as shown in Figure 2.3. The numerical layer representing the top soil is two feet thick and therefore its bottom lies two feet below the topographic elevation of Figure 2.3.

2. The stratigraphic layer representing the bottom of the upper higher conductivity SAS unit (also the top of the lower conductivity SAS unit beneath it) is shown in Figure 2.4. This layer elevation was obtained as an interpolation of the first occurrence of lower permeability materials in wells across the site. This elevation is generally consistent with observations in the Lake Marden Basin area and modeling thereof by P. B. Water Inc. (2000), that the upper third of the SAS is delineated to be more conductive than the lower part. This SAS unit (between the bottom of the topsoil layer and the bottom of the upper SAS unit) was subdivided into two numerical layers of equal thickness.
3. The bottom of the lower SAS unit (which is also the top of the ICU) was obtained as an interpolation of ICU top elevations measured from wells across the site. This elevation is different from that used in the ECF model (McGurk and Presley, 2002) and includes recent USGS interpretations deemed more accurate than data used by previous work (B. McGurk, personal communication), in delineating the ICU as first appearance of the Hawthorn unit from borehole geophysical log data. Final modifications of this elevation

were performed to ensure positive thicknesses for the overlying SAS unit. This surface, as shown in Figure 2.5 was used to model the bottom elevation of the SAS system. The USGS interpretation of this surface provides an ICU thickness that was generally thinner in the NE portions and somewhat thicker in the SW portions of the active WOSC model area, than used in the ECF model of McGurk and Presley (2002).

4. The top of the UFA-UZ was shown in Figure 2.6. The difference between this and the respective value obtained from the ECF model's BCF file, though small, was due to use of a revised and updated map of this layer which contains newer information/interpretation than the maps used when the ECF model was constructed (B. McGurk, personal communication).

5. The bottom of the UFA-UZ was coincident with the top of the UFA-DZ, which was shown in Figure 2.7. The difference between this and the respective value obtained from the ECF model's BCF file was small and may be attributed to differences in interpolation methodologies.

6. The bottom of the UFA-DZ is coincident with the top of the MSCU, which is shown in Figure 2.8. The difference between this and the respective value obtained from the ECF model's BCF file is small and may be attributed to differences in interpolation methodologies.

7. The top of the LFA is coincident with the bottom of the MSCU which is shown in Figure 2.9. The difference between this and the respective value obtained from the ECF model's BCF file is small and may be attributed to differences in interpolation methodologies.

8. The bottom of the LFA/freshwater model domain is shown in Figure 2.2 and was obtained from the bottom elevation of the LFA and the elevation of the saltwater interface as discussed earlier. The difference between this and the respective value obtained from the ECF model's BCF file is small in proportion to the thickness of the modeled LFA, and is due to use of a revised and updated saltwater interface map which contains newer information than the maps used when the ECF model was constructed (B. McGurk, personal communication).

2.3 HYDROGEOLOGIC PARAMETERS

Horizontal hydraulic conductivities of the various aquifer units were maintained as per the District's ECF model's BCF file for initial model conceptualization, except for the SAS unit. The coarse-block hydraulic conductivity zonation of the ECF model was maintained in the finer model grid used in this study. This is appropriate for the current modeling effort because there is no justification or additional data/interpretations available to change this conceptualization. The horizontal hydraulic conductivity of the SAS in the ECF model of a uniformly 20 ft/d was refined in the WOSC-ISGM to contain an upper unit of higher hydraulic conductivity that may be unsaturated (parameterization of which is discussed later), and a lower unit having a hydraulic conductivity value of 2 ft/d distributed uniformly over the model area, as per the P. B. Water (2000) modeling study. Having a uniform low conductivity value for the lower SAS unit is justified because the water-table resides in the overlying higher conductivity SAS zone which would exert more control on water-levels. The horizontal hydraulic conductivity distribution of the UFA-UZ is shown in Figure 2.10, the horizontal hydraulic conductivity distribution of the UFA-DZ is shown in Figure 2.11, and the horizontal hydraulic conductivity distribution of the LFA, is shown in Figure 2.12. A slight adjustment of the zonation has been performed for the UFA-UZ in Figure 2.10 in the region around Wekiva and Miami Springs due to the finer grid of the current model. The adjustment allows these springs to remain in the same conductivity zone as they do in the ECF model of McGurk and Presley (2002).

Vertical leakances through the ICU and MSCU aquitard units are specified in the ECF MODFLOW model via the BCF file. Rather than use them directly in the current study, it was decided to convert the information to the vertical hydraulic conductivities of the respective hydrostratigraphic aquitard units, which are the basic flow parameters. The general interpolated thicknesses of the ICU and MSCU as obtained from District files were used for this conversion, with the vertical conductivity being equal to the leakance multiplied by the thickness of the respective confining unit, as used in the ECF model. The vertical hydraulic conductivities thus obtained for the ICU and the MSCU are shown in Figure 2.13 and 2.14 respectively. These conductivities were then used to compute leakance for the respective confining units, on any finer/modified grid that was used in the current study. In this manner, even though the subsurface numerical model may not be identical to the District's ECF model due to modifications in hydrostratigraphic elevations, the physical parameters are identical (i.e., the models may be slightly dissimilar in terms of leakance but they are identical in terms of hydraulic conductivities). It is noted here that the vertical hydraulic conductivity of the ICU is later altered during the calibration process since the new ICU thicknesses affect SAS water levels which are sensitive to leakance through the ICU.

Vertical hydraulic conductivities used for the upper and lower SAS units, and for the UFA-UZ and UFA-DZ were taken as one-tenth of the respective horizontal hydraulic conductivities.

The hydrostratigraphic data and conceptualization discussed in this section were maintained during development and calibration of the WOSC-ISGM. Therefore, adjustments were not made to hydraulic conductivity values of the aquifer and aquitard units beneath the ICU thus maintaining consistency with the District's regional ECF groundwater flow model. The sensitivity of these parameters at a regional scale is noted in McGurk and Presley (2002), and associated uncertainties for the current modeling effort should not be different over the local area of the current model, from those of the ECF model since their values and roles are the same in both models. However, the SAS conceptualization of the current study was more refined from that of the ECF flow model and therefore the conductivity values (horizontal and vertical) of the SAS units may be varied within reasonable limits during calibration. In the Lake Marden area study (P. B. Water, Inc, 2000), these horizontal hydraulic conductivity values range from 20 to 90 ft/d for the upper layer (a value of 40 ft/d was used as a conservative estimate) and about 0.1 to 5 ft/d in the lower SAS layer (a value of 2 ft/d is used in the model). The horizontal hydraulic conductivity of the upper sandy SAS layer was obtained using pseudo-transfer functions from soil type information available over the region.

2.4 POTENTIOMETRIC LEVELS

The potentiometric surfaces for the SAS, the UFA-UZ, the UFA-DZ, and the LFA for average 1995 conditions, were obtained from the District's ECF model results, as shown in Figures 2.15 through 2.18. These surfaces are useful for identifying similarities and differences between the ECF model and results of the current study. They also help to systematically understand the cause and effect relationships on the potentiometric surface, of the various steps that were taken to convert the ECF groundwater flow model to an ISGM. The potentiometric levels of various observation wells penetrating the various aquifers (as depicted in Figures 4 and 5 and Appendix C of McGurk and Presley (2002), and used in calibrating their model for average 1995 conditions) are provided in Table 2.1 for the WOSC model domain and were used for investigating various calibration statistics as the ISGM was being developed.

3.0 WATER BALANCE DATA AND CONCEPTUALIZATION

The conceptual model and initial parameterization for the various water balance components of the hydrologic cycle in the WOSC domain are provided in this section. Each major element of the water balance component or conceptualization is numbered with sub-components indicated by letters, in the discussion below.

1. Precipitation/rainfall, (P), is the major source of water to the modeled system, and was input to the surficial layer or surface water features of the model. Precipitation information has been organized into Thiessen polygons over the model area for total 1995 rainfall conditions as used in the ECF groundwater flow model. The distribution of P, as provided on the ECF model's grid-block scale, was smoothened over the fine grid of the current study area as shown in Figure 3.1. The Thiessen polygons of Figure 3.1 were used to parameterize rainfall in the current model for the steady-state simulation as employed in the ECF model, to allow for a systematic understanding of the differences between the ECF model and the current modeling effort (including the grid-scale effects). Information on transient daily rainfall is available via Doppler data collected over the 1995 through 1999 period and was used and is discussed later during transient calibration.

2. Another source of water to the surficial layer includes R_{rib} representing water applied to rapid infiltration basins (RIBs). This information was available for average 1995 conditions, as applied over the ECF model grid. To resolve scale issues for the various grids used in this study, the RIB information was re-evaluated by the District, and supplied on the finest scale grid-resolution for the current study, for average 1995 conditions. The re-evaluation of R_{rib} on the finer-scale grid was performed by the District as follows (B. McGurk, personal communication):

   There are 4 sites within the current study area, where the ECF regional model was assigned RIB flow. Estimation of these flows was performed individually for each site as noted below:

   a. <u>Longwood</u> (ECF model cell id values 11142 & 11143): The ECF model RIB flow was re-assigned to the appropriate cells of the local model using 1995 & 2000 photo-imagery. Furthermore, a field inspection of this site indicated that the basins were somewhat elevated above the surrounding area and contained little or no standing water; however, the bottoms of each of the basins contained abundant vegetation, indicating that much of the reclaimed water disposal is lost via ET in the basins. Therefore, water applied to this basin was not treated as RIB flow, but as a discharge to percolation ponds which was included as a separate attribute named "pondflow" to represent average 1995 flow to percolation ponds. This segregation was performed because percolation ponds (made up of the "pondflow" type of reclaimed water disposal and reclaimed spray irrigation at percolation ponds) will be treated separately in future ECF regional model simulations.

b. Winter Springs west (ECF model cell id = 11343): A field inspection indicated that this site should be treated in the same fashion as the Longwood site. Note, however, that the average flow rate at this site has been revised to equal 0.259 mgd, from the rate used previously in the ECF model.

c. Greenwood Lakes (ECF cell id = 10560): The ECF model RIB flow was re-assigned to the appropriate cells of the local model using 1995 & 2000 photo-imagery.

d. Orange County NWSA (ECF cell id = 13448, 13449, & 13643): Average 1995 RIB flow rates were taken from Table 4.2.1 of P. B. Water (2000). These flow rates were assigned to the local model grid cells using Figure 5.3.1 of the same report, and 1995 & 2000 photo-imagery.

3. Yet another source of water to the surficial layer is R_{app} representing water applied to the land surface as irrigation. R_{app} is the sum of agricultural and golf-course irrigation R_{ag}, and total landscape irrigation (representing R_{spray}, R_{psli}, and R_{ssdli}, respectively, where R_{spray} represents landscape irrigation or spray-field irrigation derived from reclaimed water distribution systems, R_{psli} represents landscape irrigation using water derived from Floridan aquifer system public-water supply withdrawal and R_{ssdli} represents landscape irrigation derived from Floridan aquifer system self-supplied domestic well withdrawal). This information was available from the ECF model grid, but was re-evaluated by the District on the finer grid of the local model, to resolve the scale issues of the various grids used in this study. Note that "pondflow", is now included with R_{app} to represent RIBs that behave as percolation ponds (as discussed above), and reclaimed water spray irrigation as discussed below. The re-evaluation of the various components of R_{app} on the finer-scale grid of the local model was performed by the District. A write-up of how this data was altered was provided by B. McGurk (personal communication) and is reproduced here to provide continuity with the ECF model of McGurk and Presley (2002).

a. R_{spray}: R_{spray}, values from the ECF regional model were distributed among the appropriate local model grid cells in the following manner:

b. For reclaimed spray irrigation on residential and/or recreational land uses, the following method was applied:
   - For each ECF public-water-supply service area, model cells with R_{spray} values for 1995 were first selected.
   - Then local model grid cells within the selected ECF grid cells and with a percentage of "urbanized" land use (FLUCCS codes 1100-1490 & 1700-1890) greater than 50 were selected next. The land use coverages are discussed later in Section 4 when addressing surface flow conceptualization.
   - The total volumetric flux assigned to each group of ECF cells with the same R_{spray} values (usually the same in each public-water-supply service area) was recalculated and reassigned to the selected local model grid cells.

- This process was repeated for each public-water-supply service area within the local model domain.
- Where an ECF model cell covers only a portion of the local model domain (near the local model boundaries), the percentage of urbanized area within the ECF cell covered by the local model cells was estimated; this percentage of the R_{spray} flow rate was then distributed to the active local model cells.

c. For reclaimed spray irrigation at specific percolation ponds, the volumetric flow rate corresponding to the ECF model R_{spray} value was distributed among the appropriate local model cells using 1995 & 2000 photo-imagery. The exception to this method is Winter Springs east (ECF model cells 11926 & 11927) where percolation pond flow was assigned to a single cell (cell 11927) in the ECF model. Photo-imagery shows ponds at this site extending into the adjoining cell 11926 - therefore total flow was assigned to local model cells covering all percolation ponds at the site.

d. $\underline{R_{psli}}$: Estimation of public-supply landscape irrigation followed the same procedure as that used for reclaimed spray irrigation on residential and/or recreational land uses.

e. $\underline{R_{ssdli}}$: In the ECF model, it was assumed that self-supplied domestic landscape irrigation (R_{ssdli}) occurs as a portion of (50%) the self-supplied domestic withdrawal. The remaining 50% of self-supplied domestic withdrawal is attributed to $R_{septic}95$, the septic tank effluent. Further, it was assumed that the water withdrawn is re-applied onto the same grid block (areally) from which it is extracted, for both $R_{septic}95$ and R_{ssdli}. Therefore, the treatment of R_{ssdli} was identical to that of $R_{septic}95$ which is discussed later.

f. $\underline{R_{ag}}$: Estimation of irrigation from agricultural, golf course, landscape irrigation, or recreational Floridan Aquifer System withdrawals for the local model cells was performed by the District as follows. Wells with use categories A, G, L, or R and located within the active local model domain were joined with the irrigation estimates and a linear flux value (inches/year) for the R_{ag} was calculated from the 1995 volumetric well flux for the grid cell in which each well is located. This linear flux assigned to the cell in which the well was located was, for most well locations, redistributed among the local model grid cells included within the corresponding Consumptive Use Permit (CUP) project area (with the appropriate land uses). The use of 1995 vs. 2000 photo-imagery further revealed that 2 agricultural/golf course sites were not yet in operation in 1995. For these cases the 1995 well flux was changed to zero, but was maintained for the 2020 simulation case.

The sum of R_{rib} and R_{app} was applied as inflow to the surficial (overland flow) layer of the model as shown in Figure 3.2.

4. Additional input of water to the model due to R_{septic} (septic tank effluent) occurs in the upper SAS layer beneath the topsoil (second subsurface model layer). In the ECF model, it was assumed that R_{septic} occurs as a portion of (50%) the self-supplied domestic withdrawal. Information on the distribution of R_{septic} for average 1995 conditions over the current model area was available at the resolution of the ECF model grid-block but was recalculated over the finer local model grid-block scale (shown in Figure 3.3). The recalculation was performed by the District to accommodate the finer grid scale as follows:

   a. For each county in the local model domain (Orange & Seminole), the ECF regional model cells that contain non-zero R_{septic} values were selected.

   b. The total volumetric flux attributed to these cells (cfd) was then computed.

   c. The local model grid cells located inside the selected regional model cells that have a percent of residential/urban land use (FLUCCS codes 1000-1299) greater than 50%, or that have an agricultural land use with evidence from photo-imagery of residential dwellings were selected.

   d. The total volumetric flux was divided by the net area of local model grid cells selected, to obtain an estimated linear flux for each of the selected local model grid cells (in/yr).

   This procedure of scaling down R_{septic} from the ECF model values is consistent with the assumptions made in evaluating them for the District's regional ECF model simulations, where it was further ensured that the ECF model grid-cell did not contain a public water supply service area, for it to contain septic tank recharge.

5. Hydraulic characteristics of the surficial layer and the moisture state and properties of the topsoil layer determine how water applied to the surface is partitioned into overland runoff (O) along the surficial layer, and infiltration (I) into the topsoil layer. The integrated surface/subsurface model, when appropriately parameterized, internally determines the partitioning of P (and other water applied to the surface of $R_{rib} + R_{app}$) into O and I. In the ECF model, these parameters were user-inputs whereby O was calculated according to the SCS curve number approach. This value of O may be subtracted from the net applied recharge to the ECF model ($P + R_{rib} + R_{app} + R_{septic}$), to estimate a distribution of "I" as applied in the ECF model, shown in Figure 3.3. This distribution was compared to infiltration calculated by the current modeling effort, to systematically note differences in infiltration rates resulting from an integrated surface/subsurface conceptualization.

6. A major outflow of water from the system under investigation is evapotranspiration (ET).

7. ET was conceptualized as a combination of transpiration and evaporation, and the amount of ET cannot exceed the reference crop evapotranspiration which is the maximum annual evapotranspiration rate, ET_o or ET_{max} (note that FAO guidelines [Allen

et al, 1998] discourages the use of terminology such as Potential Evapotranspiration (PET) due to ambiguities in their definition). Information on the distribution of annual average ET_{max} was available from the ECF model's data assimilation effort, and is shown in Figure 3.5 over the current model area. This data was used to parameterize ET_{max} for the current modeling effort, and thus maintains consistency with the assumptions of the ECF groundwater flow model of the District to represent predevelopment, average 1995, and 2025 predictive conditions.

8. Evaporation is the mechanism that extracts an ET_{max} amount of water from surface water bodies or low-lying wetland regions, up to a point where the surface water body goes dry, at which stage only as much evaporation occurs, as is possible to maintain the dry conditions (i.e., Surface water evaporation, EV_s, cannot extract more water than is available at any given location at any time, and hence $EV_s < ET_{max}$).

9. Transpiration plus evaporation (from detention storage in the surficial layer and from the subsurface including the topsoil, and the upper SAS layer) are the mechanisms that extract water from the saturated and unsaturated zones in the upland regions. The maximum amount of water that can be withdrawn by both transpiration and evaporation from these regions is ET_{max}.

10. Transpiration is a function of the following parameters:

    a. the vegetation's Leaf Area Index (LAI) – larger leaf area index allows for greater transpiration;

    b. the available moisture (Q) – transpiration reduces when moisture becomes unavailable;

    c. field capacity (Q_{fc}) and wilting point (Q_{wp}) in the topsoil, and the upper SAS layers – transpiration is largest at field capacity, and lowest at the soil's wilting point moisture content; and

    d. the root-zone distribution function (RDFI) which defines the fraction of active root penetration among the subsurface layers – larger amount of active roots at a given depth promotes more transpiration from the associated model layer. Values range from zero to one.

Land use and soils data (SSURGO database) were used to aerially distribute these parameters to the topsoil and upper SAS model layers. LAI is correlated to land use, and Q_{fc} and Q_{wp} are correlated to soil type. Land use data shown in Figure 3.6 includes delineation of the land into citrus, abandoned trees, nurseries, residential, row field crops, urban/commercial/industrial/paved, and wetlands for 1995 conditions. Initial values of LAI were obtained from Scurlock et al. (2001). Table 3.1 lists all land use codes in the model area and the assigned LAI value. Soil data were provided via the Soil Conservation Service (SCS) hydrologic soil groups (as shown in Figure 3.7) which categorizes the runoff potential. Initial values of field capacity and wilting point were obtained from Carsel and others (1988). Table 3.2 lists the hydrologic soil groups and the assigned field capacity and wilting point. For initial parameterization of the transpiration model, RDFI was assigned 0.8 for the topsoil (layer 1) and 0.2 for the upper SAS (layer 2). The parameter values were varied upon calibration within an acceptable range of values.

11. Evaporation is a function of the following parameters:

    a. the LAI – larger leaf area allows for less energy penetration to the surface causing less evaporation;

    b. the Q_{e1}, Q_{e2} and Q – evaporation is larger when available moisture is more. It is largest at the soil's energy limiting stage, Q_{e1}, which is taken equal to the field capacity moisture content, and lowest at the soil's limiting moisture content, Q_{e2}, which is taken equal to the wilting point moisture content; and

    c. an energy penetration function (EDFI) up to an extinction depth. Typically, energy penetration into the soil is small, with most of the energy for evaporation dissipating within a foot or so of the land surface. Therefore, the EDFI was set to unity for the topsoil layer, and to zero for the two SAS layers below. Variations may be made during calibration, due to the uncertainty of this parameter (which in conjunction with RDFI directly correlates to the extinction depth concept in MODFLOW whereby it is inherently assumed that energy cannot penetrate beyond an extinction depth).

12. Information on groundwater ET_{sat} for average 1995 conditions as estimated by the ECF model was available as a volumetric flux along with the ECF model ET_{unsat} estimates. The groundwater ET_{sat} and ET_{unsat} were added to give the total ET from the region, as shown in Figure 3.8. This information was compared to net ET distributions calculated in the current model, to note differences in net ET rates resulting from a more rigorous unsaturated/saturated ET conceptualization.

13. The remaining portion of infiltration (I), after accounting for ET, is the net groundwater recharge to the SAS. This water further recharges the UFA and subsequently, the LFA, in regions where the potential gradients are downward between these units. Water also discharges from the LFA to the UFA and from the UFA to the SAS in regions where the potential gradients are upward between these units. Discharge also occurs from the UFA directly into rivers and springs (the surficial layer, or the surface water features) in regions where the ICU is thin or breached. The location of springs within the study area is shown in Figure 3.9. Higher conductivity connection features between the UFA and the SAS were specified at these locations (i.e., vertical fractures of higher conductivity connect the UFA and the SAS). Each spring also has some or all of the following data attributes: Flow rate (cfs); potential difference; top elevation; and aquifer. The first two were used as calibration targets for the current study, assuming they represent average 1995 conditions. Spring data from Table 5 (McGurk and Presley, 2002) of the ECF study were also used as calibration targets.

14. Although modeled as such in the ECF model and previous USGS models, there is no documentation of breaches in the ICU along the Wekiva River in the immediate vicinity of Wekiva Spring and Island Spring. Measurements taken during low-flow periods in recent years did not indicate an increase in flow along the stretch of the river downstream of the Little Wekiva (B. McGurk, personal communication). Therefore, the river cells that were modeled in the District's ECF groundwater flow study as occurring within the Upper Floridan Aquifer within this area were not modeled within this study. Rather, the current model allows for diffuse leakage through a thinner ICU, to represent the same water discharge mechanism in a more realistic fashion.

15. A substantial outflow of water from the system occurs as a result of pumping. Pumping information, for average 1995 conditions, may be a result of several distinctly categorized types of average 1995 pumping. Point data coverage for all withdrawal locations is shown in Figure 3.10 with 1995 average withdrawal rates shown in Table 3.3. This information was provided on a cell-by-cell basis for the ECF model grid, and was used for the initial coarse grid simulations. However, updated information was made available for the various components of well flux for average 1995 conditions, which was assimilated to create the various well files used in model development for the WOSC-ISGM. The following types of wells were present in the ECF model and are considered for the current study:

    a. Withdrawal well fluxes and locations were updated using revised information supplied by the District. The new information updates a total of 13 well locations and 7 withdrawal fluxes from the set used in the ECF model of McGurk and Presley (2002) with the remaining wells having same locations and pumping rates. These well fluxes were further updated with irrigation withdrawal estimates, for the WOSC-ISGM simulations.

    b. DRN (Drainage) well fluxes were initially used as input to the model till the point the model was fully developed to include the surface water regime, after which the drainage well fluxes are internal to the system and therefore not required as a boundary flux in the input files.

    c. FFW (Free Flowing wells) locations and fluxes were directly used in the MODFLOW simulations well files, as obtained from the ECF model of McGurk and Presley (2002).

    d. SSD (Self-Supplied Domestic) well locations and fluxes were directly used in the MODFLOW simulations well files, as obtained from the ECF model of McGurk and Presley (2002).

16. Other components of inflow and outflow to the system occur via the lateral boundaries of the subsurface. These boundaries were obtained as prescribed heads from a regional simulation of the ECF model, for similar stress conditions so that the effects of regional pumping on the regional potentiometric surface (and associated groundwater fluxes) were

included in the WOSC-ISGM. The saltwater boundary in model layer 4 was conceptualized in a similar manner to the District's ECF model, using a GHB condition. Flux into the model from this "saltwater GHB" boundary is a surrogate to represent the inland movement of the saltwater from this location. However, it is noted that there actually were no such GHB boundaries within the WOSC domain.

17. Data available on the drainage wells is important for locating and parameterizing (via the attributes depth, casing, and diameter) these features in the conjunctive model. Drainage wells were used as sources of water to the UFA in the ECF model, but are an internal feature of the integrated surface/subsurface flow model.

The water budgets terms P, R_{rib}, R_{app}, R_{septic}, ET_{max}, pumping stresses, and boundary flows (heads) were not altered during the calibration process from the ECF model values. Thus, the assumptions of the District's regional ECF modeling effort and consistency with the coarser scale regional study were maintained. Parameters that quantify other water budget terms including LAI, Q_{fc}, Q_{wp}, RDFI, and EDFI were varied during the calibration process because initial parameterization from literature values has a large range of variation for a particular soil, land use or crop type. However, areal distributions of each of these parameters were not changed from the conceptualization discussed above.

4.0 SURFACE FLOW DATA AND CONCEPTUALIZATION

A physically-based, spatially-distributed (PBSD) approach was used for quantifying the surface-water flow domain. This is consistent with the PBSD approach used for the subsurface. The model discretization therefore requires one more layer which represents this surficial layer (the overland flow surface), which communicates water to and from the subsurface. Furthermore, to accommodate small scale hydrology features (compared to the grid-block size), the model includes a surface-water body layer to represent small lakes, ponds, rivers, canals and streams which communicate water with both the overland surface as well as the subsurface. Conceptualization and parameterization of these surficial water flow domains and their interactions are discussed in this section.

4.1 OVERLAND FLOW SURFACE

The diffusion wave approximation is used to simulate flow of water along the surficial layer, thus neglecting the inertial terms of the Saint Venant equations. The inertial term is usually negligible except for flash flooding or dam-break cases, at early times, and the diffusion wave equation is sufficient for long-term water resource analysis such as the current study. Manning's equation is used to parameterize the friction term for overland flow, while Darcy's Law allows for infiltration of water into the topsoil layer. Therefore, runoff generation is a function of both the land cover features that determine the friction term as well as of the soil surface's and top-soil's overall drainage characteristics (note that this is also the case for the Curve Number in the SCS Curve Number approach). When the water level of the first subsurface cell is higher than the topographic surface (such as in depressional features or near the bottom of steep ridges), water seeps out of the subsurface as governed by Darcy's Law. Conversely, at higher elevations where the topmost soil layer is unsaturated, or in regions where water head gradients are downward, water infiltrates into the subsurface.

The diffusion wave equation is parameterized by a Manning's coefficient, and by the slope of the land surface and the depth of flow. Land slope and depth of flow are directly related to the topography (including for dry conditions) which is shown in Figure 2.3. Land use coverages were used to areally distribute the Manning's coefficient. Initial values of Manning's coefficient were obtained from Chow (1959). Table 4.1 lists all land use codes in the model area and the associated Manning's coefficients. Figure 4.1 shows the areal distribution of Manning's coefficient across the WOSC study area resulting from the area-weighted average distribution of the values of Table 4.1 onto each overland flow surface grid-block.

Boundary conditions to the surficial model layer are no-flow conditions along the lateral edges of the study area. The domain extent was specifically chosen to be aligned with basin boundaries to allow for implementation of this condition, because upstream boundaries are otherwise difficult to define.

4.2 SURFACE HYDRAULICS CHARACTERIZATION

All features of the land surface can conceptually be represented by the overland flow surface, including surface water features such as ponds, lakes, reservoirs, rivers, streams and canals. However, there is an issue of scale, whereby there is a minimum practical limit on the areal grid-block size, for the overland flow surface as well as for the subsurface layers. Therefore, to accurately simulate surface water features which may be smaller than a grid-block size, and to convey water through canals or conveyance structures (whose widths are much finer than the grid-block scale or whose orientation may not conform well with the finite difference grid structure), a surface-water-features layer was added on top of the surficial model layer. The surface water features that are present within the study area include small lakes and ponds, which may be characterized by their stage-volume (or stage-surface area) relationships. These surface water features may be internally drained, or may be connected via conveyance structures (channels, weirs, culverts, drop structures) to other similar features or to channels, streams, and rivers (themselves surface water features).

Conveyance of water between surface water features (including among river, stream and channel segments) is a function of the friction characteristics of the beds, and/or of the depth of flow within them and their geometry. The diffusion wave equation is used to characterize flow along rivers or streams and is parameterized by a Manning's coefficient, the streambed slope, the cross-sectional geometry of the channel (specifically relations between the flow depth, cross-sectional area, wetted perimeter and top width), and the depth of flow. Manning's coefficient values may be obtained from available site-specific data or from literature values provided by Chow (1959). Tabulated stage-discharge relations provide characterization of flow across various structures where flow is a function of upstream head only, or of both upstream and downstream heads. This general relationship allows for a wide variety of structures and their designs to be accommodated. Finally, Darcy's Law allows for interaction of water with the subsurface, and weir equations quantify the interactions of channels or ponds with the overland flow surface across the banks of the respective channel or surface-water body.

Geometric details of surface water features, and the conveyance flow and geometry characteristics, as well as linkage among surface-water features (including channels, streams and rivers) have been compiled for several basins by various County and State organizations, for use in storm-water management simulations using a model called ICPR (acronym for Inter Connected Pond Routing model). The latest available data is periodically field-checked by these organizations and their contractors (for instance, to examine the condition of storm-water drain blockages or culvert collapse), and updated via photographs and imagery, where information is unavailable from standard sources. In addition, some of this information is available via reach-files downloadable from the EPA or from the County's hydrography shape-files. The level of detail available through the reachfiles, though not as extensive as the local information available from the storm-water runoff ICPR models, should be sufficient for long-term water resource evaluations and was used in locations where ICPR data was unavailable. Hence the EPA reach-files provide the hydraulic data where ICPR models were not used. For the WOSC-ISGM, the surface hydraulic components were assembled as follows:

1. ICPR models exist for Soldiers Creek, Gee Creek, Little Wekiva, Lake Sherwood, and Lake Horseshoe basins as database files in .DBF format. An ICPR model for the Ocoee area was provided too late for incorporation into the current study. Figure 4.2 shows the coverage provided by these ICPR models. The node and hydraulic data (network, channel cross-sections, weirs, culverts, drop structures, lakes, etc) from these database files was first transferred to a Microsoft ACCESS database. Then, the spatial co-ordinate

information was extracted from geo-referenced AutoCAD drawings with the aid of appropriate pre-processors and GIS software. A utility (ReadDXF) was used to extract spatial co-ordinate information from the network drawings (.DXF format) for the Soldier's Creek and Gee Creek models. However, since the AutoCAD drawings for the Little Wekiva, Lake Sherwood and Lake Horseshoe basins are not assigned 'object handles', these drawings were re-digitized using GIS software (ARCMAP) to extract the required spatial co-ordinate information. Lastly, a utility (CalcDAPW) was used to process channel cross-section data into Depth, Area, Perimeter, and Top-width relationships for valid channel cross-sections. Finally, error checking was performed to ensure the integrity of the data in the database.

2. After all the ICPR model data was transferred to the Microsoft ACCESS database, it was imported into ViewHMS, a graphical user interface for the MODHMS software. Custom tables and queries were added to the database to organize the data. Following the guidelines specified in the 'ICPR to ViewHMS' document, the data from the ICPR database was transferred to ViewHMS and linked with the groundwater model for the region. This new model containing both groundwater and surface water data was saved as the preliminary model with missing data subsequently filled.

3. The software model BASINS (USEPA, 2002) was used to generate reach files for catalog units 03080101 and 03080102 in the model area. This data was added to the preliminary surface water model in 2 steps. In the first step, the river networks were isolated and pre-processed with ArcHMS (a GIS based MODHMS pre-processor) and the processed data were added to the preliminary surface-water model. Processing involves connecting river segments to reaches, connecting reaches to junctions, and applying other available information to the respective segments via interpolation. In the second step, the surface water bodies (lakes, ponds) in the region were added to the model. However, the reach files do not have data for some smaller lakes in the region which we finally added to the model from the hydrography shape file supplied by the District (note that this hydrography file was used to provide the hydrographic features on the base-map of all figures).

4. Since cross-sectional details for reaches imported from the reachfiles are not available, these channel cross-sections were assumed to be rectangular with a depth of 15ft and a width of 50ft. These values reflect the average of various channel cross-sections in the adjacent ICPR models. The Manning's roughness coefficient for these reaches was assumed to be 0.035 ($s/m^{1/3}$) from the roughness coefficient value for similar channels. The leakance value of the channel bed was assumed to be 0.01/day as an initial estimate. This number is a calibration parameter which will be varied during calibration to produce appropriate observed behavior. The bank elevations were obtained from the 1ft contour shape-file. The bed elevations were calculated by subtracting the channel depth from the bank elevations.

5. Since information on lake geometry with depth was unavailable for the surface water bodies incorporated from the reach-files or the hydrography shape-file, the surface water bodies in the model were represented as circular cones. The cross-sectional area at the

bottom was assumed to be zero. At the surface, the lake was assumed to be a circle whose perimeter is equal to the actual perimeter of the lake as provided by the attribute '*LENGTH_M'* in the reach files. For the lakes that are added from the hydrography shape file, the perimeter was calculated by measuring the length of the polyline representing the lake. The surface area of the lake (area of the circle) was then back-calculated from the perimeter. The Seminole county water atlas (http://www.seminole.wateratlas.usf.edu) is a useful reference for determining lake depths. By comparing the lake depths from this website and at the depths from the lakes in the ICPR models, surface area and depth were correlated. The leakance value of the lake bed was assumed to be 0.12/day as an initial estimate. This number is a calibration parameter which will be varied during calibration to produce appropriate observed behavior. The bank elevations were obtained from the 1ft contour shape-file. The bed elevations were calculated by subtracting the lake depths from the bank elevations.

6. Once all the data was entered in the channel package file, the control flags were modified to be consistent with the new dataset. Error checking was performed to ensure the integrity of data. Bed and bank elevations were corrected for a few channel segments where the data resulted in physically infeasible flow scenarios. Local changes to the assumed parameters (leakance, depth, roughness) were made during calibration.

Figure 4.3 summarizes these steps as needed to develop detailed hydraulics for the WOSC-ISGM. Figure 4.4 shows the surface-water features as implemented into the model. It may be noted that Soldiers Creek, Gee Creek and the Unnamed Lake District include several of these features, while the other basins are sparser. These other basins are internally drained and therefore do not have many connecting hydraulic features.

Surface water gauging information is available for lake levels from June 1995 through September 1999. Not all fields of these data are populated, with zeros indicating a lack of observation. Information that is available was averaged or extrapolated to represent annual 1995 conditions as shown in Table 4.2. Locations of these sites are provided in Figure 4.5. Head and/or flow information available from these sites was used to evaluate steady-state calibration of the integrated surface/subsurface flow model. Transient surface water flow data is also available from gauging stations on perennial streams. This information was used and is discussed later during transient calibration.

Boundary conditions for surface-water features, specifically streams and rivers include a flux or head boundary at the upstream reaches where water enters the domain, and zero-depth-gradient, or critical depth conditions (as appropriate) where water leaves the domain. For features draining to Lake Jessup, prescribed head conditions were used since the heads (stage) of these relatively large lakes is controlled.

The surface-water features information (lake and pond information, as well as river and channel sectional and connectivity information) was not changed during the calibration process. Manning's coefficients for the overland flow surface and for channel and river beds was varied due to the large range of values exhibited by various soil cover and channel bed types. Areal distributions were not changed, however, from the conceptualization provided above. Leakances of the surface water features, of springs, and of the land cover were treated as calibration parameters, since no information is available for these parameters. General guidance was used (for instance a paved surface has very low leakance), and drain/river leakances used in the ECF model were examined to evaluate the ranges used therein, to provide the initial estimates.

5.0 UNSATURATED ZONE DATA AND CONCEPTUALIZATION

Unsaturated flow occurs within large portions of the topsoil layer, and possibly also within the upper two SAS layers. The unsaturated zone was conceptualized for flow of water according to the three-dimensional Richard's equation. Thus, unsaturated zone moisture movement is dependent on the saturated conductivity of the soil, as well as on the moisture content within the soil. The moisture content, in turn, is a function of the capillarity of the soil. Therefore, the state of the system (in terms of the available moisture at any location) is also an important governing process controlling the movement of water within the unsaturated zone. Water entering the unsaturated zone from the surficial layer travels down to the water table as groundwater recharge and also travels laterally within the subsurface as interflow, depending on the moisture state of the system and on the capillary potentials within the unsaturated zone.

Data required to characterize the unsaturated flow of the soil (given the soil's potentiometric state) include the saturated hydraulic conductivity, and the moisture retention and relative permeability curves. The moisture retention was parameterized by the van Genuchten curve and the relative permeability was parameterized using the Brooks-Corey relation, for the topsoil and the upper SAS layer materials. The SCS hydrologic soil groups found in the SSURGO soil database was used to categorize the upper three subsurface numerical layers. Initial values of hydraulic conductivity and van Genuchten parameters were obtained from Carsel and Parrish (1988) (as shown in Table 5.1) for the different soil types. Parameter values were distributed within each grid-block as per the areal weighted average of soil-type distributions within the grid-block. These values have a large uncertainty, due to the fairly large range of literature values for a soil type. Averaging of these effects over a grid-block containing several fine-scale heterogeneities further adds to the uncertainty and therefore they are subject to change during calibration. It is noted that the upper SAS layer may be above or below the water table. For saturated portions of this unit, only the saturated hydraulic conductivity input is necessary and the Richard's equation reduces to the groundwater flow equation.

6.0 MODEL DEVELOPMENT AND CALIBRATION

6.1 MODEL TRANSFER AND GRID REFINEMENT

Model development for the WOSC-ISGM was performed in a systematic step-by-step manner starting with the District's ECF groundwater flow model of McGurk and Presley (2002). Results of the ECF model study were first examined only over the WOSC-ISGM study area, to quantify the state of the system via the various mass balance components, head levels, and residuals for the ECF study, as reported in data column 1 of Table 6.1. Next, the District's ECF model data and conceptualization were transferred onto the local WOSC-ISGM domain, at the same grid scale as the District's ECF model (2500 ft by 2500 ft areal grid-block size). Boundary conditions for the telescopic local model were taken as prescribed heads, with head values obtained from the regional model. This model was run for steady-state 1995 conditions (as done for the ECF model), and the state of the system (mass balance components, heads within the domain, and head residuals as compared to average 1995 observed heads within the study area) was compared with that of the regional model to ensure a consistent conversion. As noted in Table 6.1, the resultant head values (data column 2 of Table 6.1) were within 1 foot of the ECF model head values for all aquifer units, volumetric budget flux values were within a fraction of a percent from the ECF model simulation, and the observed residuals were practically the same between the two models over the WOSC-ISGM domain. Thus, translation of the ECF model to the local WOSC-ISGM domain is accurate, with the same flow behavior being exhibited by both regional and local models.

The second simulation performed for model development uses the same data-set as the first one, but applies the model using MODHMS options for solving groundwater flow instead of the traditional MODFLOW options, including use of a different matrix solver (since the MODFLOW solvers are not suitable for the integrated model). Significant results of this simulation are presented in data column 3 of Table 6.1, with heads, volumetric budget component fluxes, and residuals being virtually identical to the first simulation. Thus, a change towards MODHMS options does not affect the results of the simulation for the WOSC-ISGM study area.

The third simulation of model development updates stratigraphic data (as per Section 2.2) and the recharge values (as per Section 3) from more recently obtained information. Pertinent results for this simulation are also noted in data column 4 of Table 6.1, and are comparable to results of the previous simulation, indicating that updates to the ECF model stratigraphy and recharge do not have a significant impact to the WOSC groundwater flow system. A notable exception is the SAS head in the Lake Marden basin area, which was about 10 ft higher than for the previous simulation. This is attributed to the updated recharge applied in the region which was higher than for the previous model simulation. Flow in/out of ponds, rivers, drains, and evapotranspiration boundaries were affected by the generally higher water table values which result from a generally thicker (less leakance) ICU. Table 6.2, which provides a more detailed break-up of the flux components as pertaining to the exchange of water between the SAS and the UFA-UZ, also shows the reduction of exchange of water between the 2 units as a result of the generally thicker ICU used in this simulation. It is noted that the value of "flow-between-constant-head-cells" was different from previous simulations, because of a change in the modeling option which does not allow for flux computations between 2 adjacent constant head cells. This was done because of the difficulty in comparing lateral boundary fluxes when both grid and boundary are refined for further simulations.

The fourth step of model development is grid refinement. A finer grid was first designed (by doubling the number of nodes in the x- and y-directions), and the conceptual model (from GIS files) of the previous simulation was translated onto this finer grid for two simulations of the same problem. As a first simulation, the lateral prescribed head boundary was not refined, with this being done for the second simulation of this set, to provide a quality control check on translation of the model as noted by the mass-balance components summary. The grid size for this simulation set is 1250 ft by 1250 ft areally. Results provided in data columns 5 and 6 of Table 6.1 for these two steps respectively, show that the system behavior was affected only slightly by grid refinement, except for the Lake Marden basin area within the SAS, where the heads were about 10 ft higher than those of the previous model development simulation. The higher heads in this region are mainly due to refinement of the RIB fluxes on the refined grid. The larger computed fluxes from constant head nodes noted in Table 6.1 are due to local boundary effects. In general, heads and fluxes within the domain were comparable between the coarse and fine grid simulations. A comparison of the coarse boundary and refined boundary simulations (data columns 5 and 6 of Table 6.1) shows that the active domain area was changed with an associated change in the net flux computations for the various volume budget components within the active area.

An even finer grid was designed for the next simulation of model development, by further doubling the number of nodes areally in the domain. Grid-block sizes are 625 ft by 625 ft areally, for this case. The conceptual model (from the GIS data) was then translated onto this grid for a simulation of steady-state 1995 conditions to note the effects of even further grid refinement as provided in data column 7 of Table 6.1. The state of the system as compared to the previous simulation in Table 6.1 shows that further refinement of the grid from 1250 ft to 625 ft areal cell sizes does not significantly affect the results. Heads within the domain were about 2 ft higher in the Lake Marden basin area within the SAS for this case than for the previous simulation case that uses a 1250 ft grid size. Head differences among the grid-refinement simulations were less than a foot for the UFA, and were negligible for the LFA. Thus, the simulations seem to be grid-converged for the 625 ft by 625 ft areal grid size, for the scale of material property heterogeneity and recharge application, as provided in the conceptual model. Mounding due to recharge and depressions due to pumping were adequately addressed, and do not seem to change much with grid size for a reduction to 625 ft, as it does for a reduction of the ECF model grid (from 2500 ft) to 1250 ft. Differences in mass balance component fluxes between the 1250 ft grid and the 625 ft grid result from the change in the active domain area caused by refinement along lateral prescribed head boundaries. The large difference in the flow to/from constant head boundaries is attributable to local circulation effects that occurred with boundary head refinement in the refined grid as noted by the approximately equal increases in the inflow term and the outflow term.

6.2 DEVELOPMENT OF UNSATURATED ZONE FLOW AND RIGOROUS ET

The next step in model development enhances the conceptualization of the SAS to account for two hydrogeologic units – a lower unit comprising silty-sands and clays that occur below the first occurrence of clay in the SAS, and an upper unit comprising sands immediately beneath the surface. The segregation of the SAS into upper and lower units results in a 5 layer model which was translated onto the 625 ft by 625 ft areal grid. This step of model development was also done in two stages. For the first stage, the lower unit was given a uniform horizontal hydraulic conductivity value of 2 ft/d, and the upper unit was given a uniform horizontal hydraulic conductivity value of 40 ft/d as per average values of the Lake Marden study of P. B. Water (2000). For the second stage, the horizontal hydraulic conductivity of the upper sand unit was varied spatially, according to the area-weighted hydrologic soil groups encountered within any grid cell as noted from Figure 3.7. The pseudo-transfer function between hydrologic soil groups and horizontal hydraulic conductivity values used in the simulation is tabulated in Table 5.1. Vertical hydraulic conductivities were maintained as one-tenth of the horizontal hydraulic conductivities for both stages of enhancing the SAS conceptualization. Result summaries for these simulations are incorporated into data column 8 Table 6.1. Results of the first stage of this step of model development do not deviate significantly from the 1-layer SAS conceptualization results, with notable differences occurring only for the ET, river and pond fluxes. The second stage of this model development step (wherein the hydraulic conductivities of the top SAS layer vary areally) is summarized in data column 9 of Table 6.1 and shows similar head patterns as the previous stage, though the flux deviations were larger. The RMS error for this case however, is larger than for previous cases, with a maximum absolute error of about 15 ft. A calibration effort on the hydraulic conductivities of the first layer of the SAS could reduce this error, however, the overall system response as noted by head contours, was not significantly different from other previous simulations, and therefore the 1-layer vs the 2-layer conceptualization of the SAS was not adversely sensitive to the head and flow results.

The next step of model development incorporates two additional numerical grid layers in the upper SAS unit, but still maintains the unconfined groundwater flow model. Adjustments were made to the lateral constant heads in that they were not applied along model layers 1 and 2, which are possibly unsaturated. Further, ET was temporarily moved to layer 3 to avoid attempting extraction of water from dry layers. Note that the MODFLOW saturated zone ET function will be removed later in the model development process, when ET is represented by the physically-based ET conceptualization discussed in Chapter 3.0. Results of this simulation noted in data item 10 of Table 6.1 were almost identical to the 5-layer model of the previous development step thus ensuring that the newly created 7-layer model was accurate. A notable difference is the fluxes to ponds which show larger inflows and smaller outflows than the previous simulations, resulting from lowering the constant head nodes into layer 3. Note that the "constant head" conceptualization of ponds is removed later in model development process, when the ponds are represented explicitly by the surface-water modules.

The next simulation incorporates real soil functions into the SAS upper unit, to represent unsaturated zone flow conditions. The van Genuchten parameters were provided to each grid block according to the area-weighted hydrologic soil group encountered within any grid cell, where soil groups were related to the moisture retention and relative permeability parameters according to the pseudo-transfer functions of Table 5.1. Water levels in the SAS and fluxes throughout the domain resulting from this simulation as summarized in data item 11 of Table 6.1, were very similar to the previous case and were not affected by the use of real unsaturated moisture movement or vertical equilibrium assumptions (noting that MODFLOW's groundwater ET function was still being used to extract ET from the saturated zone).

At this stage of model development, the hydraulic conductivity values of the upper SAS layer were re-evaluated based on site conditions and noted to be high. Thus, the hydraulic conductivity of the upper SAS layer was halved to better represent site drainage conditions. The resulting areal distribution of horizontal hydraulic conductivity used in the simulation is shown in Figure 6.1, and better represent the average value of 40 ft/d and spread of 5 to 80 ft/d noted in the Lake Marden basin study of P. B. Water (2000). The mass balance component fluxes were not much different from the previous simulation values as seen in data item 12 of Table 6.1, however, the RMS and maximum error of the entire model for this case drop significantly. Table 6.2 shows that the improvement in RMS and maximum errors was significant in the SAS system for this case and indeed, the hydraulic conductivity values of the upper SAS layer being lower produces better head matches with SAS observations.

The next simulation removes the unsaturated zone ET assumptions made for the ECF model, and uses instead, the transpiration and evaporation functions of MODHMS that relate ET to actual vegetation and moisture conditions. For this case, therefore, the MODFLOW saturated zone ET package was disconnected, and the MODHMS IPT package for computation of both saturated and unsaturated ET was attached. Further, the recharge applied to the model now includes the unsaturated zone ET which was conceptually removed apriori from the ECF groundwater model. The computation of comprehensive evapotranspiration from moisture availability conditions uses field capacity and wilting point moisture conditions to determine the actual ET from the system. These were obtained according to the area-weighted hydrologic soil group encountered within any grid cell, where soil groups are related to the required moisture conditions according to the pseudo-transfer functions of Table 3.2. Additional parameters required for ET computations are provided in Table 6.3. These parameters are obtained from the literature, and adjusted slightly to provide similar total ET behavior to the previous simulation. The resulting head and flux components for this simulation are shown in data column 4 of Table 6.4. The first few columns of this table show these results for the following cases:

- the base-case ECF model (over the WOSC domain) is shown in data column 1,
- the updated fine-grid groundwater flow model with a single layer for the SAS (to note the differences that occur in updating the ECF model parameters and withdrawals with most recent information) is shown in data column 2, and
- the previous simulation (which uses a refined conceptualization and spatially varying parameterization of the SAS, but with the MODFLOW ET function) is shown in data column 3.

These columns provide comparison (note that the groundwater elements of these fluxes are noted earlier in Table 6.1 when the focus of model development was on the groundwater aspects of the project) of the hydrologic cycle fluxes for the entire model development process initiated from the ECF model of McGurk and Presley (2002). It is noted that overall ET flux and other flux components were similar between the last two simulations, and thus the overall water balances have been preserved through the model development stages. Figure 6.2 shows the water levels within the SAS for this simulation, which are similar to the ECF model results of Figure 2.15 except for the localized mounding adjacent to the RIBS within the Lake Marden basin. Hence model development till this stage has not significantly affected SAS water level patterns even though water levels were noted to differ by as much as 10 ft between the two simulations.

6.3 INCORPORATION OF SURFACE WATER FLOW

The next simulation of model development includes the overland flow surface (which accommodates generation of runoff), the surface-water bodies such as lakes and ponds and the surficial drainage features such as streams, canals, rivers, pipes, culverts and manholes. The drain and river boundary conditions of MODFLOW were removed from this simulation since these are now an internal component of the ISGM domain. The prescribed head nodes representing ponds and prescribed drainage-well fluxes were also removed from the simulation since ponds and drainage-wells are now a part of the hydrologic system being modeled. Further, the recharge applied to the simulation now includes the runoff portion of precipitation which was excluded in the earlier subsurface simulations. Also, the septic tank recharge is now applied separately to the subsurface (model layer 2) as were RIBS (model layer 1). This simulation was performed in transient mode, since the one-step steady-state simulation mode does not converge. Modifications made to this simulation, to provide a global match of the mass balance component fluxes and heads include:

1. The bottom leakance of the overland flow surface was increased from the initial estimates to allow more water into the subsurface since initial simulations indicate low groundwater heads and less net infiltration as compared with the ECF groundwater flow model over the WOSC model domain. The leakance was increased till net infiltration values were similar to those of the ECF model. Note that this leakance is a calibration parameter, and was deliberately initialized at low values, to avoid numerical difficulties that arise with extremely high leakances.

2. The bottom leakance of all surface drainage features (channels and ponds) was increased from the initial estimates to lower the groundwater heads around drainage features. Note that this leakance is a calibration parameter, and was deliberately initialized at low values, to avoid numerical difficulties that arise with extremely high leakances.

3. The observations for surface-water features and springs were included in the model to further refine the model. Also, for each Upper Floridan Aquifer spring, the surface (all in-stream river nodes in this case), was provided a connection to subsurface model layer 5 at the spring location and the leakance of the connection was adjusted to match with observed average 1995 spring discharge rates. The hydraulic conductivity zonation of Upper Floridan Aquifer nodes adjacent to Miami and Wekiva Springs (see Figure 3.9) was also adjusted at this stage (to produce the map of Figure 2.10) because the finer grid of the WOSC-ISGM study places the spring in a different property zone from that of the ECF model of McGurk and Presley (2002). This adjustment allows for the correct

amount of water to discharge from the spring, and also produces correct head values in the aquifer, as observed or interpreted from the earlier model development stages.

4. Some channel and pipe segments that are numerically problematic were identified. It is noted that their properties were incorrect (typically bottom elevations were inconsistent with adjacent segments creating a damming effect), which was fixed to the point of removing the inconsistency.

5. Errors in bed and bank elevations at individual ponds and lakes were corrected to the point of removing the inconsistency (some bed elevations were noted to be above the observed water levels, while other bank elevations were noted to be below the observed water levels in the lake, which identified these problems). Guidance was also provided by District personnel (B. McGurk, personal communication).

6. Flow characteristics of connected features were also adjusted on an individual basis, to reflect the observed surface-water heads, as water flows from one lake or pond to another. Problems associated with flow connectivity are identified when sharp water-level declines are associated with a structure (weir or culvert) having a higher bottom elevation in the simulation, than occurs in the field creating a larger damming effect than is present. In this manner, the surface-water heads were calibrated to within 5 ft of their average 1995 estimates, unless other factors such as lateral boundary effects prevent meeting this water-level target.

6.4 INCORPORATION OF TRANSIENTS

The steady-state model representing average 1995 conditions was further developed to include transient simulations from June 1995 through September 1999. Average 1995 conditions were taken as initial conditions for the simulation, and transient boundary conditions were provided for precipitation, lateral prescribed head boundaries, applied recharge and pumping conditions. Precipitation information was provided on a daily basis for this time period, from NEXRAD data supplied on a grid of size 6250 by 6250 ft. This data was assimilated into the WOSC-ISGM at the same spatial and temporal scales of the raw information, to maintain the resolution of this data. Figure 6.3 shows the various NEXRAD zones and Figure 6.4 shows the cumulative volumetric flux over these zones from June 1995 through September 1999, applied as a result of the NEXRAD precipitation data. Note that the steady-state simulations instead use precipitation values obtained using Thiessen polygons (Figure 3.1) created from data at five rain-gauging stations within and adjacent to the WOSC domain.

A transient simulation for the same time period (June 1995 through September 1999) was performed by the District on the ECF model (McGurk, personal communication) to provide lateral subsurface boundary conditions to the WOSC-ISGM. Head results from the transient ECF model for the SAS, UFA-UZ, UFA-DZ and LFA were interpolated spatially onto the lateral boundaries of the finer grid of the WOSC model domain, and are varied on a monthly stress period. Pumping information and applied recharge values (R_{rib}, R_{app}, and R_{septic}), were also supplied by the District for this time period, on a monthly basis, which were assimilated into the WOSC-ISGM transient simulation data-files on a monthly stress period. The well locations are as noted in Figure 3.10, and the cumulative volumetric flux over all wells from June 1995 through September 1999 is shown in Figure 6.5.

All WOSC-ISGM transient simulation were performed using an adaptive time-stepping that allows the time-step size to vary depending on the difficulty of solution. The time-stepping however adjusts to account for daily changes in precipitation, except when multi-day hiatus periods are present in the data. It is noted that the simulations may take time-step sizes as small as a minute to resolve the large changes in the state of the system when large recharge events begin or end, indicating that use of a decoupled solution to the system using fixed time-step sizes larger than a minute, may lead to erroneous results for these periods. Transient simulation results were compared with available lake levels, groundwater levels, and stream fluxes from June 1995 through September 1999. These levels and their trends were visually inspected to identify model performance, and comparisons were made with available observations from June 1995 through June 1997 for model calibration, and from July 1997 through September 1999 for model verification.

6.5 MODEL CALIBRATION

After the model was assembled, it was calibrated to steady-state 1995 conditions and to transient conditions from June 1995 through September 1999. A series of exploratory sensitivity analysis was first performed to note the effect of various parameters to the model results. The following was noted regarding these initial simulations:

- Lake levels and SAS head results for steady or transient simulations were not very sensitive to horizontal and vertical hydraulic conductivity values of the upper or lower SAS units, within acceptable ranges of their values.

- Groundwater heads in the SAS and lake levels were sensitive to the evaporation distribution function (EDFI) and the root-zone distribution function (RDFI).

- In general, the initial simulation required more ET (and associated lower heads) when water-table was higher (location-wise, and during transients) and less ET (with associated higher heads) when the water-table was deeper or becomes deeper through time. In other words, the shallow water levels were too high and the deep water levels were too low as compared to observations. Thus, the EDFI and RDFI were made non-zero only in the top layer to compensate for this general behavior. The values in the topmost layer were then calibrated to provide for similar bulk ET flux magnitudes over the model domain, as for the ECF model conceptualization.

- Groundwater heads in the SAS as well as lake levels were sensitive to the field capacity and wilting point saturations with higher ET at lower values of these parameters and vice versa. Higher ET generally causes lower water levels in lakes and in the SAS.

- Groundwater heads in the SAS, lake levels and stream fluxes were sensitive to the leakance values of the ICU, however, heads in the Upper Floridan Aquifer were less sensitive to this parameter. Larger leakance values cause larger interaction fluxes between the SAS and UFA-UZ, causing lake levels and SAS heads to drop if gradients are downward. On the other hand, larger leakance values cause lake levels and SAS heads to rise if gradients are upward and flow is from the UFA to the SAS.

- Fluctuations of lake levels were somewhat sensitive to the porosity of the SAS for smaller lakes, but insensitive to the porosity of the SAS for larger lakes with significant associated storage.

- Groundwater heads in the SAS and lake levels were significantly controlled by lateral boundary conditions applied to the WOSC-ISGM for observations that fall within 2 connected nodes of the prescribed lateral boundary. This effect diminished when the observation is greater than 4 connected nodes away from a lateral prescribed head boundary.

These initial simulations governed how calibration was performed. Leakance values of the ICU and the field capacity and wilting point saturations that govern evapotranspiration were treated as the major calibration parameters, after the EDFI and RDFI were set in the topmost layer only and calibrated to represent similar bulk ET fluxes as conceptualized by the ECF model. The leakance value was varied locally during calibration, within ranges established from the ECF model, in the model development stage. Head differences between the UFA-UZ and the SAS, and the leakance fluxes were checked in the output cell-by-cell flow term file to determine if leakance changes would affect simulated results further. A typical case during calibration was that lake water levels were too low and ICU leakances were adjusted locally to raise them into the respective lake or water body. Evapotranspiration was controlled by locally adjusting the field-capacity and wilting-point saturations within ranges established for the model from available literature values. A uniform EDFI and RDFI used in the simulation avoids complexity, and therefore the field-capacity and wilting-point saturations were used as surrogates to further control ET locally. Thus, if less ET was required from an area, the field-capacity and wilting-point saturations were increased to allow less ET from available soil moisture, in lieu of reducing the EDFI or RDFI locally. The evapotranspiration fluxes were checked in the output cell-by-cell flow term file to determine if these changes would affect simulated results further.

During calibration, it was further noticed that the top elevation of the overland flow surface (and adjacent overland flow nodes) was below the high lake level of the connecting surface-water body at some of the observations. These OLF node elevations were increased to be at the highest water level in the pond or lake, otherwise the storage of this node is counted twice – once in the lake, and the second time on the connecting overland flow surface which is inundated. When other connecting node elevations are also below the lake level the storage effects are quite large thus dampening or totally flattening fluctuations in lake levels and therefore, all connecting nodes have their elevation raised accordingly. Other changes involved with calibration include:

- The storage-area relationships of Steer, Sherwood, the lake immediately upstream of Sherwood, Rose, Bear, Lil Bear, Cub, Bosse, Gandy, Lockhart, Searcy, Island, Myrtle, Mirror, Rock, Irene and Horseshoe were altered to have less storage at the same depth to allow for more lake fluctuations. Storage-area relationship for Cranes Roost was increased to decrease fluctuations noted in early simulations. Note that the storage-area relationships for lakes that were not imported from ICPR datasets have been estimated during model development from pond perimeters supplied with the hydrography shapefiles as discussed in bullet item 5 of section 4.2. In addition, pond storages developed from ICPR models are noted to have erroneous bottom elevations which in turn may have affected the storage capacity at the given pond depth. It is noted that several ponds in the ICPR database were provided a bottom elevation of exactly 13 ft, even in regions where the land surface elevation is greater than 100 ft.

- The bed elevations for Long and Crooked were increased to known dry bed elevations from deep incorrect numbers encountered with model development from the ICPR databases.

- The leakance values of lakebeds for Searcy, Hodge, Bosse (and upstream connected lakes and ponds), Cub and Lil Bear were reduced to reduce the interaction of these lakes with groundwater.

- The depth-discharge relationships of the structures on the downstream side of Cub and Bosse were reduced to slow down huge fluxes noted to exit from these lakes during initial simulations. The radius of the pipe downstream of Mirror was also reduced to slow down huge fluxes noted in initial simulations.

- The overland flow surface leakance was not calibrated further from what was noted in the first bullet of section 6.3.

Table 6.5 shows the calibration parameters and their ranges. Figure 6.6 shows the resulting leakance distribution of the ICU and Figure 6.7 shows the related vertical hydraulic conductivity which may be compared with Figure 2.13 to note differences with the ECF model. The ICU vertical conductance of both models is similar in that it is higher in the Long Lake, Gee Creek, Soldier Creek and Cranes Roost Outlet sub-basins and lower in Trout Lake Outlet, Wekiva River, Lake Apopka Outlet and southern portions of the Unnamed Lake District sub-basin. The range of values is also similar, however, the calibrated values are different between models reflecting the new ICU thicknesses. Figures 6.8 and 6.9 show the field capacity and wilting point saturations respectively for the calibrated WOSC-ISGM – other local changes are as noted above. The resulting ISGM of the WOSC region is taken as the calibrated model which was used further for sensitivity analyses and examining predictions till the year 2025. Each component of the net volumetric budget for the simulation representing steady-state 1995 conditions (except for prescribed head boundaries) was within a few percent of the respective volumetric fluxes obtained from the earlier model development stages as noted in Table 6.4 and therefore, the WOSC-ISGM conceptually reflects the steady-state ECF model simulation results in terms of the various components of inflow and outflow. The increased groundwater inflow from prescribed head boundaries for the final simulation in Table 6.4 occurs mainly in the UFA-UZ and SAS, which is balanced by a corresponding increase in the outflow from rivers and streams. The largest single component of this extra inflow occurs in the region of Barrel and Wekiva Springs from adjacent prescribed head boundaries, to supply water to the river as observed at Wekiva River Marina. This large flux is not accounted for in the ECF model. Other surface-water systems that are located close to lateral boundaries also induce local changes in the final simulation, to fluxes occurring from lateral prescribed head boundary nodes in the SAS and the UFA-UZ.

7.0 CALIBRATED STEADY-STATE WOSC-ISGM

The steady-state WOSC-ISGM was developed and calibrated by incorporating all available data. Table 7.1 shows the subsurface head residuals, Table 7.2 shows the water-level residuals for the surface-water bodies, and Table 7.3 shows the spring flux and surface water flow residuals of the calibrated WOSC-ISGM. Figures 7.1, 7.2, and 7.3 show the observed versus simulated subsurface heads, water-levels for surface-water bodies and spring fluxes respectively. It is noted that the residuals are low, and that simulated conditions generally match the observed average 1995 estimates. The maximum error for the subsurface observations was 7 ft with an RMS of 3.2 ft. The maximum error for the surface-water observations of 14.85 ft occurs at Rutherford which is close to a lateral prescribed head boundary. The RMS error for the surface water domain was 3.17 ft. Spring fluxes were calibrated to within 0.5 cfs of their respective average 1995 observed values, except for Wekiva Spring which has a larger error for steady-state conditions, but better matches the transient results. Surface water flows also show larger errors for the steady-state results, to better match the transient 1995 to 1999 conditions. Figure 7.4 shows the spatial distribution of head residuals in the subsurface and Figure 7.5 shows the spatial distribution of water-level residuals in lakes and ponds for the calibrated steady-state simulation. The calibration was not spatially biased in the subsurface observations at the scale of the WOSC domain, though a positive bias is noted for water-levels in lakes in the south-east portions of the domain in Orange County for steady-state conditions. The model is statistically representative of average 1995 field conditions for surface and subsurface water levels and for spring flows and is therefore considered calibrated for average 1995 steady-state conditions.

Figures 7.6, 7.7, 7.8, and 7.9 show the steady-state, average 1995 simulated head values in the SAS, the UFA-UZ, the UFA-DZ, and the LFA respectively. A comparison of these head values with the respective values from the ECF model over the WOSC model domain (Figures 2.15 through 2.18) shows excellent matches for the UFA-UZ, UFA-DZ and LFA with less than a foot of difference between the two simulations for each of the aquifers. An areally larger cone of depression was however noted in the WOSC-ISGM in the UFA-UZ for the region draining Barrel and Wekiva Springs, and the region draining Sanlando, Palm and Starbuck Springs as located in Figure 3.9. The WOSC-ISGM SAS water levels have regional trends that are similar to the SAS water levels of the ECF model of McGurk and Presley (2002); however, water levels at any location may be different by as much as 10 ft and in small localized areas, by as much as 30 ft. A comparison of Figure 7.6 with Figure 6.2 (depicting the pre-final development stage, before the overland surface and associated drainage features were incorporated) shows the same regional similarities with large local deviations. Inclusion of the overland surface and its drainage features has a significant influence on SAS water-levels resulting mainly from the detailed drainage features that cut through the water table. For instance, the recharge mound in the Lake Marden basin area was substantially smaller in the integrated model than seen in Figure 6.2. Water levels in this region were also generally lower than those of Figure 2.15 for the ECF model. This occurs because the land surface elevation in the region was lower than the resulting SAS water levels of Figures 6.2 or 2.15, causing water to drain to the nearby lakes via overland runoff, in the ISGM results of Figure 7.6.

Table 7.4 shows the mass balance results for the simulation, as well as its breakup into the subsurface, overland, and channel domains. Flow between the surface and subsurface domains are internal to the system and are therefore not presented in the total volumetric budget but only in the individual domain budgets. The rate of change of storage for the subsurface, the overland flow surface (OLF) and the channel domain (which includes all surface water features such as ponds, lakes, rivers and other drainage features and is denoted by the acronym CHF) were negligible compared to the other flux components indicating that flow within these domains is very close to steady-state conditions. The overall hydrologic mass balance was less than 6% of the boundary fluxes to the integrated model. Mass balance errors within each of the domains are smaller compared to their respective boundary fluxes. It is noted that most of the mass balance flux error occurs in the CHF domain, probably resulting from high fluxes that occur in the rivers and springs – in such regions, high conductances coupled with low gradients create mass balance errors during back-calculation.

The areal distribution of infiltration and ET fluxes for the WOSC-ISGM was further checked against the ECF model results, to note the similarities and differences between the two models. Figure 7.10 shows the spatial distribution of infiltration through the overland flow surface as computed by the ISGM. Trends are noted to be similar to the results of the ECF model of McGurk and Presley (2002), shown in Figure 3.4, whereby infiltration is larger in the Lake Apopka Outlet, Long Lake, Unnamed Lake District, Soldiers Creek, Gee Creek, Cranes Roost Outlet and Mirror Lake Outlet basins than in the Wekiva River, Little Wekiva River, Lake Lovley Outlet, and Trout Lake Outlet basins. The differences are attributed to the following reasons:

- The ISGM solves the entire hydrologic cycle mass balance and therefore provides full accountability of all water in the system whereas the distribution shown in Figure 3.4 is a calculation performed independent of the groundwater flow model and therefore does not reflect the groundwater interactions or seepage.

- The SCS curve number approach includes approximations which do not reflect the local (grid-scale) state of water movement in the system, including runoff in closed basins.

- Low-lying areas along the Wekiva River are discharge areas. In surrounding areas, the ISGM shows very low infiltration, while the calculations input to the ECF groundwater model show high infiltration rates that are contrary to discharge areas.

Figure 7.11 shows the spatial distribution of total ET as computed by the ISGM. ET was more uniform for this case than for the ECF model of McGurk and Presley (2002), shown in Figure 3.8. The typical ET rate in the WOSC-ISGM was around 37 in/yr with pockets of lower ET occurring throughout the domain, while for the ECF model a typical ET rate was around 33 in/yr with pockets of higher ET occurring throughout the domain. However, the variation in ET in the ECF model is only around 3 in/yr around its mean value, and further, the total ET from the domain is similar for the two models as noted by the mass balance components in Table 6.4.
The steady-state model presented above was used further for sensitivity analyses and as initial conditions for transient simulations from 1995 through 1999.

8.0 STEADY-STATE WOSC-ISGM SENSITIVITY ANALYSIS

A parameter sensitivity analysis was conducted on the calibrated steady-state WOSC-ISGM to identify the model input groups that have the most significant impact on the model calibration and on model results. The sensitivity analysis focuses on the ISGM, and therefore the groundwater flow parameters were not evaluated in this study – the sensitivity of these parameters to the groundwater flow system was evaluated in the ECF model by McGurk and Presley (2002) and is not likely to change for the ISGM, because the values and roles of these parameters are the same in both models. Parameter sets were individually altered to their minimum expected and maximum expected values, to bracket their effects on the results.

The parameter sensitivity study is summarized in Table 8.1. The first column of the table shows the parameters that were chosen for the sensitivity, followed by their selected variations in the second column. The remaining columns summarize calibration statistics and model predictions for the various parameters that were evaluated. The last column for each domain categorizes the various parameters into one of the four sensitivity categories (i.e., Type I, II, III, or IV) as defined by ASTM (1994) guidelines. The first row of Table 8.1 provides results for the calibrated model (termed as the base case), while subsequent rows discuss the various parameter sensitivities. Figures 8.1 through 8.9 provide significant calibration statistics and the results of model predictions for each of the parameter sensitivities separately within surface and subsurface domains as indexed by "a" and "b" respectively. These calibration statistics include those that were evaluated during the model calibration process – i.e., the residual mean error and root-mean-squared error (RMS). Further, the absolute sum of all head values in the domain was used as a surrogate for available water within the system, and is the measure of model prediction used in this sensitivity analysis. Henceforth, this statistic is referred to as the total head measure. For more specific objectives, their specific measures may be evaluated with respect to the parameter sensitivities (for instance, if modeled water-level prediction at a particular lake are of importance, the head at that lake may be taken as the measure of model prediction that is evaluated with respect to the parameter sensitivities).

The most sensitive parameter for prediction of a total head measure within both surface and subsurface domains is the leakance value of the ICU. However, as noted in Figures 8.9a and 8.9b, the calibration statistics are also sensitive to a variation of this parameter therefore providing a significantly less calibrated model when the parameter value deviates from the base case. Hence, the sensitivity to this parameter is of Type III which is not of concern in terms of model reliability.

The second most sensitive parameter for prediction of a total head measure within both surface and subsurface domains is the moisture parameter controlling ET within the domain - i.e., the wilting point and field capacity saturations of the top three model layers. However, as noted in Figures 8.5a and 8.5b, the calibration statistics are also sensitive to a variation of this parameter therefore providing a significantly less calibrated model when the parameter value deviates from the base case. Hence, the sensitivity to this parameter is of Type III which is not of concern in terms of model reliability. It is noted here that the effect primarily comes from the wilting point moisture content which when increased, raises the minimum moisture level at which ET can occur thereby retaining greater water storage in both surface and subsurface domains, reflected in the associated higher total head measure. Figure 8.10 shows the spatial distribution of actual ET from the site for the case of increasing the wilting point and field capacity saturations by a factor of 2. This distribution has similar trends to that of the ECF model (Figure 3.8) with highest ET occurring in the Wekiva River, Little Wekiva River Gee Creek and Soldiers Creek basins and variable ET fluxes in the other basins within the WOSC domain. Net ET however, is about 20 percent lower for this sensitivity case.

The third most sensitive parameter for evaluation of a total head measure within the surface domain is the channel bottom leakance. However, as noted in Figures 8.3, the calibration statistics are also sensitive to a variation of this parameter therefore providing a significantly less calibrated model when the parameter value deviates from the base case. Hence, the sensitivity to this parameter is of Type III which is not of concern in terms of model reliability. Further, the total head measure within the subsurface domain is insensitive to the channel bottom leakance with a Type I sensitivity which is not of consequence to model reliability.

The next most sensitive parameter for evaluation of a total head measure within both surface and subsurface domains is the characteristic of the relative permeability curve - i.e., the Brooks Corey exponent used to define relative permeability. However, as noted in Figures 8.8a and 8.8b, the calibration statistics are also sensitive to a variation of this parameter therefore providing a significantly less calibrated model when the parameter value deviates from the base case. Hence, the sensitivity to this parameter is of Type III which is not of concern in terms of model reliability. Sensitivity to the Brooks Corey exponent term is very likely related to ET within the system. A lower value allows for water flow in the unsaturated zone (primarily to deeper layers of the SAS as well as the deeper aquifers), at lower water saturations thereby retaining larger storage in the subsurface (Figure 8.8b) and to some extent the surface (Figure 8.8a) domains of the simulation.

The next most sensitive parameter for prediction of a total head measure within the surface domain is the leakance of the overland flow surface. This parameter is also sensitive for subsurface predictions, though the van Genuchten "alpha" parameter shows more sensitivity in the subsurface, but little sensitivity to the surface domain. Overland flow surface leakance has Type III sensitivity in both domains, and van Genuchten "alpha" parameter has Type III sensitivity in the subsurface with Type II sensitivity in the surface. These parameters therefore are not of consequence in terms of model reliability for prediction of the total head measure.

The remaining sensitivities are all of Type I whereby calibration as well as prediction are insensitive and therefore of little concern with respect to model reliability for prediction of the total head measure.

9.0 TRANSIENT WOSC-ISGM SIMULATIONS FOR 1995 THROUGH 1999

The WOSC-ISGM was further used to evaluate transient conditions from June 1995 through September 1999. The water level distribution in the SAS for May 1999 and September 1999 conditions are shown Figures 9.1 and 9.2 respectively, depicting conditions during the driest and wettest months respectively. The SAS water levels for May 1999 are noted to be up to 10 ft lower than for September 1999, which in turn are generally slightly higher than the average steady-state 1995 results of Figure 7.6. The largest difference between May 1999 and September 1999 SAS results, is about 20 ft and occurs in the Trout Lake Outlet and Long Lake Basins. The fluctuations between May 1999 and September 1999 are generally lowest in the Unnamed Lake District, Lake Apopka Outlet and Soldier Creek Basins. The head distribution in the UFA-UZ for May 1999 and September 1999 conditions are shown in Figures 9.3 and 9.4 respectively. The lowest UFA-UZ heads occur in May 1999, and the highest heads occur in September 1999 with largest differences of 2 to 4 ft occurring in the Long Lake Basin. September 1999 conditions are however lower than average 1995 conditions of Figure 7.7 by as much as 3 ft in the Unnamed Lake District and Lake Apopka Outlet Basins, and by about 2 ft in Trout Lake Outlet, Lake Lovely Outlet, Soldier Creek and Gee Creek Basins for the UFA-UZ. Heads do not change significantly from 1995 to 1999 or between seasons in the immediate region surrounding Wekiva and Barrel Springs. The head distribution in the LFA for May 1999 and September 1999 conditions are shown in Figures 9.5 and 9.6 respectively. September 1999 results are generally about a foot higher than May 1999 results in the LFA throughout the domain. A comparison of September 1999 LFA results (Figure 9.6) with average 1995 conditions (Figure 7.9) shows that LFA head declines are about half a foot in the north-east of the domain (Northern end of Soldier Creek Basin), which increases in a southwesterly direction to about 4 ft in the south-west of the domain (western end of Unnamed Lake District).

Figure 9.7 shows the locations of observations for the subsurface and surface domains where transient data is available between June 1995 and September 1999 and Table 9.1 identifies the model layer number and aquifer unit of the simulated subsurface observations. Figures 9.8 show the water level fluctuations at these subsurface and surface-water locations for the transient simulation. The first thirty-five observations are subsurface observation wells, the next 52 observations (Observation Numbers 36 through 87) reflect surface-water levels, the next observation (Observation Number 88) is for the spring flux at Wekiva Spring, the next 6 observations (Observation Numbers 89 through 95) are for gauged stream fluxes and the last observation (Observation Number 96) depicts the flux down the drainage well at Lake Orienta. The measured stages or fluxes, and those computed by the transient ECF model (McGurk, personal communication) are also included on Figures 9.8. The WOSC-ISGM simulation did an excellent job of depicting water levels and fluctuations for subsurface and surface observations as well as for stream-flow and spring flux at Wekiva Spring. Simulated water levels were generally within 5 feet of observed conditions and fluxes were generally within a few percent of observed conditions throughout the simulation. Even where simulated errors were larger, the temporal trends are noted to follow observed trends. It should be noted that observations that lie on lateral prescribed head boundaries, exactly follow the prescribed head temporal trends supplied to the WOSC-ISGM by interpolation from results of the transient ECF model. Therefore, these observations cannot perform better (or different) from the transient input provided to the model. Boundary effects were also dominant for observation locations that are only one or two grid-block connections away from a lateral prescribed head boundary and these effects diminish for observations that are greater than four grid-block connections away from a lateral prescribed head boundary. Observation Numbers 1, 10, 11, 20, 21, 22, 27, 29, 30, 37, 63, 76 and 77 are within 2 grid-block connections from a lateral prescribed head boundary, and Observation Numbers 15, 18, 33 and 64 are within 4 grid-block connections from a lateral prescribed head boundary.

Aside from nodes that are within the influence of a lateral prescribed head boundary, Observation Numbers 14, 23, 25, 42, 65, 79 and 82 performed poorest in the simulation. The first 3 observations are groundwater heads while the last 4 are lake levels. A brief note on these observations follows:

- Observation Number 14 is at the Greenwood Lake well with simulated heads as much as 7 ft below observed conditions. This well lies in an area of very flat water levels and even though the temporal trends are greatly muted in the simulation, the fluctuations have similar trends to observed fluctuations.

- Observation Number 23 is at the Rock Springs Well with simulated heads consistently 3 ft above observed conditions. Leakance is not an effective calibration parameter in this location, because heads in the SAS and in the UFA-UZ are both above observed values. The ET flux was also at its maximum limit in the region and hence head could not be lowered by allowing more ET. Fluctuations at this well however have similar trends to observed fluctuations.

- Observation Number 25 is at the Sanlando Softball W3 well with simulated heads around 8 ft higher than observed conditions. This well is close to the Wekiva River and heads in the SAS and in the UFA-UZ are such that these heads cannot be reduced further via adjustment of leakance. The ET flux was also at its maximum limit in the region and hence head could not be lowered by allowing more ET. Simulated temporal trends are similar to observed conditions, though considerably muted.

- Observation Number 42 is at Lake Searcy, where observed heads are generally lower than simulated by as much as 4 ft. The transients depicted by the simulation do not match observed trends and further investigation of the hydraulics and hydrogeology in the area will be required to determine the appropriate flow-field at this lake.

- Observation Number 65 is at Cranes Roost where observed water levels are insufficient to judge trends. Simulated levels are noted to steadily increase from 1995 through 1999. This depiction may be inaccurate because the area around Cranes Roost has been developed in this period, which is not reflected by changing land uses in the model (McGurk, personal communication).

- Observation Number 79 is at Long Lake where simulated heads rapidly rise and remain at high levels, while Long Lake observations show declining trends (in fact, it is noted to be dry after 1999, McGurk, personal communication). A Local examination of the hydrogeology surrounding Long Lake will be required to properly calibrate this lake to observed trends.

- Observation Number 82 at Lake Prairie has only one observed point and therefore no judgment can be made regarding its behavior.

It is also noted that some pond levels react severely, immediately at the start of the simulation (Long Lake discussed above also shows this reaction). This behavior reflects the fact that the precipitation is provided at different resolutions between the calibrated steady-state system and the transient simulation, and in the immediate vicinity of such surface-water bodies, the precipitation value of the steady-state model does not reflect the average of the 1995 precipitation from the transient data. The steady-state calibration should be rerun using average 1995 rainfall calculated from Doppler-derived radar data, for further adjustments to the system.

10.0 TRANSIENT WOSC-ISGM SENSITIVITY ANALYSIS

The first transient sensitivity analysis conducted for the WOSC-ISGM investigates its behavior to different time-scales of input. Specifically, the daily rainfall values were averaged over a monthly period for each NEXRAD grid and this monthly variation was provided to the model as precipitation. This is important for long-term water-resource evaluation investigations of five to twenty-five years, since it may be computationally prohibitive to evaluate the system for long time spans with small input time-scales. Conversely, the effect of averaging even smaller time-scale input of hourly rainfall into daily values may also be inferred from this sensitivity study. Other parameters of the simulation were identical to the transient simulation case discussed in Chapter 9.0, with initial conditions taken as the average 1995 simulation. The water level distribution in the SAS for May 1999 and September 1999 conditions are shown Figures 10.1 and 10.2 respectively, for this simulation. These are generally similar to the water level distribution of the base case transient study of Figures 9.1 and 9.2 for the same time periods. Discrepancies are as noted below.

For May 1999 conditions, the difference in SAS heads for daily versus monthly-averaged rainfall simulations was largest in the regions between Wekiva/Orlando and Lawne (see Figures 4.5 and 9.7 for locations) where the sensitivity results for heads are about 10 ft less than the base case; locally around Big Fairview, Silver, and Lake Brantley where sensitivity results were around 5 ft less than the base case; and locally around Alpharetta, Mitchell, and Long where sensitivity results were between 10 and 20 ft higher than for the base case. In the Upper Floridan Aquifer, the sensitivity results differed from the base case by about 1.5 ft locally around Long, Alpharetta, Mitchell and Pleasant with a half foot increase in the Long Lake Basin, and very small differences in the rest of the domain for May 1999 conditions. Lower Floridan Aquifer heads for the sensitivity case show negligible difference from base case results.

For the September 1999 case, the difference in SAS heads for daily versus monthly-averaged rainfall simulations was less than 1 foot over most of the domain. Exceptions include the regions between Wekiva/Orlando and Lawne (see Figures 4.5 and 9.7 for locations) where the sensitivity results for heads are about 16 ft less than the base case; locally around Big Fairview, Silver, Little Bear Lake, Bear Lake and Lake Brantley where sensitivity results were around 10 ft less than the base case; and locally around Alt. Springs Elem. Sch., Hammer, Mitchell, and Long where sensitivity results were between 10 and 20 ft higher than for the base case. In the Upper Floridan Aquifer, the sensitivity results differed from the base case by about 1 ft locally around Long, Alpharetta and Hammer with less than half a foot difference in the rest of the domain for September 1999 conditions. Lower Floridan Aquifer heads for the sensitivity case show negligible difference from base case results.

Figures 10.3 show the water level, stream-flow and spring flux fluctuations at the various observation locations of Figure 9.3, for the transient sensitivity study. Base case results and observed values are also provided on Figures 10.3 for comparison. In general, the results are very similar to base-case values providing confidence that time-scale issues for rainfall input are not significant to general water levels or fluxes. However, it is noted that some of the peaks were muted in the sensitivity study, than for the base case simulation. This is more noticeable in the stream-flow results where base-flow and low flow conditions are accurately depicted, but peak flow is severely muted. This indicates that time-scales may be important in accurately determining peak flows and therefore it may be inferred that daily averaging of hourly input may further mute water-level fluctuations that may be important for flood analyses. However, for long-term water resource evaluations, the monthly averaged input of rainfall data does not alter results from daily rainfall input in a significant way. Exceptions include Observation Number 14 at Greenwood Lake Sch., and Observation Number 42 at Lake Searcy where sensitivity results are more muted than for the base case; and Observation Number 78 at Long Lake and Observation Number 82 at Prairie where the results do not even follow similar trends. It should be noted that these same observation locations were flagged in Chapter 9 as being unable to match observed conditions. Aside from these locations, and considering the closeness of the results of daily rainfall versus monthly-averaged rainfall input for the remaining observations, all further analyses use monthly averaged rainfall input to provide faster simulations. Monthly-averaged rainfall input simulations typically run eight times faster than the daily rainfall input base case.

The second transient sensitivity analysis investigates the effects of ICU leakance on the results. Leakance values were globally multiplied and divided by a factor of 3 to provide two simulations that bound the effects of ICU leakance on water levels and fluxes. Initial conditions for these simulations were taken from the respective 1995 steady-state sensitivity results. Figures 10.4 show the results of this sensitivity study along with observed values and results of the first sensitivity study with monthly averaged rainfall input (which is referred to as the base-case henceforth in this report). ICU leakance is noted to be sensitive to some observations, and insensitive to others. Further, increasing the ICU leakance tends to decrease heads at all lake observations, but can increase or decrease heads in subsurface observation locations depending on the direction of gradients between the SAS and the UFA-UZ. ICU leakance did not have a significant impact on spring flux at Wekiva Spring or on the flux at Observation Number 89 at Wekiva River Marina with larger differences noted at other flux observations. Increasing the leakance of the ICU tended to decrease the flux at these gauge stations, with larger differences occurring for peak flow than for baseflow conditions.

The third transient sensitivity analysis investigates the effects of SAS porosity values on the results. The porosity values were globally multiplied and divided by a factor of 2 to provide two simulations that bound the effects of SAS porosity on water levels and fluxes. Initial conditions for these simulations were taken from the 1995 steady-state base-case results which are not affected by porosity as a result of them depicting steady-state conditions. Figures 10.5 show the results of this sensitivity study along with observed values and base-case results. SAS porosity is an insensitive parameter for spring flux and stream flow results. However, it had an effect on groundwater heads and lake levels, with smaller porosity values showing larger fluctuations than larger porosity conditions. Sensitivity to porosity however, is not as dramatic as for ICU leakance.

The fourth transient sensitivity analysis investigates the effects of field capacity and wilting point saturations (dominant ET parameters) on the results. The field capacity and wilting point saturation values were globally multiplied and divided by a factor of 2 to provide two simulations that bound the effects of their variation on water levels and fluxes. Initial conditions for these simulations were taken from the respective 1995 steady-state sensitivity results. Figures

10.6 show the results of this sensitivity study along with observed values and base-case results. The flux at Wekiva Spring was not sensitive to this parameter, however, stream-flows at the gauging stations are noted to be affected at peak as well as at baseflow conditions. Reducing the moisture parameters allowed for more ET in the domain with associated lower heads in the subsurface and water levels in lakes. This sensitivity is noted to be large for some observations and very small for others, and no consistent trend is noted with respect to the fluctuations.

11.0 PREDICTIVE TRANSIENT WOSC-ISGM SIMULATIONS TILL THE YEAR 2025

The calibrated transient WOSC-ISGM was used to evaluate potential changes to the flow system due to projected changes in withdrawals and water use practices from 1999 through 2025. The results of the transient simulation discussed in Chapter 9.0 at September 1999 conditions were used as initial conditions for predictive runs and transient boundary conditions were provided for precipitation, lateral prescribed head boundaries, applied recharge, and pumping rates. Transient boundary conditions for precipitation were obtained by recycling available data from the four year period of September 1995 to September 1999 as being a representative time period consisting of seasonal variations, as well as wet and dry years. The daily precipitation values for each NEXRAD grid (Figure 6.3) were averaged on a monthly basis for this study due to their noted lack of effect for water management evaluations during the transient sensitivity analysis, the large uncertainty in future rainfall evaluations, and to provide all inputs at the same average monthly time-scale. Figure 11.1 shows the cumulative volumetric flux added over the NEXRAD zones of Figure 6.3 from October 1999 through December 2025, applied as a result of the monthly-averaged NEXRAD precipitation data.

The predictive simulations consist of two cases – one where public supply pumping is projected to increase from 1999 through 2025, and the other where the public supply pumping is maintained at conditions between 1995 and 1999. These cases are henceforth referred to as the predicted pumping case, and the recycled pumping case respectively. A comparison of water levels and flows for these two cases delineates the effect of pumping increase on the transients in the results, from transients that occur due to monthly variations in precipitation. For the predictive pumping case, a transient simulation was conducted for the same time period by the District on the ECF model (McGurk, personal communication), and the head results for the SAS, UFA-UZ, UFA-DZ, and LFA were interpolated spatially, to provide lateral subsurface boundary conditions for these aquifer units on a monthly time period. Estimated well withdrawals and applied recharge values (R_{rib}, R_{app}, and R_{septic}) were supplied by the District for this time period on a monthly basis (McGurk, personal communication) and were assimilated into the datasets for the predictive simulation study. The public supply withdrawal estimates generally increase from 1999 through 2025, while commercial and agricultural withdrawals, and RIB and septic injection values were estimated by recycling the respective values from October 1995 through September 1999. For the recycled pumping case, the lateral subsurface boundary conditions in the SAS, UFA-UZ, UFA-DZ, and LFA were implemented by recycling the information from October 1995 through September 1999, which was obtained as discussed in Section 6.4. The pumping information from October 1995 through September 1999 was also recycled for this case and therefore, an ECF model simulation was not required to provide boundary conditions. The cumulative volumetric flux over all wells (including septic tank and RIB application) from October 1999 through December 2025 is shown in Figure 11.2 for both predicted pumping and recycled pumping cases, with well locations as noted in Figure 3.10.

The water level distribution in the SAS for May 2025 and September 2025 conditions are shown Figures 11.3 and 11.4 respectively, the head distribution in the UFA-UZ for May 2025 and September 2025 conditions are shown in Figures 11.5 and 11.6 respectively, and the head distribution in the LFA for May 2025 and September 2025 conditions are shown in Figures 11.7 and 11.8 respectively, for the predicted pumping case. The difference between these figures and the respective ones from Figures 9.1 through 9.6 provide the respective drawdown from 1999 through 2025 conditions. The drawdown from 1999 through 2025 is shown in Figures 11.9 and 11.10 for May and September conditions respectively in the SAS, in Figures 11.11 and 11.12 for May and September conditions respectively in the UFA-UZ, and in Figures 11.13 and 11.14 for May and September conditions respectively in the LFA. SAS water levels are noted to drop by around 10 ft in Unnamed Lake District and southern portions of Long Lake Basin for May and September conditions, but have risen locally by around 5 ft in Trout Lake Outlet for September conditions and also in Mirror Lake Outlet, Cranes Roost Outlet, Wekiva River, and Little Wekiva River Basins for May conditions. Water levels have declined throughout the domain in the UFA and the LFA, from 1999 through 2025. UFA declines range from around 1 ft near Wekiva and Barrel Springs to around 11 ft in Unnamed Lake District and southern Trout Lake Outlet Basins. General declines ranged from 4 to 8 ft throughout the domain in the UFA for May and September conditions. LFA heads have declined by about 9 ft throughout the domain with larger declines of about 10 ft in SE portions of the WOSC area and smaller declines of about 7 ft in NW portions of the WOSC domain.

Figures 11.9 show the water level fluctuations at various subsurface and surface-water observation locations (shown in Figure 9.7) for the transient predictive simulations. Gradually declining trends are noted in most of the water levels for the predicted pumping case as compared with the recycled pumping case. However, it is noted that several lakes and observation wells do not show a significant difference between the results of the two pumping cases. Further, some lakes are noted to exhibit declines during low water-level conditions (in the predictive pumping case as compared to the recycled pumping case), but fill up to the same level during high water-level periods for both pumping cases. It should also be noted that observations have been provided through 2003 for some water levels and stream fluxes, however, the simulations did not consider actual rainfall conditions after September 1999 and therefore comparisons between simulated and observed levels are not made for the predictive simulations.

12.0 PREDICTIVE TRANSIENT WOSC-ISGM SENSITIVITY ANALYSIS

A predictive sensitivity analysis was conducted to note the effects of various surface-subsurface interaction parameters on the results of the WOSC-ISGM simulation. The evaluation was not performed on the Floridan Aquifer parameters, since these parameters were evaluated in the transient ECF model study of the District (currently ongoing by McGurk, personal communication) and their effects are not likely to change for the ISGM, because the values and roles of these parameters are the same in both models. The most sensitive parameters from the sensitivity study of Chapter 8 were selected here to bracket the behavior of the system for most sensitive conditions. This includes the ICU leakance and the ET moisture parameters (field capacity moisture content and wilting point moisture content). The parameters were applied in combination such that their individual effect was to generally lower the average head in one simulation, and to raise the average head in the other, to bracket the extreme behavior of the predictive runs, for uncertainty evaluation. Therefore, the ICU leakance was multiplied by a factor of 3 along with ET parameters (field capacity and wilting point saturations) being divided by a factor of 2 for one case and the ICU leakance was divided by a factor of 3 along with ET parameters being multiplied by a factor of 2 for the other. It should be noted that for Type III parameters, the calibration effort itself determines good calibrated values for these parameters and therefore their predictive uncertainty is not of significance unless predictive results fall outside of the range in which the model was calibrated. Figures 12.1 show the water level fluctuations at various subsurface and surface-water observation locations (shown in Figure 9.7) for the base-case predictive scenario as well as the upper and lower bracketing sensitivity simulations. The range of head results bracketed by these sensitivities is narrow at some observations and extremely large at others. Further, the base-case results are closer to the low water-level sensitivity case at some observations, closer to the high water-level sensitivity case at other locations and in between the two at still other locations. Therefore, no consistent trend is noted between observation locations, and the sensitivity needs to be analyzed for each observation location individually. However, the simulations are noted to be relatively insensitive to the flux results for Wekiva Spring flux, and for the streamflows at Observation Locations 89 through 95.

13.0 SUMMARY AND CONCLUSIONS

An integrated surface/subsurface flow model was developed for the WOSC area. The model domain was selected to coincide with major basins of interest and is a subset of the East Central Florida groundwater flow model domain. The model was developed in a step-by-step manner starting from the groundwater model of McGurk and Presley (2002), with inclusion of additional details within the SAS and addition of the surface water domain to address the interactions between pumping of the Floridan Aquifer and water levels in the SAS or in numerous lakes and wetlands in the region.

All objectives set forth for this study have been achieved. As listed in Chapter 1, this includes:

1. The model simulates the surface and groundwater flow systems within the areas of interest. The model was calibrated to steady-state conditions as noted in Chapter 7 and its sensitivity was tested with respect to parameters of the integrated system as discussed in Chapter 8.

2. The model characterizes trends of stage in groundwater and surface water and was calibrated against available data from June 1995 through September 1999 as noted in Chapter 9. The effects of time-scales of precipitation input are noted in Chapter 10, to determine errors caused by time averaging of voluminous amounts of information. Other transient sensitivities depict the effect of various parameters on the observations analyzed in this study.

3. The model predicts the effects of projected future pumping within the Floridan Aquifer system, on water-table elevations and on connected lakes and wetlands as discussed in Chapter 11, and provides an uncertainty range on these results via a sensitivity analysis described in Chapter 12.

4. Model development addresses the grid-scale errors of the regional flow model by systematically reducing the grid dimensions and noting their effects on the resulting potentiometric levels and water budgets as discussed in Chapter 6.

5. The step-by-step approach to model development addresses the conceptual errors of a groundwater flow model as it was developed into an integrated model. At each step, the errors of potentiometric levels and of water budgets were evaluated in Chapter 6 to provide a measure of the effect of each approximation, individually.

6. The model examines the long-term transient effects of increased Floridan Aquifer pumping upon the water table and on connected lakes and wetlands. By performing simulations of recycled pumping conditions and predictive pumping conditions in Chapter 11, the long term water-level and stream flux trends as well as their changes due to predictive pumping changes, may be noted.

Further enhancements to the model include using NEXRAD data for average 1995 conditions instead of the Thiessen Polygons of Figure3.1; assimilating precipitation and pumping data from

1999 through 2004 and using this period to further validate model results; examining if transient potential ET input would provide even better calibration; and including a larger set of observations from within the WOSC-ISGM domain in model calibration.

This model may be used further for additional evaluations in the WOSC-ISGM study area. For observations that match well, the model should give good predictions, and for observations where the calibrated match is poorer, the predictions should be treated with larger uncertainty. For un-gauged locations, the predictions should also be treated with larger uncertainty, specifically for water-bodies that are not connected to other gauged systems since such bodies can have behavior that is totally independent of other gauged areas, and may need some level of individual calibration to reduce errors. In addition, it should be recognized that the model is developed at a regional scale, with similar scale for input data variability. Further, it is noted from the transient sensitivity analysis and the predictive sensitivity analysis that results at some observation locations have larger variability than others, and this too should be taken into consideration when deciding upon the certainty of results for lake levels, groundwater heads, spring fluxes or stream flows. It should however be noted that parameters that are sensitive may not be highly uncertain to the results if they have a Type II or III sensitivity. Finally, observation locations that are close to the lateral boundary may be influenced by the prescribed boundary value and hence predictions at such locations should be evaluated accordingly. It was noted that observations that are within 2 nodal connections from a prescribed head boundary were highly influenced by the boundary value and the effect diminished beyond 4 nodal connections from a prescribed head boundary.

13.1 MODEL LIMITATIONS

The WOSC-ISGM is a surface/subsurface model that represents the hydrologic system under study, by a series of equations that approximate the flow of water in surface and subsurface regimes, and the interactions between these regimes. The Floridan Aquifer System representation of the WOSC-ISGM is the same as for the ECF model, with associated limitations in representation including neglecting preferential flow zones caused by secondary porosity features such as fractures and solution conduits at a local scale. Further limitations of the model include grid-scale effects, inaccuracies of measurements and uncertainties of parameter distributions and coarse-scale estimates of pumping/applied recharge. Some of these limitations are addressed by sensitivity analysis (for instance, grid-scale effects and effects to some parameter value uncertainties) while others (for instance effects of parameter distribution uncertainties or inaccuracies of measurements) will need more elaborate measures to address.

14.0 REFERENCES

Allen, R.G., L.S. Pereira, D. Raes, and M. Smith, 1998. Crop Evapotranspiration – Guidelines for computing crop water requirements – FAO Irrigation and drainage paper 56, Food and Agriculture Organization of the United Nations, Rome.

Carsel, R. F., R. S. Parrish, R. L. Jones, J. L. Hansen, and R. L. Lamb, 1988. Characterizing the uncertainty of pesticide movement in agriculture soils, Journal of Contaminant Hydrology, vol. 2, 111-124.

Carsel, R. F., and R. S. Parrish, 1988. Developing joint probability distributions of soil water retention characteristics, Water Resources Research, vol. 24, no. 5, 755-769.

Chow, V. T., 1959. Open-channel Hydraulics, McGraw-Hill, Inc., New York, 680 pages.

Kristensen, K. J., and S. E. Jensen, 1975. A model for estimating actual evapotranspiration from potential evapotranspiration, Royal Veterinary and Agricultural University, Nordic Hydrology, 6, p. 170-188.

McGurk, B. and P. F. Presley, 2002. Simulation of the Effects of Groundwater Withdrawals on the Floridan Aquifer System: Model Expansion and Revision, Technical Publication SJ2002-03, St. Johns River Water Management District, Palatka, FL, 196 pages.

P. B. Water, Inc, 2000. Groundwater Modeling in Support of Reclaimed Water Recharge Capacity expansion at Northwest Water Reclamation Facility for Orange County Utilities.

Scurlock, J. M. O., G. P. Asner, and S. T. Gower. 2001. Worldwide Historical Estimates and Bibliography of Leaf Area Index, 1932-2000. ORNL Technical Memorandum TM-2001/268, Oak Ridge National Laboratory, Oak Ridge, Tennessee, U.S.A.

USEPA, 2002. http://www.epa.gov/waterscience/basins/basinsv3.htm

Van Genuchten, M. T., 1980. A closed-form equation for predicting the hydraulic conductivity of unsaturated soils, *Soil Sci. Am. J.*, v44, 892-898.

TABLES

Table 2.1
Average 1995 Water Levels in Observation Wells within the WOSC-ISGM Study Area

Site Name	X	Y	Layer	Row	Column	Average 1995 Observed Water Level (Feet)
Long Lake	454680	3165980	3	94	55	70.02
Lake Meadow	449120	3163740	3	106	26	75.5
Lake Hiawassee	452945	3155940	3	147	46	77.15
Lake Orlando	457690	3163555	3	107	71	83.2
Starke Lake	447600	3160700	3	122	18	100.4
Bear Lake	456175	3169650	3	75	63	104.73
CHARLOTTE STREET - S-1015	465266	3172858	3	58	111	78.01
284533081204801	466156.7	3181353.1	5	14	115	35.01
284440081175901	470735	3179710	5	22	139	36.66
OR0548 - Wekiva Springs St Park	454495.3	3176037.4	5	42	54	21.85
284244081234901	461231	3176168	5	41	90	37.5
284207081174401	471131	3175000	5	47	142	35.17
S-0125	464149.3	3174434.2	5	50	105	44.77
CHARLOTTE STREET - S-1017	465267	3172857	5	58	111	44.55
284012081264601	456411	3171507	5	65	64	49.63
S-1056	473177	3170352	5	71	152	45.33
283920081232501	461861	3169887	5	74	93	48.73
283654081260801	457420	3165410	5	97	70	57.63
283417081331401	445877.3	3160625.6	5	122	9	73.44
283326081262101	457044	3159010	5	131	68	51.71
283121081311601	449010	3155200	5	151	25	72.06
CHARLOTTE STREET - S-1016	465268	3172856	6	58	111	47.16
Orlo Vista - 283253081283401	453446.9	3158038.9	6	136	49	65

Table 3.1
Leaf Area Index Values for Different Land Uses

LUCODE	Description	LAI*	Note
1009	Urban and Built-Up	2.08	Shrub
1100	Residential, Low Density Less than two dwelling units per acre	2.08	Shrub
1110	Residential, Low Density Less than two dwelling units per acre	2.08	Shrub
1130	Residential, Low Density Less than two dwelling units per acre	2.08	Shrub
1200	Residential, Med. Density Two to five dwelling units per acre	2.08	Shrub
1210	Residential, Med. Density Two to five dwelling units per acre	2.08	Shrub
1290	Residential, Med. Density Two to five dwelling units per acre	2.08	Shrub
1300	Residential, High Density	2.08	Shrub
1310	Residential, High Density	2.08	Shrub
1330	Residential, High Density	2.08	Shrub
1340	Residential, High Density	2.08	Shrub
1400	Commercial and Services. Condominiums and Motels combined	2.08	Shrub
1410	Commercial and Services. Condominiums and Motels combined	2.08	Shrub
1411	Commercial and Services. Condominiums and Motels combined	2.08	Shrub
1423	Commercial and Services. Condominiums and Motels combined	2.08	Shrub
1430	Commercial and Services. Condominiums and Motels combined	2.08	Shrub
1460	oil and gas storage: except those areas associated with industrial use or manufacturing	1.31	Desert
1470	oil and gas storage: except those areas associated with industrial use or manufacturing	1.31	Desert
1480	Cemeteries	2.08	Shrub
1510	food processing	1.31	Desert
1520	timber processing.	1.31	Desert
1550	other light industry	1.31	Desert
1560	other heavy industrial	1.31	Desert
1562	prestressed concrete plants	1.31	Desert
1600	Extractive	1.31	Desert
1611	clays	1.31	Desert
1620	sand and gravel pits	1.31	Desert
1630	rock quarries	1.31	Desert
1650	reclaimed lands	2.08	Shrub
1670	abandoned lands	2.08	Shrub
1700	Institutional	2.08	Shrub
1710	Institutional	2.08	Shrub
1720	Institutional	2.08	Shrub
1730	military	2.08	Shrub

Table 3.1 (continued)
Leaf Area Index Values for Different Land Uses

LUCODE	Description	LAI*	Note
1740	military	2.08	Shrub
1750	governmental	2.08	Shrub
1800	Recreational	2.08	Shrub
1820	golf course	2.08	Shrub
1830	race tracks	2.08	Shrub
1840	marinas and fish camps	2.08	Shrub
1850	parks and zoos	2.08	Shrub
1860	parks and zoos	2.08	Shrub
1870	stadiums: those facilities not associated with high schools, colleges, or universities	2.08	Shrub
1900	Open Land	2.08	Shrub
1910	Open Land	2.08	Shrub
1920	inactive land with street pattern but without structures	3.08	Shrub
1930	inactive land with street pattern but without structures	4.08	Shrub
1940	inactive land with street pattern but without structures	5.08	Shrub
2110	improved pastures	2.5	Grassland
2120	unimproved pastures	2.08	Shrub
2130	woodland pastures	2.5	Grassland
2140	row crops	4.22	crops
2150	field crops	4.22	crops
2160	mixed crops: used if crop type cannot be determined	4.22	crops
2200	Tree Crops	8.72	Plantation
2210	citrus groves	8.72	Plantation
2240	abandoned tree crops	4.22	crops
2310	cattle feeding operations	2.5	Grassland
2320	poultry feeding operations	2.5	Grassland
2400	Nurseries and Vineyards	8.72	Plantation
2410	tree nurseries	8.72	Plantation
2430	ornamentals	2.08	Shrub
2450	floriculture	2.08	Shrub
2500	Specialty Farms	4.22	crops
2510	horse farms	2.5	Grassland
2540	aquaculture	2.08	Shrub
2610	fallow cropland	4.22	crops
3100	Herbaceous	2.08	Shrub
3200	Shrub and Brushland	2.08	Shrub
3210	Shrub and Brushland	2.08	Shrub
3290	Shrub and Brushland	2.08	Shrub
3300	Mixed Rangeland	2.08	Shrub
4110	pine flatwoods	6.7	Forest, temperate evergreen needle leaf
4120	longleaf pine xeric oak	6.7	Forest, temperate evergreen needle leaf
4130	sand pine	6.7	Forest, temperate evergreen needle leaf

Table 3.1 (continued)
Leaf Area Index Values for Different Land Uses

LUCODE	Description	LAI*	Note
4140	sand pine	6.7	Forest, temperate evergreen needle leaf
4200	Upland Hardwood Forest (4200 4399)	6.7	Forest, temperate evergreen needle leaf
4210	xeric oak	6.7	Forest, temperate evergreen needle leaf
4250	xeric oak	6.7	Forest, temperate evergreen needle leaf
4270	xeric oak	6.7	Forest, temperate evergreen needle leaf
4340	upland mixed coniferous/hardwood	6.7	Forest, temperate evergreen needle leaf
4380	australian pine	6.7	Forest, temperate evergreen needle leaf
4410	coniferous pine	6.7	Forest, temperate evergreen needle leaf
4430	forest regeneration	6.7	Forest, temperate evergreen needle leaf
5100	streams and waterways	2.08	Shrub
5200	lakes	2.08	Shrub
5210	lakes	2.08	Shrub
5220	lakes	2.08	Shrub
5230	lakes	2.08	Shrub
5240	lakes	2.08	Shrub
5300	reservoirs	2.08	Shrub
5330	reservoirs	2.08	Shrub
5340	reservoirs less than 10 acres (4 hectares) which are dominant features	2.08	Shrub
5600	slough waters	6.34	Wetlands
6110	bay swamps	6.34	Wetlands
6150	river/lake swamp (bottomland)	6.34	Wetlands
6170	mixed wetland hardwoods	6.34	Wetlands
6172	mixed wetland hardwoods	6.34	Wetlands
6200	wetland coniferous forest	6.34	Wetlands
6210	cypress	6.7	Forest, temperate evergreen needle leaf
6220	forested depressional pine	6.7	Forest, temperate evergreen needle leaf
6240	forested depressional pine	6.7	Forest, temperate evergreen needle leaf
6300	wetland forested mixed	6.34	Wetlands
6410	freshwater marshes	6.34	Wetlands
6430	wet prairies	6.34	Wetlands
6439	wet prairies	6.34	Wetlands
6440	emergent aquatic vegetation	6.34	Wetlands
6460	mixed scrub shrub wetland	6.34	Wetlands
7200	sand other than beaches	2.08	Shrub
7400	disturbed land	2.5	Grassland
7410	rural land in transition without positive indicators of intended activity	2.5	Grassland

Table 3.1 (continued)
Leaf Area Index Values for Different Land Uses

LUCODE	Description	LAI*	Note
7420	borrow areas	2.5	Grassland
7430	spoil areas	2.5	Grassland
8110	airports	2.08	Shrub
8120	railroads	2.08	Shrub
8140	roads and highways	2.08	Shrub
8160	canals and locks	2.08	Shrub
8180	auto parking facilities when not directly related to other land uses	1.31	Desert
8191	highways	2.08	Shrub
8200	Communications	2.08	Shrub
8210	Communications	2.08	Shrub
8220	Communications	2.08	Shrub
8310	Electrical Power Facilities	2.08	Shrub
8320	Electrical Power Transmission Lines	2.08	Shrub
8330	Water Supply Plants	2.08	Shrub
8340	Sewage Treatment Plants	2.08	Shrub
8350	Solid Waste Disposal	2.08	Shrub

* The reference for the LAI values is listed below:
Scurlock, J. M. O., G. P. Asner, and S. T. Gower. 2001. Worldwide Historical Estimates and Bibliography of Leaf Area Index, 1932-2000. ORNL Technical Memorandum TM-2001/268, Oak Ridge National Laboratory, Oak Ridge, Tennessee, U.S.A.
Note: The leaf area index values used in the calibrated model are ½ of the values shown above.
Note: The land-use codes are generally classified as follows:

1000-1999 Urban and Built Up
2000-2999 Agricultural
3000-3999 Rangeland
4000-4999 Upland Forests
5000-5999 Water
6000-6999 Wetlands
7000-7999 Barren land
8000-8999 Transportation, Communication and Utilities
9999 Unmapped

Table 3.2
Field Capacity and Wilting Point Moisture Content Values for Different Soil Types

SCS Hydrologic Soil Group	Field Capacity Moisture Content [1]	Wilting Point Moisture Content [1]	Porosity	Saturation at Field Capacity[2]	Saturation at Wilting Point[2]
A	0.118	0.041	0.41	0.29	0.10
B	0.195	0.09	0.43	0.45	0.21
C	0.224	0.108	0.39	0.57	0.28
D	0.241	0.146	0.45	0.54	0.32

[1] Mean values from Carsel and others, 1988
[2] Saturation = Moisture Content/Porosity

Table 3.3
Average 1995 Pumping Rates for the WOSC-ISGM Model

Well ID	Permit Number	Owner	Well Type	X	Y	Aquifer	Average 1995 Withdrawal (Ft^3/Day)
4335	3835	ALAQUA LAKES DEVELOPMENT COMPANY	Withdrawal	462109	3180416	UFUZ	0.0
3992	8337	SEMINOLE COMMUNITY COLLEGE	Withdrawal	470495	3180015	UFUZ	0.0
4309	8460	ALAQUA COUNTRY CLUB INC.	Withdrawal	460868	3180010	UFUZ	0.0
4310	8460	ALAQUA COUNTRY CLUB INC.	Withdrawal	460779	3179922	UFUZ	0.0
4308	8460	ALAQUA COUNTRY CLUB INC.	Withdrawal	461599	3179709	UFUZ	0.0
3989	8337	SEMINOLE COMMUNITY COLLEGE	Withdrawal	470035	3179706	UFUZ	0.0
3991	8337	SEMINOLE COMMUNITY COLLEGE	Withdrawal	469918	3179618	UFUZ	0.0
3990	8337	SEMINOLE COMMUNITY COLLEGE	Withdrawal	470035	3179529	UFUZ	0.0
5871	8213	SEMINOLE COUNTY PWD	Withdrawal	466206	3179351	UFUZ	-33,155.0
5871	8213	SEMINOLE COUNTY PWD	Withdrawal	466206	3179351	UFDZ	-33,155.0
5873	8213	SEMINOLE COUNTY PWD	Withdrawal	466040	3179263	UFUZ	-17,613.5
5873	8213	SEMINOLE COUNTY PWD	Withdrawal	466040	3179263	UFDZ	-17,613.5
5874	8213	SEMINOLE COUNTY PWD	Withdrawal	466147	3179074	LF	-20,722.0
5875	8213	SEMINOLE COUNTY PWD	Withdrawal	466966	3178485	UFUZ	-42,480.0
5875	8213	SEMINOLE COUNTY PWD	Withdrawal	466966	3178485	UFDZ	-42,480.0
5870	8213	SEMINOLE COUNTY PWD	Withdrawal	467776	3178483	UFUZ	-41,912.0
5872	8213	SEMINOLE COUNTY PWD	Withdrawal	467805	3178460	UFUZ	-27,941.0
6021	8238	WINTER SPRINGS CITY OF	Withdrawal	469420	3176140	UFUZ	0.0
5869	160	SANLANDO UTILITIES CORP	Withdrawal	463052	3176070	UFUZ	0.0
6019	8238	WINTER SPRINGS CITY OF	Withdrawal	469068	3176053	UFUZ	-33,534.0
6019	8238	WINTER SPRINGS CITY OF	Withdrawal	469068	3176053	UFDZ	-33,534.0
5957	8274	LONGWOOD CITY OF	Withdrawal	464701	3175666	UFUZ	-59,395.0
5861	160	SANLANDO UTILITIES CORP	Withdrawal	463207	3175638	UFUZ	-43,822.0
5861	160	SANLANDO UTILITIES CORP	Withdrawal	463207	3175638	UFDZ	-43,822.0
5956	8274	LONGWOOD CITY OF	Withdrawal	464672	3175633	UFUZ	-59,395.0
5955	8274	LONGWOOD CITY OF	Withdrawal	464701	3175600	UFUZ	-29,697.5
5955	8274	LONGWOOD CITY OF	Withdrawal	464701	3175600	UFDZ	-29,697.5
5860	160	SANLANDO UTILITIES CORP	Withdrawal	463069	3175428	UFUZ	-39,032.0
5860	160	SANLANDO UTILITIES CORP	Withdrawal	463069	3175428	UFDZ	-39,032.0
5858	160	SANLANDO UTILITIES CORP	Withdrawal	463235	3175361	UFDZ	-28,741.5

Table 3.3 (Continued)
Average 1995 Pumping rates for the WOSC-ISGM Model

Well ID	Permit Number	Owner	Well Type	X	Y	Aquifer	Average 1995 Withdrawal (Ft^3/Day)
5858	160	SANLANDO UTILITIES CORP	Withdrawal	463235	3175361	LF	-28,741.5
5859	160	SANLANDO UTILITIES CORP	Withdrawal	463265	3175361	UFUZ	-65,822.0
5859	160	SANLANDO UTILITIES CORP	Withdrawal	463265	3175361	UFDZ	-65,822.0
6000	8369	SEMINOLE PINES MHP	Withdrawal	473569	3175211	UFUZ	-2,674.0
6001	8369	SEMINOLE PINES MHP	Withdrawal	473598	3175144	UFUZ	-1,337.0
6001	8369	SEMINOLE PINES MHP	Withdrawal	473598	3175144	UFDZ	-1,337.0
3994	8338	RICHARD I. AND KIM O. WINOKUR	Withdrawal	455127	3175046	UFUZ	-1,212.0
5954	8274	LONGWOOD CITY OF	Withdrawal	466271	3174764	UFUZ	-22,309.5
5954	8274	LONGWOOD CITY OF	Withdrawal	466271	3174764	UFDZ	-22,309.5
5953	8274	LONGWOOD CITY OF	Withdrawal	466115	3174643	UFUZ	-44,619.0
4330	8486	ORLANDO RESORT CORPORATION	Withdrawal	459950	3174507	UFUZ	0.0
5867	160	SANLANDO UTILITIES CORP	Withdrawal	457479	3174483	UFUZ	-146,008.0
5867	160	SANLANDO UTILITIES CORP	Withdrawal	457479	3174483	UFDZ	-146,008.0
5867	160	SANLANDO UTILITIES CORP	Withdrawal	457479	3174483	LF	-146,008.0
5863	160	SANLANDO UTILITIES CORP	Withdrawal	463261	3174375	UFUZ	-3,641.0
5863	160	SANLANDO UTILITIES CORP	Withdrawal	463261	3174375	UFDZ	-3,641.0
5862	160	SANLANDO UTILITIES CORP	Withdrawal	463046	3174342	UFUZ	-1,149.5
5862	160	SANLANDO UTILITIES CORP	Withdrawal	463046	3174342	UFDZ	-1,149.5
4324	8483	FRANCIS & LEOLA BOWMAN	Withdrawal	457144	3174180	UFUZ	-11,669.0
5996	8361	FLORIDA WATER SERVICES	Withdrawal	457829	3174149	UFUZ	-2,562.0
4329	8486	ORLANDO RESORT CORPORATION	Withdrawal	460086	3174141	UFUZ	-7,061.0
4314	3812	ROLLING HILLS GOLF CLUB	Withdrawal	463641	3174008	UFUZ	-7,910.0
3947	8283	WEKIVA HUNT CLUB CONDOMINIUMS ASSOCIATIONS	Withdrawal	456500	3173966	UFUZ	-1,819.0
4323	8483	FRANCIS & LEOLA BOWMAN	Withdrawal	456988	3173720	UFUZ	-5,834.5
4323	8483	FRANCIS & LEOLA BOWMAN	Withdrawal	456988	3173720	UFDZ	-5,834.5
4292	8438	GARDEN ARTS NURSERY	Withdrawal	457953	3173661	UFUZ	-16,398.0
5868	160	SANLANDO UTILITIES CORP	Withdrawal	457016	3173598	UFUZ	-62,897.0

Table 3.3 (Continued)
Average 1995 Pumping rates for the WOSC-ISGM Model

Well ID	Permit Number	Owner	Well Type		Y	Aquifer	Average 1995 Withdrawal (Ft^3/Day)
5868	160	SANLANDO UTILITIES CORP	Withdrawal	457016	3173598	UFDZ	-62,897.0
4291	8438	GARDEN ARTS NURSERY	Withdrawal	457881	3173564	UFUZ	-16,398.0
4312	3812	ROLLING HILLS GOLF CLUB	Withdrawal	462878	3173545	UFUZ	-7,910.0
4313	3812	ROLLING HILLS GOLF CLUB	Withdrawal	462878	3173489	UFUZ	-7,910.0
5864	160	SANLANDO UTILITIES CORP	Withdrawal	457182	3173476	UFUZ	-39,080.0
5864	160	SANLANDO UTILITIES CORP	Withdrawal	457182	3173476	UFDZ	-39,080.0
5994	8359	FLORIDA WATER SERVICES	Withdrawal	459517	3173467	UFUZ	-35,695.0
6020	8238	WINTER SPRINGS CITY OF	Withdrawal	470263	3173280	UFUZ	-34,209.0
6020	8238	WINTER SPRINGS CITY OF	Withdrawal	470263	3173280	UFDZ	-34,209.0
6018	8238	WINTER SPRINGS CITY OF	Withdrawal	470204	3173214	UFUZ	-31,577.5
6018	8238	WINTER SPRINGS CITY OF	Withdrawal	470204	3173214	UFDZ	-31,577.5
4311	3812	ROLLING HILLS GOLF CLUB	Withdrawal	463531	3173210	UFUZ	-7,910.0
5865	160	SANLANDO UTILITIES CORP	Withdrawal	456937	3173200	UFUZ	-39,080.0
5865	160	SANLANDO UTILITIES CORP	Withdrawal	456937	3173200	UFDZ	-39,080.0
4315	3812	ROLLING HILLS GOLF CLUB	Withdrawal	462281	3173115	UFUZ	-7,910.0
5866	160	SANLANDO UTILITIES CORP	Withdrawal	456770	3173045	UFUZ	-46,815.0
5866	160	SANLANDO UTILITIES CORP	Withdrawal	456770	3173045	UFDZ	-46,815.0
5966	8284	CASSELBERRY CITY OF	Withdrawal	468630	3172941	UFUZ	-56,679.0
5965	8284	CASSELBERRY CITY OF	Withdrawal	468572	3172886	UFUZ	-56,679.0
4050	8387	SEMINOLE COUNTY SCHOOL BOARD	Withdrawal	458616	3172795	UFUZ	-3,916.0
4051	8387	SEMINOLE COUNTY SCHOOL BOARD	Withdrawal	458645	3172761	UFUZ	-3,916.0
5967	8284	CASSELBERRY CITY OF	Withdrawal	468493	3172697	LF	-113,358.0
4049	8384	SEMINOLE COUNTY SCHOOL BOARD	Withdrawal	458341	3172397	UFUZ	-848.5
4049	8384	SEMINOLE COUNTY SCHOOL BOARD	Withdrawal	458341	3172397	UFDZ	-848.5
1960	1619	GREEN MASTERS	Withdrawal	452781	3172385	UFUZ	-606.0
1960	1619	GREEN MASTERS	Withdrawal	452781	3172385	UFDZ	-606.0
6022	8238	WINTER SPRINGS CITY OF	Withdrawal	474247	3172373	UFUZ	-63,778.0
1959	1619	GREEN MASTERS	Withdrawal	452801	3172318	UFUZ	-606.0
1959	1619	GREEN MASTERS	Withdrawal	452801	3172318	UFDZ	-606.0
5980	8349	UTILITIES INC OF FLORIDA	Withdrawal	459210	3172205	UFUZ	-1,894.0
5987	50281	FLORIDA WATER SERVICES	Withdrawal	461652	3172197	UFUZ	-13,686.5
5987	50281	FLORIDA WATER SERVICES	Withdrawal	461652	3172197	UFDZ	-13,686.5

Table 3.3 (Continued)
Average 1995 Pumping rates for the WOSC-ISGM Model

Well ID	Permit Number	Owner	Well Type	X	Y	Aquifer	Average 1995 Withdrawal (Ft^3/Day)
5986	50281	FLORIDA WATER SERVICES	Withdrawal	461623	3172164	UFUZ	-16,728.0
5986	50281	FLORIDA WATER SERVICES	Withdrawal	461623	3172164	UFDZ	-16,728.0
5991	8357	FLORIDA WATER SERVICES	Withdrawal	464993	3172032	UFUZ	-1,559.5
5991	8357	FLORIDA WATER SERVICES	Withdrawal	464993	3172032	UFDZ	-1,559.5
4317	8467	HIGHLAND MEMORY GARDENS INC	Withdrawal	456277	3171817	UFUZ	-4,243.0
4316	8467	HIGHLAND MEMORY GARDENS INC	Withdrawal	456336	3171817	UFUZ	-4,243.0
6006	8372	ALTAMONTE SPRINGS CITY OF	Withdrawal	463009	3171694	UFUZ	0.0
3927	8216	TENN-FLA PARTNERS	Withdrawal	462598	3171640	UFUZ	-6,304.0
6009	8372	ALTAMONTE SPRINGS CITY OF	Withdrawal	463037	3171484	UFUZ	0.0
6009	8372	ALTAMONTE SPRINGS CITY OF	Withdrawal	463037	3171484	UFDZ	0.0
3948	8288	ALL FAITHS MEMORIAL PARK	Withdrawal	470033	3171430	UFUZ	-1,940.0
5919	8241	SEMINOLE COUNTY PWD	Withdrawal	455923	3171320	UFUZ	0.0
5920	8241	SEMINOLE COUNTY PWD	Withdrawal	456031	3171320	UFUZ	0.0
5918	8241	SEMINOLE COUNTY PWD	Withdrawal	455484	3171266	UFUZ	0.0
5990	8356	FLORIDA WATER SERVICES	Withdrawal	458581	3171222	UFUZ	-10,695.0
4289	8436	POST PROPERTIES INC.	Withdrawal	457359	3171016	UFUZ	-10,548.0
6007	8372	ALTAMONTE SPRINGS CITY OF	Withdrawal	459635	3170974	UFUZ	-4,996.5
6007	8372	ALTAMONTE SPRINGS CITY OF	Withdrawal	459635	3170974	UFDZ	-4,996.5
6010	8372	ALTAMONTE SPRINGS CITY OF	Withdrawal	459723	3170974	UFUZ	-11,659.0
6010	8372	ALTAMONTE SPRINGS CITY OF	Withdrawal	459723	3170974	UFDZ	-11,659.0
5922	8241	SEMINOLE COUNTY PWD	Withdrawal	456381	3170953	UFUZ	-29,523.0
5922	8241	SEMINOLE COUNTY PWD	Withdrawal	456381	3170953	UFDZ	-29,523.0
6002	8372	ALTAMONTE SPRINGS CITY OF	Withdrawal	464961	3170891	UFUZ	0.0
4290	8436	POST PROPERTIES INC.	Withdrawal	457329	3170883	UFUZ	-10,548.0
5921	8241	SEMINOLE COUNTY PWD	Withdrawal	456352	3170831	UFUZ	-29,523.0
5921	8241	SEMINOLE COUNTY PWD	Withdrawal	456352	3170831	UFDZ	-29,523.0
6003	8372	ALTAMONTE SPRINGS CITY OF	Withdrawal	464902	3170769	UFUZ	0.0
6003	8372	ALTAMONTE SPRINGS CITY OF	Withdrawal	464902	3170769	UFDZ	0.0
5627	3217	APOPKA CITY OF	Withdrawal	452608	3170690	UFUZ	0.0
6011	8372	ALTAMONTE SPRINGS CITY OF	Withdrawal	464852	3170680	UFUZ	0.0
6011	8372	ALTAMONTE SPRINGS CITY OF	Withdrawal	464852	3170680	UFDZ	0.0
5992	3769	FLORIDA WATER SERVICES	Withdrawal	462487	3170466	UFUZ	-2,340.0

Table 3.3 (Continued)
Average 1995 Pumping rates for the WOSC-ISGM Model

Well ID	Permit Number	Owner	Well Type	X	Y	Aquifer	Average 1995 Withdrawal (Ft^3/Day)
5993	3769	FLORIDA WATER SERVICES	Withdrawal	462487	3170466	UFUZ	-2,340.0
5976	8346	UTILITIES INC OF FLORIDA	Withdrawal	460180	3170352	UFUZ	-14,518.0
5976	8346	UTILITIES INC OF FLORIDA	Withdrawal	460180	3170352	UFDZ	-14,518.0
5975	8346	UTILITIES INC OF FLORIDA	Withdrawal	460239	3170352	UFUZ	-8,710.5
5975	8346	UTILITIES INC OF FLORIDA	Withdrawal	460239	3170352	UFDZ	-8,710.5
4215	8419	SEMINOLE COUNTY SCHOOL BOARD	Withdrawal	468838	3170292	UFUZ	-2,546.0
5979	8348	UTILITIES INC OF FLORIDA	Withdrawal	456457	3170277	UFUZ	-4,289.0
5979	8348	UTILITIES INC OF FLORIDA	Withdrawal	456457	3170277	UFDZ	-4,289.0
4044	8365	FLORIDA DEER RUN INC. DBA DEER RUN COUNTRY CLUB	Withdrawal	470382	3170111	UFUZ	-19,652.0
6008	8372	ALTAMONTE SPRINGS CITY OF	Withdrawal	458087	3169805	UFUZ	-79,908.0
6008	8372	ALTAMONTE SPRINGS CITY OF	Withdrawal	458087	3169805	UFDZ	-79,908.0
6013	8372	ALTAMONTE SPRINGS CITY OF	Withdrawal	458058	3169750	LF	-324,475.0
4969	7351	JV FURNITURE CO.	Withdrawal	454422	3169609	UFUZ	-960.5
4969	7351	JV FURNITURE CO.	Withdrawal	454422	3169609	UFDZ	-960.5
5625	3217	APOPKA CITY OF	Withdrawal	452603	3169427	LF	-117,313.0
5630	3217	APOPKA CITY OF	Withdrawal	450971	3169346	UFUZ	0.0
5630	3217	APOPKA CITY OF	Withdrawal	450971	3169346	UFDZ	0.0
5995	8360	FLORIDA WATER SERVICES	Withdrawal	465141	3169228	UFUZ	-5,459.0
1764	50167	HERMANN ENGELMANN GREENHOUSES INC.	Withdrawal	449015	3168977	UFUZ	-1,477.0
1765	50167	HERMANN ENGELMANN GREENHOUSES INC.	Withdrawal	449015	3168977	UFUZ	-88.0
6005	8372	ALTAMONTE SPRINGS CITY OF	Withdrawal	463870	3168900	UFUZ	-32,255.5
6005	8372	ALTAMONTE SPRINGS CITY OF	Withdrawal	463870	3168900	UFDZ	-32,255.5
6004	8372	ALTAMONTE SPRINGS CITY OF	Withdrawal	463762	3168867	UFUZ	-32,255.5
6004	8372	ALTAMONTE SPRINGS CITY OF	Withdrawal	463762	3168867	UFDZ	-32,255.5
6012	8372	ALTAMONTE SPRINGS CITY OF	Withdrawal	463811	3168867	LF	-219,686.0
1767	50167	HERMANN ENGELMANN GREENHOUSES INC.	Withdrawal	448858	3168801	UFUZ	-88.0
1766	50167	HERMANN ENGELMANN GREENHOUSES INC.	Withdrawal	448858	3168801	UFUZ	-1,477.0
5978	8347	UTILITIES INC OF FLORIDA	Withdrawal	455455	3168774	UFUZ	-2,311.5
5978	8347	UTILITIES INC OF FLORIDA	Withdrawal	455455	3168774	UFDZ	-2,311.5
5653	3317	OCU	Withdrawal	450294	3168761	UFUZ	-1,671.0

Table 3.3 (Continued)
Average 1995 Pumping rates for the WOSC-ISGM Model

Well ID	Permit Number	Owner	Well Type	X	Y	Aquifer	Average 1995 Withdrawal (Ft^3/Day)
1768	50167	HERMANN ENGELMANN GREENHOUSES INC.	Withdrawal	449013	3168678	UFUZ	-1,477.0
1769	50167	HERMANN ENGELMANN GREENHOUSES INC.	Withdrawal	449013	3168678	UFUZ	-88.0
1810	3240	O.F. NELSON AND SONS NURSERY	Withdrawal	451681	3168634	UFUZ	-5,375.0
5977	8347	UTILITIES INC OF FLORIDA	Withdrawal	455884	3168617	UFUZ	-4,623.0
1809	3240	O.F. NELSON AND SONS NURSERY	Withdrawal	451407	3168568	UFUZ	-5,375.0
1812	3240	O.F. NELSON AND SONS NURSERY	Withdrawal	451759	3168511	UFUZ	-5,375.0
1808	3240	O.F. NELSON AND SONS NURSERY	Withdrawal	451622	3168412	UFUZ	-5,375.0
1825	3250	DEWAR NURSERIES INC.	Withdrawal	448797	3168402	UFUZ	-612.0
2089	3412	PATRICIA THAKUR	Withdrawal	450429	3168362	UFUZ	-393.5
2089	3412	PATRICIA THAKUR	Withdrawal	450429	3168362	UFDZ	-393.5
1826	3250	DEWAR NURSERIES INC.	Withdrawal	448767	3168303	UFUZ	-612.0
1811	3240	O.F. NELSON AND SONS NURSERY	Withdrawal	451514	3168291	UFUZ	-5,375.0
1827	3250	DEWAR NURSERIES INC.	Withdrawal	448718	3168281	UFUZ	-306.0
1827	3250	DEWAR NURSERIES INC.	Withdrawal	448718	3168281	UFDZ	-306.0
2088	3412	PATRICIA THAKUR	Withdrawal	450321	3168274	UFUZ	-787.0
1935	3327	W & A AGRI-GROWTH	Withdrawal	446793	3168256	UFUZ	-6,643.5
1935	3327	W & A AGRI-GROWTH	Withdrawal	446793	3168256	UFDZ	-6,643.5
1828	3250	DEWAR NURSERIES INC.	Withdrawal	448718	3168181	UFUZ	-306.0
1828	3250	DEWAR NURSERIES INC.	Withdrawal	448718	3168181	UFDZ	-306.0
4973	3255	HYDRO CONDUIT CORP	Withdrawal	454064	3168125	UFUZ	-383.0
5674	3317	OCU	Withdrawal	452051	3168078	LF	0.0
5671	3317	OCU	Withdrawal	452138	3168078	LF	0.0
4998	3403	FINFROCK ROBERT D	Withdrawal	454855	3168034	UFUZ	-686.0
2074	3397	ORANGE COUNTY PUBLIC SCHOOLS	Withdrawal	453252	3168007	UFUZ	-512.0
5669	3317	OCU	Withdrawal	451942	3167957	LF	-250,000.0
5675	3317	OCU	Withdrawal	452079	3167956	LF	0.0
5672	3317	OCU	Withdrawal	452245	3167955	LF	0.0
4972	3255	HYDRO CONDUIT CORP	Withdrawal	454122	3167948	UFUZ	0.0
1774	1613	STATE OF FLORIDA	Withdrawal	446381	3167948	UFUZ	-2,910.0
1829	3250	DEWAR NURSERIES INC.	Withdrawal	448903	3167936	UFUZ	-612.0
4999	3403	FINFROCK ROBERT D	Withdrawal	454826	3167879	UFUZ	-686.0
1718	3185	JACOBSONS PLANTS INC.	Withdrawal	451453	3167837	UFUZ	-1,311.0
5605	3203	JELLYSTONE CONDO ASSOC INC	Withdrawal	450642	3167807	UFUZ	-17,374.0
5670	3317	OCU	Withdrawal	452030	3167801	LF	-250,000.0
5676	3317	OCU	Withdrawal	452167	3167801	LF	0.0
5673	3317	OCU	Withdrawal	452352	3167800	LF	0.0

Table 3.3 (Continued)
Average 1995 Pumping rates for the WOSC-ISGM Model

Well ID	Permit Number	Owner	Well Type	X	Y	Aquifer	Average 1995 Withdrawal (Ft^3/Day)
5606	3203	JELLYSTONE CONDO ASSOC INC	Withdrawal	450671	3167774	UFUZ	-17,374.0
1743	3201	ROBERT R. HOGSETTE III	Withdrawal	452811	3167732	UFUZ	0.0
1742	3201	ROBERT R. HOGSETTE III	Withdrawal	452811	3167732	UFUZ	-3,844.0
1741	3201	ROBERT R. HOGSETTE III	Withdrawal	452948	3167731	UFUZ	0.0
1741	3201	ROBERT R. HOGSETTE III	Withdrawal	452948	3167731	UFDZ	0.0
1740	3201	ROBERT R. HOGSETTE III	Withdrawal	452948	3167731	UFUZ	-1,922.0
1740	3201	ROBERT R. HOGSETTE III	Withdrawal	452948	3167731	UFDZ	-1,922.0
1776	3214	O. F. NELSON & SONS NURSERY	Withdrawal	451374	3167560	UFUZ	-4,799.0
1777	3214	O. F. NELSON & SONS NURSERY	Withdrawal	451374	3167560	UFUZ	-131.0
5704	3405	ORANGE COUNTY COMMISSIONERS	Withdrawal	446320	3167549	UFUZ	-47.0
5704	3405	ORANGE COUNTY COMMISSIONERS	Withdrawal	446320	3167549	UFDZ	-47.0
5664	3317	OCU	Withdrawal	458646	3167499	UFUZ	-26,328.0
1729	3195	NATURAL BEAUTY OF FLORIDA	Withdrawal	451329	3168170	UFUZ	-3,976.0
5665	3317	OCU	Withdrawal	458734	3167432	LF	-51,010.0
2070	3393	APOPKA NURSERY PROPERTY ASSOCIATION	Withdrawal	451539	3167404	UFUZ	-2,098.0
5666	3317	OCU	Withdrawal	458733	3167377	LF	-87,211.0
1988	3349	SEIL & MISUN CHIN	Withdrawal	451314	3167283	UFUZ	-720.0
1987	3349	SEIL & MISUN CHIN	Withdrawal	451314	3167283	UFUZ	-720.0
1948	1618	DAVID RUBRIGHT	Withdrawal	447296	3167179	UFUZ	-265.5
1948	1618	DAVID RUBRIGHT	Withdrawal	447296	3167179	UFDZ	-265.5
1947	1618	DAVID RUBRIGHT	Withdrawal	447296	3167179	UFUZ	-329.5
1947	1618	DAVID RUBRIGHT	Withdrawal	447296	3167179	UFDZ	-329.5
1941	1618	DAVID RUBRIGHT	Withdrawal	447139	3167047	UFUZ	-659.0
1942	1618	DAVID RUBRIGHT	Withdrawal	447139	3167047	UFUZ	-531.0
1946	1618	DAVID RUBRIGHT	Withdrawal	447110	3166958	UFUZ	-265.5
1946	1618	DAVID RUBRIGHT	Withdrawal	447110	3166958	UFDZ	-265.5
1945	1618	DAVID RUBRIGHT	Withdrawal	447110	3166958	UFUZ	-329.5
1945	1618	DAVID RUBRIGHT	Withdrawal	447110	3166958	UFDZ	-329.5
1944	1618	DAVID RUBRIGHT	Withdrawal	447246	3166924	UFUZ	-531.0
1943	1618	DAVID RUBRIGHT	Withdrawal	447246	3166924	UFUZ	-659.0
5612	50258	MAITLAND CITY OF	Withdrawal	460872	3166815	LF	-110,851.0
1930	3320	LINDA MOTCHECK	Withdrawal	451752	3166750	UFUZ	-2,400.0
1929	3320	LINDA MOTCHECK	Withdrawal	451752	3166750	UFUZ	-2,400.0
5613	50258	MAITLAND CITY OF	Withdrawal	460872	3166627	LF	0.0
1837	3254	RONALD J. VAUGHN	Withdrawal	451936	3166450	UFUZ	-248.0
1833	3254	RONALD J. VAUGHN	Withdrawal	452044	3166416	UFUZ	-248.0
1834	3254	RONALD J. VAUGHN	Withdrawal	452073	3166416	UFUZ	-248.0
1835	3254	RONALD J. VAUGHN	Withdrawal	451916	3166328	UFUZ	-124.0

Table 3.3 (Continued)
Average 1995 Pumping rates for the WOSC-ISGM Model

Well ID	Permit Number	Owner	Well Type		Y	Aquife r	Average 1995 Withdrawal (Ft^3/Day)
1835	3254	RONALD J. VAUGHN	Withdrawal	451916	3166328	UFDZ	-124.0
1836	3254	RONALD J. VAUGHN	Withdrawal	451935	3166228	UFUZ	-124.0
1836	3254	RONALD J. VAUGHN	Withdrawal	451935	3166228	UFDZ	-124.0
1902	3293	SAMUEL WALKER	Withdrawal	454868	3166217	UFUZ	-292.0
1851	7419	SHERWOOD STARBIRD	Withdrawal	447134	3165917	UFUZ	-437.0
1849	7419	SHERWOOD STARBIRD	Withdrawal	447105	3165850	UFUZ	-437.0
1850	7419	SHERWOOD STARBIRD	Withdrawal	447026	3165795	UFUZ	-437.0
1738	50106	G.I. GILLIAM INC.	Withdrawal	448374	3165535	UFUZ	-1,249.0
1738	50106	G.I. GILLIAM INC.	Withdrawal	448374	3165535	UFDZ	-1,249.0
1739	50106	G.I. GILLIAM INC.	Withdrawal	448374	3165535	UFUZ	-1,849.0
1739	50106	G.I. GILLIAM INC.	Withdrawal	448374	3165535	UFDZ	-1,849.0
2093	309	SCI FUNERAL SERVICES OF FLORIDA INC.	Withdrawal	447698	3165261	UFUZ	-285.0
4993	4619	RINKER MATERIALS CORPORATION	Withdrawal	458178	3165218	UFUZ	-2,586.0
2094	309	SCI FUNERAL SERVICES OF FLORIDA INC.	Withdrawal	447669	3165205	UFUZ	-285.0
4995	7689	UNIWES INC.	Withdrawal	450811	3163895	UFUZ	-8,382.0
1732	50083	ARTHUR LEONHARDT JR.	Withdrawal	450595	3163708	UFUZ	-691.0
1732	50083	ARTHUR LEONHARDT JR.	Withdrawal	450595	3163708	UFDZ	-691.0
5617	3216	OCOEE CITY OF	Withdrawal	450810	3163563	LF	-63,465.0
5618	3216	OCOEE CITY OF	Withdrawal	450868	3163563	UFUZ	-63,465.0
5621	3216	OCOEE CITY OF	Withdrawal	450898	3163563	LF	-63,465.0
1908	3298	J.M. & M. NADINE KNOX JR.	Withdrawal	453497	3163209	UFUZ	-765.0
1910	3298	J.M. & M. NADINE KNOX JR.	Withdrawal	453614	3163142	UFUZ	-765.0
1909	3298	J.M. & M. NADINE KNOX JR.	Withdrawal	453526	3163120	UFUZ	-382.5
1909	3298	J.M. & M. NADINE KNOX JR.	Withdrawal	453526	3163120	UFDZ	-382.5
1803	3237	DALE CHANG/ROSEMONT GOLF & COUNTRY CLUB	Withdrawal	458033	3162948	UFUZ	-2,259.0
1801	3237	DALE CHANG/ROSEMONT GOLF & COUNTRY CLUB	Withdrawal	457925	3162826	UFUZ	-2,259.0
1802	3237	DALE CHANG/ROSEMONT GOLF & COUNTRY CLUB	Withdrawal	458170	3162825	UFUZ	-2,259.0
2013	3367	DIOCESE OF ORLANDO-BISHOP	Withdrawal	461611	3162379	UFUZ	-78.0
2012	3367	DIOCESE OF ORLANDO-BISHOP	Withdrawal	461864	3162159	UFUZ	-78.0
5615	3216	OCOEE CITY OF	Withdrawal	448388	3162155	UFUZ	-32,420.0
5615	3216	OCOEE CITY OF	Withdrawal	448388	3162155	UFDZ	-32,420.0
5616	3216	OCOEE CITY OF	Withdrawal	448388	3162155	UFUZ	-32,420.0
5616	3216	OCOEE CITY OF	Withdrawal	448388	3162155	UFDZ	-32,420.0
1995	306	CITY OF ORLANDO	Withdrawal	462655	3161880	UFUZ	-1,377.0
1994	306	CITY OF ORLANDO	Withdrawal	462537	3161825	UFUZ	-1,377.0
1775	4589	ARMADA REALTY DBA SEVILE PLACE II	Withdrawal	455808	3161505	UFUZ	0.0

Table 3.3 (Continued)
Average 1995 Pumping rates for the WOSC-ISGM Model

Well ID	Permit Number	Owner	Well Type		Y	Aquifer	Average 1995 Withdrawal (Ft^3/Day)
		APARTMENTS					
1796	3232	RICHARD F KNUTH	Withdrawal	451074	3161368	UFUZ	-1,063.0
4994	3377	FRITO-LAY	Withdrawal	459171	3161215	UFUZ	-17,776.0
1927	3315	W. C. DAVIS TRUSTEE	Withdrawal	449528	3161164	UFUZ	-792.0
1927	3315	W. C. DAVIS TRUSTEE	Withdrawal	449528	3161164	UFDZ	-792.0
1737	7252	D.A.B.I. INC.	Withdrawal	449037	3160579	UFUZ	-1,169.5
1737	7252	D.A.B.I. INC.	Withdrawal	449037	3160579	UFDZ	-1,169.5
5518	3159	OUC	Withdrawal	455501	3160464	LF	-402,406.0
1797	3233	JERRY BROWN	Withdrawal	445749	3160284	UFUZ	-14,882.0
5516	3159	OUC	Withdrawal	455422	3160221	LF	-402,406.0
1824	3249	COUNTRY CLUB VILLAS - OWNERS ASSOCIATION	Withdrawal	460663	3159925	UFUZ	-57.0
5515	3159	OUC	Withdrawal	455362	3159911	LF	-402,406.0
2008	7645	MARGARET W. MULVEY	Withdrawal	449171	3159870	UFUZ	-3,189.0
5614	3216	OCOEE CITY OF	Withdrawal	446558	3159704	UFUZ	0.0
5614	3216	OCOEE CITY OF	Withdrawal	446558	3159704	UFDZ	0.0
5519	3159	OUC	Withdrawal	455420	3159689	LF	-402,406.0
5525	3159	OUC	Withdrawal	455664	3159633	LF	0.0
5517	3159	OUC	Withdrawal	455908	3159410	LF	-402,406.0
2100	3416	HOMART DEVELOPMENT COMPANY	Withdrawal	449706	3159380	UFUZ	0.0
2100	3416	HOMART DEVELOPMENT COMPANY	Withdrawal	449706	3159380	UFDZ	0.0
2101	3416	HOMART DEVELOPMENT COMPANY	Withdrawal	449736	3159313	UFUZ	0.0
2101	3416	HOMART DEVELOPMENT COMPANY	Withdrawal	449736	3159313	UFDZ	0.0
2049	126	WEST ORANGE GIRLS CLUB	Withdrawal	446166	3159332	UFUZ	-142.0
2099	3416	HOMART DEVELOPMENT COMPANY	Withdrawal	449735	3159258	UFUZ	0.0
2099	3416	HOMART DEVELOPMENT COMPANY	Withdrawal	449735	3159258	UFDZ	0.0
1704	3179	MARY LUCY HAWTHORNE TRUST	Withdrawal	447581	3158955	UFUZ	-1,245.0
1704	3179	MARY LUCY HAWTHORNE TRUST	Withdrawal	447581	3158955	UFDZ	-1,245.0
5662	3317	OCU	Withdrawal	452496	3157429	LF	-20,183.0
5661	3317	OCU	Withdrawal	452584	3157429	LF	-343,106.0
5660	3317	OCU	Withdrawal	452633	3157429	UFUZ	-70,639.5
5660	3317	OCU	Withdrawal	452633	3157429	UFDZ	-70,639.5
1974	3341	WOODLAWN MEMORIUM	Withdrawal	449833	3156942	UFUZ	-2,688.0
1973	3341	WOODLAWN MEMORIUM	Withdrawal	449833	3156942	UFUZ	-676.0
1967	3341	WOODLAWN MEMORIUM	Withdrawal	450077	3156886	UFUZ	-676.0
1968	3341	WOODLAWN MEMORIUM	Withdrawal	450077	3156886	UFUZ	-2,688.0
1969	3341	WOODLAWN MEMORIUM	Withdrawal	450185	3156785	UFUZ	-676.0

Table 3.3 (Continued)
Average 1995 Pumping rates for the WOSC-ISGM Model

Well ID	Permit Number	Owner	Well Type		Y	Aquifer	Average 1995 Withdrawal (Ft^3/Day)
1970	3341	WOODLAWN MEMORIUM	Withdrawal	450185	3156785	UFUZ	-2,688.0
1971	3341	WOODLAWN MEMORIUM	Withdrawal	449644	3156234	UFUZ	-338.0
1971	3341	WOODLAWN MEMORIUM	Withdrawal	449644	3156234	UFDZ	-338.0
1972	3341	WOODLAWN MEMORIUM	Withdrawal	449644	3156234	UFUZ	-1,344.0
1972	3341	WOODLAWN MEMORIUM	Withdrawal	449644	3156234	UFDZ	-1,344.0
2082	3404	ORANGE CO. PUBLIC SCHOOLS	Withdrawal	450162	3156143	UFUZ	-277.0
2083	3404	ORANGE CO. PUBLIC SCHOOLS	Withdrawal	449996	3156088	UFUZ	-277.0
1794	3230	CHARLES E. AND MABEL RINEHART	Withdrawal	448675	3156170	UFUZ	-372.0
1794	3230	CHARLES E. AND MABEL RINEHART	Withdrawal	448675	3156170	UFDZ	-372.0
1793	3230	CHARLES E. AND MABEL RINEHART	Withdrawal	448476	3156067	UFUZ	-372.0
1793	3230	CHARLES E. AND MABEL RINEHART	Withdrawal	448476	3156067	UFDZ	-372.0
1414	0	DYKES CECIL CARLTON AND	Withdrawal	449011	3154708	UFUZ	-3,374.0
1414	0	DYKES CECIL CARLTON AND	Withdrawal	449011	3154708	UFDZ	-3,374.0
1416	0	DYKES KENNETH A.	Withdrawal	449686	3154605	UFUZ	-4,961.5
1416	0	DYKES KENNETH A.	Withdrawal	449686	3154605	UFDZ	-4,961.5
1417	0	ROUSE ETHEL	Withdrawal	450037	3154293	UFUZ	-15,877.0
S-0861	-	DNR	Free Flowing	459397	3181097	UFUZ	-442.8
S-0862	-	DNR	Free Flowing	459342	3180974	UFUZ	-442.8
S-0863	-	DNR	Free Flowing	459123	3180329	UFUZ	-442.8
OR0535	-	DNR	Free Flowing	459150	3180267	UFUZ	-423.6
S-0864	-	DNR	Free Flowing	459040	3179867	UFUZ	-442.8
OR0517	-	ROCK SPRINGS DNR	Free Flowing	455540	3179511	UFUZ	-423.6
OR0539	-	DNR	Free Flowing	458957	3179498	UFUZ	-423.6
S-0865	-	DNR	Free Flowing	458875	3179191	UFUZ	-442.8
S-0870	-	DNR	Free Flowing	458820	3178976	UFUZ	-442.8
OR0536	-	DNR	Free Flowing	458466	3178638	UFUZ	-423.6
OR0537	-	DNR	Free Flowing	458411	3178546	UFUZ	-423.6
OR0538	-	DNR	Free Flowing	458193	3178239	UFUZ	-423.6
S-0866	-	DNR	Free Flowing	458002	3177963	UFUZ	-442.8
S-0869	-	DNR	Free Flowing	457511	3177165	UFUZ	-442.8
S-0868	-	UNDETERMINED	Free Flowing	457348	3176950	UFUZ	-442.8
S-0867	-	DNR	Free Flowing	457266	3176858	UFUZ	-442.8

Table 3.3 (Continued)
Average 1995 Pumping rates for the WOSC-ISGM Model

Well ID	Permit Number	Owner	Well Type		Y	Aquife r	Average 1995 Withdrawal (Ft^3/Day)
-	-	-	Self-Supplied Domestic	460555	3180706	UFUZ	-413.8
-	-	-	Self-Supplied Domestic	460746	3180706	UFUZ	-413.8
-	-	-	Self-Supplied Domestic	460555	3180516	UFUZ	-413.8
-	-	-	Self-Supplied Domestic	460746	3180516	UFUZ	-413.8
-	-	-	Self-Supplied Domestic	460555	3180325	UFUZ	-413.8
-	-	-	Self-Supplied Domestic	460746	3180325	UFUZ	-413.8
-	-	-	Self-Supplied Domestic	460746	3180135	UFUZ	-413.8
-	-	-	Self-Supplied Domestic	460936	3180135	UFUZ	-413.8
-	-	-	Self-Supplied Domestic	447220	3166800	UFUZ	-1,591.0
-	-	-	Self-Supplied Domestic	450649	3166800	UFUZ	-1,591.0
-	-	-	Self-Supplied Domestic	450840	3166800	UFUZ	-1,591.0
-	-	-	Self-Supplied Domestic	451030	3166800	UFUZ	-1,591.0
-	-	-	Self-Supplied Domestic	447220	3166609	UFUZ	-1,591.0
-	-	-	Self-Supplied Domestic	450649	3166609	UFUZ	-1,591.0
-	-	-	Self-Supplied Domestic	450840	3166609	UFUZ	-1,591.0
-	-	-	Self-Supplied Domestic	446839	3166419	UFUZ	-1,591.0
-	-	-	Self-Supplied Domestic	447030	3166419	UFUZ	-1,591.0
-	-	-	Self-Supplied Domestic	447220	3166419	UFUZ	-1,591.0
-	-	-	Self-Supplied Domestic	450649	3166419	UFUZ	-1,591.0
-	-	-	Self-Supplied Domestic	446839	3166228	UFUZ	-1,591.0
-	-	-	Self-Supplied Domestic	447030	3166228	UFUZ	-1,591.0
-	-	-	Self-Supplied Domestic	447220	3166228	UFUZ	-1,591.0

Table 3.3 (Continued)
Average 1995 Pumping rates for the WOSC-ISGM Model

Well ID	Permit Number	Owner	Well Type		Y	Aquifer	Average 1995 Withdrawal (Ft^3/Day)
-	-	-	Self-Supplied Domestic	446839	3166038	UFUZ	-1,591.0
-	-	-	Self-Supplied Domestic	448173	3164704	UFUZ	-1,591.0
-	-	-	Self-Supplied Domestic	448363	3164704	UFUZ	-1,591.0
-	-	-	Self-Supplied Domestic	448554	3164704	UFUZ	-1,591.0
-	-	-	Self-Supplied Domestic	448363	3164514	UFUZ	-1,591.0
-	-	-	Self-Supplied Domestic	448554	3164323	UFUZ	-1,591.0
-	-	-	Self-Supplied Domestic	448363	3164133	UFUZ	-1,591.0
-	-	-	Self-Supplied Domestic	448554	3164133	UFUZ	-1,591.0

Table 4.1
Manning's Coefficient Values for Different Land-Use Types

Lucode	Description	Manning's n*	Note
1009	Urban and Built-Up	0.027	Short Grass, Few Weeds
1100	Residential, Low Density Less Than Two Dwelling Units Per Acre	0.027	Short Grass, Few Weeds
1110	Residential, Low Density Less Than Two Dwelling Units Per Acre	0.027	Short Grass, Few Weeds
1130	Residential, Low Density Less Than Two Dwelling Units Per Acre	0.027	Short Grass, Few Weeds
1200	Residential, Med. Density Two and Five Dwelling Units Per Acre	0.027	Short Grass, Few Weeds
1210	Residential, Med. Density Two and Five Dwelling Units Per Acre	0.027	Short Grass, Few Weeds
1290	Residential, Med. Density Two and Five Dwelling Units Per Acre	0.027	Short Grass, Few Weeds
1300	Residential, High Density	0.027	Short Grass, Few Weeds
1310	Residential, High Density	0.027	Short Grass, Few Weeds
1330	Residential, High Density	0.027	Short Grass, Few Weeds
1340	Residential, High Density	0.027	Short Grass, Few Weeds
1400	Commercial and Services. Condominiums and Motels Combined	0.013	Concrete, Trowel Finish
1410	Commercial and Services. Condominiums and Motels Combined	0.013	Concrete, Trowel Finish
1411	Commercial and Services. Condominiums and Motels Combined	0.013	Concrete, Trowel Finish
1423	Commercial and Services. Condominiums and Motels Combined	0.013	Concrete, Trowel Finish
1430	Commercial and Services. Condominiums and Motels Combined	0.013	Concrete, Trowel Finish
1460	Oil and Gas Storage: Except Those Areas Associated With Industrial Use Or Manufacturing	0.013	Concrete, Trowel Finish
1470	Oil and Gas Storage: Except Those Areas Associated With Industrial Use Or Manufacturing	0.013	Concrete, Trowel Finish
1480	Cemeteries	0.03	Pasture, No Brush, Short Grass
1510	Food Processing	0.013	Concrete, Trowel Finish
1520	Timber Processing.	0.013	Concrete, Trowel Finish
1550	Other Light Industry	0.013	Concrete, Trowel Finish
1560	Other Heavy Industrial	0.013	Concrete, Trowel Finish
1562	Prestressed Concrete Plants	0.013	Concrete, Trowel Finish
1600	Extractive	0.03	Earth Bottom And Rubble Sides
1611	Clays	0.03	Earth Bottom And Rubble Sides
1620	Sand and Gravel Pits	0.03	Earth Bottom And Rubble Sides
1630	Rock Quarries	0.035	Rock Cuts, Smooth And Uniform
1650	Reclaimed Lands	0.03	Excavated Or Dredged Earth. Grass And Some Weeds
1670	Abandoned Lands	0.03	Pasture, No Brush, Short Grass
1700	Institutional	0.013	Concrete, Trowel Finish
1710	Institutional	0.013	Concrete, Trowel Finish
1720	Institutional	0.013	Concrete, Trowel Finish

Table 4.1 (continued)
Manning's Coefficient Values for Different Land-Use Types

Lucode	Description	Manning's n*	Note
1730	Military	0.013	Concrete, Trowel Finish
1740	Military	0.013	Concrete, Trowel Finish
1750	Governmental	0.013	Concrete, Trowel Finish
1800	Recreational	0.013	Concrete, Trowel Finish
1820	Golf Course	0.03	Pasture, No Brush, Short Grass
1830	Race Tracks	0.013	Asphalt, Smooth
1840	Marinas and Fish Camps	0.07	Sluggish Reaches, Weedy Deep Pools
1850	Parks and Zoos	0.03	Pasture, No Brush, Short Grass
1860	Parks and Zoos	0.03	Pasture, No Brush, Short Grass
1870	Stadiums: Those Facilities Not Associated With High Schools, Colleges, Or Universities	0.03	Earth, Grass, Some Weeds
1900	Open Land	0.03	Pasture, No Brush, Short Grass
1910	Open Land	0.03	Pasture, No Brush, Short Grass
1920	Inactive Land With Street Pattern But Without Structures	0.03	Pasture, No Brush, Short Grass
1930	Inactive Land With Street Pattern But Without Structures	0.03	Pasture, No Brush, Short Grass
1940	Inactive Land With Street Pattern But Without Structures	0.03	Pasture, No Brush, Short Grass
2110	Improved Pastures	0.03	Pasture, No Brush, Short Grass
2120	Unimproved Pastures	0.03	Pasture, No Brush, Short Grass
2130	Woodland Pastures	0.03	Pasture, No Brush, Short Grass
2140	Row Crops	0.035	Mature Row
2150	Field Crops	0.04	Mature Field
2160	Mixed Crops: Used If Crop Type Cannot Be Determined	0.0375	Average Of Row, Field
2200	Tree Crops	0.15	Dense Willows, Summer, Straight
2210	Citrus Groves	0.15	Dense Willows, Summer, Straight
2240	Abandoned Tree Crops	0.06	Cleared Land With Tree Stumps, Heavy Growth Of Sprouts
2310	Cattle Feeding Operations	0.03	Pasture, No Brush, Short Grass
2320	Poultry Feeding Operations	0.03	Pasture, No Brush, Short Grass
2400	Nurseries and Vineyards	0.03	Pasture, No Brush, Short Grass
2410	Tree Nurseries	0.03	Pasture, No Brush, Short Grass
2430	Ornamentals	0.03	Pasture, No Brush, Short Grass
2450	Floriculture	0.03	Pasture, No Brush, Short Grass
2500	Specialty Farms	0.03	Pasture, No Brush, Short Grass
2510	Horse Farms	0.03	Pasture, No Brush, Short Grass
2540	Aquaculture	0.07	Sluggish Reaches, Weedy Deep Pools
2610	Fallow Cropland	0.03	Cultivated Areas, No Crop
3100	Herbaceous	0.07	Medium and Dense Brush, In Winter
3200	Shrub and Brushland	0.07	Medium and Dense Brush, In Winter
3210	Shrub and Brushland	0.07	Medium and Dense Brush, In Winter
3290	Shrub and Brushland	0.07	Medium and Dense Brush, In Winter
3300	Mixed Rangeland	0.07	Medium and Dense Brush, In Winter
4110	Pine Flatwoods	0.15	Dense Willows, Summer, Straight
4120	Longleaf Pine Xeric Oak	0.15	Dense Willows, Summer, Straight
4130	Sand Pine	0.15	Dense Willows, Summer, Straight
4140	Sand Pine	0.15	Dense Willows, Summer, Straight
4200	Upland Hardwood Forest (4200 4399)	0.15	Dense Willows, Summer, Straight
4210	Xeric Oak	0.15	Dense Willows, Summer, Straight

Table 4.1 (continued)
Manning's Coefficient Values for Different Land-Use Types

Lucode	Description	Manning's n*	Note
4250	Xeric Oak	0.15	Dense Willows, Summer, Straight
4270	Xeric Oak	0.15	Dense Willows, Summer, Straight
4340	Upland Mixed Coniferous/Hardwood	0.15	Dense Willows, Summer, Straight
4380	Australian Pine	0.15	Dense Willows, Summer, Straight
4410	Coniferous Pine	0.15	Dense Willows, Summer, Straight
4430	Forest Regeneration	0.15	Dense Willows, Summer, Straight
5100	Streams and Waterways	0.045	Streams With Some Weeds And Stones And Rifts
5200	Lakes	0.045	Streams With Some Weeds And Stones And Rifts
5210	Lakes	0.045	Streams With Some Weeds And Stones And Rifts
5220	Lakes	0.045	Streams With Some Weeds And Stones And Rifts
5230	Lakes	0.045	Streams With Some Weeds And Stones And Rifts
5240	Lakes	0.045	Streams With Some Weeds And Stones And Rifts
5300	Reservoirs	0.03	Clean. Straight, Full Stage, No Rifts Or Deep Pools
5330	Reservoirs	0.03	Clean. Straight, Full Stage, No Rifts Or Deep Pools
5340	Reservoirs Less Than 10 Acres (4 Hectares) Which Are Dominant Features	0.03	Clean. Straight, Full Stage, No Rifts Or Deep Pools
5600	Slough Waters	0.07	Sluggish Reaches, Weedy Deep Pools
6110	Bay Swamps	0.07	Sluggish Reaches, Weedy Deep Pools
6150	River/Lake Swamp (Bottomland)	0.07	Sluggish Reaches, Weedy Deep Pools
6170	Mixed Wetland Hardwoods	0.1	Sluggish Reaches, Weedy Deep Pools With Heavy Stand Of Timber And Underbrush
6172	Mixed Wetland Hardwoods	0.1	Sluggish Reaches, Weedy Deep Pools With Heavy Stand Of Timber And Underbrush
6200	Wetland Coniferous Forest	0.1	Sluggish Reaches, Weedy Deep Pools With Heavy Stand Of Timber And Underbrush
6210	Cypress	0.1	Sluggish Reaches, Weedy Deep Pools With Heavy Stand Of Timber And Underbrush
6220	Forested Depressional Pine	0.1	Sluggish Reaches, Weedy Deep Pools With Heavy Stand Of Timber And Underbrush
6240	Forested Depressional Pine	0.1	Sluggish Reaches, Weedy Deep Pools With Heavy Stand Of Timber And Underbrush
6300	Wetland Forested Mixed	0.1	Sluggish Reaches, Weedy Deep Pools With Heavy Stand Of Timber And Underbrush
6410	Freshwater Marshes	0.1	Sluggish Reaches, Weedy Deep Pools With Heavy Stand Of Timber And Underbrush

Table 4.1 (continued)
Manning's Coefficient Values for Different Land-Use Types

Lucode	Description	Manning's n*	Note
6430	Wet Prairies	0.035	Pasture, No Brush, High Grass
6439	Wet Prairies	0.035	Pasture, No Brush, High Grass
6440	Emergent Aquatic Vegetation	0.05	Scattered Brush Heavy Weeds
6460	Mixed Scrub Shrub Wetland	0.07	Sluggish Reaches, Weedy Deep Pools
7200	Sand Other Than Beaches	0.04	Bottom, Gravels, Cobbles And A Few Boulders
7400	Disturbed Land	0.03	Pasture, No Brush, Short Grass
7410	Rural Land In Transition Without Positive Indicators Of Intended Activity	0.03	Pasture, No Brush, Short Grass
7420	Borrow Areas	0.03	Pasture, No Brush, Short Grass
7430	Spoil Areas	0.03	Pasture, No Brush, Short Grass
8110	Airports	0.013	Asphalt, Smooth
8120	Railroads	0.013	Asphalt, Smooth
8140	Roads and Highways	0.013	Asphalt, Smooth
8160	Canals and Locks	0.013	Concrete, Trowel Finish
8180	Auto Parking Facilities When Not Directly Related and Other Land Uses	0.013	Asphalt, Smooth
8191	Highways	0.013	Asphalt, Smooth
8200	Communications	0.013	Concrete, Trowel Finish
8210	Communications	0.013	Concrete, Trowel Finish
8220	Communications	0.013	Concrete, Trowel Finish
8310	Electrical Power Facilities	0.013	Concrete, Trowel Finish
8320	Electrical Power Transmission Lines	0.013	Concrete, Trowel Finish
8330	Water Supply Plants	0.013	Concrete, Trowel Finish
8340	Sewage Treatment Plants	0.013	Concrete, Trowel Finish
8350	Solid Waste Disposal	0.013	Concrete, Trowel Finish

* Manning's roughness values were obtained from following reference:
Chow, V.T ., Open Channel Hydraulics, McGraw Hill Book Company (1959)
Note: The Manning's coefficient values in the calibrated model are 7.9e-6 times the values in the above table, to convert from SI units of $s/m^{1/3}$ to model units of $d/ft^{1/3}$.
Note: The land-use codes are generally classified as follows:

1000-1999 Urban and Built Up
2000-2999 Agricultural
3000-3999 Rangeland
4000-4999 Upland Forests
5000-5999 Water
6000-6999 Wetlands
7000-7999 Barren land
8000-8999 Transportation, Communication and Utilities
9999 Unmapped

Table 4.2
Average 1995 Surface-Water Elevations within the WOSC-ISGM Study Area

Site Name	Model Segment	Average 1995 Observed Surface Water Elevation (feet)	Comments
Greenwood Lake	935	40.43	
Lake Bingham	904	41.63	
Lake Myrtle East	989	49.15	
Lake Ruth	1190	60.44	
Boat Lake	906	51.39	
West Lake	1216	59.71	
Lake Searcy	1192	69.31	
East Lake	916	59.01	
Rock Lake	1188	80.89	
Lake Winsor	1220	82.09	
Lake Talmo	1208	55.02	
Lake Irene	944	59.44	
Lake Wildmere	1219	59.28	
Lake Hodge	942	53.21	
Fairy Lake	922	53.74	
Island Lake Heathrow	946	81.63	
Lake Kathryn	949	50.50	approximation based on 1994 and 1997 (1995 and 1996 observations not available)
Lake Griffin	936	75.75	
Trout Lake	1211	79.18	
Lake Ellen	918	68.03	
Lake Lotus	967	57.37	
Lake Concord	909	58.20	
Secret Lake	1193	51.14	
Triplet	1209	51.24	
Lost Lake	966	51.47	
Lake Yvonne	1222	54.16	
Queens Mirror Lake	1183	51.24	
Crystal Bowl Lake	912	61.42	
Prairie Lake	1181	86.89	
Cranes Roost	1654	47.89	
Lake Orienta	1655	61.94	
Spring Lake	1207	64.29	
Lake Brantley	1623	45.98	observations for 1995 not available - values for 1993 used
Mirror Lake	987	60.92	
Bear Lake	903	104.76	
Cub Lake	913	101.20	
Little Bear Lake	953	103.81	
Cortez	1626	59.13	observations for 1995 not available - values for 1994 used

Table 4.2 (Continued)
Surface-Water Elevations within the WOSC-ISGM Study Area

Site Name	Model Segment	Average 1995 Observed Surface Water Elevation (feet)	Comments
Blue	1628	79.70	observations for 1995 not available - values for 1994 used
Page	1631	79.7	observations for 1995 not available - values for 1994 used
Pleasant	1622	72.56	observations for 1995 not available - values for 1994 used
Jewel	1639	67.65	observations for 1995 not available - values for 1994 used
Rutherford	1642	60.64	observations for 1995 not available - values for 1994 used
Bosse	907	60.16	
Gandy	925	72.36	
Lockhart	965	72.53	
Big Fairview	921	87.81	
Little Fairview	954	89.25	
Silver	1195	91.98	
Mitchell	1646	59.43	observations for 1995 not available - values for 1994 used
Alpharetta	1613	62.28	
Long	1636	71.57	
Trout	1610	60.71	
Sparling	1206	62.17	observations for 1995 not available - values for 1994 used
Crooked	911	70.48	
Horseshoe	943	69.96	
Prairie	1616	75.61	approximate based on 1994 and 1996 (1995 observations not available
Stanley	1617	78.41	observations for 1995 not available - values for 1994 used
Lucy	1618	70.12	
Florence	1619	70.74	observations for 1995 not available - values for 1994 used
Johio	1621	114.45	observations for 1995 not available - values for 1994 used
Starke	1648	100.15	observations for 1995 not available - values for 1994 used
Olympia	1660	97.65	observations for 1995 not available - values for 1994 used
Lawne	950	87.55	
Sherwood	973	77.74	
Olivia	957	93.77	observations for 1995 not available - values for 1994 used
Rose	971	81.87	
Steer	1198	82.16	approximation based on 1994 and 1996 (1995 observations not available)
Miami	1521	4.50	Springs_Cropped.SHP
Wekiva	1538	68.90	Springs_Cropped.SHP
Starbuck	1000	14.60	Springs_Cropped.SHP

Table 4.2 (Continued)
Surface-Water Elevations within the WOSC-ISGM Study Area

Site Name	Model Segment	Average 1995 Observed Surface Water Elevation (feet)	Comments
Palm	1002	8.50	Springs_Cropped.SHP
Sanlando	1005	19.10	Springs_Cropped.SHP

Table 5.1
Hydraulic Conductivity and van Genuchten Parameter Values for Different Soil Types

SCS Hydrologic Soil Group	SCS Texture Classification	Hydraulic Conductivity [1,4] (ft/d)	van Genuchten Alpha Parameter[1,2] (1/ft)	van Genuchten Beta Parameter [1,2]	van Genuchten Residual Saturation[1,2,5]	Porosity[1]
A	Sandy loam	4.42	2.25	1.89	0.158	0.41
B	Loam	1.04	1.08	1.56	0.181	0.43
C	Sandy clay loam	1.31	1.77	1.48	0.256	0.39
D	Silt loam	0.45	0.6	1.41	0.149	0.45
Rest (urban, pond)	Loam	2[3]	1.08	1.56	0.181	0.43

[1] Mean values from Carsel and Parrish, 1988
[2] van Genuchten, 1980
[3] Average K value used for soils under urban development and ponds
[4] The Hydraulic Conductivity values for the calibrated model are 10 times the values shown in the above table.
[5] The van Genuchten Residual Saturation values for the calibrated model are 0.63 times the values shown in the above table.

Table 6.1
Groundwater Model Mass Balance Components, Heads and Residual Statistics for Model Development Simulations

		Base Case [2]	2500 ft Grid			1250 ft Grid		625 ft Grid
		ECF Regional Model	MODFLOW Option	MODHMS Option	Updated Data	Coarse Boundary	Refined Boundary	Refined Boundary
	Column Number	1	2	3	4	5	6	7
Maximum Head Error[1]								
	SAS	-	1	0	10	10	0	2
	UFA-UZ	-	2	0	1	<1	0	<1
	UFA-DZ	-	2	0	1	<1	0	0
	LFA	-	<1	0	0	0	0	0
Mass Balance								
Inflow:	Well	705,352	705,288	705,288	703,911	720,816	894,096	901,884
		24,651,973	23,313,409	23,399,658	17,495,096	26,042,076	25,497,124	34,542,144
		15,349	14,579	14,940	6,151	4,538	4,770	11,294
	Recharge	18,708,918	18,718,709	18,718,709	19,899,245	19,899,245	21,061,552	21,889,542
	Total	44,081,592	42,751,985	42,838,595	38,104,403	46,666,675	47,457,543	57,344,865
Outflow:								
	Well	6,965,165	6,972,738	6,972,738	6,921,240	6,938,145	6,994,085	7,395,147
	Constant Head [3]	20,480,765	24,095,670	24,205,532	15,635,012	25,107,235	25,458,282	35,107,216
		36,392	37,311	42,288	69,306	95,084	94,338	127,625
	River	1,359,034	1,381,722	1,405,232	2,581,557	2,088,776	2,244,135	2,166,318
	Drain	4,143,753	4,230,397	4,234,516	6,119,277	5,600,941	5,500,683	5,192,185
	Evapotranspiration	5,818,766	6,034,150	5,978,289	6,778,010	6,836,494	7,166,018	7,356,372
	Total	38,803,875	42,751,990	42,838,598	38,104,403	46,666,676	47,457,543	57,344,866
Head Residuals								
	Average	1.8972	-1.2878	1.3182	1.1607	0.8309	0.6954	0.929
	RMS	3.4311	3.168	3.1824	4.6572	4.4325	4.5267	4.38
	Absolute Maximum Error	8.127	7.94	8.11	13.5	11.68	11.78	11.8

Table 6.1 (Continued)
Groundwater Model Mass Balance Components, Heads and Residual Statistics for Model Development Simulations

	5 Layer Model Uniform Upper SAS Conductivity	5 Layer Model Variable Upper SAS Conductivity	Finer Upper SAS Vertical Discretization	Unsaturated SAS Simulation	Calibrated Upper SAS
Column Number	8	9	10	11	12
Maximum Head Error[1]					
SAS[5]	5(U)/2(L)	10(U)/5(L)	5(U)/1(L)	0(U)/0(L)	0(U)/0(L)
UFA-UZ	0	2	<1	0	0
UFA-DZ	0	2	0	0	0
LFA	0	0	0	0	0
Mass Balance					
Well	901,884	901,884	901,884	901,884	901,884
	34,665,021	35,162,296	35,112,570	34,974,989	33,932,744
	10,009	10,087	129,568	124,834	142,517
Recharge	21,889,542	21,889,543	23,549,521	23,549,521	23,549,521
Total	57,466,457	57,963,810	59,693,543	59,551,228	58,526,666
Outflow:					
Well	7,395,147	7,395,147	7,395,148	7,395,148	7,395,148
Constant Head [3]	36,201,299	36,706,349	38,840,045	38,711,845	37,873,500
	132,627	143,753	72,966	79,576	50,680
River	1,226,323	1,121,650	1,305,796	1,287,238	1,135,146
Drain	5,213,219	5,216,497	5,234,469	5,235,283	5,238,369
Evapotranspiration	7,297,839	7,380,413	6,845,167	6,842,290	6,833,900
Total	57,466,457	57,963,810	59,693,592	59,551,381	58,526,744
Head Residuals					
Average	0.1869	-0.2003	0.4065	0.3964	0.9966
RMS	4.3876	4.903	4.2888	4.1958	3.4277
Absolute Maximum Error	12.73	14.864	9.762	9.573	8.261

[1] Maximum Head Error is based on visual inspection of the head contours and is compared to previous run (previous column on this sheet). For example results for 2500ft grid are compared to the Base Case.
[2] Values in Mass Balance differ slightly from local (smaller) model because polyline marked to digitize area of interest in GW Vistas is approximate.
[3] Constant Head in Base Case (regional model) is the sum of Xmin, Xmax, Ymin, and Ymax as given by GW Vistas when the regional model is digitized right along the Local Boundary. In all other cases Constant Head represents the mass-balance across all lateral boundaries of the local model.
[4] Inflow and outflow for Ponds is obtained by digitizing area just around two locations with Constant Heads that are present in the SAS.
[5] The SAS is divided into an upper more conductive unit (U) and a Lower less conductive unit (L) for simulations including and after Column 8.
Note: Head values are in feet; flux values are in ft^3/day

Table 6.2
Flux Components in the SAS of WOSC-ISGM Development Simulations

Surficial Aquifer System	2500 ft Grid		1250 ft grid		625 ft Grid	5 Layer Model Uniform Upper SAS Conductivity	5 Layer Model Variable Upper SAS Conductivity	Finer Upper SAS Vertical Discretization	d SAS Simulation	Calibrated Upper SAS
	MODHMS Option	Updated Data	Coarse Boundary	Refined Boundary	Refined Boundary					
Column Number	1	2	3	4	5	6	7	8	9	10
Inflow:						**For Layers 1 and 2**		**For Layers 1 to 4**		
Bottom	841,718	1,458,551	1,094,283	1,152,717	1,124,266	425,179	377,538	608,235	602,853	577,753
Constant Head	3,792,798	774,872	1,211,981	1,020,539	1,126,102	1,777,397	2,411,825	2,854,909	2,695,763	1,513,035
Recharge	18,718,709	19,899,245	19,899,245	21,061,551	21,889,542	21,889,542	21,889,542	23,549,521	23,549,521	23,549,521
Total	23,353,225	22,132,668	22,205,509	23,234,809	24,139,910	24,092,118	24,678,905	27,012,665	26,848,137	25,640,309
Outflow:										
	15,764,481	12,552,622	12,844,803	13,499,459	14,035,466	14,949,877	15,368,056	16,545,208	16,485,990	15,931,669
Constant Head	510,905	522,434	739,097	666,781	930,854	971,325	1,162,144	2,670,094	2,586,244	2,093,239
River	1,099,549	2,279,601	1,785,115	1,902,550	1,817,218	873,077	768,293	952,198	933,616	781,502
Evapotranspiration	5,978,289	6,778,010	6,836,493	7,166,018	7,356,372	7,297,840	7,380,413	6,845,167	6,842,290	6,833,900
Total	23,353,226	22,132,668	22,205,510	23,234,810	24,139,911	24,092,119	24,678,906	27,012,667	26,848,139	25,640,311
Head Residuals:										
Average	1.35	0.80	-0.29	-0.16	0.61	-1.49	-2.64	-0.63	-0.67	1.17
RMS	3.3224	6.9799	6.4171	6.4186	6.1279	6.1555	7.2797	5.9837	5.7729	3.8618
Absolute Maximum Error	8.11	13.51	11.68	11.78	11.81	12.73	14.86	9.76	9.57	8.26

Note: Flux values are in ft^3/day

Table 6.3
Parameters Used Uniformly for ET Conceptualization of the WOSC-ISGM

Model Layer	Evaporation Distribution Function[1]	Root Zone Distribution Function[1]	Parameter for Evapotranspiration		
			C1[2]	C2[2]	C3 (ft/day)[3]
1	0.4	0.6	0.3	0.2	0.05
2	0.3	0.3	0.3	0.2	0.05
3	0.1	0.07	0.3	0.2	0.05

[1] Values are within the range of values and have been calibrated to fit the model conceptualization. Note that these are further tuned during final calibration.
[2] Values suggested by Kristensen and Jensen (1975).
[3] Value selected such that $C3/E_p$ is within the range of values suggested by Kristensen and Jensen (1975).

Table 6.4
Total Hydrologic Cycle Mass Balance Components, Heads and Residual Statistics for Model Development Simulations

Row #			Regional Model[2]	5 Layer Model Uniform Upper SAS	Unsaturated with Adjusted Upper SAS	With Physically-based ET	With Surface Water Flow
1	**Maximum Head Error[1]**						
	(visual inspection)	Model Layer 3 (SAS)	-	-	0	0-10 (lower for peaks only)	0-10 ft (higher generally but lower for peaks)
3		Model Layer 4 (SAS)	-	-	0	0-10 (lower for peaks only)	0-10 ft (higher generally but lower for peaks)
4		Model Layer 5 (UFUZ)	-	-	0	0	0-5 ft higher
5		Model Layer 6 (UFDZ)	-	-	0	0	0-5 ft higher
6		Model Layer 7 (LFA)	-	-	0	0	0
7	**Total Mass Balance**						
	Inflow:	Well	705,352	901,884	901,884	901,884	481,526 [9,10]
9		Constant Head GW	24,651,973	34,665,021	33,932,744	34,734,205	65,204,644
10		Constant Head Ponds [2]	15,349	10,009	142,517	34,686	- [7]
11		Precipitation (A)	56,972,743	56,987,618	56,987,618	56,987,618	56,892,391
12		Other recharge components (B1)		4,253,825	4,253,825	4,253,825	4,253,825
13		Septic & Ribs (B2)		481,526	481,526	481,526	- [9]
14		Net recharge (A) + (B)		61,722,970	61,722,970	61,722,970	61,146,216
15							
	Outflow:						
		Well	6,965,165	7,395,147	7,395,148	7,395,148	7,395,148
18		Constant Head GW	20,480,765	36,201,299	37,873,500	36,925,207	35,904,364
19		Constant Head Ponds [2]	36,392	132,627	50,680	122,056	- [7]
20		River	1,359,034	1,226,323	1,135,146	1,251,833	-
21		Drain	4,143,753	5,213,219	5,238,369	5,266,867	-
22		Groundwater Evapotranspiration	5,818,766	7,297,839	6,833,900	- [4]	- [4]
23		Et unsat	32,570,622	32,570,622	32,570,622	- [4]	- [4]
24		Total actual ET	38,389,388	39,868,461	39,404,522	41,164,972	38,660,728

Table 6.4 (Continued)
Total Hydrologic Cycle Mass Balance Components, Heads and Residual Statistics for Model Development Simulations

Row #			Base Case ECF Regional Model[2]	5 Layer Model Uniform Upper SAS	Unsaturated with Adjusted Upper SAS	With Physically-based ET	With Surface Water Flow
27	**Internal or other balance components**						
		Potential Evapotranspiration	50,190,853	50,190,853	50,190,853	50,188,544 [5]	50,188,544 [5]
30		GW Recharge	18,708,918	21,889,542	23,549,521	-	
31		Infiltration into subsurface	51,279,540	54,460,164	56,120,143	56,120,143	48,137,396
32							
		Overland runoff	5,962,294	5,962,294	5,962,294	5,962,294	8,163,776 [8]
35	**Head Residuals**						
36		Average	1.8972	0.1869	0.9966	1.8117	1.11
37		RMS	3.4311	4.3876	3.4277	4.4748	3.1742
38		Absolute Maximum Error	8.127	12.73	8.261	13.815	14.37

1 Maximum Head Error is based on visual inspection of the head contours and is compared to previous run (previous column on this sheet).
2 Inflow and outflow for Ponds is obtained by digitizing area just around two locations with Constant Heads that are present in Layer 1.
3 Evapotranspiration as used in ECF model (McGurk & Presley, "Simulation of the Effects of Groundwater Withdrawals on the Floridan Aquifer System in East-Central Florida: Model expansion and revision", Technical Publication SJ2002-03, St. Johns River Water Management District, Palatka, FL, 196 pages.).
4 Simulation computes total ET as a comprehensive water budget.
5 Roundoff error due to the use of multiplication factor of 2.283e-4 (in/yr -> ft/day).
6 Precipitation lesser because of new constant head cells in OLF (model row 38-40 and col 140-145). Recharge on constant head cells is not accounted in mass balance calculations.
7 Ponds are no longer provided as constant head boundary conditions.
8 Calculated as net inflow to the CHF domain from the overland surface.
9 Septic and Ribs contribution modeled as wells injecting in layer 2. In the earlier runs Septic and Ribs were a part of recharge.
10 Drainage wells removed from well file as CHF package has links to groundwater.
Note: Head values are in feet; flux values are in ft^3/day

Table 6.5
Calibration Parameters and Plausible Range of Values

Parameter	Expected Value	Low Value	High Value
ICU Leakance	Anywhere within range	2×10^{-5} / day	2×10^{-3} / day
Evaporation Distribution Function – Top Layer	Closer to unity	0	1
Evaporation Distribution Function – Lower Layers	Closer to zero	0	1
Root Zone Distribution Function – Top Layer	Closer to unity	0	1
Root Zone Distribution Function – Lower Layers	Closer to zero	0	1
Field Capacity / Wilting Point Saturations	Anywhere within range	0.29 / 0.1	0.54 / 0.32
Vertical Leakance of Lake or Pond Bottom, Channel Bed and Pipes	Anywhere within range	0 /day	10^{8} /day
Area of Lake at maximum depth – Also affects areas at lower depths in Depth – Area Relationship	Anywhere within range	10^{3} ft^{2}	10^{8} ft^{2}
Radius of Pipe	Anywhere within range	0.5 ft	8 ft
Field Capacity / Wilting Point Saturations – Used as surrogates for local RDFI and EDFI changes to raise ET levels	Anywhere within range	0.54 / 0.32	0.65 / 0.95
Leakance of Overland Flow Surface	Anywhere within range	0	10^{8} /day

Table 7.1
Groundwater Head Residuals for the Steady-State WOSC-ISGM Representing Average 1995 Conditions

Observation #	Site Name	Layer	Row	Column	Observed Head (Feet)	Simulated Head (Feet)	Residual (Obs-Sim)
1	Long Lake	3	94	55	70.02	68.33	1.6879
2	Lake Meadow	3	106	26	75.5	77.60	-2.09842
3	Lake Hiawassee	3	147	46	77.15	80.44	-3.29223
4	Lake Orlando	3	107	71	83.2	83.77	-0.56846
5	Starke Lake	3	122	18	100.4	100.31	0.0937
6	Bear Lake	3	75	63	104.73	104.78	-0.0463
7	CHARLOTTE STREET - S-1015	3	58	111	78.01	78.43	-0.41822
8	284533081204801	5	14	115	35.01	35.08	-0.06892
9	284440081175901	5	22	139	36.66	34.34	2.31554
10	OR0548 - Wekiva Springs St Park	5	42	54	21.85	24.38	-2.5323
11	284244081234901	5	41	90	37.5	35.23	2.26527
12	284207081174401	5	47	142	35.17	37.30	-2.13209
13	S-0125	5	50	105	44.77	37.72	7.05147
14	CHARLOTTE STREET - S-1017	5	58	111	44.55	40.77	3.77909
15	284012081264601	5	65	64	49.63	45.35	4.27615
16	283920081232501	5	74	93	48.73	45.62	3.10646
17	283654081260801	5	97	70	57.63	54.73	2.89628
18	283417081331401	5	122	9	73.44	70.87	2.56931
19	283326081262101	5	131	68	51.71	57.34	-5.6334
20	283121081311601	5	151	25	72.06	73.75	-1.68845
21	CHARLOTTE STREET - S-1016	6	58	111	47.16	40.70	6.46106
22	283253081283401 – Orlo Vista well	6	136	49	65	64.40	0.59605

Head Residuals	
Average	0.846
RMS	3.188
Absolute Maximum Error	7.05

Table 7.2
Water-Level residuals in Ponds and Lakes for the Steady-State WOSC-ISGM Representing Average 1995 Conditions

Observation #	Name	Model Segment	Observed Head (feet)	Simulated Head (feet)	(Obs-Sim)
101	Greenwood Lake	935	40.43	40.05	0.38
102	Lake Bingham	904	41.63	43.63	-2.00
103	Lake Myrtle East	989	49.15	49.07	0.08
104	Lake Ruth	1190	60.44	58.51	1.93
105	Boat Lake	906	51.39	48.86	2.54
106	West Lake	1216	59.71	58.52	1.19
107	Lake Searcy	1192	69.31	67.46	1.85
108	East Lake	916	59.01	58.28	0.73
109	Rock Lake	1188	80.89	80.28	0.60
110	Lake Winsor	1220	82.09	82.71	-0.61
111	Lake Talmo	1208	55.02	54.49	0.53
112	Lake Irene	944	59.44	56.50	2.93
113	Lake Wildmere	1219	59.28	58.29	0.99
114	Lake Hodge	942	53.21	50.20	3.01
115	Fairy Lake	922	53.74	53.07	0.67
116	Island Lake	946	81.63	80.66	0.96
118	Lake Kathryn	949	50.50	50.35	0.15
119	Lake Griffin	936	75.75	75.77	-0.03
120	Trout Lake	1211	79.18	79.22	-0.04
121	Lake Ellen	918	68.03	67.22	0.81
122	Lake Lotus	967	57.37	56.79	0.58
123	Lake Concord	909	58.20	57.89	0.31
124	Secret Lake	1193	51.14	51.83	-0.69
125	Triplet	1209	51.24	50.72	0.53
126	Lost Lake	966	51.47	50.77	0.70
127	Lake Yvonne	1222	54.16	53.05	1.12
128	Queens Mirror Lake	1183	51.24	50.83	0.41
129	Crystal Bowl Lake	912	61.42	59.14	2.29
131	Prairie Lake	1181	86.89	86.17	0.72
133	Cranes Roost	1654	47.89	46.33	1.55
134	Lake Orienta	1655	61.94	60.42	1.51
135	Spring Lake	1207	64.29	64.06	0.23
136	Lake Brantley	1623	45.98	45.86	0.12
137	Mirror Lake	987	60.92	60.33	0.59
138	Bear Lake	903	104.76	103.84	0.91
139	Cub Lake	913	101.20	100.52	0.68
140	Little Bear Lake	953	103.81	103.84	-0.03
141	Cortez	1626	59.13	60.25	-1.13
145	Blue	1628	79.70	80.33	-0.63
146	Page	1631	79.70	80.13	-0.43
147	Pleasant	1622	72.56	73.62	-1.06
149	Jewel	1639	67.65	63.49	4.16
151	Rutherford	1642	60.64	75.00	-14.37
153	Bosse	907	60.16	60.22	-0.06
155	Gandy	925	72.36	70.39	1.98
156	Lockhart	965	72.53	70.39	2.15
161	Big Fairview	921	87.81	87.63	0.19

Table 7.2 (Continued)
Water-Level residuals in Ponds and Lakes for the Steady-State WOSC-ISGM Representing Average 1995 Conditions

Observation #	Name	Model Segment	Observed Head (feet)	Simulated Head (feet)	Residuals (Obs-Sim)
162	Little Fairview	954	89.25	88.31	0.94
163	Silver	1195	91.98	92.03	-0.05
164	Mitchell	1646	59.43	62.30	-2.87
167	Alpharetta	1613	62.28	59.38	2.90
168	Long	1636	71.57	60.75	10.82
169	Trout	1610	60.71	63.17	-2.47
173	Sparling	1206	62.17	59.00	3.16
174	Crooked	911	70.48	65.88	4.60
175	Horseshoe	943	69.96	67.05	2.91
178	Prairie	1616	75.61	72.99	2.62
179	Stanley	1617	78.41	72.50	5.91
180	Lucy	1618	70.12	69.70	0.43
181	Florence	1619	70.74	69.53	1.21
182	Johio	1621	114.45	103.99	10.46
184	Starke	1648	100.15	100.87	-0.72
185	Olympia	1660	97.65	94.73	2.91
186	Lawne	950	87.55	85.66	1.89
188	Sherwood	973	77.74	72.82	4.92
191	Olivia	957	93.77	93.27	0.50
192	Rose	971	81.87	79.06	2.80
194	Steer	1198	82.16	78.24	3.92

Head Residuals	
Average	1.11
RMS	3.17
Absolute Maximum Error	14.37

Table 7.3
Spring Flux and Surface Water Flow residuals for the Steady-State WOSC-ISGM Representing Average 1995 Conditions

Observation #	Spring Name	Model Segment	Observed Spring Flow (cfs)	Simulated Spring Flow (cfs)	Residual (Obs-Sim)	Percent Error
196	Miami	1521	4.50	4.52	-0.0187	-0.42%
197	Wekiva	1538	68.90	47.40	21.5005	31.2 %
198	Barrel	1497		20.51		
199	Starbuck	1000	14.60	14.67	-0.0735	-0.50%
200	Palm	1002	8.50	8.10	0.4007	4.71%
201	Sanlando	1005	19.10	19.59	-0.4933	-2.58%

Spring Flow Residuals	
Average	4.26
RMS	9.62
Absolute Maximum Error	21.5

Table 7.4
Mass Balance Results for the Steady-State WOSC-ISGM
Representing Average 1995 Conditions

Rates for This Time Step	Total	Overland Flow Surface	Surface Water Bodies	Subsurface
IN:				
Storage	242			242
Constant Head	65,204,700			65,204,700
CHF Storage	87		87	
From CHF To GW			53,771,976	
From GW To CHF				19,577,280
From CHF To OLF			165,618,124	
From OLF To CHF		155,243,758		
Source-Sinks CHF	5,438,016		5,438,016	
Wells	481,526.5			481,526.5
OLF Storage	140	140		
Lake Jessup Prescribed Head	490,093	490,093		
From OLF To GW		24,410,186		
From GW To OLF				72,553,040
OLF Recharge	61,146,216	61,146,216		
Total In	132,760,933.5	241,290,393	224,828,203	157,816,788.5
OUT:				
Storage	367			367
Constant Head	35,904,292			35,904,292
CHF Storage	2,050		2,050	
From CHF To GW			19,577,280	
From GW To CHF				53,771,976
From CHF To OLF			155,243,758	
From OLF To CHF		165,618,124		
CHF Outflow Boundary	64,608,956		64,608,956	
Wells	7,395,148			7,395,148
OLF Storage	165	165		
Lake Jessup Prescribed Head	3,071,732	3,071,732		
From OLF To GW		72,553,040		
From GW To OLF				24,410,186
ET and EVP Flux	38,660,736	Subdivision into individual domains is not available		
Total Out	149,643,281	241,243,061	239,432,044	160,142,705
IN - OUT	-16,882,347.5	47,332	-14,603,841	-2,325,916.5
Percent Discrepancy	-5.98	0.01	-3.14	-0.73

Note: Flow rates are in ft3/day.
Note: CHF represents the surface-water bodies such as lakes, ponds, canals, streams, and rivers.
Note: OLF represents the overland flow plane which facilitates runoff and infiltration.
Note: GW, or lack of specific domain acronym represents the subsurface domain of the simulation.

Table 8.1
Scenarios and Results of Parameter Sensitivity Analyses for the Steady-State WOSC-ISGM Representing Average 1995 Conditions

Sensitivity Parameter	Multiplication factor	Surface Domain					Subsurface Domain				
		Residual (ft)		Total Head (ft)			Residual (ft)		Total Head (ft)		
		Average	RMS	Head	Change (final-base)	Sensitivity Type	Average	RMS	Head	Change (final-base)	Sensitivity Type
Base Case	1	1.1149	3.1743	1,050,705	0		0.8463	3.1886	5,194,945	0	
Overland leakance	0.2	0.6734	2.5877	1,051,220	516	III	0.6703	3.3015	5,176,036	-18,908	III
	5	1.1571	3.5026	1,050,595	-110		1.0467	3.4911	5,200,375	5,430	
Overland Manning's coefficient	0.2	1.0826	3.2697	1,050,674	-31	I	0.8462	3.1790	5,194,778	-167	I
	5	1.1779	2.9304	1,050,741	36		0.8611	3.2095	5,195,086	141	
Channel leakance	0.01	0.6183	3.3557	1,051,473	768	I	-0.3440	2.5933	5,232,879	37,935	III
	100	1.3097	3.2731	1,050,926	221		1.2203	3.6344	5,181,978	-12,967	
Channel roughness coefficient	0.2	1.1052	3.1815	1,050,601	-104	I	0.8490	3.1879	5,194,821	-124	I
	5	1.1083	3.1919	1,050,970	265		0.8416	3.1923	5,195,195	250	
Moisture parameters (WP, FC)	0.5	1.4006	3.4414	1,050,412	-293	III	1.1198	3.4840	5,172,451	-22,494	III
	2	-0.9085	3.6029	1,052,922	2,217		0.1758	3.1858	5,285,586	90,641	
Leaf area index	0.5	1.0918	3.1727	1,050,730	26	I	0.8254	3.1781	5,196,026	1,081	I
	2	1.1409	3.2246	1,050,634	-70		0.8888	3.2178	5,192,742	-2,203	
Van Ganuchten alpha	0.5	1.2836	3.4774	1,050,538	-167	II	1.0751	3.4826	5,169,428	-25,516	III
	2	0.8702	3.0635	1,050,909	204		0.6350	3.2213	5,210,249	15,304	
Brook's number	0.5	0.0531	3.7122	1,051,873	1,169	III	0.2747	3.2833	5,208,394	13,449	III
	2	0.9686	3.0937	1,050,773	68		0.7105	3.1990	5,204,281	9,336	
ICU leakance	0.333	-2.2498	5.3167	1,055,642	4,938	III	-0.1200	4.6620	5,303,521	108,576	III
	3	5.7085	8.0235	1,044,538	-6,167		3.5867	6.0304	5,026,723	-168,222	

Table 9.1
Model Layer Number for Transient Subsurface Observations from 1995 through 1999.

Observation Number	Well Name	Model layer	Aquifer Unit
1	840-120-02 well	5	UFA-UZ
2	Alt Springs Elem Sch	3	SAS
3	bear lake elem.	3	SAS
4	boyles	5	UFA-UZ
5	c.benton inc. well	5	UFA-UZ
6	Charlotte Street	3	SAS
7	Charlotte Street	5	UFA-UZ
8	Charlotte Street	6	UFA-DZ
9	Charlotte Street	7	LFA
10	Crate Mill	3	SAS
11	Crate Mill	5	UFA-UZ
12	ecolog utilities	5	UFA-UZ
13	gilbert principe	5	UFA-UZ
14	Greenwood Lake sch	3	SAS
15	lake orienta elem.	3	SAS
16	longwood elem.	3	SAS
17	mr. neely well	5	UFA-UZ
18	Orlo Vista	6	UFA-DZ
19	rock lake middle	3	SAS
20	Rock Springs St Preserve	3	SAS
21	Rock Springs St Preserve	5	UFA-DZ
22	Rock Springs St Preserve	6	UFA-DZ
23	Rock Springs well (Anderson well)	5	UFA-DZ
24	sabal point elem.	3	SAS
25	sanlando softball_mw3	3	SAS
26	span. trail apts	5	UFA-DZ
27	state foliage I181	5	UFA-DZ
28	tenneco well	3	SAS
29	the forest well	5	UFA-DZ
30	transportation dept	3	SAS
31	USGS Seminole County	5	UFA-DZ
32	wekiva elem.	3	SAS
33	Wekiva State Park	5	UFA-DZ
34	Wekiva State Park	7	LFA
35	woodlands elem.	3	SAS

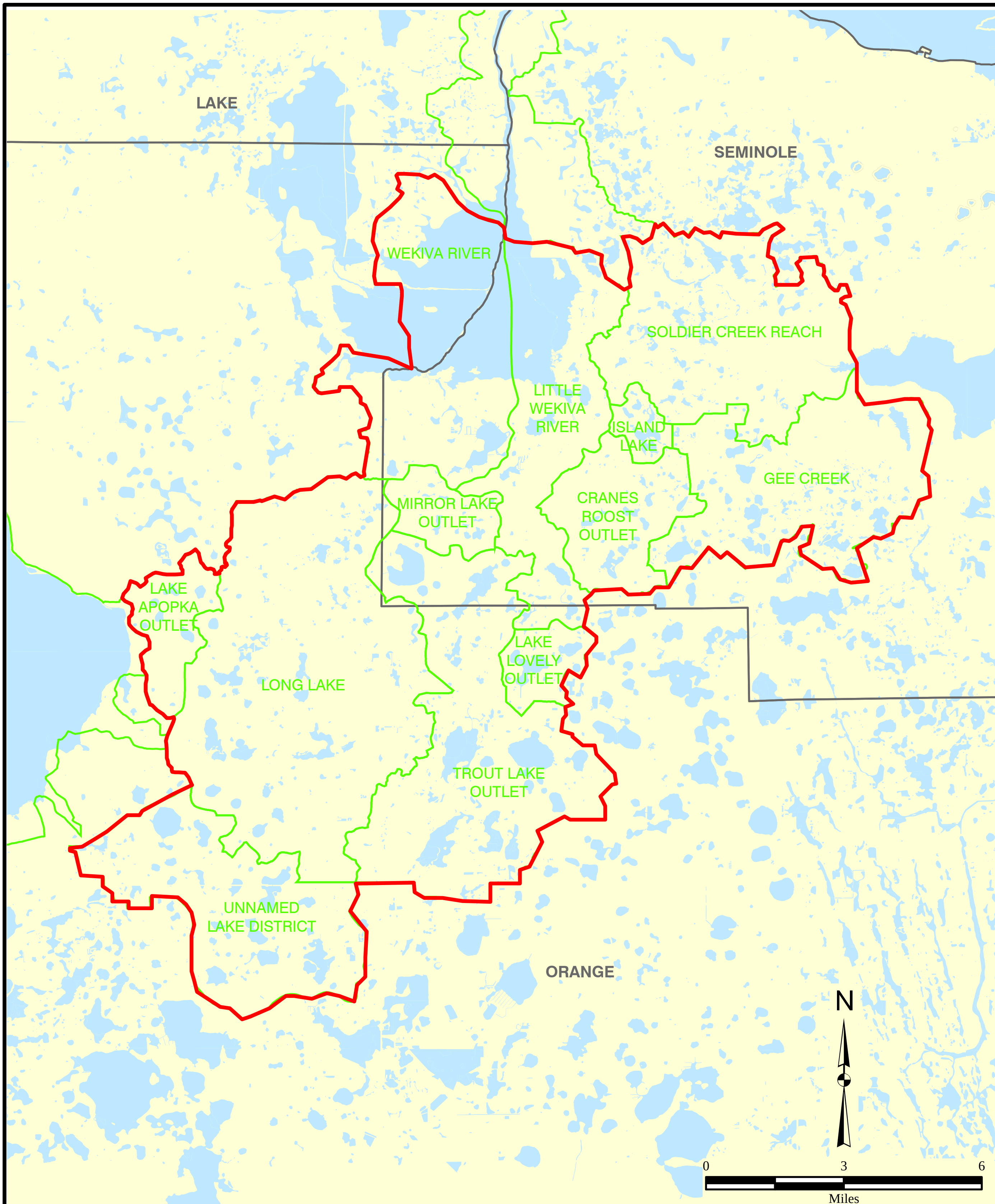

Source:
Filename: X:/SJR017/TO1/Maps/ Conceptual_model_report/Study_region.mxd
Project: SJR017-001-99
Revised: 11/30/04 TB

Legend

- Model Boundary
- Surface Water Basin
- County Boundary
- Surface Water Bodies and Wetlands

Figure 1.1
Study Region and Delineation of the Model Domain

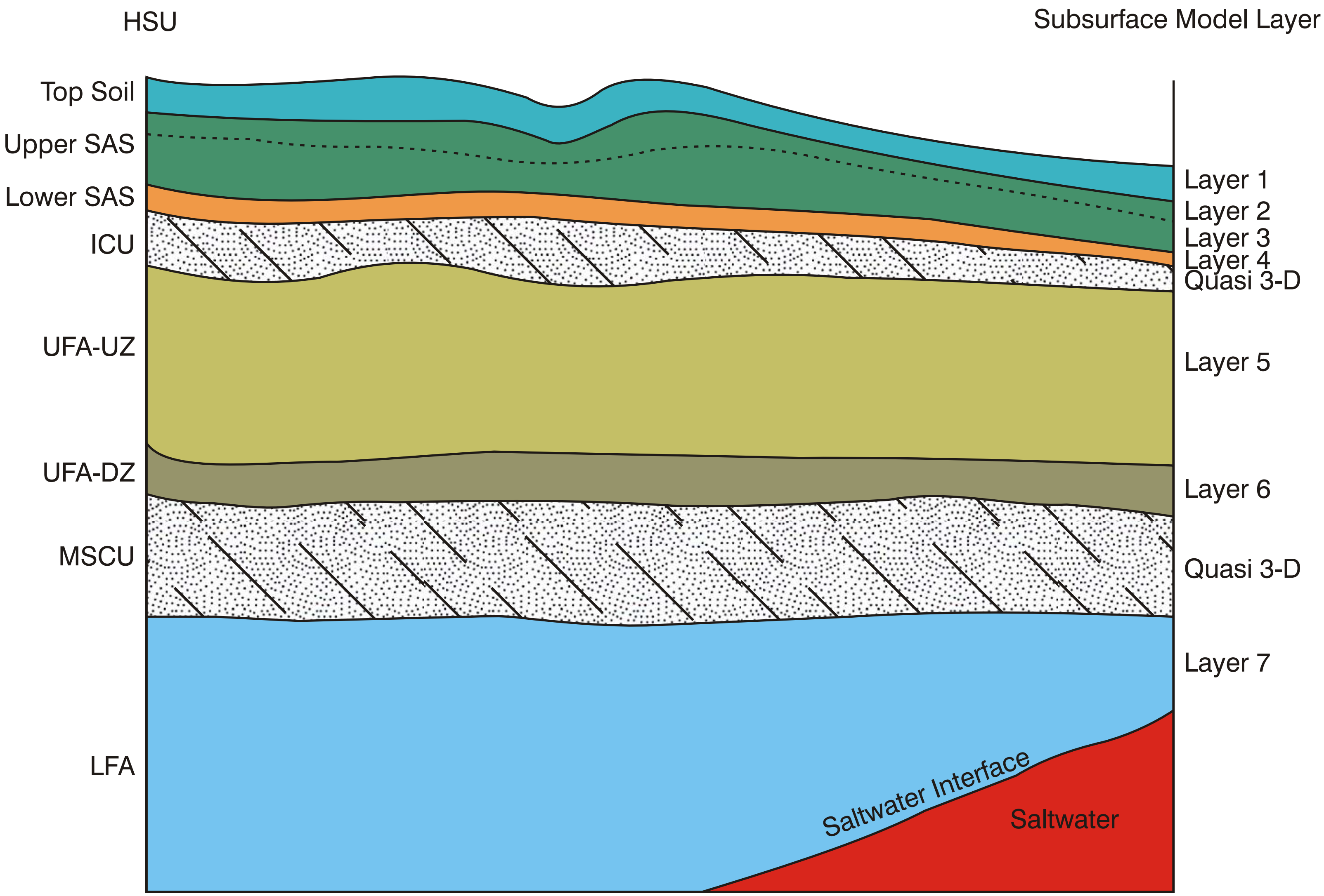

Filename: X:\SJR017\TO1\Maps
\Conceptual_model_report\model_concept.cdr
Project: SJR017-001-06
Revised: 09/09/04 CF
Source: HydroGeoLogic, Inc.

Figure 2.1

Subsurface Model Conceptualization

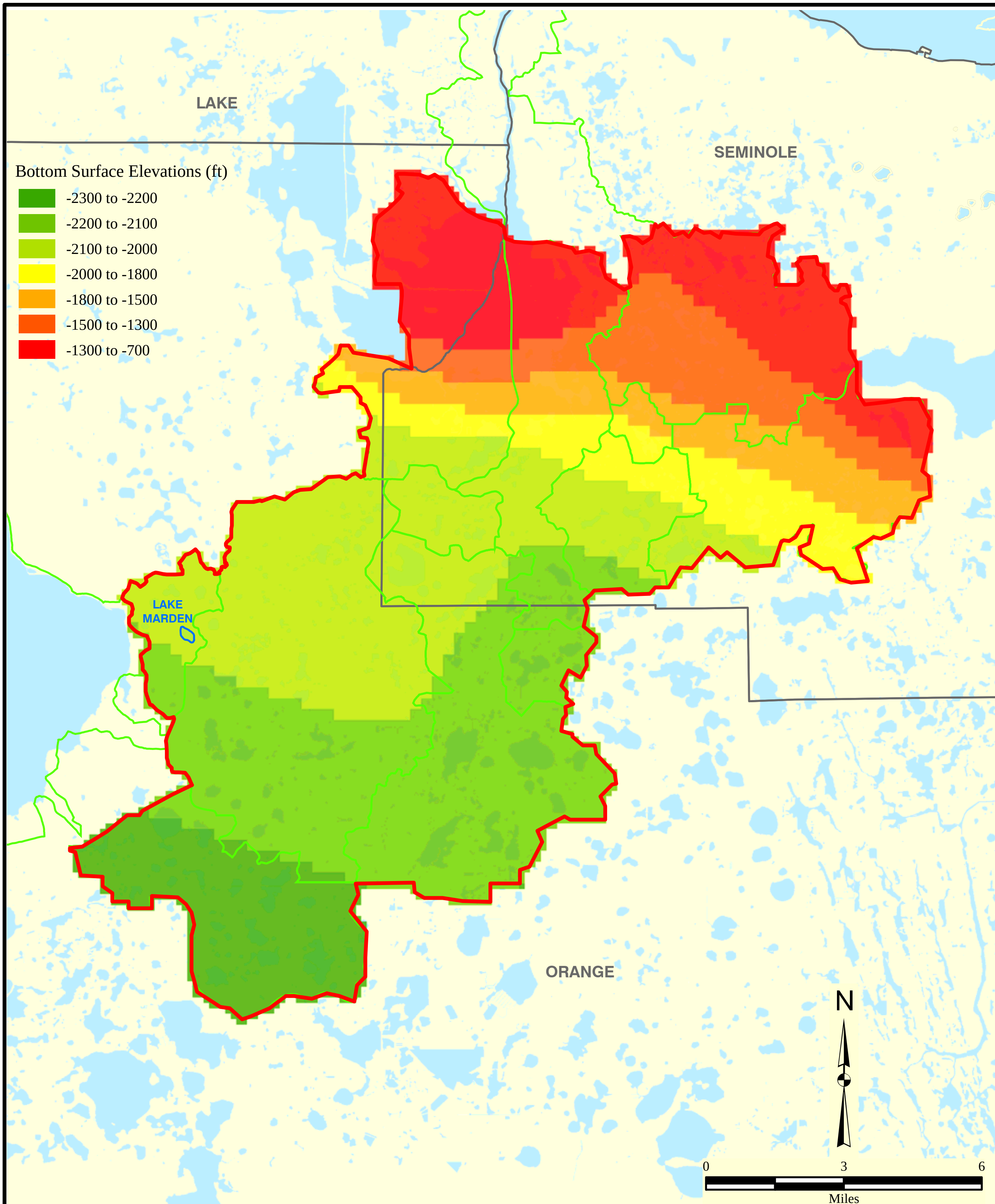

Source:
Filename: X:/SJR017/TO1/Maps/
Conceptual_model_report/BotSurface.mxd
Project: SJR017-001-99
Revised: 11/30/04 TB

Legend

- Model Boundary
- Surface Water Basin
- County Boundary
- Surface Water Bodies and Wetlands

Figure 2.2
Bottom Surface Elevations of the Freshwater Model Domain

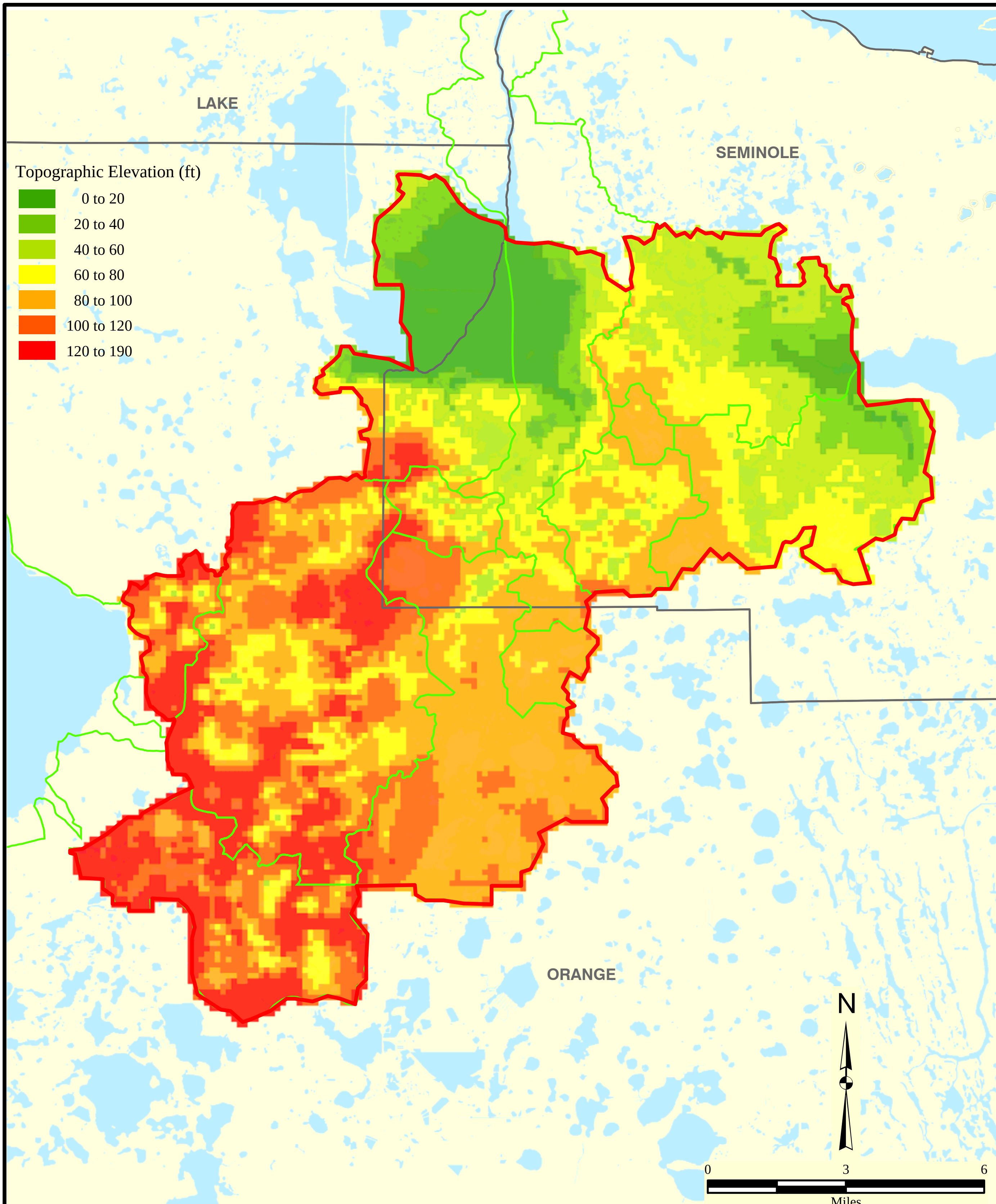

Source:
Filename: X:/SJR017/TO1/Maps/
Conceptual_model_report/TopElev.mxd
Project: SJR017-01-06
Revised: 09/13/04 TB

Legend

Model Boundary
Surface Water Basin
County Boundary
Surface Water Bodies and Wetlands

Figure 2.3
Topographic Elevation of the Study Area

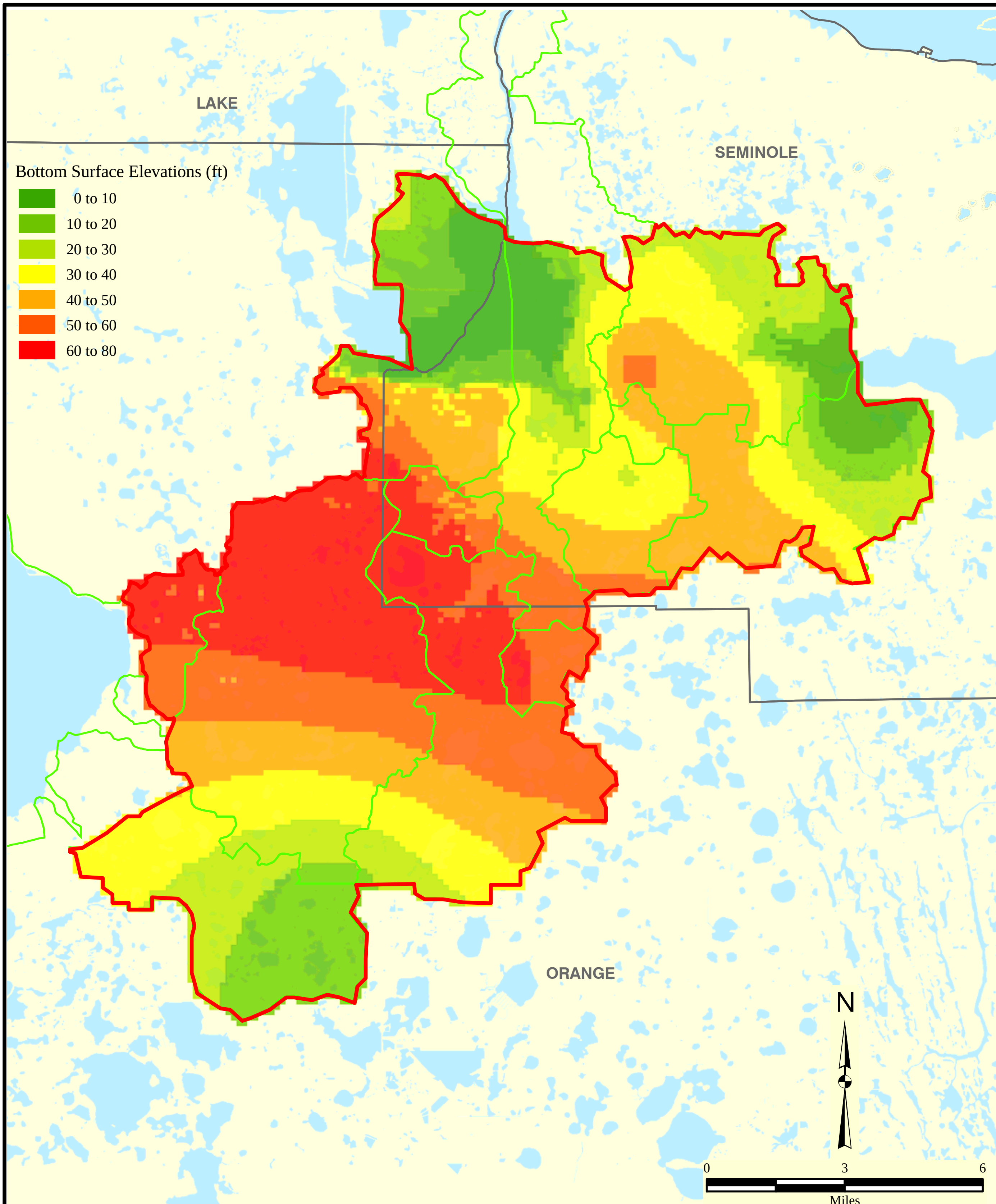

Source:
Filename: X:/SJR017/TO1/Maps/
Conceptual_model_report/BotSurfaceUHCSAS.mxd
Project: SJR017-01-06
Revised: 09/13/04 TB

Legend

- Model Boundary
- Surface Water Basin
- County Boundary
- Surface Water Bodies and Wetlands

Figure 2.4
Bottom Surface Elevation of the Upper Higher Conductivity SAS Unit

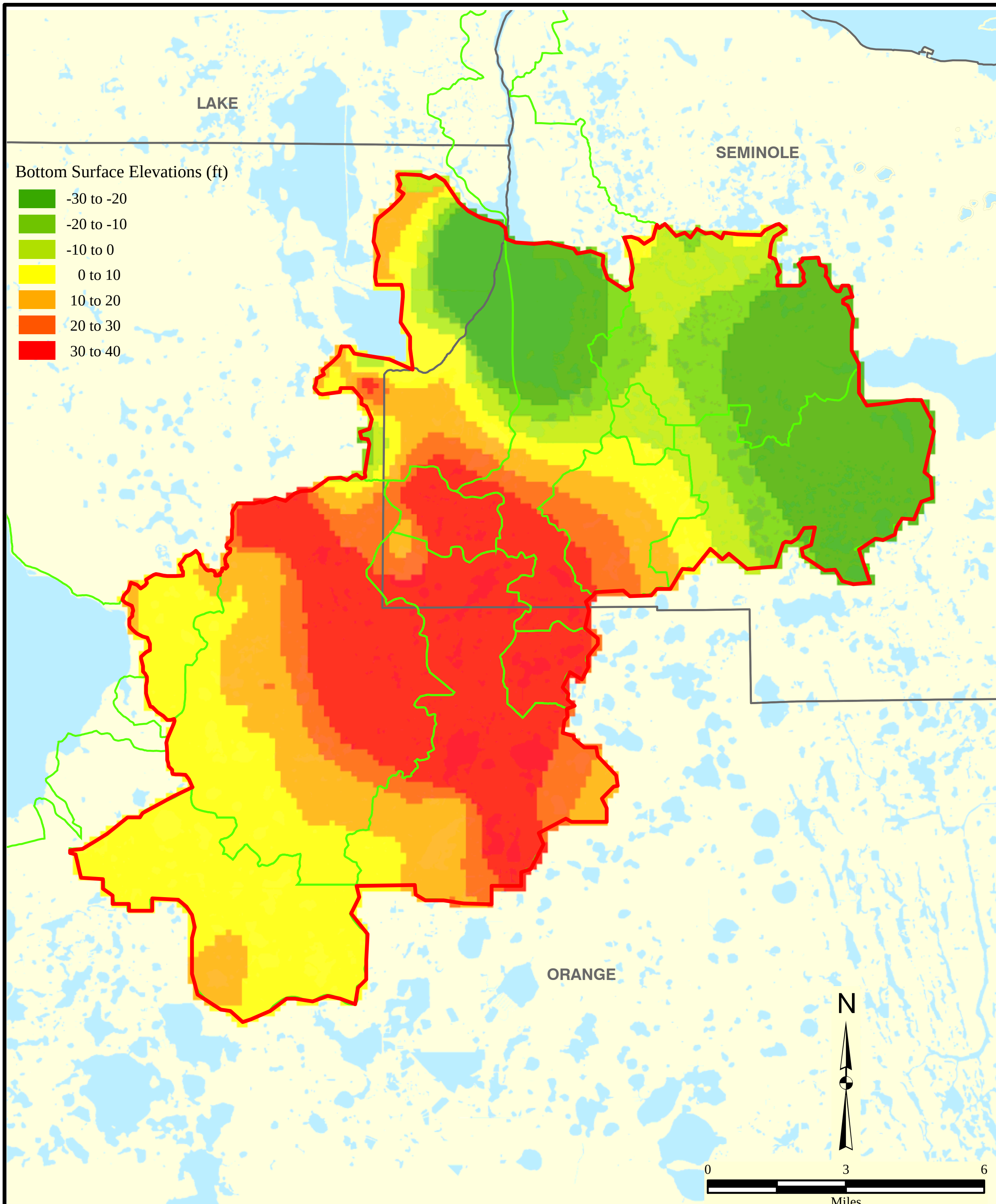

Source:
Filename: X:/SJR017/TO1/Maps/
Conceptual_model_report/BotSurfaceSAS.mxd
Project: SJR017-01-06
Revised: 09/13/04 TB

Legend

Model Boundary
Surface Water Basin
County Boundary
Surface Water Bodies and Wetlands

Figure 2.5
Bottom Surface Elevation of the SAS

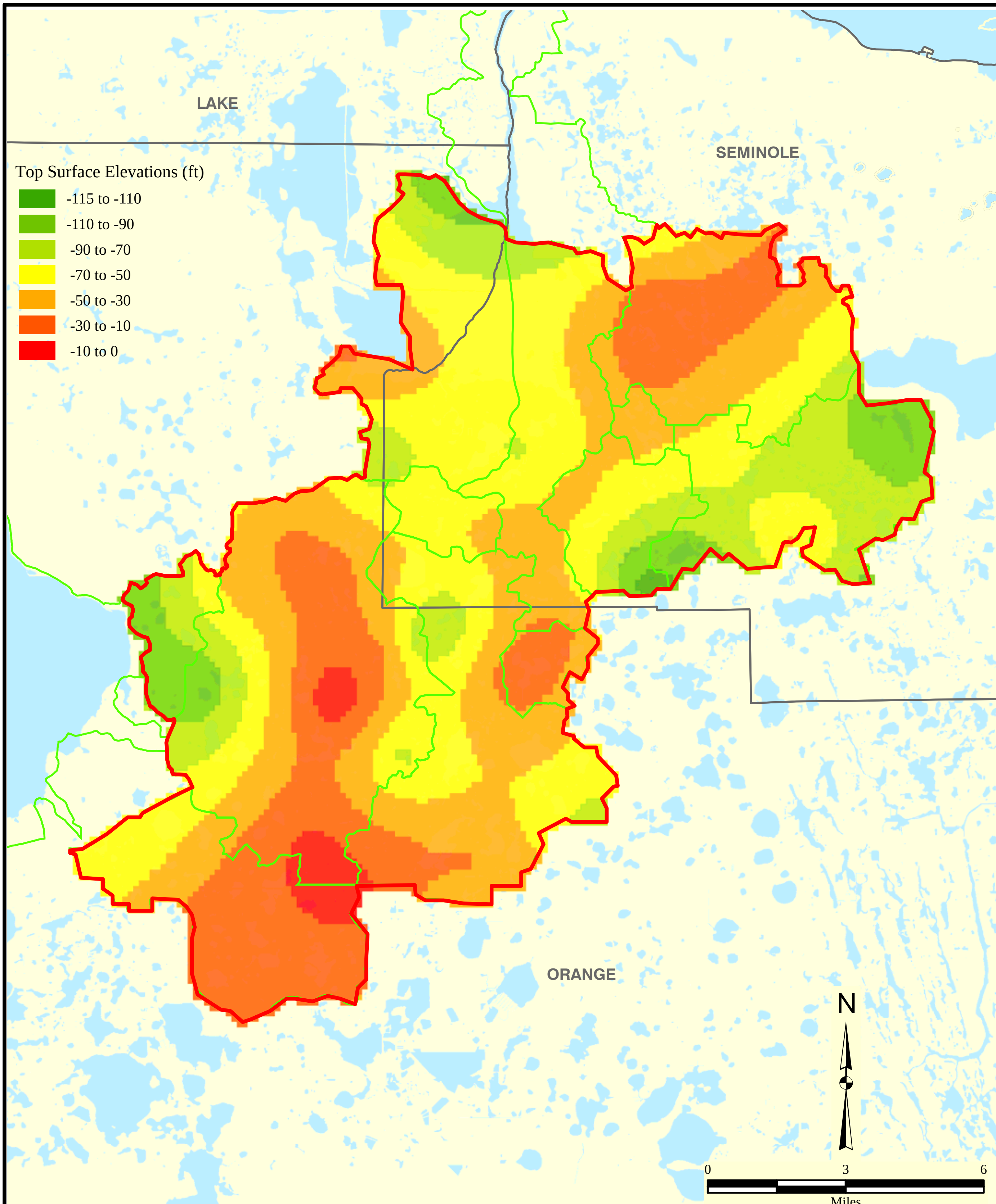

Source:
Filename: X:/SJR017/TO1/Maps/
Conceptual_model_report/TopSurfaceUFA-UZ.mxd
Project: SJR017-01-06
Revised: 09/13/04 TB

Legend

- Model Boundary
- Surface Water Basin
- County Boundary
- Surface Water Bodies and Wetlands

Figure 2.6
Top Surface
Elevation of the
UFA-UZ

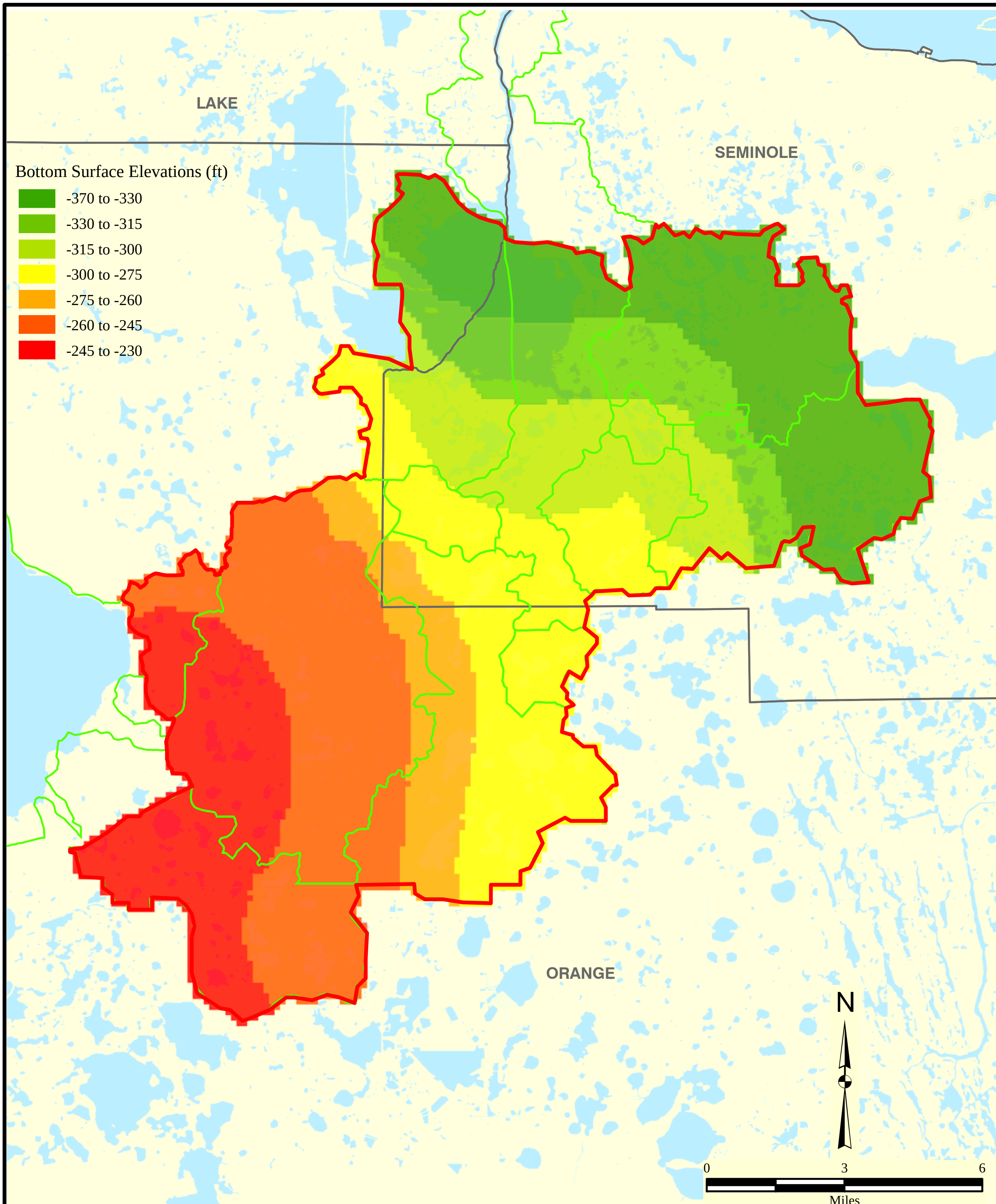

Source:
Filename: X:/SJR017/TO1/Maps/
Conceptual_model_report/BotSurfaceUFA-UZ.mxd
Project: SJR017-01-06
Revised: 09/13/04 TB

Legend

- Model Boundary
- Surface Water Basin
- County Boundary
- Surface Water Bodies and Wetlands

Figure 2.7
Bottom Surface Elevation of the UFA-UZ

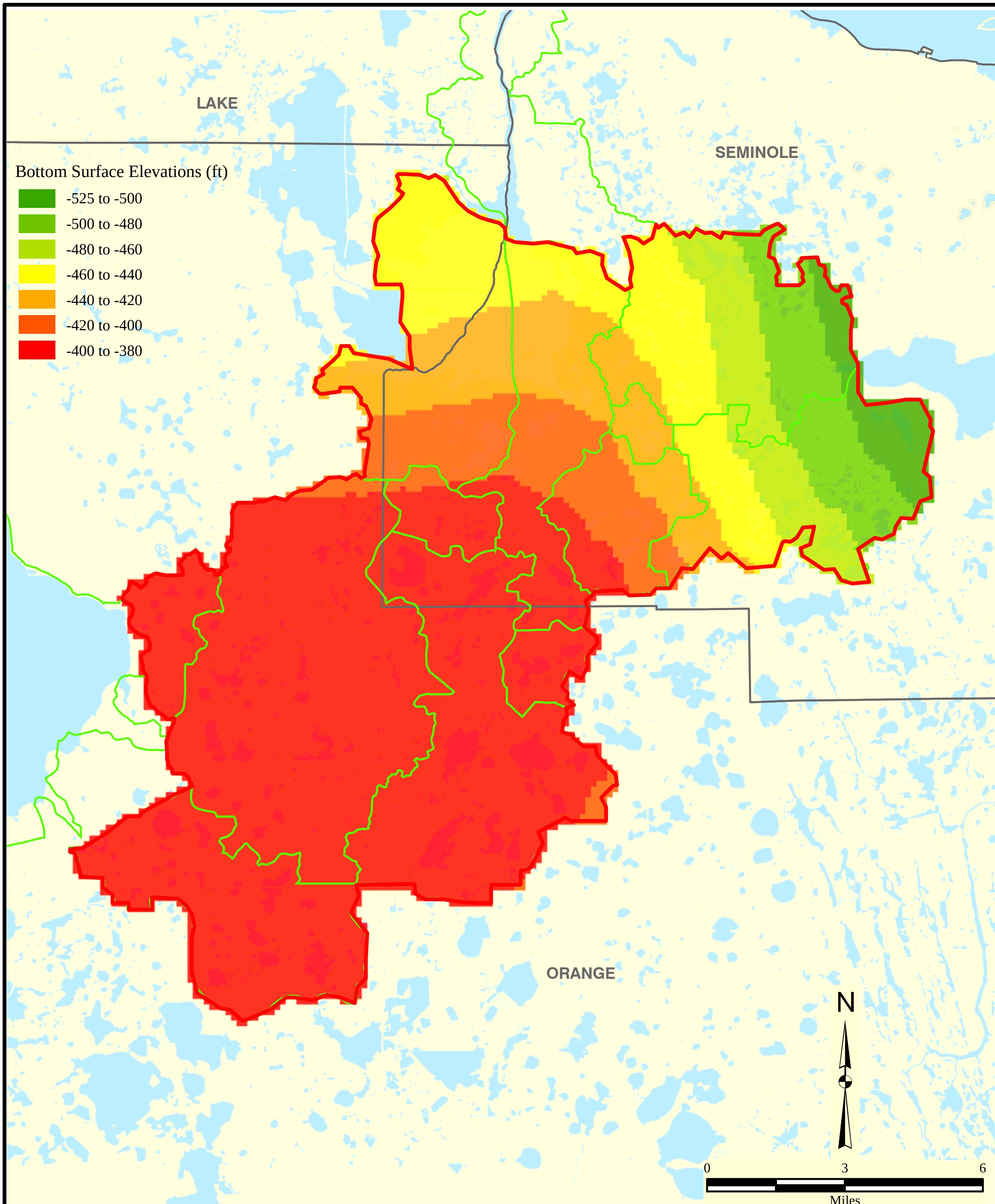

Source:
Filename: X:/SJR017/TO1/Maps/
Conceptual_model_report/BotSurfaceUFA-DZ.mxd
Project: SJR017-01-06
Revised: 09/13/04 TB

Legend

- Model Boundary
- Surface Water Basin
- County Boundary
- Surface Water Bodies and Wetlands

Figure 2.8
Bottom Surface Elevation of the UFA-DZ

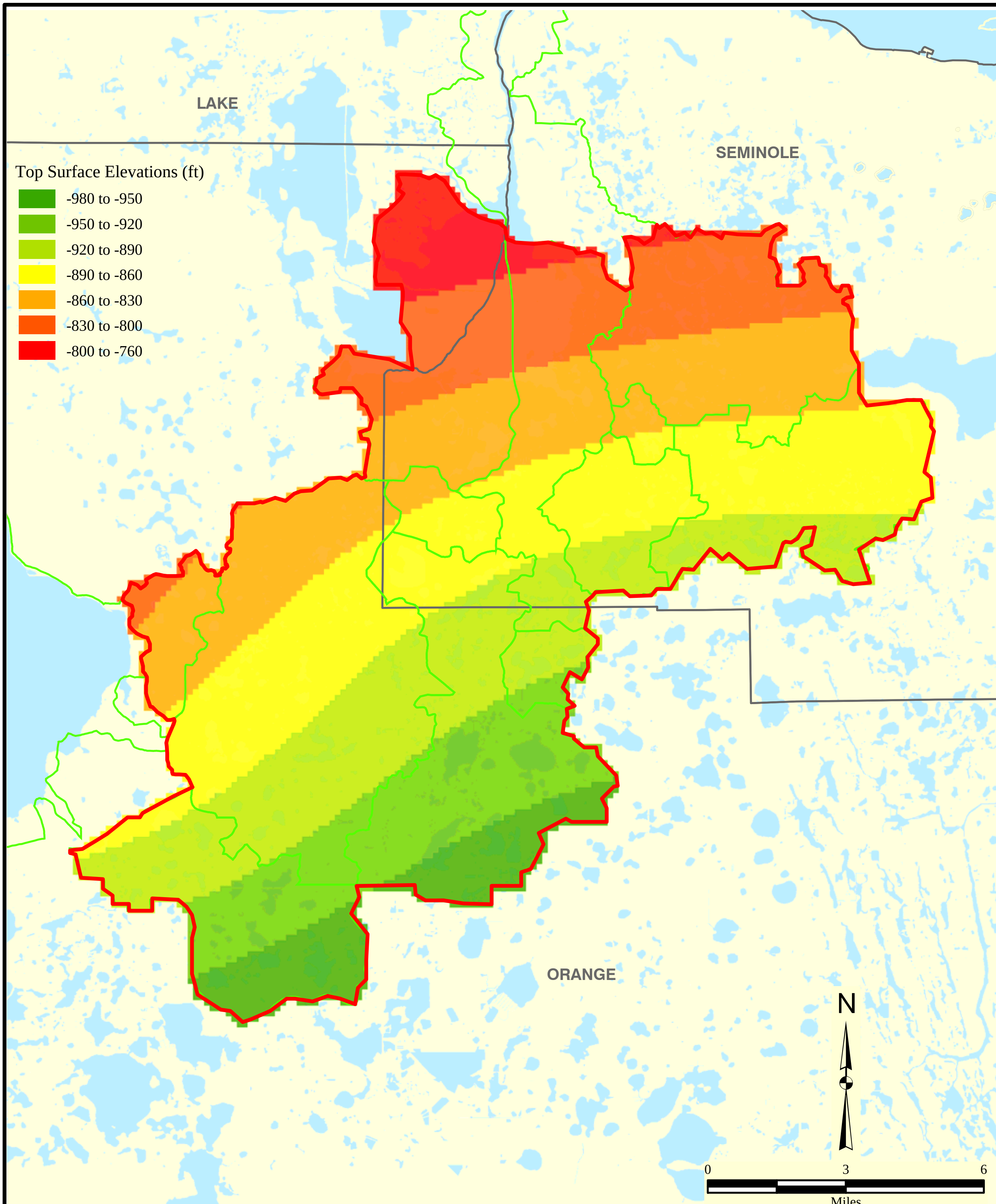

Source:
Filename: X:/SJR017/TO1/Maps/
Conceptual_model_report/TopSurfaceElev-LFA.mxd
Project: SJR017-01-06
Revised: 09/13/04 TB

Legend

- Model Boundary
- Surface Water Basin
- County Boundary
- Surface Water Bodies and Wetlands

Figure 2.9
Top Surface
Elevation of the
LFA

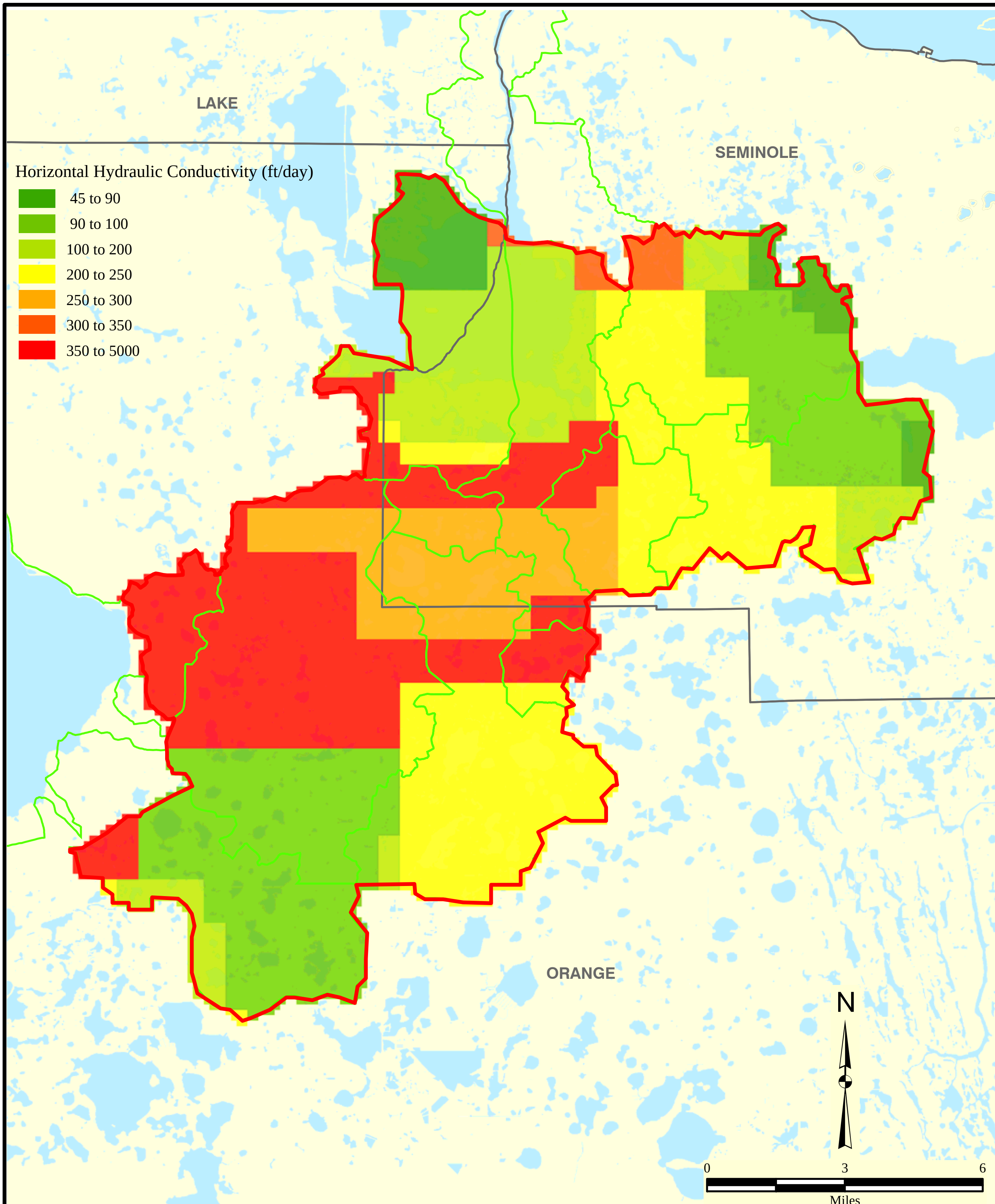

Source:
Filename: X:/SJR017/TO1/Maps/
Conceptual_model_report/HHC-UFA-UZ.mxd
Project: SJR017-01-06
Revised: 09/13/04 TB

Legend

- Model Boundary
- Surface Water Basin
- County Boundary
- Surface Water Bodies and Wetlands

Figure 2.10
Horizontal Hydraulic Conductivity of UFA-UZ

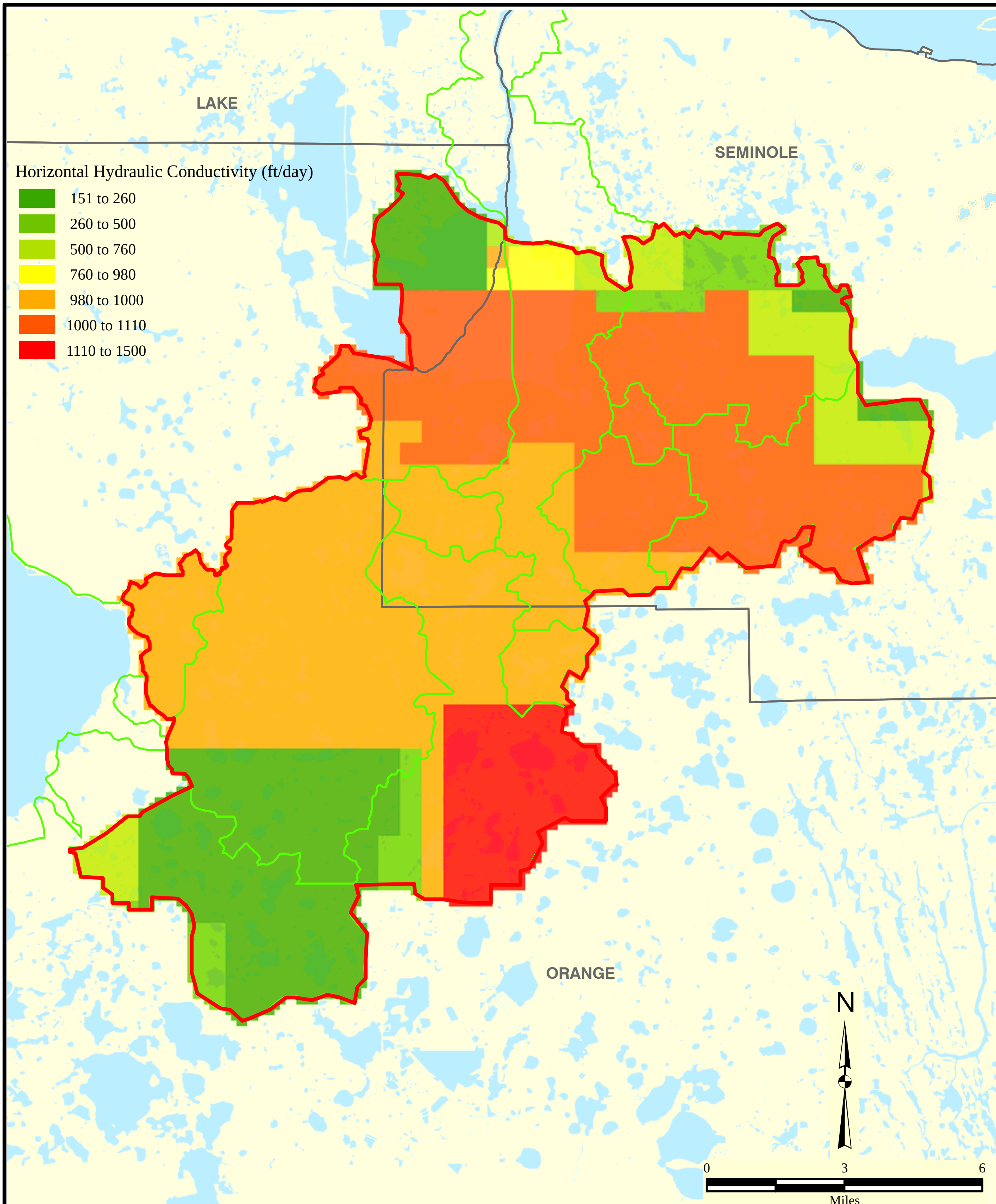

Source:
Filename: X:/SJR017/TO1/Maps/
Conceptual_model_report/HHC-UFA-UZ.mxd
Project: SJR017-01-06
Revised: 09/13/04 TB

Legend

- Model Boundary
- Surface Water Basin
- County Boundary
- Surface Water Bodies and Wetlands

Figure 2.11
Horizontal Hydraulic Conductivity of UFA-DZ

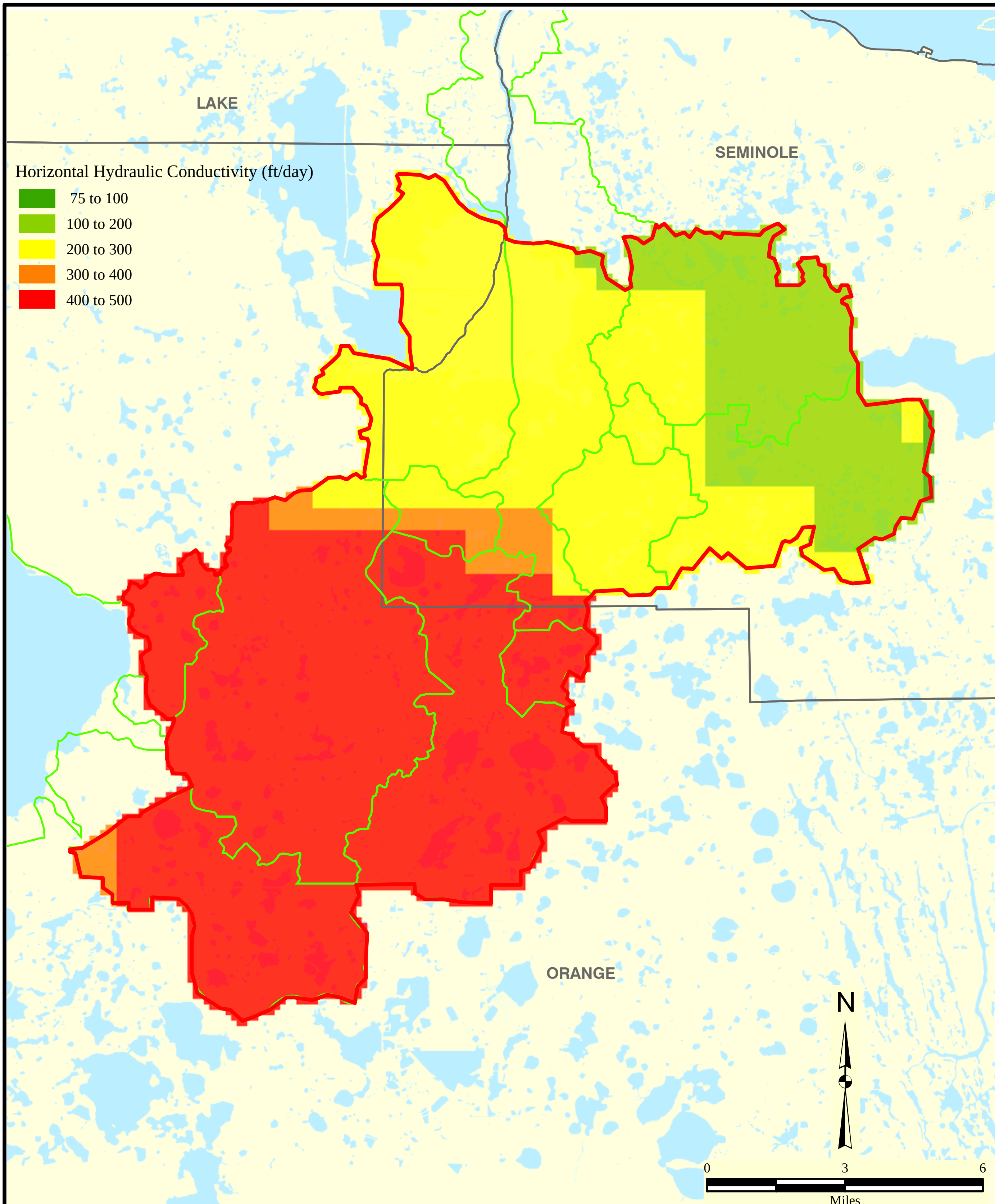

Source:
Filename: X:/SJR017/TO1/Maps/
Conceptual_model_report/HHC-LFA.mxd
Project: SJR017-01-06
Revised: 09/13/04 TB

Legend

- Model Boundary
- Surface Water Basin
- County Boundary
- Surface Water Bodies and Wetlands

Figure 2.12
Horizontal Hydraulic Conductivity of LFA

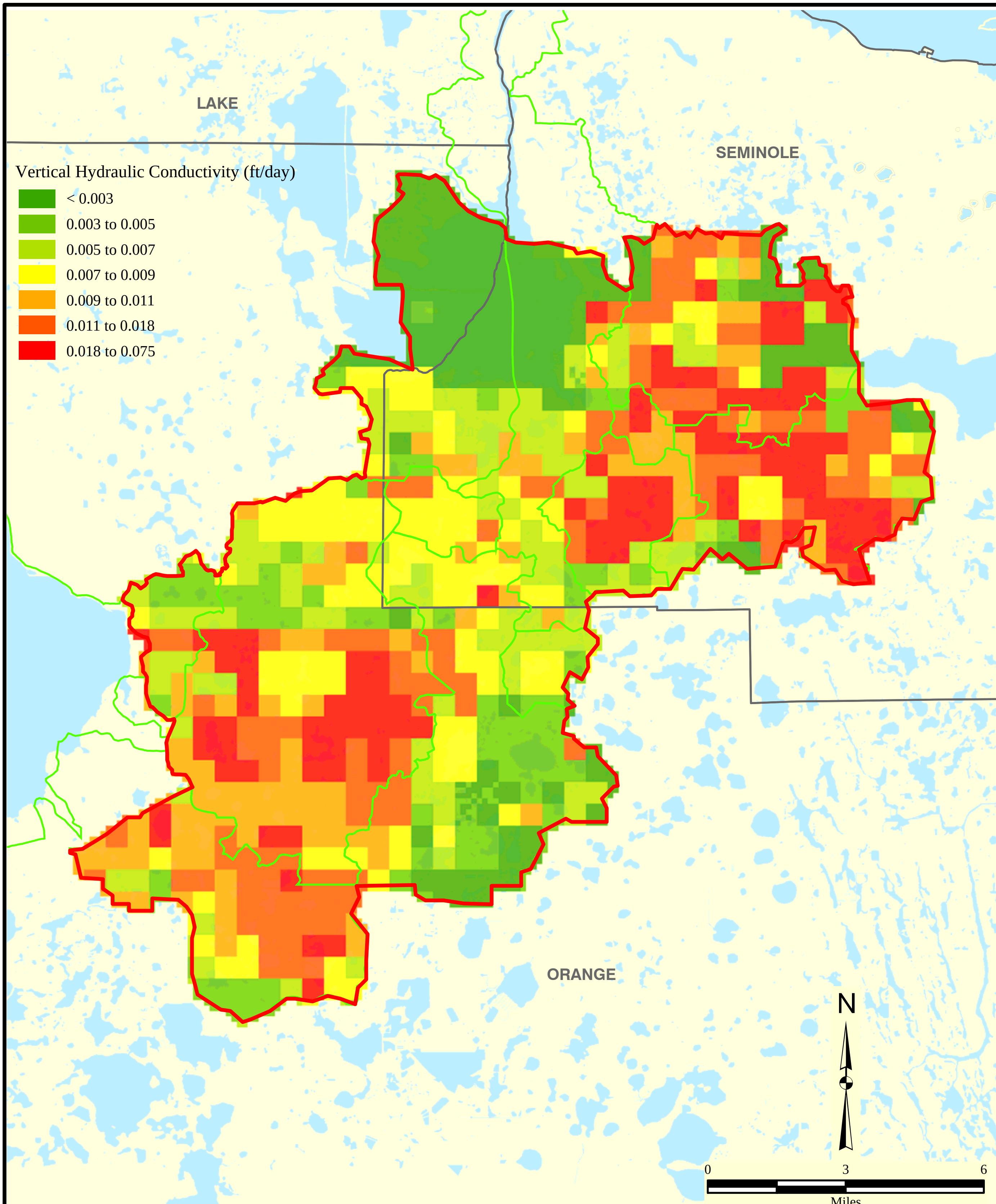

Source:
Filename: X:/SJR017/TO1/Maps/
Conceptual_model_report/VHC-ICU.mxd
Project: SJR017-01-06
Revised: 09/13/04 TB

Legend

- Model Boundary
- Surface Water Basin
- County Boundary
- Surface Water Bodies and Wetlands

Figure 2.13
Vertical Hydraulic Conductivity of the ICU

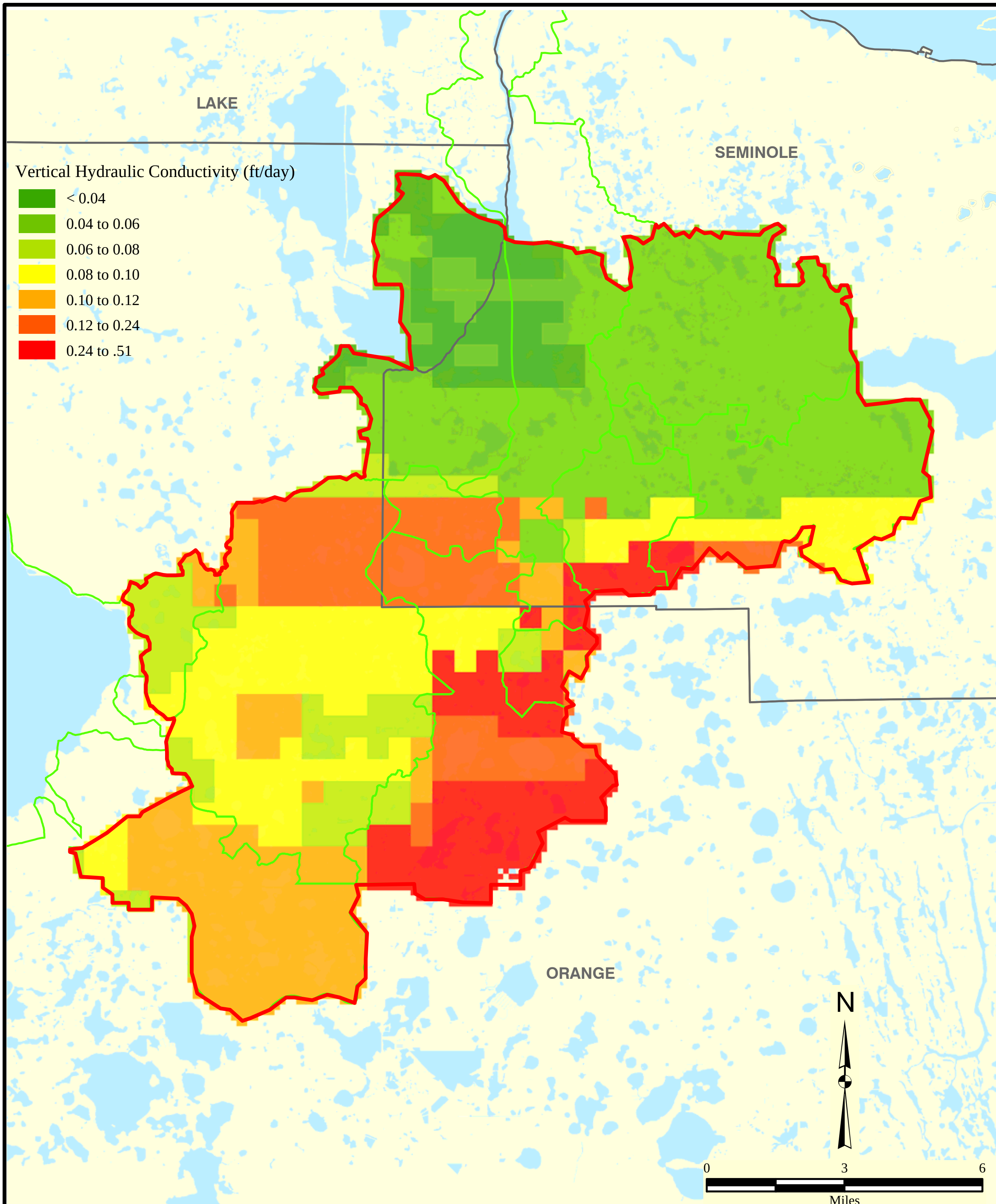

Source:
Filename: X:/SJR017/TO1/Maps/ Conceptual_model_report/VHC-MSCU.mxd
Project: SJR017-01-06
Revised: 09/13/04 TB

Legend

- Model Boundary
- Surface Water Basin
- County Boundary
- Surface Water Bodies and Wetlands

Figure 2.14
Vertical Hydraulic Conductivity of the MSCU

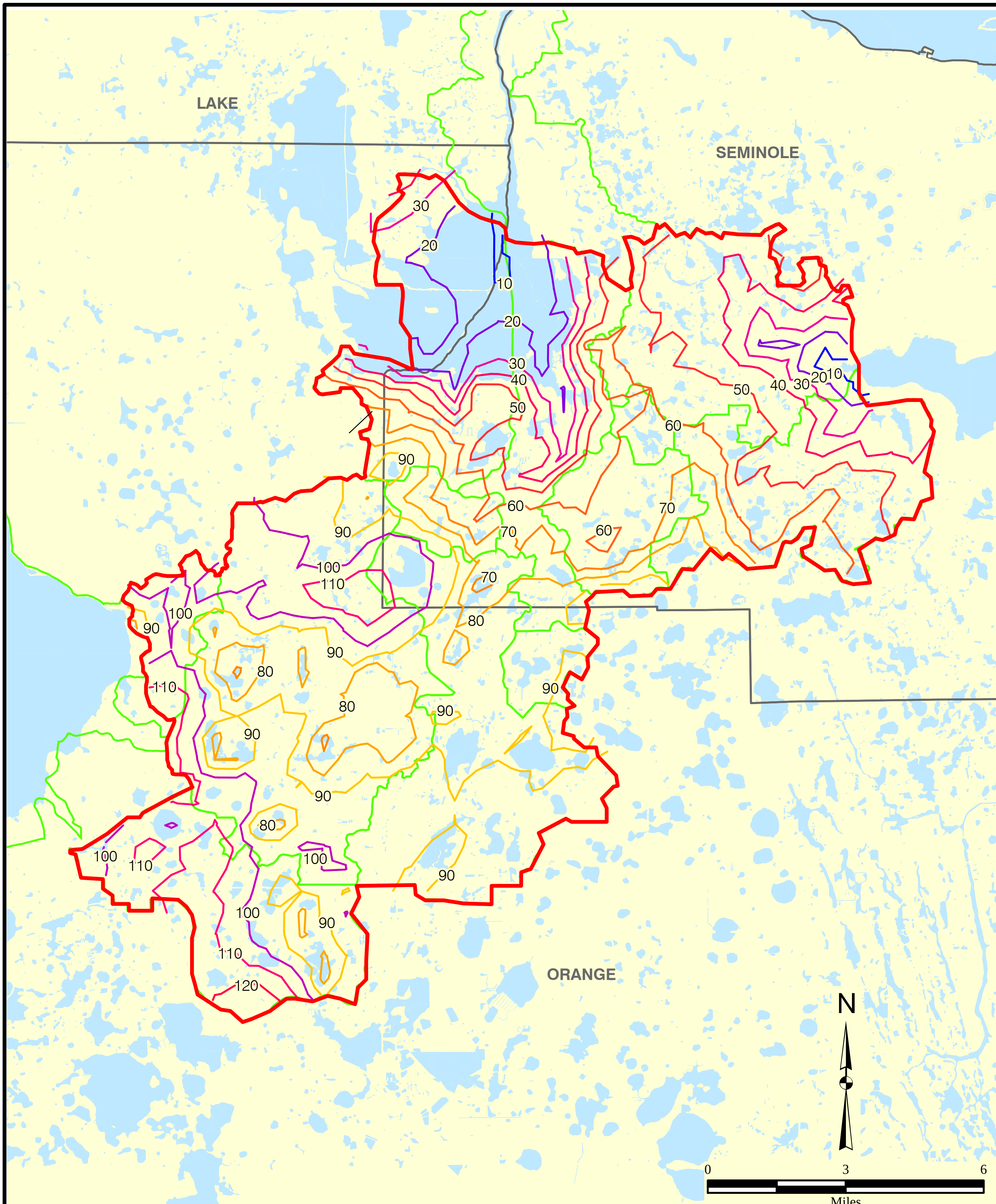

Source:
Filename: X:/SJR017/TO1/Maps/
Conceptual_model_report/Pot-SAS.mxd
Project: SJR017-001-06
Revised: 09/13/04 TB

Legend

- Model Boundary
- Surface Water Basin
- County Boundary
- 50 Potentiometric Contour (ft)
- Surface Water Bodies and Wetlands

Figure 2.15
Potentiometric Surface of the SAS for Average 1995 Conditions (ECF Model Simulation)

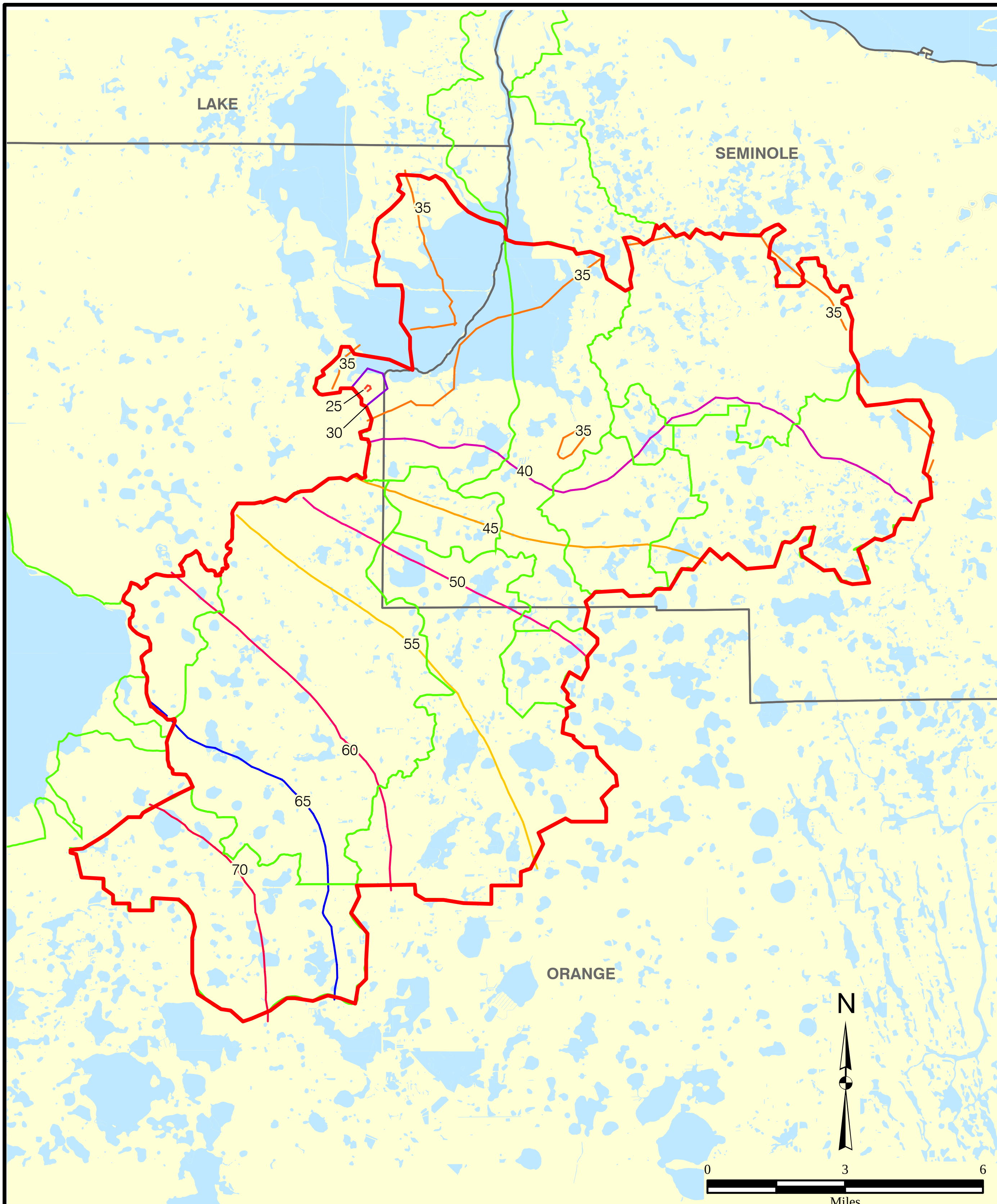

Source:
Filename: X:/SJR017/TO1/Maps/
Conceptual_model_report/Pot-UFA.mxd
Project: SJR017-001-06
Revised: 09/13/04 TB

Legend

- Model Boundary
- Surface Water Basin
- County Boundary
- 50 Potentiometric Contour (ft)
- Surface Water Bodies and Wetlands

Figure 2.16
Potentiometric Surface of the UFA-UZ for Average 1995 Conditions (ECF Model Simulation)

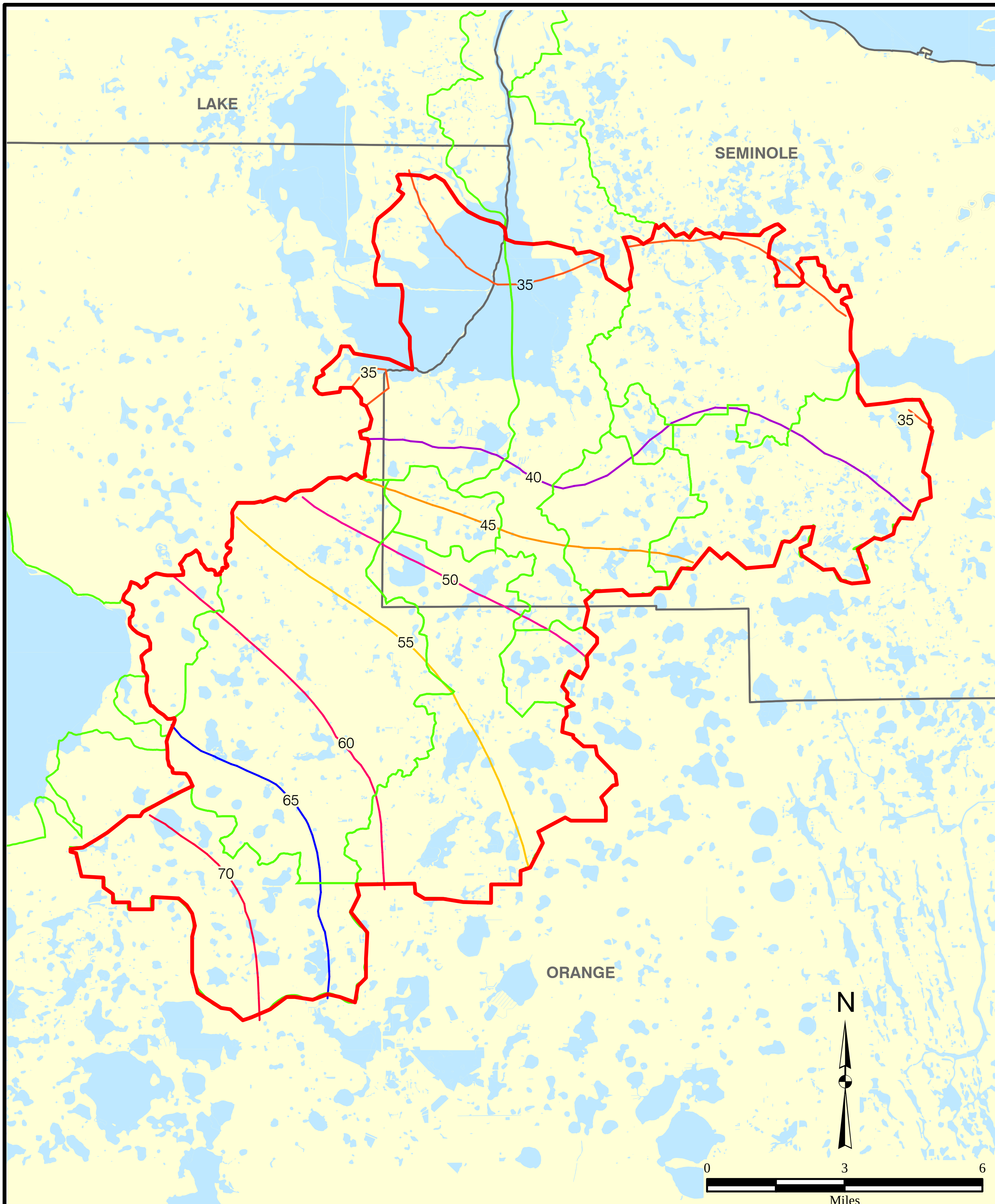

Source:
Filename: X:/SJR017/TO1/Maps/
Conceptual_model_report/Pot-UFA-DZ.mxd
Project: SJR017-001-06
Revised: 09/13/04 TB

Legend

- Model Boundary
- Surface Water Basin
- County Boundary
- 50 Potentiometric Contour (ft)
- Surface Water Bodies and Wetlands

Figure 2.17
Potentiometric Surface of the UFA-DZ for Average 1995 Conditions (ECF Model Simulation)

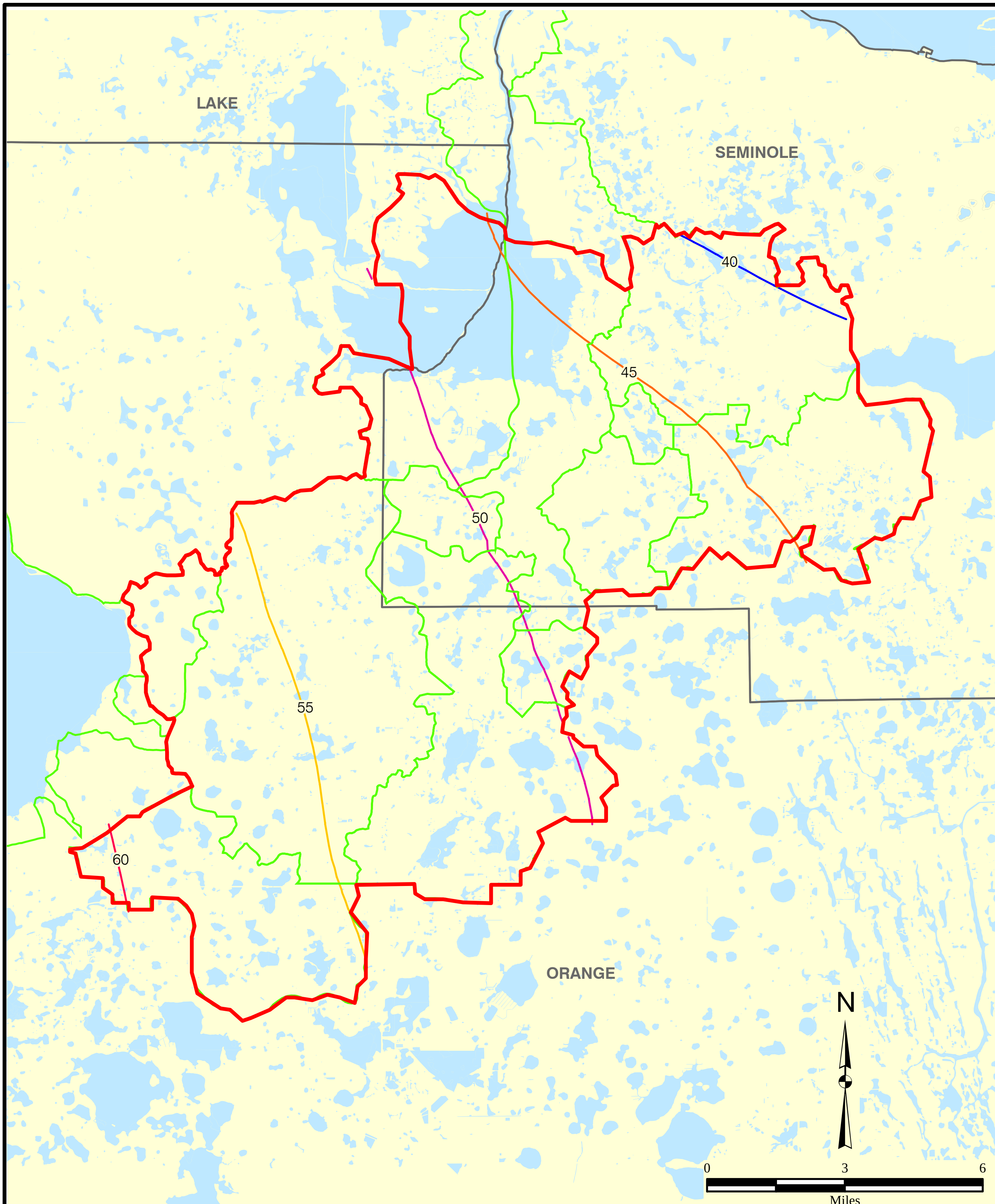

Source:
Filename: X:/SJR017/TO1/Maps/
Conceptual_model_report/Pot-LFA.mxd
Project: SJR017-001-06
Revised: 09/13/04 TB

Legend

- Model Boundary
- Surface Water Basin
- County Boundary
- 50 Potentiometric Contour (ft)
- Surface Water Bodies and Wetlands

Figure 2.18
Potentiometric Surface of the LFA for Average 1995 Conditions (ECF Model Simulation)

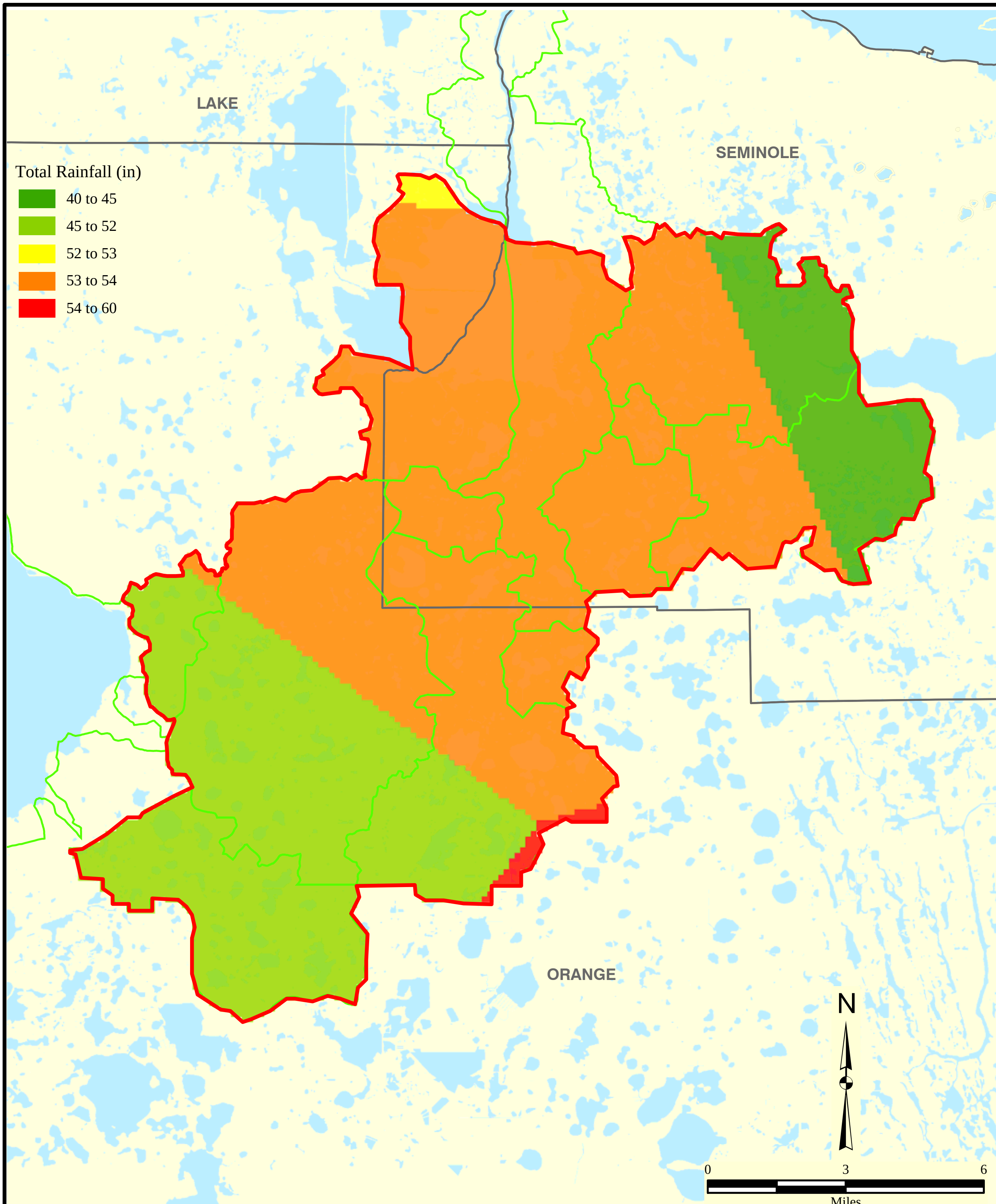

Source:
Filename: X:/SJR017/TO1/Maps/
Conceptual_model_report/Total_Rain.mxd
Project: SJR017-01-06
Revised: 09/13/04 TB

Legend

Model Boundary
Surface Water Basin
County Boundary
Surface Water Bodies and Wetlands

Figure 3.1
Distribution of Total Rainfall for Average 1995 Conditions

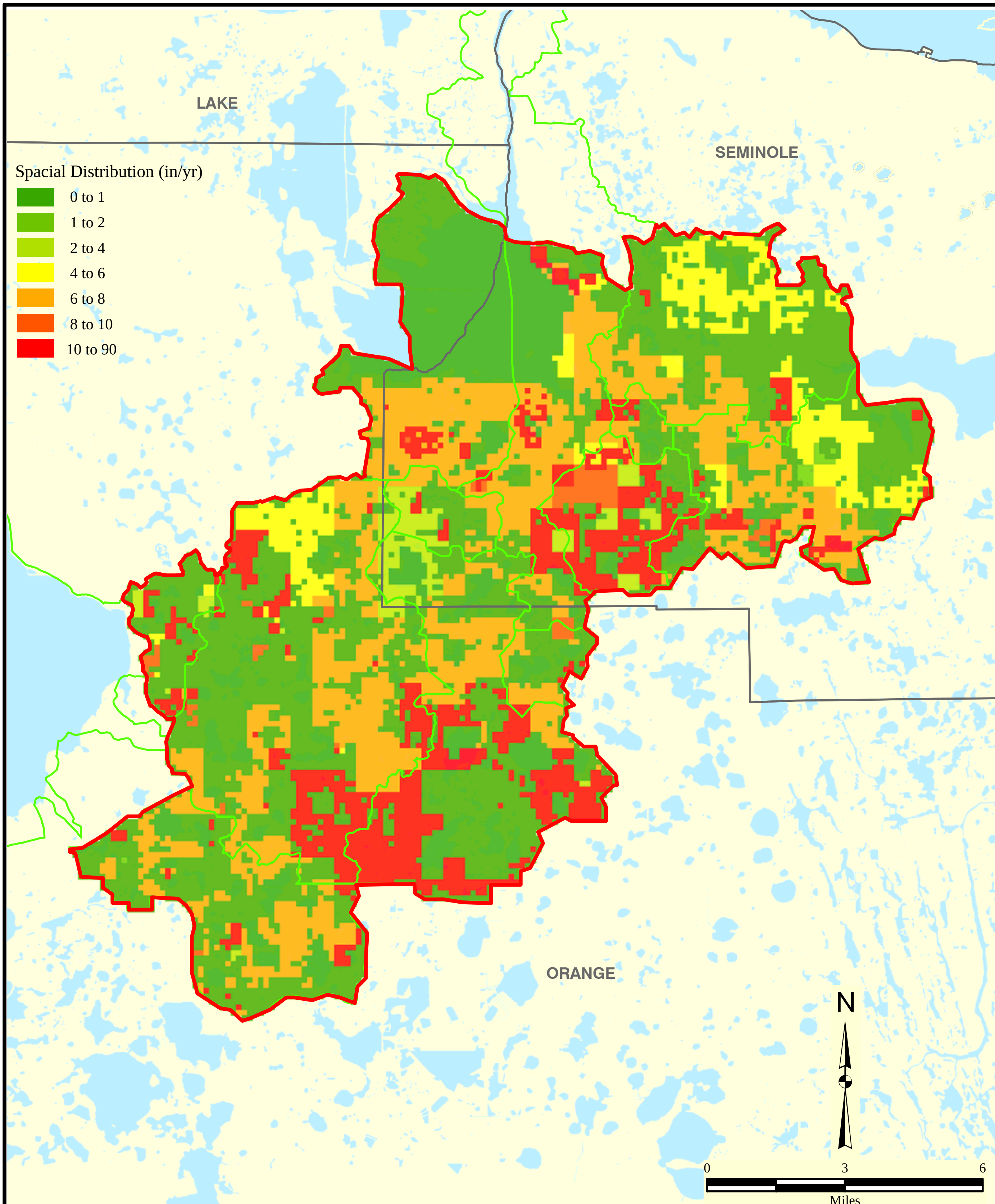

Source:
Filename: X:/SJR017/TO1/Maps/
Conceptual_model_report/RIBAPP.mxd
Project: SJR017-01-06
Revised: 09/13/04 TB

Legend

- Model Boundary
- Surface Water Basin
- County Boundary
- Surface Water Bodies and Wetlands

Figure 3.2
Spatial Distribution of the Average 1995 Water Application to the Surfical Layer of the Model, aside from the Precipitation (RIB & APP)

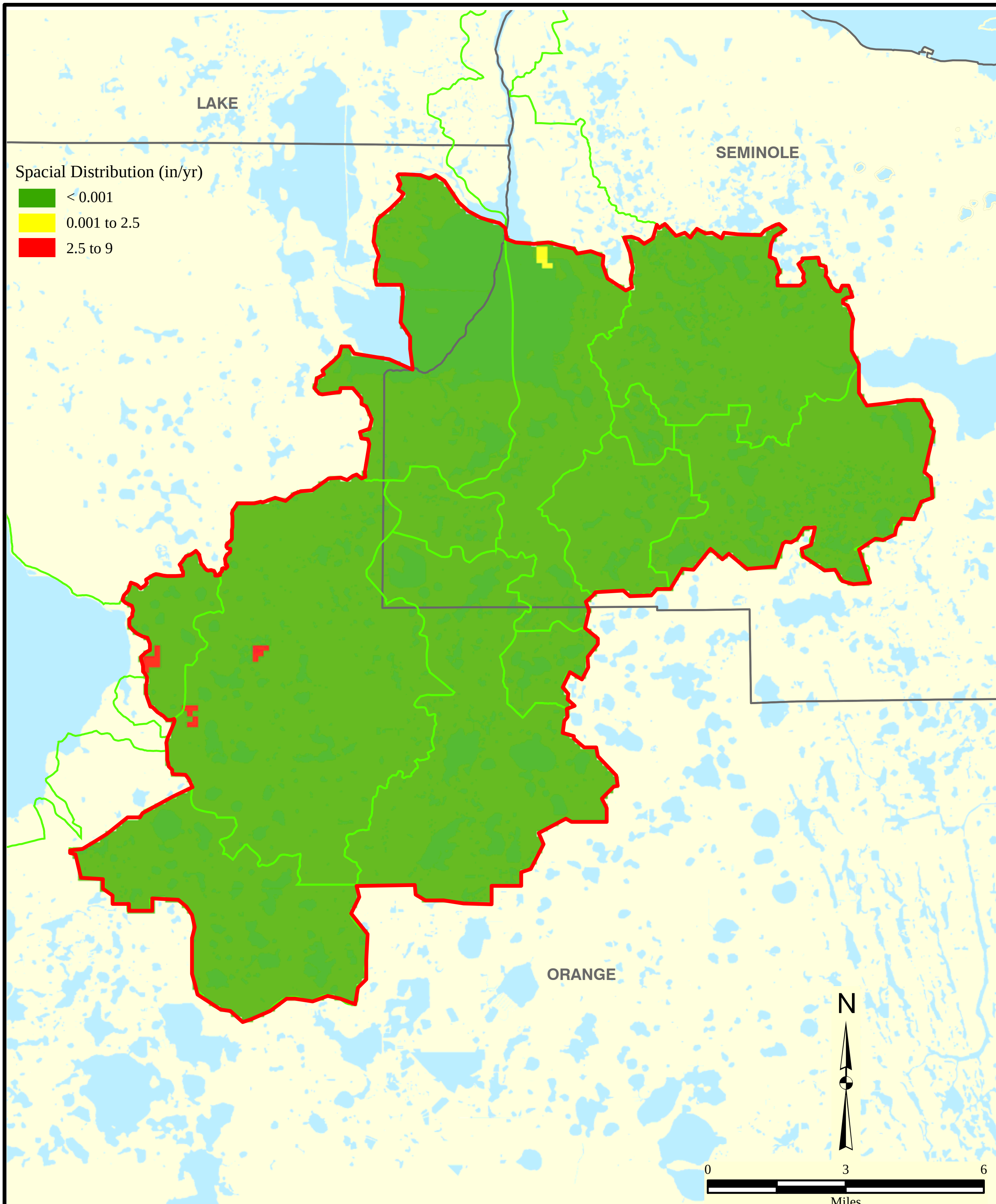

Source:
Filename: X:/SJR017/TO1/Maps/
Conceptual_model_report/Septic.mxd
Project: SJR017-001-06
Revised: 09/13/04 TB

Legend

- Model Boundary
- Surface Water Basin
- County Boundary
- Surface Water Bodies and Wetlands

Figure 3.3
Spatial Distribution of Estimated Average 1995 Septic Tank Effluent

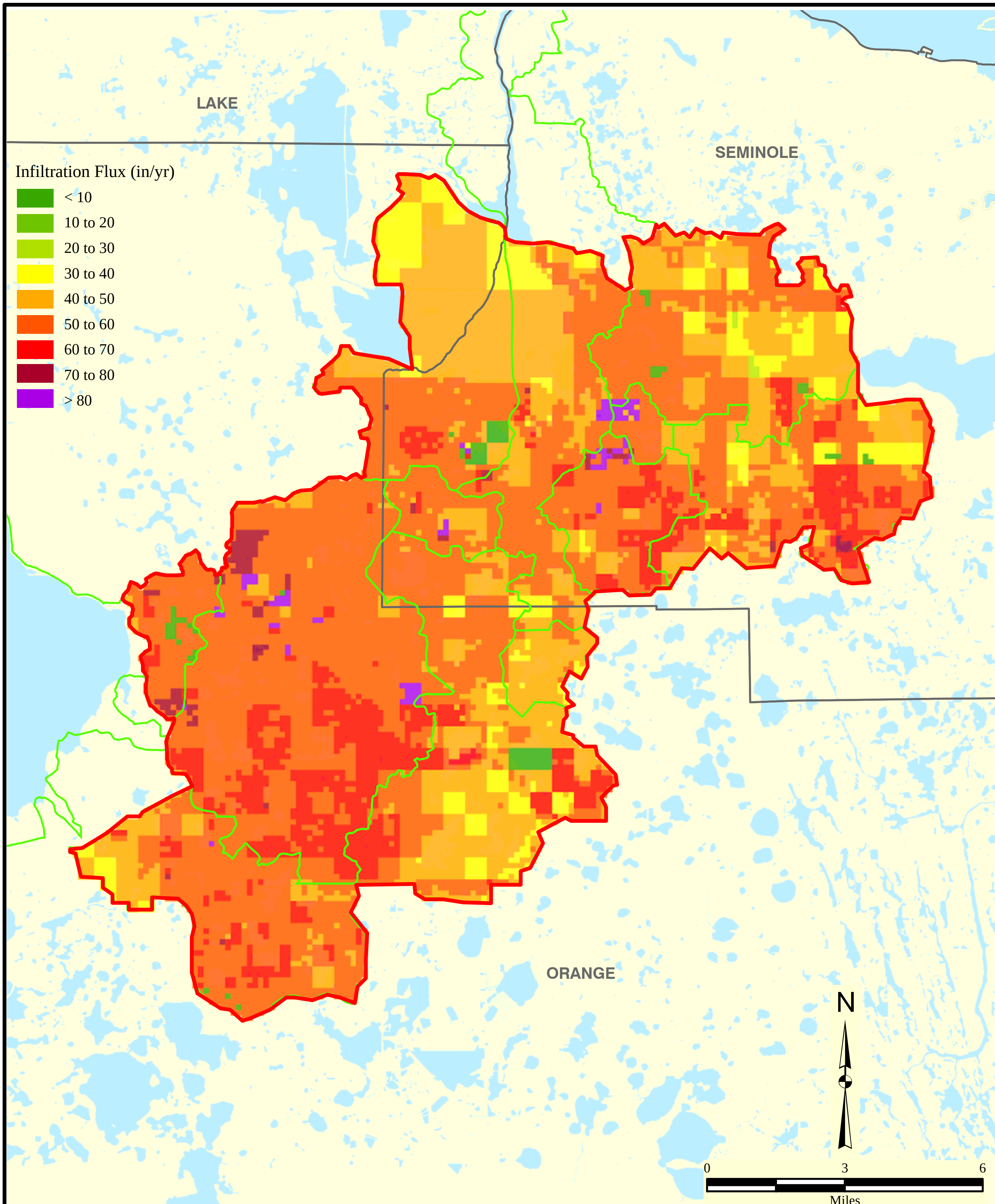

Source:
Filename: X:/SJR017/TO1/Maps/
Conceptual_model_report/Infil.mxd
Project: SJR017-001-06
Revised: 09/13/04 TB

Legend

- Model Boundary
- Surface Water Basin
- County Boundary
- Surface Water Bodies and Wetlands

Figure 3.4
Spatial Distribution of Infiltration as Calculated in the ECF Model

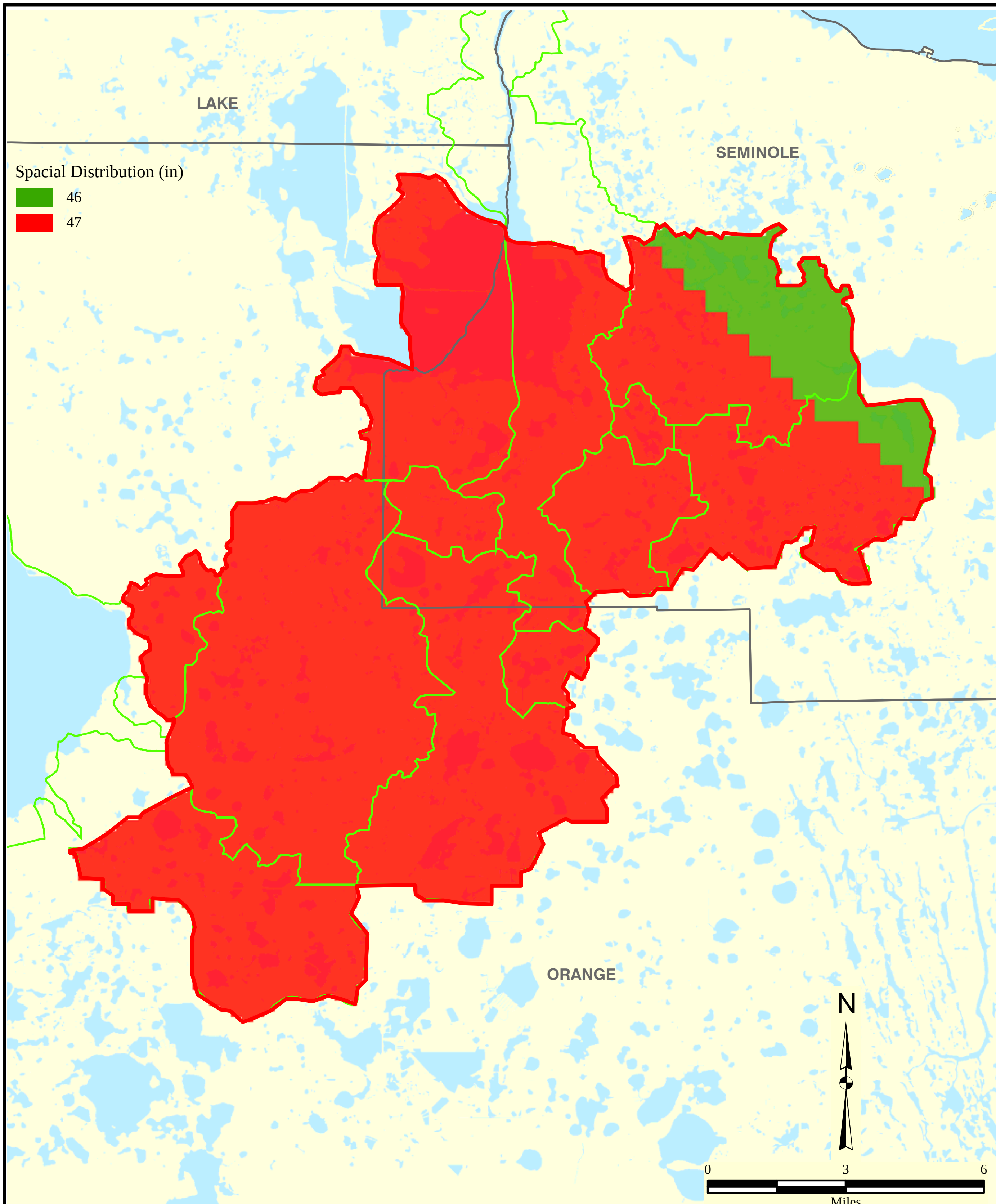

Source:
Filename: X:/SJR017/TO1/Maps/
Conceptual_model_report/MaxEvap.mxd
Project: SJR017-001-06
Revised: 09/08/04 TB

Legend

Model Boundary
Surface Water Basin
County Boundary
Surface Water Bodies and Wetlands

Figure 3.5
Spatial Distribution of Maximum Annual Evapotranspiration

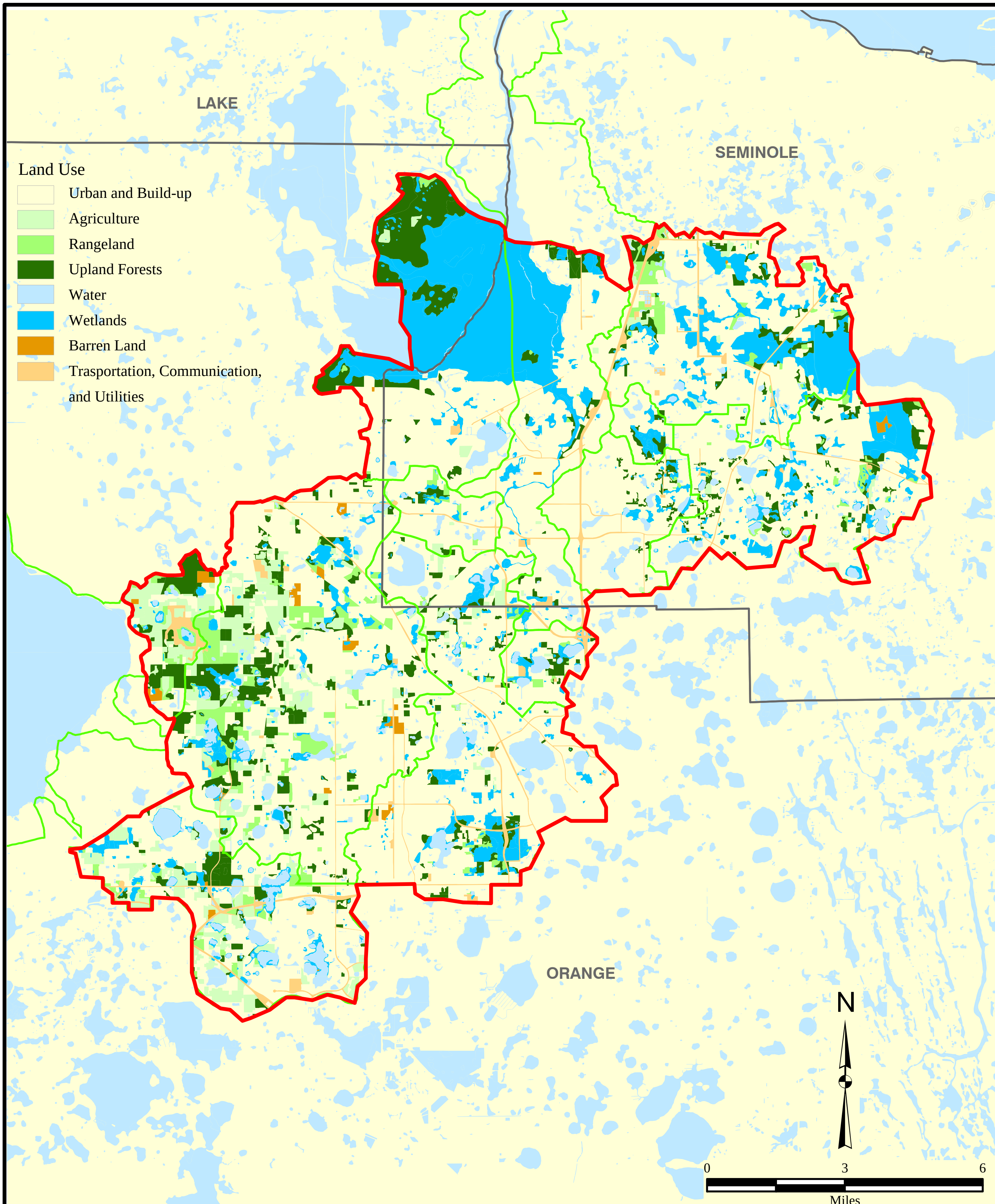

Source:
Filename: X:/SJR017/TO1/Maps/
Conceptual_model_report/LandUse.mxd
Project: SJR017-001-06
Revised: 09/13/04 TB

Legend

Model Boundary
Surface Water Basin
County Boundary
Surface Water Bodies and Wetlands

Figure 3.6
Plot of Land Use
for 1995 Conditions

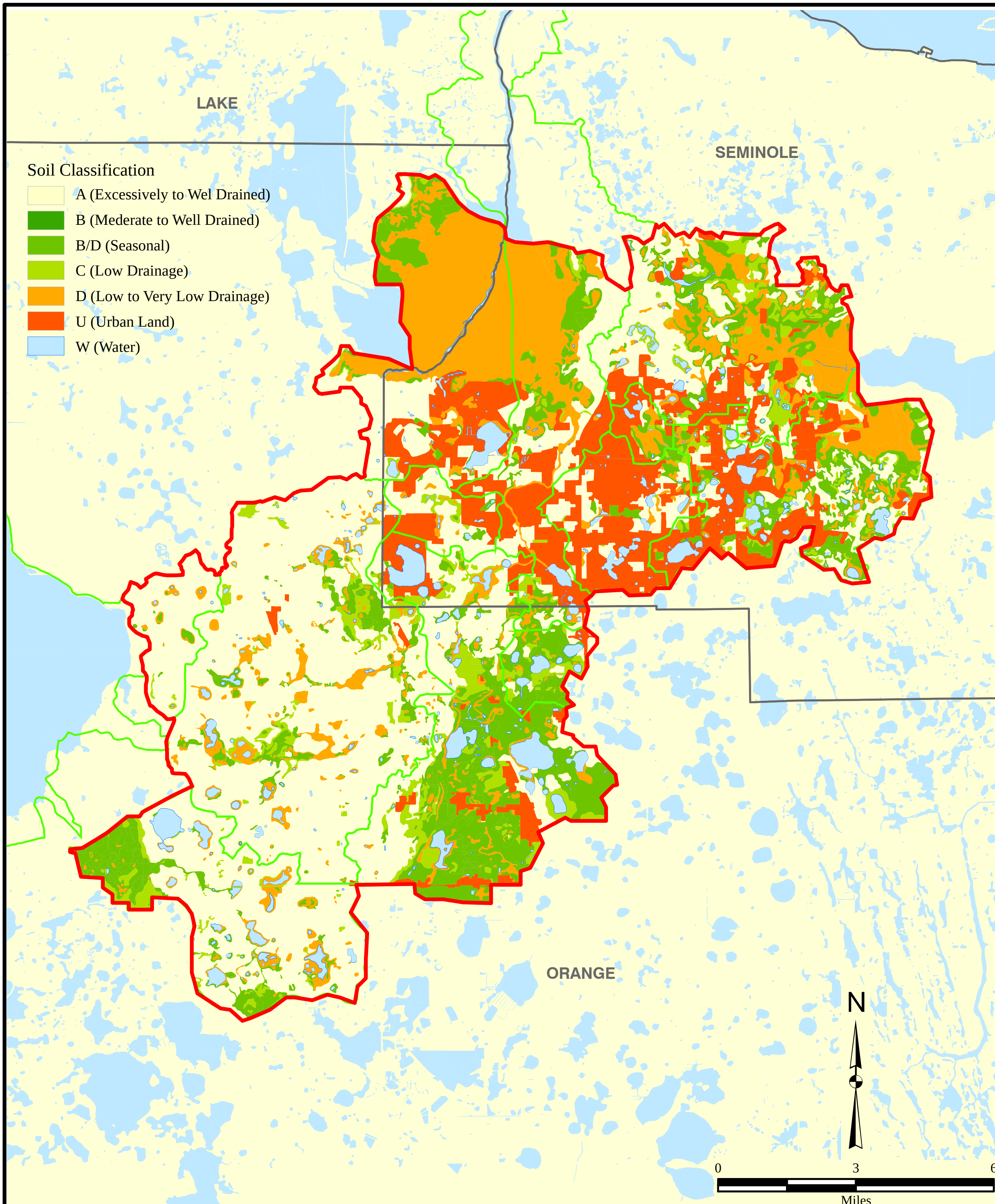

Source:
Filename: X:/SJR017/TO1/Maps/
Conceptual_model_report/Soil.mxd
Project: SJR017-001-99
Revised: 11/30/04 TB

Legend

Model Boundary
Surface Water Basin
County Boundary
Surface Water Bodies and Wetlands

Figure 3.7
Soil Classification in the Study Region
(from ECF SSURGO Database)

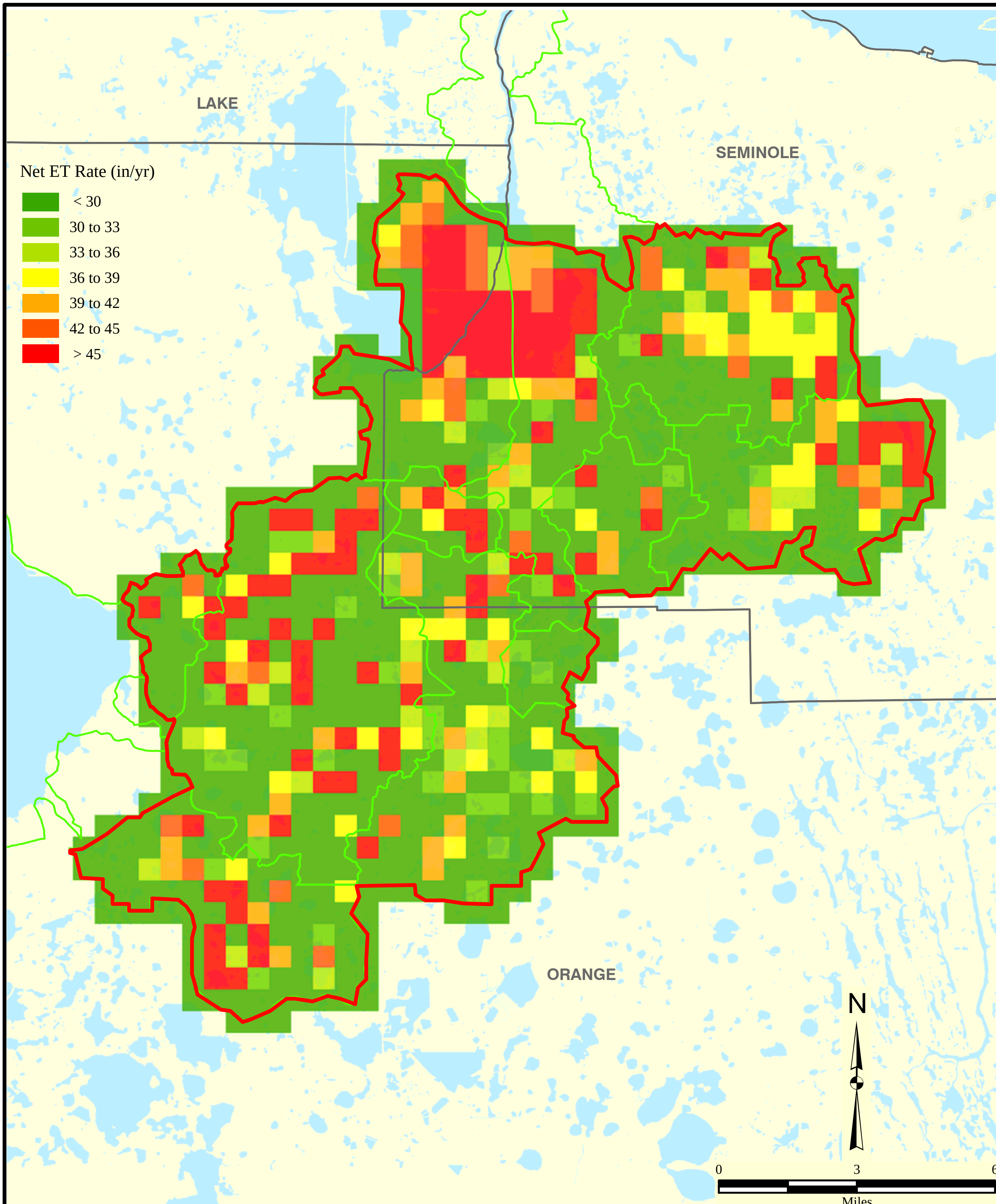

Source:
Filename: X:/SJR017/TO1/Maps/
Conceptual_model_report/ETRate.mxd
Project: SJR017-001-06
Revised: 09/13/04 TB

Legend

Model Boundary
Surface Water Basin
County Boundary
Surface Water Bodies and Wetlands

Figure 3.8
Total Evapotranspiration for the ECF Model of McGurk and Presley (2002), for Average 1995 Conditions

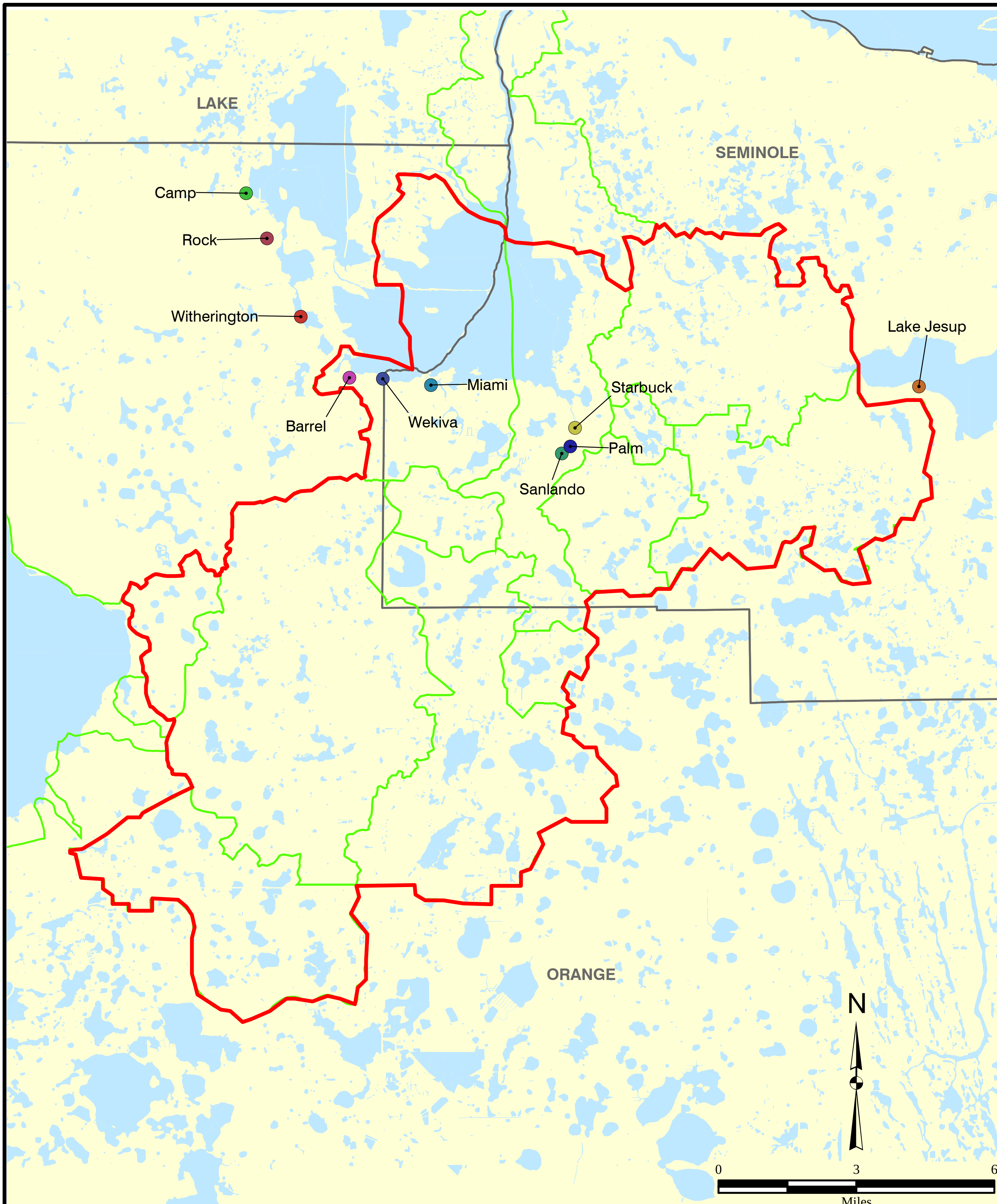

Source:
Filename: X:/SJR017/TO1/Maps/ Conceptual_model_report/Soil.mxd
Project: SJR017-001-06
Revised: 09/08/04 TB

Legend

- Model Boundary
- Surface Water Basin
- County Boundary
- Surface Water Bodies and Wetlands
- Spring Location

Figure 3.9
Locations of Springs in the Study Region

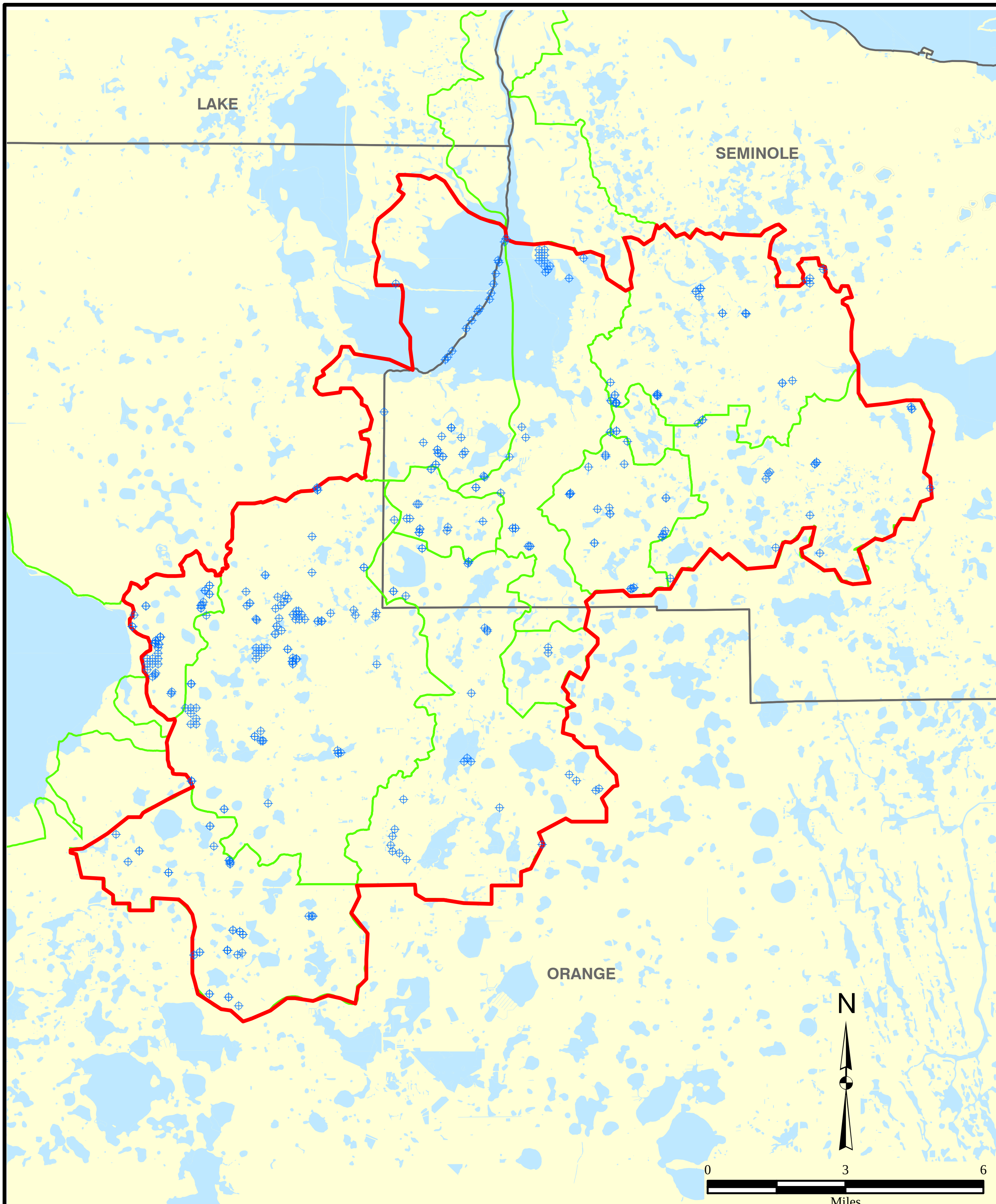

Source:
Filename: X:/SJR017/TO1/Maps/
Conceptual_model_report/Withdrawl-Well.mxd
Project: SJR017-001-99
Revised: 01/20/05 TB

Legend

- Model Boundary
- Surface Water Basin
- County Boundary
- Surface Water Bodies and Wetlands
- Withdrawal Well

Figure 3.10
Location of Withdrawal Wells in the Study Region

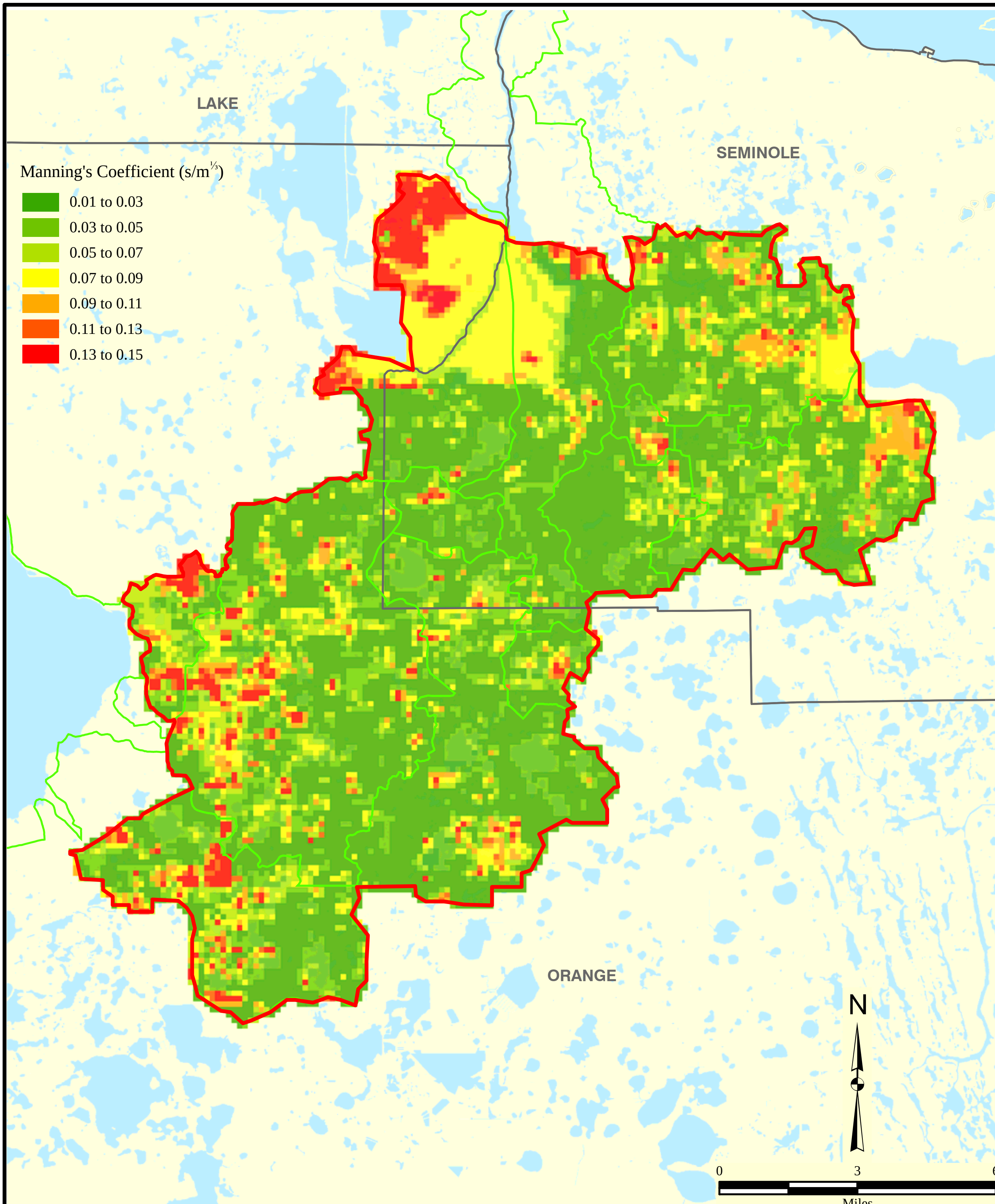

Source:
Filename: X:/SJR017/TO1/Maps/
Conceptual_model_report/MannCoDist.mxd
Project: SJR017-001-06
Revised: 09/13/04 TB

Legend

- Model Boundary
- Surface Water Basin
- County Boundary
- Surface Water Bodies and Wetlands

Figure 4.1
Manning's Coefficient Distribution Over the WOSC - ISGM Domain

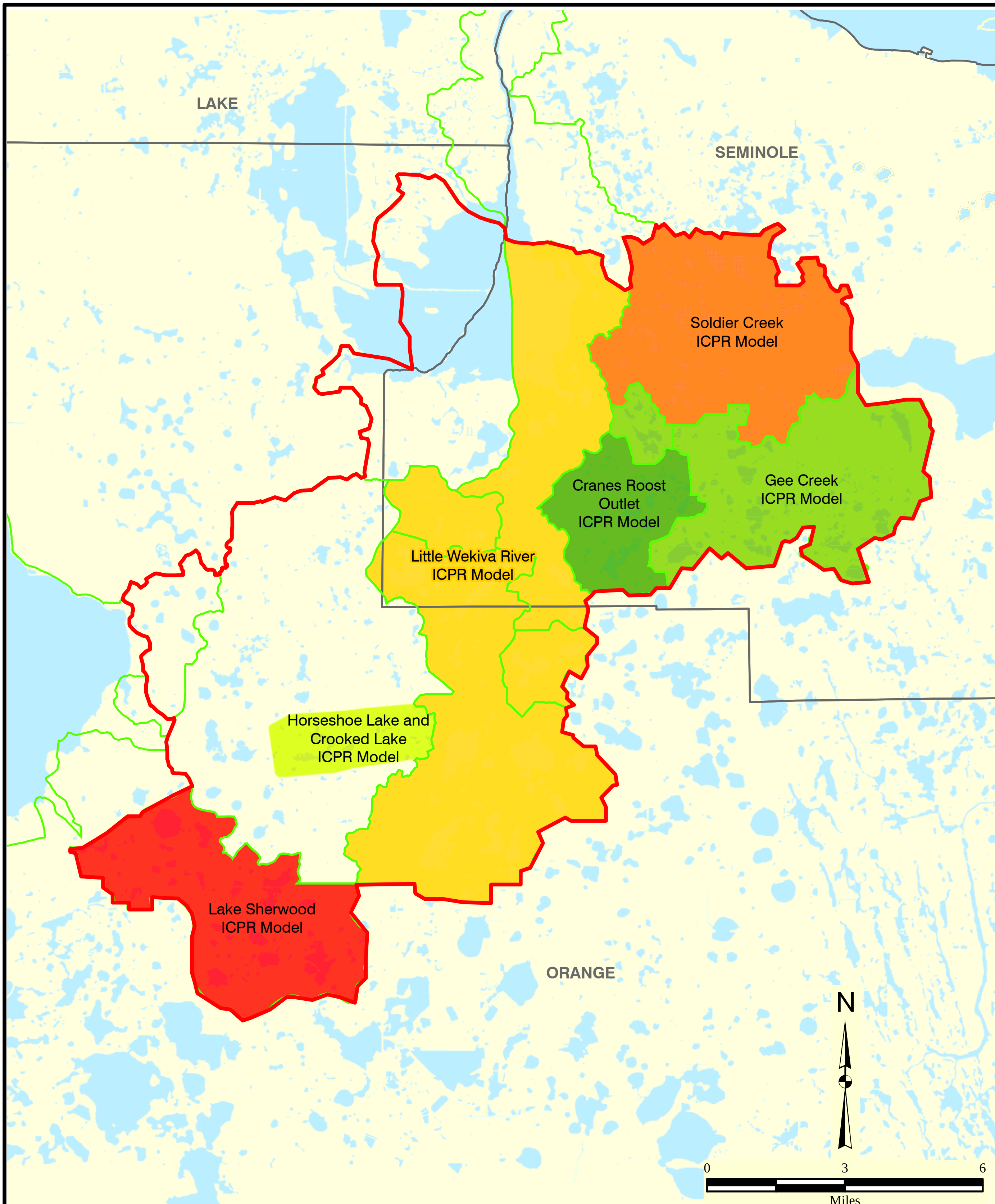

Source:
Filename: X:/SJR017/TO1/Maps/
Conceptual_model_report/ICPR_Models.mxd
Project: SJR017-01-06
Revised: 09/13/04 TB

Legend

- Model Boundary
- Surface Water Basin
- County Boundary
- Surface Water Bodies and Wetlands

Figure 4.2
Available Access Database Coverage of ICPR Models Over the WOSC-ISGM Domain

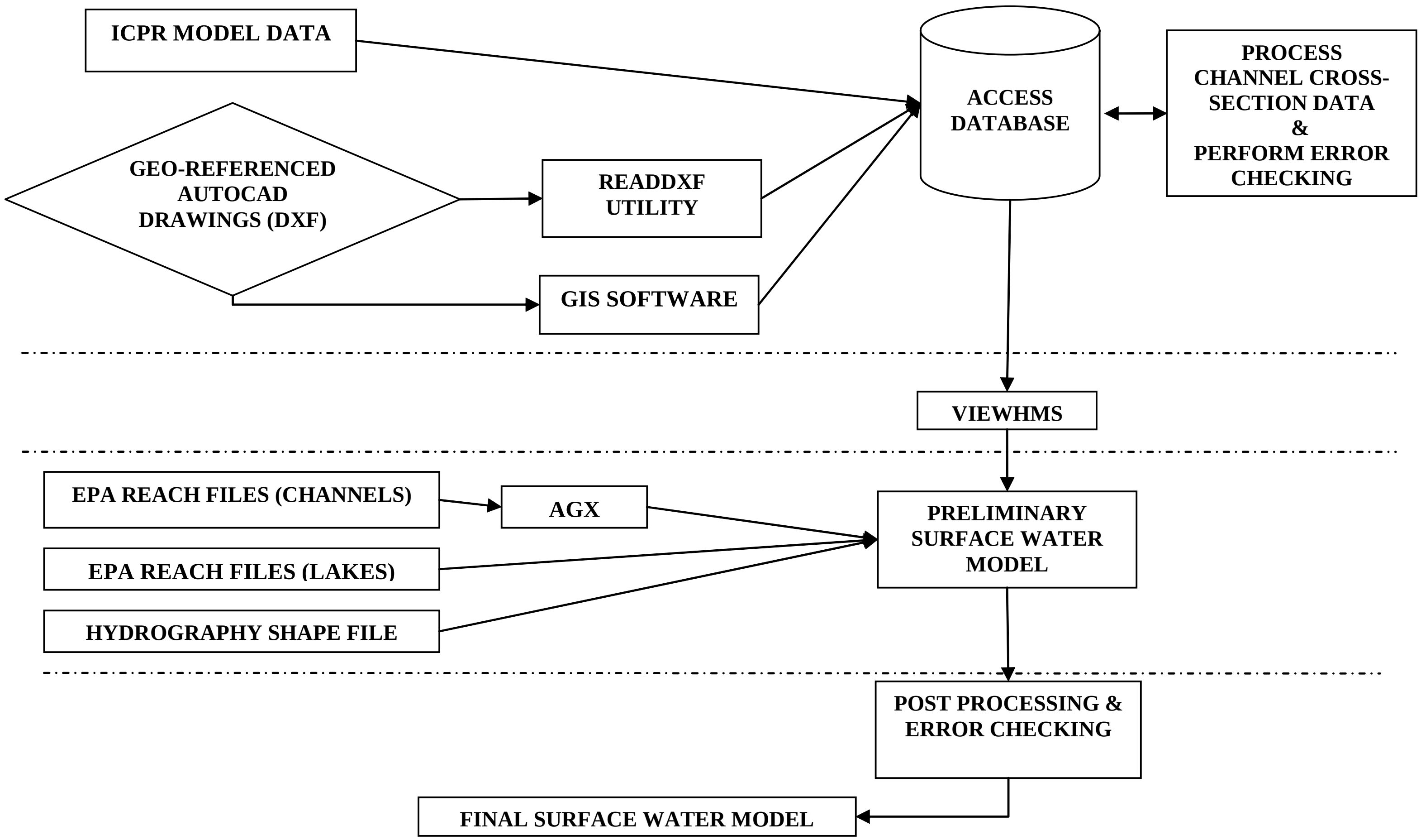

Source:
Filename: X:/SJR017/TO1/Maps/ Conceptual_model_report/Hydra_Convey_Features.mxd
Project: SJR017-001-99
Revised: 12/07/04 TB

Figure 4.3
Overview of Development of Hydraulic Conveyance Features of the WOSC-ISG

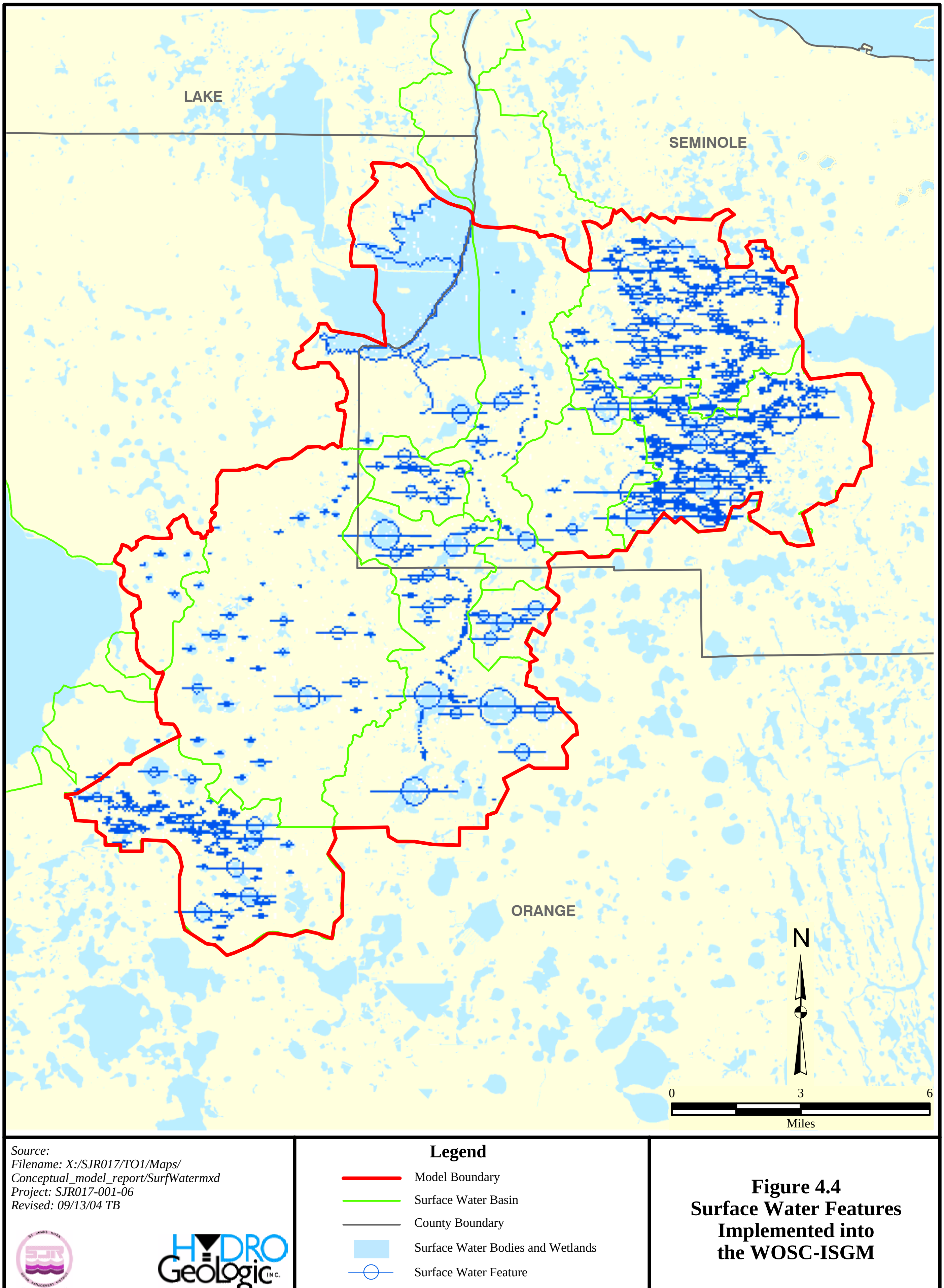

Source:
Filename: X:/SJR017/TO1/Maps/
Conceptual_model_report/SurfWatermxd
Project: SJR017-001-06
Revised: 09/13/04 TB

Figure 4.4
Surface Water Features Implemented into the WOSC-ISGM

Source:
Filename: X:/SJR017/TO1/Maps/
Conceptual_model_report/HHC_UpperSAS.mxd
Project: SJR017-001-99
Revised: 01/06/05 TB

Legend

- Model Boundary
- County Boundary
- Surface Water Basin
- Surface Water Bodies and Wetlands
- Surface-Water Stage Observations
- Surface-Water Flow - Actual Locations
- Surface-Water Flow - Locations Approximated In Model

Figure 4.5
Locations of Surface-Water Stage and Flow Observations for Steady-State Average 1995 Conditions

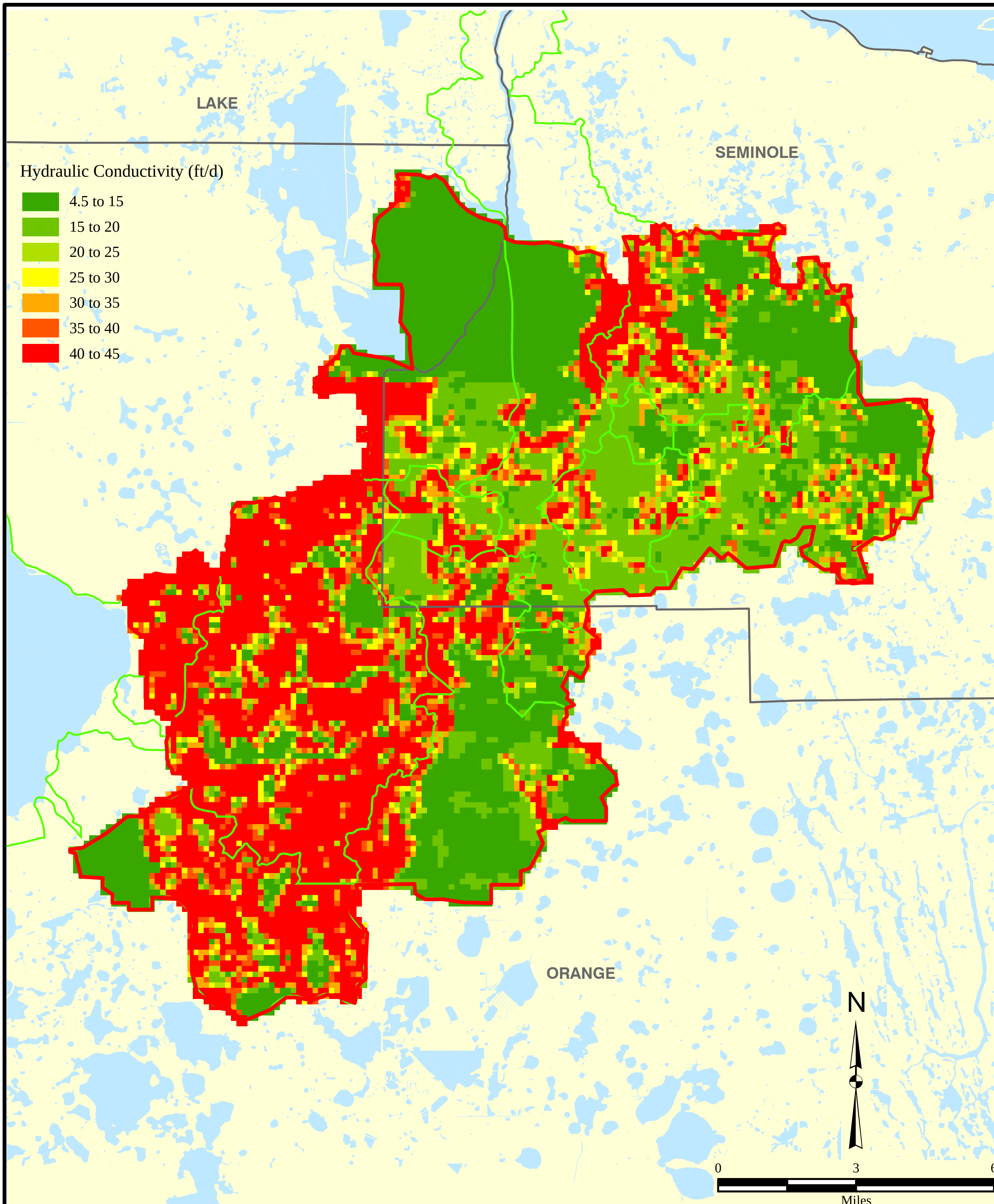

Source:
Filename: X:/SJR017/TO1/Maps/
Conceptual_model_report/HHC_Topsoil.mxd
Project: SJR017-001-06
Revised: 09/14/04 TB

Legend

Model Boundary
Surface Water Basin
County Boundary
Surface Water Bodies and Wetlands

Figure 6.1
Areal Distribution of Horizontal Hydraulic Conductivity of the Topsoil and Upper SAS Model Layers

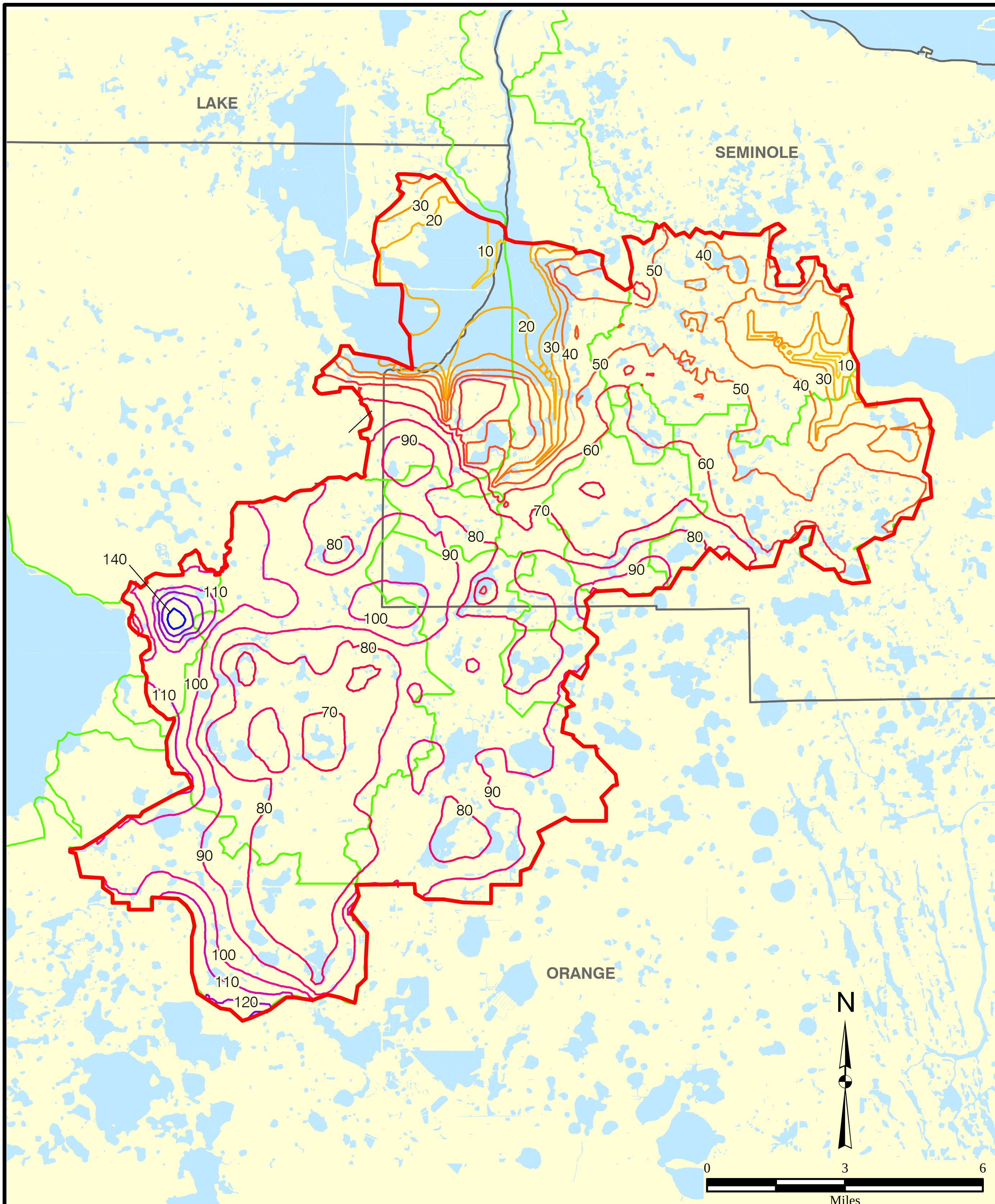

Source:
Filename: X:/SJR017/TO1/Maps/
Conceptual_model_report/SAS_WaterLevels.mxd
Project: SJR017-001-06
Revised: 09/14/04 TB

Legend

- Model Boundary
- Surface Water Basin
- County Boundary
- 50 Water Levels (ft)
- Surface Water Bodies and Wetlands

Figure 6.2
SAS Water Levels for the Second to Last Model Development Stage of Average 1995 Conditions

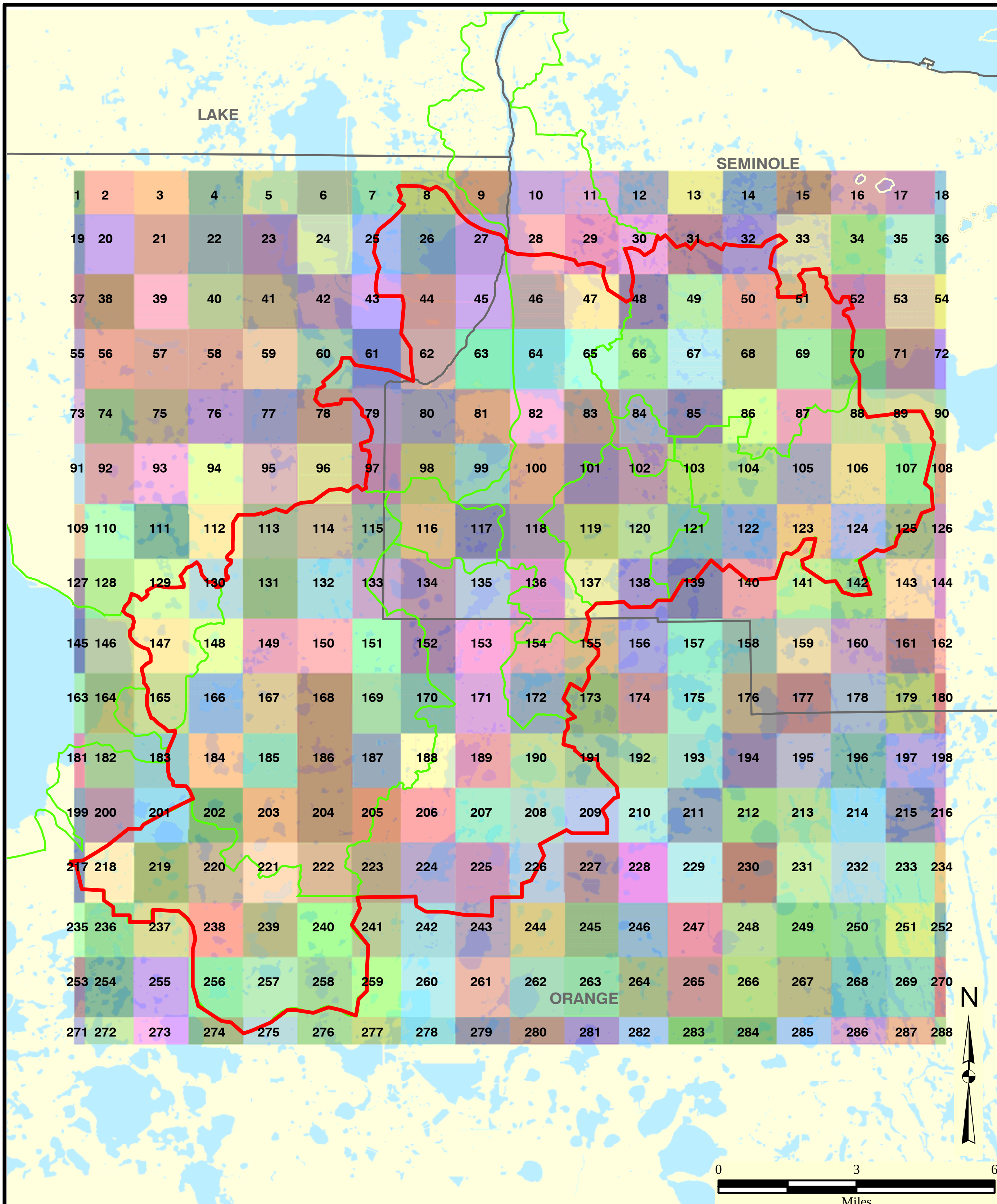

Source:
Filename: X:/SJR017/TO1/Maps/
Conceptual_model_report/NEXRADRainfall.mxd
Project: SJR017-001-99
Revised: 12/06/04 TB

Legend

- Model Boundary
- Surface Water Basin
- County Boundary
- Surface Water Bodies and Wetlands
- 42 NEXRAD Rainfall Pixels

Figure 6.3
Zones of NEXRAD Rainfall Applied on WOSC–ISGM Model Grid

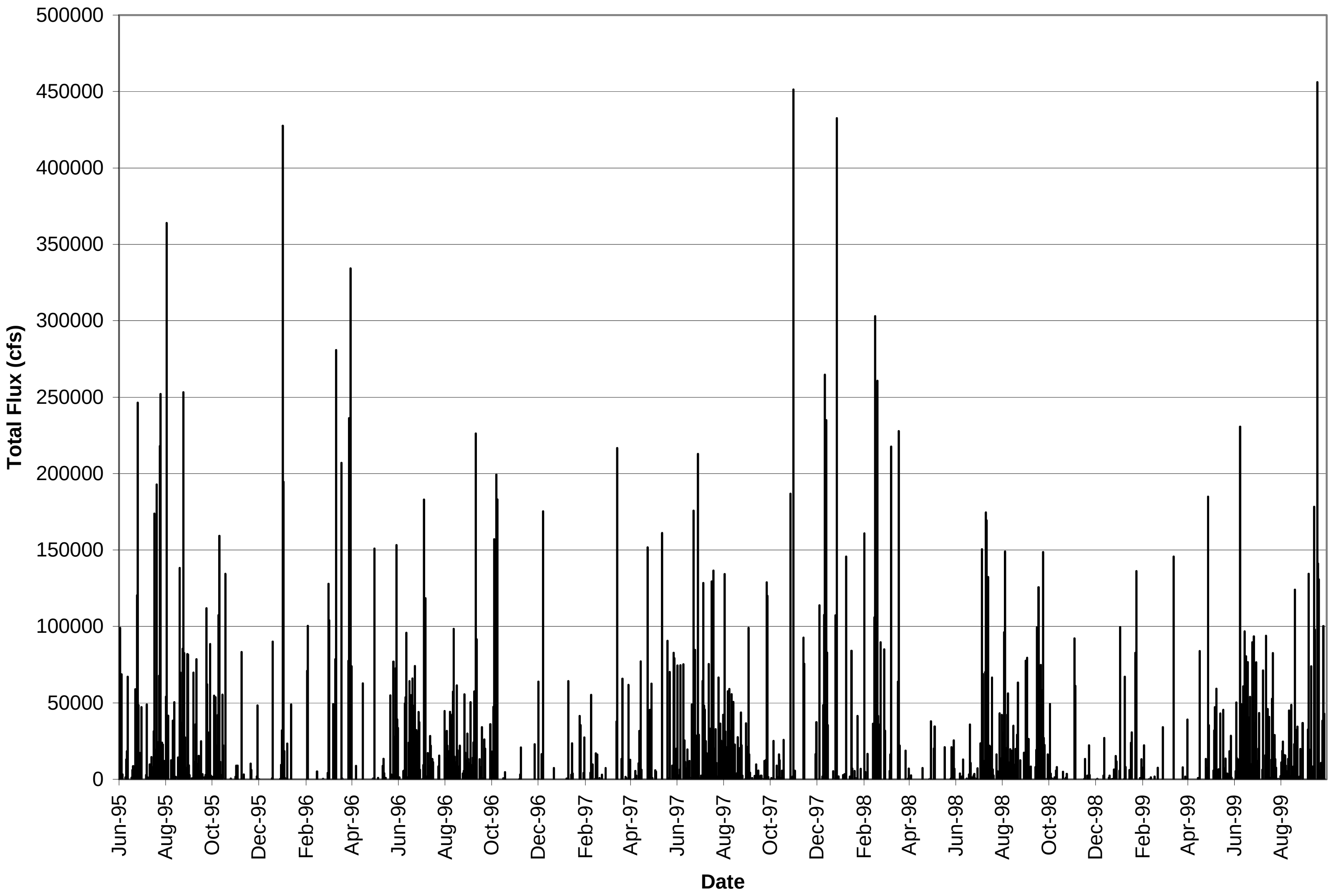

Source:
Filename: X:/SJR017/TO1/Maps/
Conceptual_model_report/Vol_Flux_NEXRAD.mxd
Project: SJR017-001-99
Revised: 12/07/04 TB

Figure 6.4
Cumulative Volumetric Flux over all NEXRAD Stations

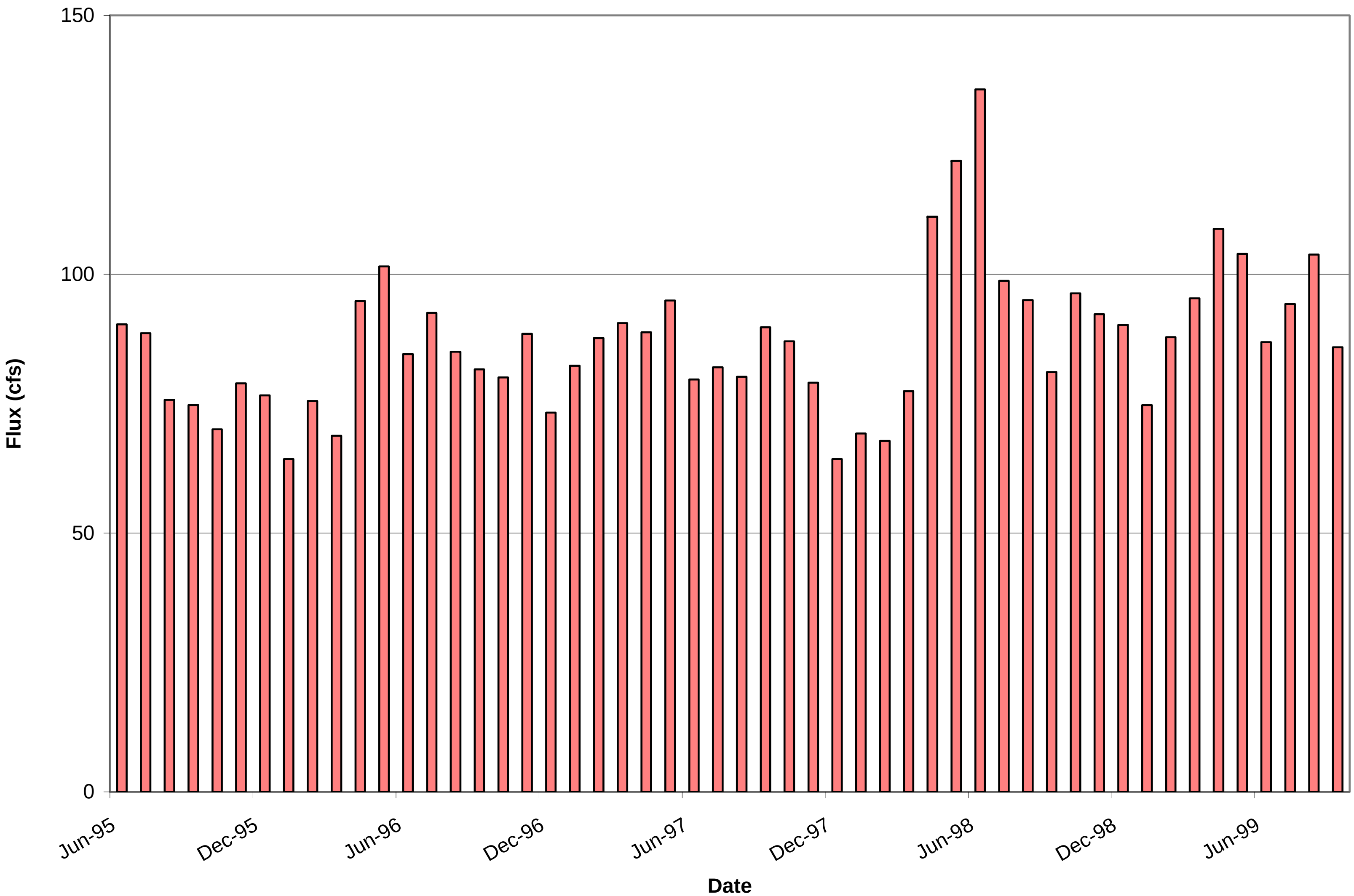

Source:
Filename: X:/SJR017/TO1/Maps/
Conceptual_model_report/Vol_Flux_AllWells.mxd
Project: SJR017-001-99
Revised: 12/07/04 TB

Figure 6.5
Cumulative Volumetric Flux
over all Wells Including RIBS
and Septic Tank Inflows

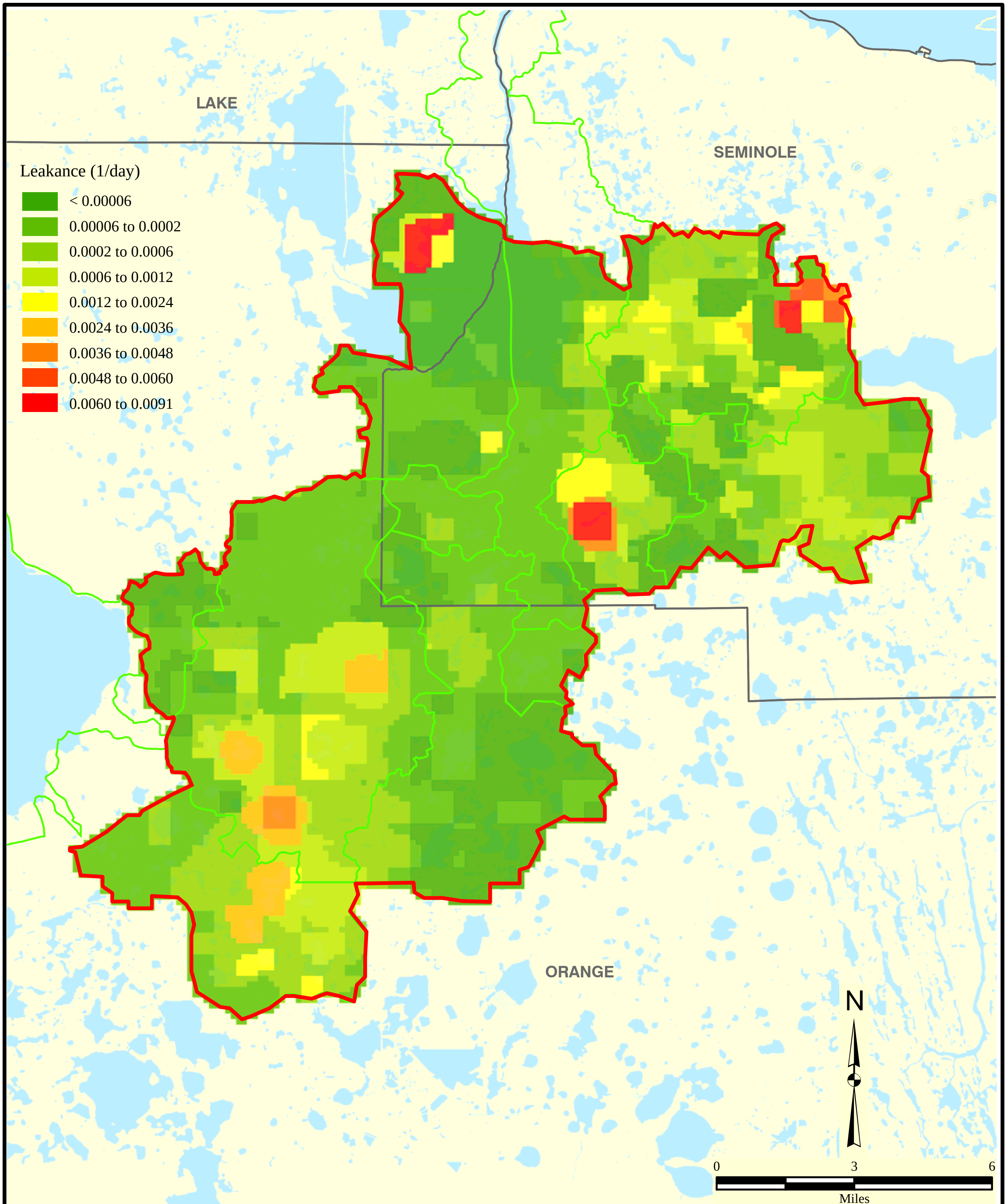

Source:
Filename: X:/SJR017/TO1/Maps/
Conceptual_model_report/Leak_ICU.mxd
Project: SJR017-001-99
Revised: 12/06/04 TB

Legend

Model Boundary
Surface Water Basin
County Boundary
Surface Water Bodies and Wetlands

Figure 6.6
Leakance Distribution of the ICU for the Calibrated WOSC-ISGM

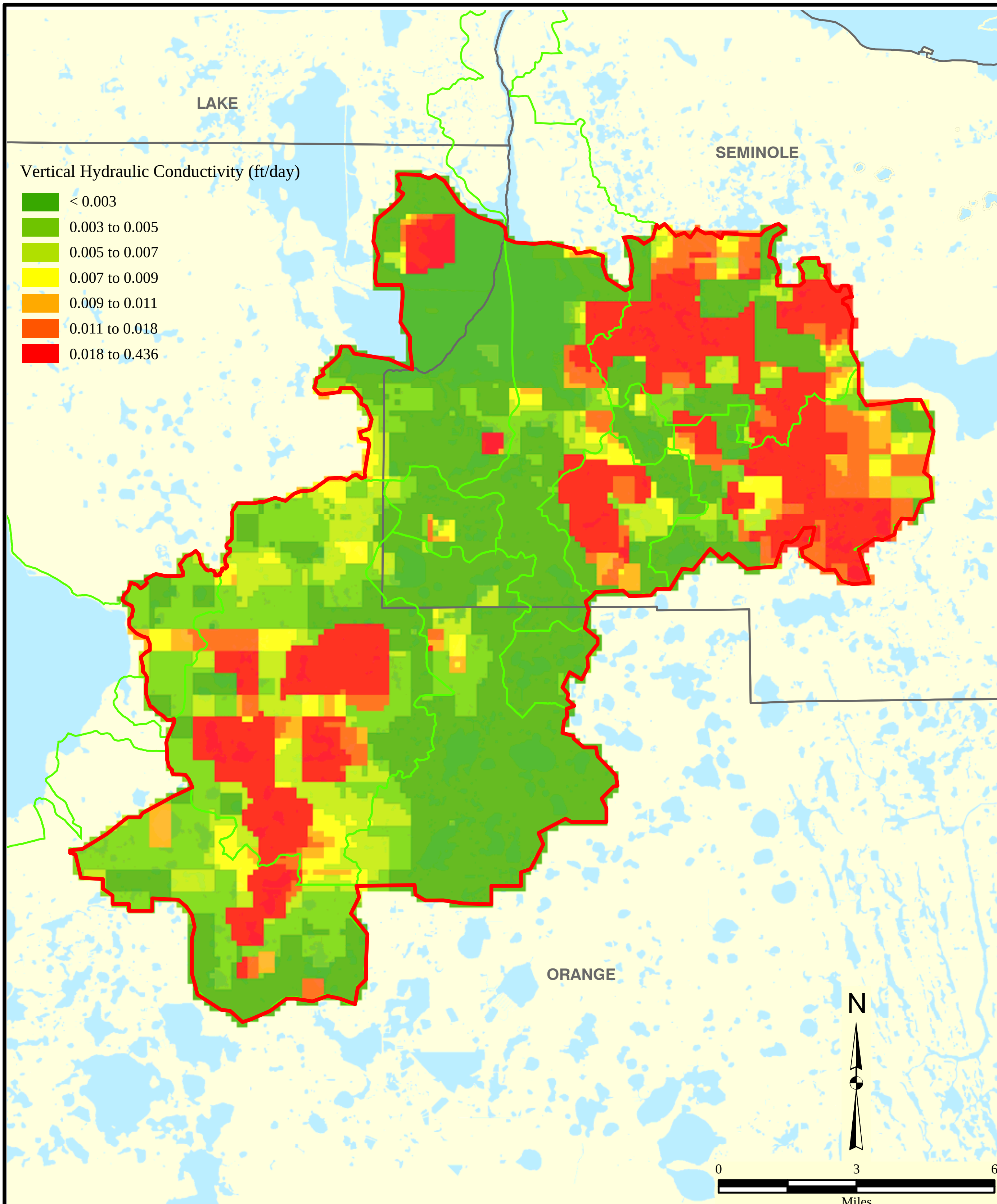

Source:
Filename: X:/SJR017/TO1/Maps/
Conceptual_model_report/Kv_ICU.mxd
Project: SJR017-001-99
Revised: 12/06/04 TB

Legend

- Model Boundary
- Surface Water Basin
- County Boundary
- Surface Water Bodies and Wetlands

Figure 6.7
Vertical Hydraulic Conductivity Distribution of the ICU for the Calibrated WOSC-ISGM

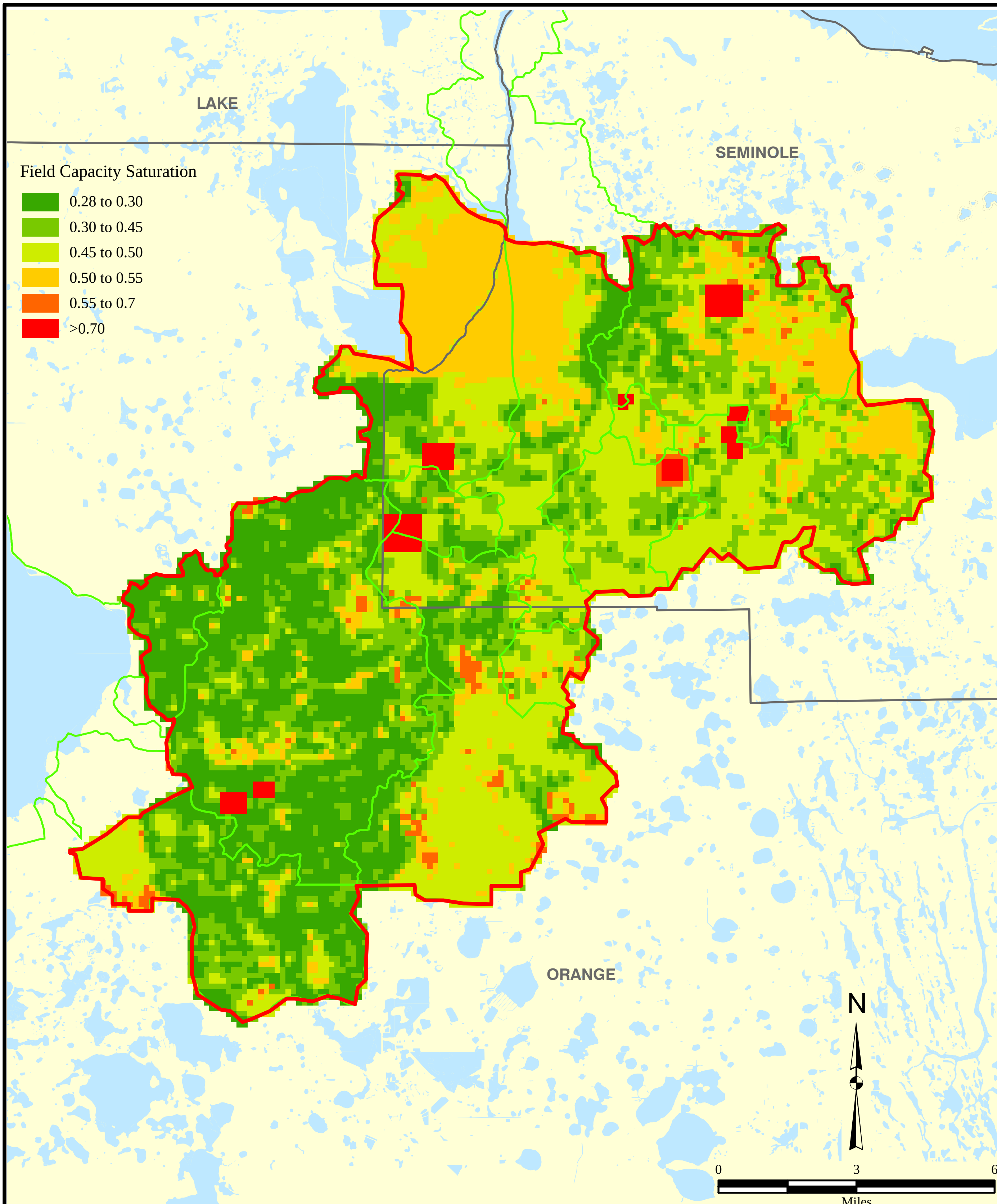

Source:
Filename: X:/SJR017/TO1/Maps/
Conceptual_model_report/S_fc.mxd
Project: SJR017-001-99
Revised: 11/30/04 TB

Legend

Model Boundary
Surface Water Basin
County Boundary
Surface Water Bodies and Wetlands

Figure 6.8
Field Capacity
Saturation Distribution
for the Calibrated
WOSC-ISGM

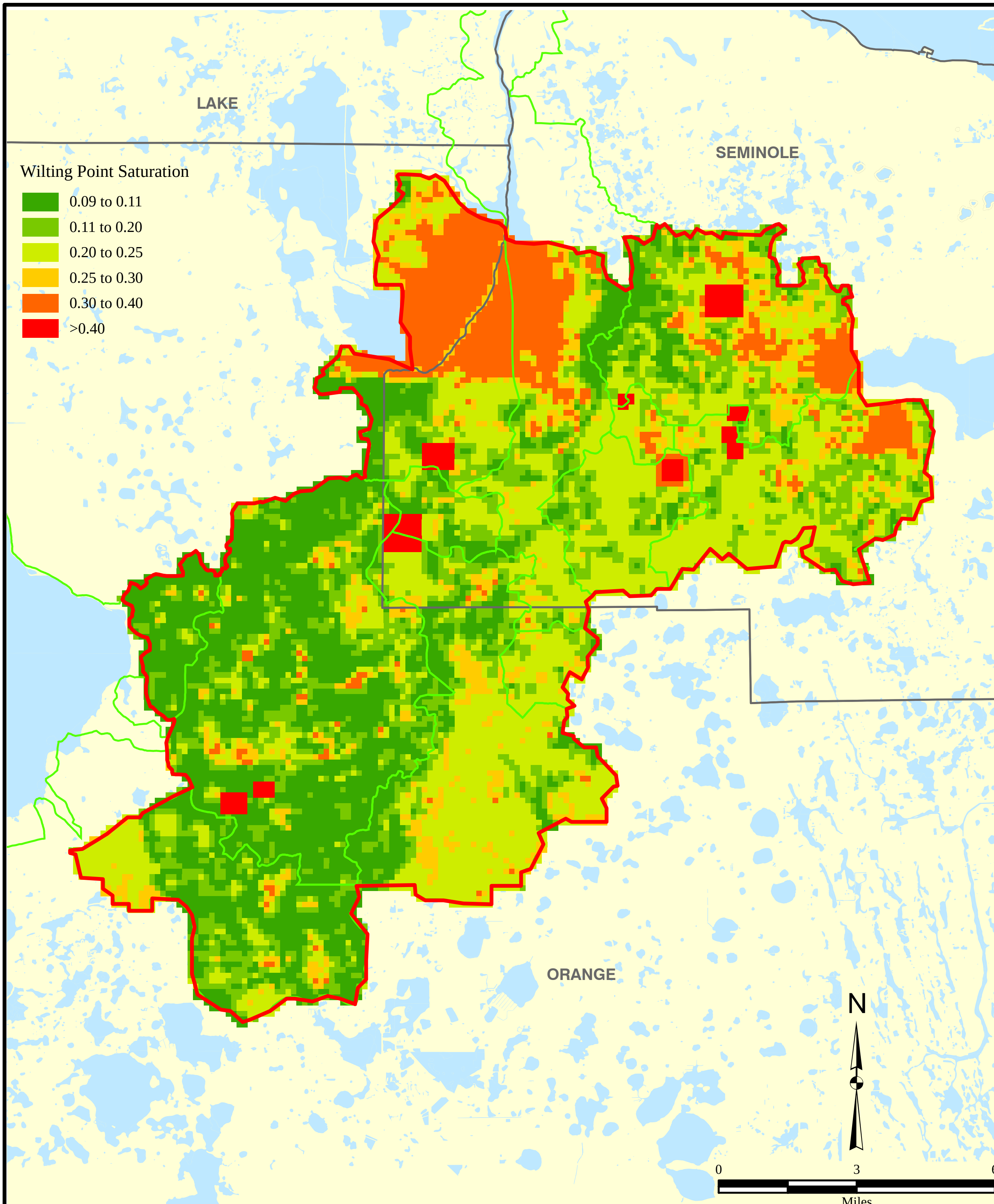

Source:
Filename: X:/SJR017/TO1/Maps/
Conceptual_model_report/S_wp.mxd
Project: SJR017-001-99
Revised: 11/30/04 TB

Legend

- Model Boundary
- Surface Water Basin
- County Boundary
- Surface Water Bodies and Wetlands

Figure 6.9
Wilting Point Saturation Distribution for the Calibrated WOSC-ISGM

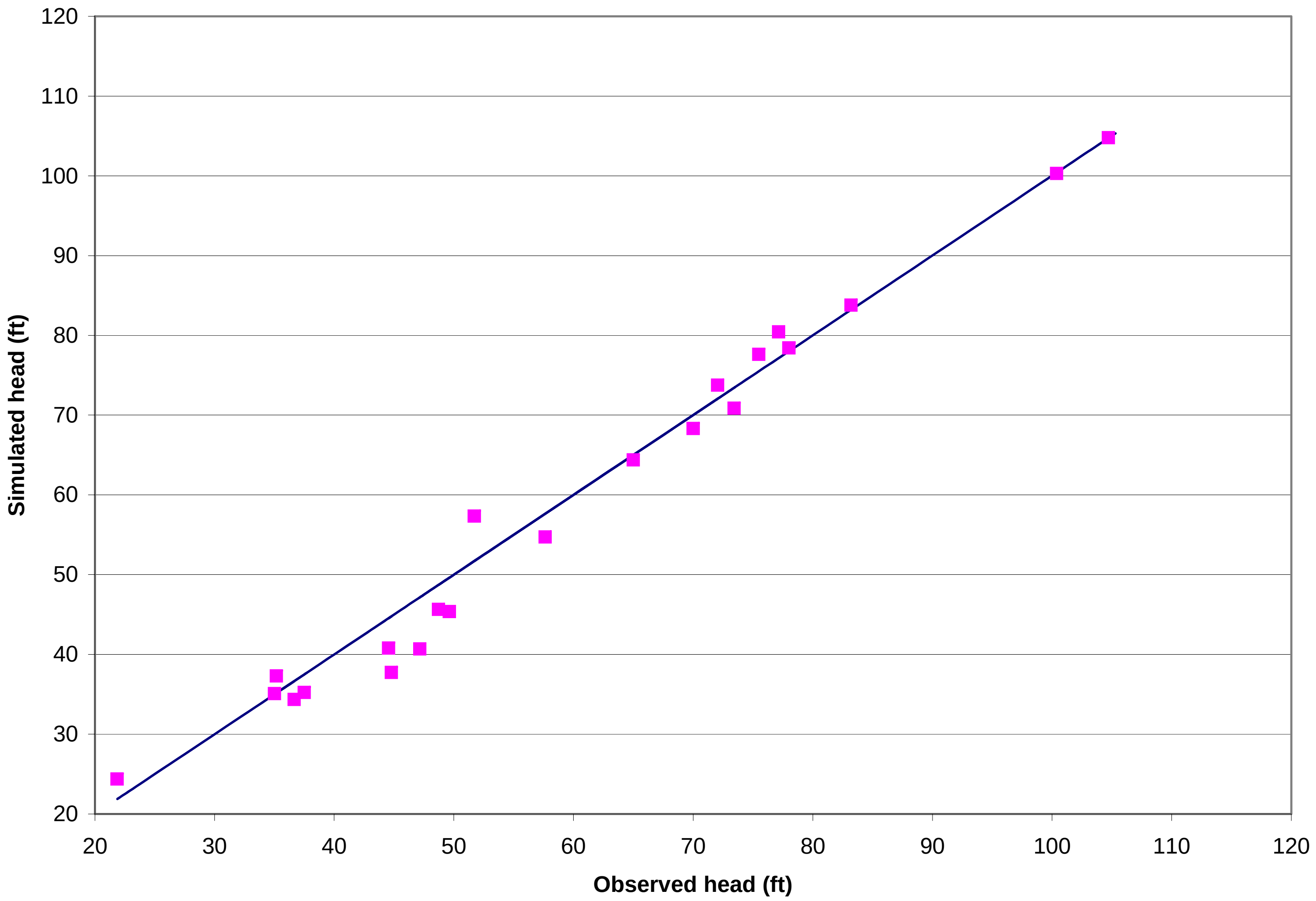

Source:
Filename: X:/SJR017/TO1/Maps/ Conceptual_model_report/residual-brook-gw1.mxd
Project: SJR017-001-99
Revised: 12/07/04 TB

Legend

Observed

Simulated

Statistics

Average = 0.85
RMS = 3.1885
Maximum = 7.05
R^2 = 0.9803

Figure 7.1
Observed versus Simulated Subsurface Heads for Steady-State Average 1995 Conditions of the WOSC-ISGM

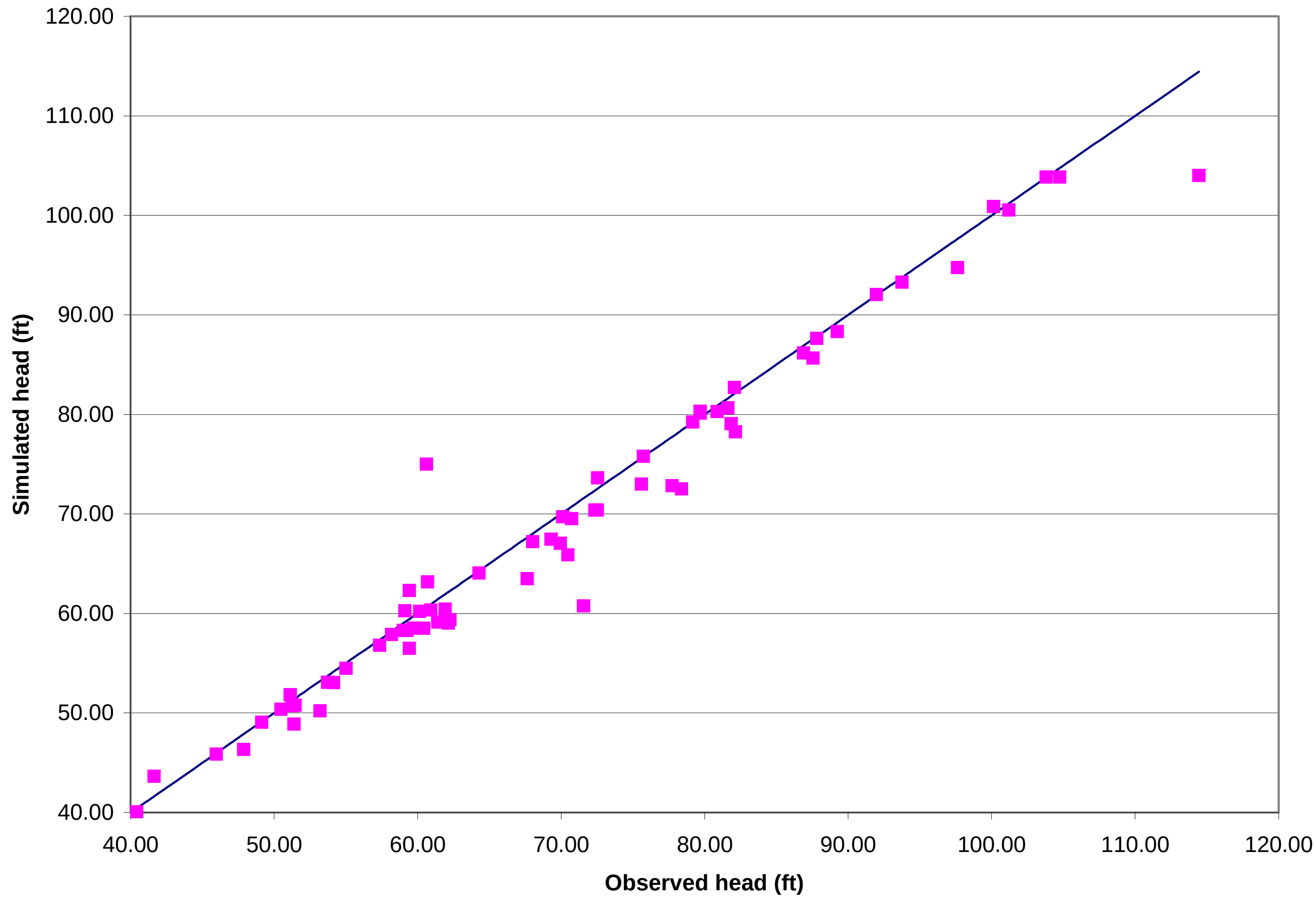

Source:
Filename: X:/SJR017/TO1/Maps/Conceptual_model_report/residual-brook-sw.mxd
Project: SJR017-001-99
Revised: 12/31/04 TB

Legend

Observed
Simulated

Statistics

Average = 1.1
RMS = 3.1742
Maximum = 14.37
R^2 = 0.967

Figure 7.2
Observed versus Simulated Water Levels of Lakes and Ponds for Steady-State Average 1995 Conditions of the WOSC-ISGM

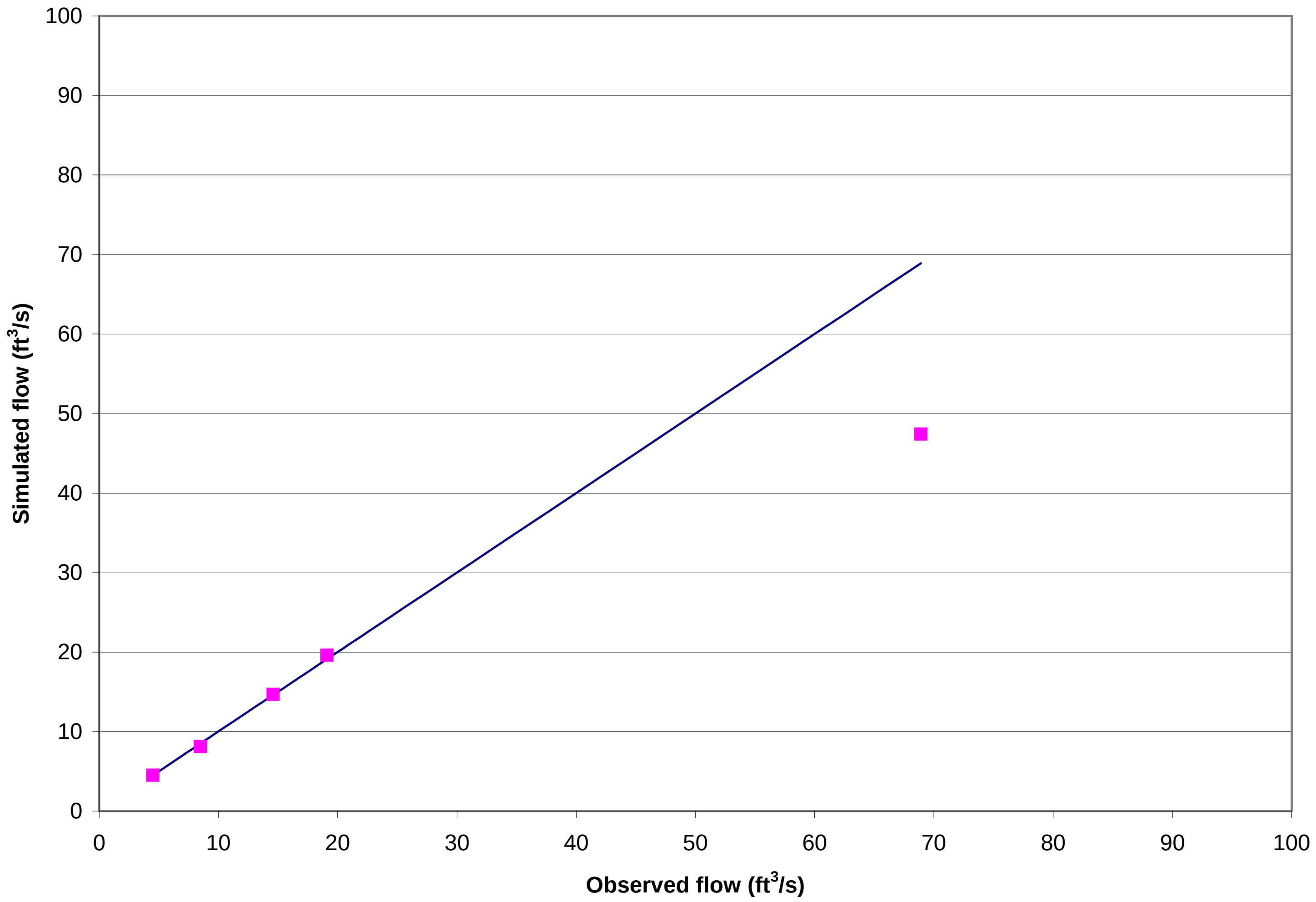

Source:
Filename: X:/SJR017/TO1/Maps/ Conceptual_model_report/residual-brook-springs.mxd
Project: SJR017-001-99
Revised: 12/31/04 TB

Legend

Observed

Simulated

Statistics

Average = 4.26
RMS = 9.6195
Maximum = 21.50
R^2 = 0.9467

Figure 7.3
Observed versus Simulated Spring Fluxes for Steady-State Average 1995 Conditions of the WOSC-ISGM

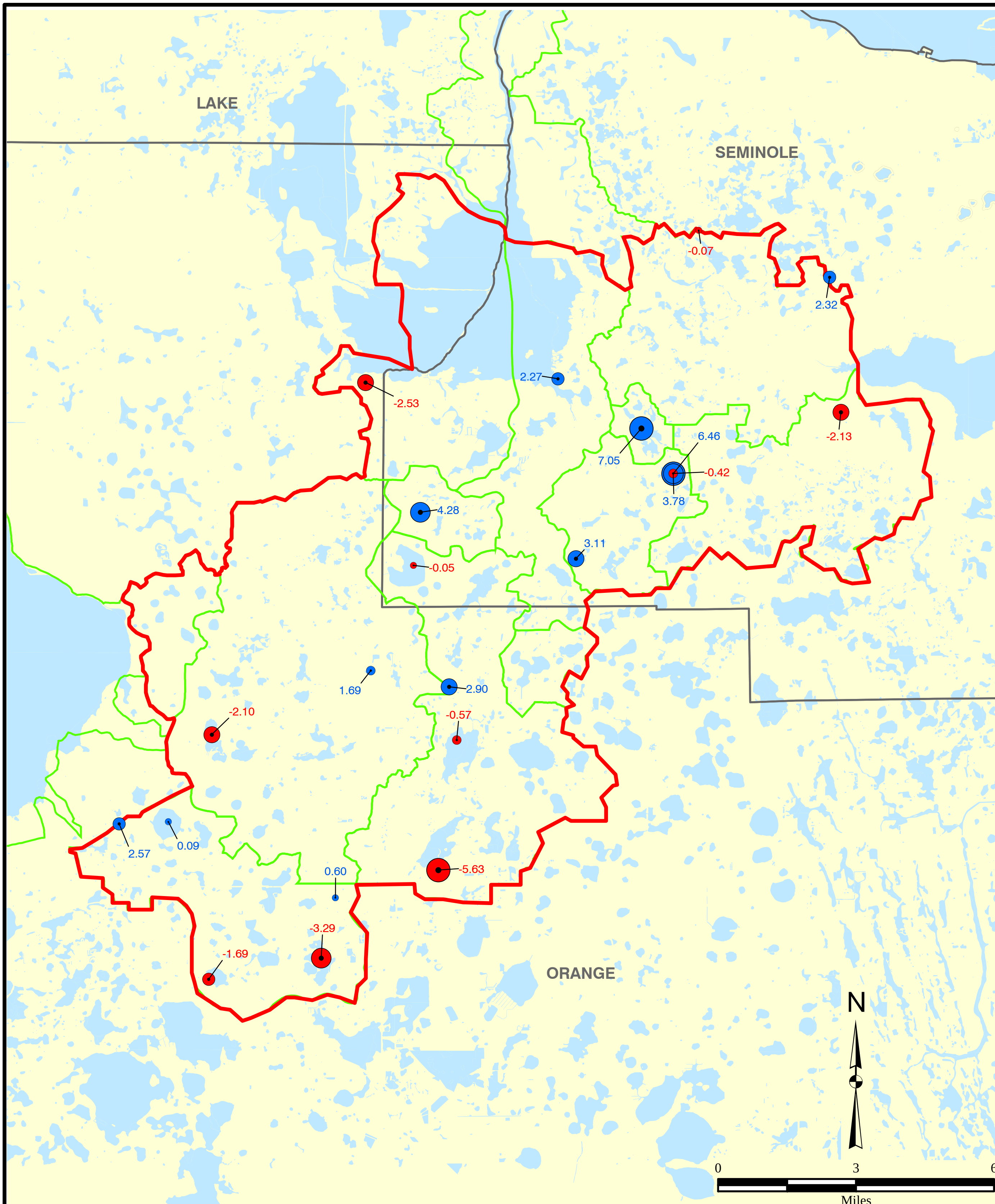

Source:
Filename: X:/SJR017/TO1/Maps/
Conceptual_model_report/Head_Resid.mxd
Project: SJR017-001-99
Revised: 12/31/04 TB

Legend

Model Boundary
Surface Water Basin
County Boundary
Surface Water Bodies and Wetlands
Head Residuals Red - Negative Blue - Positive

Figure 7.4
Spatial Distribution of Head Residuals for the Subsurface for Steady-State Average 1995 Conditions of the WOSC-ISGM

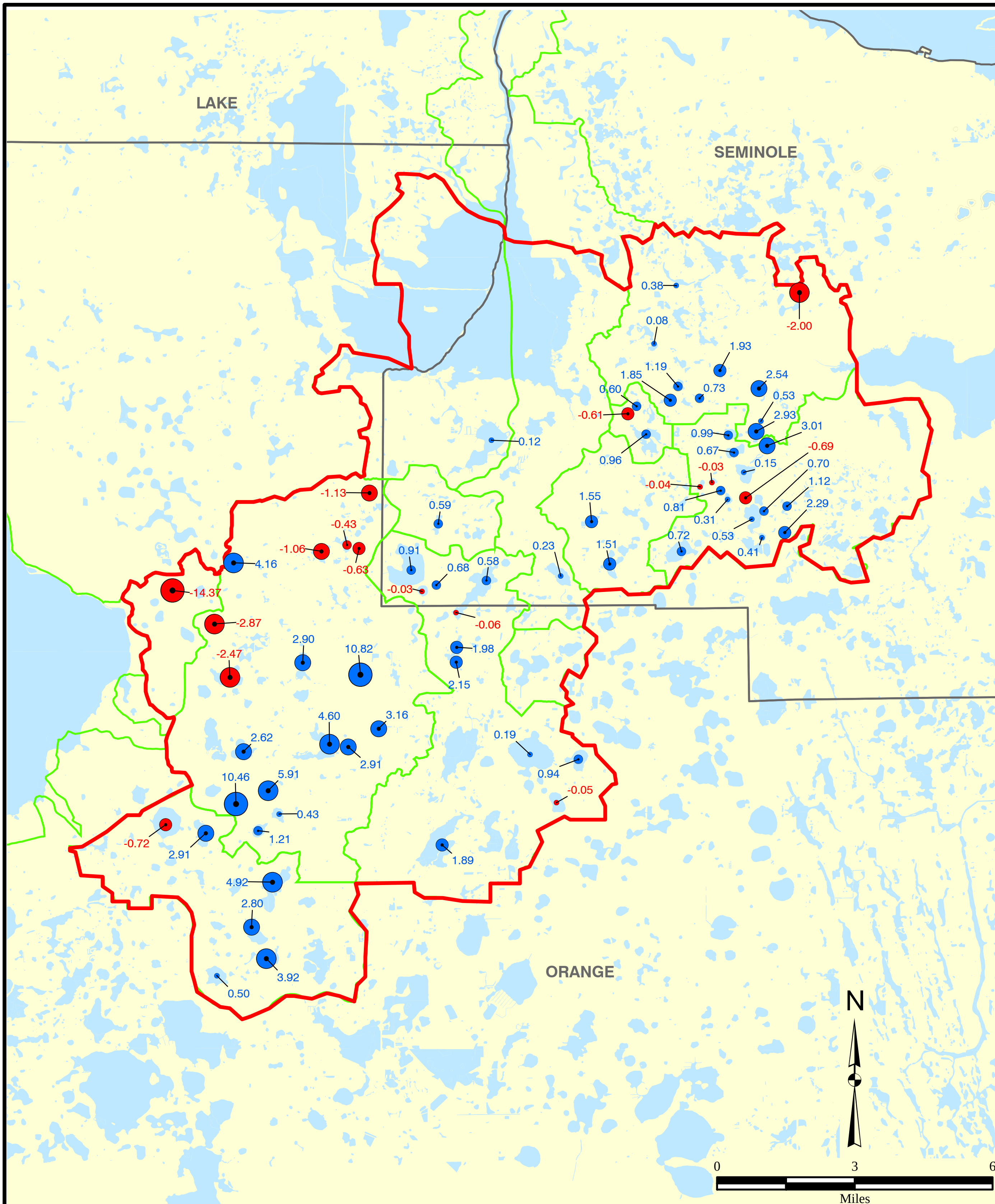

Source:
Filename: X:/SJR017/TO1/Maps/
Conceptual_model_report/WL_Resid.mxd
Project: SJR017-001-99
Revised: 12/31/04 TB

Legend

- Model Boundary
- Surface Water Basin
- County Boundary
- Surface Water Bodies and Wetlands
- Water-Level Residuals — Red - Negative; Blue - Positive

Figure 7.5
Spatial Distribution of Water-Level Residuals for Lakes and Ponds for Steady-State Average 1995 Conditions of the WOSC-ISGM

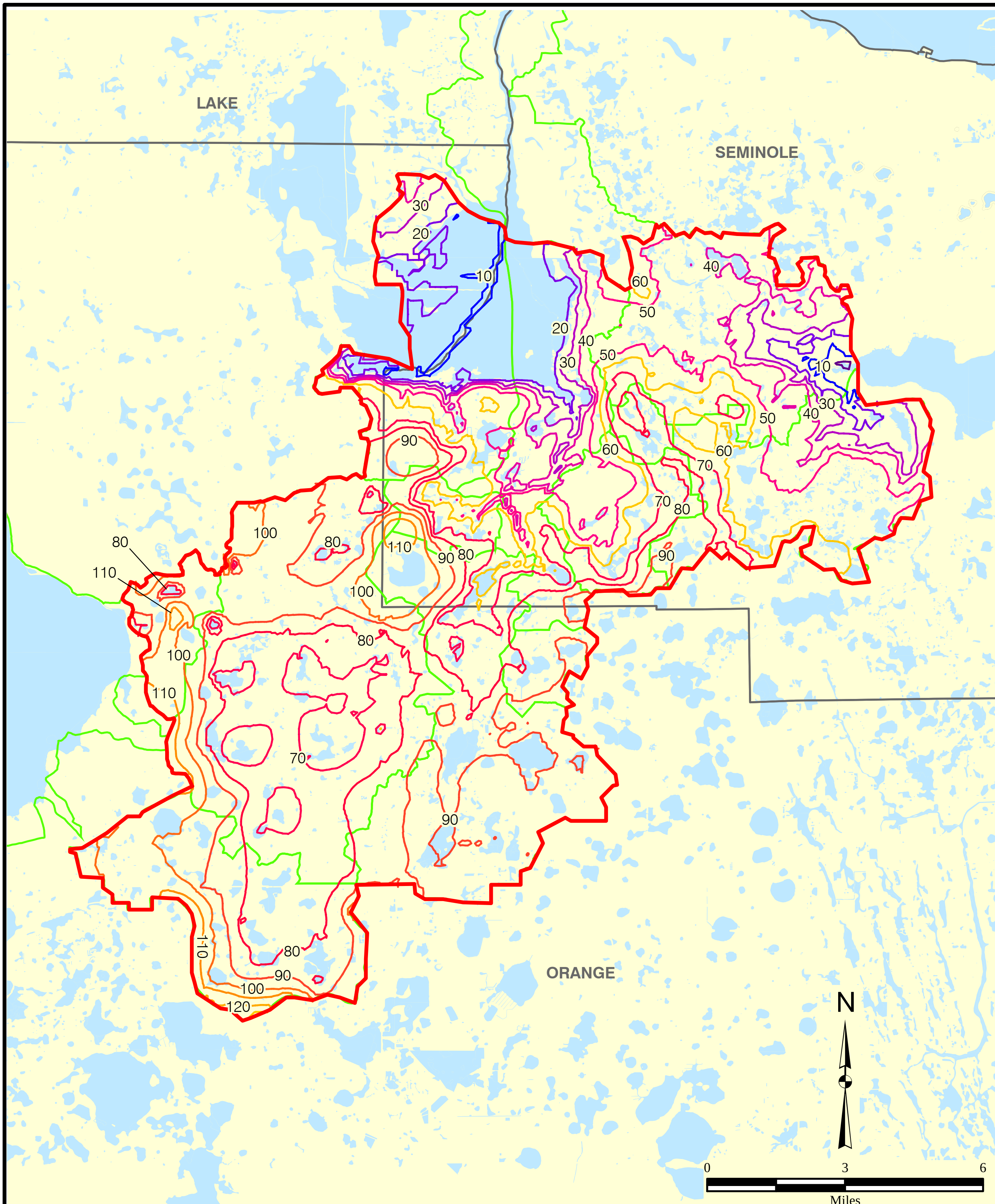

Source:
Filename: X:/SJR017/TO1/Maps/
Conceptual_model_report/HeadVal_SAS.mxd
Project: SJR017-001-99
Revised: 12/06/04 TB

Legend

Model Boundary
Surface Water Basin
County Boundary
50 Head Values (ft)
Surface Water Bodies and Wetlands

Figure 7.6
Simulated Head Values in the SAS for Steady-State Average 1995 Conditions of the WOSC-ISGM

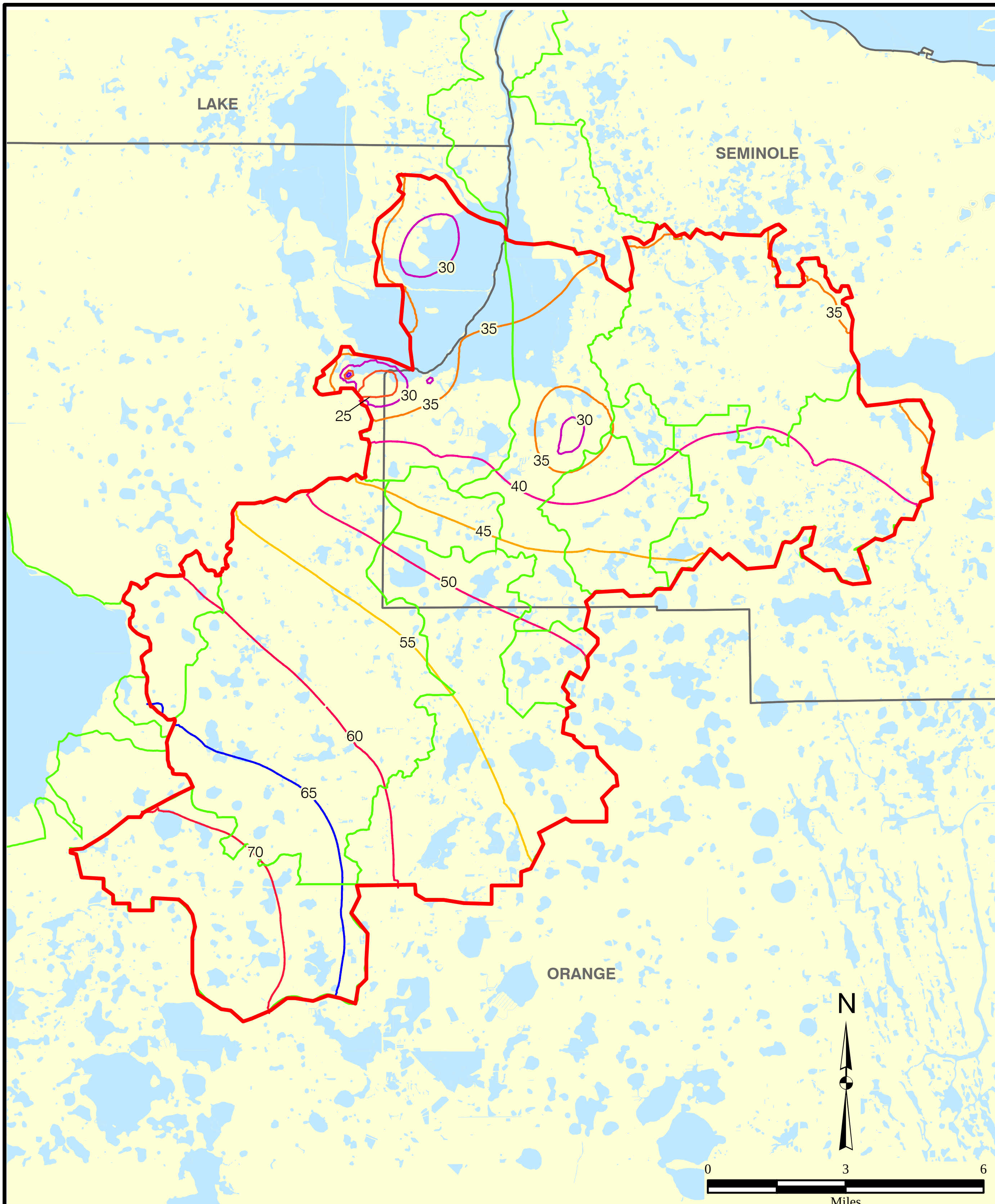

Source:
Filename: X:/SJR017/TO1/Maps/
Conceptual_model_report/HeadVal_UFA-UZ.mxd
Project: SJR017-001-99
Revised: 12/06/04 TB

Legend

Model Boundary
Surface Water Basin
County Boundary
50 Head Value (ft)
Surface Water Bodies and Wetlands

Figure 7.7
Simulated Head Values in the UFA-UZ for Steady-State Average 1995 Conditions of the WOSC-ISGM

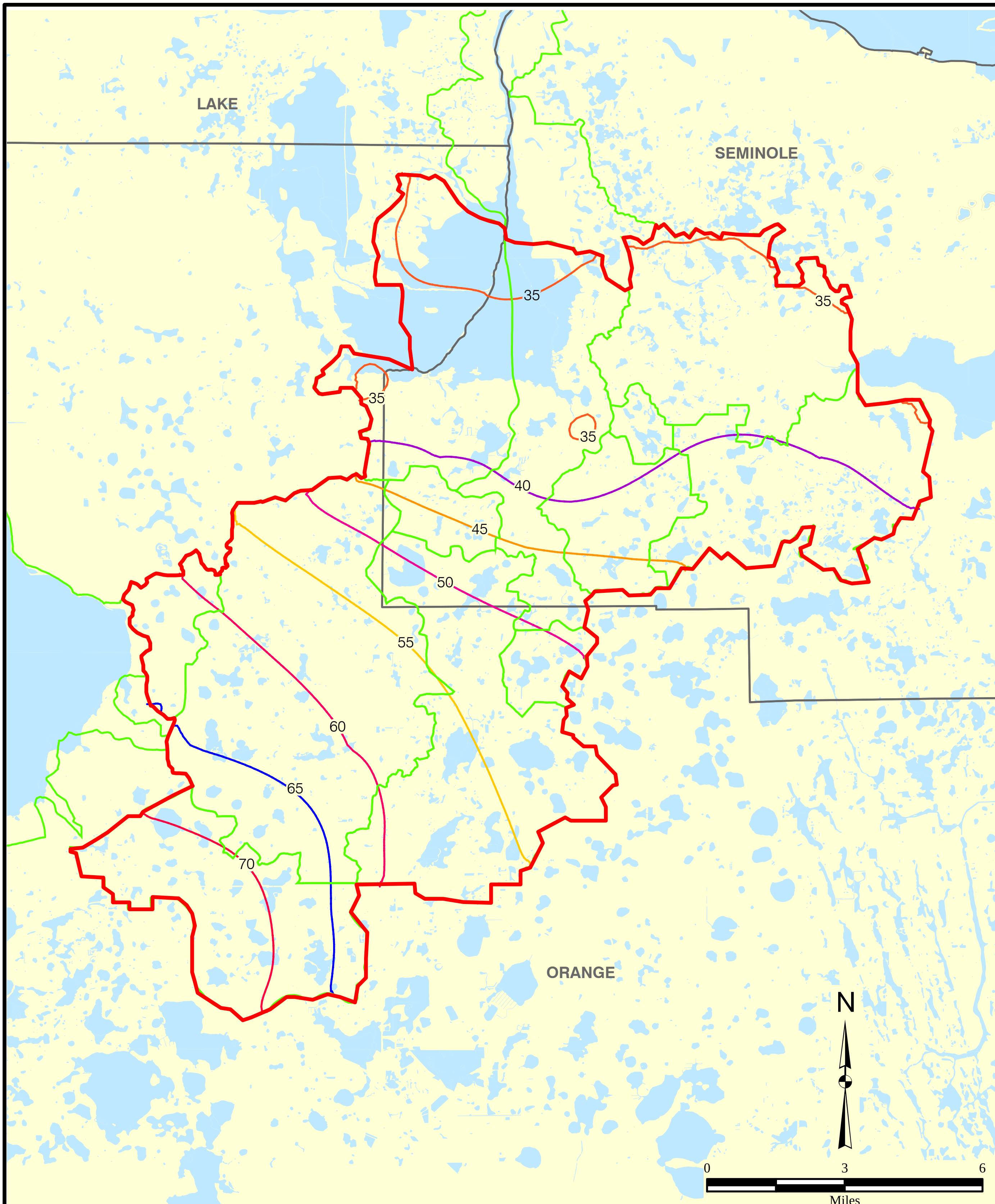

Source:
Filename: X:/SJR017/TO1/Maps/
Conceptual_model_report/HeadVal_UFA-DZmxd
Project: SJR017-001-99
Revised: 12/06/04 TB

Legend

- Model Boundary
- Surface Water Basin
- County Boundary
- 50 Head Values (ft)
- Surface Water Bodies and Wetlands

Figure 7.8
Simulated Head Values in the UFA-DZ for Steady-State Average 1995 Conditions of the WOSC-ISGM

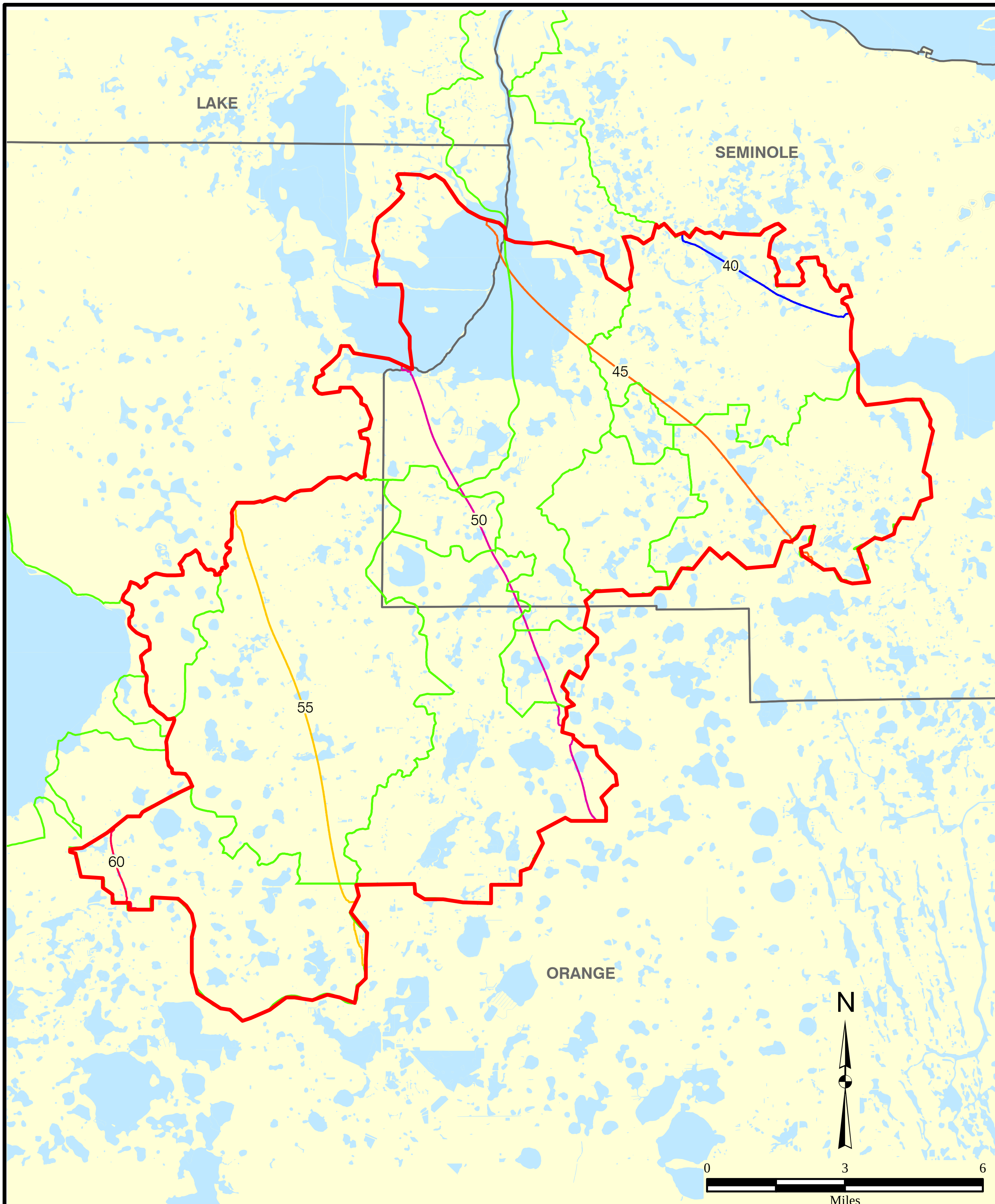

Source:
Filename: X:/SJR017/TO1/Maps/
Conceptual_model_report/HeadVal_LFA.mxd
Project: SJR017-001-99
Revised: 12/06/04 TB

Legend

- Model Boundary
- Surface Water Basin
- County Boundary
- 50 Head Value(ft)
- Surface Water Bodies and Wetlands

Figure 7.9
Simulated Head Values in the LFA for Steady-State Average 1995 Conditions of the WOSC-ISGM

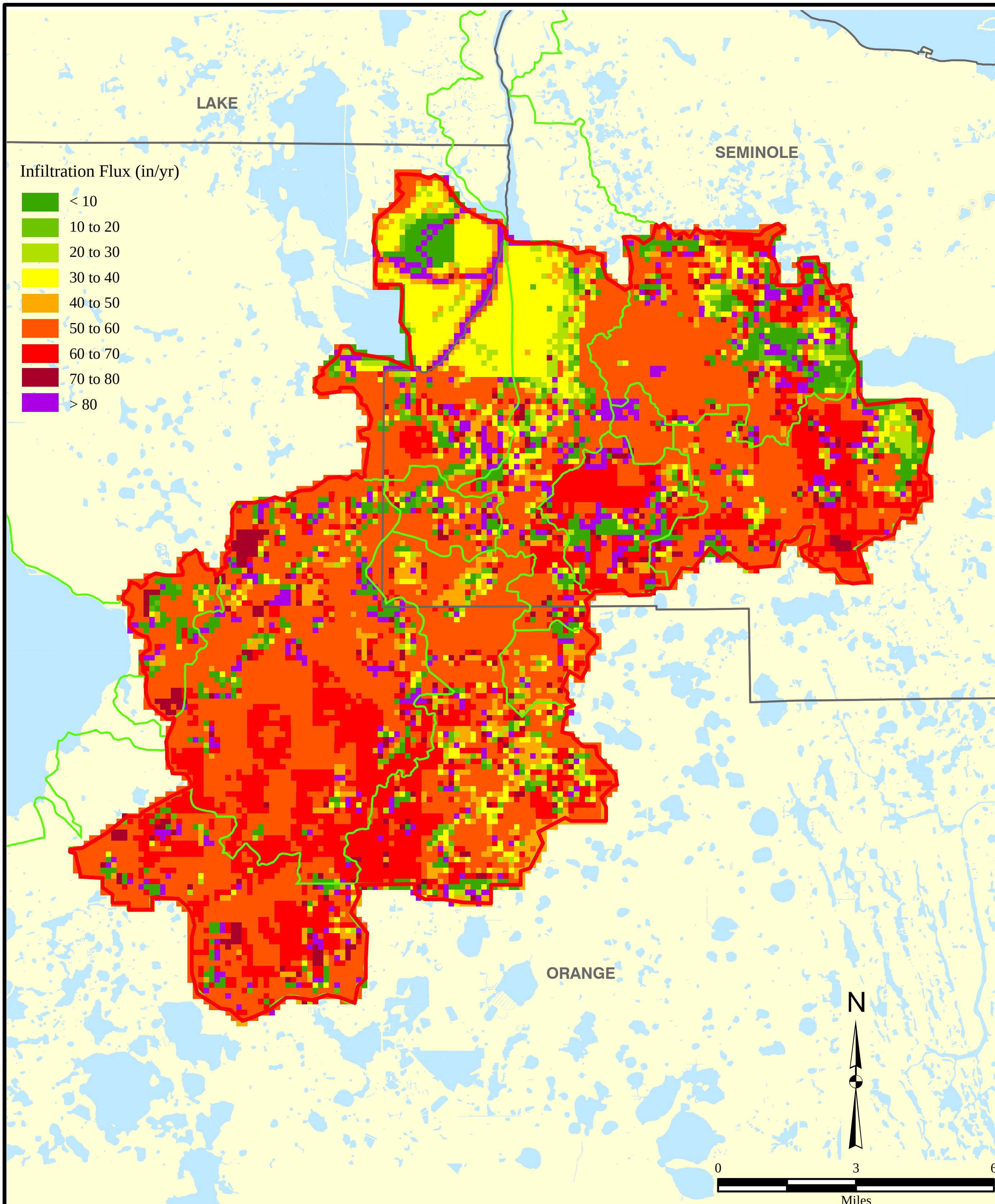

Source:
Filename: X:/SJR017/TO1/Maps/
Conceptual_model_report/SSDI.mxd
Project: SJR017-001-99
Revised: 11/30/04 TB

Legend

- Model Boundary
- Surface Water Basin
- County Boundary
- Surface Water Bodies and Wetlands

Figure 7.10
Simulated Spatial Distribution of Infiltration for Steady-State Average 1995 Conditions of the WOSC-ISGM

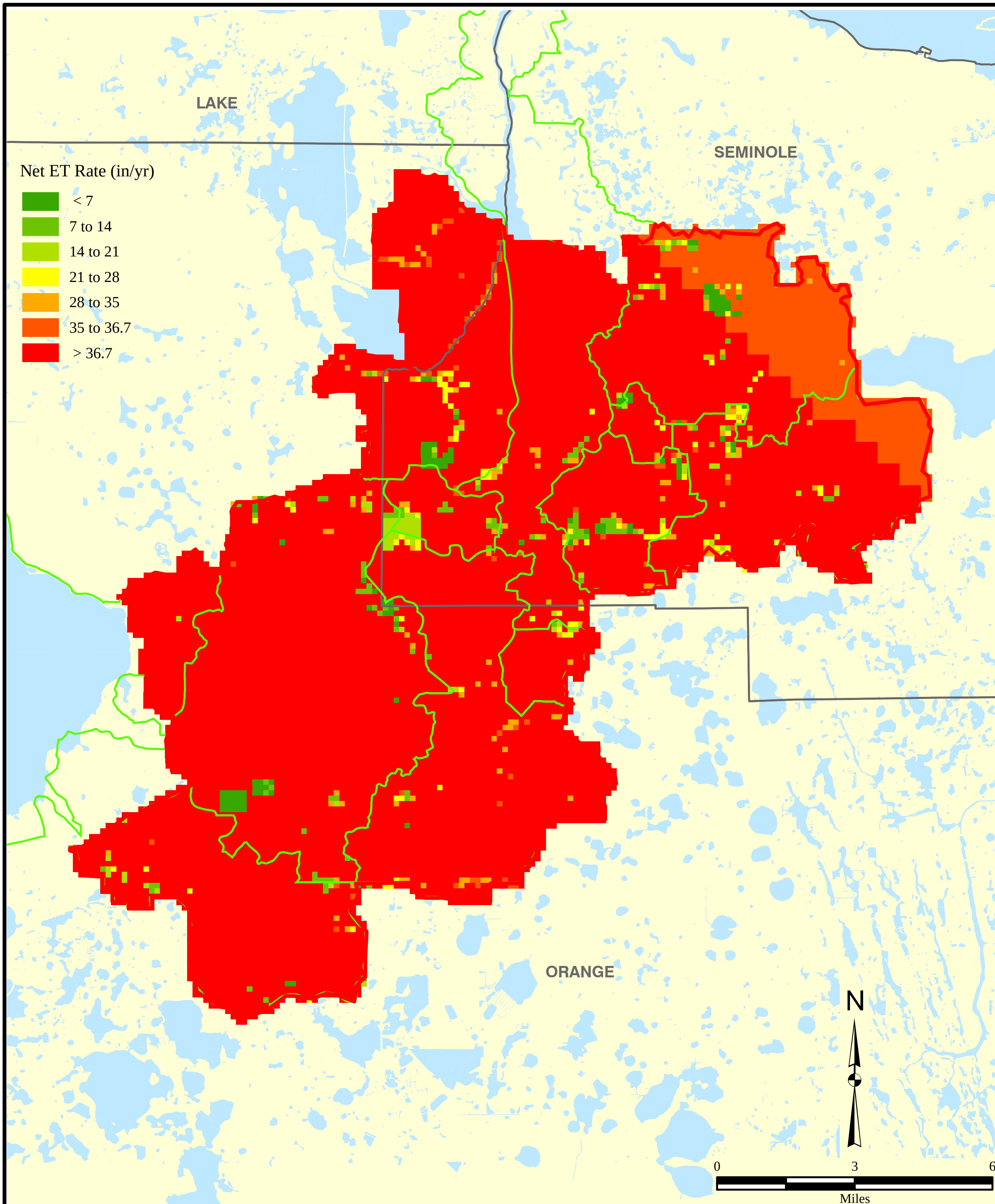

Source:
Filename: X:/SJR017/TO1/Maps/
Conceptual_model_report/SSDNetET.mxd
Project: SJR017-001-99
Revised: 11/30/04 TB

Legend

- Model Boundary
- Surface Water Basin
- County Boundary
- Surface Water Bodies and Wetlands

Figure 7.11
Simulated Spatial Distribution of Net ET for Steady-State Average 1995 Conditions of the WOSC-ISGM

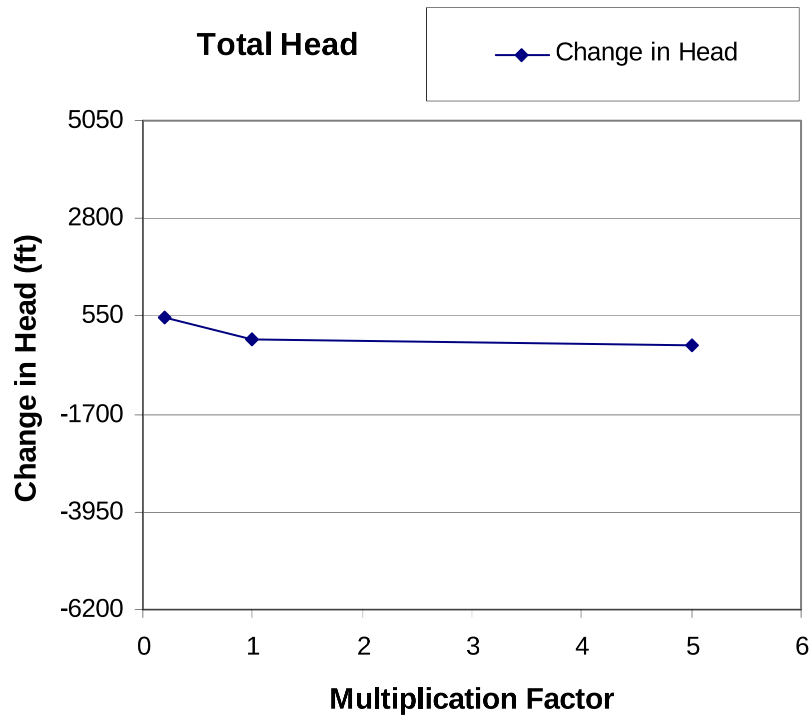

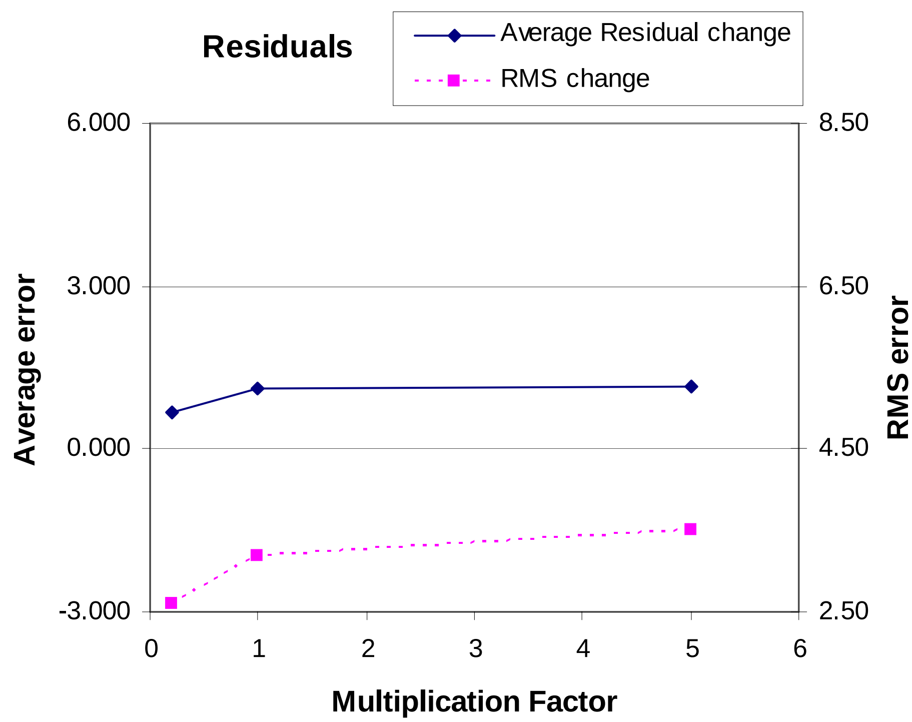

Source:
Filename: X:/SJR017/TO1/Maps/ Conceptual_model_report/Sens_OL_Surf.mxd
Project: SJR017-001-99
Revised: 12/22/04 TB

Figure 8.1a
Sensitivity to Overland Leakance in the Surface Domain

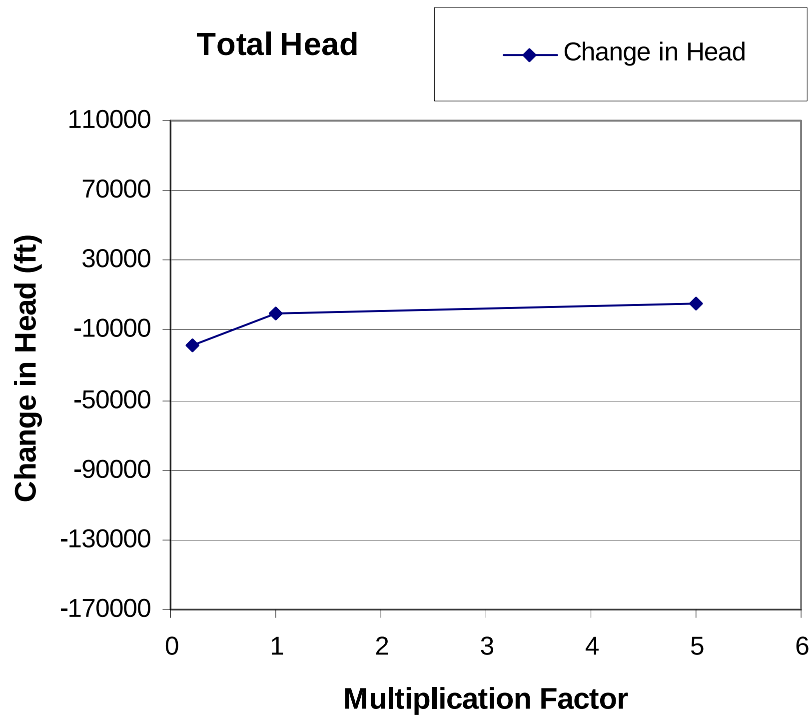

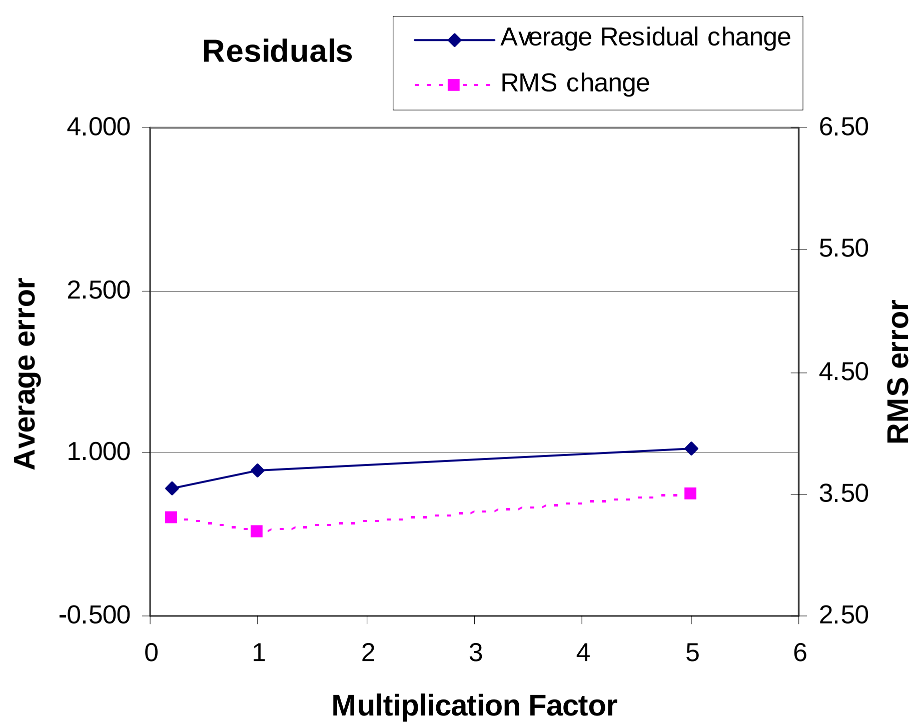

Source:
Filename: X:/SJR017/TO1/Maps/Conceptual_model_report/Sens_OL_SubSurf.mxd
Project: SJR017-001-99
Revised: 12/22/04 TB

Figure 8.1b
Sensitivity to Overland Leakance in the Subsurface Domain

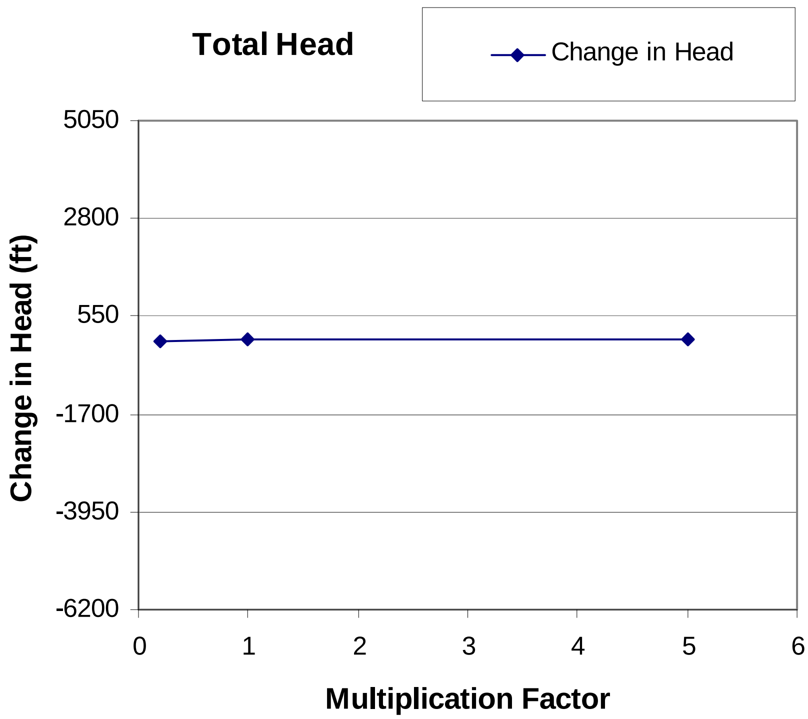

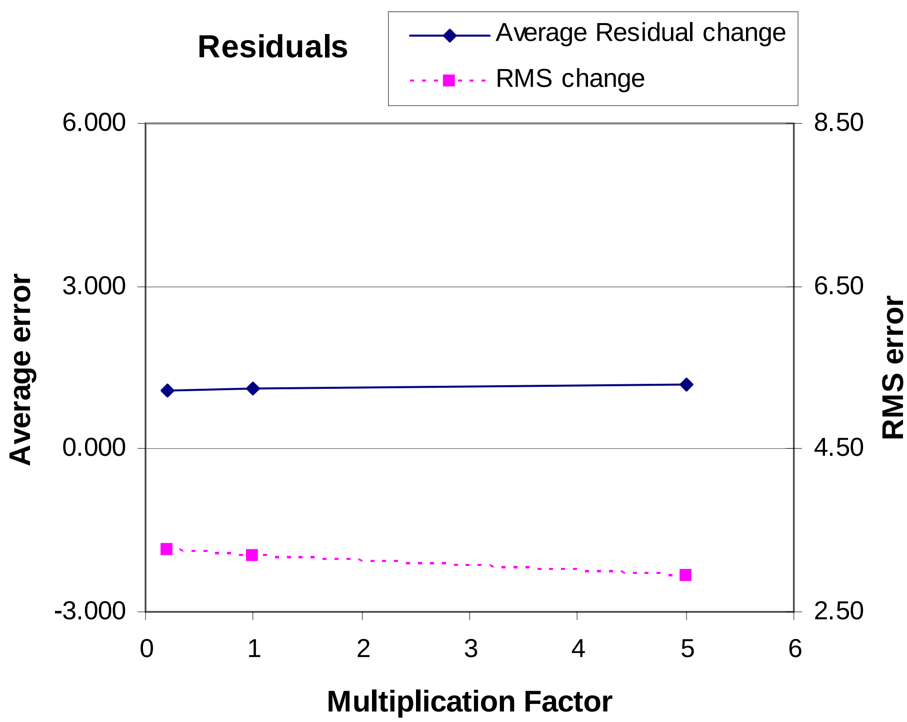

Source:
Filename: X:/SJR017/TO1/Maps/
Conceptual_model_report/Sens_OMC_Surf.mxd
Project: SJR017-001-99
Revised: 12/22/04 TB

Figure 8.2a
Sensitivity to Overland Manning's Coefficient in the Surface Domain

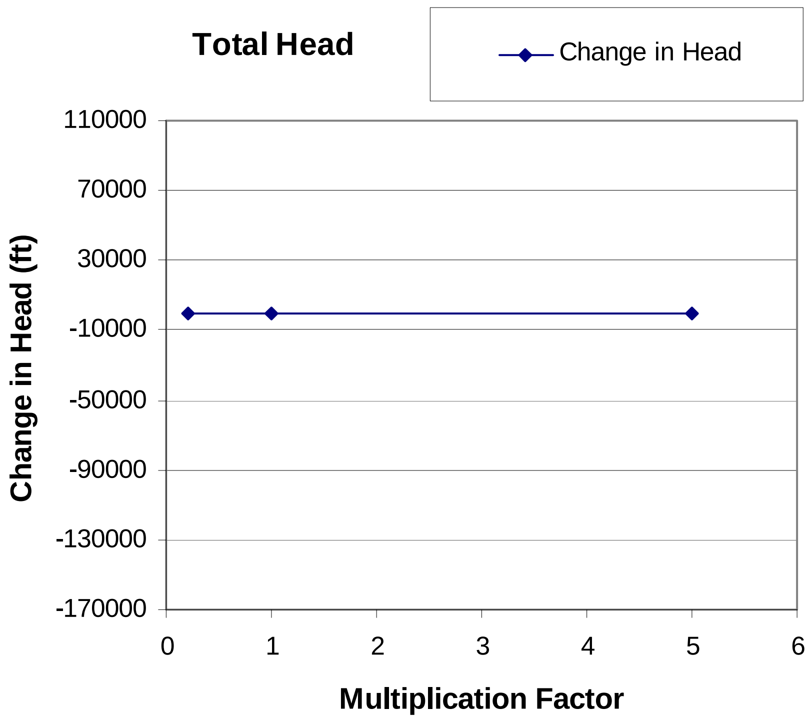

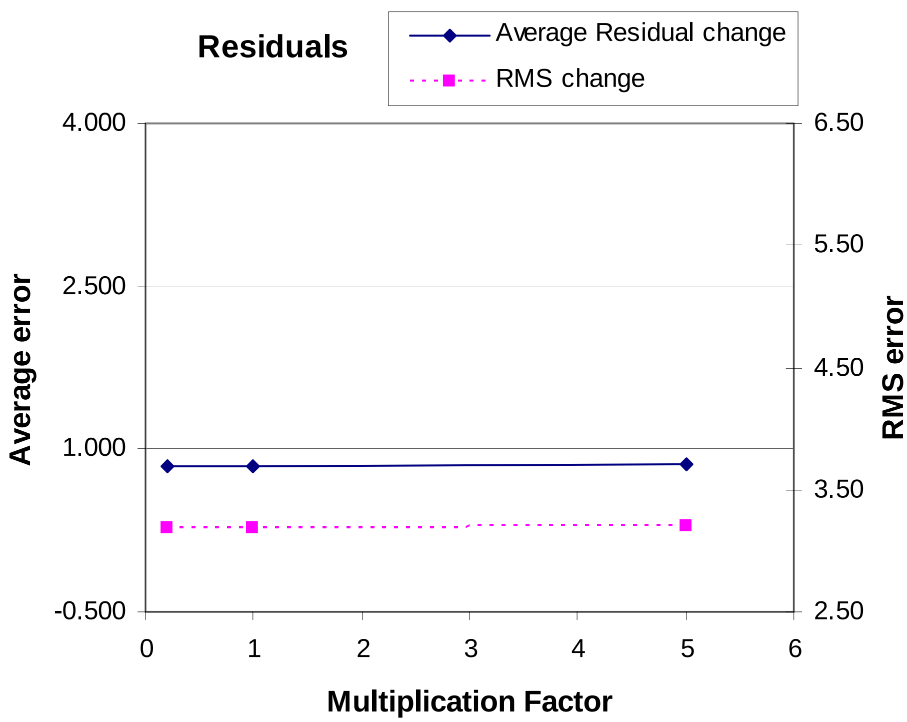

Source:
Filename: X:/SJR017/TO1/Maps/
Conceptual_model_report/Sens_OMC_SubSurf.mxd
Project: SJR017-001-99
Revised: 12/22/04 TB

Figure 8.2b
Sensitivity to Overland Manning's Coefficient in the Subsurface Domain

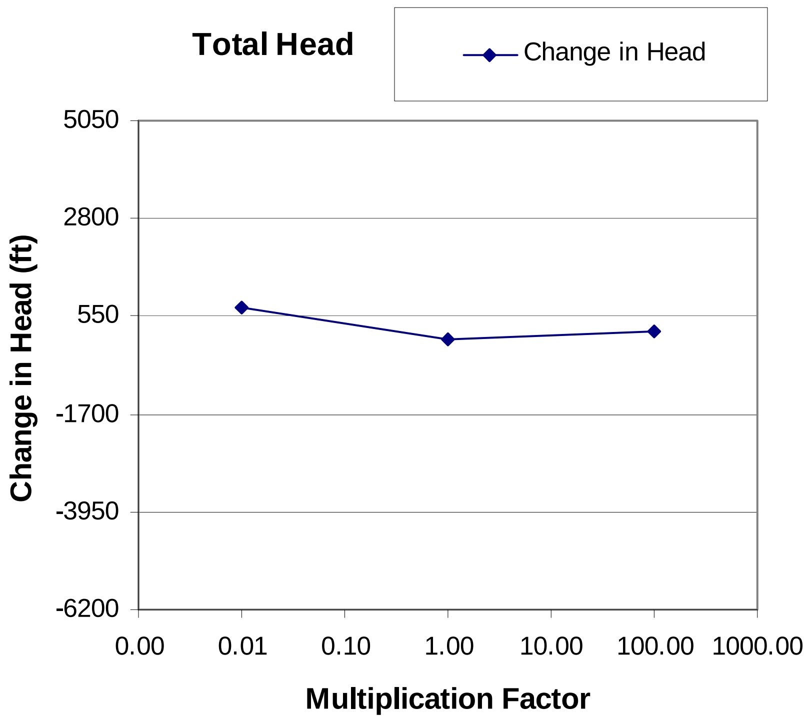

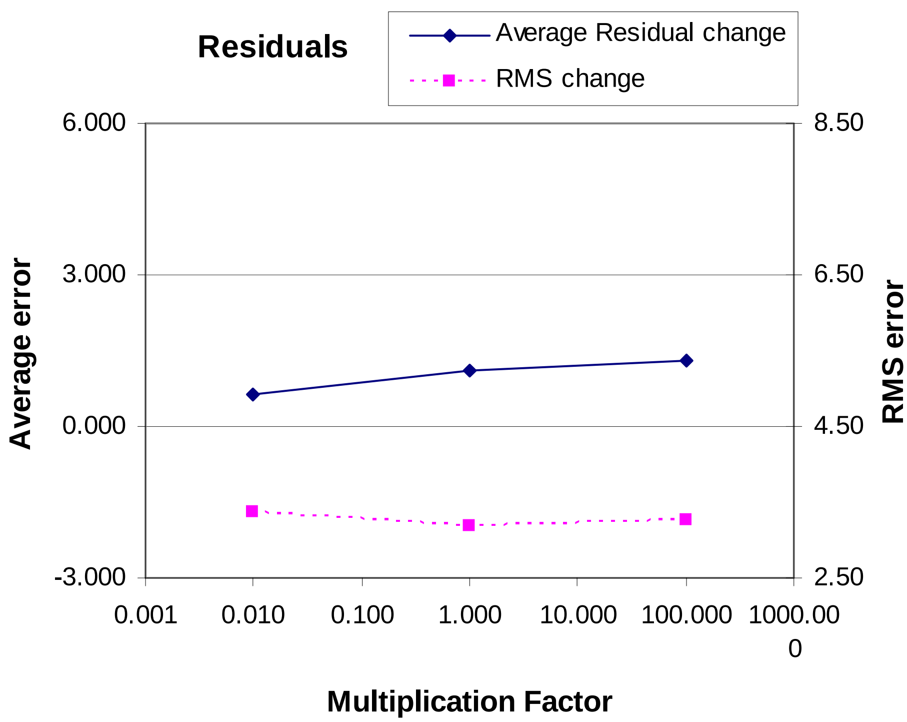

Source:
Filename: X:/SJR017/TO1/Maps/
Conceptual_model_report/Sens_CL_Surf.mxd
Project: SJR017-001-99
Revised: 12/22/04 TB

Figure 8.3a
Sensitivity to
Channel Leakance
in the Surface Domain

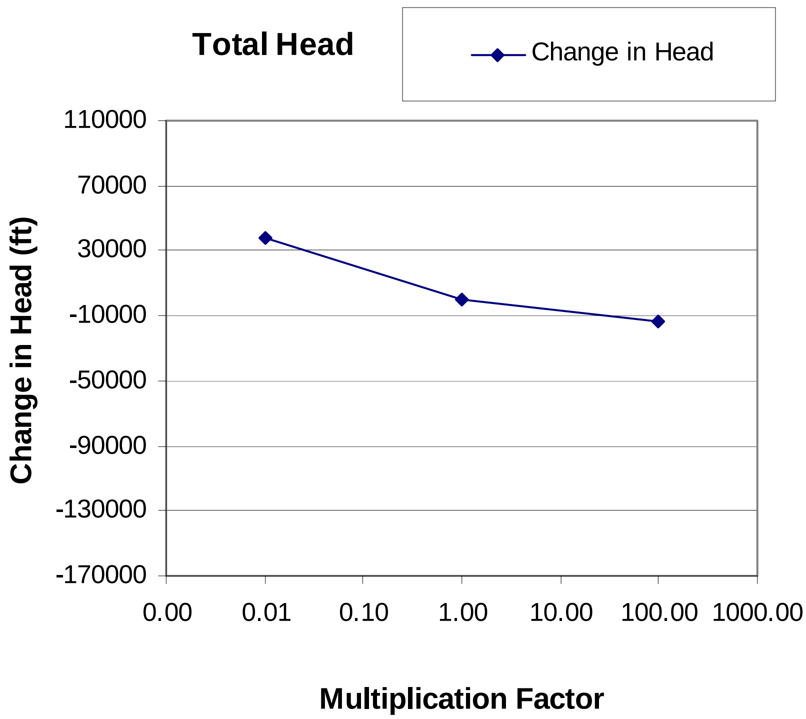

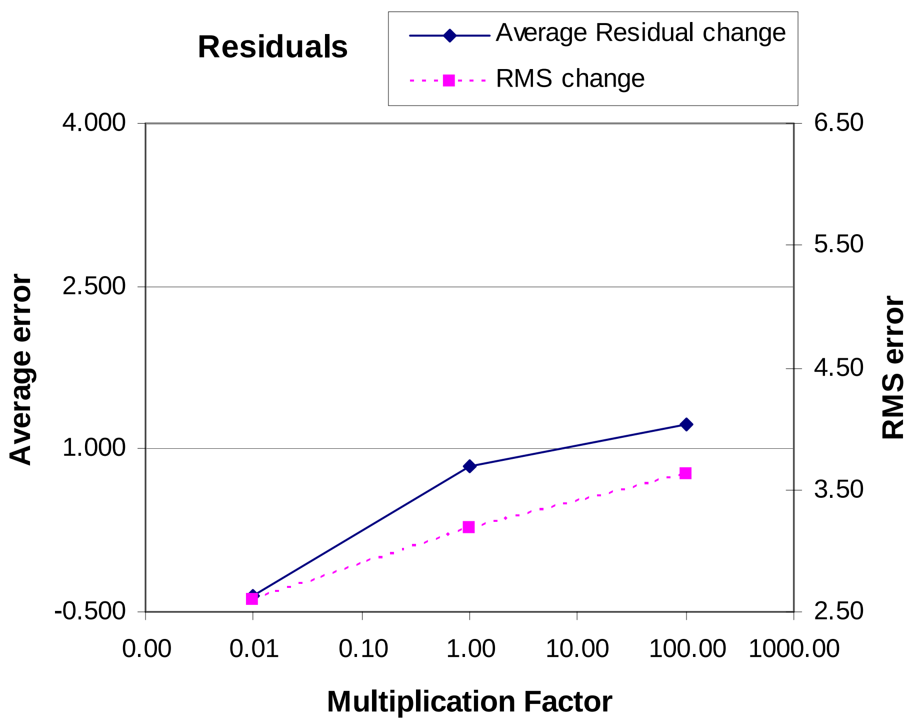

Source:
Filename: X:/SJR017/TO1/Maps/ Conceptual_model_report/Sens_CL_SubSurf.mxd
Project: SJR017-001-99
Revised: 12/22/04 TB

Figure 8.3b
Sensitivity to
Channel Leakance
in the Subsurface Domain

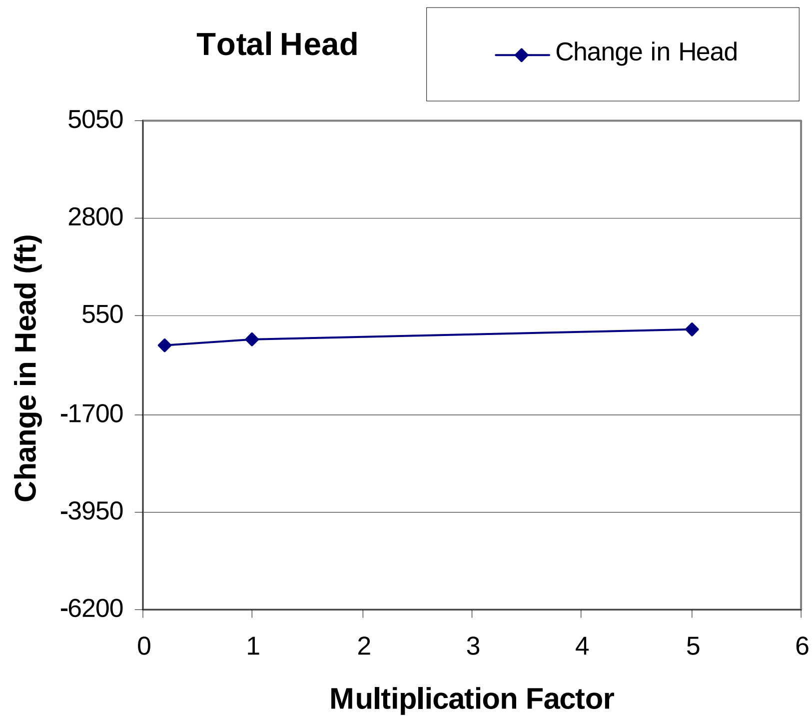

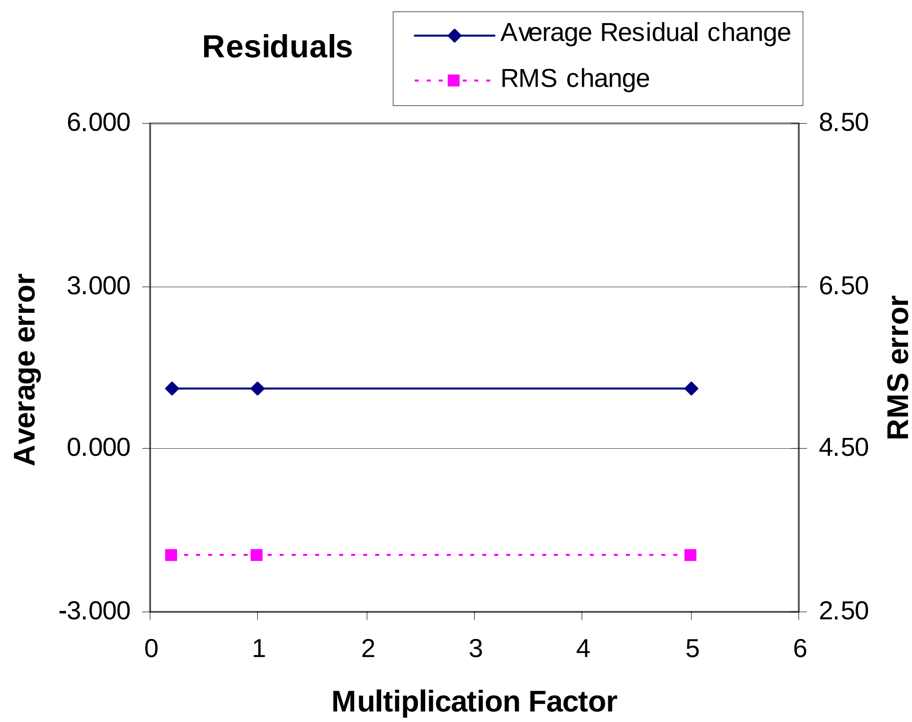

Source:
Filename: X:/SJR017/TO1/Maps/ Conceptual_model_report/Sens_CR_Surf.mxd
Project: SJR017-001-99
Revised: 12/22/04 TB

Figure 8.4a
Sensitivity to Channel Roughness in the Surface Domain

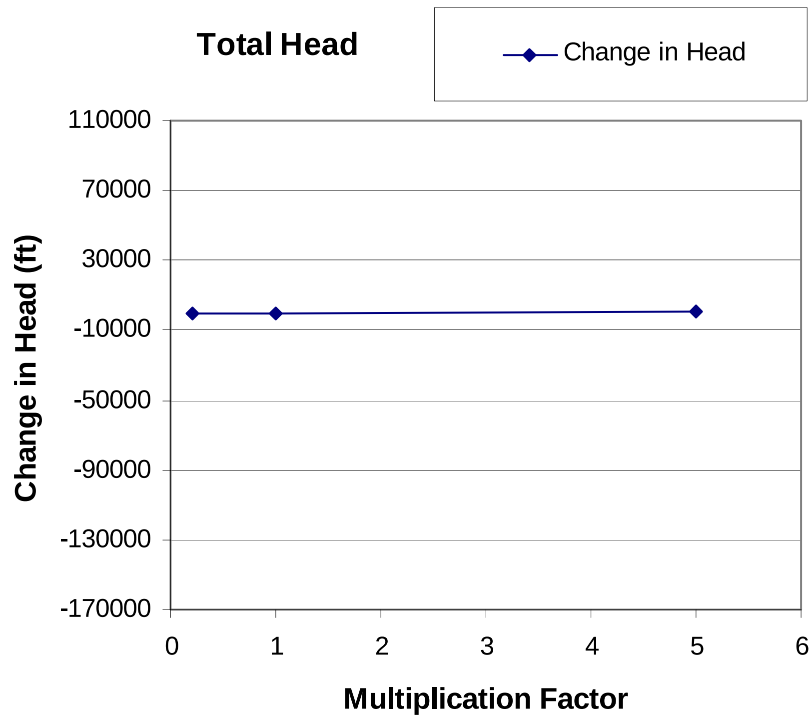

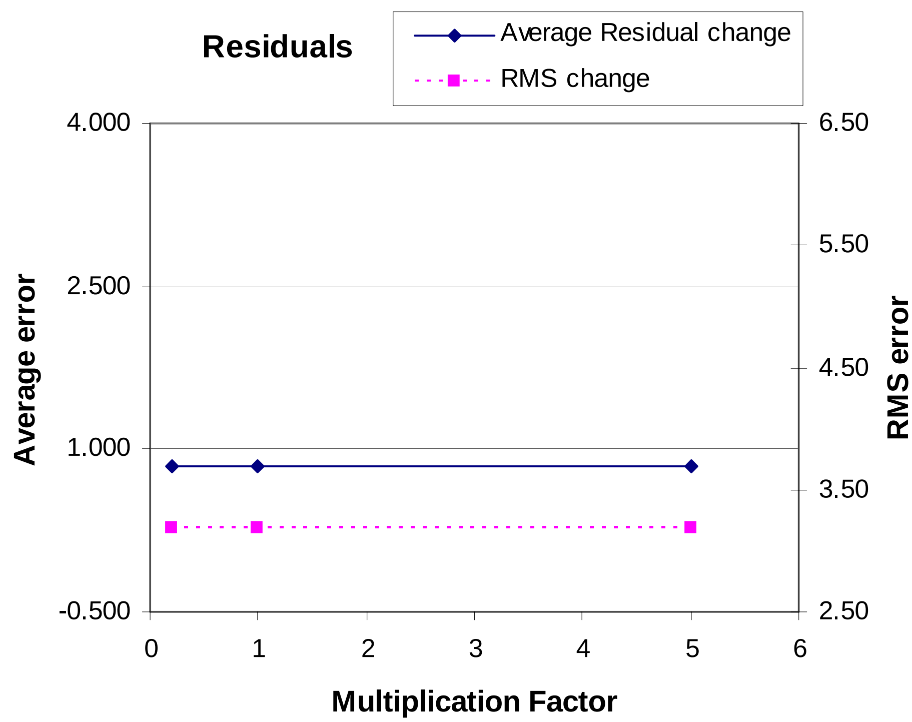

Source:
Filename: X:/SJR017/TO1/Maps/
Conceptual_model_report/Sens_CR_SubSurf.mxd
Project: SJR017-001-99
Revised: 12/22/04 TB

Figure 8.4b
Sensitivity to
Channel Roughness
in the Subsurface Domain

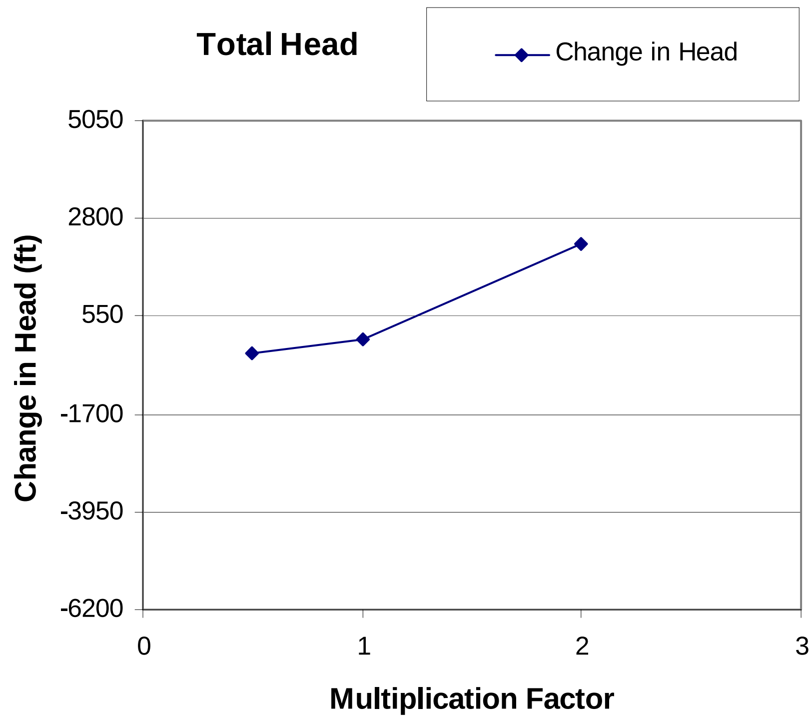

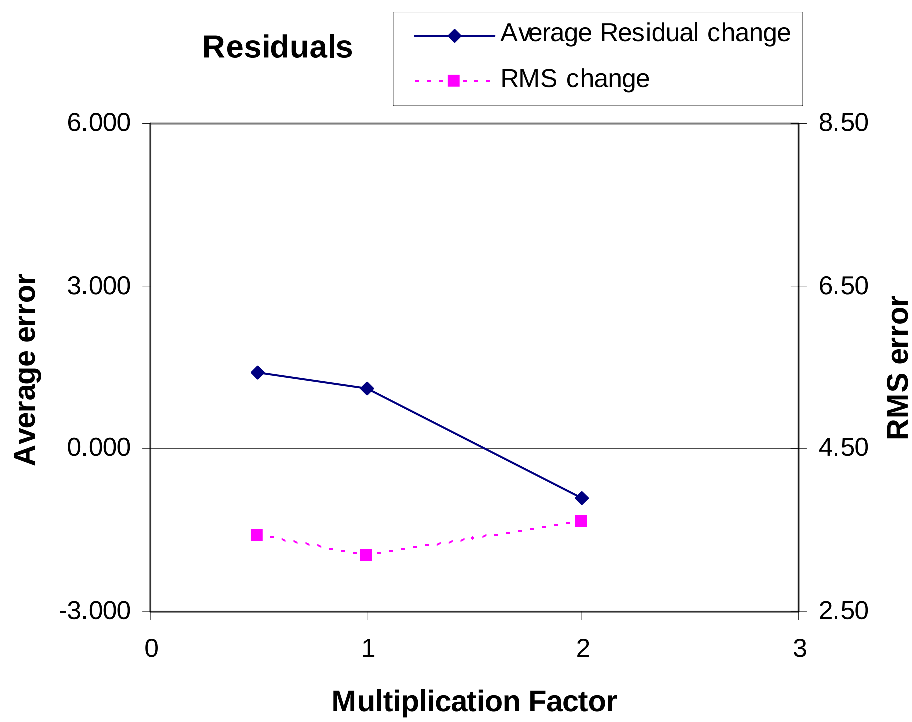

Source:
Filename: X:/SJR017/TO1/Maps/Conceptual_model_report/Sens_MP_Surf.mxd
Project: SJR017-001-99
Revised: 12/22/04 TB

Figure 8.5a
Sensitivity to Moisture Parameters (Wilting Point and Field Capacity) in the Surface Domain

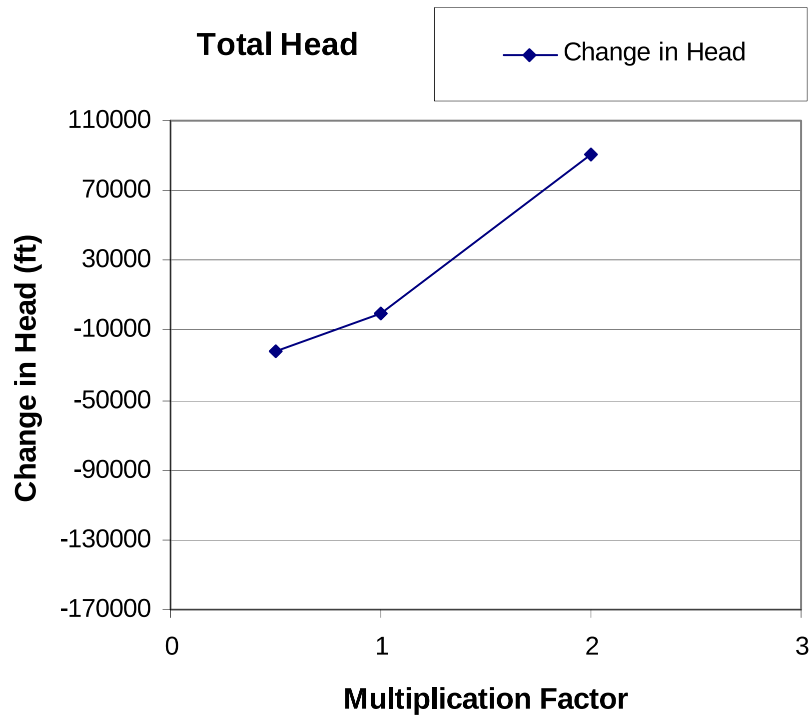

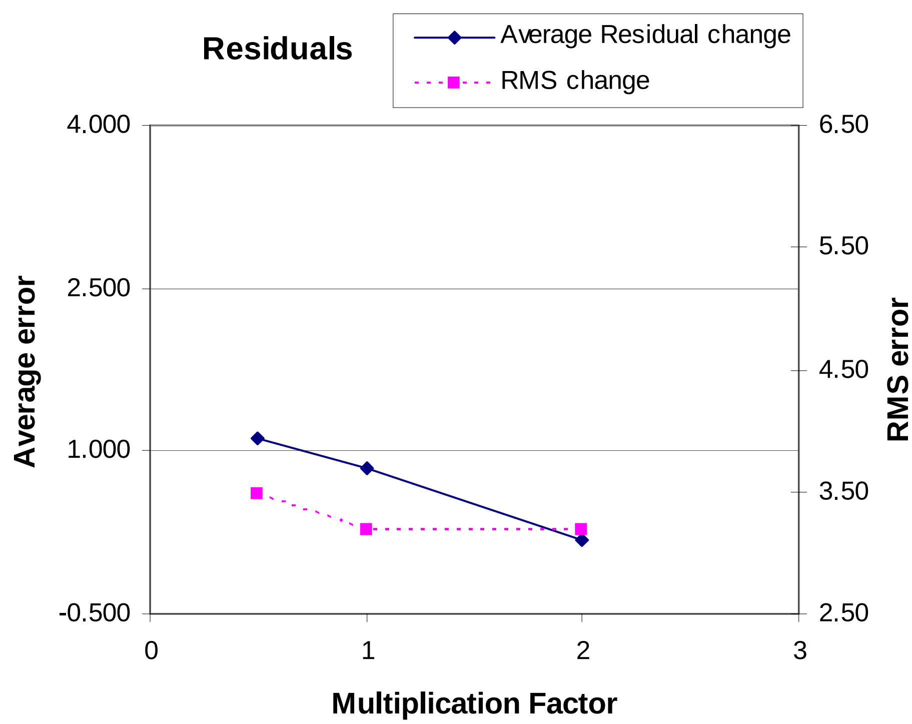

Source:
Filename: X:/SJR017/TO1/Maps/
Conceptual_model_report/Sens_MP_SubSurf.mxd
Project: SJR017-001-99
Revised: 12/22/04 TB

Figure 8.5b
Sensitivity to
Moisture Parameters
(Wilting Point and
Field Capacity)
in the Subsurface Domain

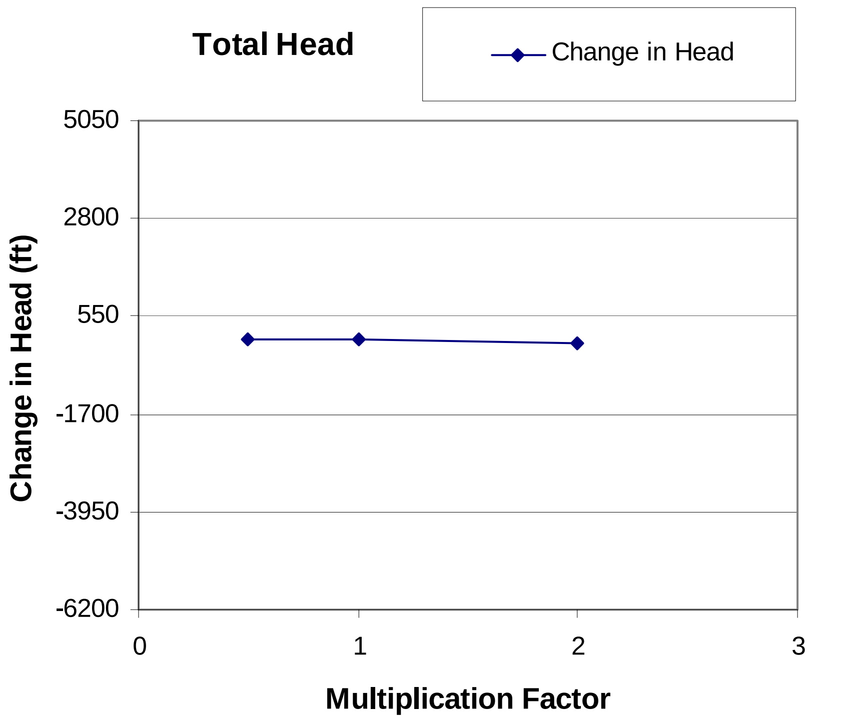

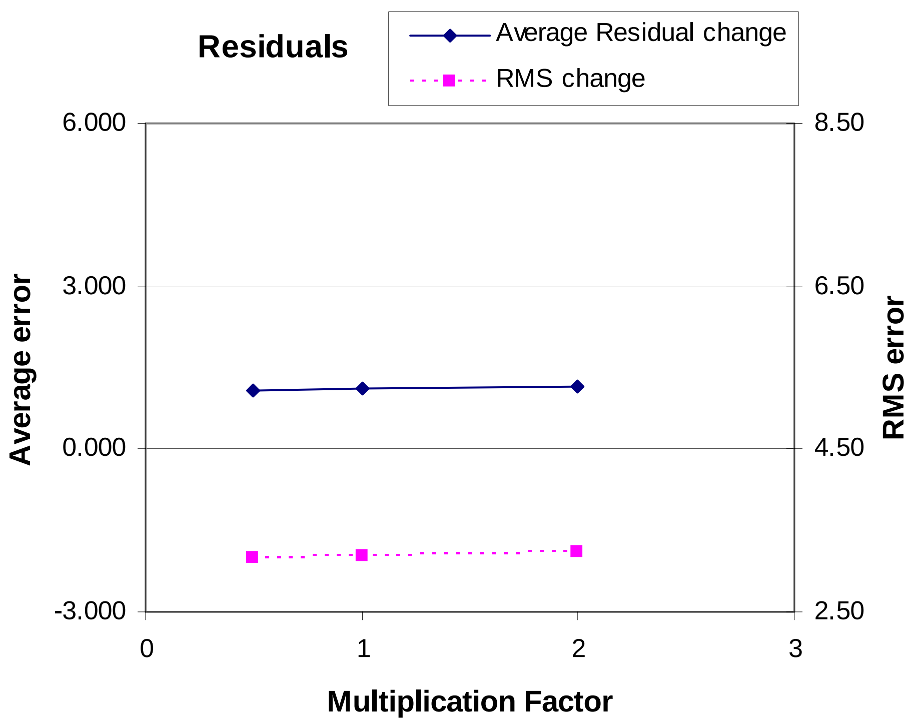

Source:
Filename: X:/SJR017/TO1/Maps/
Conceptual_model_report/Sens_LAI_Surf.mxd
Project: SJR017-001-99
Revised: 12/22/04 TB

Figure 8.6a
Sensitivity to
Leaf Area Index
in the Surface Domain

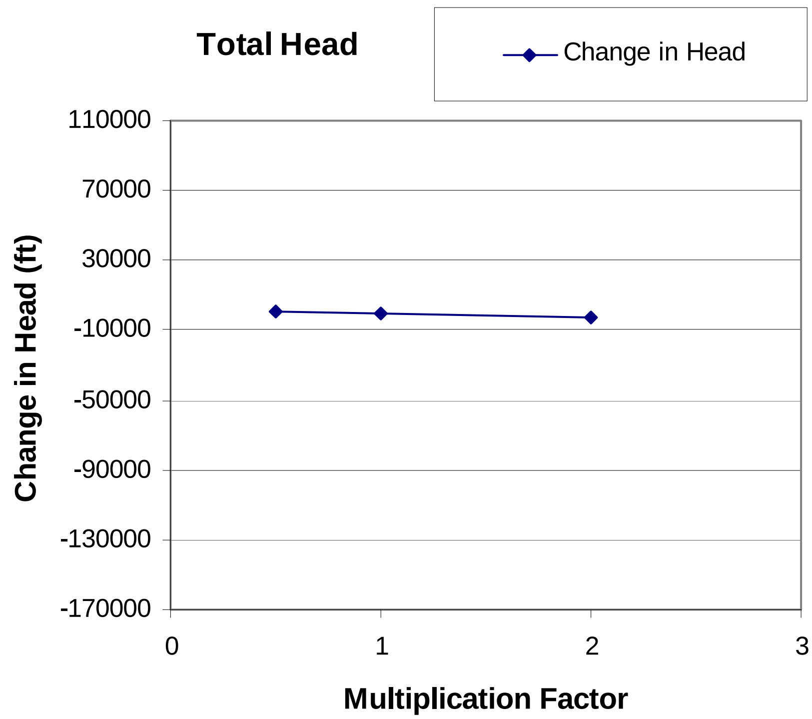

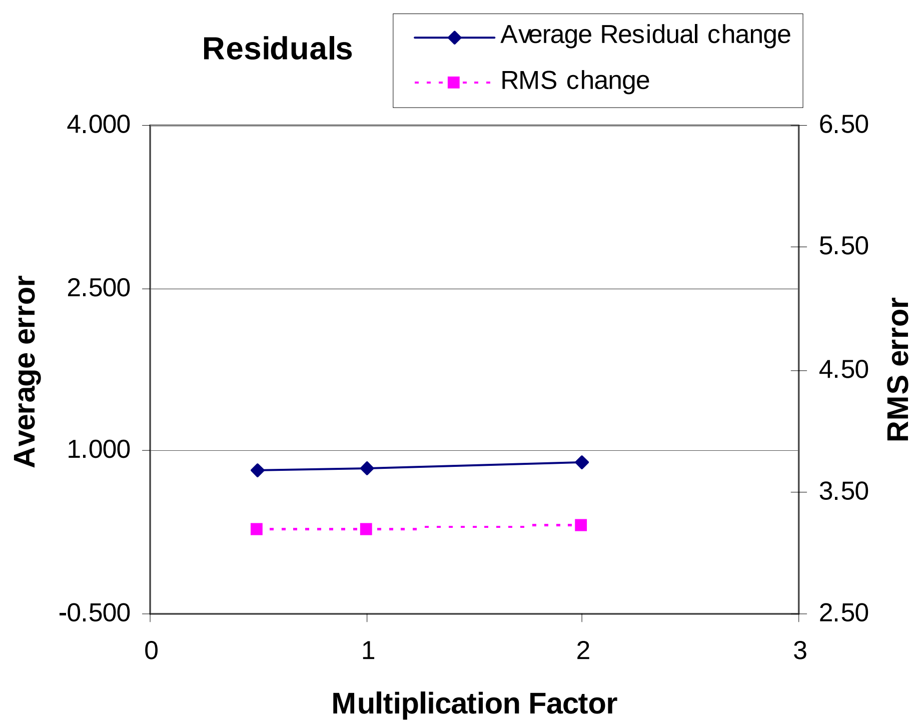

Source:
Filename: X:/SJR017/TO1/Maps/
Conceptual_model_report/Sens_LAI_SubSurf.mxd
Project: SJR017-001-99
Revised: 12/22/04 TB

Figure 8.6b
Sensitivity to
Leaf Area Index
in the Subsurface Domain

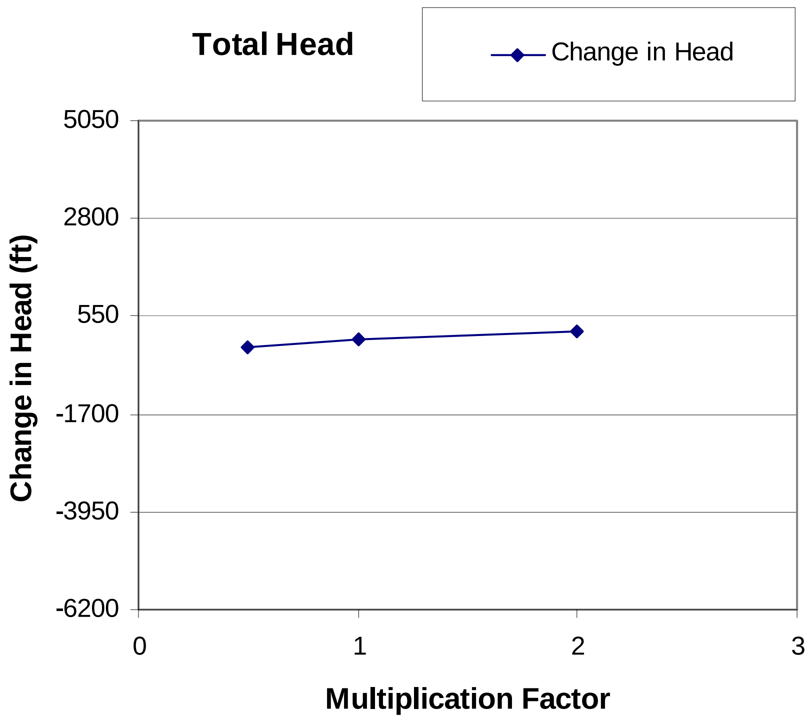

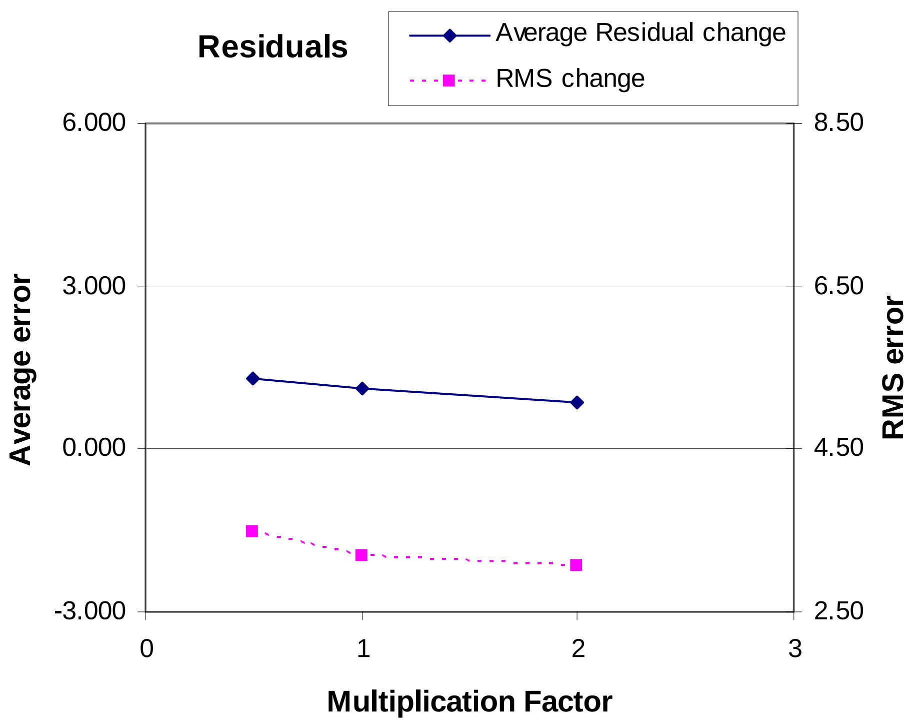

Source:
Filename: X:/SJR017/TO1/Maps/
Conceptual_model_report/Sens_vGA_Surf.mxd
Project: SJR017-001-99
Revised: 12/22/04 TB

Figure 8.7a
Sensitivity to
van Ganuchten Alpha
in the Surface Domain

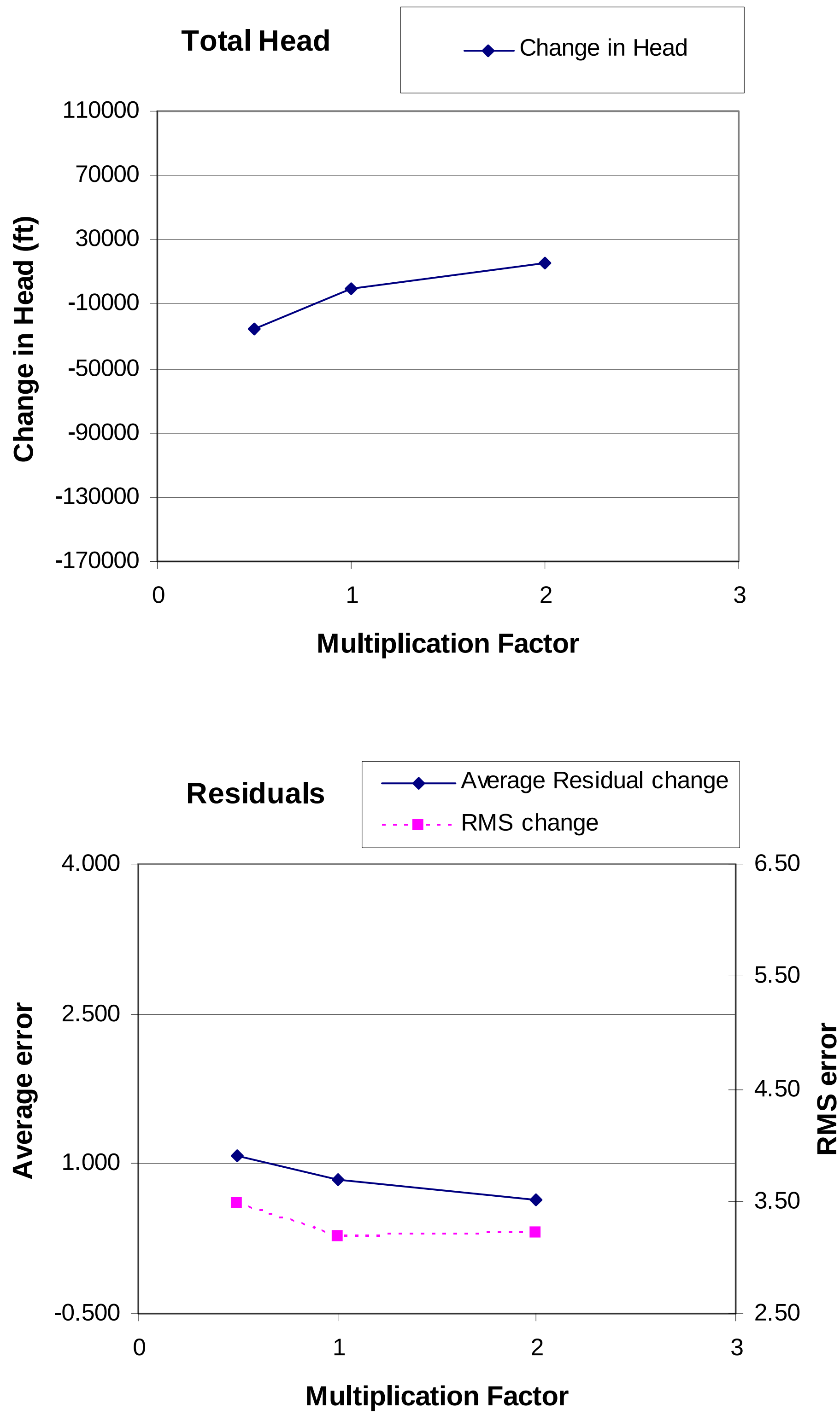

Source:
Filename: X:/SJR017/TO1/Maps/
Conceptual_model_report/Sens_vGA_SubSurf.mxd
Project: SJR017-001-99
Revised: 12/22/04 TB

Figure 8.7b
Sensitivity to
van Ganuchten Alpha
in the Subsurface Domain

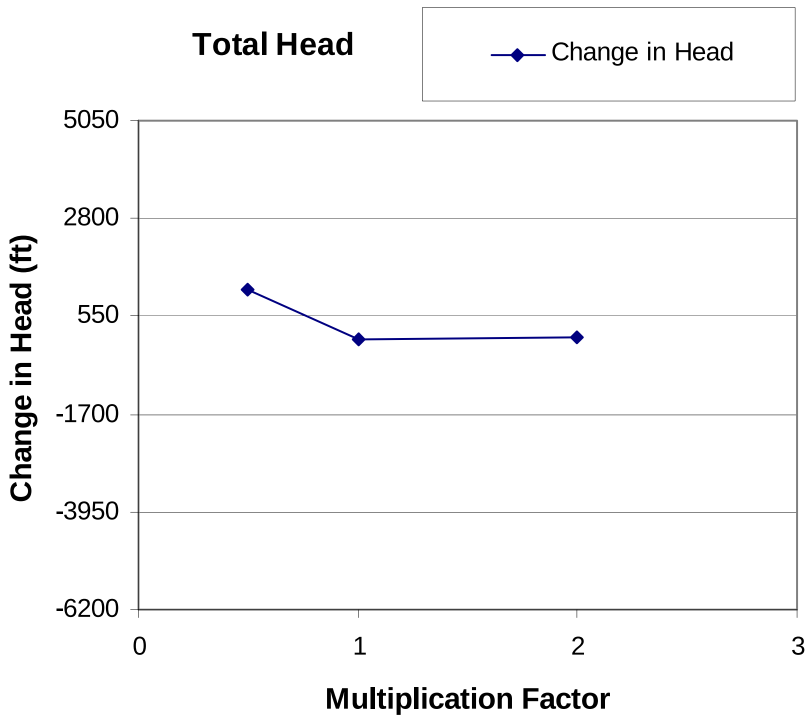

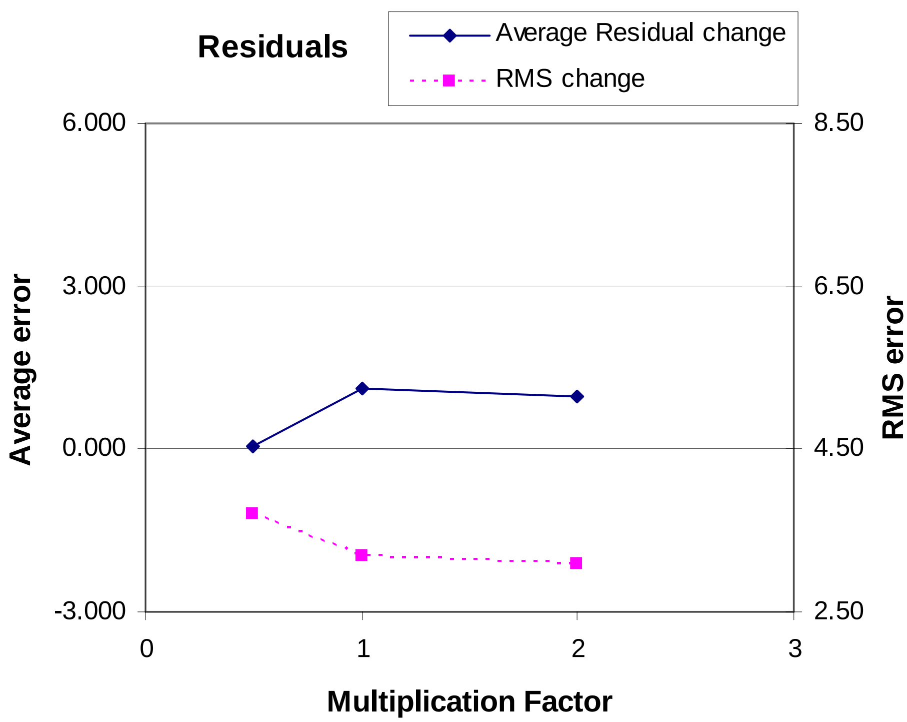

Source:
Filename: X:/SJR017/TO1/Maps/
Conceptual_model_report/Sens_BN_Surf.mxd
Project: SJR017-001-99
Revised: 12/22/04 TB

Figure 8.8a
Sensitivity to
Brook's Number
in the Surface Domain

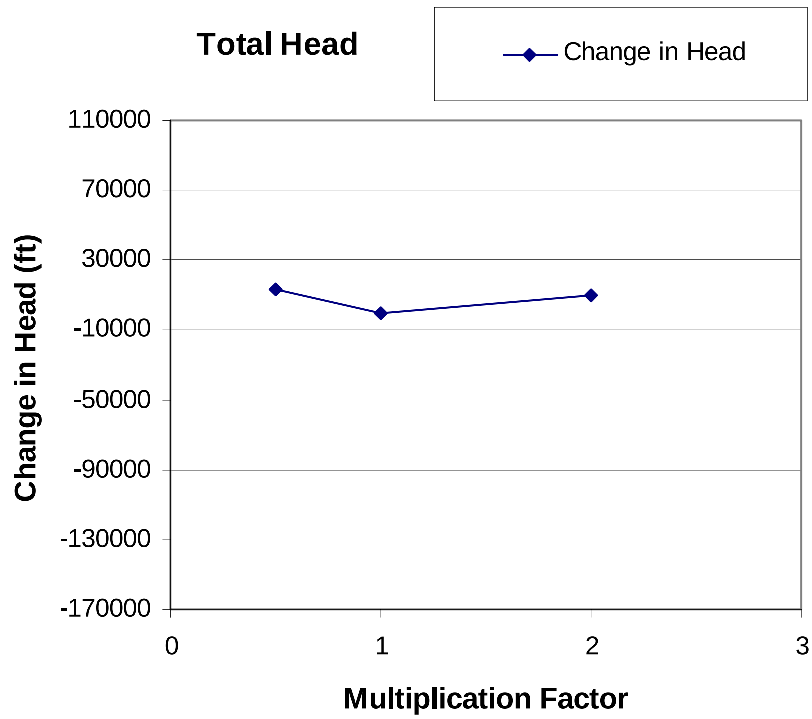

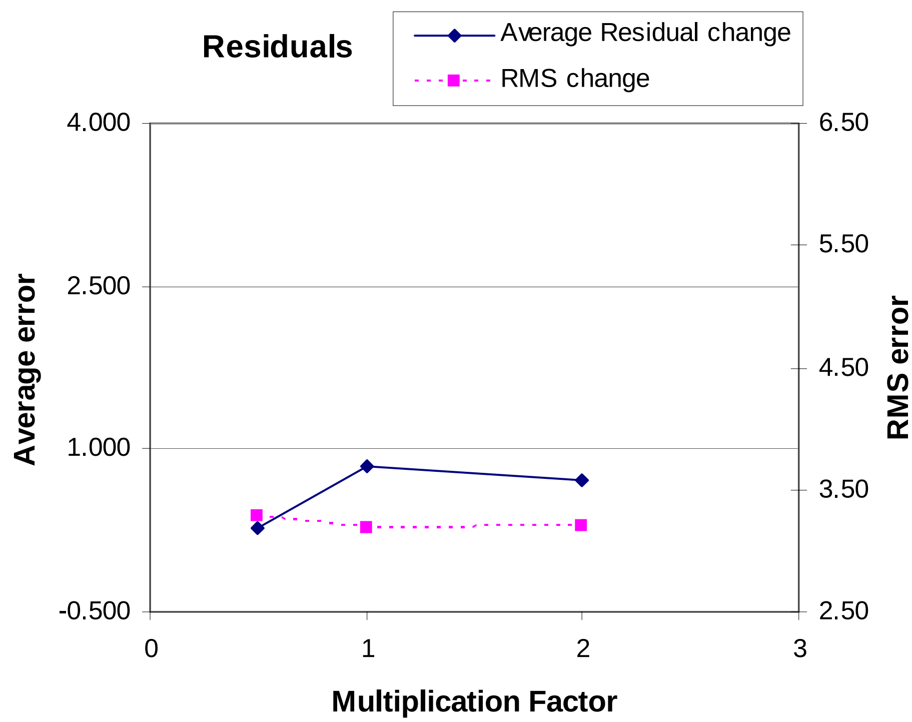

Source:
Filename: X:/SJR017/TO1/Maps/ Conceptual_model_report/Sens_BN_SubSurf.mxd
Project: SJR017-001-99
Revised: 12/22/04 TB

Figure 8.8b
Sensitivity to Brook's Number in the Subsurface Domain

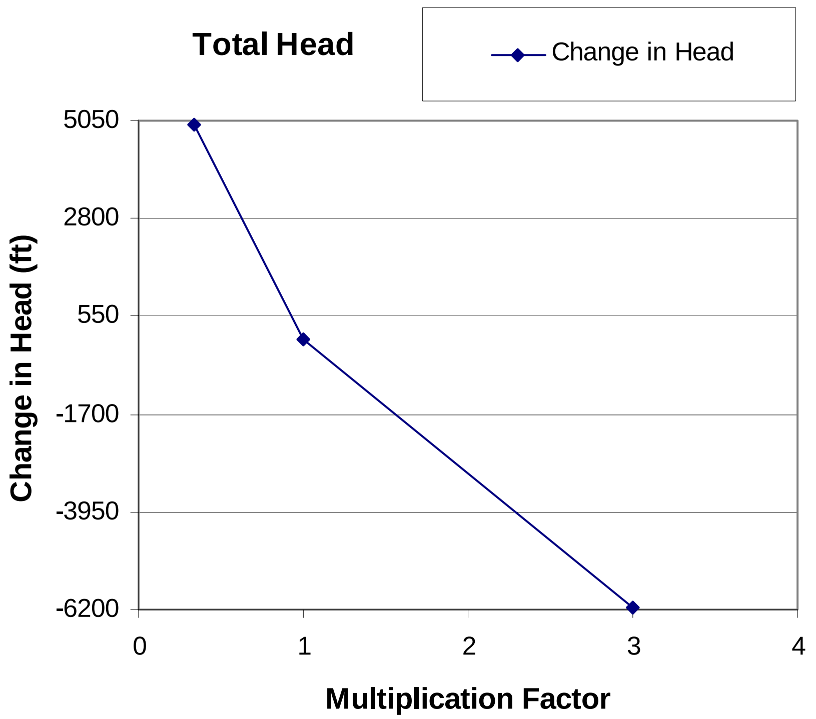

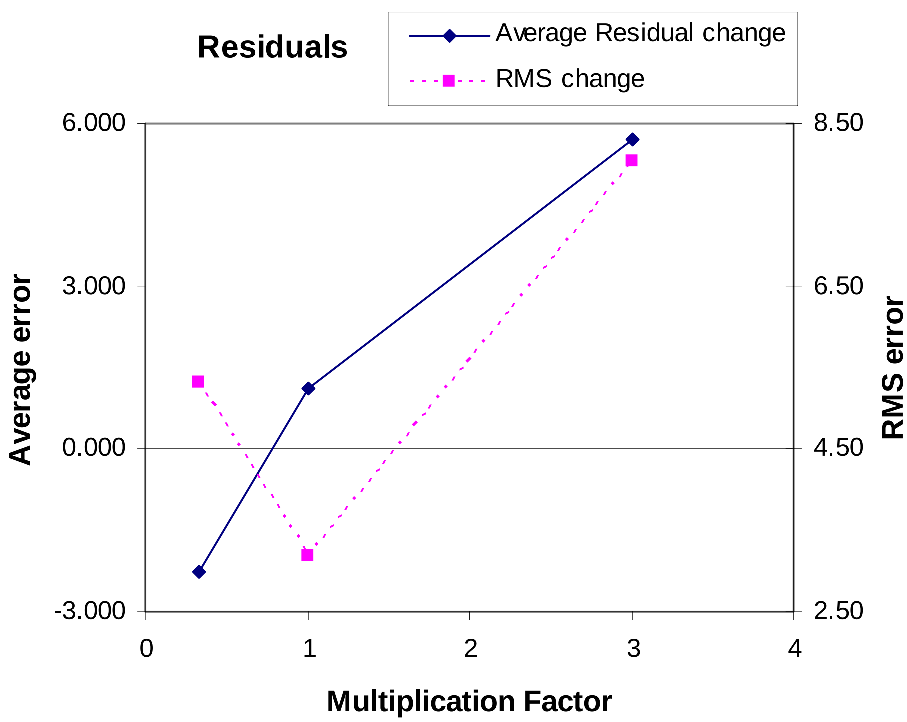

Source:
Filename: X:/SJR017/TO1/Maps/Conceptual_model_report/Sens_ICUL_Surf.mxd
Project: SJR017-001-99
Revised: 12/22/04 TB

Figure 8.9a
Sensitivity to ICU Leakance in the Surface Domain

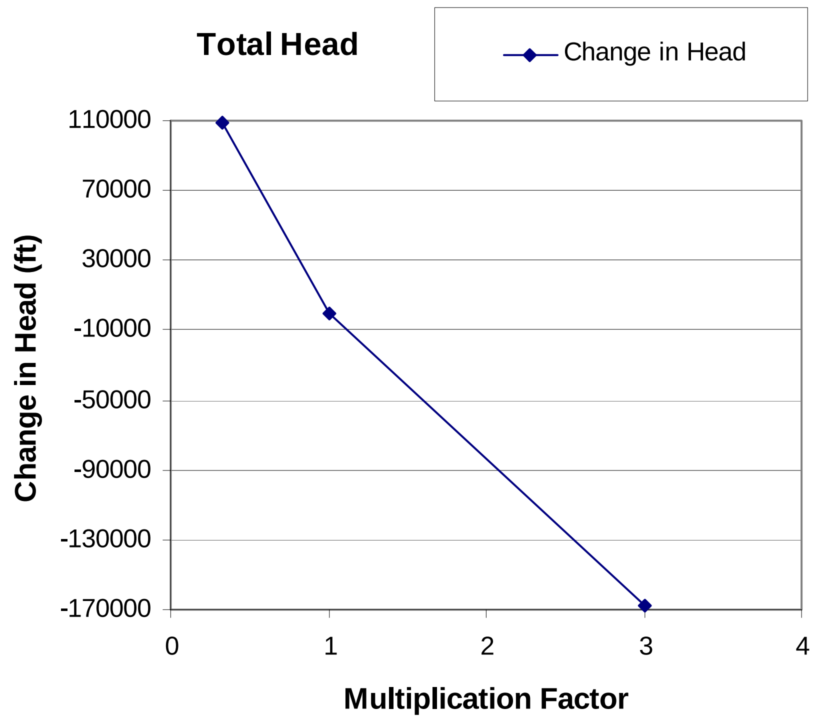

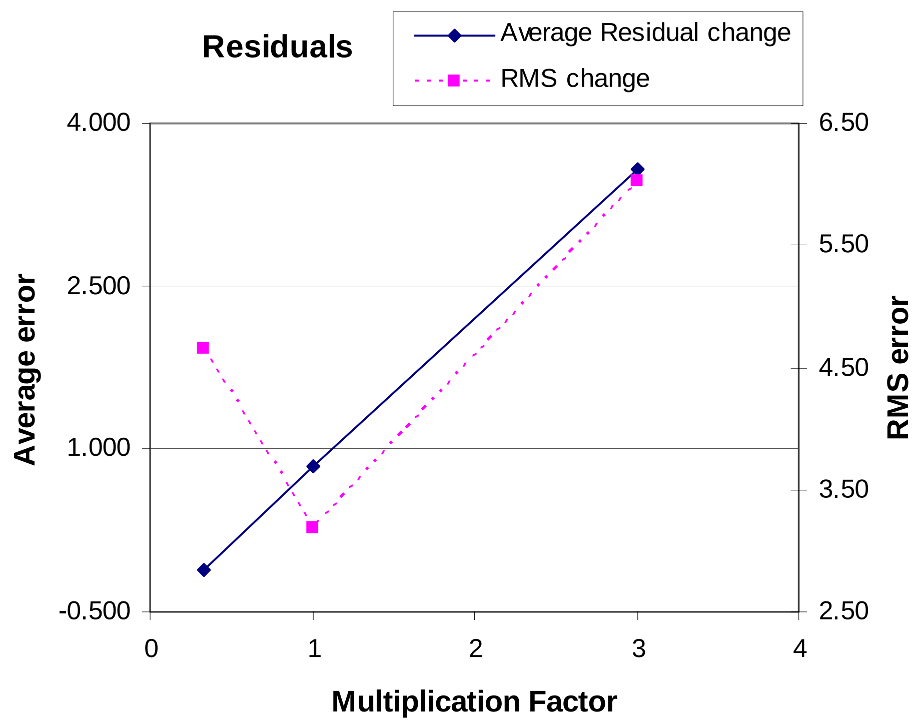

Source:
Filename: X:/SJR017/TO1/Maps/
Conceptual_model_report/Sens_ICUL_SubSurf.mxd
Project: SJR017-001-99
Revised: 12/22/04 TB

Figure 8.9b
Sensitivity to
ICU Leakance
in the Subsurface Domain

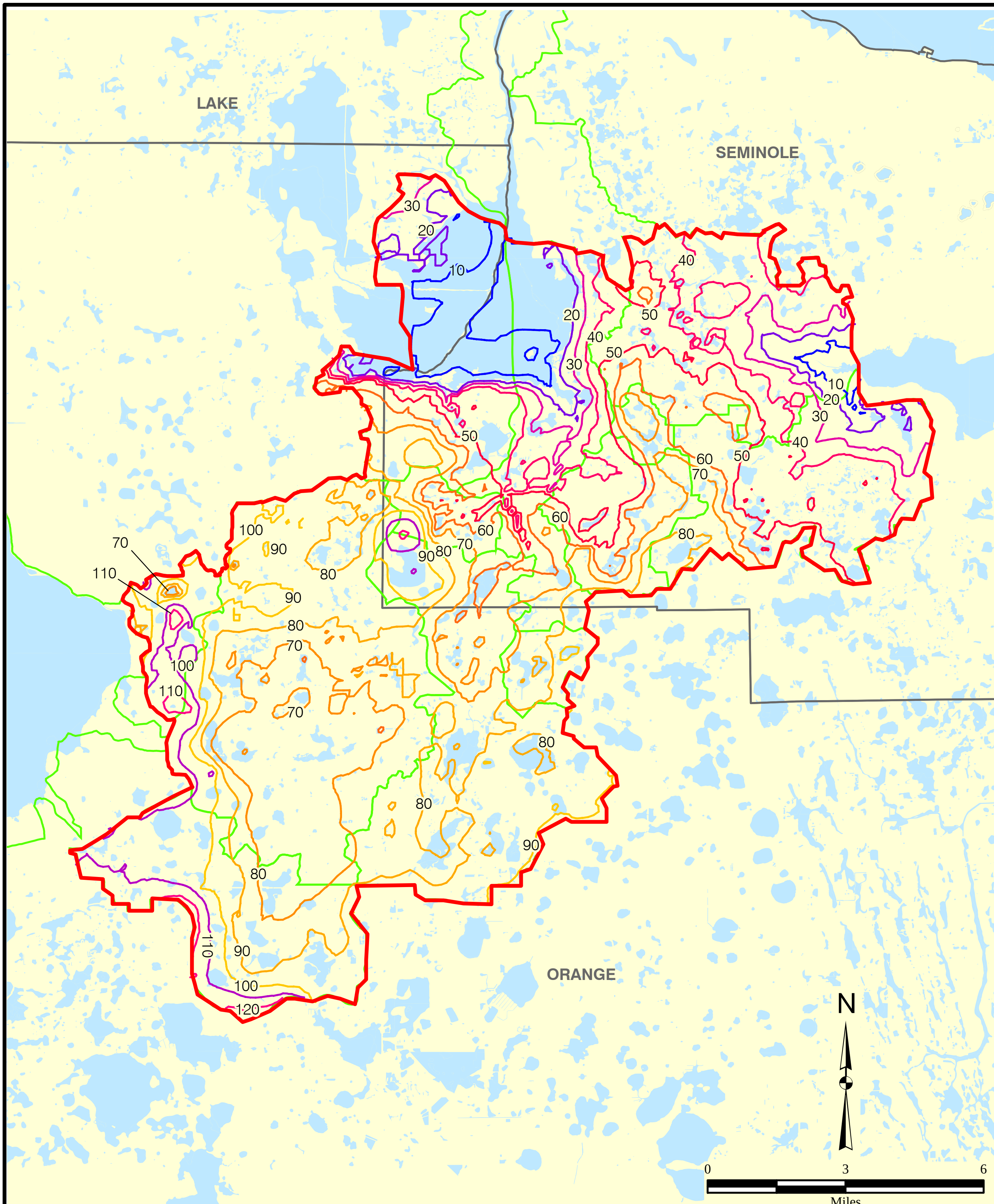

Source:
Filename: X:/SJR017/TO1/Maps/
Conceptual_model_report/WL_SAS_Mar99.mxd
Project: SJR017-001-06
Revised: 12/22/04 TB

Legend

- Model Boundary
- Surface Water Basin
- County Boundary
- 50 Water Levels (ft)
- Surface Water Bodies and Wetlands

Figure 9.1
Simulated Water Levels in the SAS for May 1999 Conditions

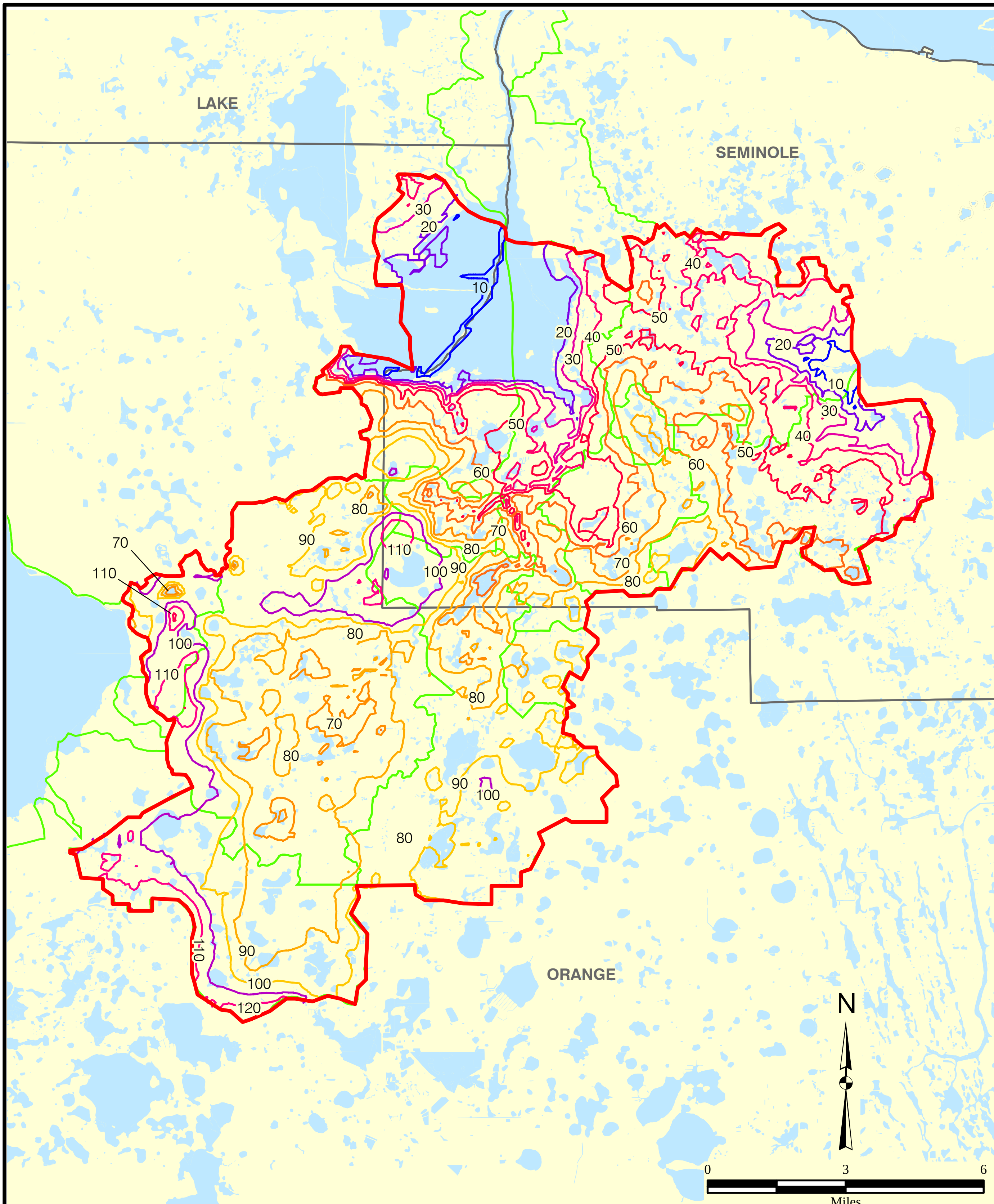

Source:
Filename: X:/SJR017/TO1/Maps/ Conceptual_model_report/WL_SAS_Mar99.mxd
Project: SJR017-001-06
Revised: 12/22/04 TB

Legend

- Model Boundary
- Surface Water Basin
- County Boundary
- 50 Water Levels (ft)
- Surface Water Bodies and Wetlands

Figure 9.2
Simulated Water Levels in the SAS for September 1999 Conditions

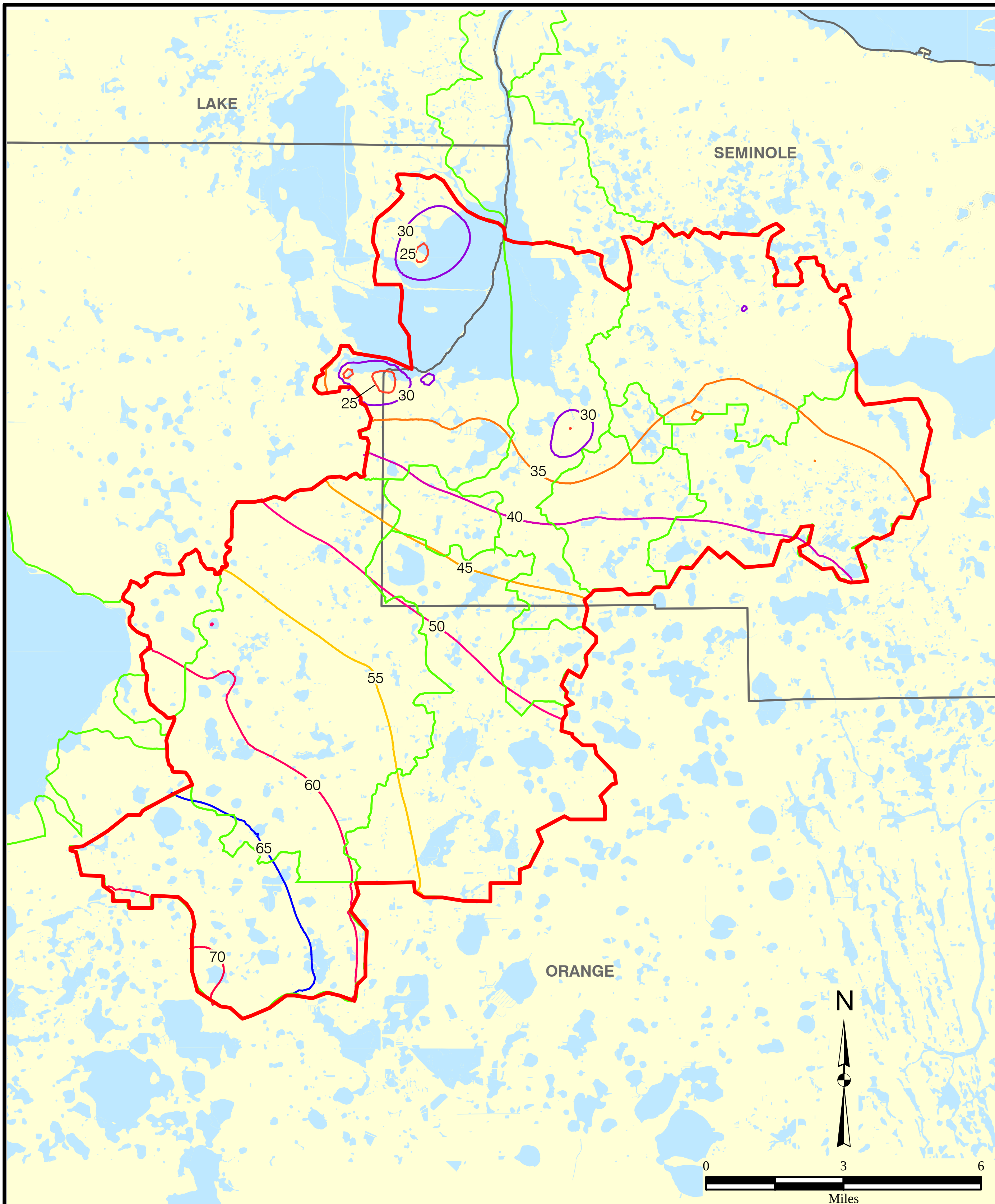

Source:
Filename: X:/SJR017/TO1/Maps/
Conceptual_model_report/WL_UFA-UZ_Mar99.mxd
Project: SJR017-001-06
Revised: 12/22/04 TB

Legend

- Model Boundary
- Surface Water Basin
- County Boundary
- 50 Water Levels (ft)
- Surface Water Bodies and Wetlands

Figure 9.3
Simulated Water Levels in the UFA-UZ for May 1999 Conditions

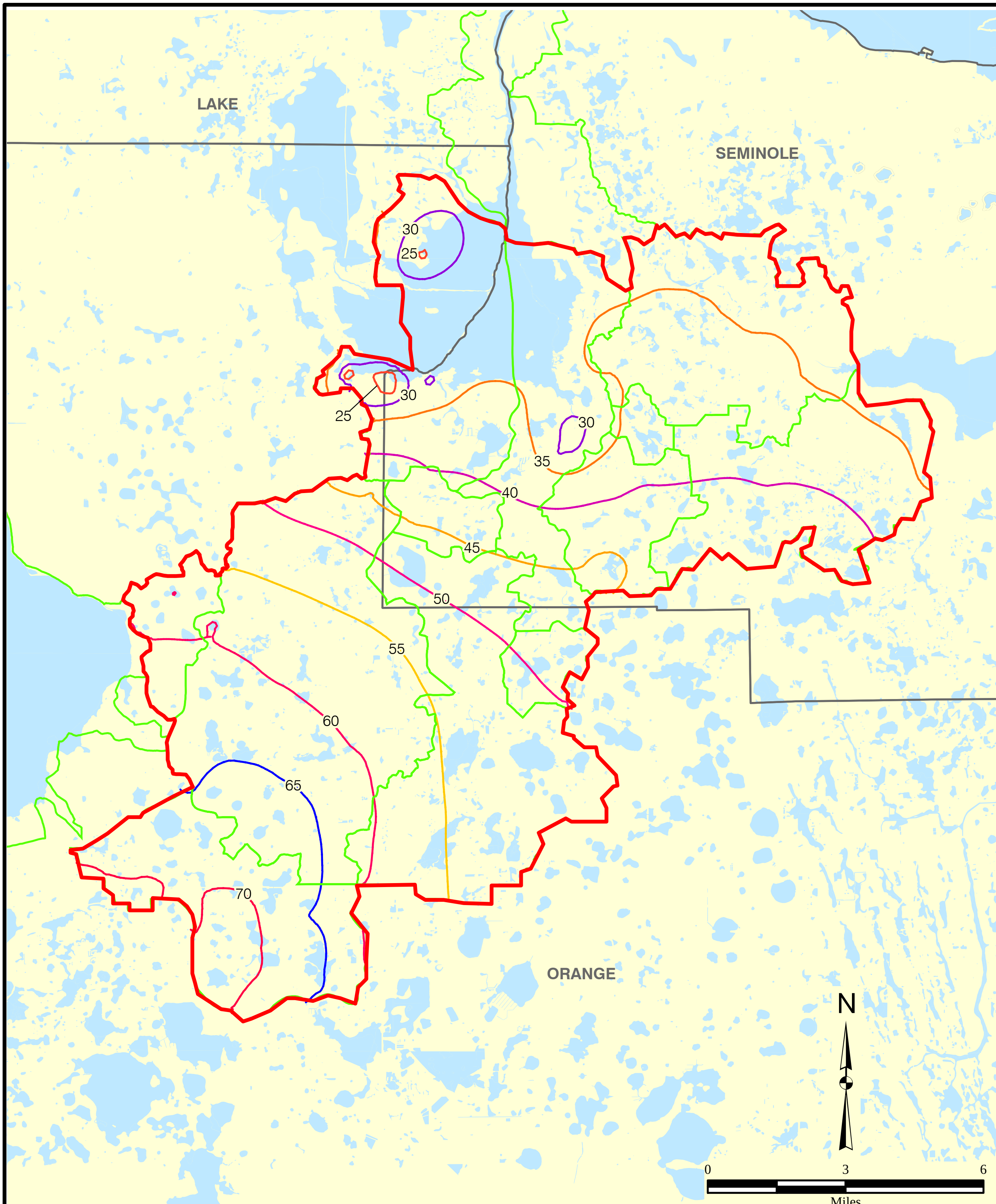

Source:
Filename: X:/SJR017/TO1/Maps/
Conceptual_model_report/WL_UFA-UZ_Sept99.mxd
Project: SJR017-001-06
Revised: 12/22/04 TB

Legend

- Model Boundary
- Surface Water Basin
- County Boundary
- 50 Water Levels (ft)
- Surface Water Bodies and Wetlands

Figure 9.4
Simulated Water Levels in the UFA-UZ for September 1999 Conditions

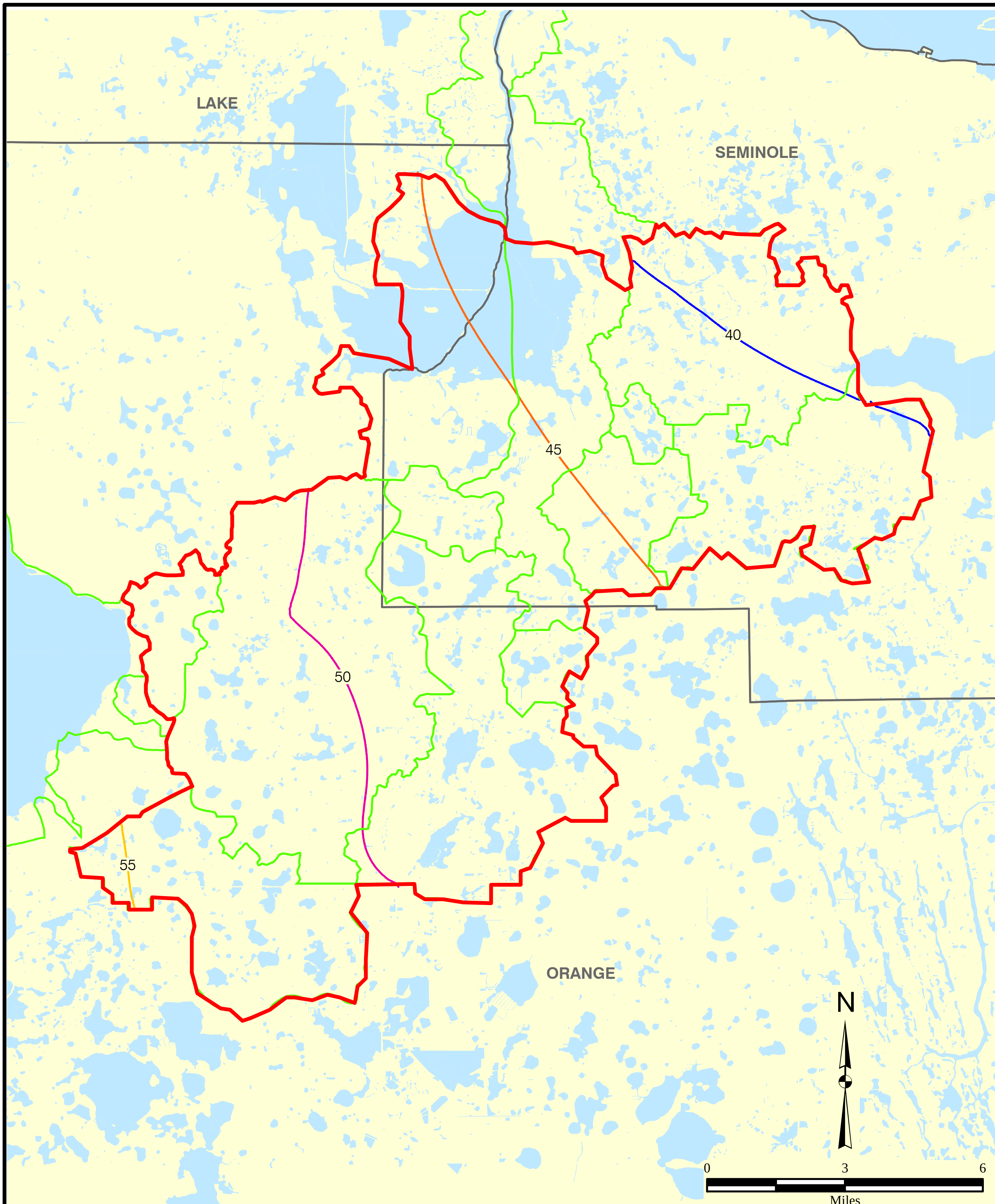

Source:
Filename: X:/SJR017/TO1/Maps/
Conceptual_model_report/WL_LFA_Mar99.mxd
Project: SJR017-001-06
Revised: 12/22/04 TB

Legend

Model Boundary
Surface Water Basin
County Boundary
50 Water Levels (ft)
Surface Water Bodies and Wetlands

Figure 9.5
Simulated Water Levels in the LFA for May 1999 Conditions

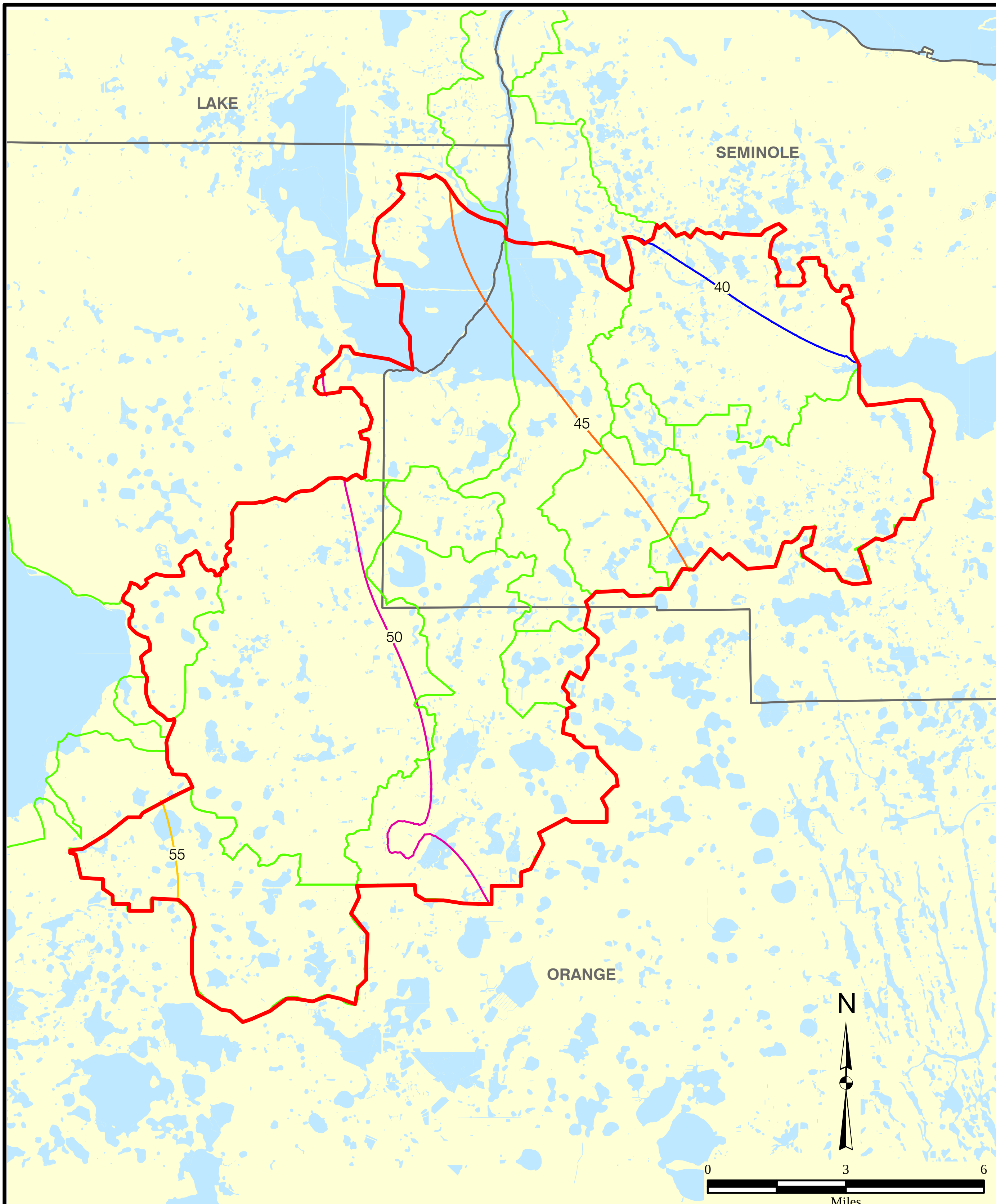

Source:
Filename: X:/SJR017/TO1/Maps/
Conceptual_model_report/WL_LFA_Sept99.mxd
Project: SJR017-001-06
Revised: 09/14/04 TB

Legend

- Model Boundary
- Surface Water Basin
- County Boundary
- 50 Water Levels (ft)
- Surface Water Bodies and Wetlands

Figure 9.6
Simulated Water Levels in the LFA for September 1999 Conditions

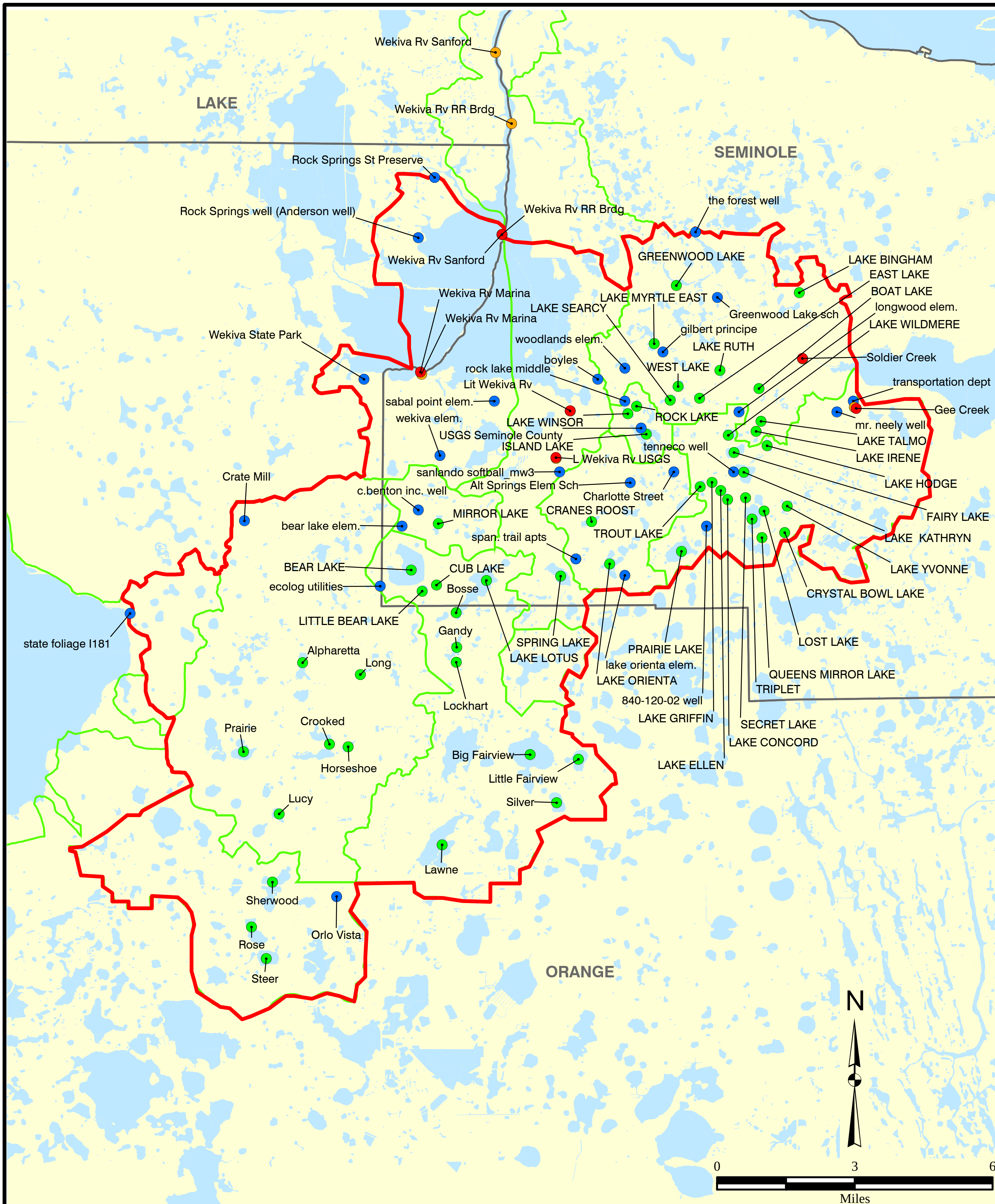

Source:
Filename: X:/SJR017/TO1/Maps/
Conceptual_model_report/Obs_Locs.mxd
Project: SJR017-001-99
Revised: 01/06/05 TB

Legend

- Model Boundary
- County Boundary
- Surface Water Basin
- Surface Water Bodies and Wetlands
- Subsurface Observation Locations
- Surface Observation Locations
- Surface-Water Flow - Actual Locations
- Surface-Water Flow - Locations Approximated In Model

Figure 9.7
Location of Flow and Water Level Observations from 1995 Through 1999

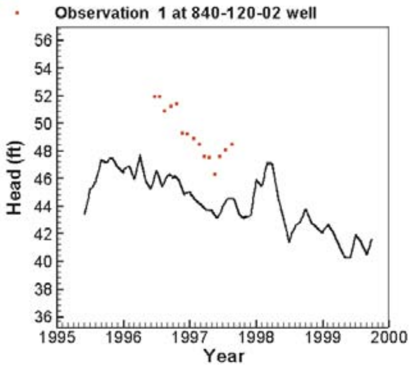

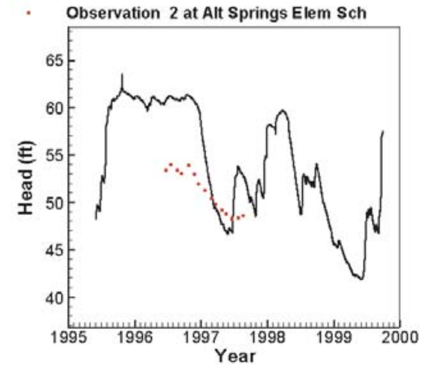

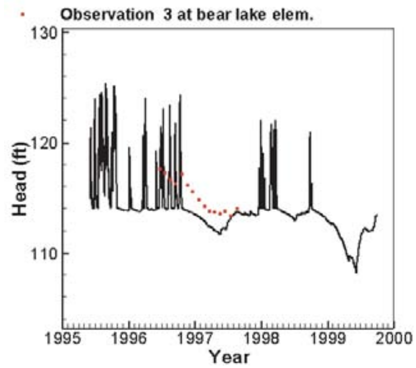

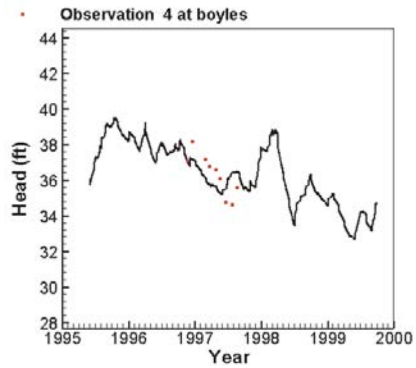

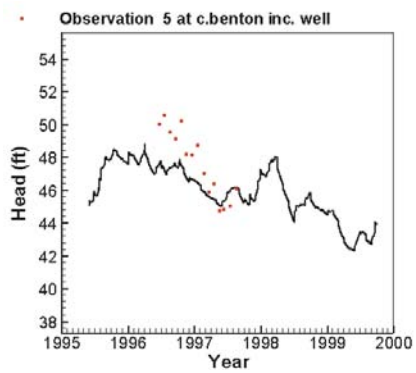

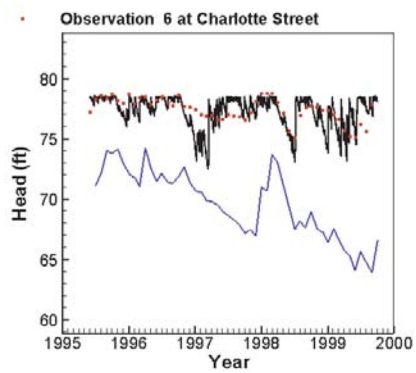

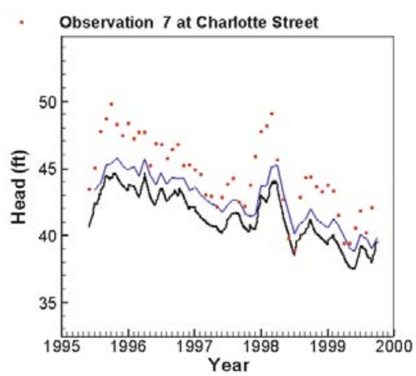

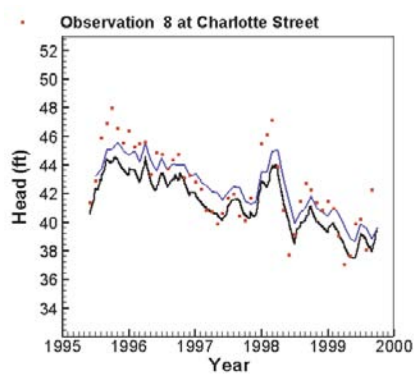

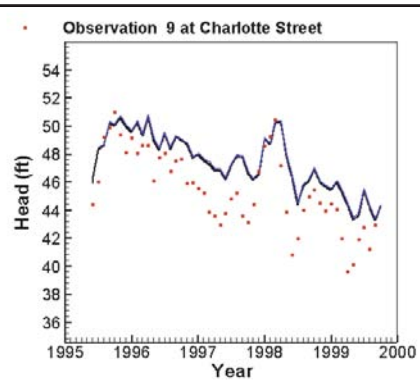

Figure 9.8 Transient Hydrographs at Observation Locations for Transient ISGM Simulation of 1995 through 1999 Conditions. (Page 1 of 11)

Observed Data

ISGM Simulation with Daily Rainfall

ECF Regional Model Simulation

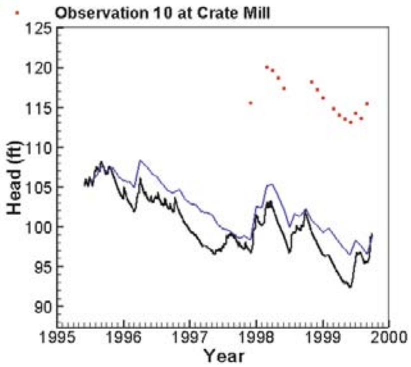

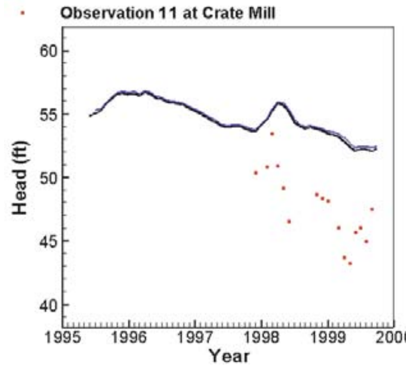

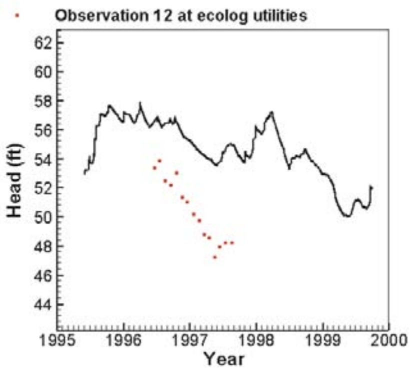

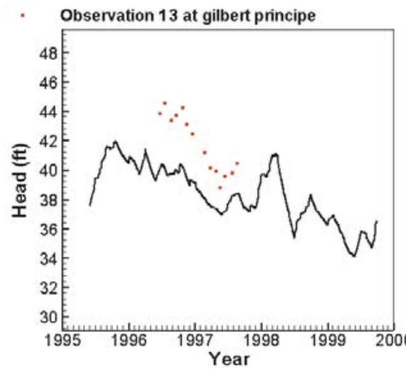

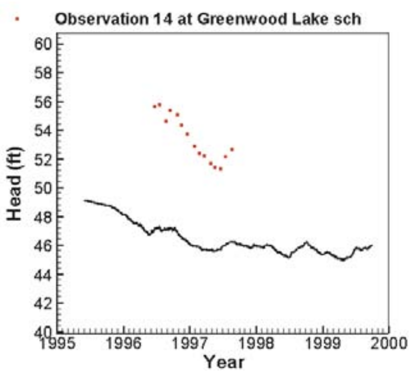

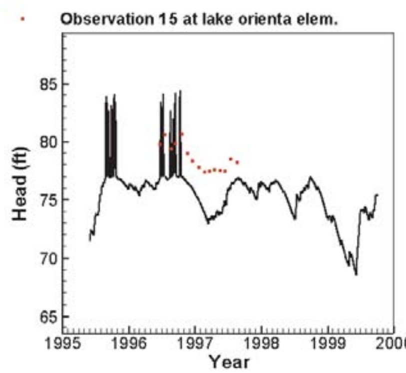

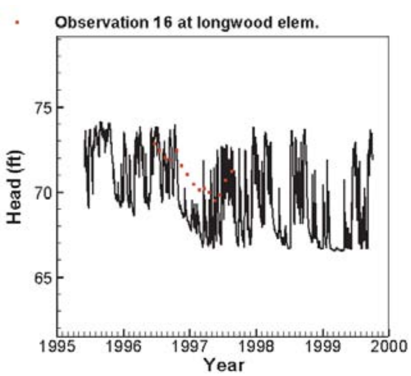

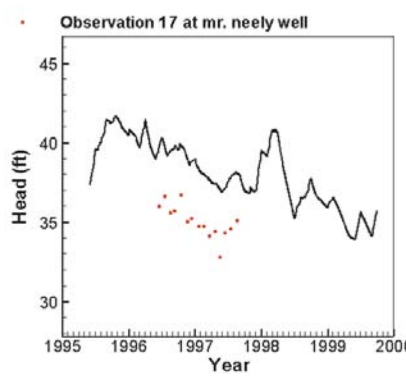

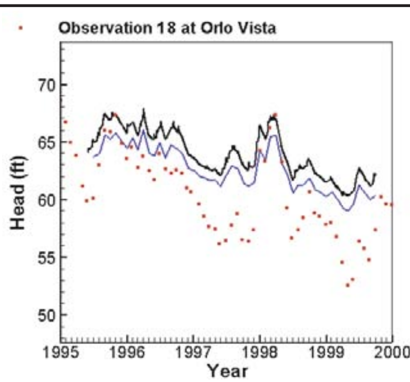

Figure 9.8 Transient Hydrographs at Observation Locations for Transient ISGM Simulation of 1995 through 1999 Conditions. (Page 2 of 11)

- Observed Data
- ISGM Simulation with Daily Rainfall
- ECF Regional Model Simulation

X:\SJR017\TO1\Maps\Conceptual_Model_Report\transient_ISGM.cdr

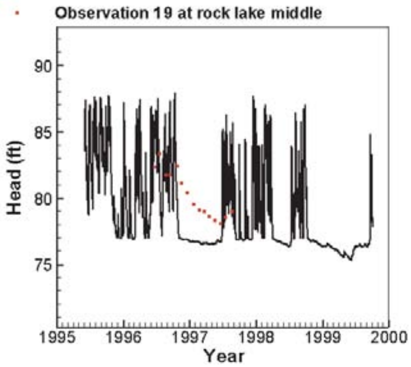

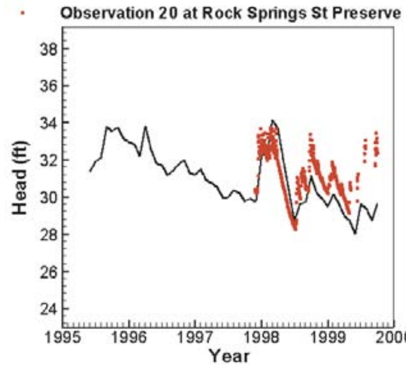

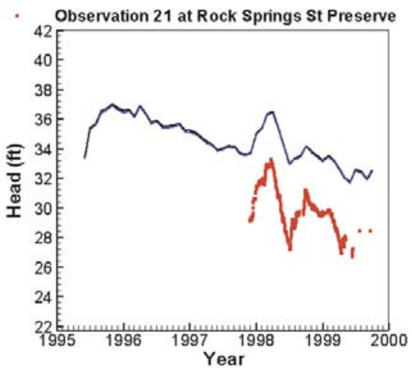

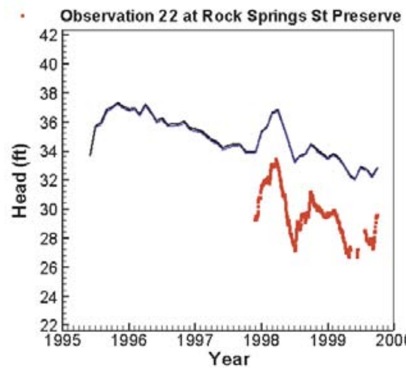

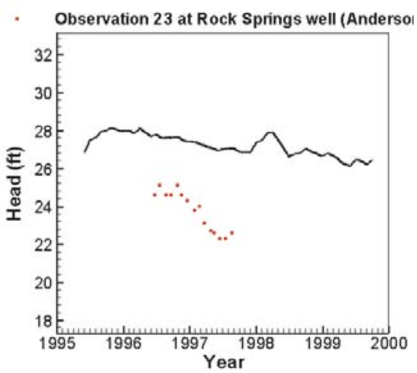

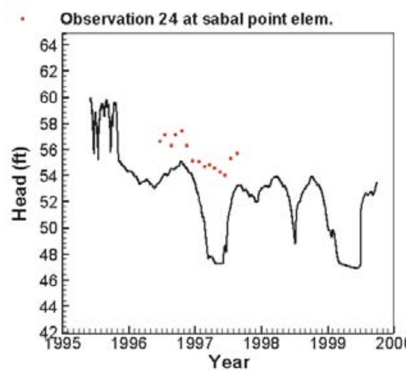

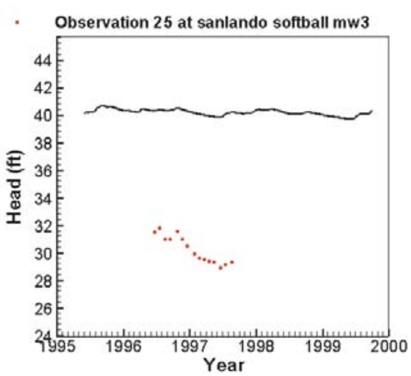

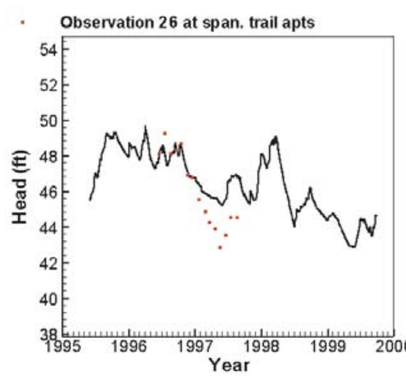

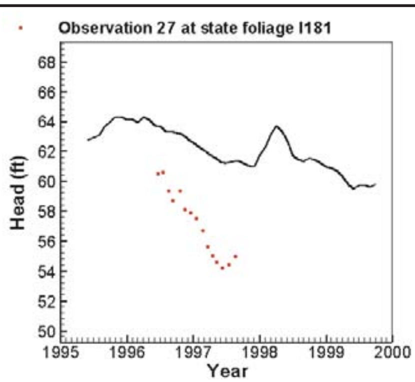

Figure 9.8 Transient Hydrographs at Observation Locations for Transient ISGM Simulation of 1995 through 1999 Conditions. (Page 3 of 11)

Observed Data

ISGM Simulation with Daily Rainfall

ECF Regional Model Simulation

X:\SJR017\TO1\Maps\Conceptual_Model_Report\transient_ISGM.cdr

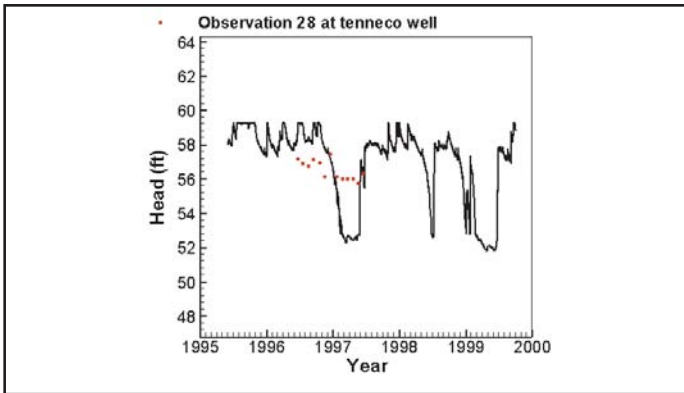

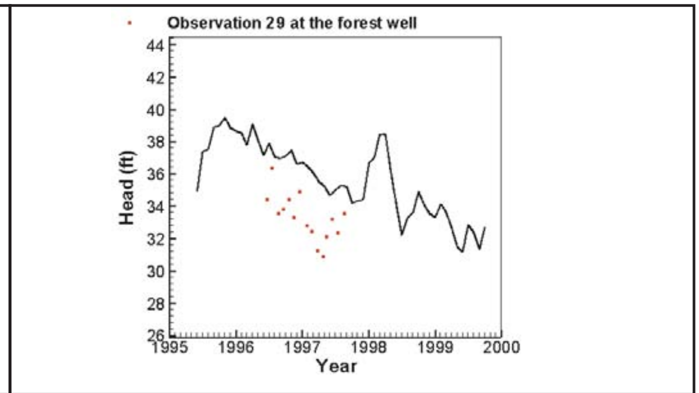

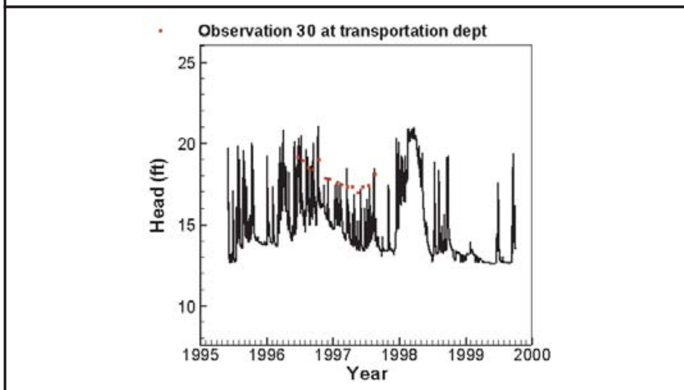

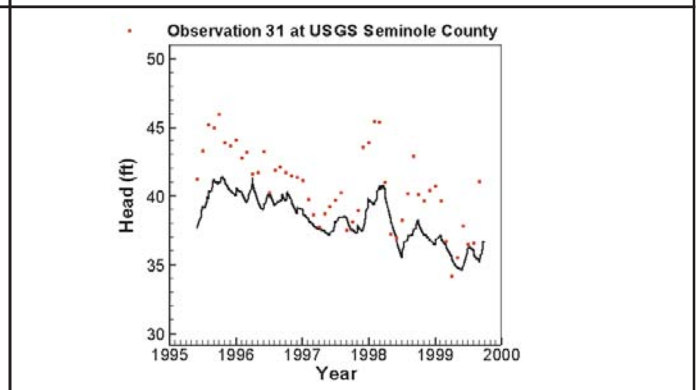

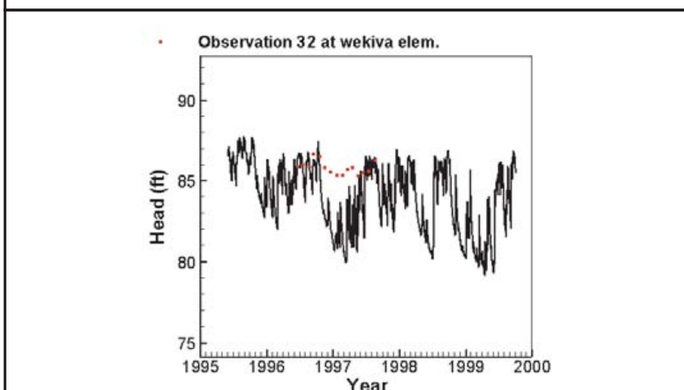

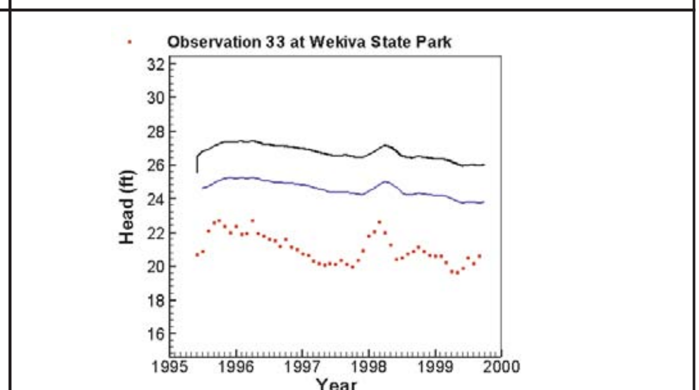

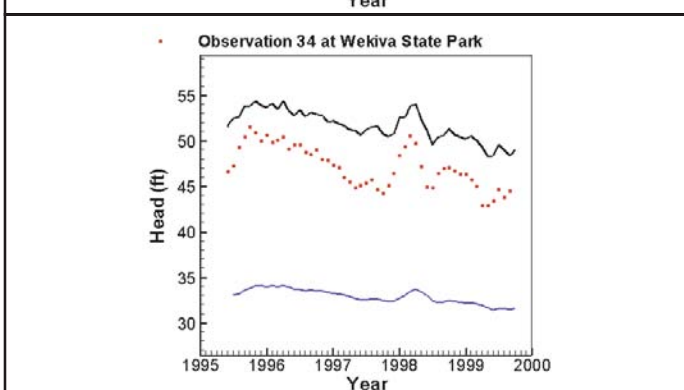

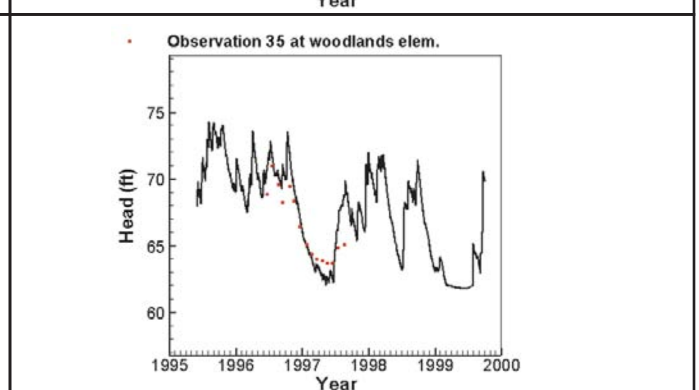

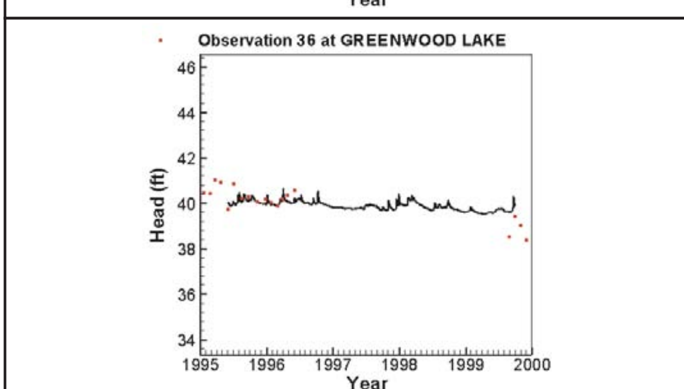

Figure 9.8 Transient Hydrographs at Observation Locations for Transient ISGM Simulation of 1995 through 1999 Conditions. (Page 4 of 11)

Observed Data

ISGM Simulation with Daily Rainfall

ECF Regional Model Simulation

X:\SJR017\TO1\Maps\Conceptual_Model_Report\transient_ISGM.cdr

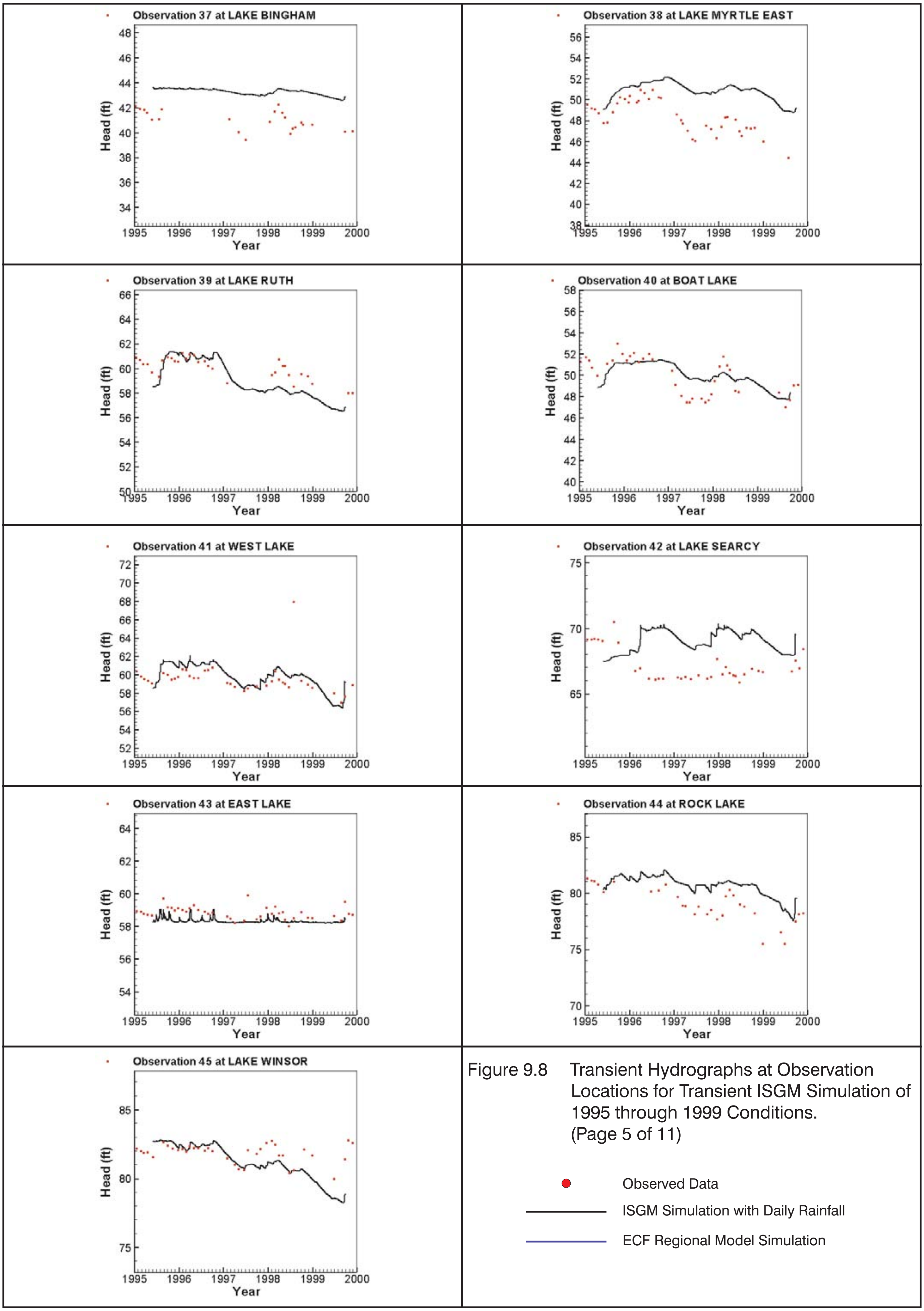

Figure 9.8 Transient Hydrographs at Observation Locations for Transient ISGM Simulation of 1995 through 1999 Conditions. (Page 5 of 11)

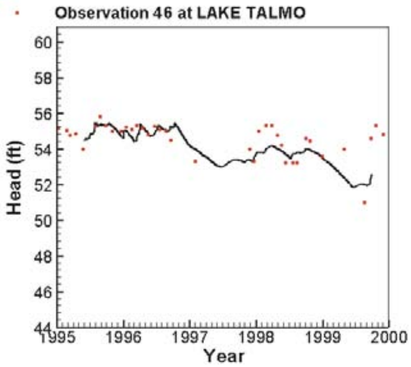

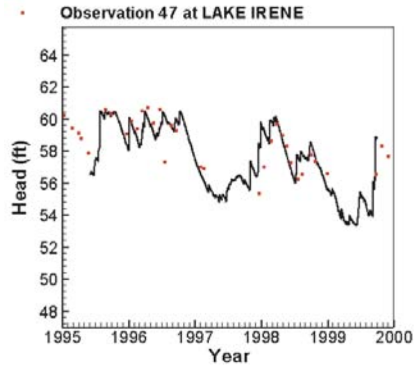

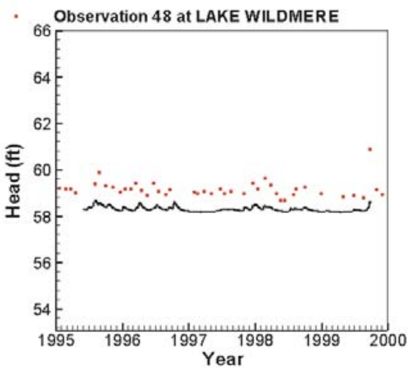

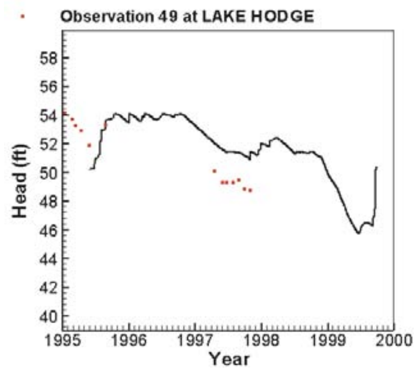

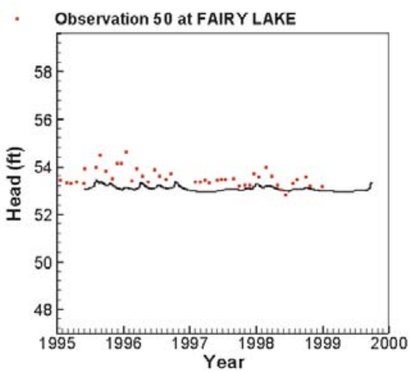

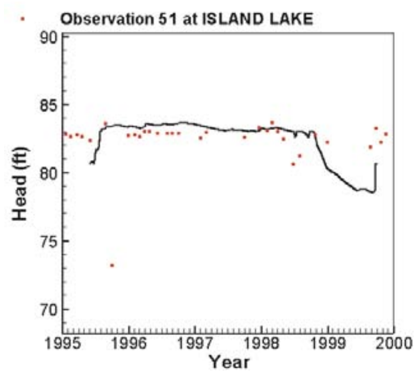

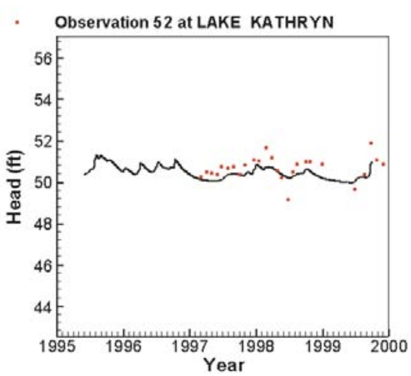

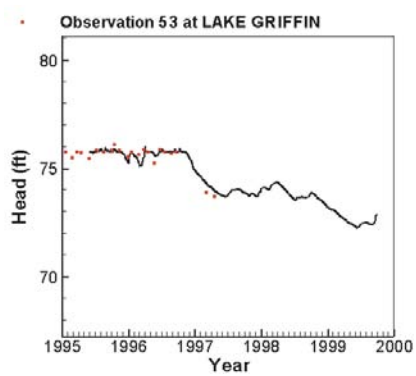

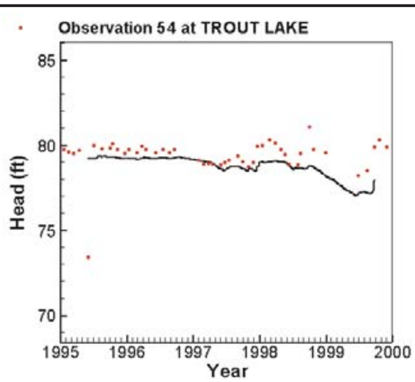

Figure 9.8 Transient Hydrographs at Observation Locations for Transient ISGM Simulation of 1995 through 1999 Conditions. (Page 6 of 11)

Observed Data

ISGM Simulation with Daily Rainfall

ECF Regional Model Simulation

X:\SJR017\TO1\Maps\Conceptual_Model_Report\transient_ISGM.cdr

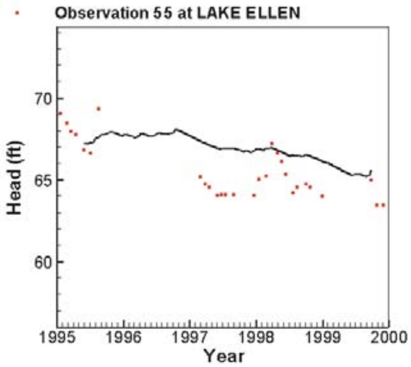

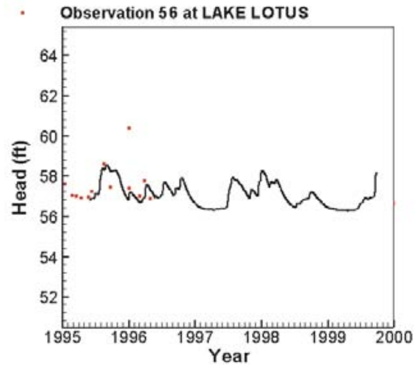

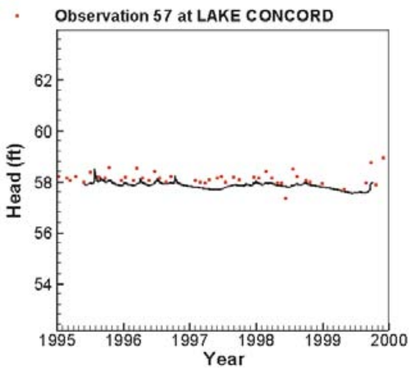

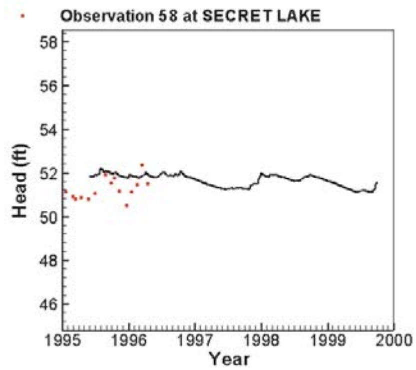

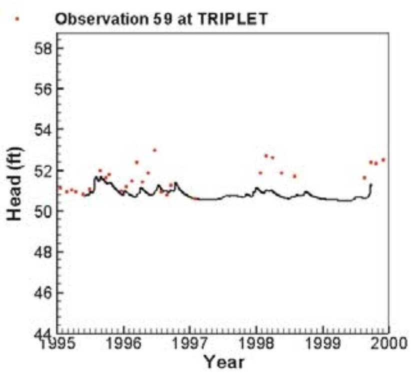

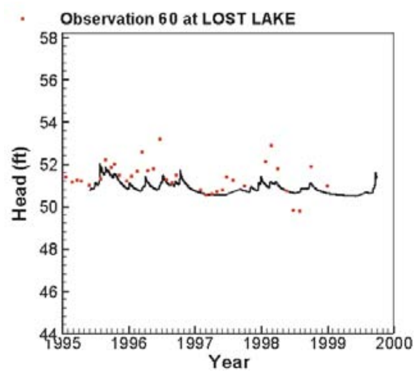

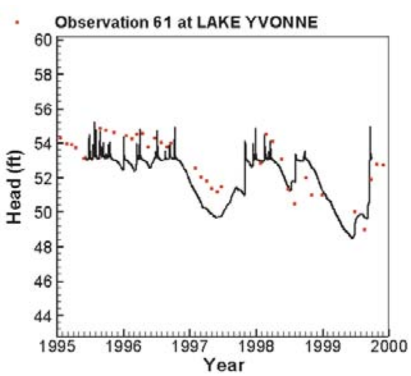

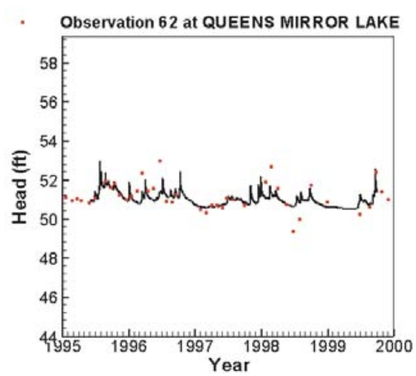

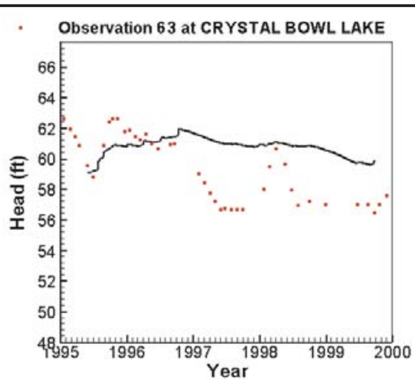

Figure 9.8 Transient Hydrographs at Observation Locations for Transient ISGM Simulation of 1995 through 1999 Conditions. (Page 7 of 11)

Observed Data

ISGM Simulation with Daily Rainfall

ECF Regional Model Simulation

X:\SJR017\TO1\Maps\Conceptual_Model_Report\transient_ISGM.cdr

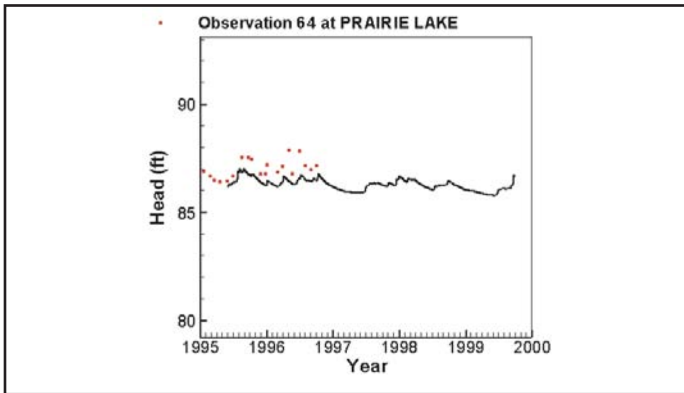

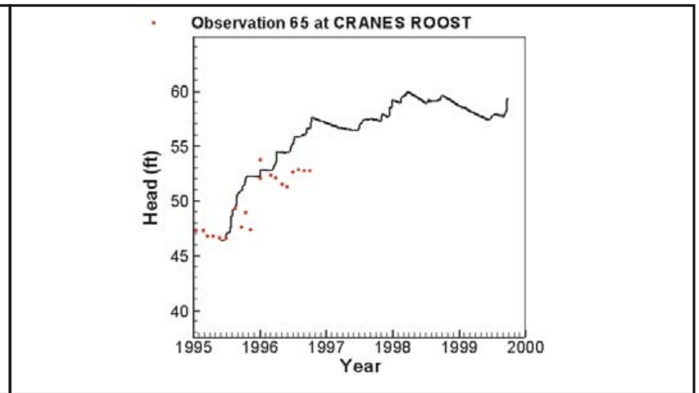

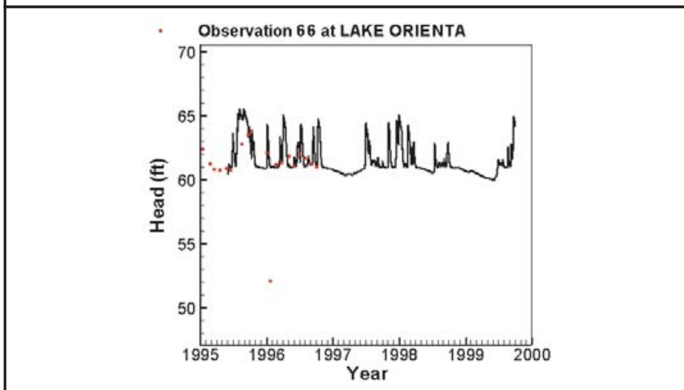

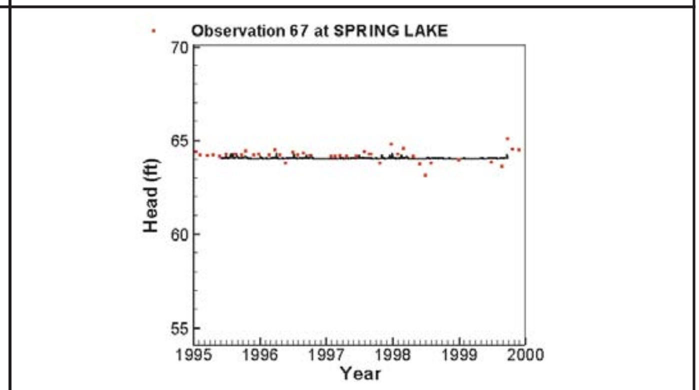

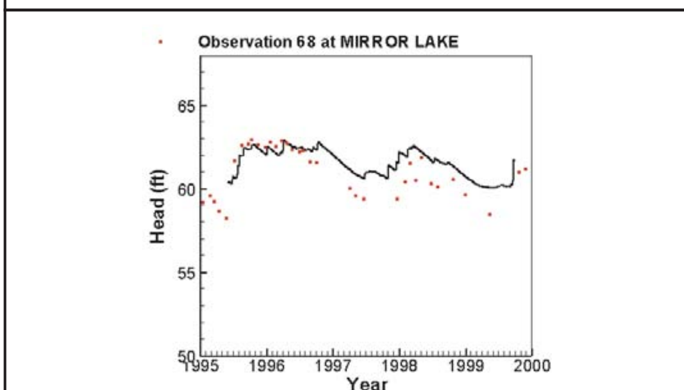

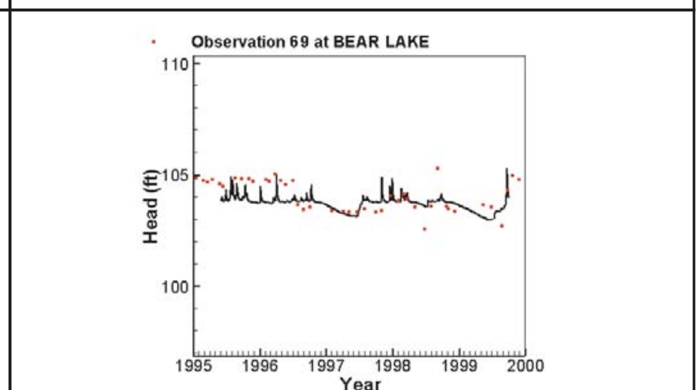

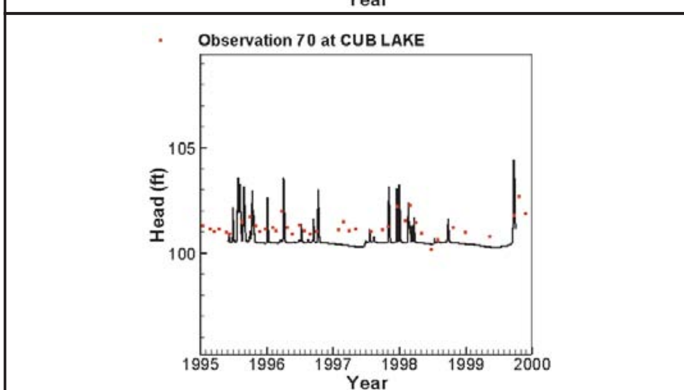

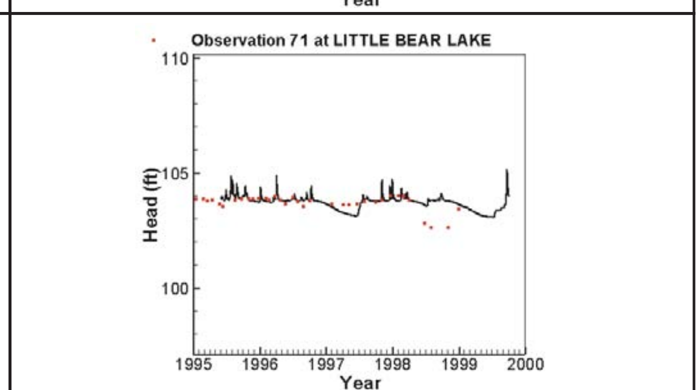

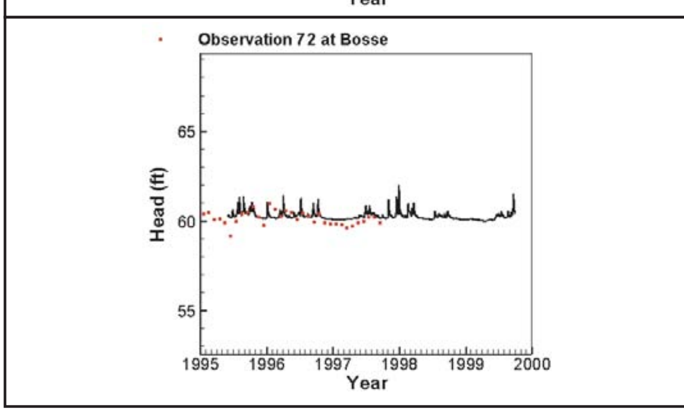

Figure 9.8 Transient Hydrographs at Observation Locations for Transient ISGM Simulation of 1995 through 1999 Conditions. (Page 8 of 11)

● Observed Data

—— ISGM Simulation with Daily Rainfall

—— ECF Regional Model Simulation

X:\SJR017\TO1\Maps\Conceptual_Model_Report\transient_ISGM.cdr

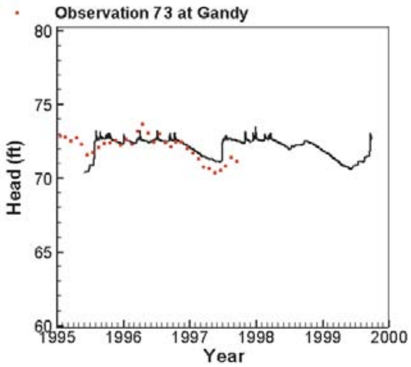

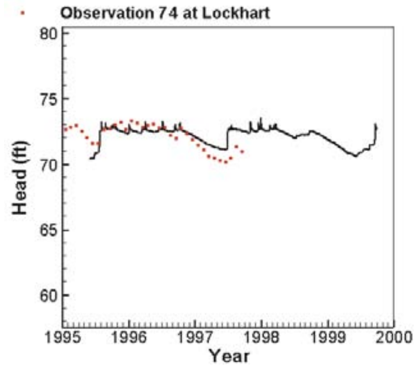

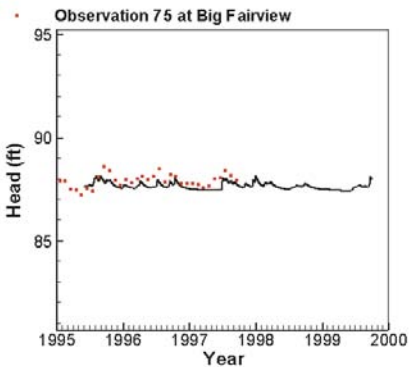

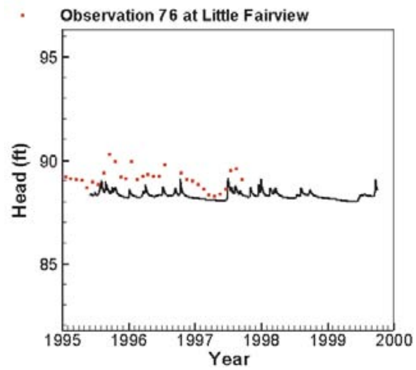

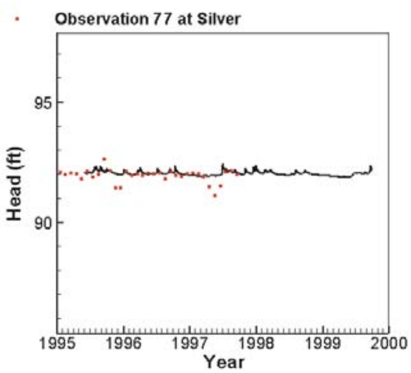

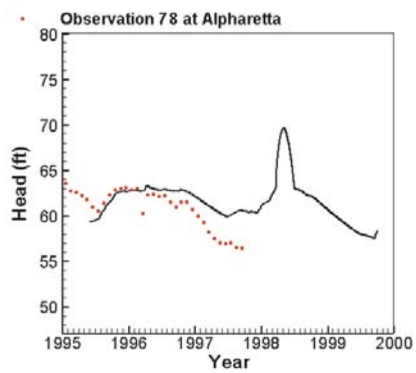

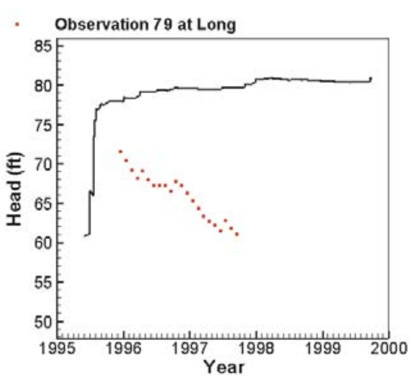

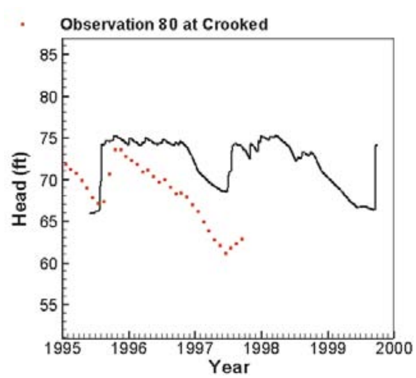

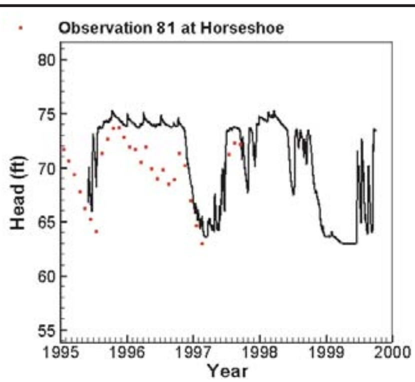

Figure 9.8 Transient Hydrographs at Observation Locations for Transient ISGM Simulation of 1995 through 1999 Conditions. (Page 9 of 11)

Observed Data

ISGM Simulation with Daily Rainfall

ECF Regional Model Simulation

X:\SJR017\TO1\Maps\Conceptual_Model_Report\transient_ISGM.cdr

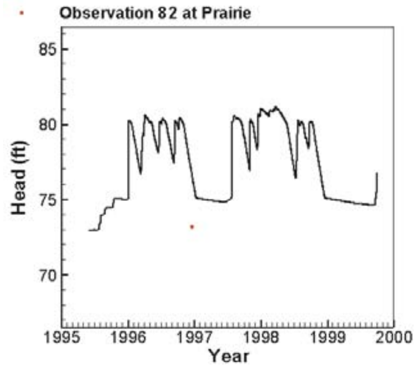

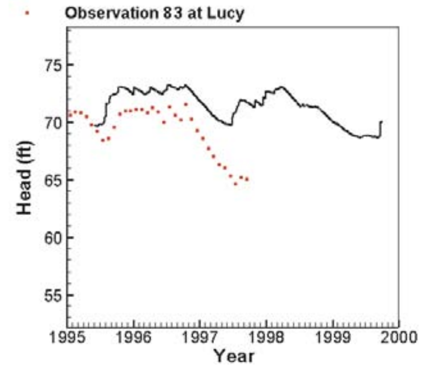

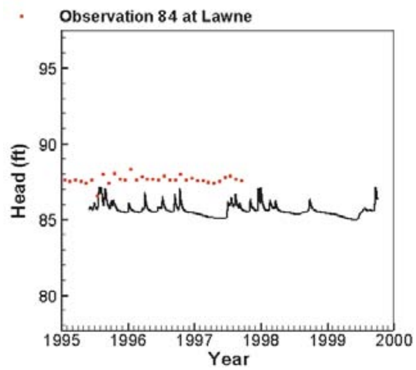

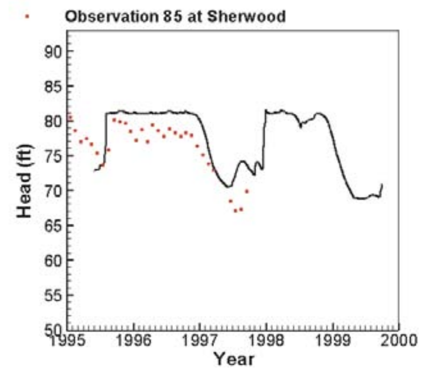

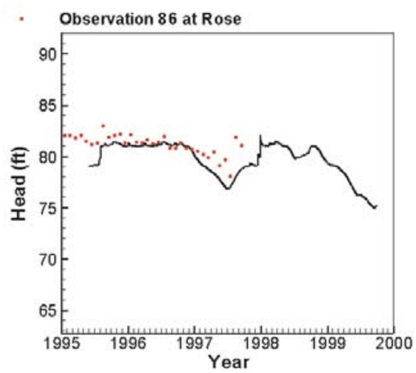

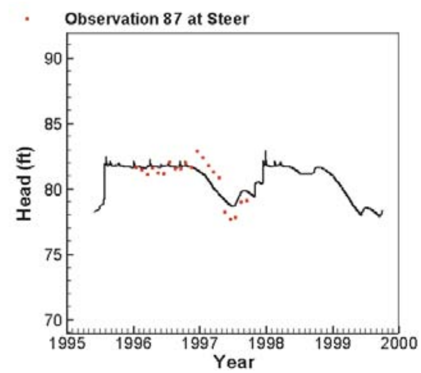

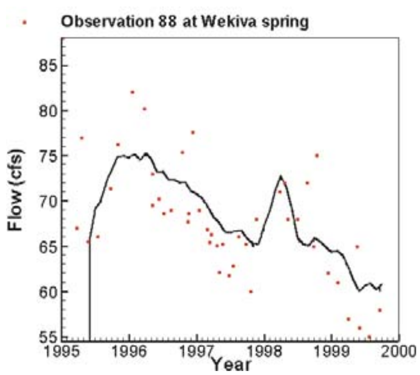

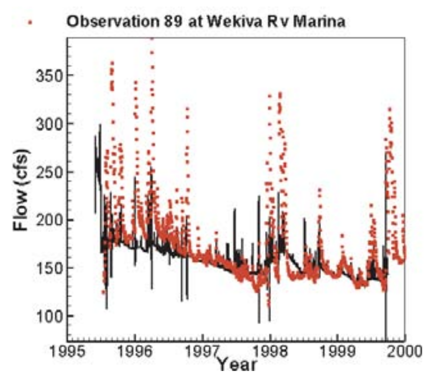

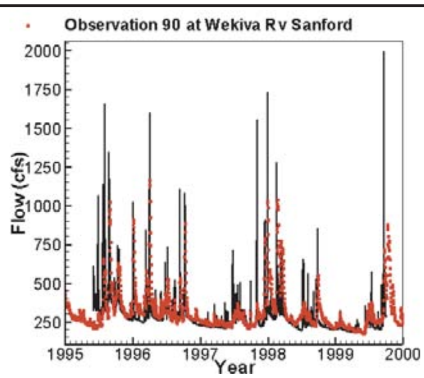

Figure 9.8 Transient Hydrographs at Observation Locations for Transient ISGM Simulation of 1995 through 1999 Conditions. (Page 10 of 11)

Observed Data

ISGM Simulation with Daily Rainfall

ECF Regional Model Simulation

X:\SJR017\TO1\Maps\Conceptual_Model_Report\transient_ISGM.cdr

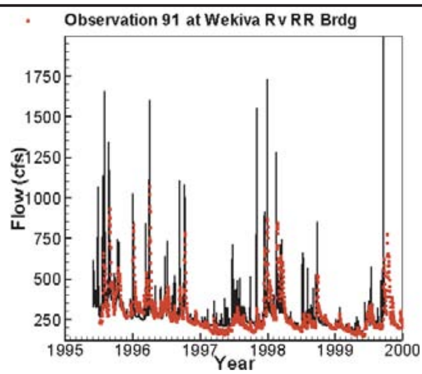

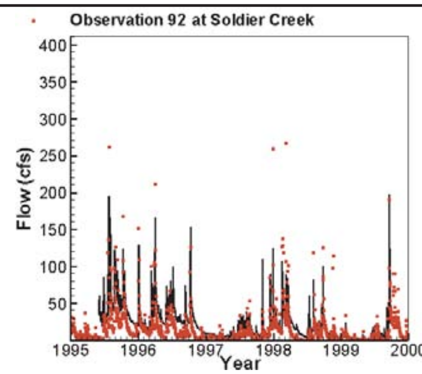

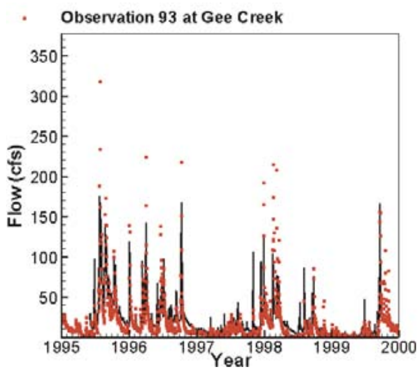

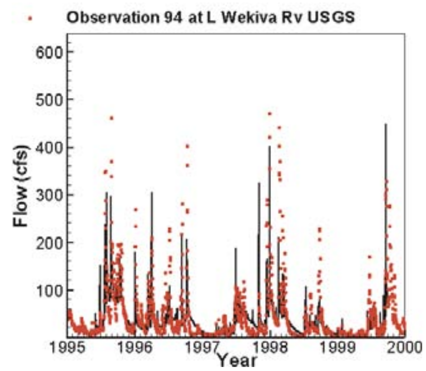

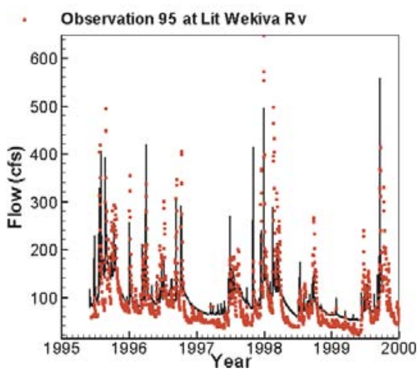

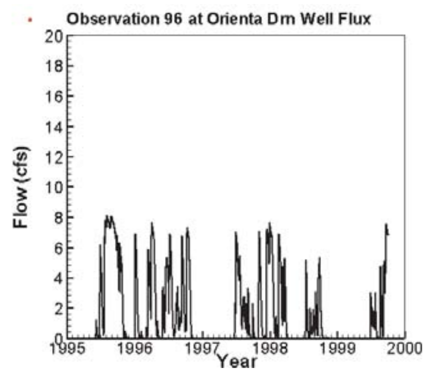

Figure 9.8 Transient Hydrographs at Observation Locations for Transient ISGM Simulation of 1995 through 1999 Conditions. (Page 11 of 11)

Observed Data
ISGM Simulation with Daily Rainfall
ECF Regional Model Simulation

X:\SJR017\TO1\Maps\Conceptual_Model_Report\transient_ISGM.cdr

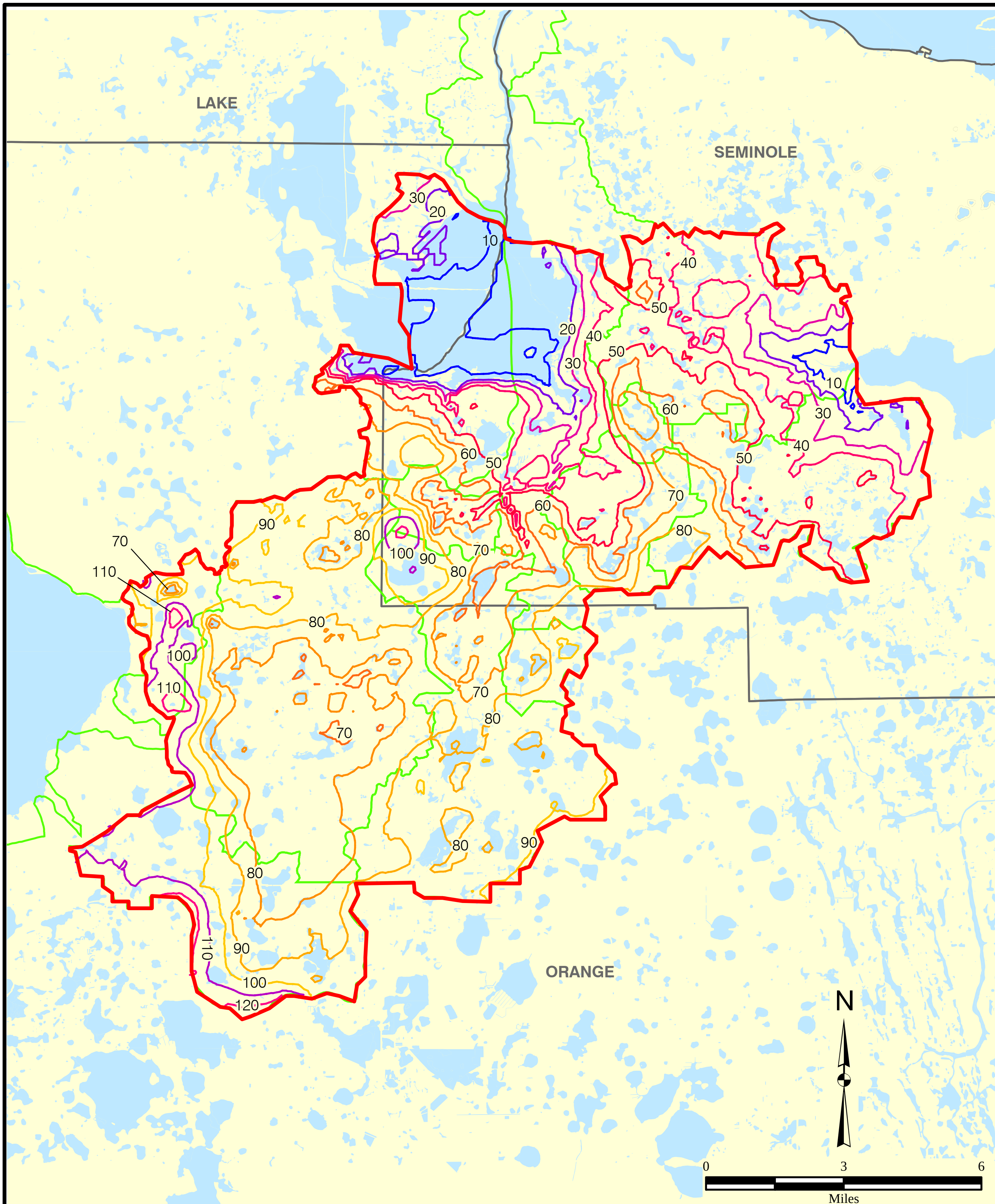

Source:
Filename: X:/SJR017/TO1/Maps/
Conceptual_model_report/WL_SAS_TS_Mar99.mxd
Project: SJR017-001-06
Revised: 12/22/04 TB

Legend

- Model Boundary
- Surface Water Basin
- County Boundary
- 50 Water Levels (ft)
- Surface Water Bodies and Wetlands

Figure 10.1
Simulated Water Levels in the SAS for May 1999 Conditions for the Transient Sensitivity Analysis of Temporal Averaging of Precipitation

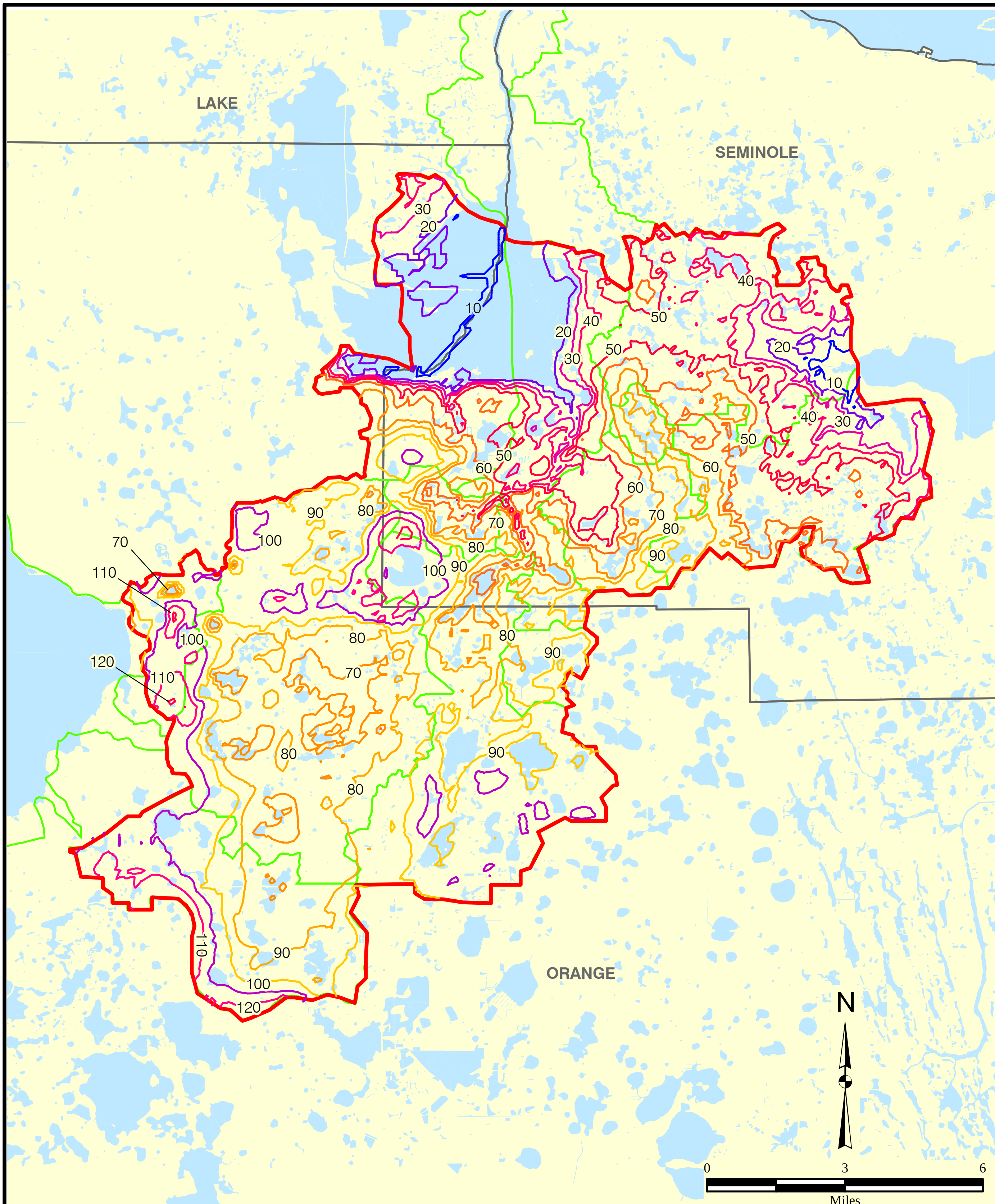

Source:
Filename: X:/SJR017/TO1/Maps/
Conceptual_model_report/WL_SAS_TS_Sept99.mxd
Project: SJR017-001-06
Revised: 12/22/04 TB

Legend

- Model Boundary
- Surface Water Basin
- County Boundary
- 50 Water Levels (ft)
- Surface Water Bodies and Wetlands

Figure 10.2
Simulated Water Levels in the SAS for September 1999 Conditions for the Transient Sensitivity Analysis of Temporal Averaging of Precipitation

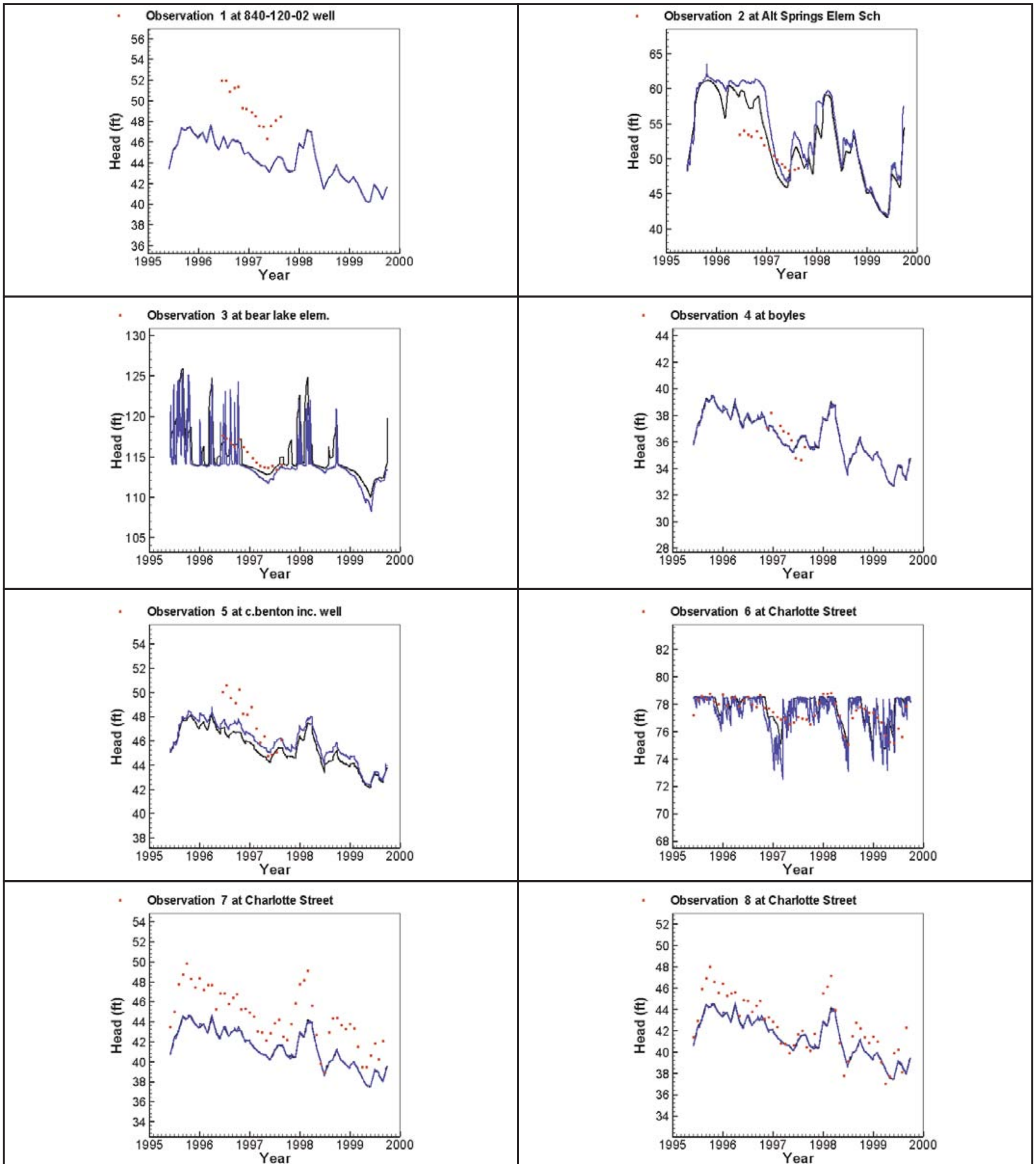

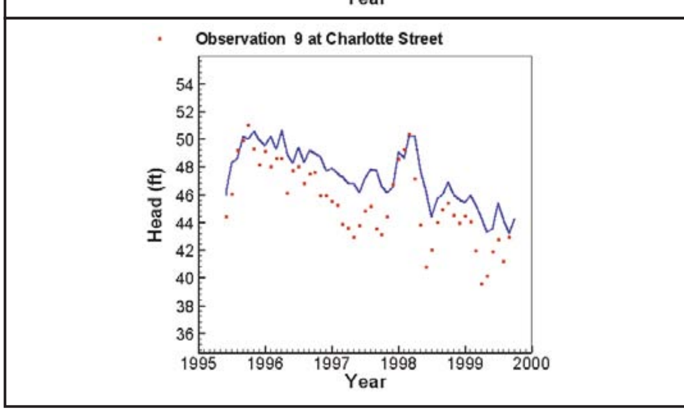

Figure 10.3 Transient Hydrographs at Observation Locations for Sensitivity to Time-Scale of Rainfall Input for Transient ISGM Simulation of 1995 through 1999 Conditions. (Page 1 of 11)

- Observed Data
- Simulation with Monthly Rainfall
- Simulation with Daily Rainfall

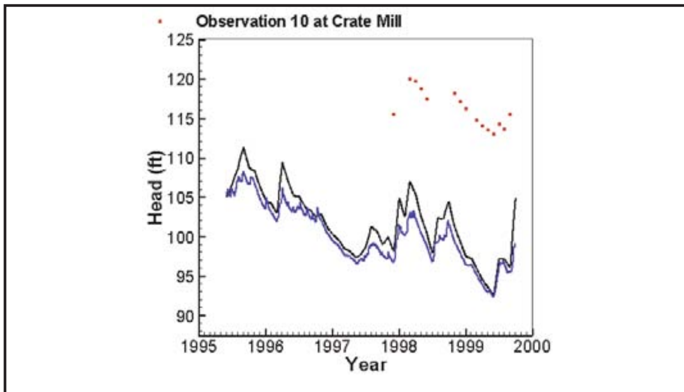

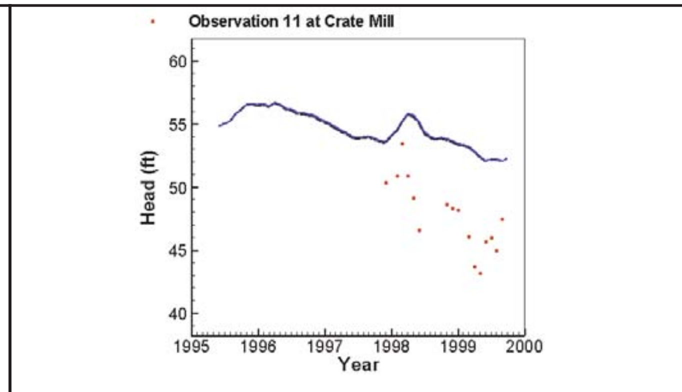

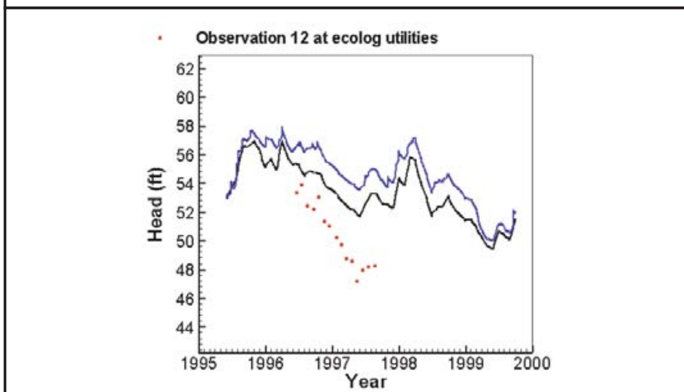

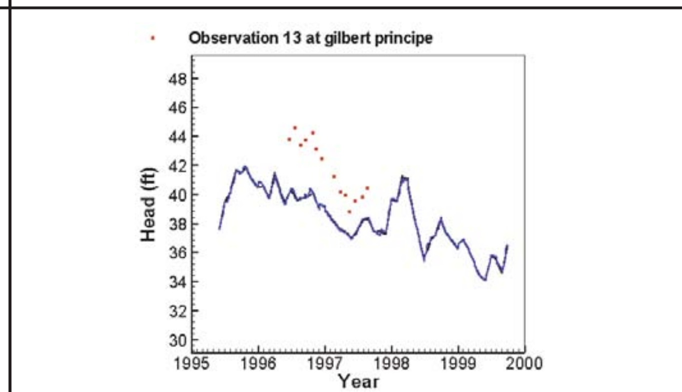

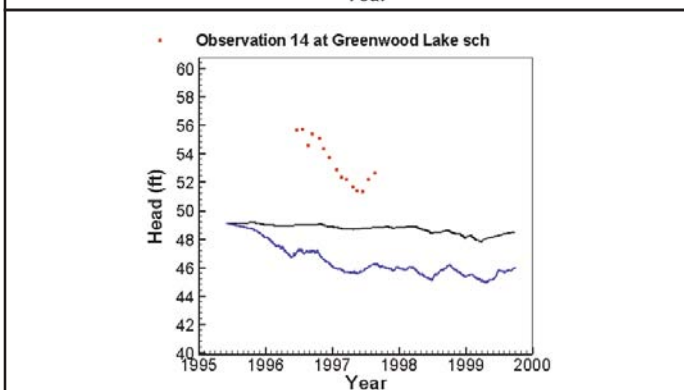

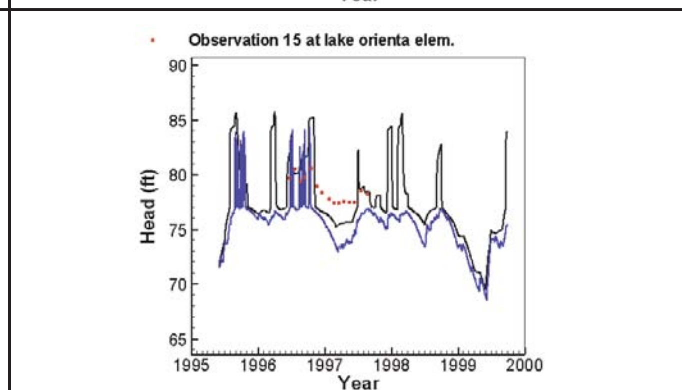

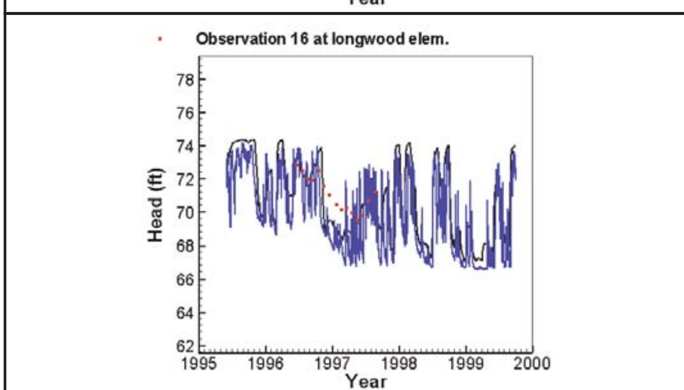

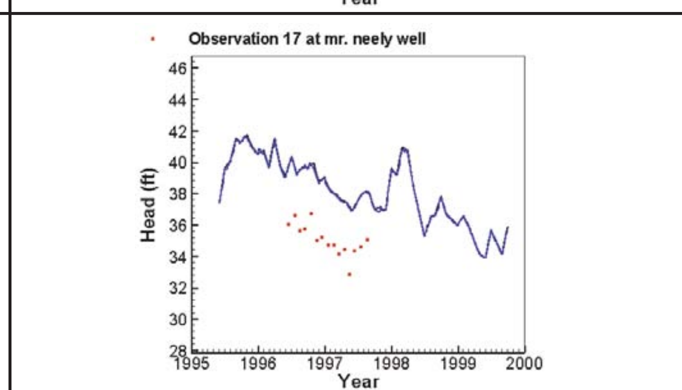

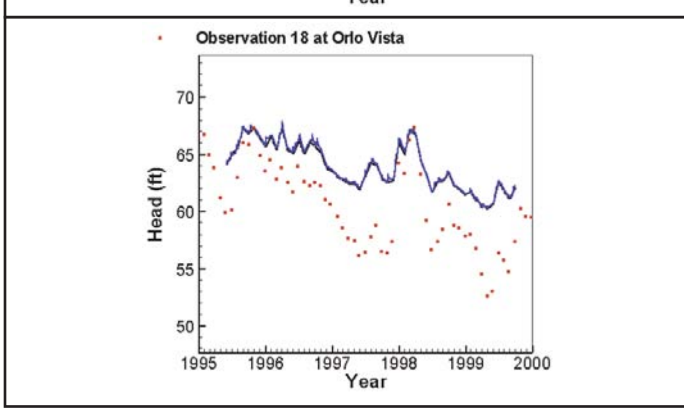

Figure 10.3 Transient Hydrographs at Observation Locations for Sensitivity to Time-Scale of Rainfall Input for Transient ISGM Simulation of 1995 through 1999 Conditions. (Page 2 of 11)

● Observed Data

Simulation with Monthly Rainfall

Simulation with Daily Rainfall

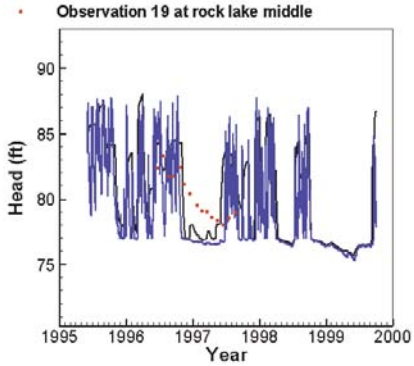

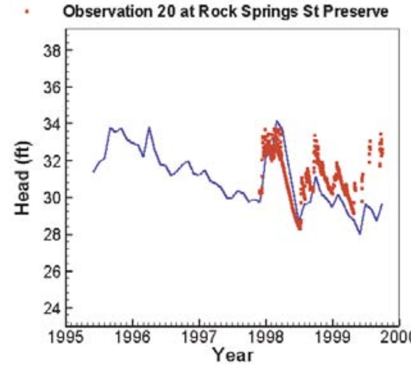

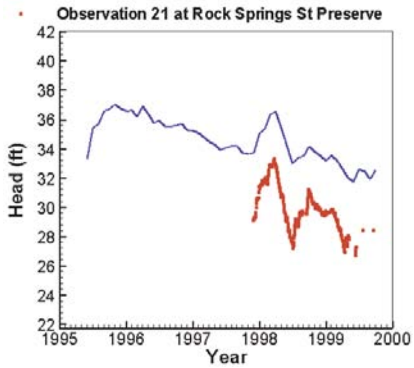

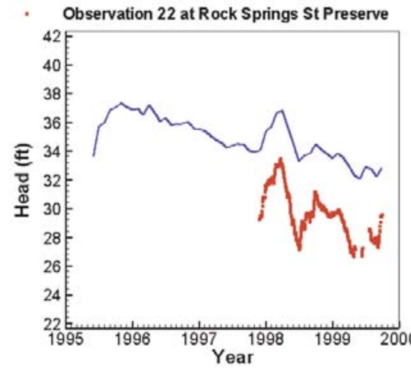

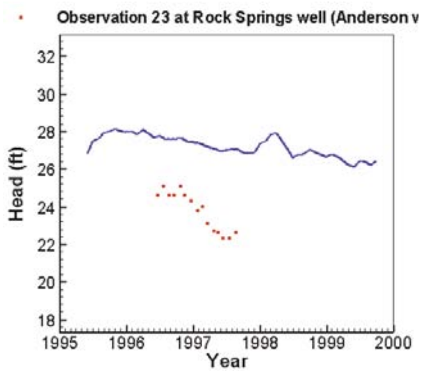

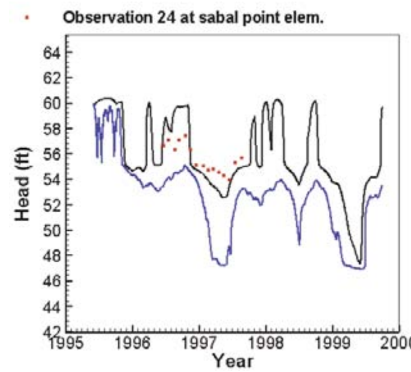

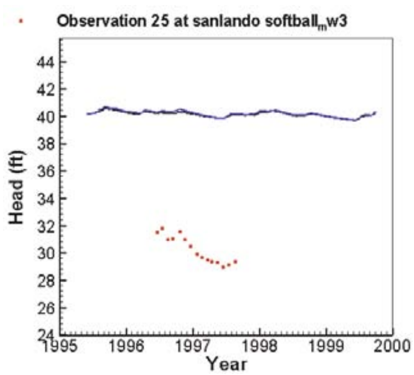

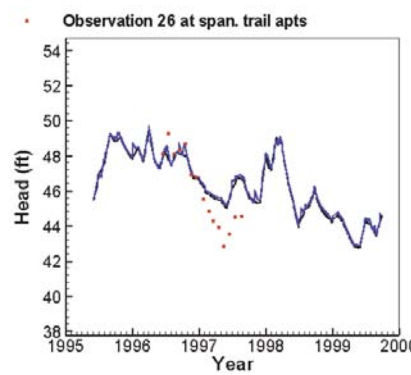

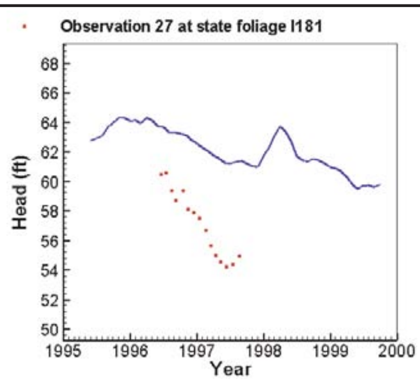

Figure 10.3 Transient Hydrographs at Observation Locations for Sensitivity to Time-Scale of Rainfall Input for Transient ISGM Simulation of 1995 through 1999 Conditions. (Page 3 of 11)

Observed Data

Simulation with Monthly Rainfall

Simulation with Daily Rainfall

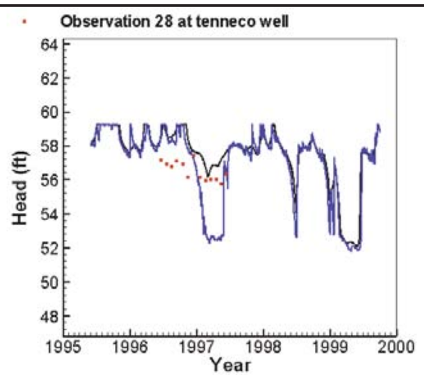

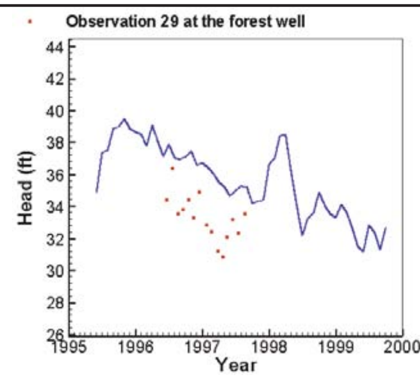

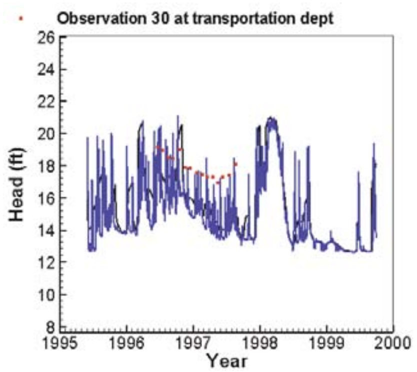

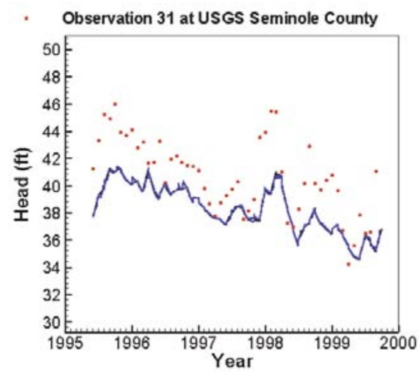

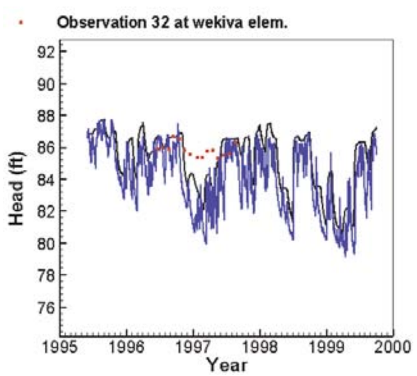

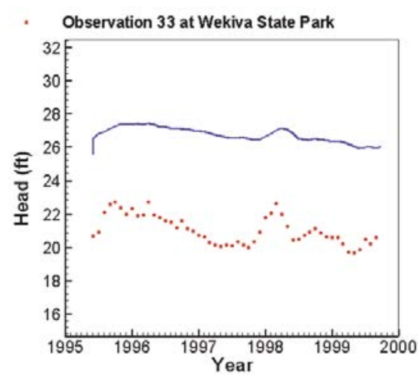

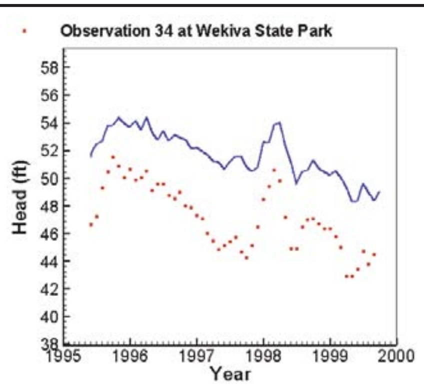

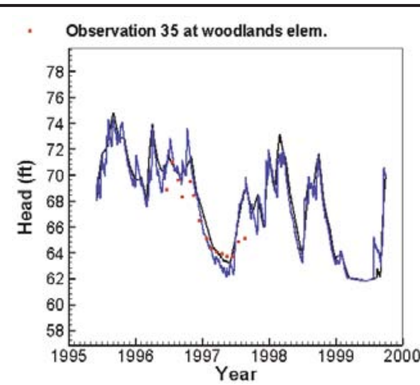

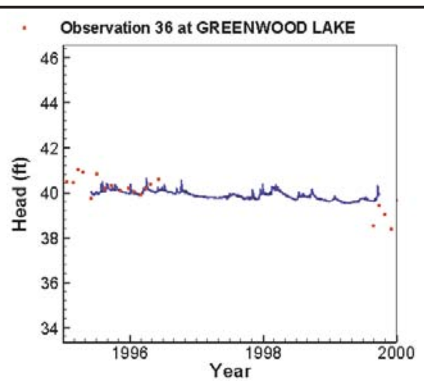

Figure 10.3 Transient Hydrographs at Observation Locations for Sensitivity to Time-Scale of Rainfall Input for Transient ISGM Simulation of 1995 through 1999 Conditions. (Page 4 of 11)

Observed Data

Simulation with Monthly Rainfall

Simulation with Daily Rainfall

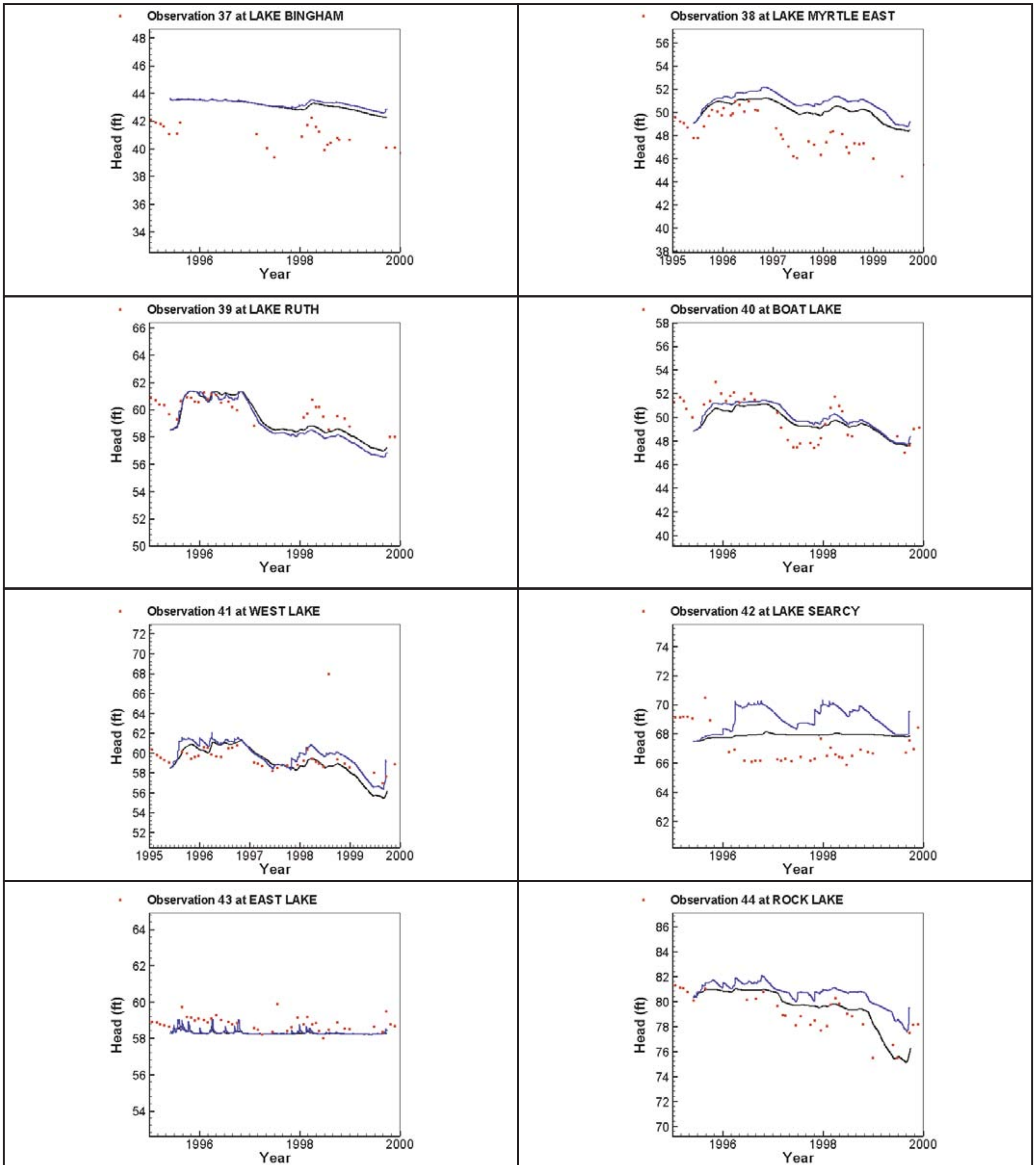

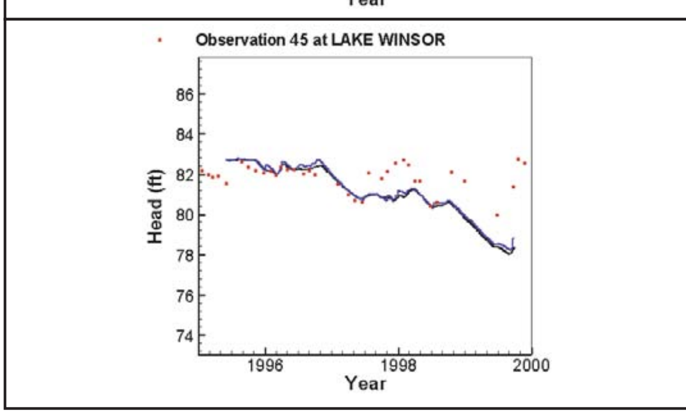

Figure 10.3 Transient Hydrographs at Observation Locations for Sensitivity to Time-Scale of Rainfall Input for Transient ISGM Simulation of 1995 through 1999 Conditions. (Page 5 of 11)

Observed Data

Simulation with Monthly Rainfall

Simulation with Daily Rainfall

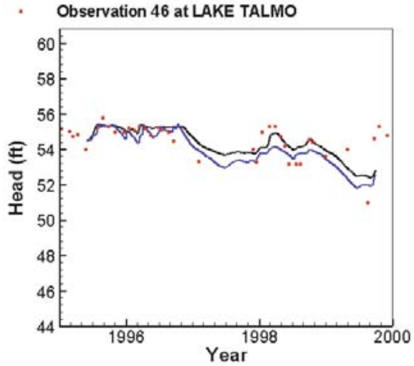

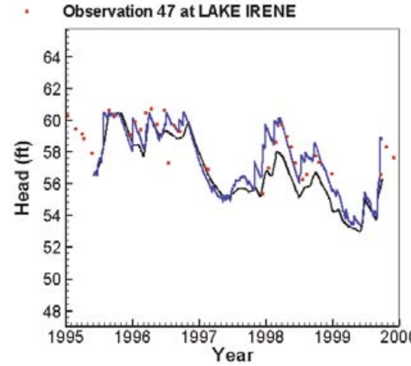

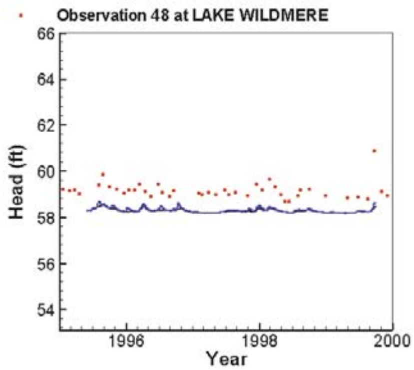

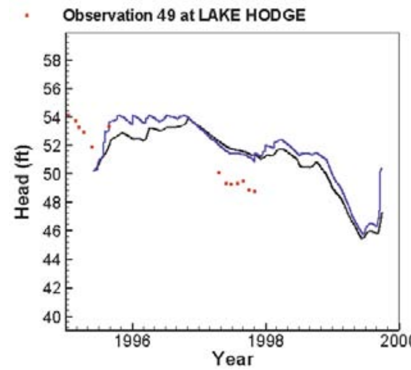

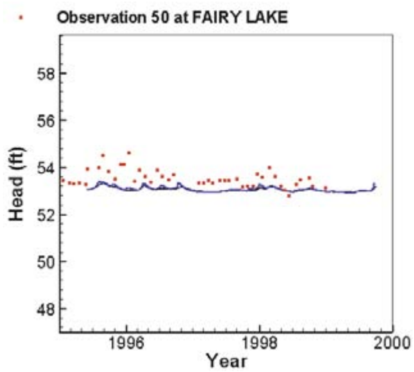

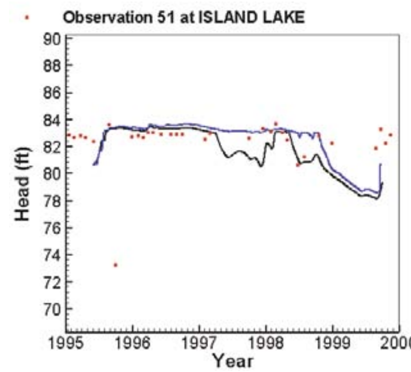

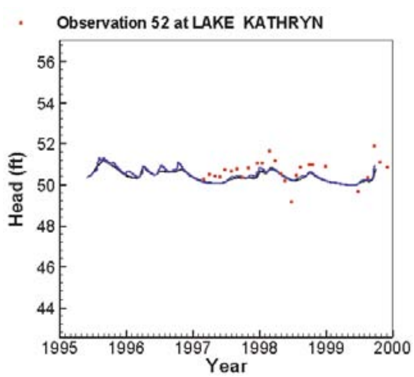

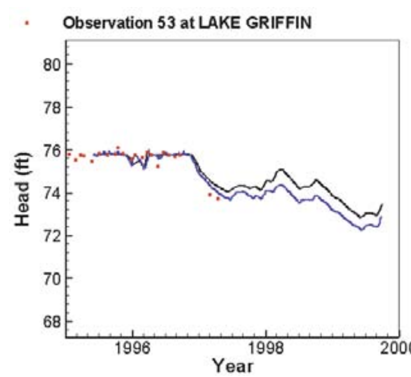

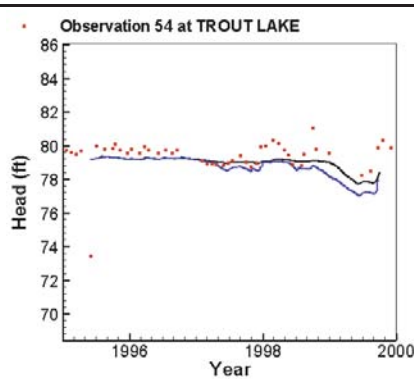

Figure 10.3 Transient Hydrographs at Observation Locations for Sensitivity to Time-Scale of Rainfall Input for Transient ISGM Simulation of 1995 through 1999 Conditions. (Page 6 of 11)

Observed Data

Simulation with Monthly Rainfall

Simulation with Daily Rainfall

X:\SJR017\TO1\Maps\Conceptual_Model_Report\graphs_day-mo.cdr

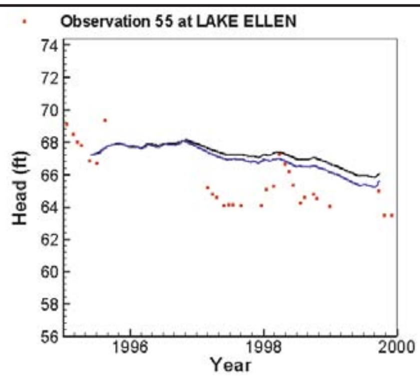

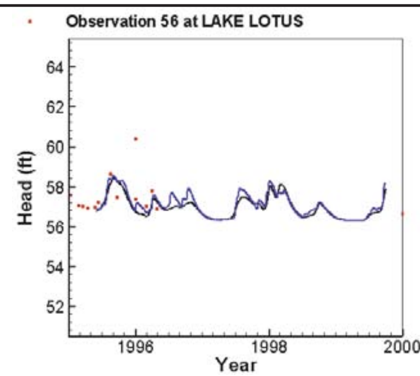

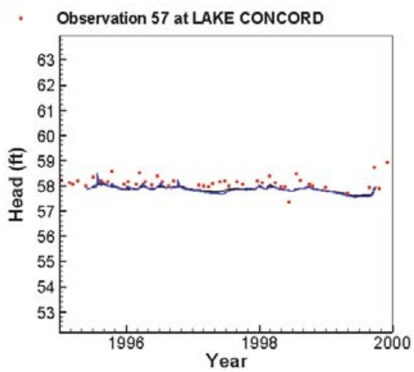

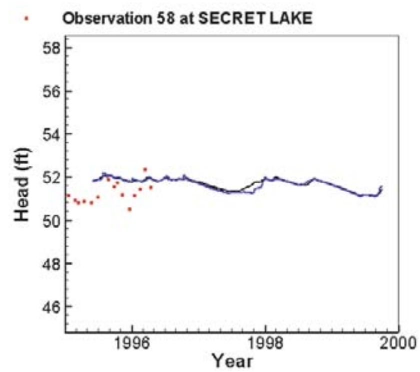

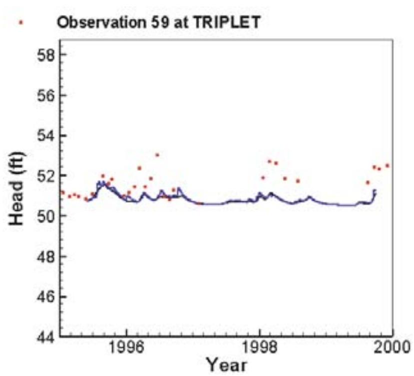

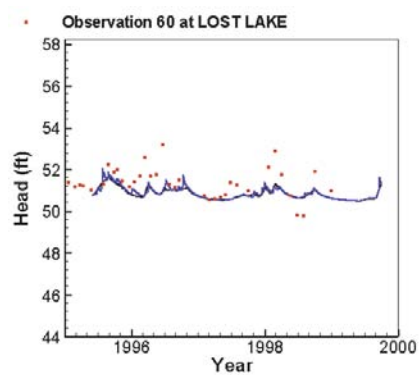

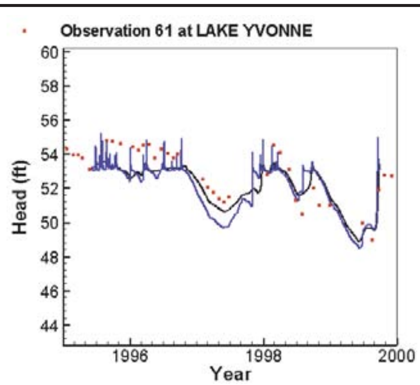

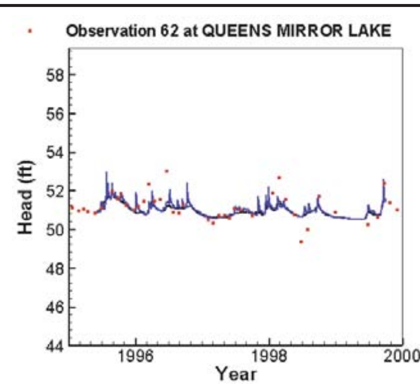

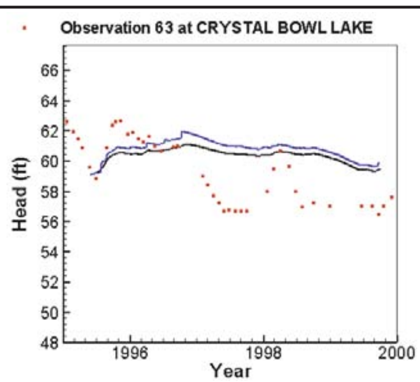

Figure 10.3 Transient Hydrographs at Observation Locations for Sensitivity to Time-Scale of Rainfall Input for Transient ISGM Simulation of 1995 through 1999 Conditions. (Page 7 of 11)

Observed Data

Simulation with Monthly Rainfall

Simulation with Daily Rainfall

X:\SJR017\TO1\Maps\Conceptual_Model_Report\graphs_day-mo.cdr

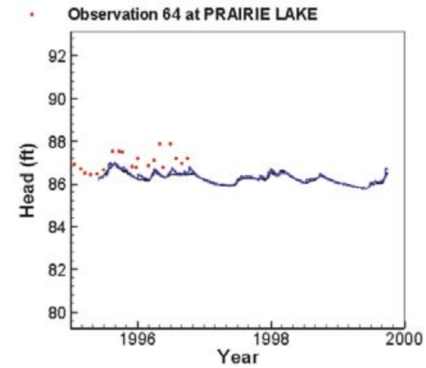

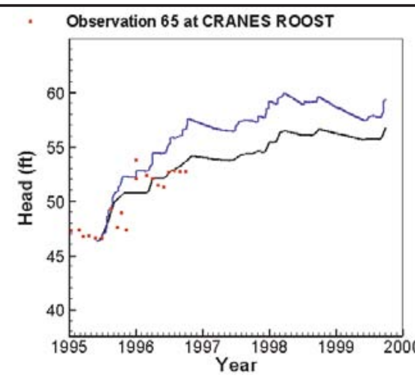

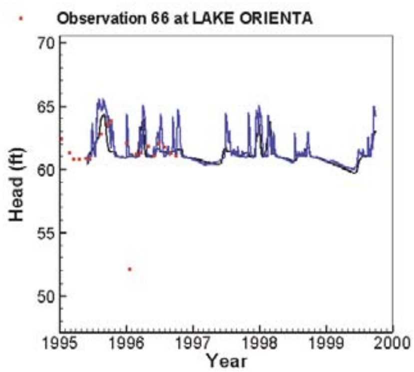

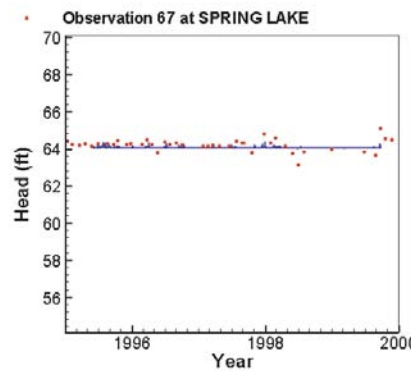

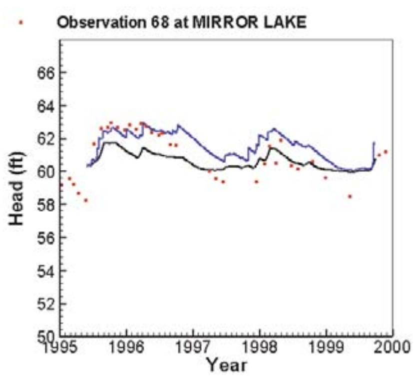

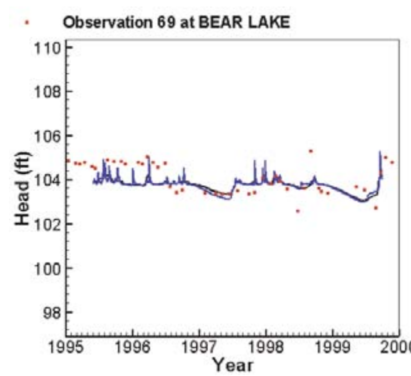

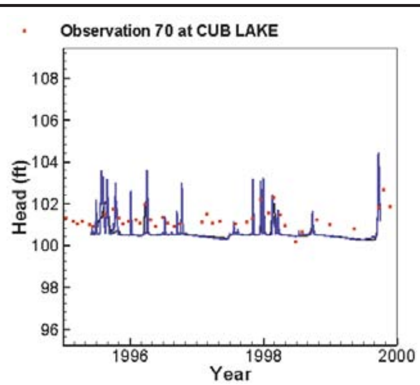

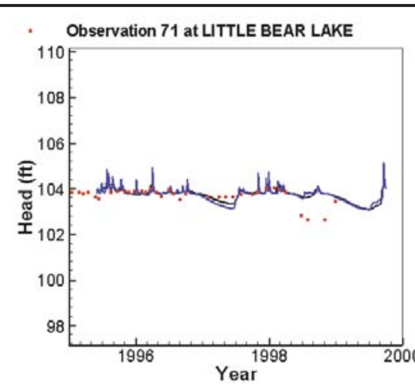

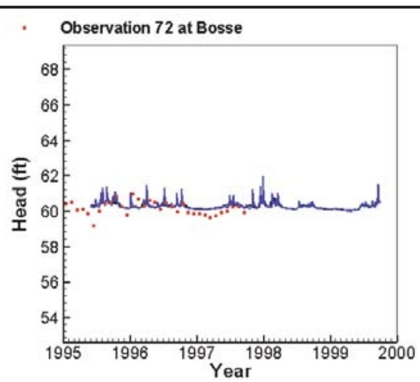

Figure 10.3 Transient Hydrographs at Observation Locations for Sensitivity to Time-Scale of Rainfall Input for Transient ISGM Simulation of 1995 through 1999 Conditions. (Page 8 of 11)

Observed Data

Simulation with Monthly Rainfall

Simulation with Daily Rainfall

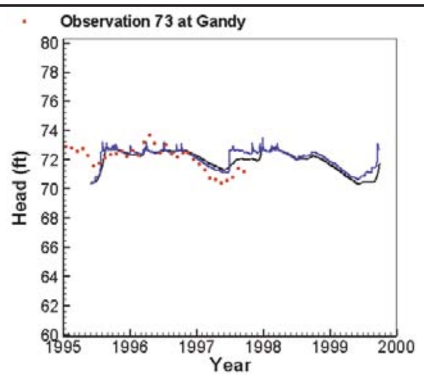

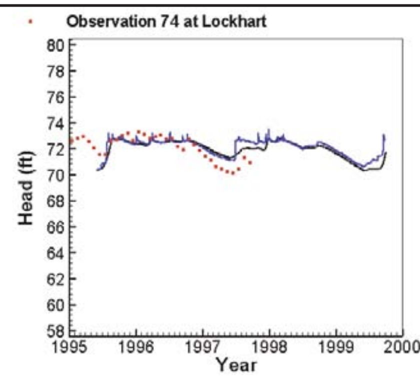

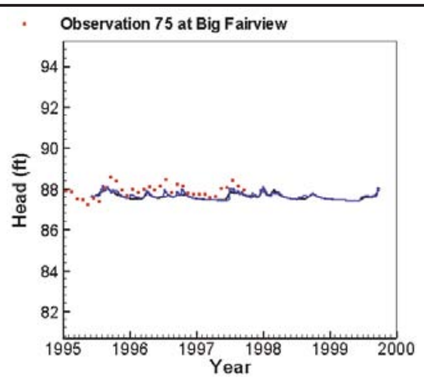

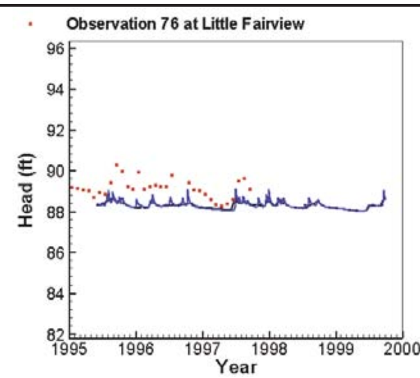

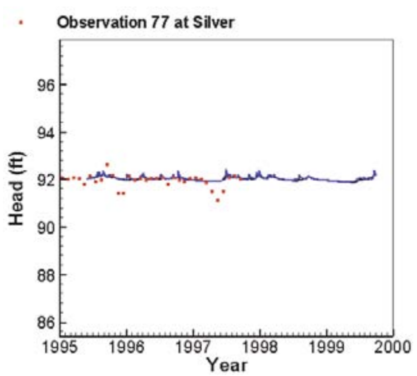

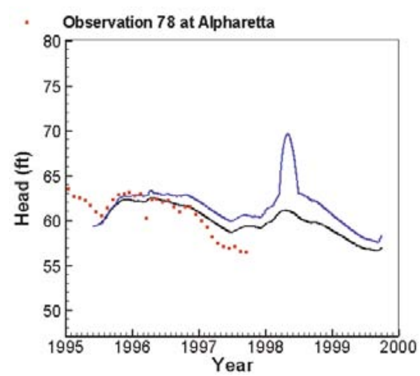

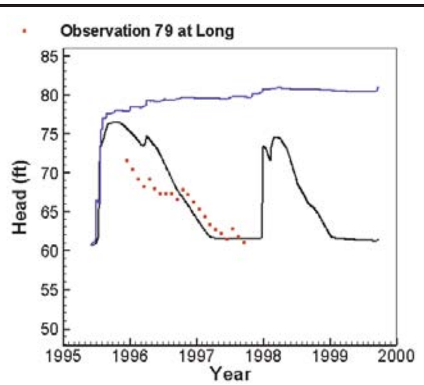

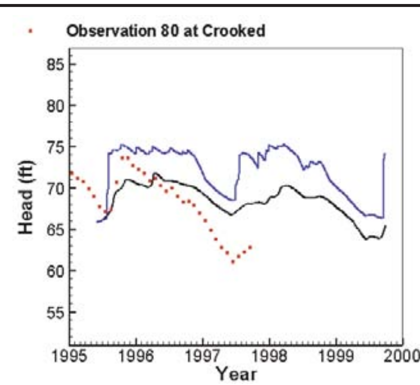

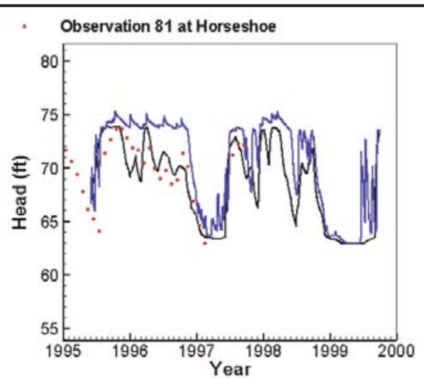

Figure 10.3 Transient Hydrographs at Observation Locations for Sensitivity to Time-Scale of Rainfall Input for Transient ISGM Simulation of 1995 through 1999 Conditions. (Page 9 of 11)

● Observed Data

Simulation with Monthly Rainfall

Simulation with Daily Rainfall

X:\SJR017\TO1\Maps\Conceptual_Model_Report\graphs_day-mo.cdr

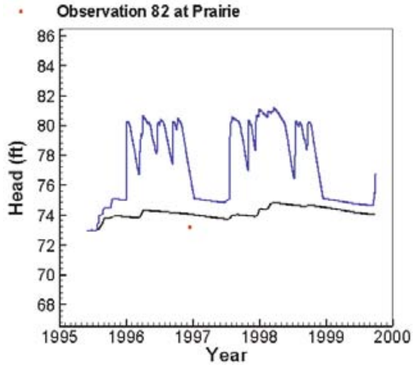

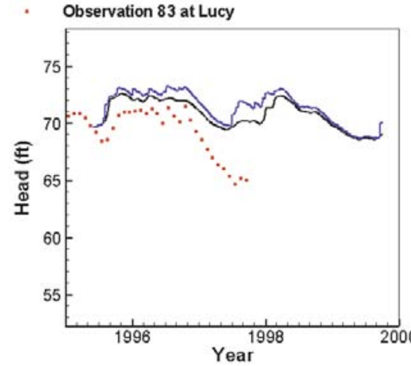

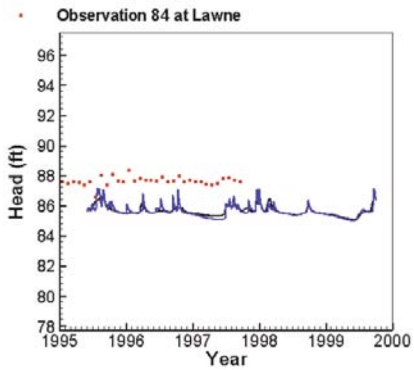

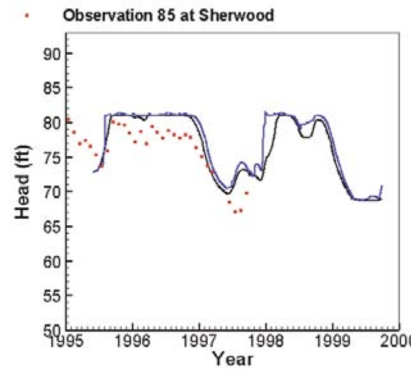

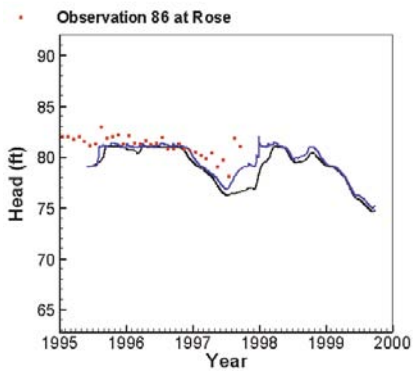

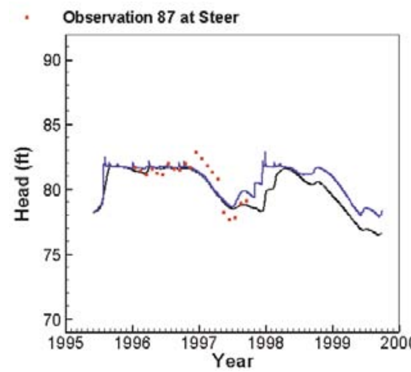

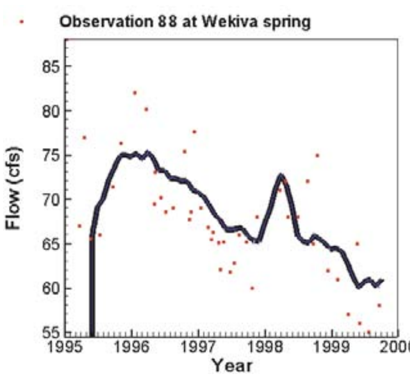

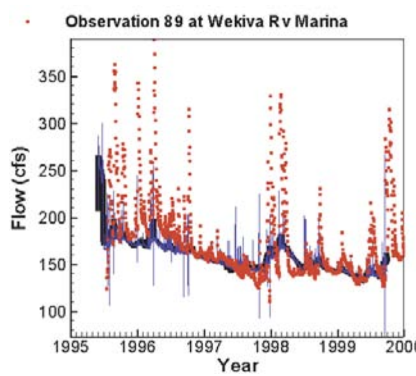

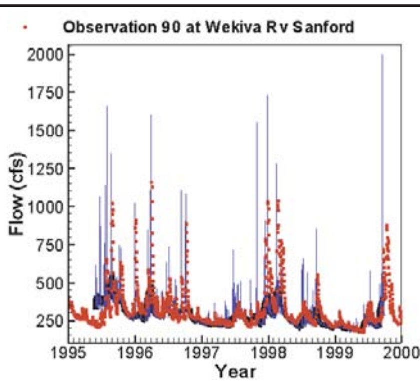

Figure 10.3 Transient Hydrographs at Observation Locations for Sensitivity to Time-Scale of Rainfall Input for Transient ISGM Simulation of 1995 through 1999 Conditions. (Page 10 of 11)

Observed Data

Simulation with Monthly Rainfall

Simulation with Daily Rainfall

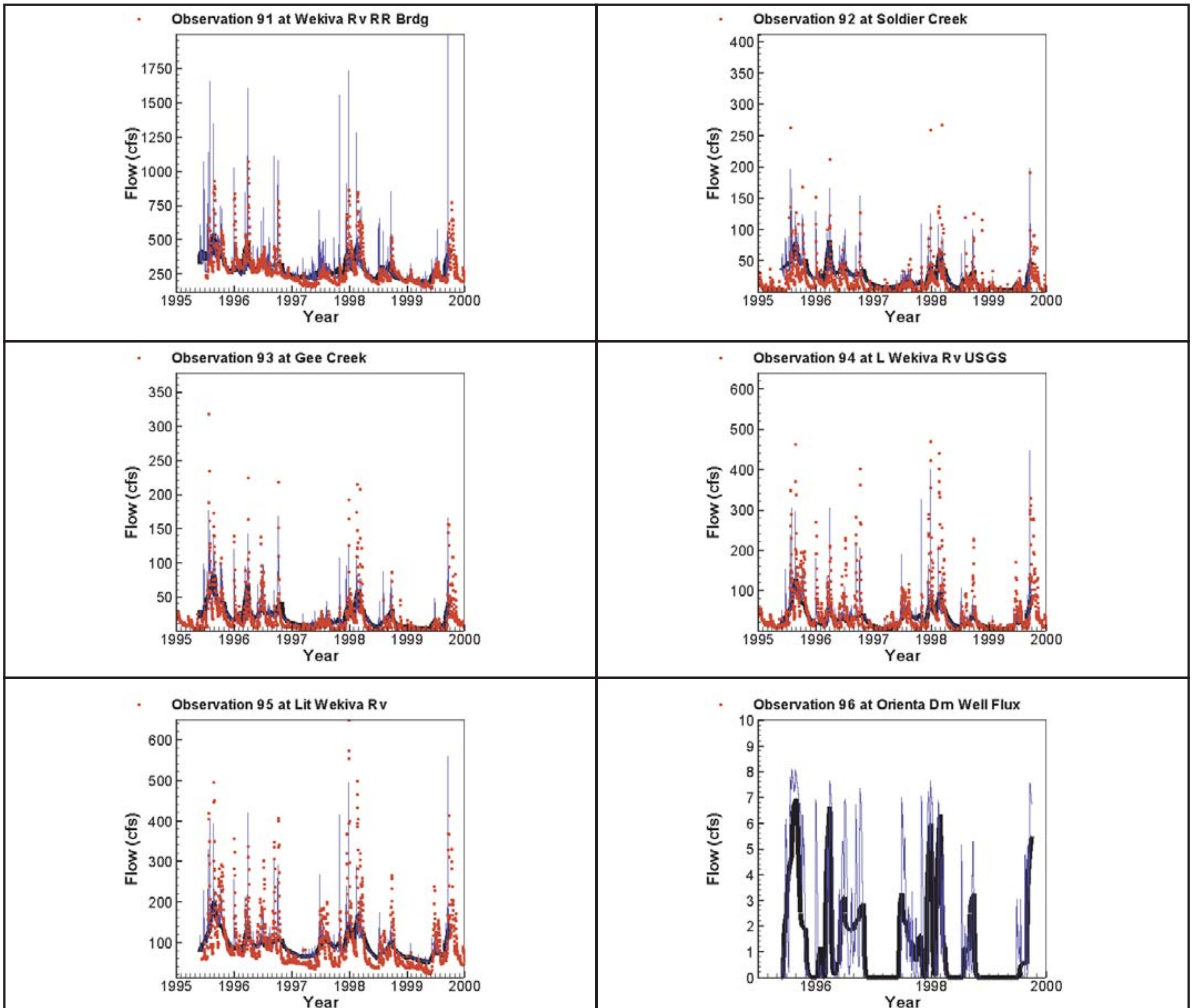

Figure 10.3 Transient Hydrographs at Observation Locations for Sensitivity to Time-Scale of Rainfall Input for Transient ISGM Simulation of 1995 through 1999 Conditions. (Page 11 of 11)

Observed Data

Simulation with Monthly Rainfall

Simulation with Daily Rainfall

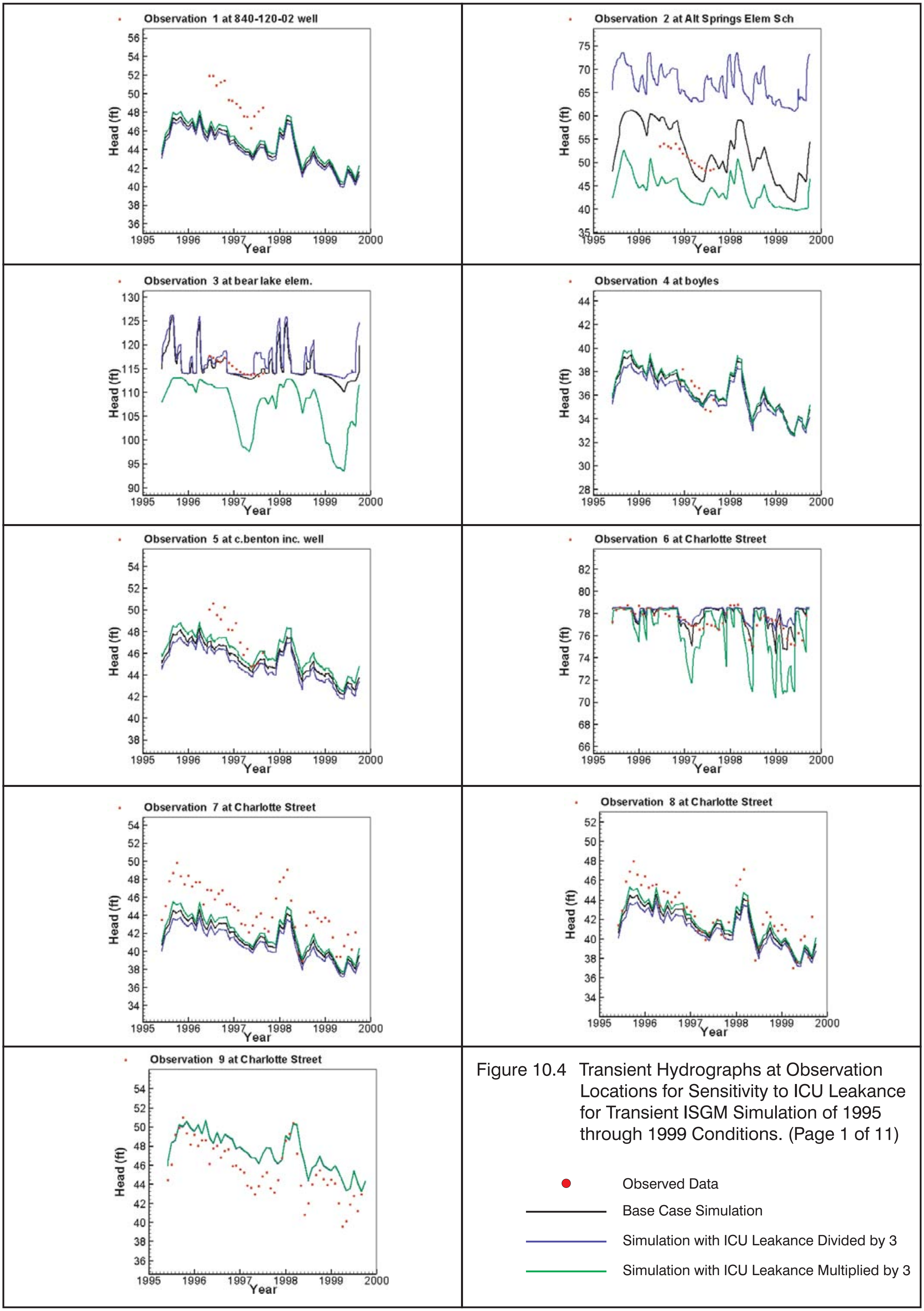

Figure 10.4 Transient Hydrographs at Observation Locations for Sensitivity to ICU Leakance for Transient ISGM Simulation of 1995 through 1999 Conditions. (Page 1 of 11)

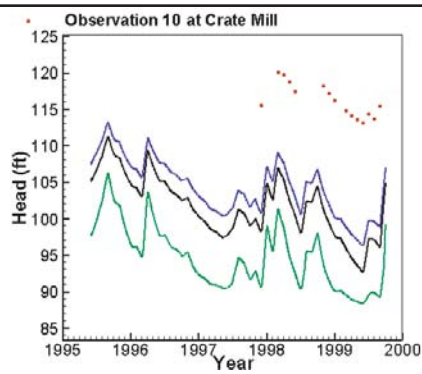

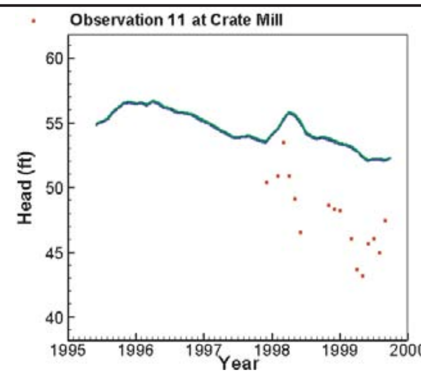

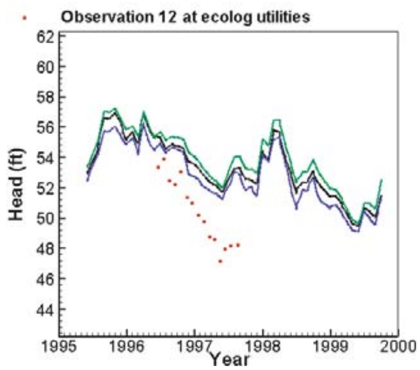

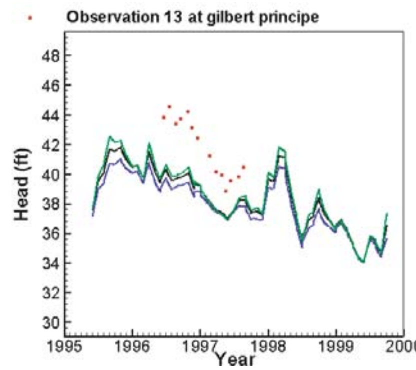

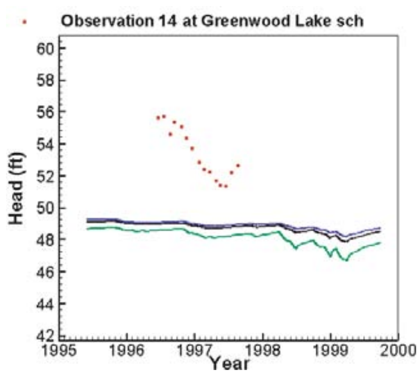

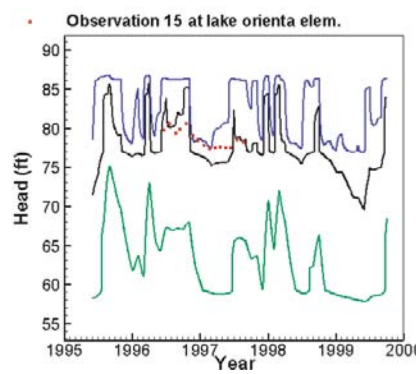

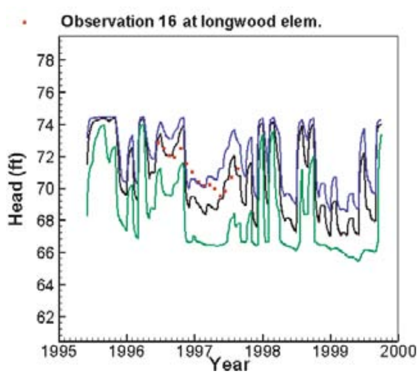

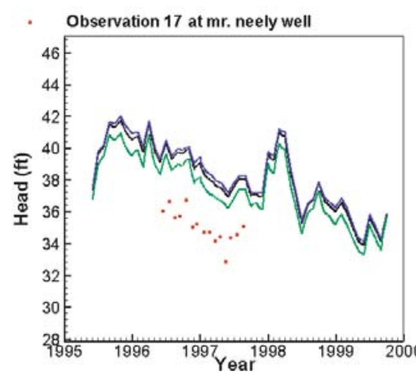

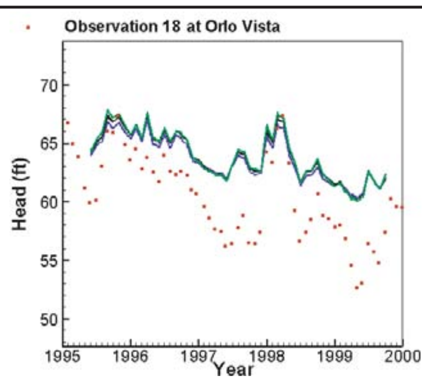

Figure 10.4 Transient Hydrographs at Observation Locations for Sensitivity to ICU Leakance for Transient ISGM Simulation of 1995 through 1999 Conditions. (Page 2 of 11)

- Observed Data
- Base Case Simulation
- Simulation with ICU Leakance Divided by 3
- Simulation with ICU Leakance Multiplied by 3

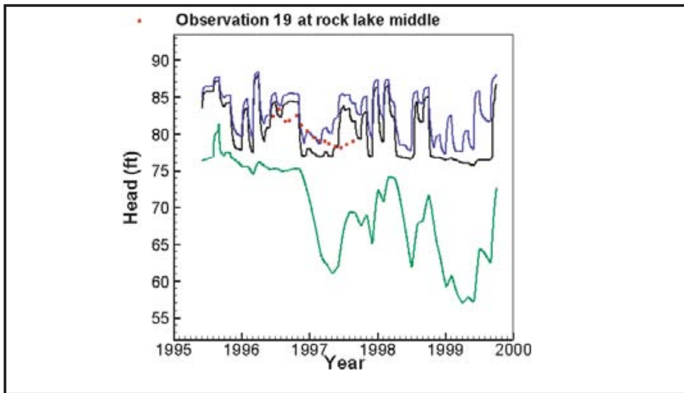

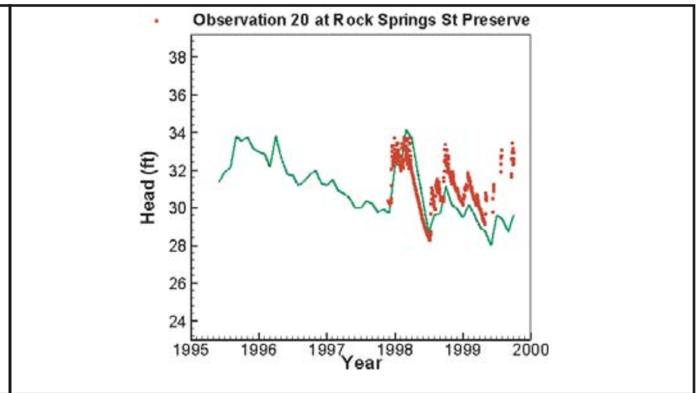

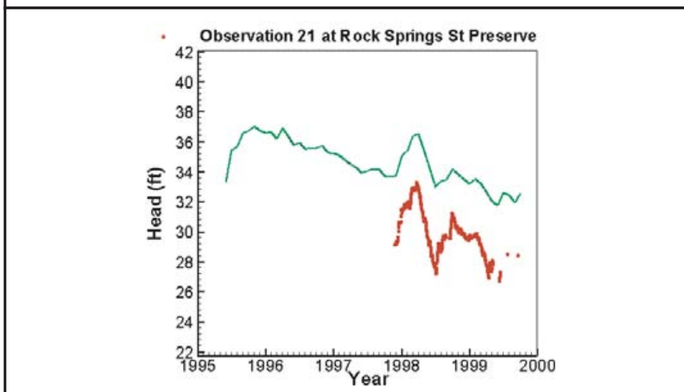

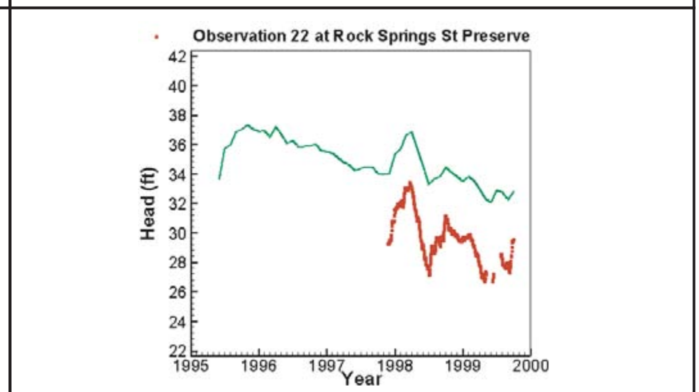

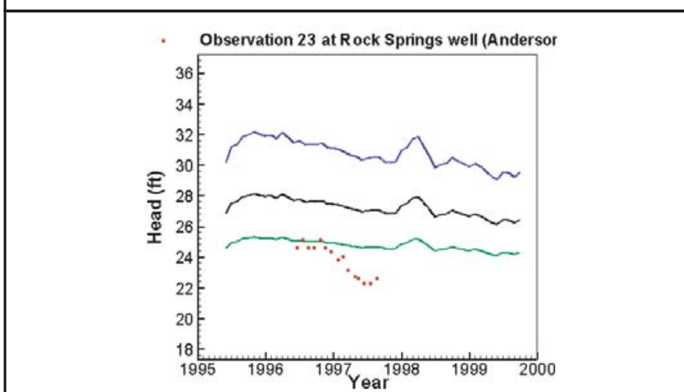

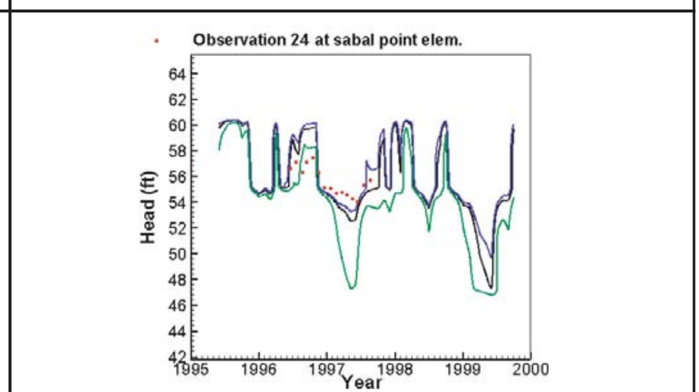

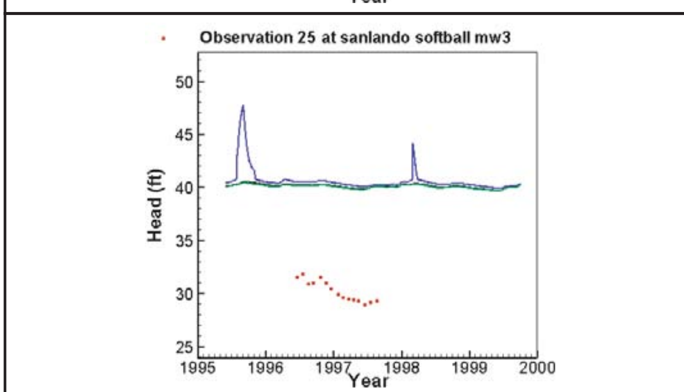

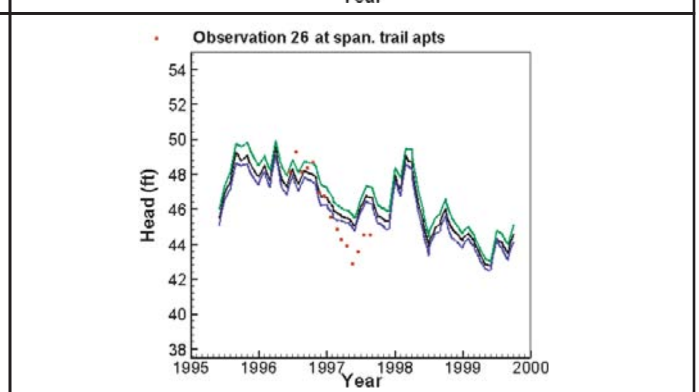

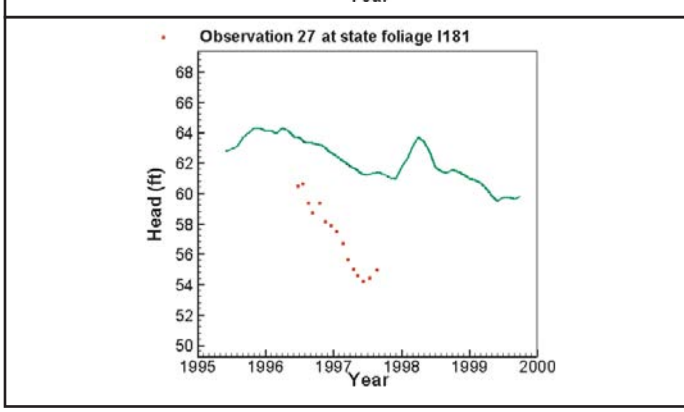

Figure 10.4 Transient Hydrographs at Observation Locations for Sensitivity to ICU Leakance for Transient ISGM Simulation of 1995 through 1999 Conditions. (Page 3 of 11)

Observed Data

Base Case Simulation

Simulation with ICU Leakance Divided by 3

Simulation with ICU Leakance Multiplied by 3

X:\SJR017\TO1\Maps\Conceptual_Model_Report\graphs_leakance.cdr

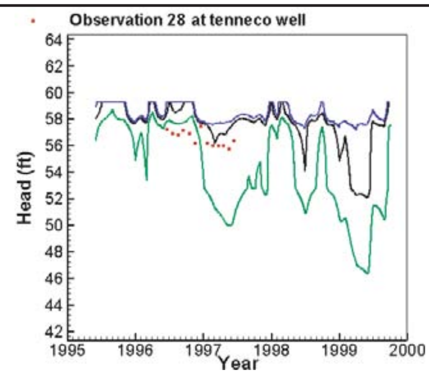

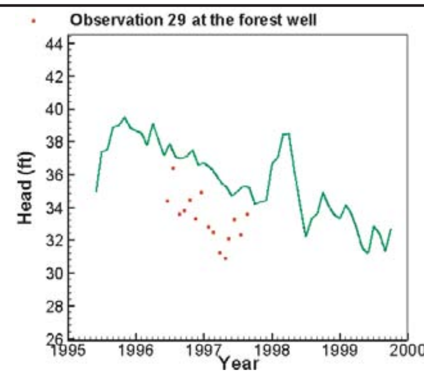

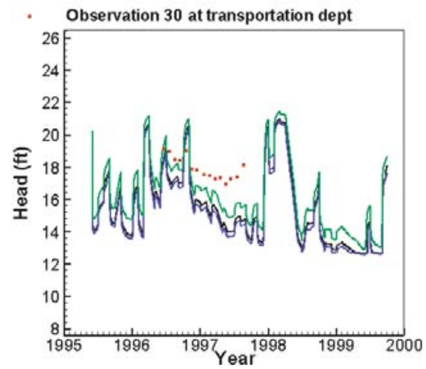

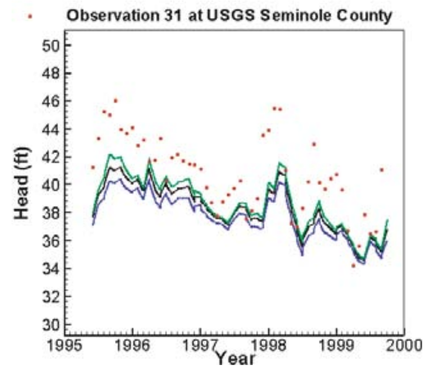

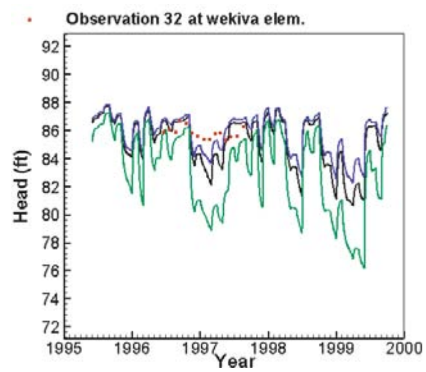

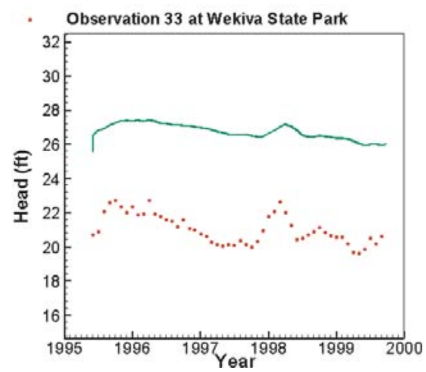

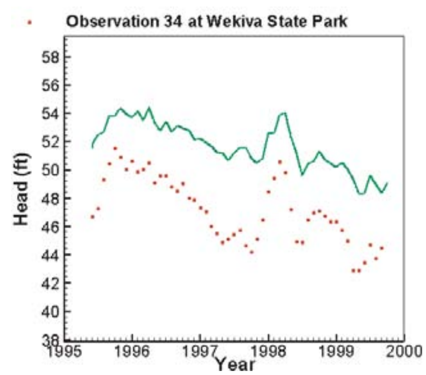

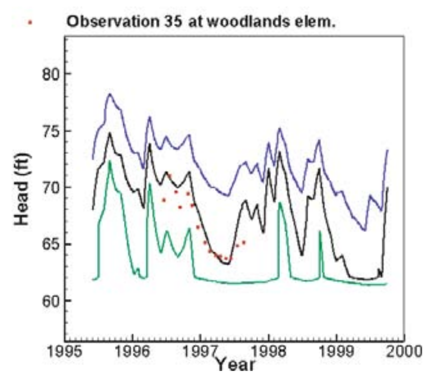

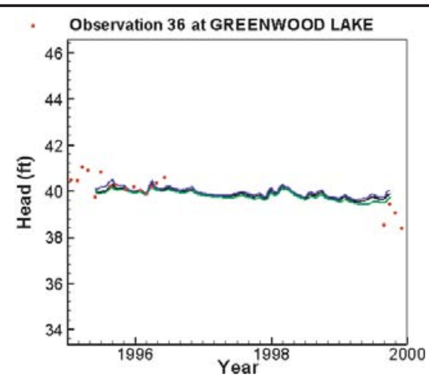

Figure 10.4 Transient Hydrographs at Observation Locations for Sensitivity to ICU Leakance for Transient ISGM Simulation of 1995 through 1999 Conditions. (Page 4 of 11)

Observed Data

Base Case Simulation

Simulation with ICU Leakance Divided by 3

Simulation with ICU Leakance Multiplied by 3

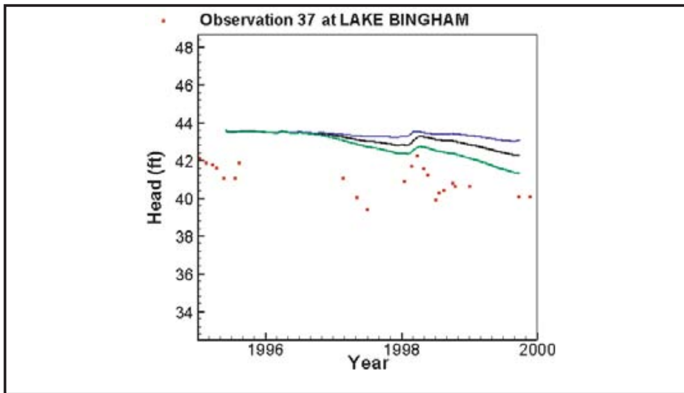

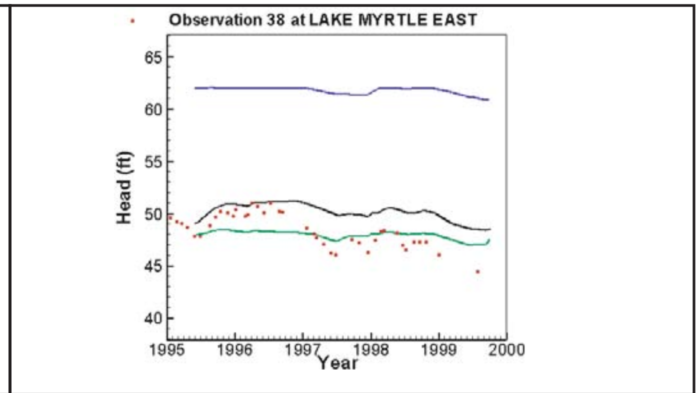

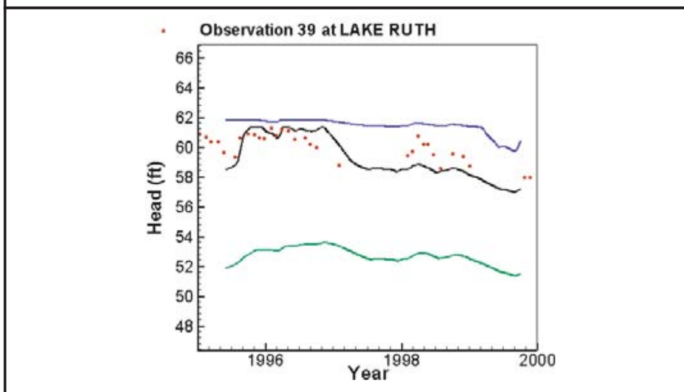

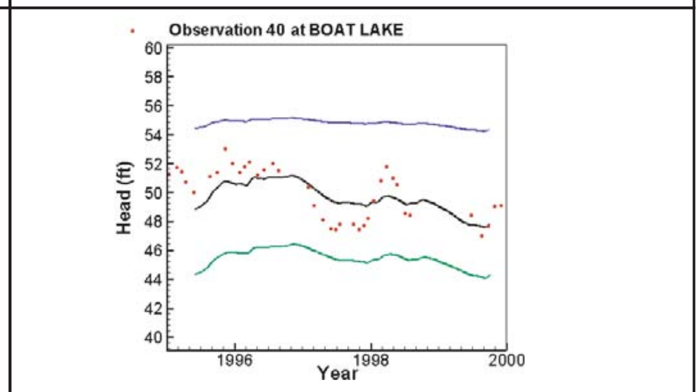

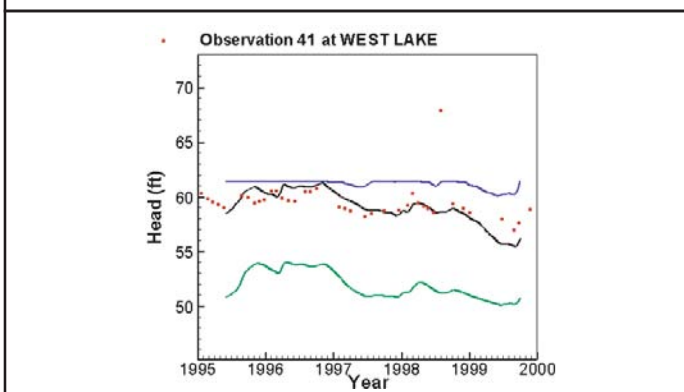

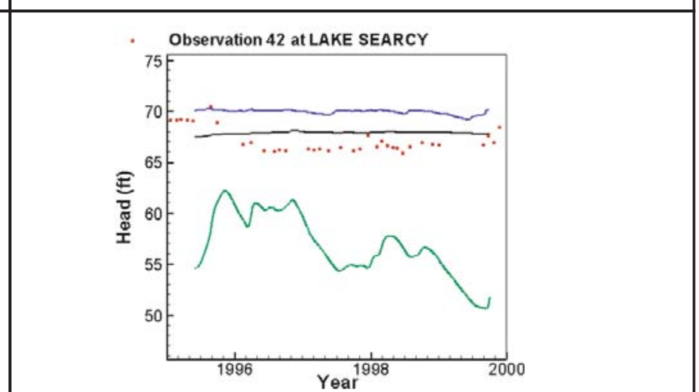

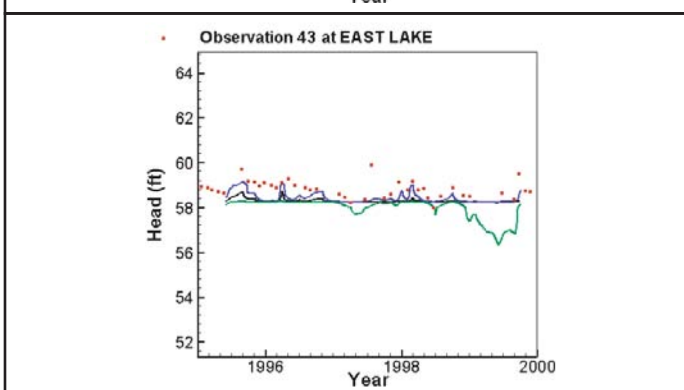

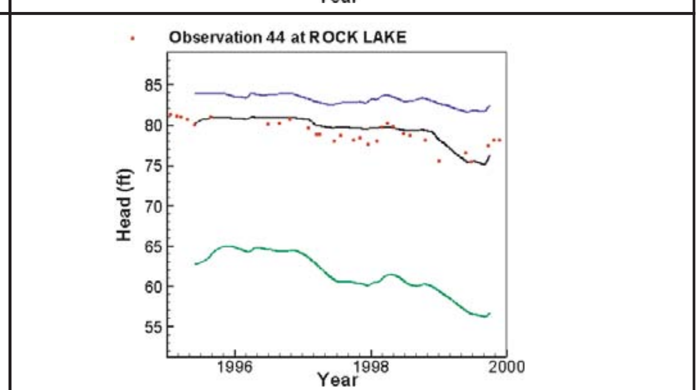

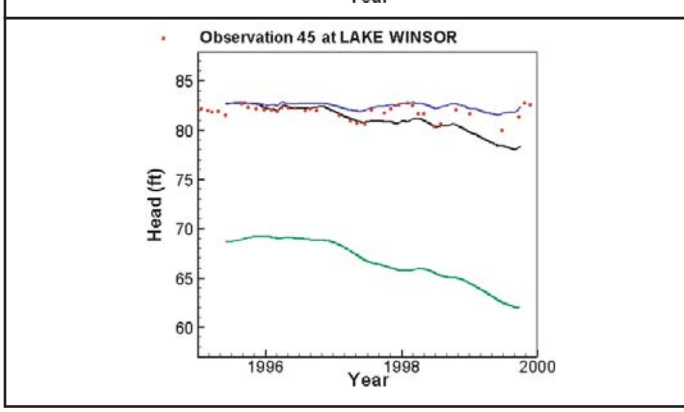

Figure 10.4 Transient Hydrographs at Observation Locations for Sensitivity to ICU Leakance for Transient ISGM Simulation of 1995 through 1999 Conditions. (Page 5 of 11)

Observed Data

Base Case Simulation

Simulation with ICU Leakance Divided by 3

Simulation with ICU Leakance Multiplied by 3

X:\SJR017\TO1\Maps\Conceptual_Model_Report\graphs_leakance.cdr

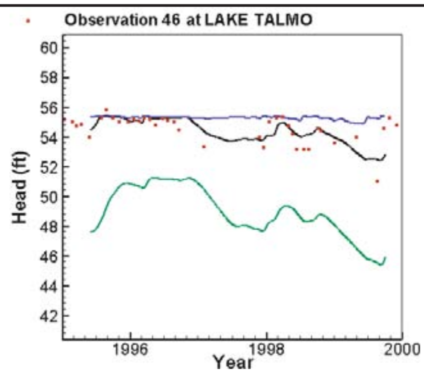

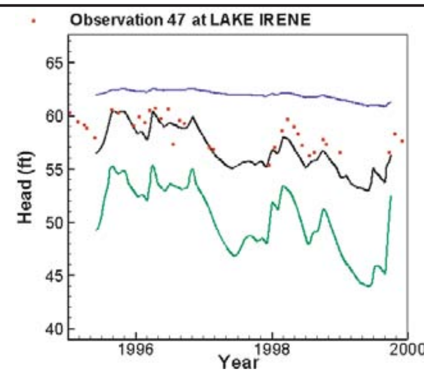

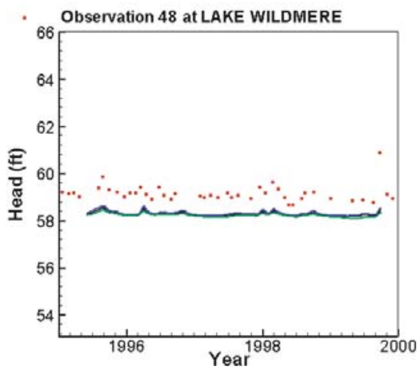

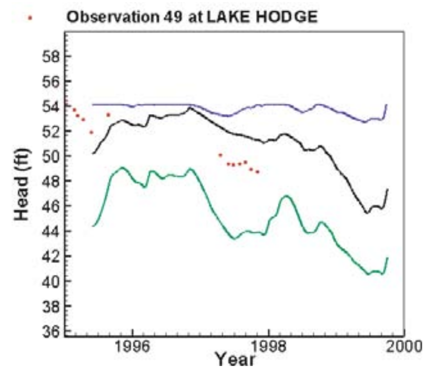

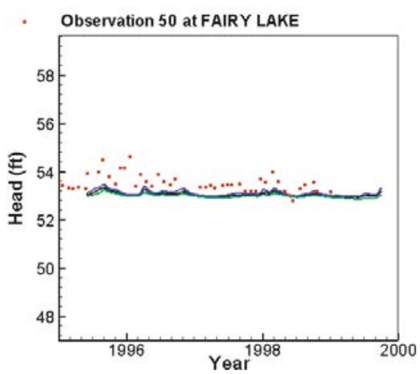

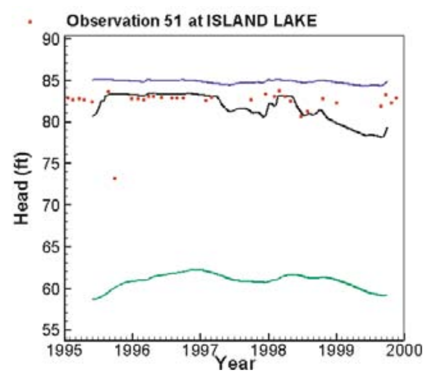

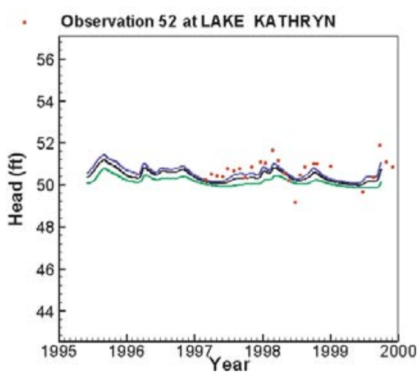

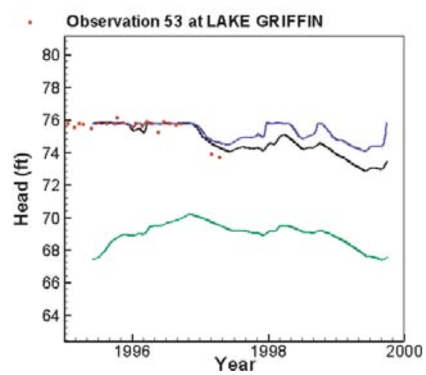

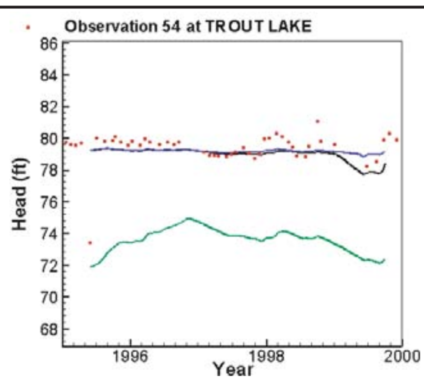

Figure 10.4 Transient Hydrographs at Observation Locations for Sensitivity to ICU Leakance for Transient ISGM Simulation of 1995 through 1999 Conditions. (Page 6 of 11)

- Observed Data
- Base Case Simulation
- Simulation with ICU Leakance Divided by 3
- Simulation with ICU Leakance Multiplied by 3

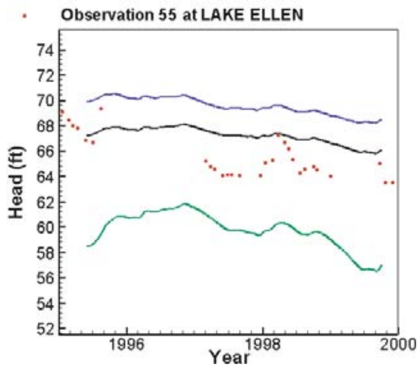

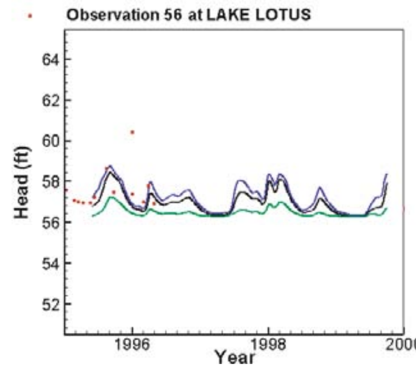

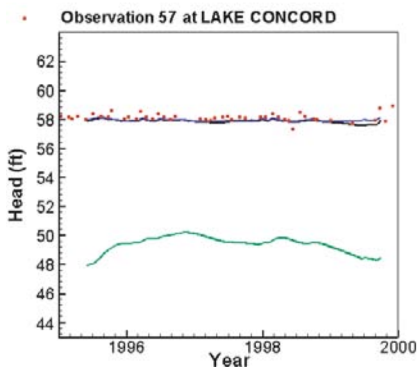

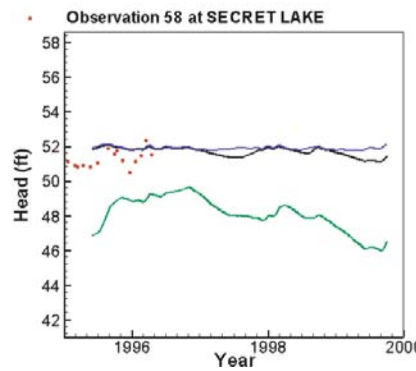

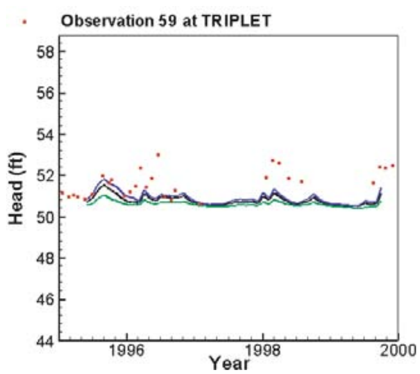

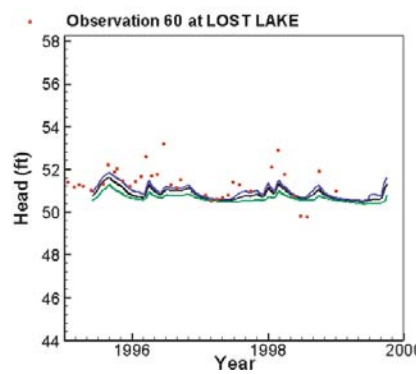

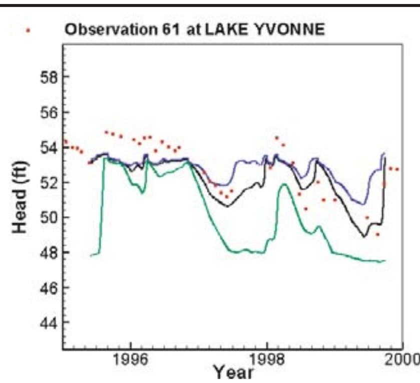

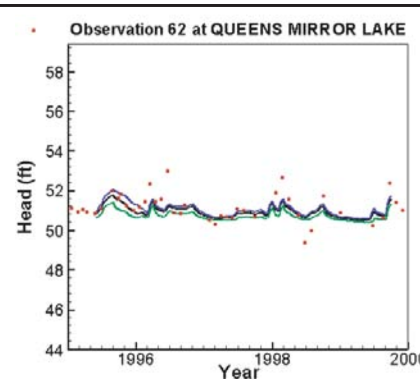

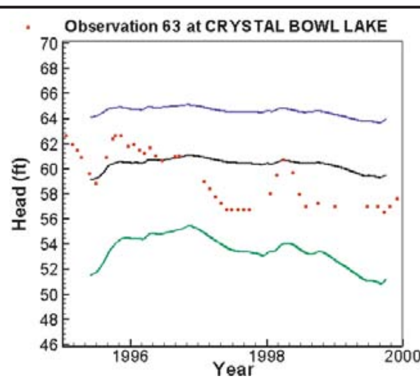

Figure 10.4 Transient Hydrographs at Observation Locations for Sensitivity to ICU Leakance for Transient ISGM Simulation of 1995 through 1999 Conditions. (Page 7 of 11)

Observed Data

Base Case Simulation

Simulation with ICU Leakance Divided by 3

Simulation with ICU Leakance Multiplied by 3

X:\SJR017\TO1\Maps\Conceptual_Model_Report\graphs_leakance.cdr

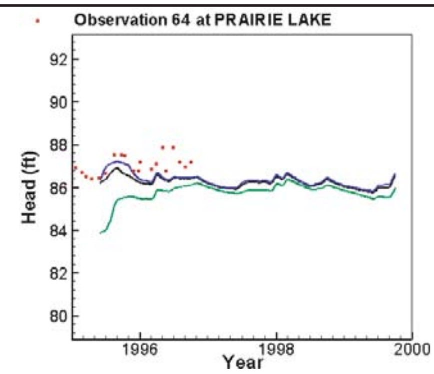

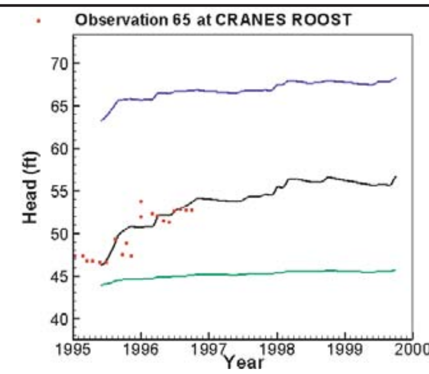

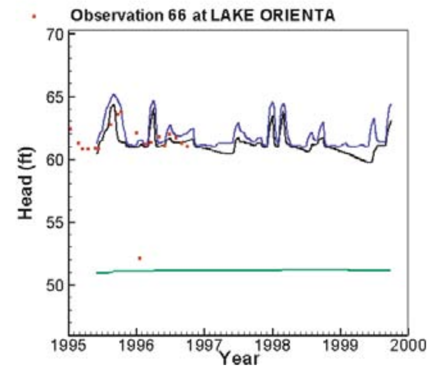

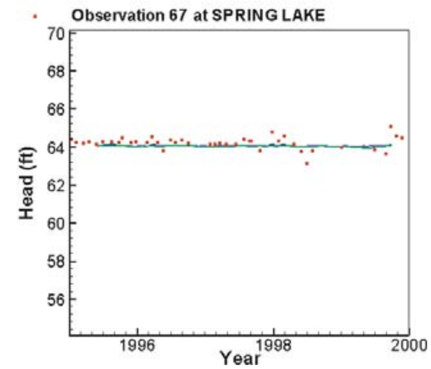

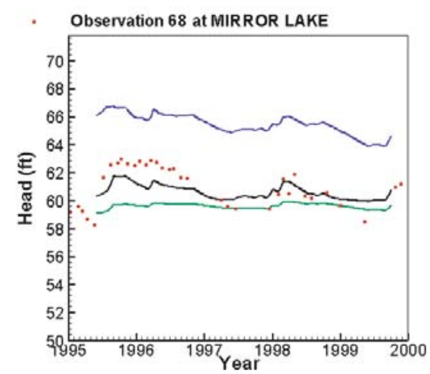

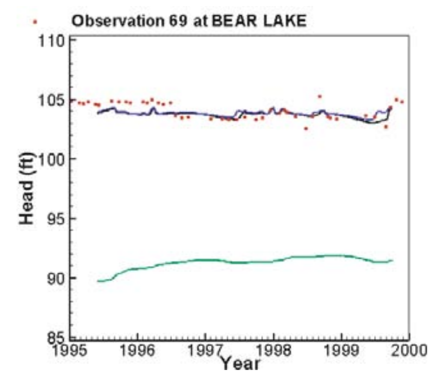

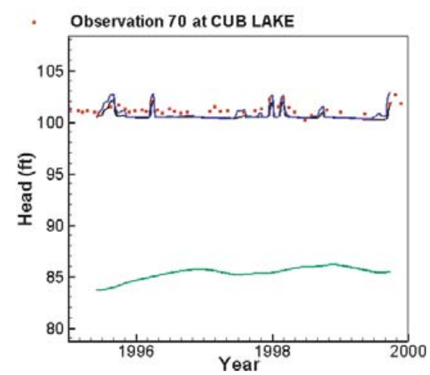

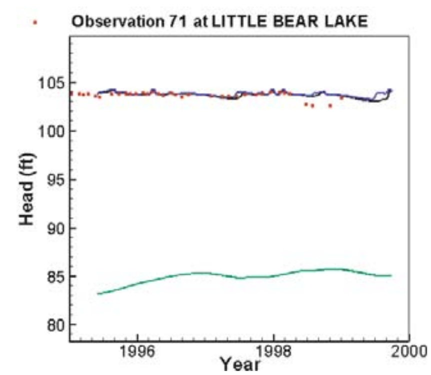

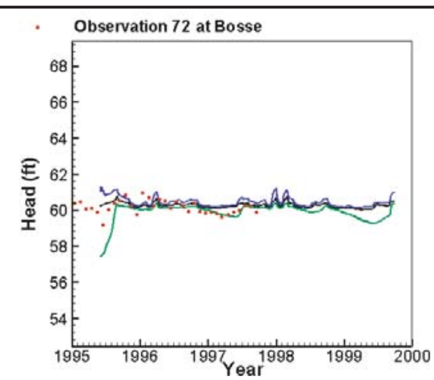

Figure 10.4 Transient Hydrographs at Observation Locations for Sensitivity to ICU Leakance for Transient ISGM Simulation of 1995 through 1999 Conditions. (Page 8 of 11)

Observed Data

Base Case Simulation

Simulation with ICU Leakance Divided by 3

Simulation with ICU Leakance Multiplied by 3

X:\SJR017\TO1\Maps\Conceptual_Model_Report\graphs_leakance.cdr

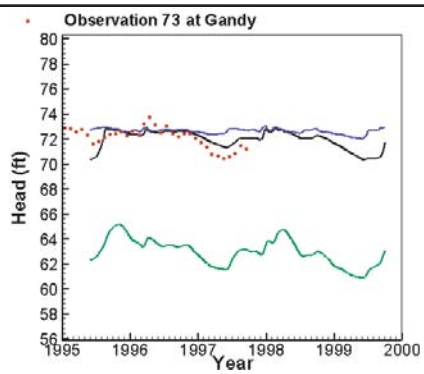

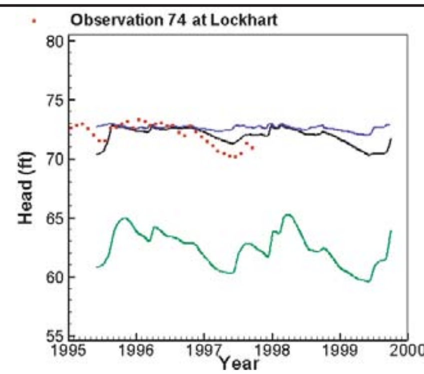

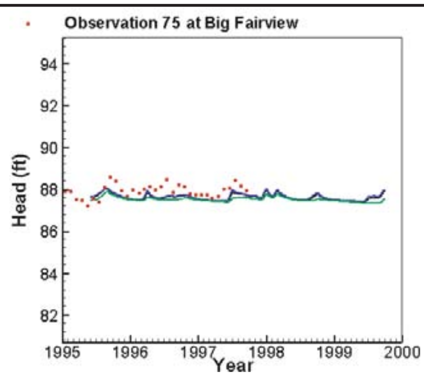

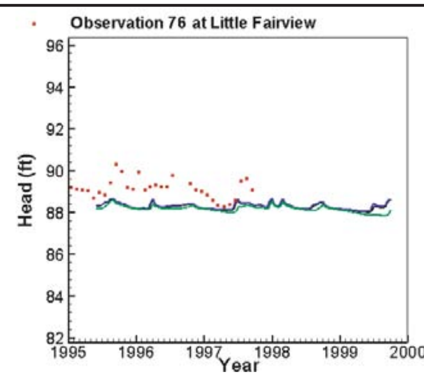

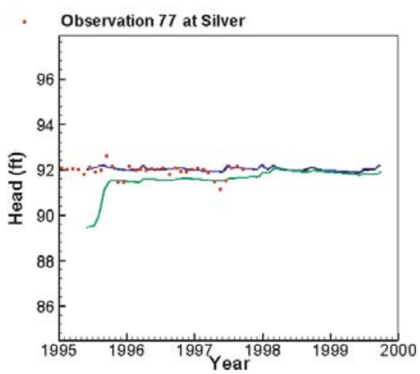

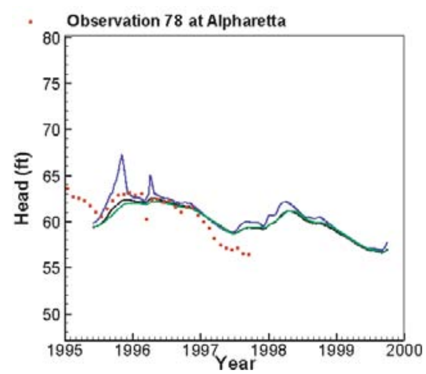

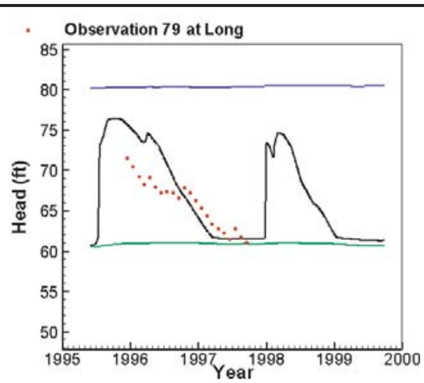

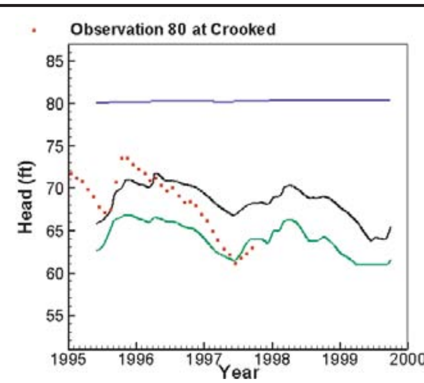

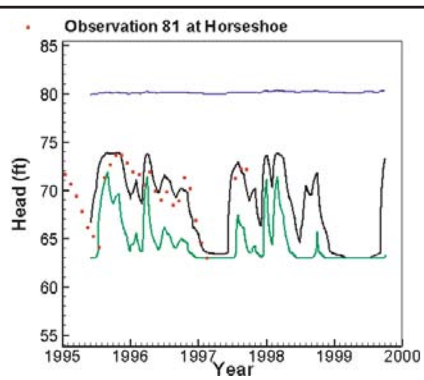

Figure 10.4 Transient Hydrographs at Observation Locations for Sensitivity to ICU Leakance for Transient ISGM Simulation of 1995 through 1999 Conditions. (Page 9 of 11)

Observed Data

Base Case Simulation

Simulation with ICU Leakance Divided by 3

Simulation with ICU Leakance Multiplied by 3

X:\SJR017\TO1\Maps\Conceptual_Model_Report\graphs_leakance.cdr

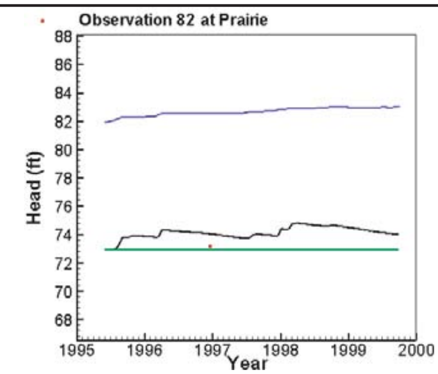

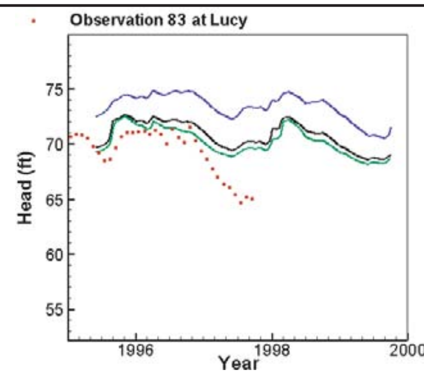

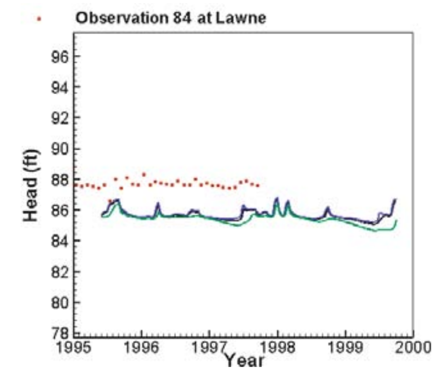

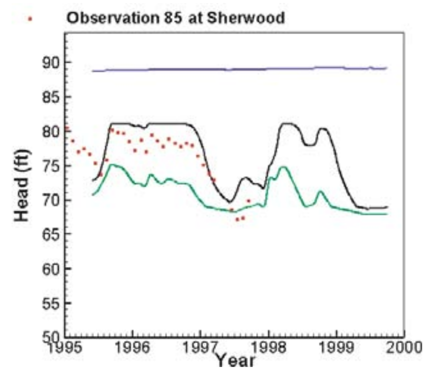

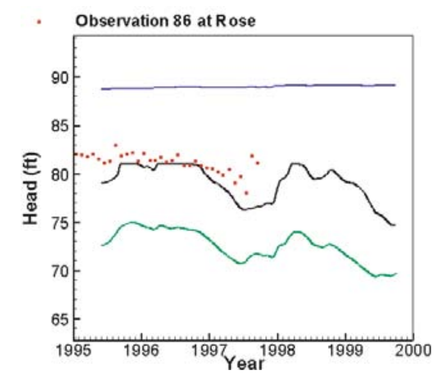

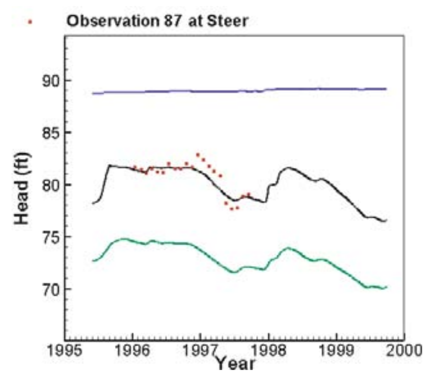

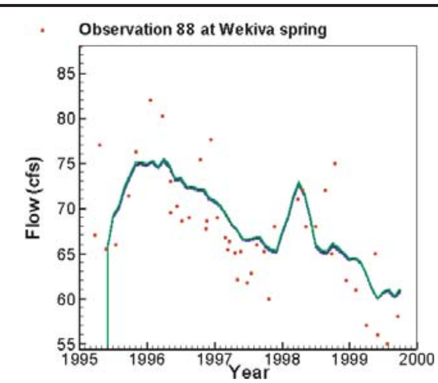

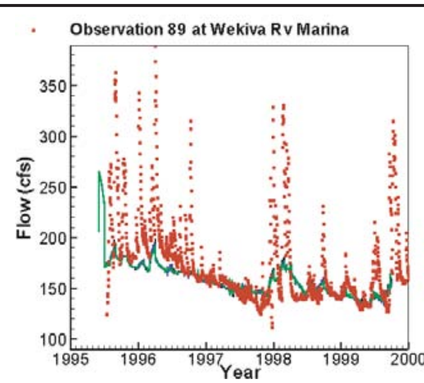

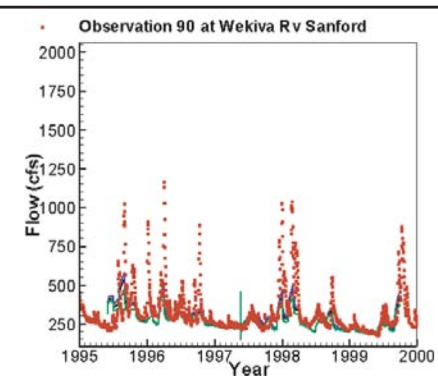

Figure 10.4 Transient Hydrographs at Observation Locations for Sensitivity to ICU Leakance for Transient ISGM Simulation of 1995 through 1999 Conditions. (Page 10 of 11)

Observed Data

Base Case Simulation

Simulation with ICU Leakance Divided by 3

Simulation with ICU Leakance Multiplied by 3

X:\SJR017\TO1\Maps\Conceptual_Model_Report\graphs_leakance.cdr

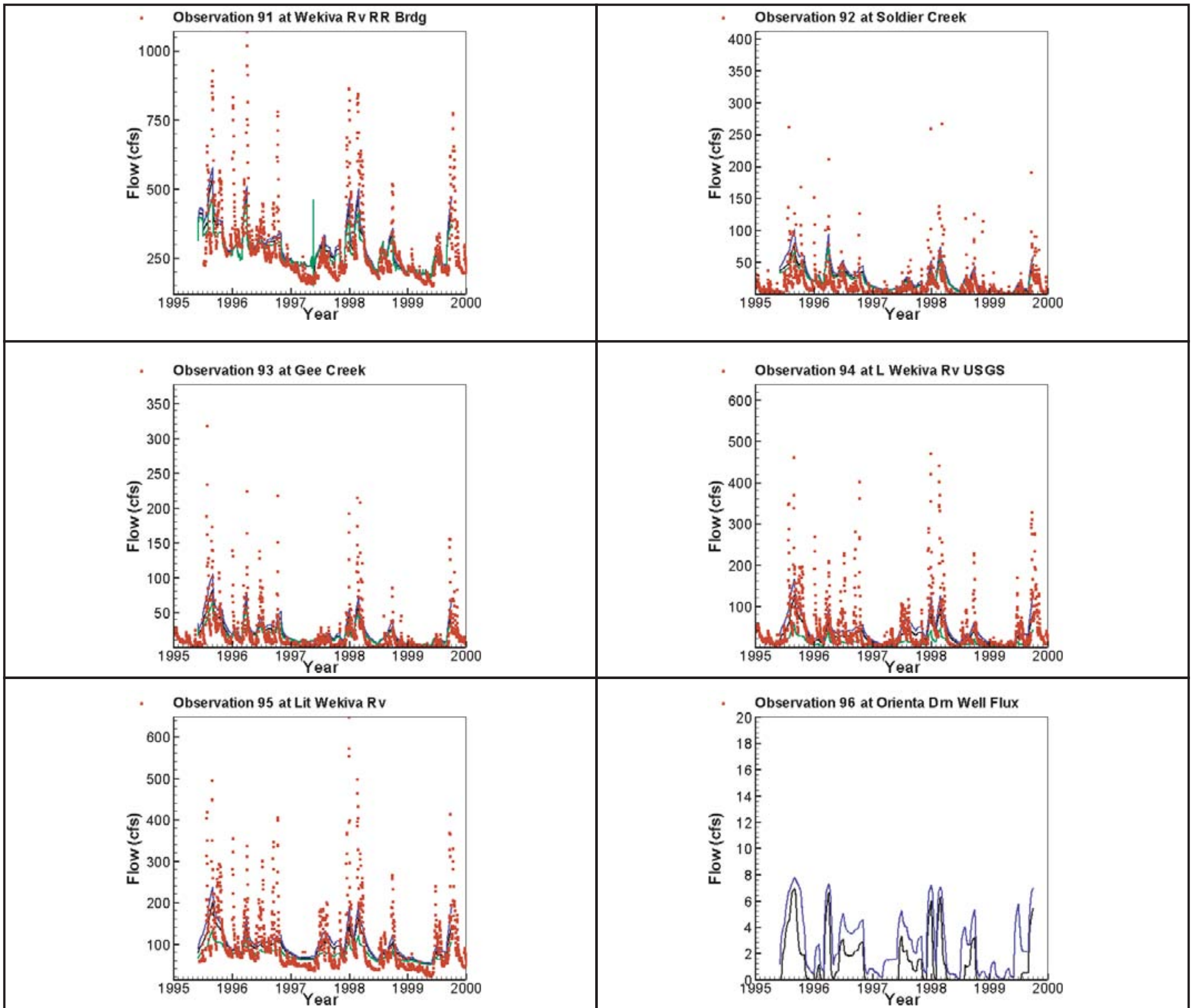

Figure 10.4 Transient Hydrographs at Observation Locations for Sensitivity to ICU Leakance for Transient ISGM Simulation of 1995 through 1999 Conditions. (Page 11 of 11)

- Observed Data
- Base Case Simulation
- Simulation with ICU Leakance Divided by 3
- Simulation with ICU Leakance Multiplied by 3

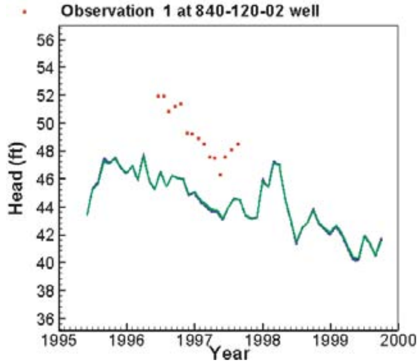

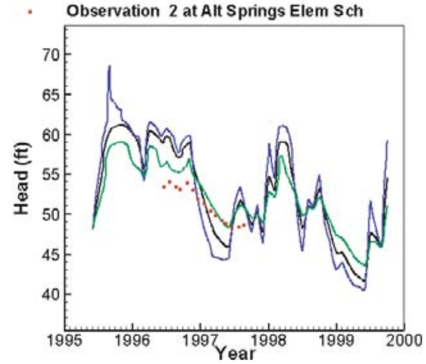

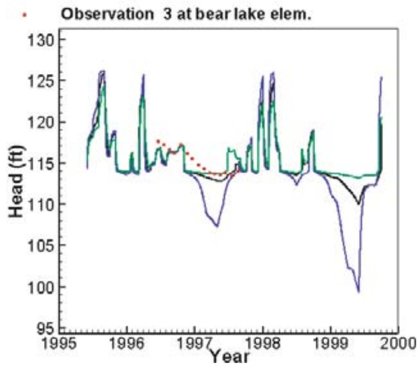

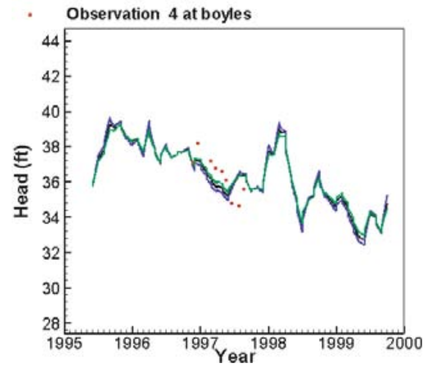

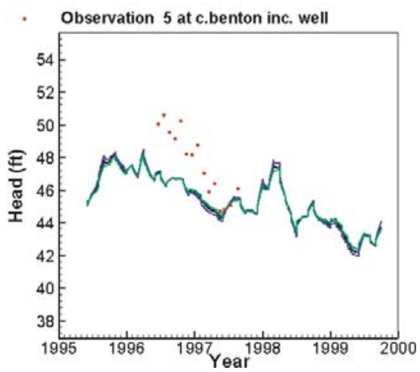

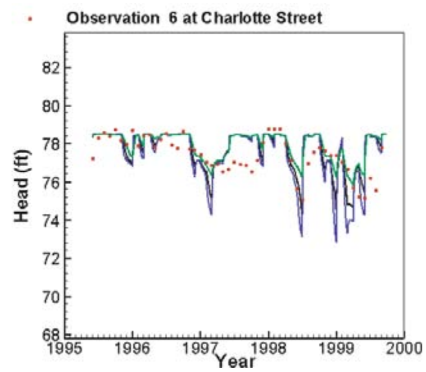

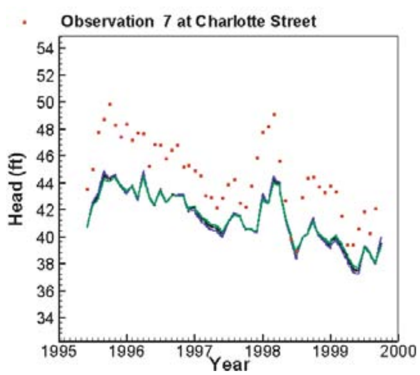

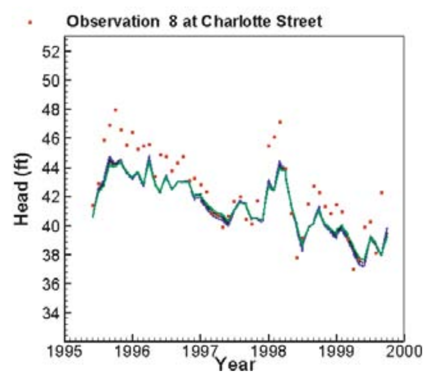

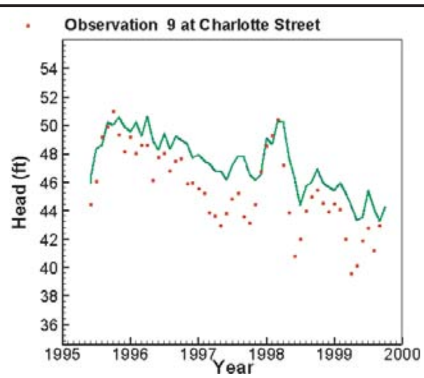

Figure 10.5 Transient Hydrographs at Observation Locations for Sensitivity to Porosity for Transient ISGM Simulation of 1995 through 1999 Conditions. (Page 1 of 11)

Observed Data

Base Case Simulation

Simulation with Porosity Divided by 2

Simulation with Porosity Multiplied by 2

X:\SJR017\TO1\Maps\Conceptual_Model_Report\graphs_porosity.cdr

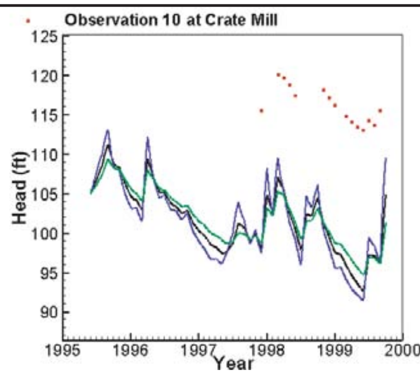

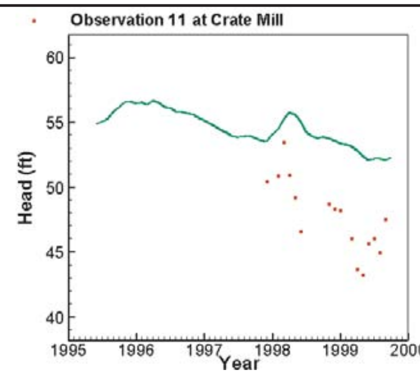

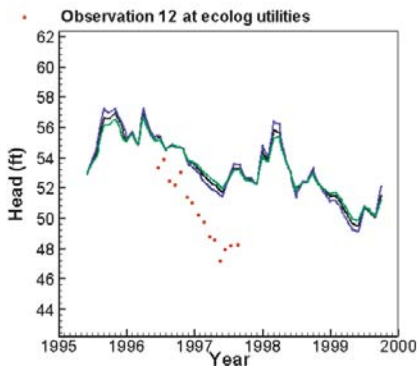

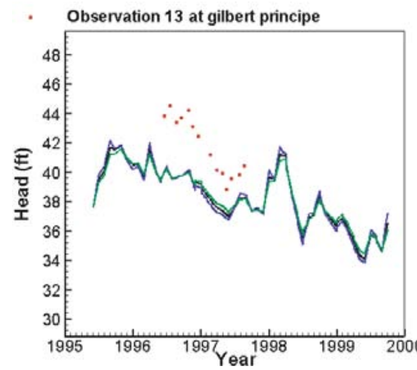

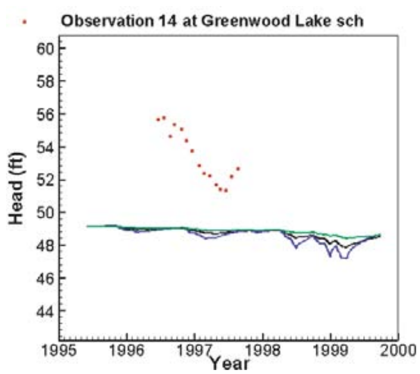

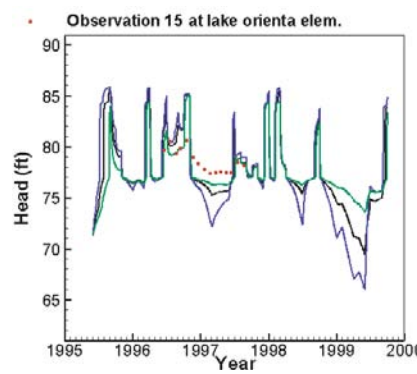

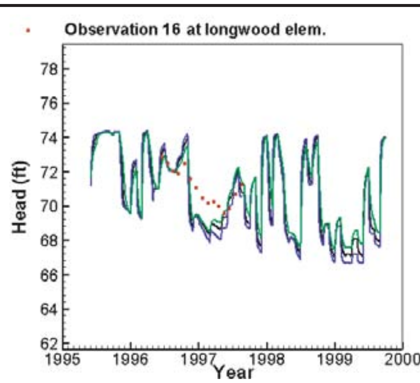

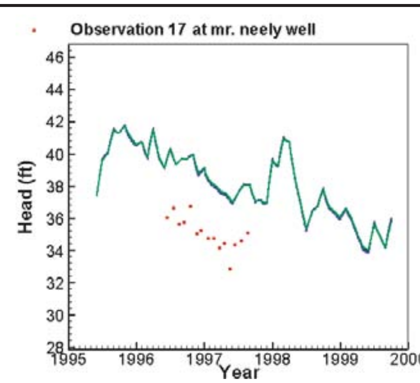

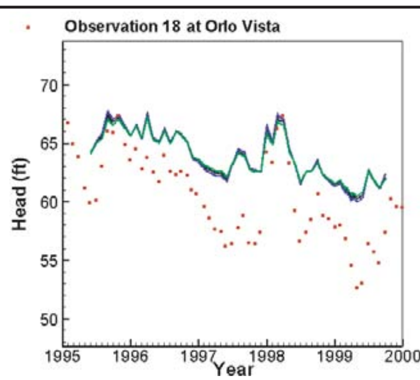

Figure 10.5 Transient Hydrographs at Observation Locations for Sensitivity to Porosity for Transient ISGM Simulation of 1995 through 1999 Conditions. (Page 2 of 11)

Observed Data

Base Case Simulation

Simulation with Porosity Divided by 2

Simulation with Porosity Multiplied by 2

X:\SJR017\TO1\Maps\Conceptual_Model_Report\graphs_porosity.cdr

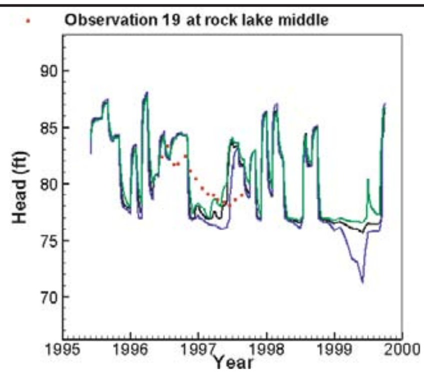

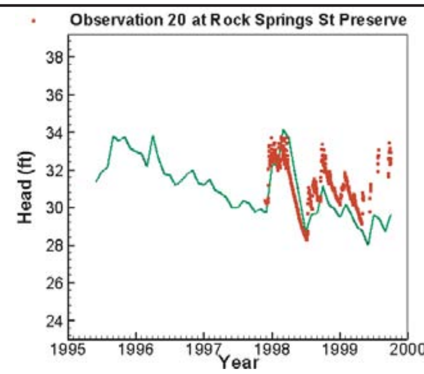

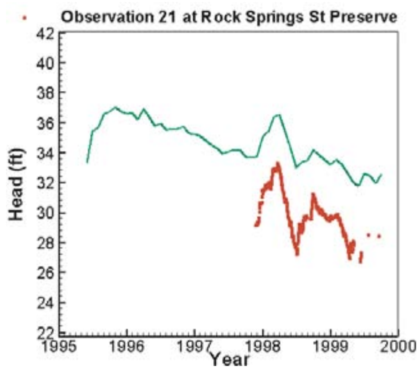

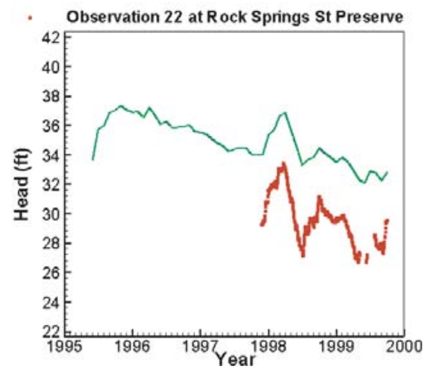

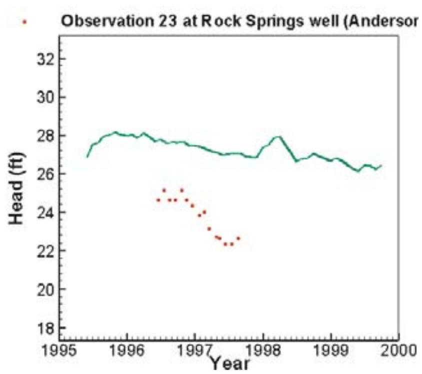

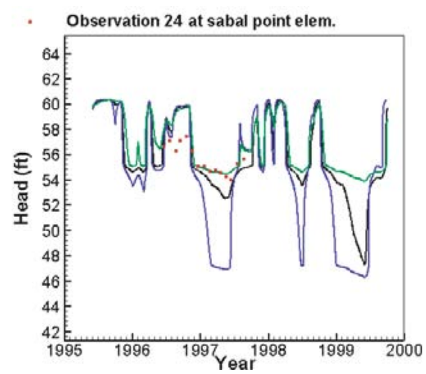

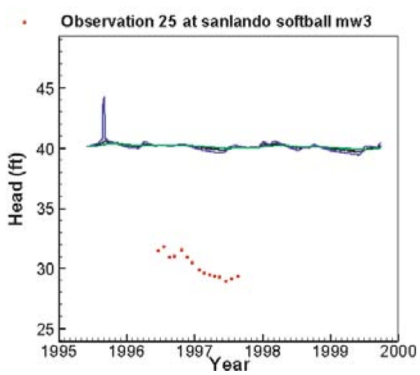

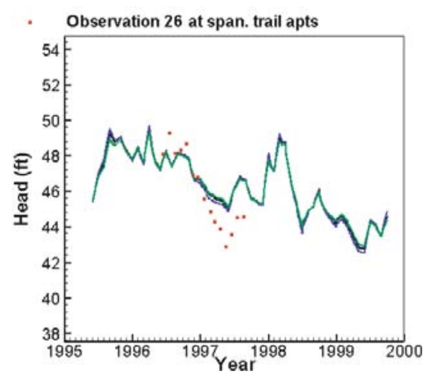

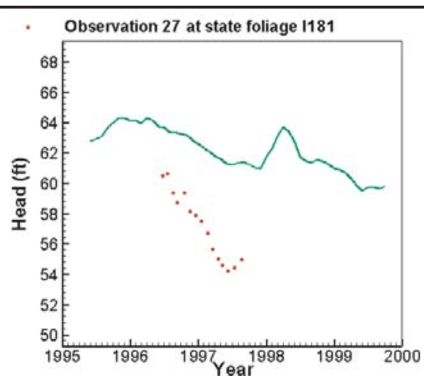

Figure 10.5 Transient Hydrographs at Observation Locations for Sensitivity to Porosity for Transient ISGM Simulation of 1995 through 1999 Conditions. (Page 3 of 11)

Observed Data

Base Case Simulation

Simulation with Porosity Divided by 2

Simulation with Porosity Multiplied by 2

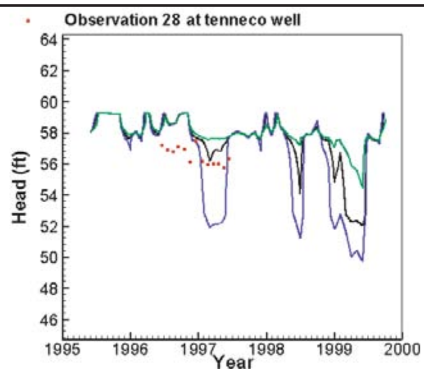

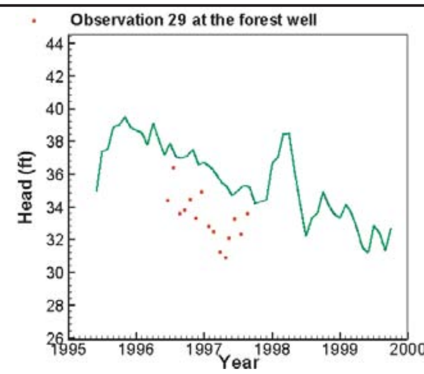

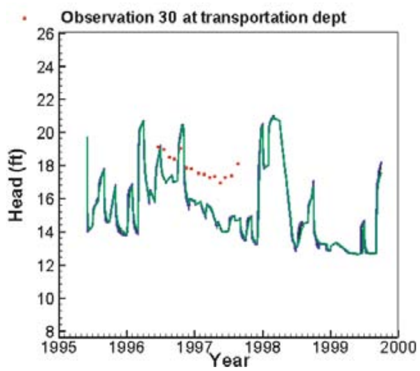

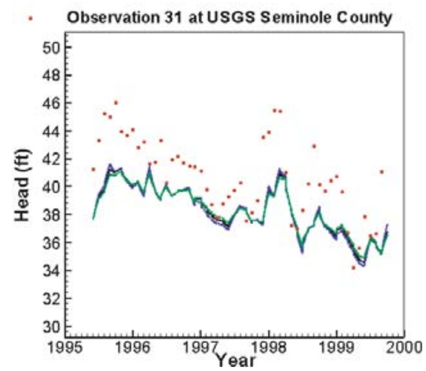

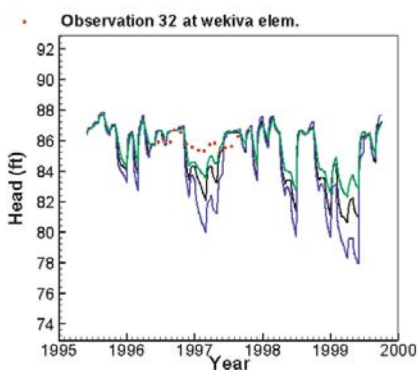

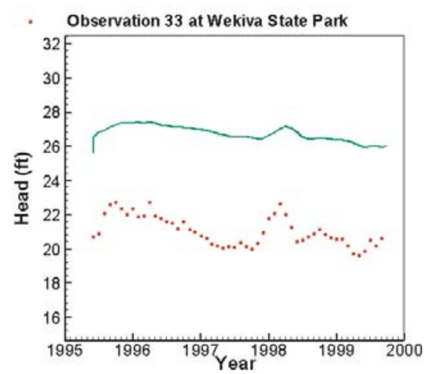

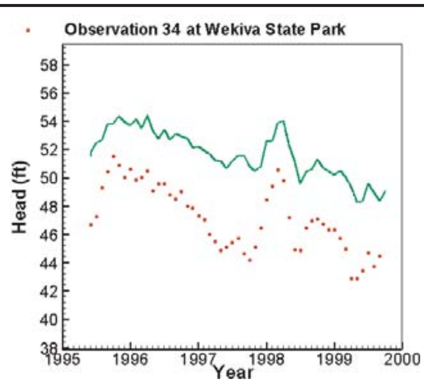

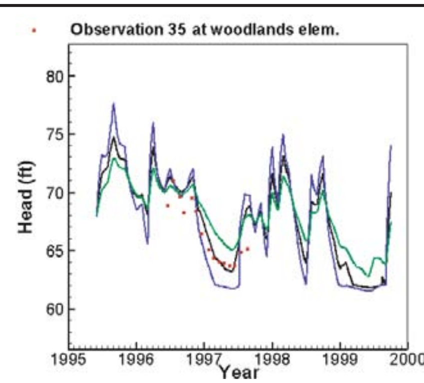

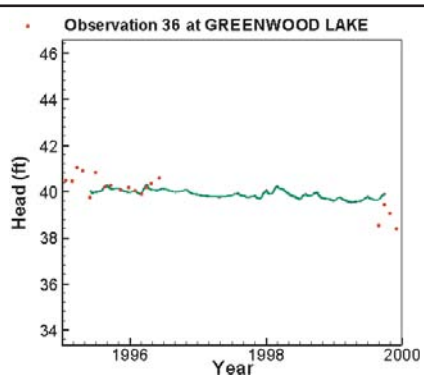

Figure 10.5 Transient Hydrographs at Observation Locations for Sensitivity to Porosity for Transient ISGM Simulation of 1995 through 1999 Conditions. (Page 4 of 11)

Observed Data

Base Case Simulation

Simulation with Porosity Divided by 2

Simulation with Porosity Multiplied by 2

X:\SJR017\TO1\Maps\Conceptual_Model_Report\graphs_porosity.cdr

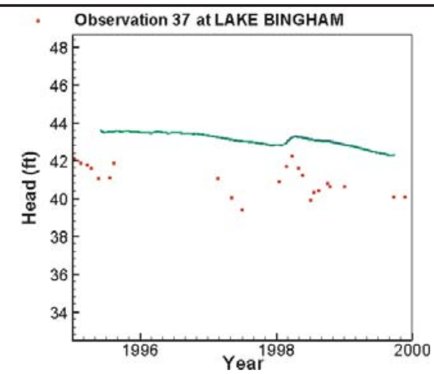

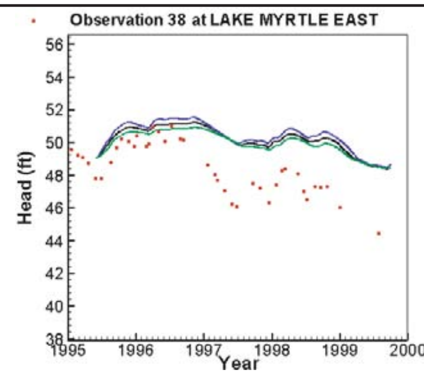

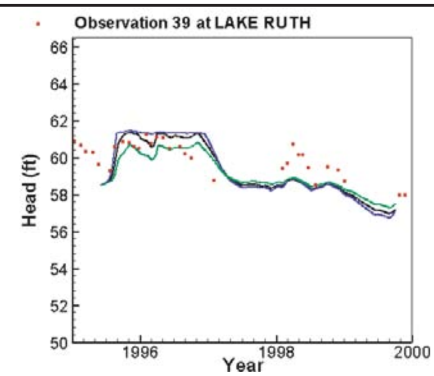

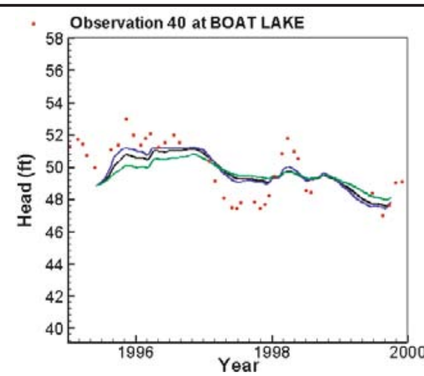

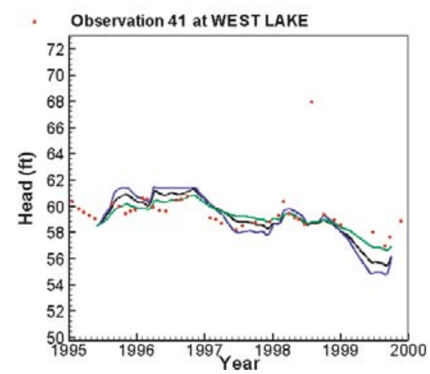

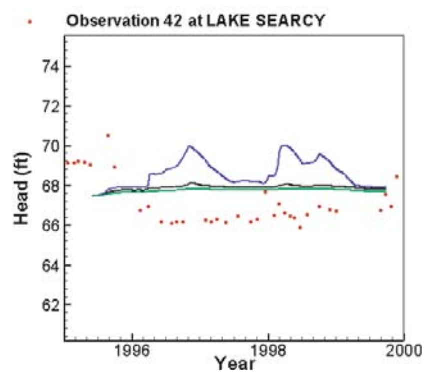

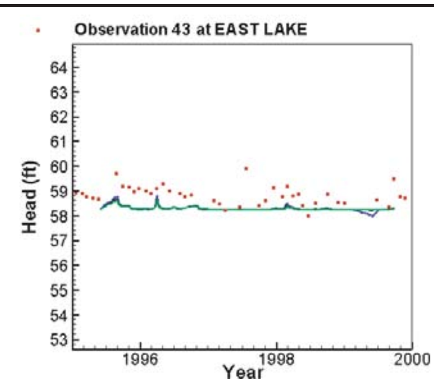

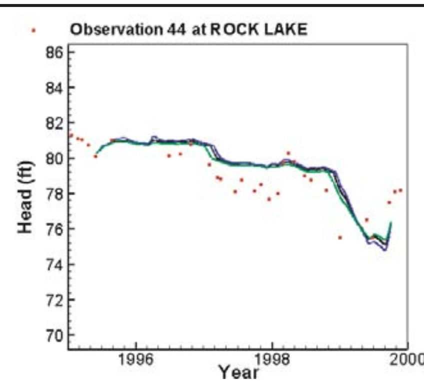

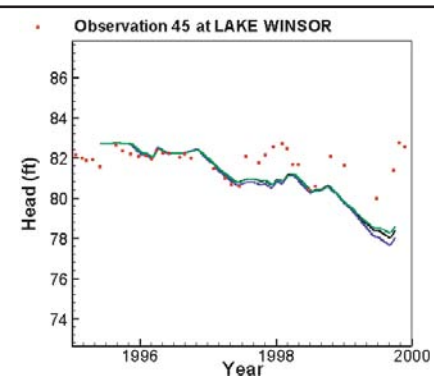

Figure 10.5 Transient Hydrographs at Observation Locations for Sensitivity to Porosity for Transient ISGM Simulation of 1995 through 1999 Conditions. (Page 5 of 11)

● Observed Data
Base Case Simulation
Simulation with Porosity Divided by 2
Simulation with Porosity Multiplied by 2

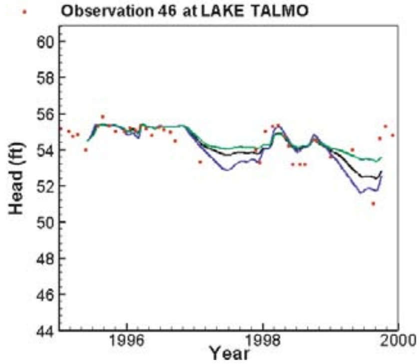

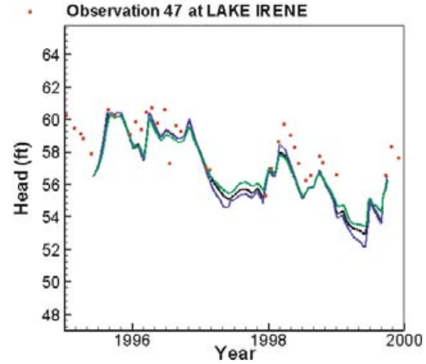

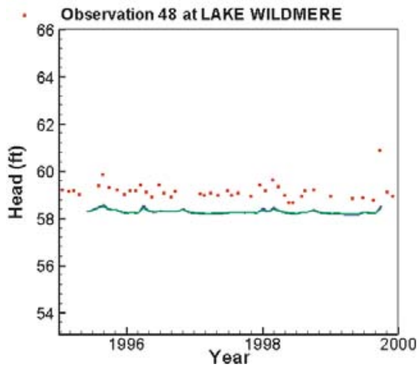

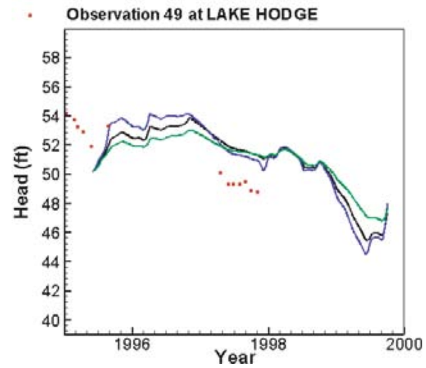

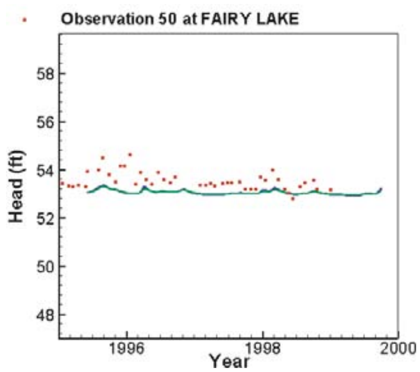

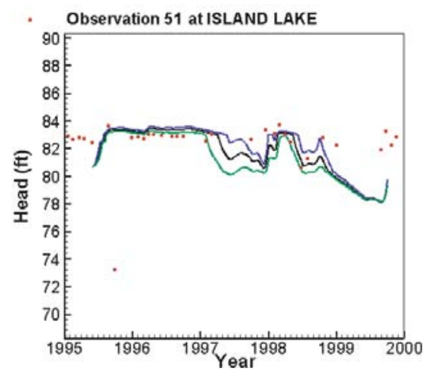

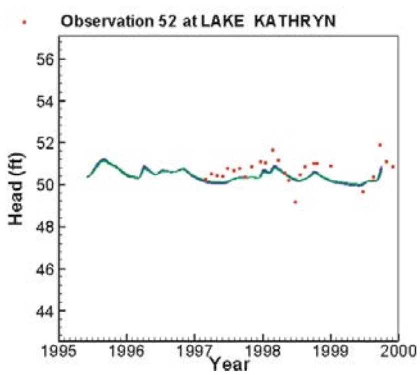

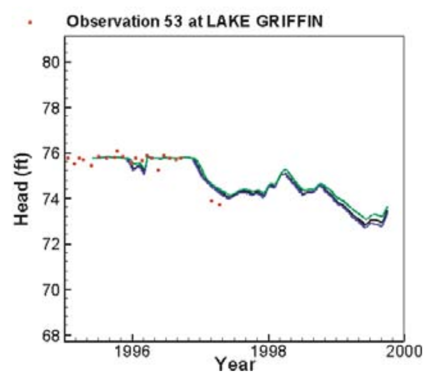

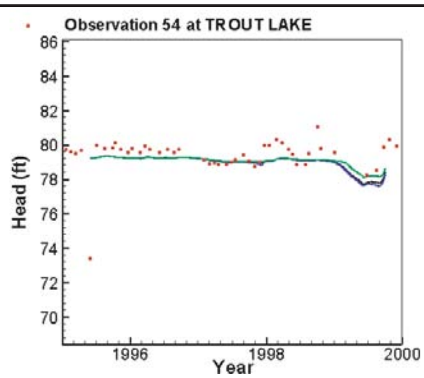

Figure 10.5 Transient Hydrographs at Observation Locations for Sensitivity to Porosity for Transient ISGM Simulation of 1995 through 1999 Conditions. (Page 6 of 11)

- Observed Data
- Base Case Simulation
- Simulation with Porosity Divided by 2
- Simulation with Porosity Multiplied by 2

X:\SJR017\TO1\Maps\Conceptual_Model_Report\graphs_porosity.cdr

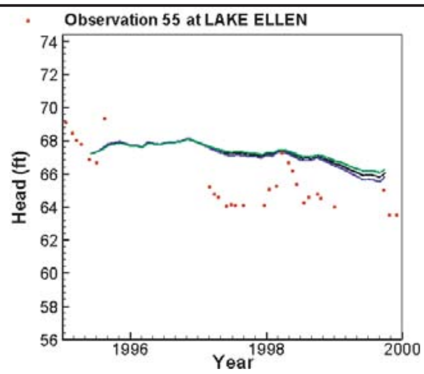

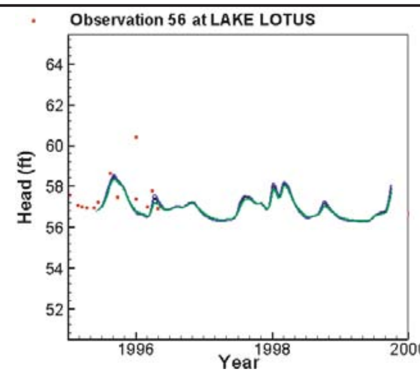

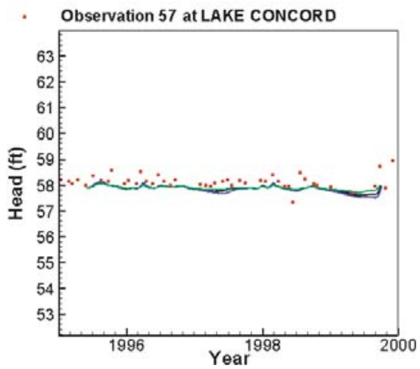

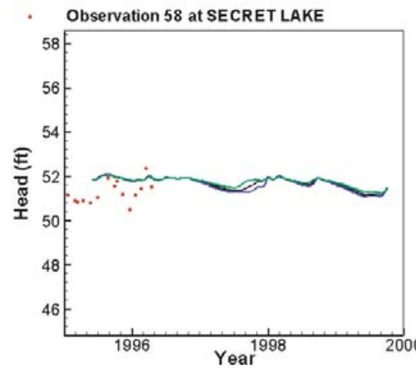

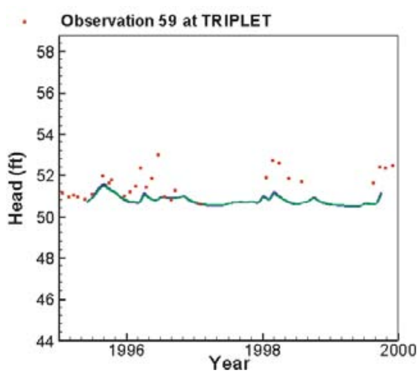

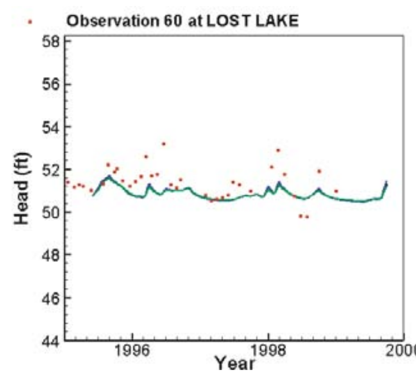

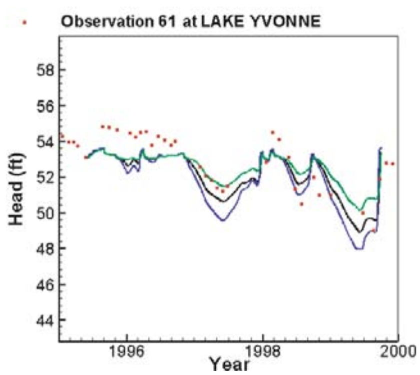

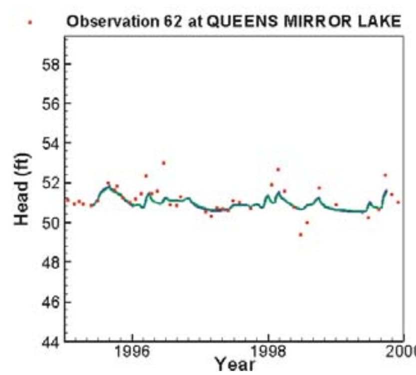

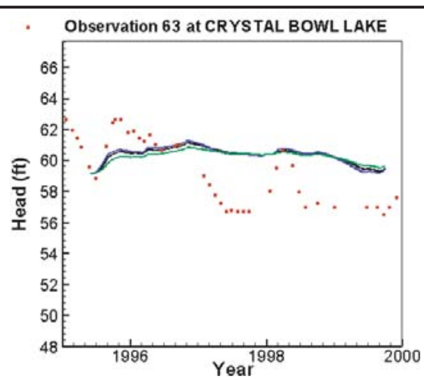

Figure 10.5 Transient Hydrographs at Observation Locations for Sensitivity to Porosity for Transient ISGM Simulation of 1995 through 1999 Conditions. (Page 7 of 11)

Observed Data

Base Case Simulation

Simulation with Porosity Divided by 2

Simulation with Porosity Multiplied by 2

X:\SJR017\TO1\Maps\Conceptual_Model_Report\graphs_porosity.cdr

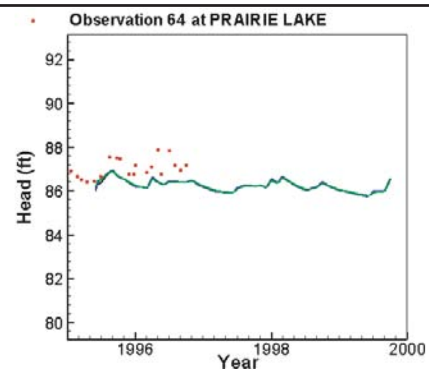

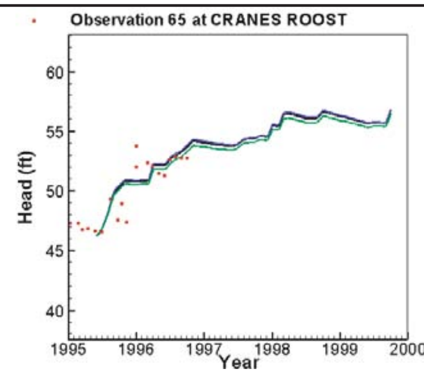

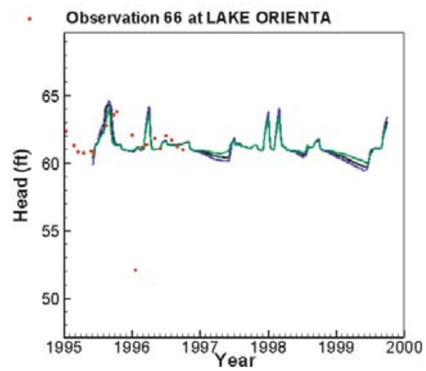

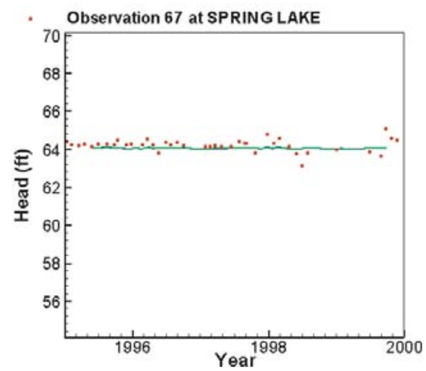

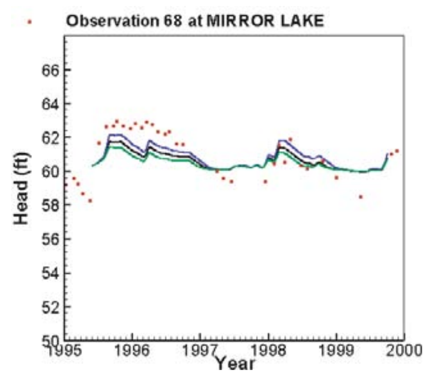

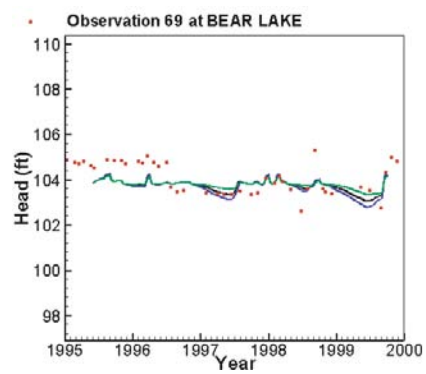

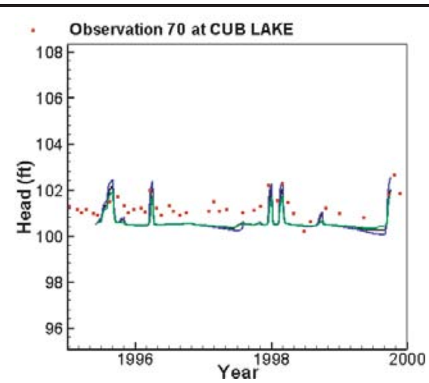

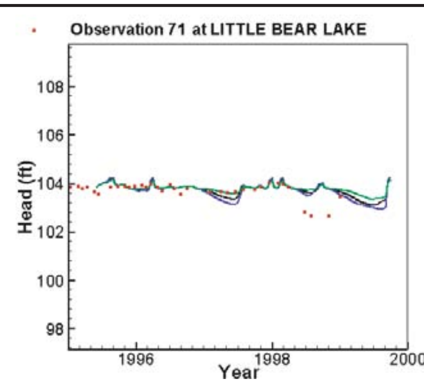

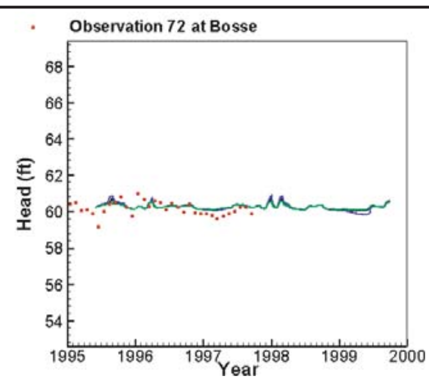

Figure 10.5 Transient Hydrographs at Observation Locations for Sensitivity to Porosity for Transient ISGM Simulation of 1995 through 1999 Conditions. (Page 8 of 11)

Observed Data

Base Case Simulation

Simulation with Porosity Divided by 2

Simulation with Porosity Multiplied by 2

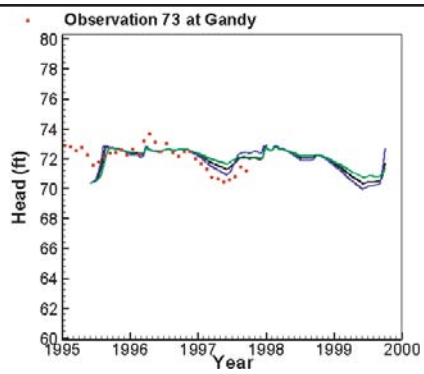

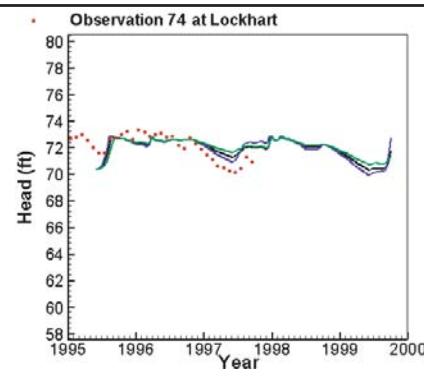

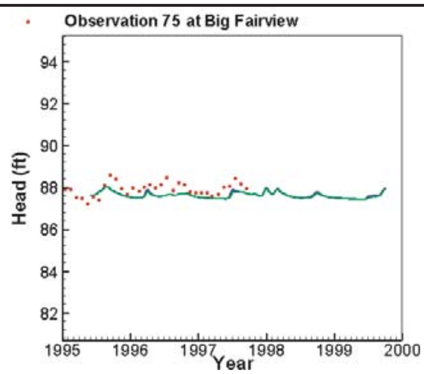

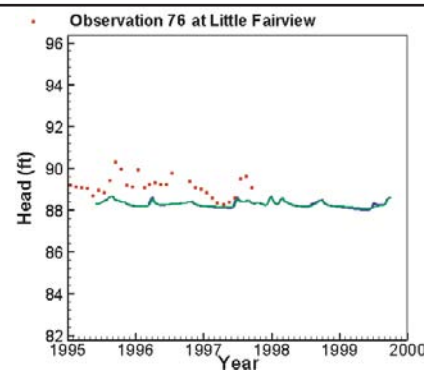

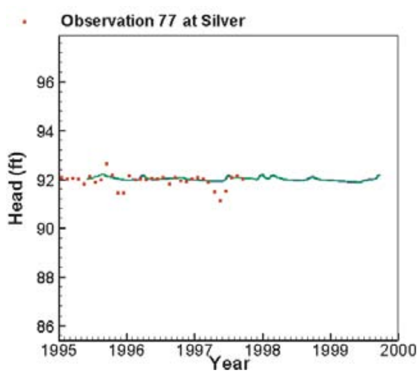

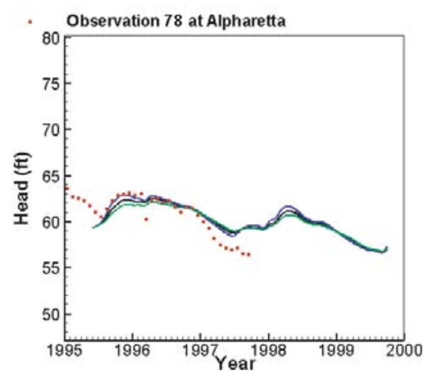

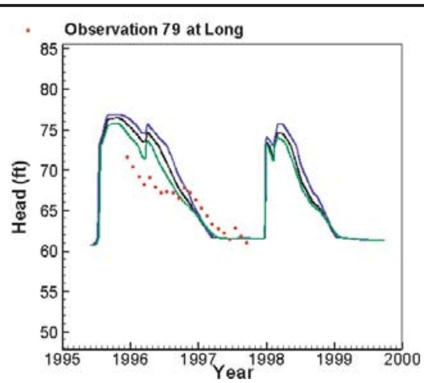

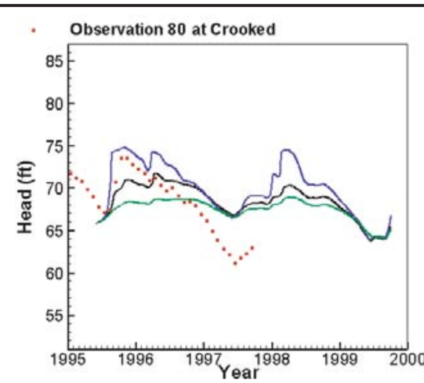

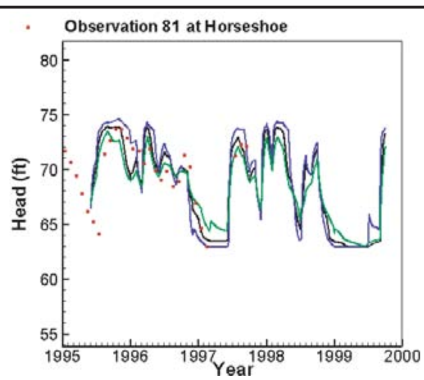

Figure 10.5 Transient Hydrographs at Observation Locations for Sensitivity to Porosity for Transient ISGM Simulation of 1995 through 1999 Conditions. (Page 9 of 11)

Observed Data

Base Case Simulation

Simulation with Porosity Divided by 2

Simulation with Porosity Multiplied by 2

X:\SJR017\TO1\Maps\Conceptual_Model_Report\graphs_porosity.cdr

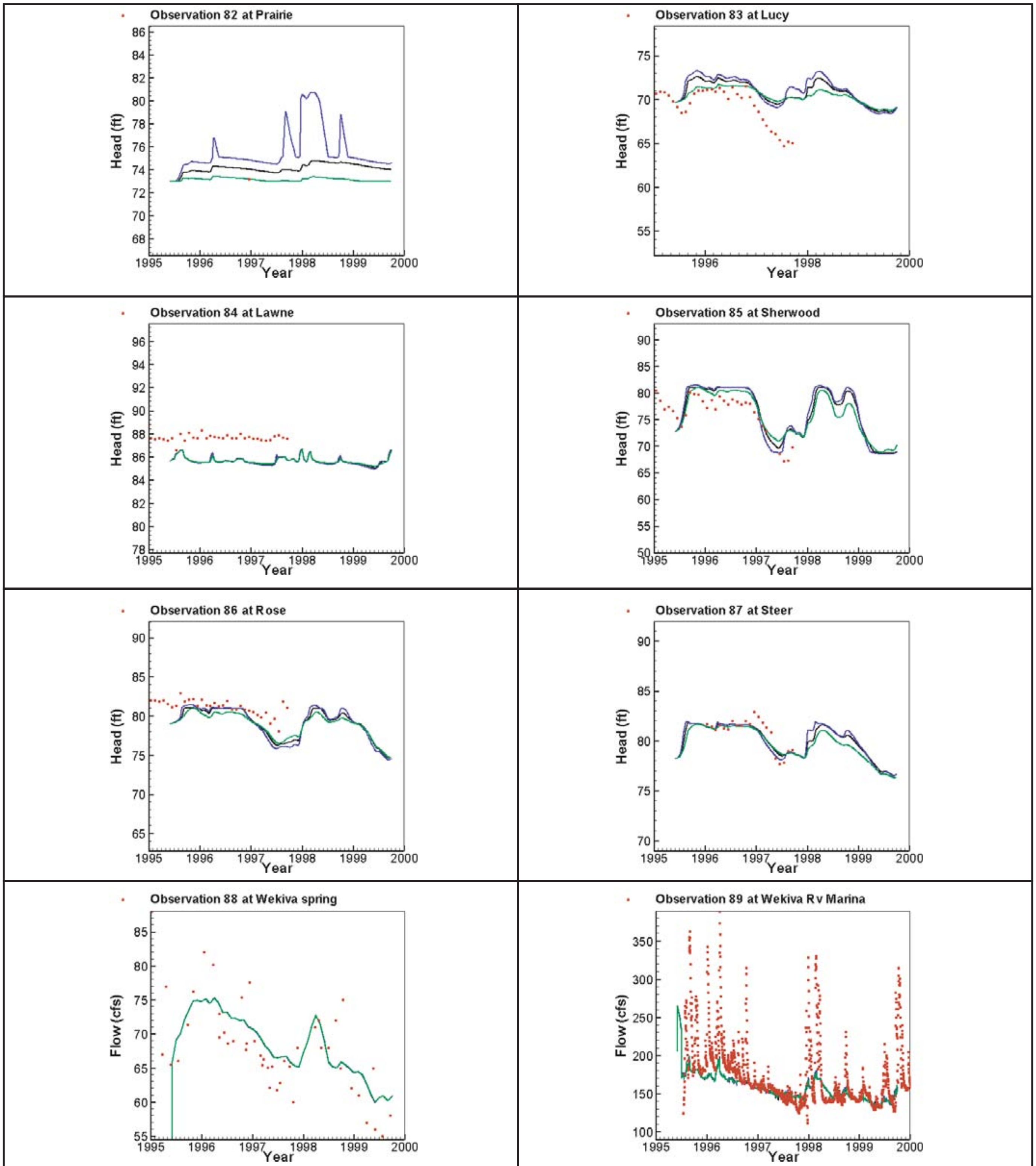

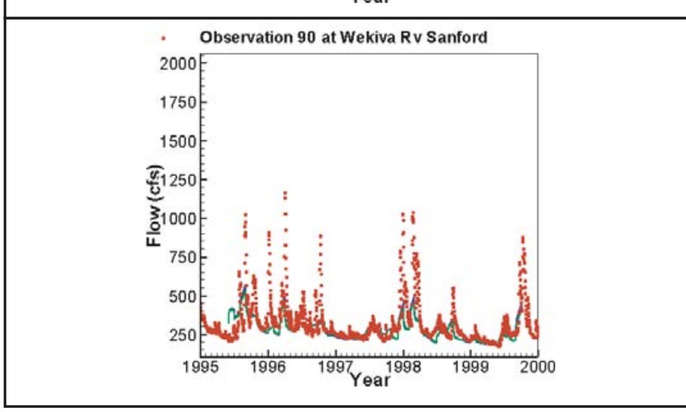

Figure 10.5 Transient Hydrographs at Observation Locations for Sensitivity to Porosity for Transient ISGM Simulation of 1995 through 1999 Conditions. (Page 10 of 11)

Observed Data

Base Case Simulation

Simulation with Porosity Divided by 2

Simulation with Porosity Multiplied by 2

X:\SJR017\TO1\Maps\Conceptual_Model_Report\graphs_porosity.cdr

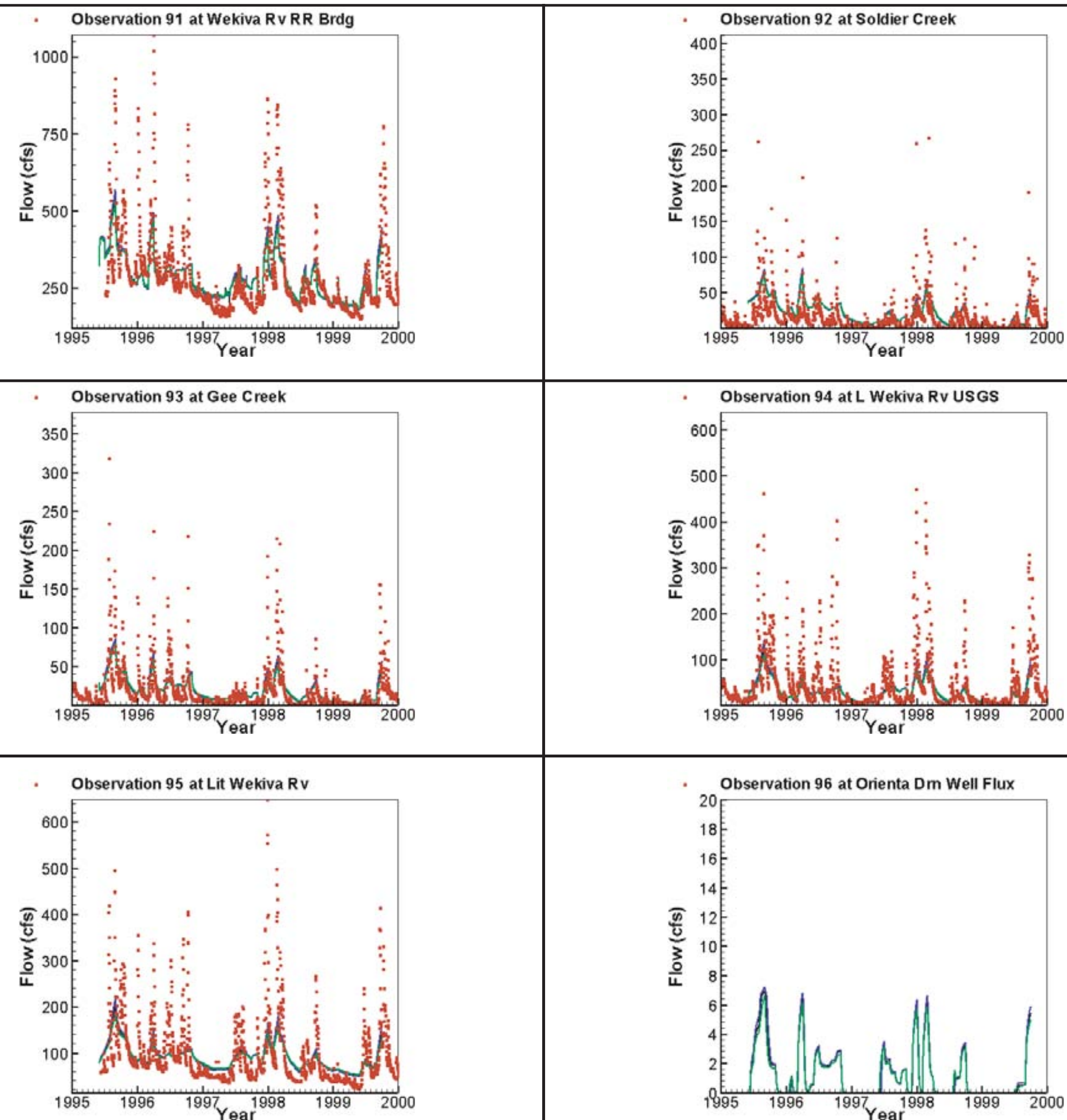

Figure 10.5 Transient Hydrographs at Observation Locations for Sensitivity to Porosity for Transient ISGM Simulation of 1995 through 1999 Conditions. (Page 11 of 11)

Observed Data

Base Case Simulation

Simulation with Porosity Divided by 2

Simulation with Porosity Multiplied by 2

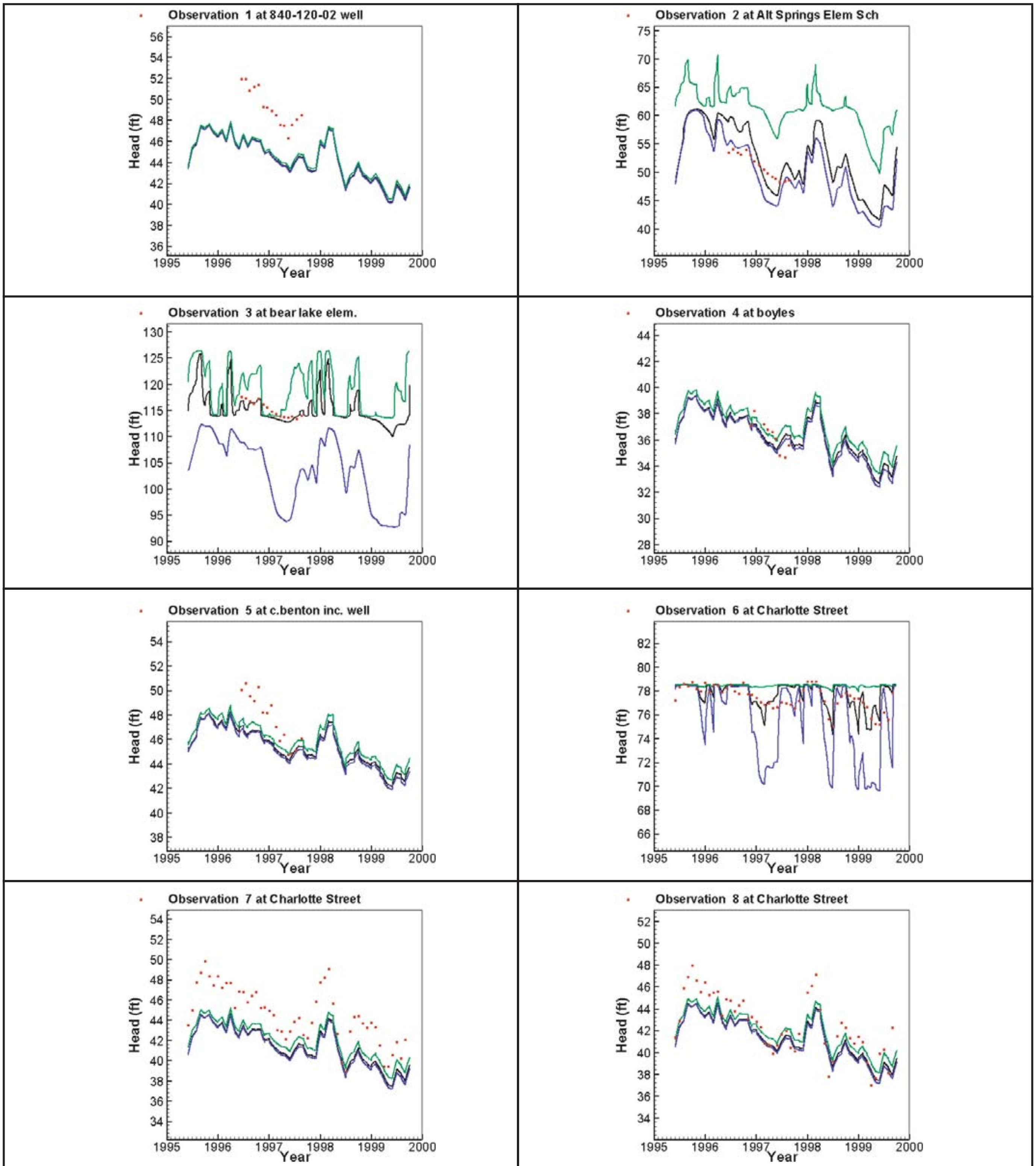

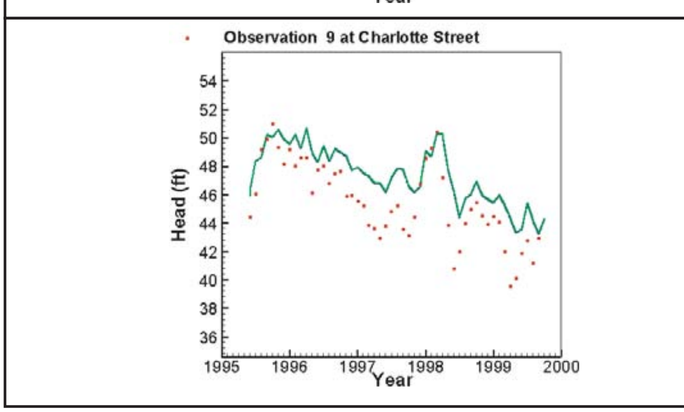

Figure 10.6 Transient Hydrographs at Observation Locations for Sensitivity to Field Capacity and Wilting Point Saturations for Transient ISGM Simulation of 1995 through 1999. (Page 1 of 11)

Observed Data

Base Case Simulation

Simulation with Field Capacity and Wilting Point Divided by 2

Simulation with Field Capacity and Wilting Point Multiplied by 2

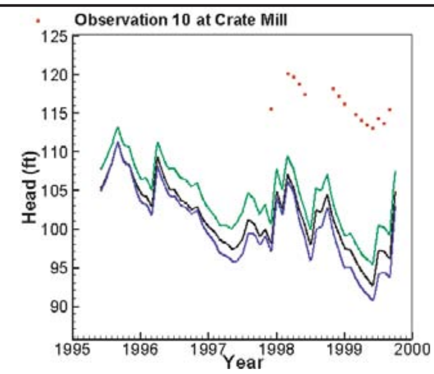

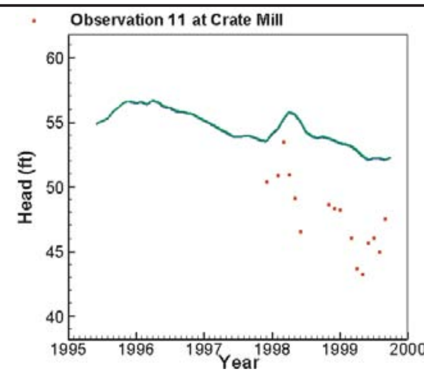

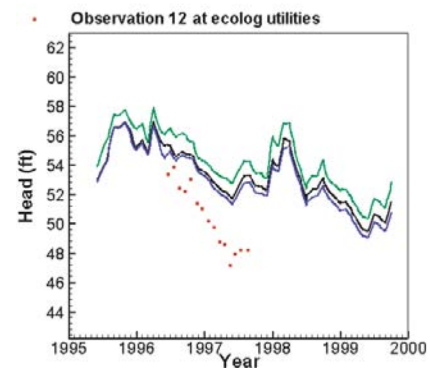

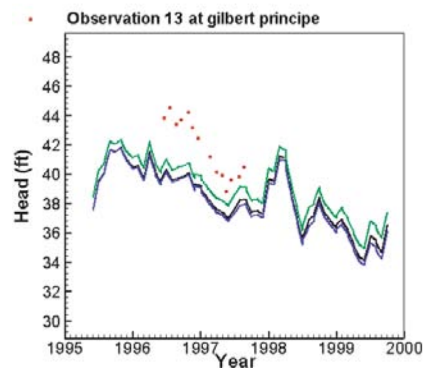

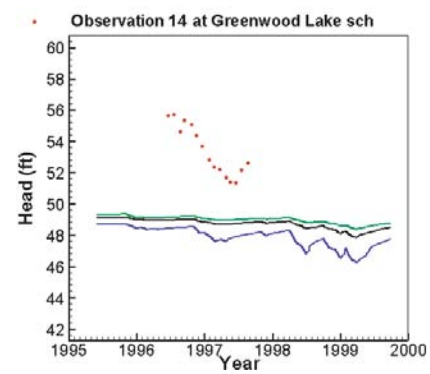

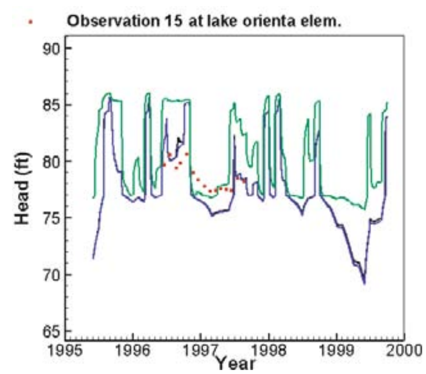

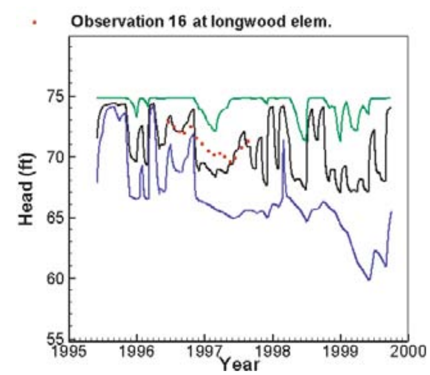

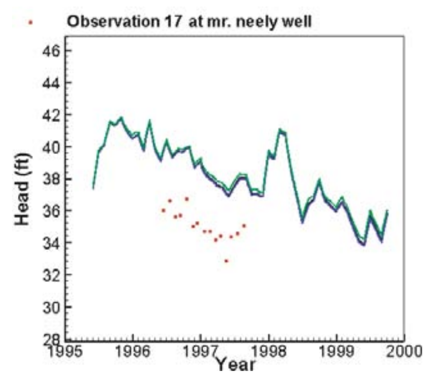

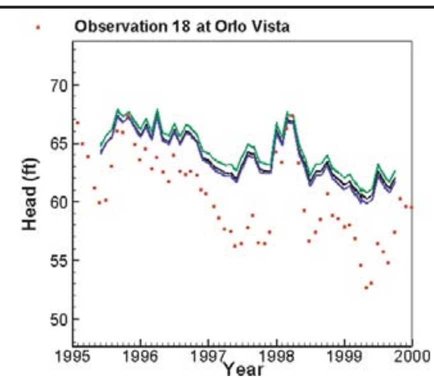

Figure 10.6 Transient Hydrographs at Observation Locations for Sensitivity to Field Capacity and Wilting Point Saturations for Transient ISGM Simulation of 1995 through 1999. (Page 2 of 11)

- Observed Data
- Base Case Simulation
- Simulation with Field Capacity and Wilting Point Divided by 2
- Simulation with Field Capacity and Wilting Point Multiplied by 2

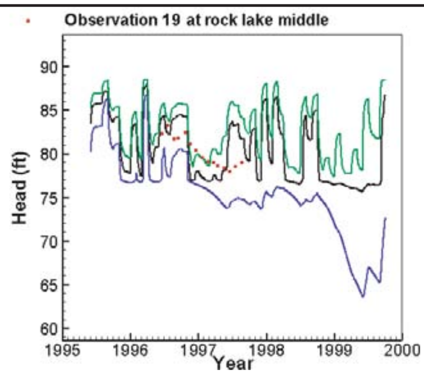

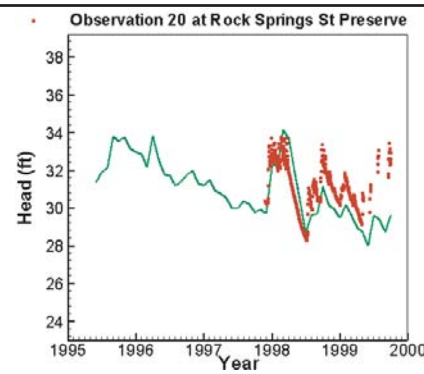

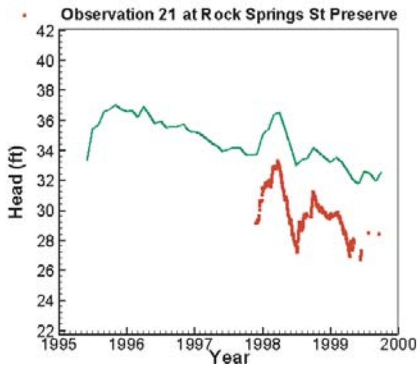

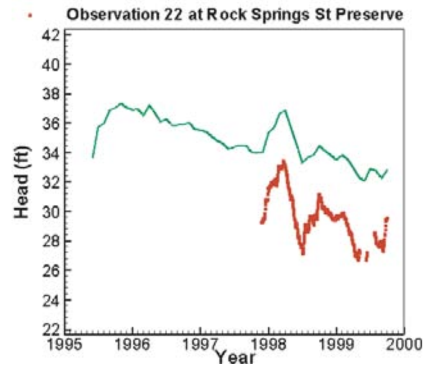

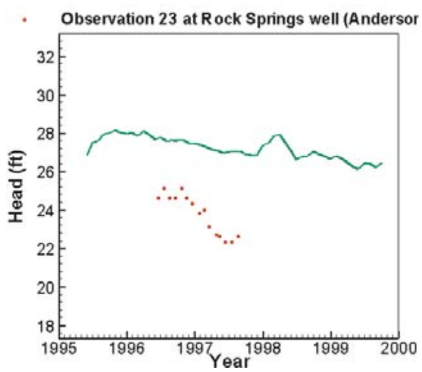

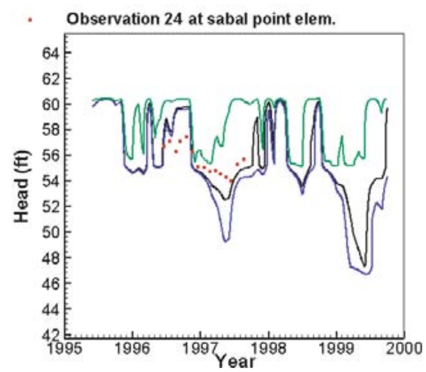

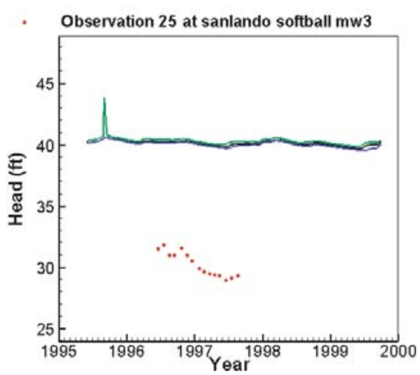

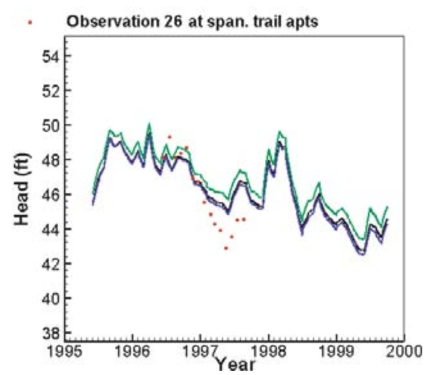

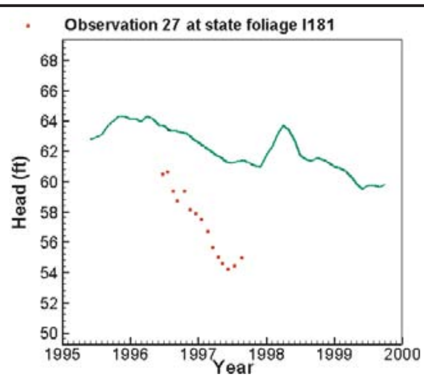

Figure 10.6 Transient Hydrographs at Observation Locations for Sensitivity to Field Capacity and Wilting Point Saturations for Transient ISGM Simulation of 1995 through 1999. (Page 3 of 11)

- Observed Data
- Base Case Simulation
- Simulation with Field Capacity and Wilting Point Divided by 2
- Simulation with Field Capacity and Wilting Point Multiplied by 2

X:\SJR017\TO1\Maps\Conceptual_Model_Report\graphs_parameters.cdr

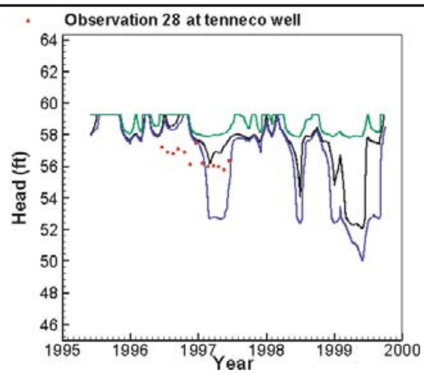

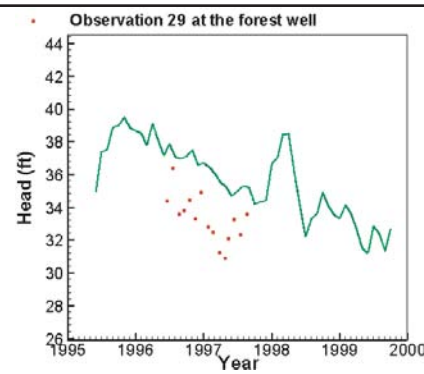

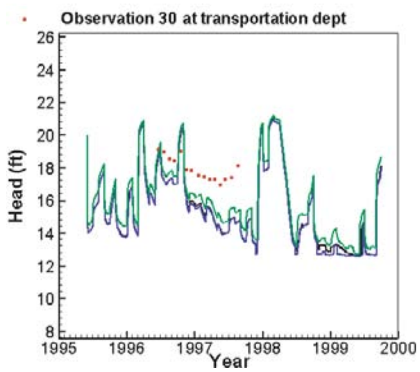

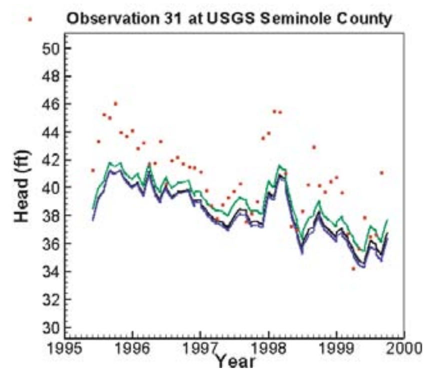

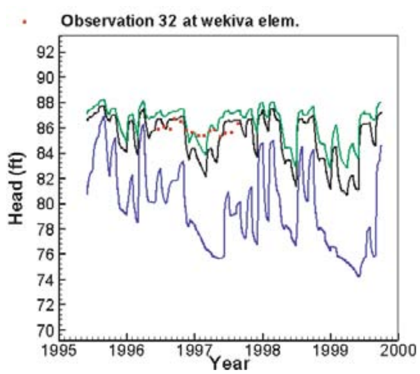

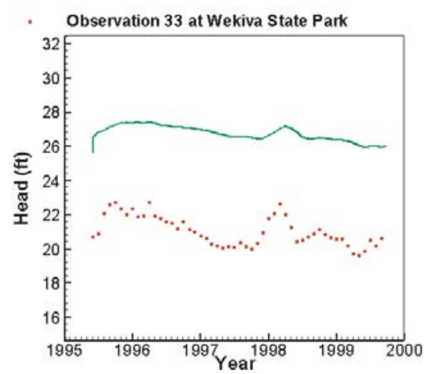

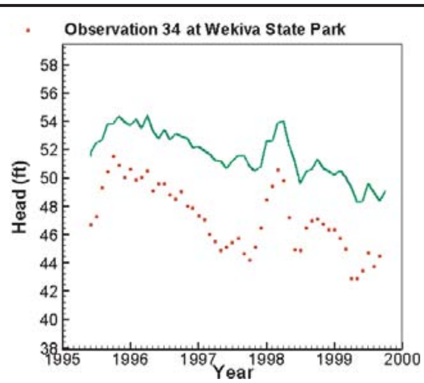

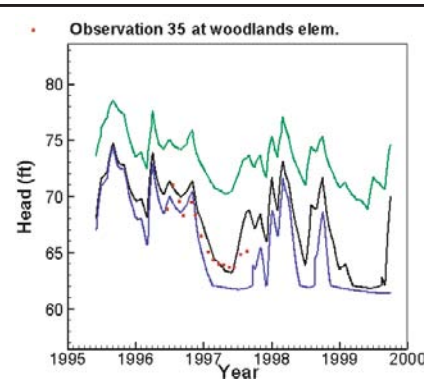

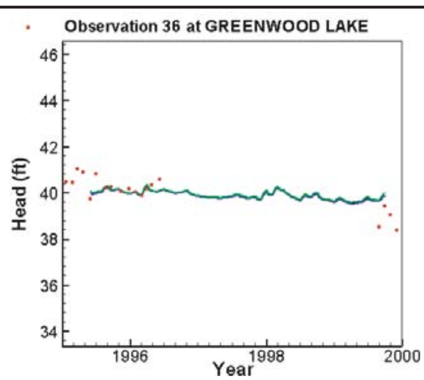

Figure 10.6 Transient Hydrographs at Observation Locations for Sensitivity to Field Capacity and Wilting Point Saturations for Transient ISGM Simulation of 1995 through 1999. (Page 4 of 11)

- Observed Data
- Base Case Simulation
- Simulation with Field Capacity and Wilting Point Divided by 2
- Simulation with Field Capacity and Wilting Point Multiplied by 2

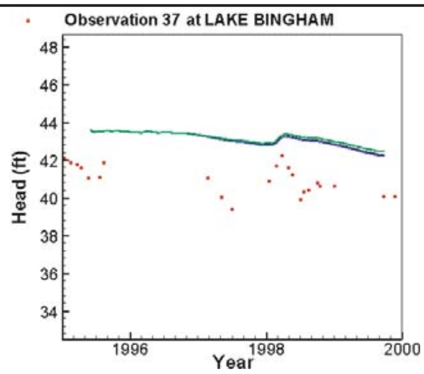

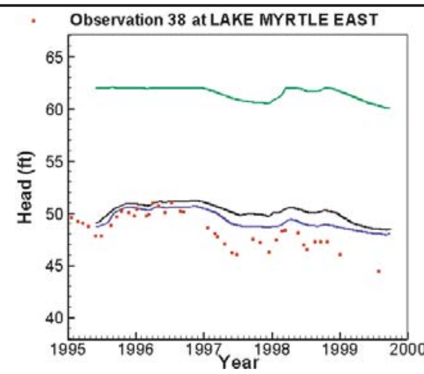

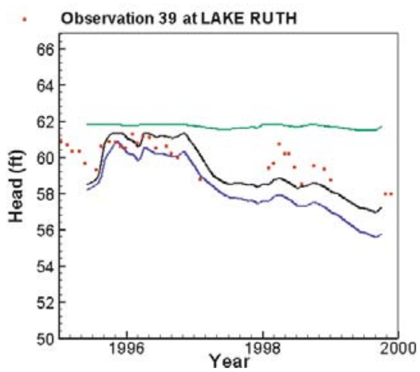

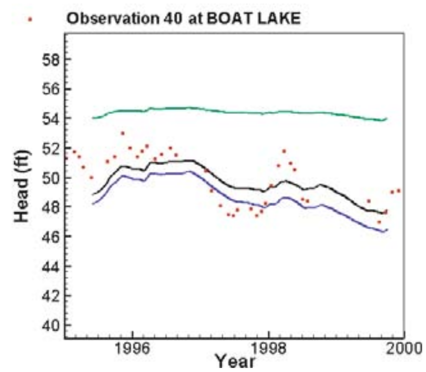

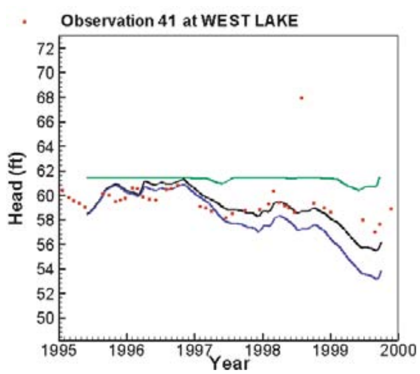

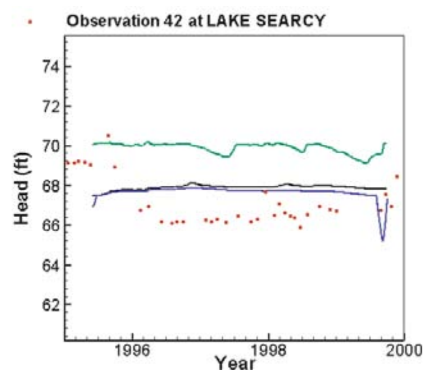

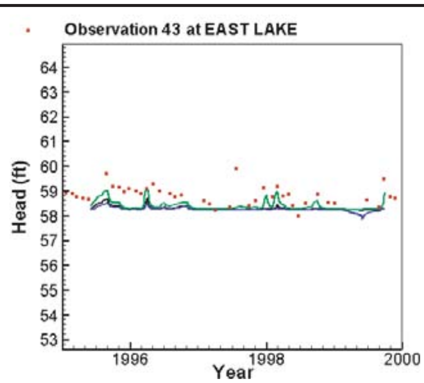

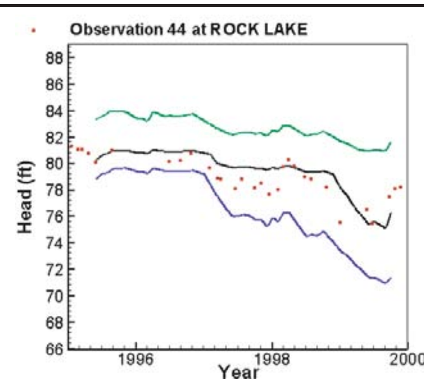

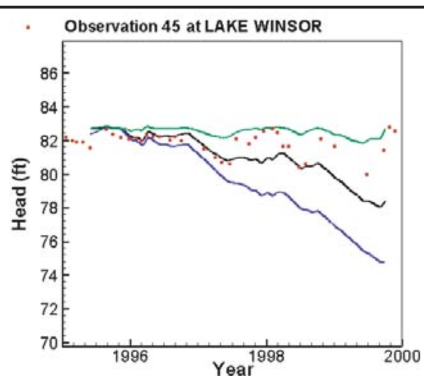

Figure 10.6 Transient Hydrographs at Observation Locations for Sensitivity to Field Capacity and Wilting Point Saturations for Transient ISGM Simulation of 1995 through 1999. (Page 5 of 11)

Observed Data

Base Case Simulation

Simulation with Field Capacity and Wilting Point Divided by 2

Simulation with Field Capacity and Wilting Point Multiplied by 2

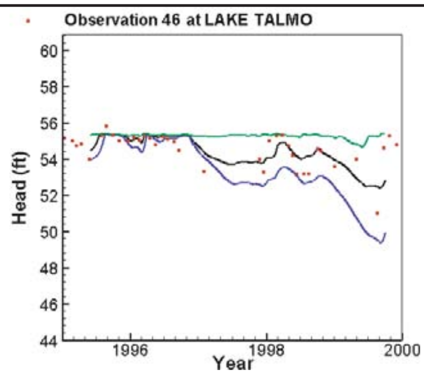

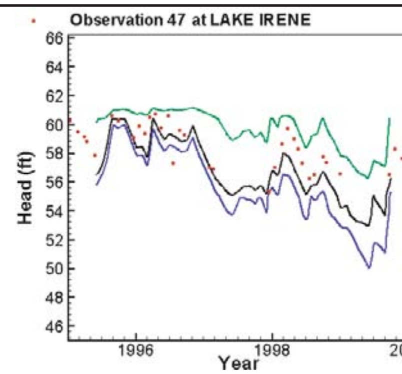

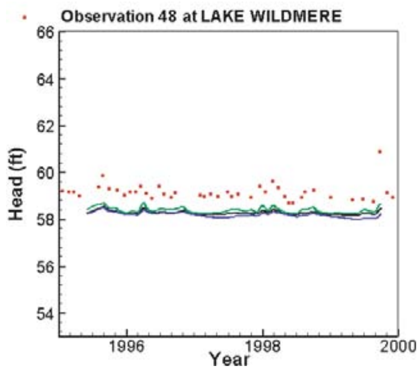

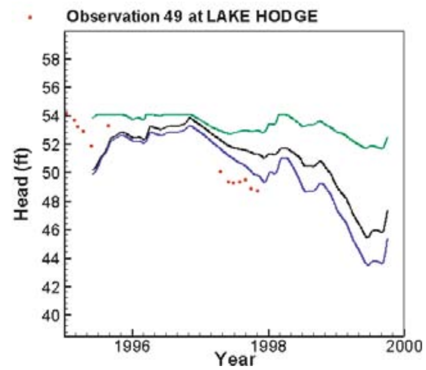

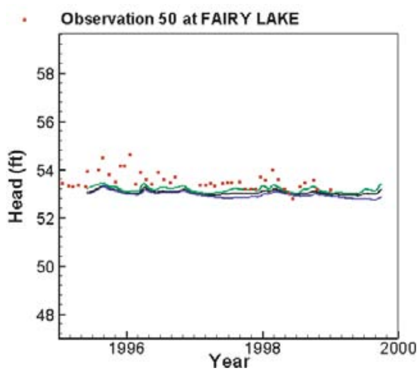

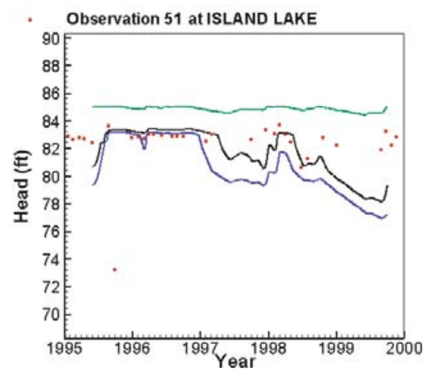

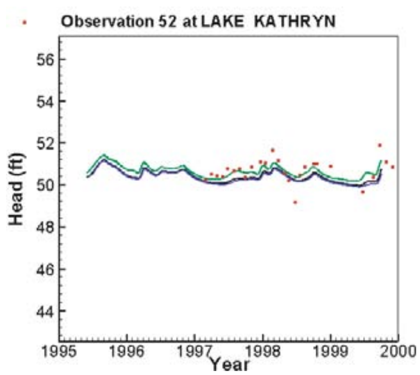

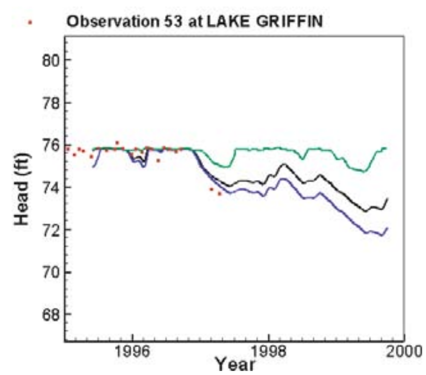

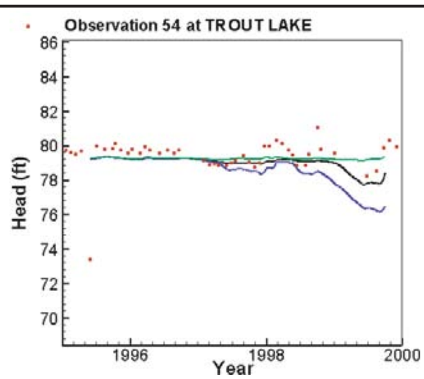

Figure 10.6 Transient Hydrographs at Observation Locations for Sensitivity to Field Capacity and Wilting Point Saturations for Transient ISGM Simulation of 1995 through 1999. (Page 6 of 11)

- Observed Data
- Base Case Simulation
- Simulation with Field Capacity and Wilting Point Divided by 2
- Simulation with Field Capacity and Wilting Point Multiplied by 2

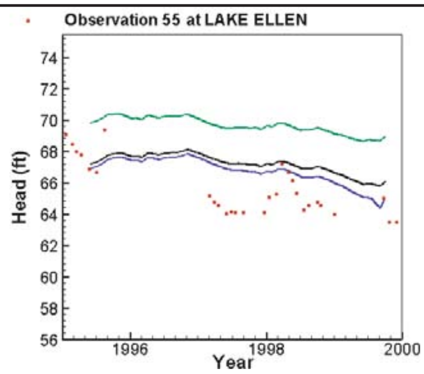

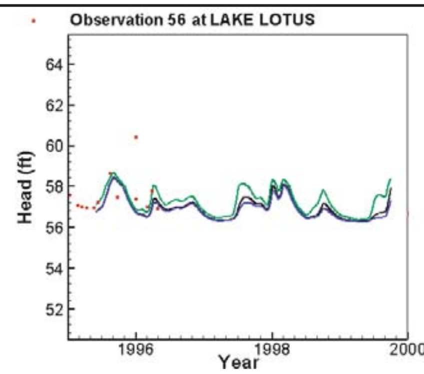

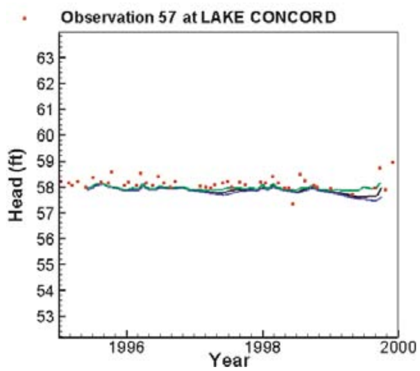

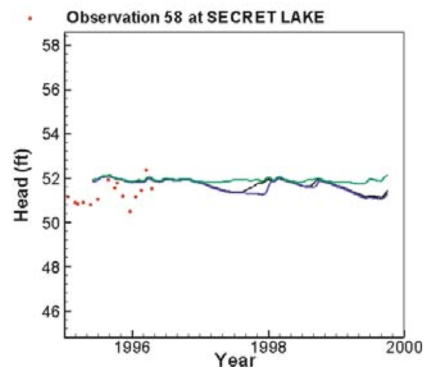

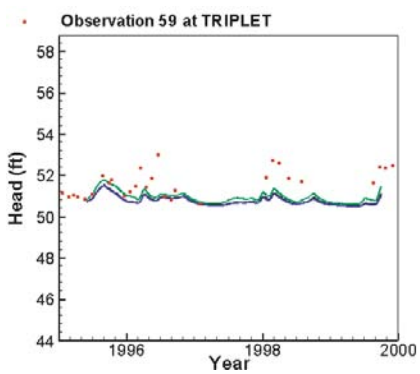

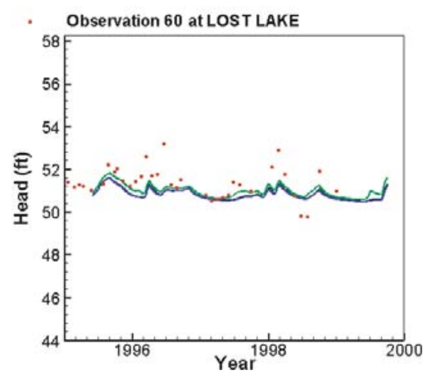

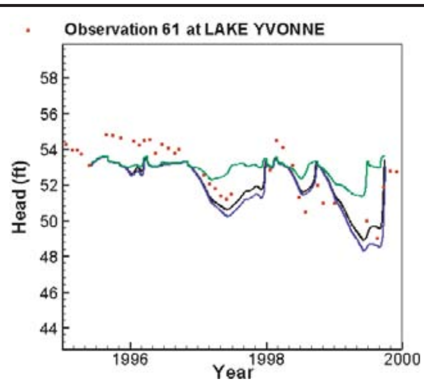

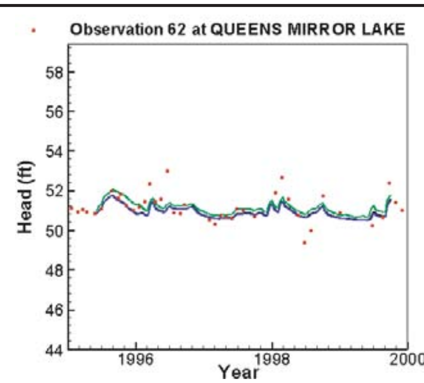

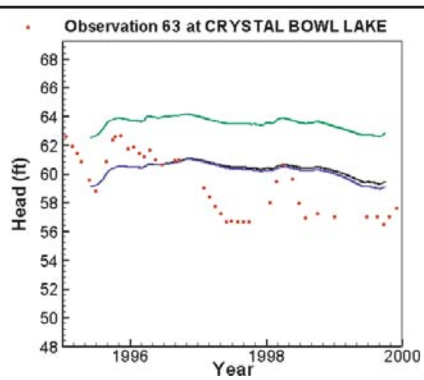

Figure 10.6 Transient Hydrographs at Observation Locations for Sensitivity to Field Capacity and Wilting Point Saturations for Transient ISGM Simulation of 1995 through 1999. (Page 7 of 11)

Observed Data

Base Case Simulation

Simulation with Field Capacity and Wilting Point Divided by 2

Simulation with Field Capacity and Wilting Point Multiplied by 2

X:\SJR017\TO1\Maps\Conceptual_Model_Report\graphs_parameters.cdr

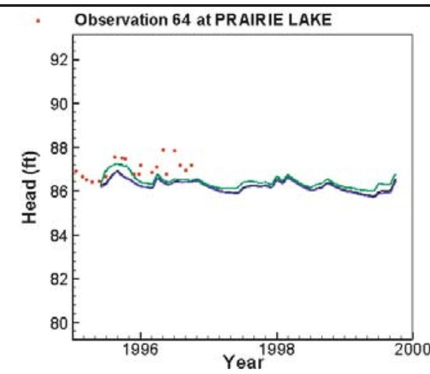

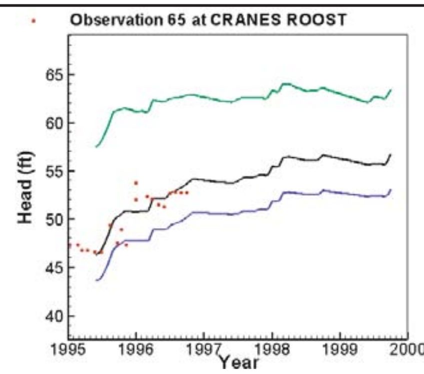

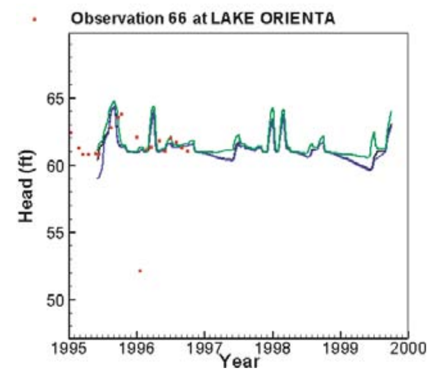

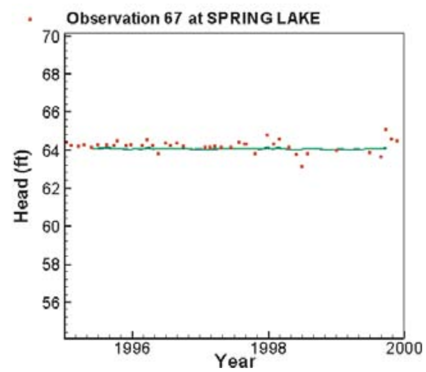

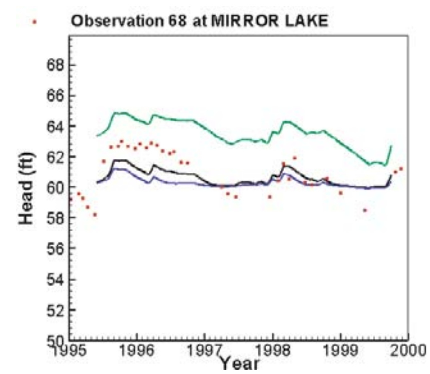

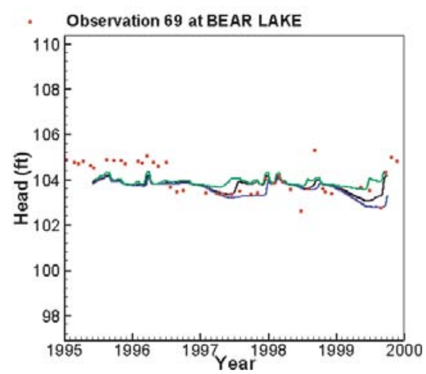

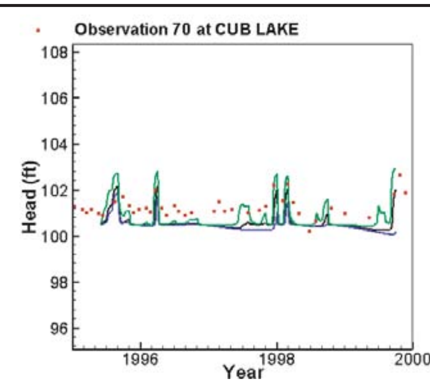

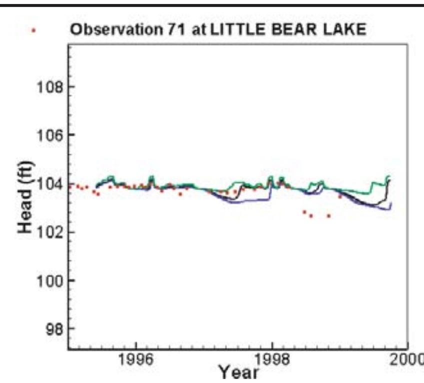

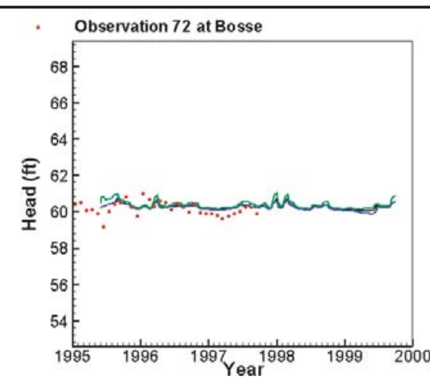

Figure 10.6 Transient Hydrographs at Observation Locations for Sensitivity to Field Capacity and Wilting Point Saturations for Transient ISGM Simulation of 1995 through 1999. (Page 8 of 11)

- Observed Data
- Base Case Simulation
- Simulation with Field Capacity and Wilting Point Divided by 2
- Simulation with Field Capacity and Wilting Point Multiplied by 2

X:\SJR017\TO1\Maps\Conceptual_Model_Report\graphs_parameters.cdr

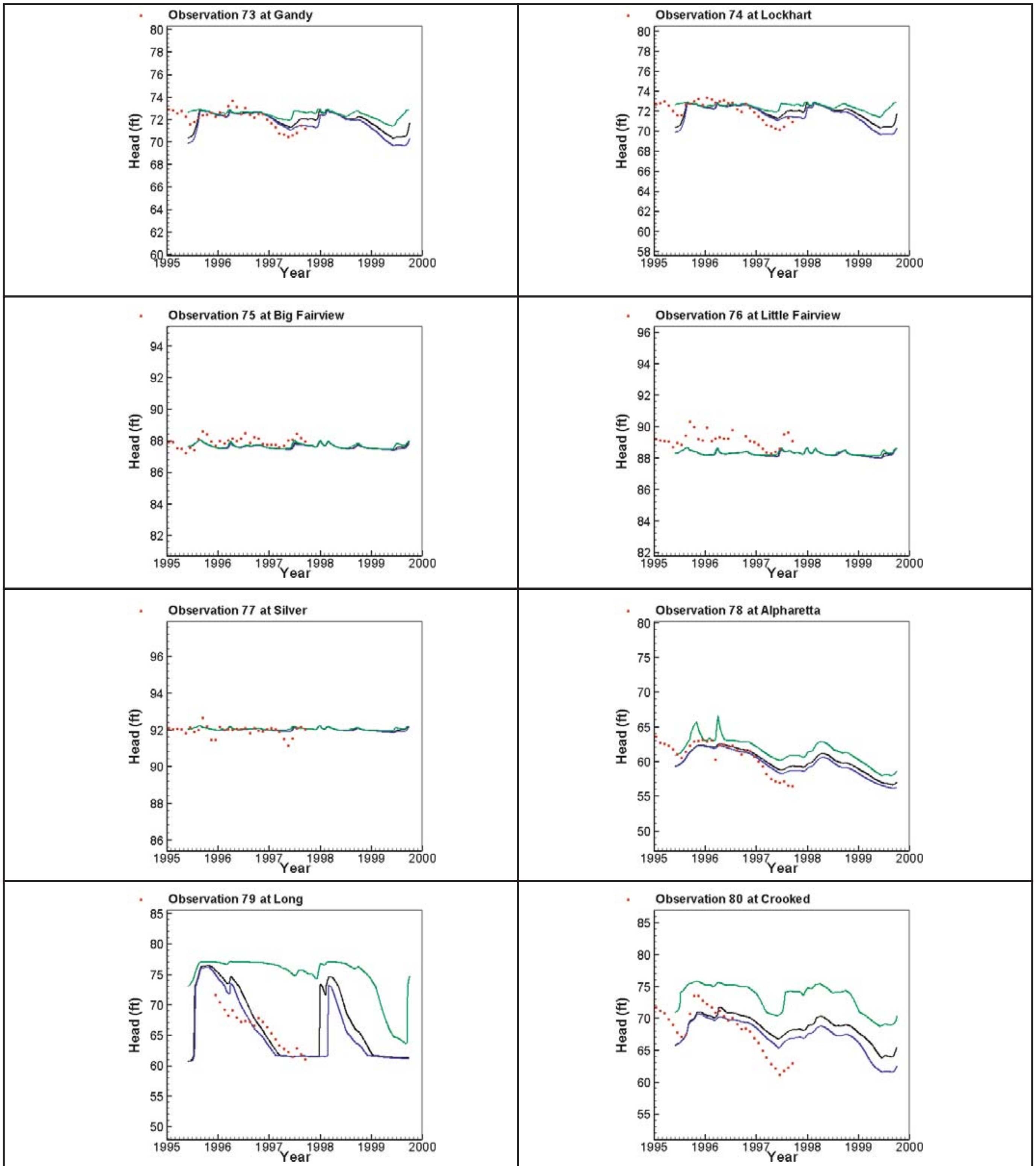

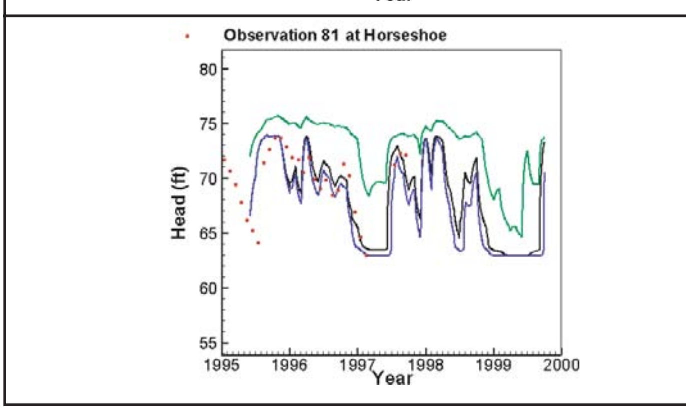

Figure 10.6 Transient Hydrographs at Observation Locations for Sensitivity to Field Capacity and Wilting Point Saturations for Transient ISGM Simulation of 1995 through 1999. (Page 9 of 11)

- Observed Data
- Base Case Simulation
- Simulation with Field Capacity and Wilting Point Divided by 2
- Simulation with Field Capacity and Wilting Point Multiplied by 2

X:\SJR017\TO1\Maps\Conceptual_Model_Report\graphs_parameters.cdr

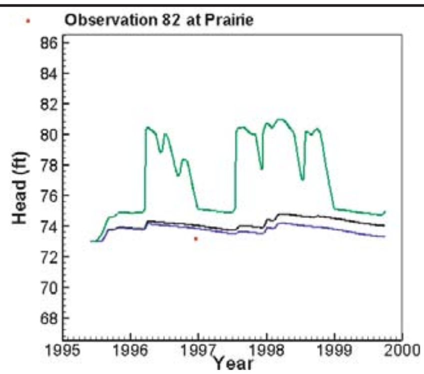

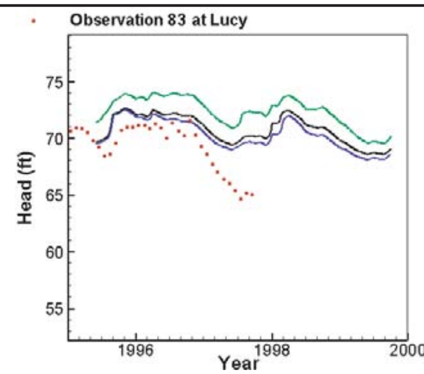

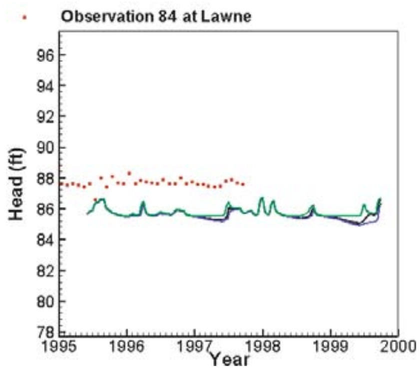

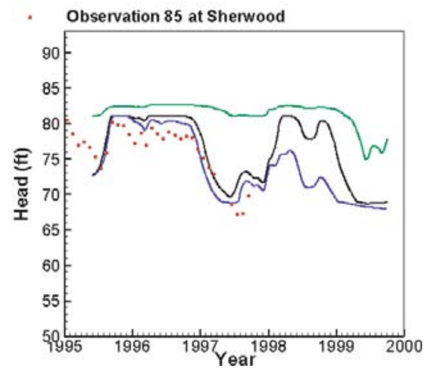

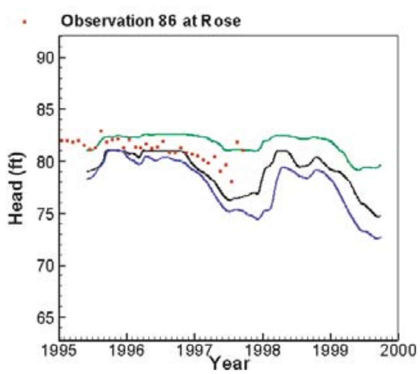

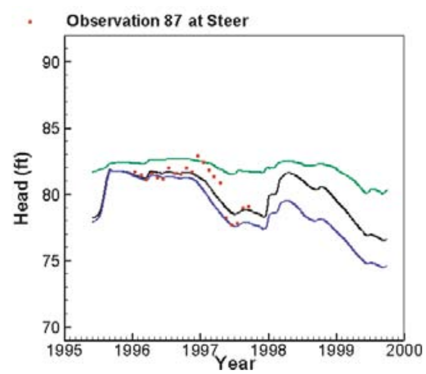

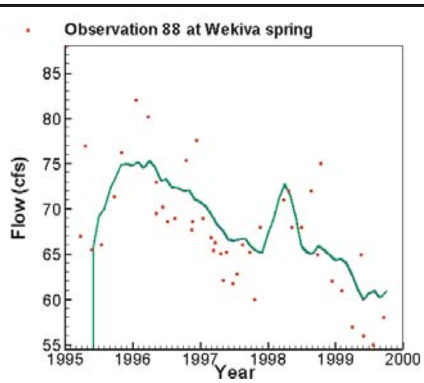

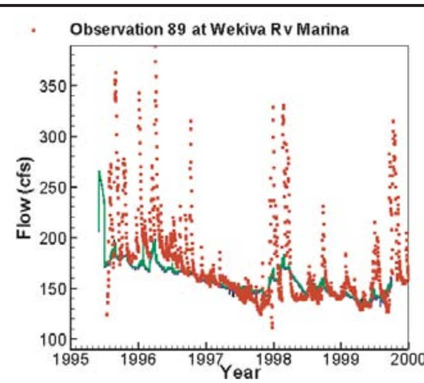

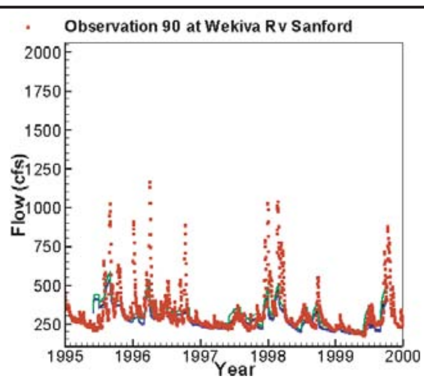

Figure 10.6 Transient Hydrographs at Observation Locations for Sensitivity to Field Capacity and Wilting Point Saturations for Transient ISGM Simulation of 1995 through 1999. (Page 10 of 11)

Observed Data

Base Case Simulation

Simulation with Field Capacity and Wilting Point Divided by 2

Simulation with Field Capacity and Wilting Point Multiplied by 2

X:\SJR017\TO1\Maps\Conceptual_Model_Report\graphs_parameters.cdr

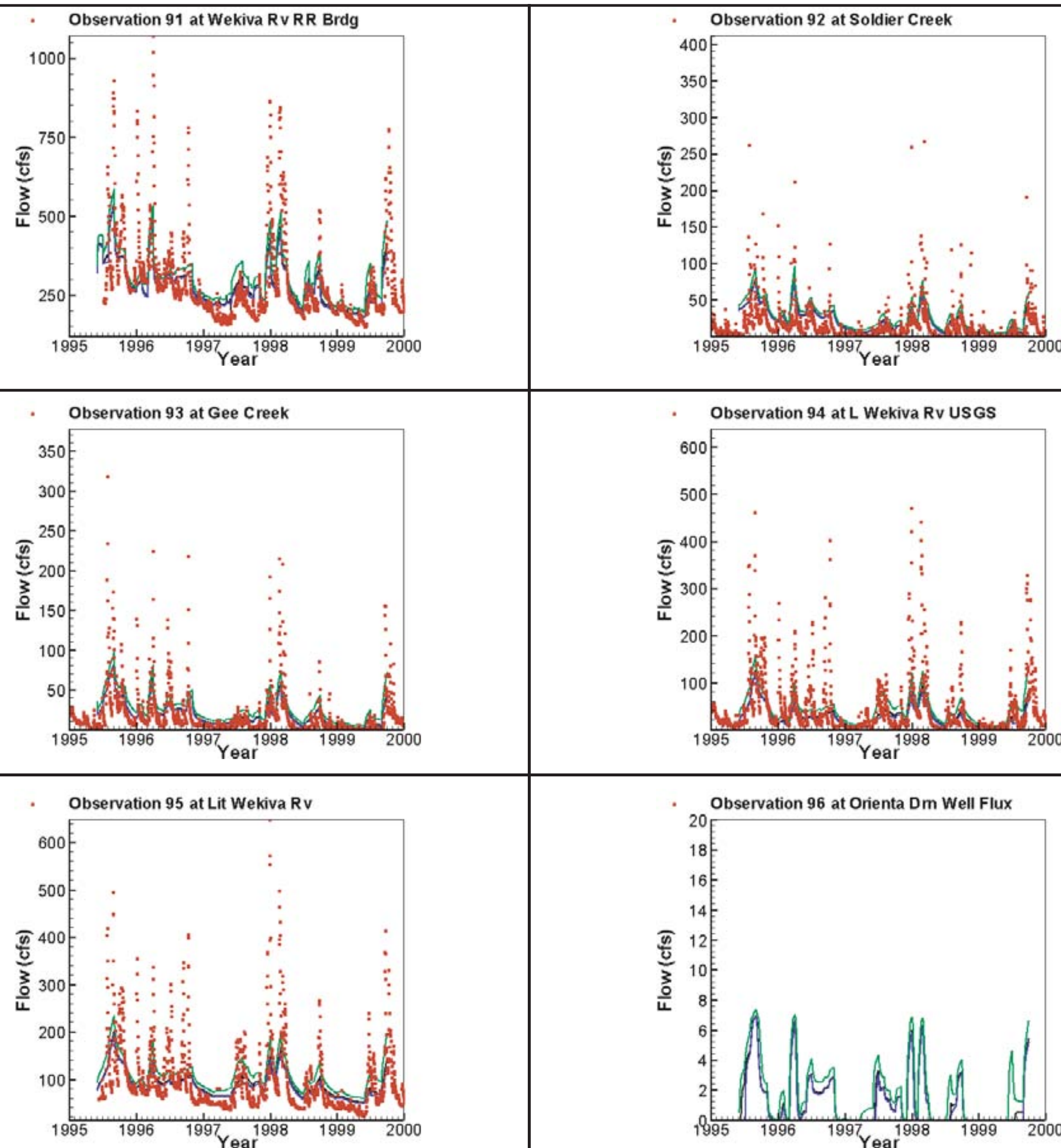

Figure 10.6 Transient Hydrographs at Observation Locations for Sensitivity to Field Capacity and Wilting Point Saturations for Transient ISGM Simulation of 1995 through 1999. (Page 11 of 11)

Observed Data

Base Case Simulation

Simulation with Field Capacity and Wilting Point Divided by 2

Simulation with Field Capacity and Wilting Point Multiplied by 2

X:\SJR017\TO1\Maps\Conceptual_Model_Report\graphs_parameters.cdr

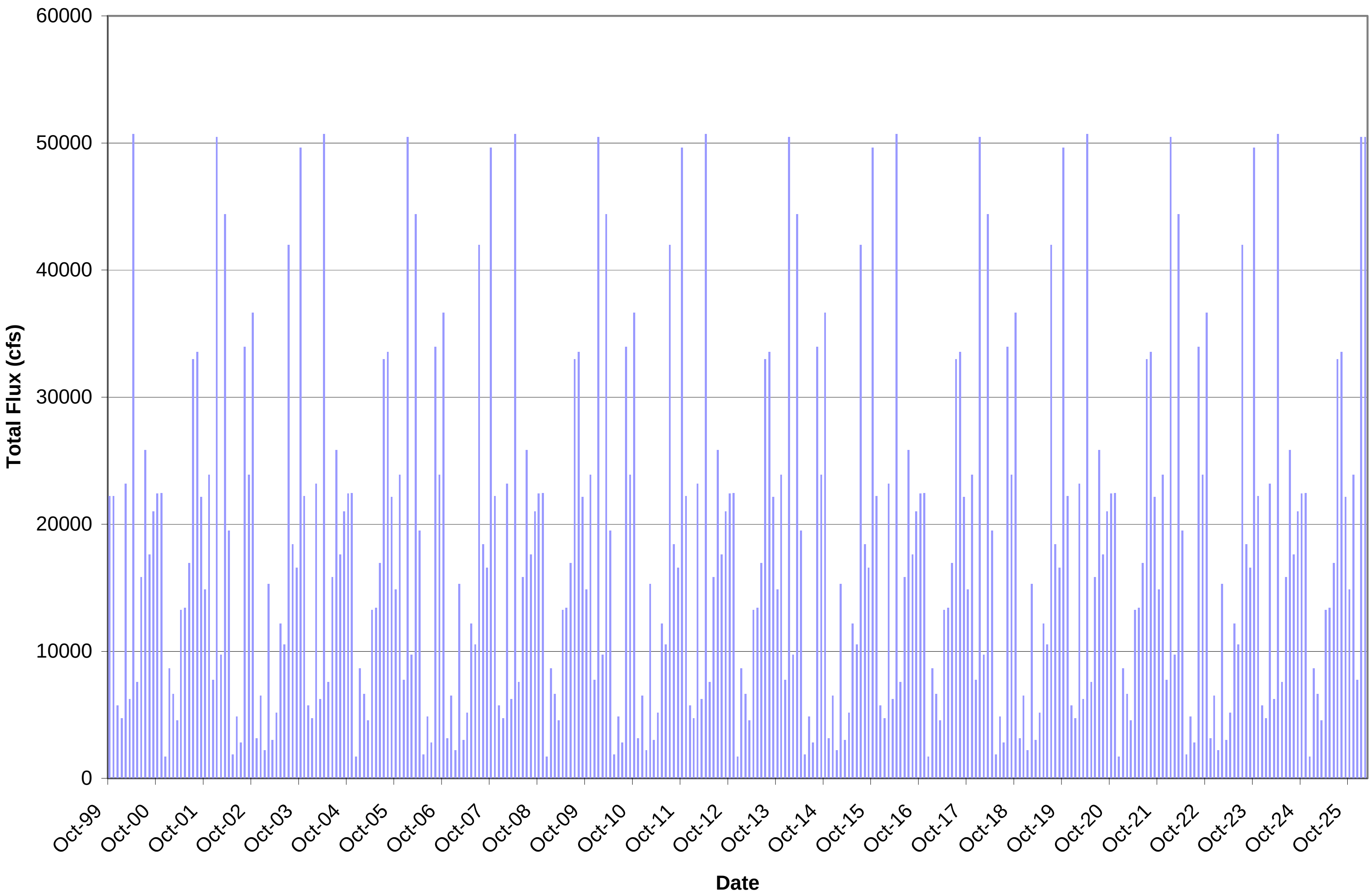

Source:
Filename: X:/SJR017/TO1/Maps/
Conceptual_model_report/sum_Monthly_RTS.mxd
Project: SJR017-001-99
Revised: 12/07/04 TB

Figure 11.1
Cumulative Volumetric Flux over all NEXRAD Stations for Predictive Simulation from 1999 through 2025

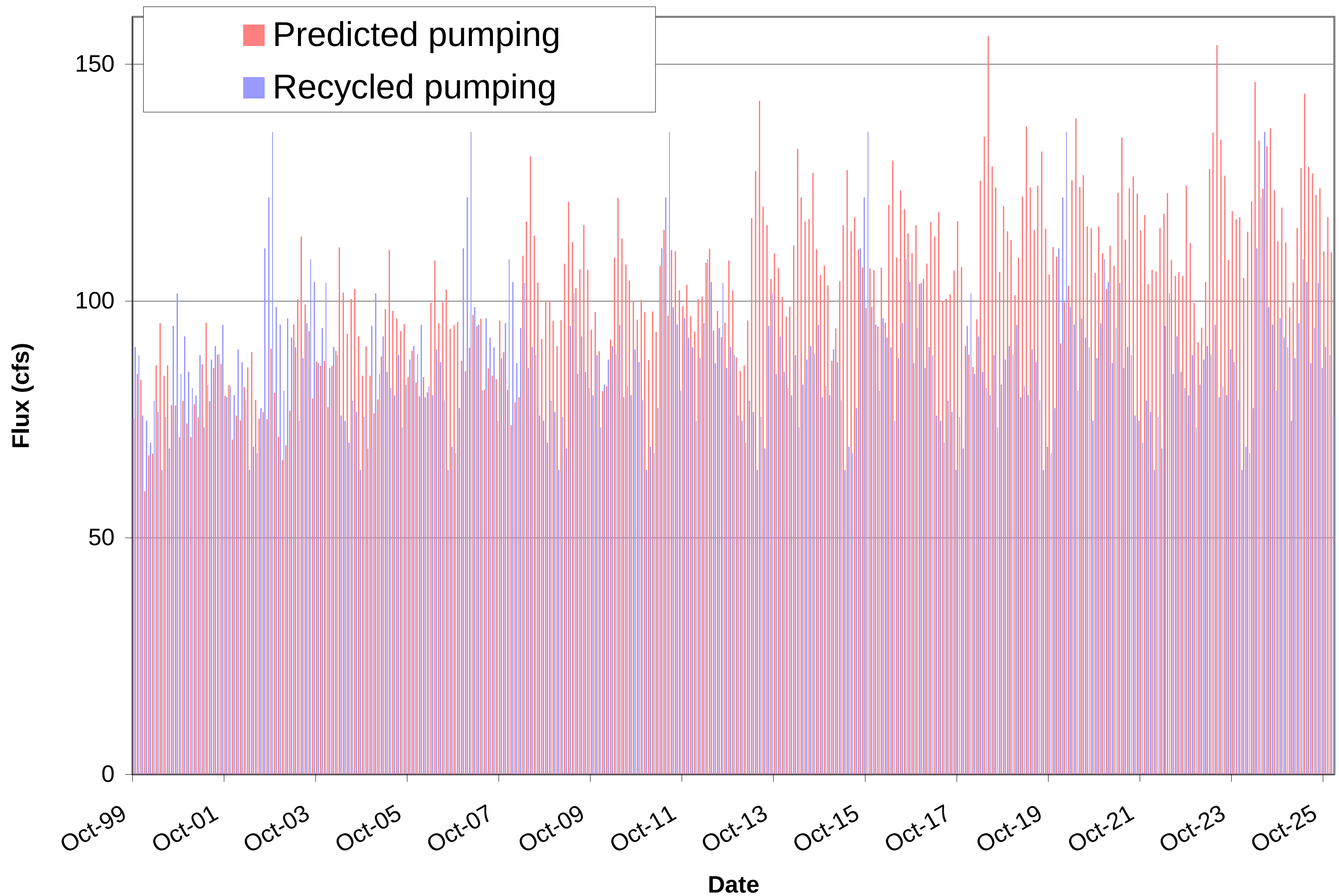

Source:
Filename: X:/SJR017/TO1/Maps/
Conceptual_model_report/Well_Totals.mxd
Project: SJR017-001-99
Revised: 12/07/04 TB

Figure 11.2
Cumulative Volumetric Flux over all Wells including RIBS and Septic Tank Inflows for Predictive Simulation from 1999 through 2025

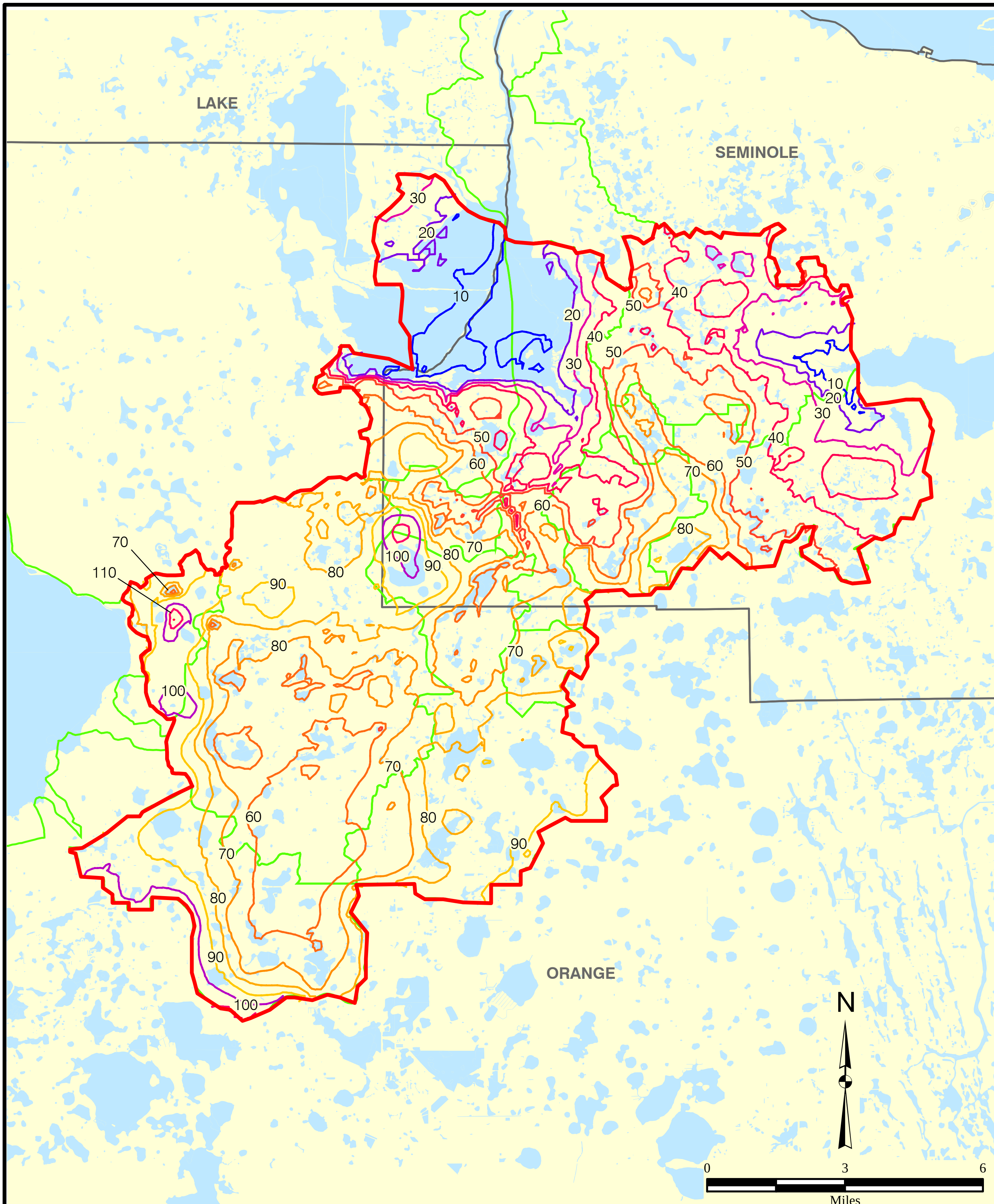

Source:
Filename: X:/SJR017/TO1/Maps/ Conceptual_model_report/WL_SAS_Mar2025.mxd
Project: SJR017-001-06
Revised: 12/27/04 TB

Legend

- Model Boundary
- Surface Water Basin
- County Boundary
- 50 Water Levels (ft)
- Surface Water Bodies and Wetlands

Figure 11.3
Simulated Water Levels in the SAS for May 2025 Conditions

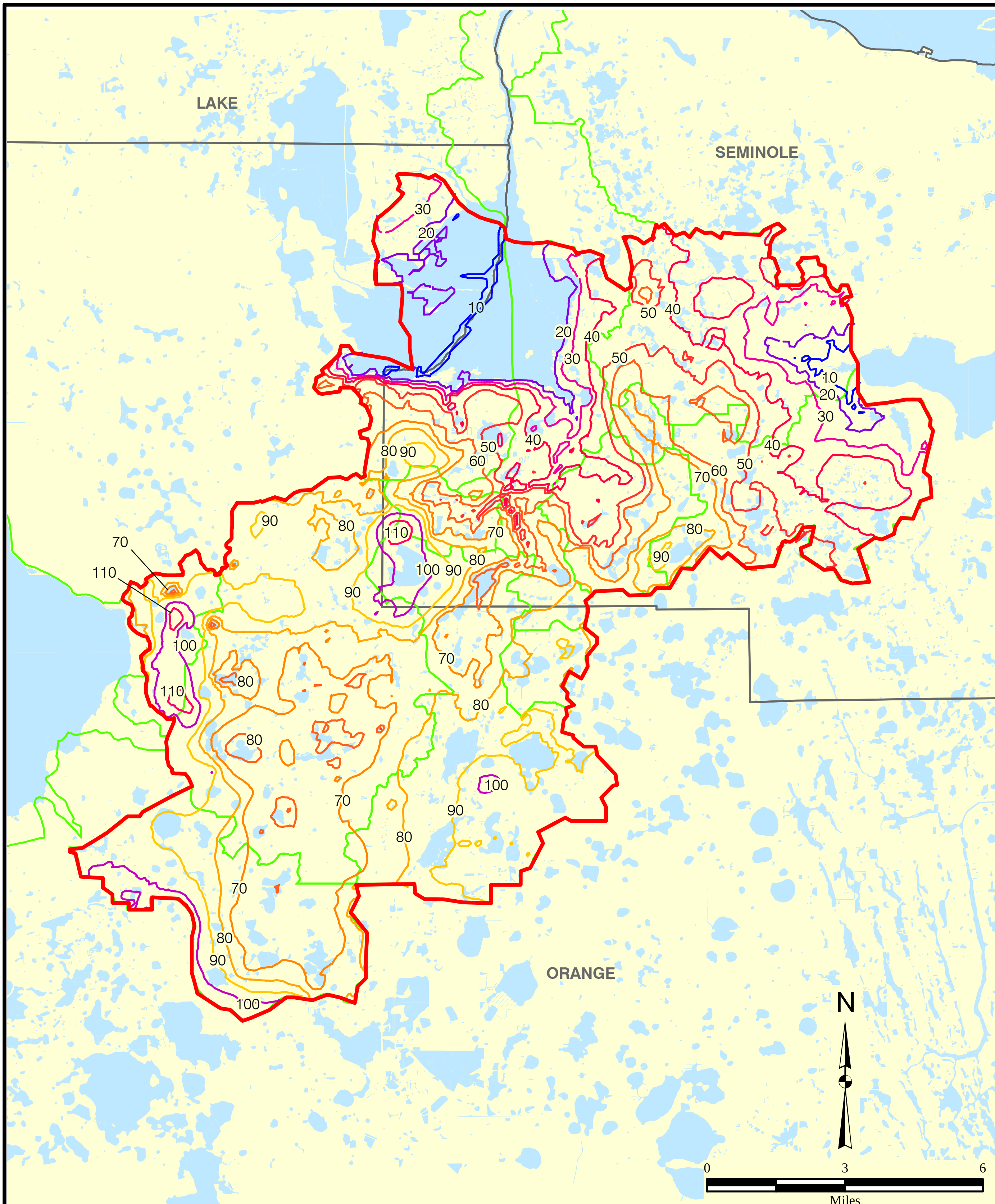

Source:
Filename: X:/SJR017/TO1/Maps/
Conceptual_model_report/WL_SAS_Mar2025.mxd
Project: SJR017-001-99
Revised: 12/27/04 TB

Legend

- Model Boundary
- Surface Water Basin
- County Boundary
- 50 Water Levels (ft)
- Surface Water Bodies and Wetlands

Figure 11.4
Simulated Water Levels in the SAS for September 2025 Conditions

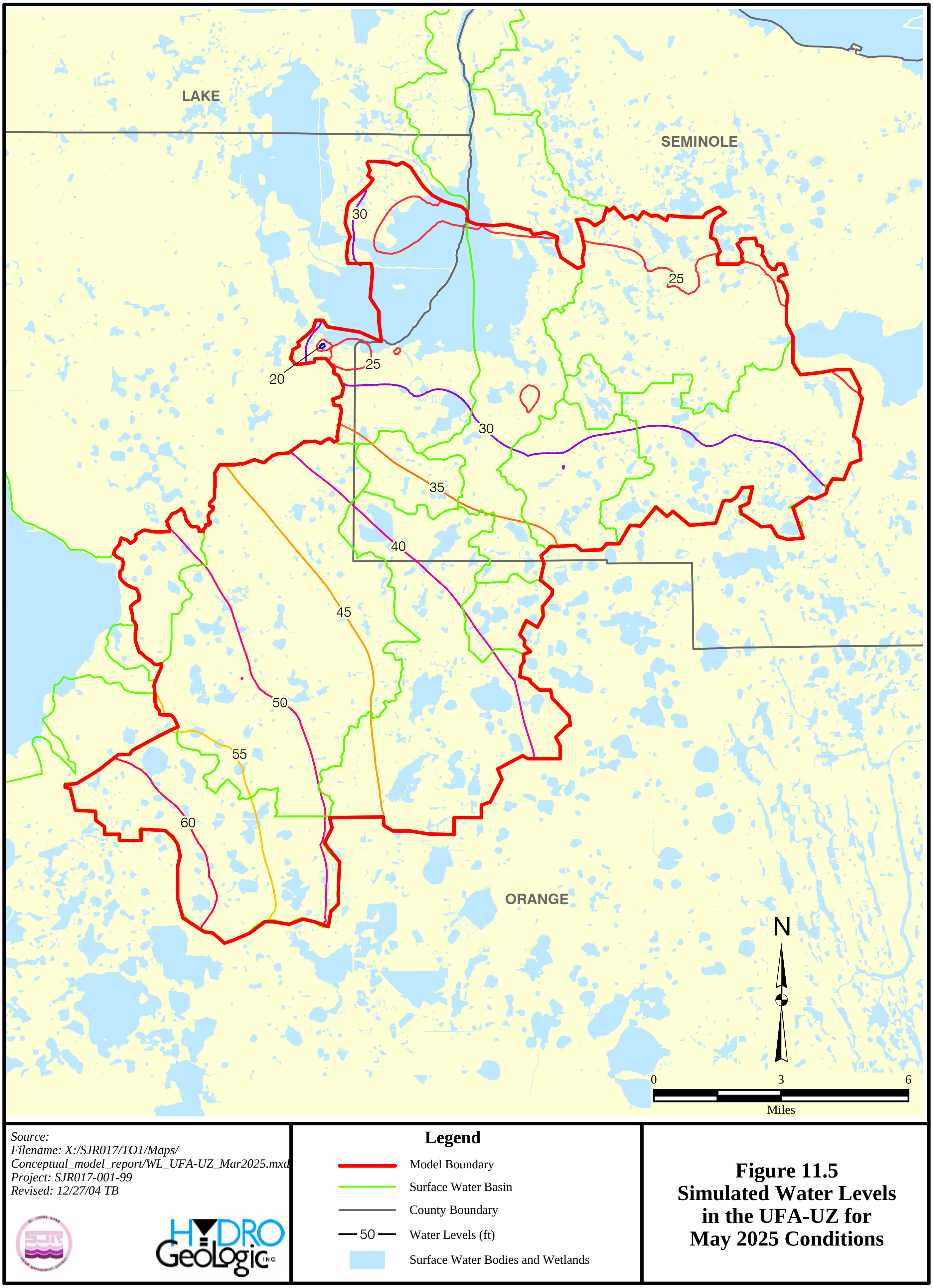

Source:
Filename: X:/SJR017/TO1/Maps/
Conceptual_model_report/WL_UFA-UZ_Mar2025.mxd
Project: SJR017-001-99
Revised: 12/27/04 TB

Figure 11.5
Simulated Water Levels in the UFA-UZ for May 2025 Conditions

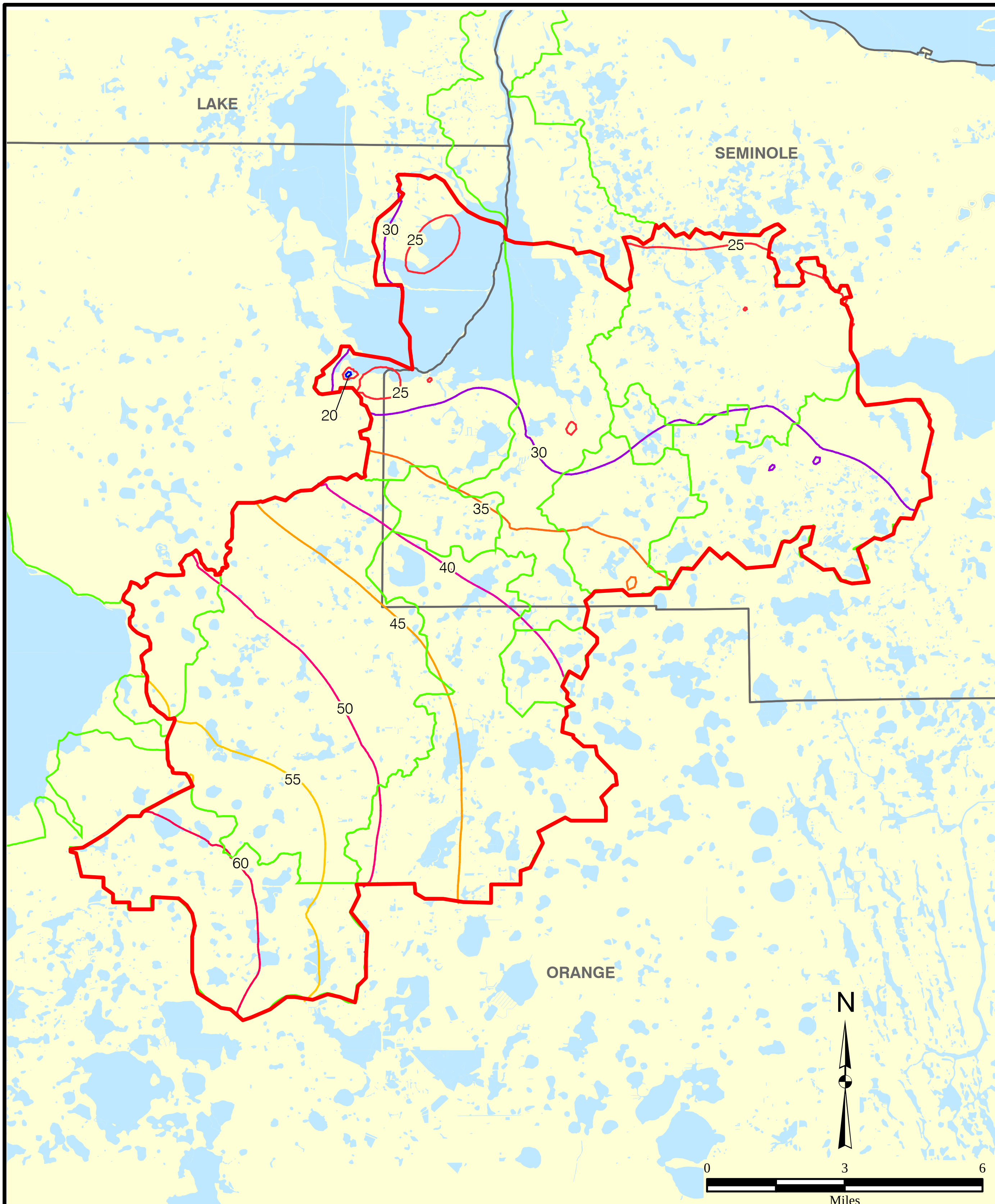

Source:
Filename: X:/SJR017/TO1/Maps/
Conceptual_model_report/WL_UFA-UZ_Sept2025.mxd
Project: SJR017-001-99
Revised: 12/27/04 TB

HYDRO GeoLogic INC.

Legend

- Model Boundary
- Surface Water Basin
- County Boundary
- 50 Water Levels (ft)
- Surface Water Bodies and Wetlands

Figure 11.6
Simulated Water Levels in the UFA-UZ for September 2025 Conditions

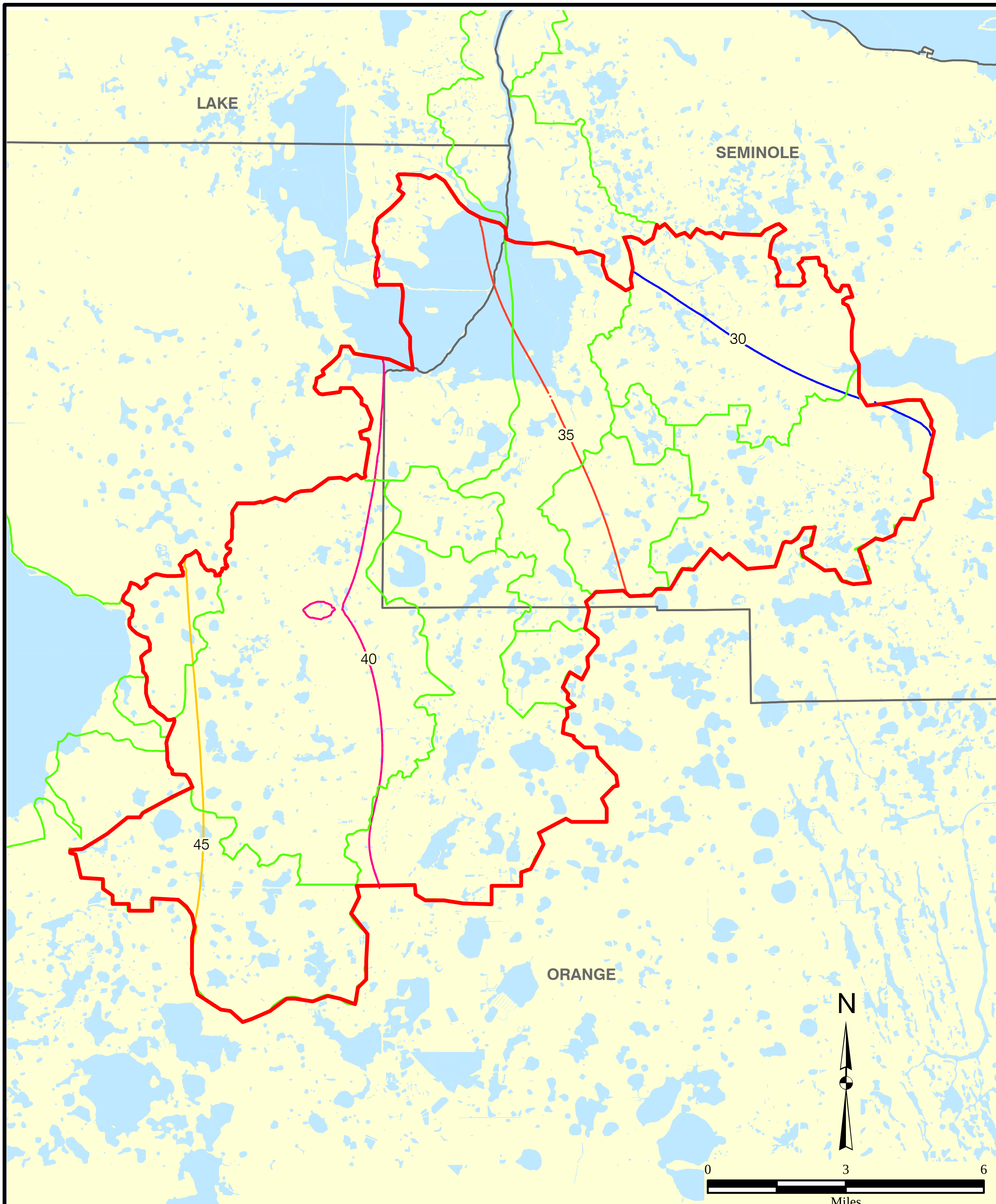

Source:
Filename: X:/SJR017/TO1/Maps/
Conceptual_model_report/WL_LFA_Mar2025.mxd
Project: SJR017-001-99
Revised: 12/27/04 TB

Legend

- Model Boundary
- Surface Water Basin
- County Boundary
- 50 Water Levels (ft)
- Surface Water Bodies and Wetlands

Figure 11.7
Simulated Water Levels in the LFA for May 2025 Conditions

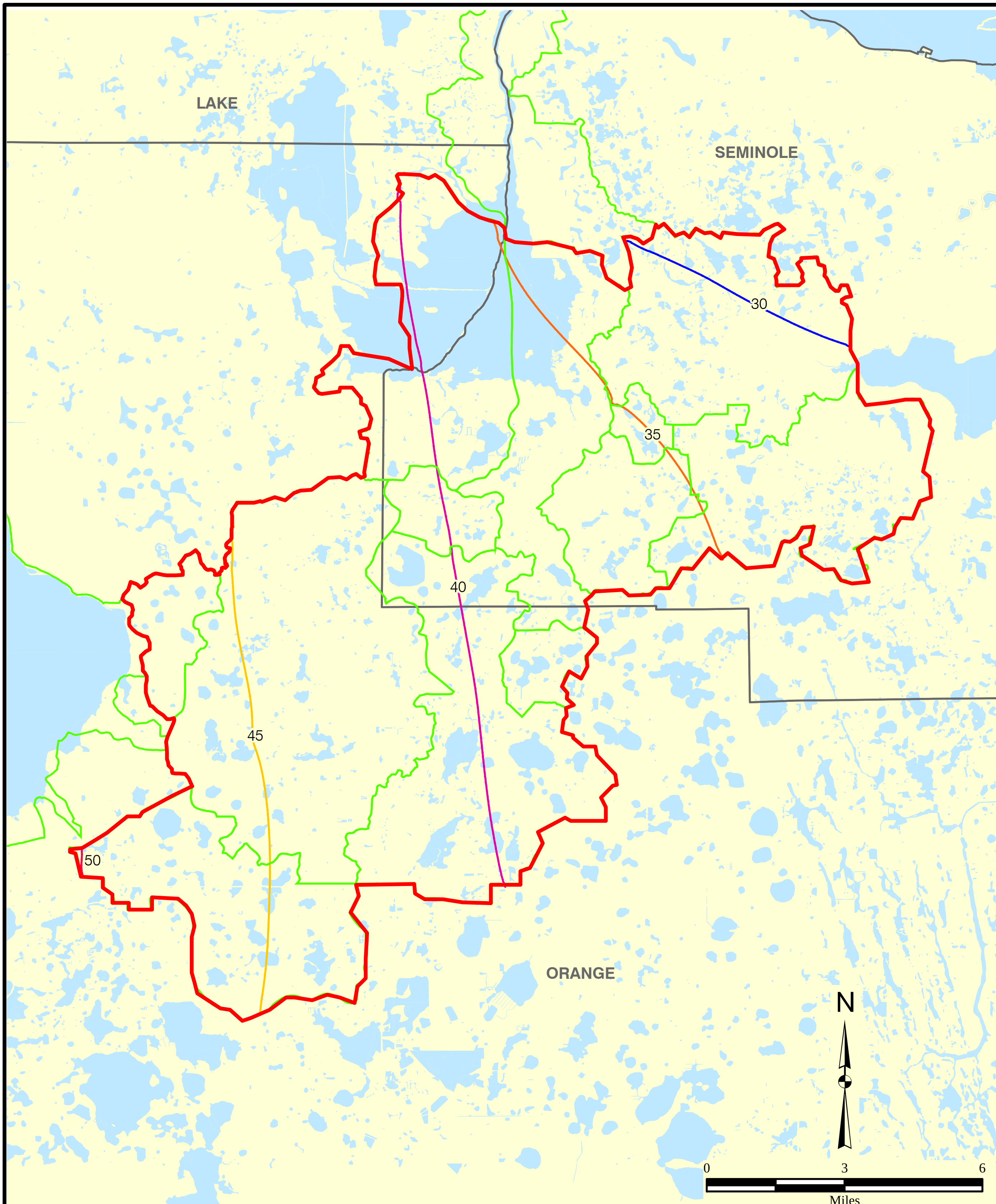

Source:
Filename: X:/SJR017/TO1/Maps/
Conceptual_model_report/WL_LFA_Sept2025.mxd
Project: SJR017-001-99
Revised: 12/27/04 TB

Legend

- Model Boundary
- Surface Water Basin
- County Boundary
- 50 Water Levels (ft)
- Surface Water Bodies and Wetlands

Figure 11.8
Simulated Water Levels in the LFA for September 2025 Conditions

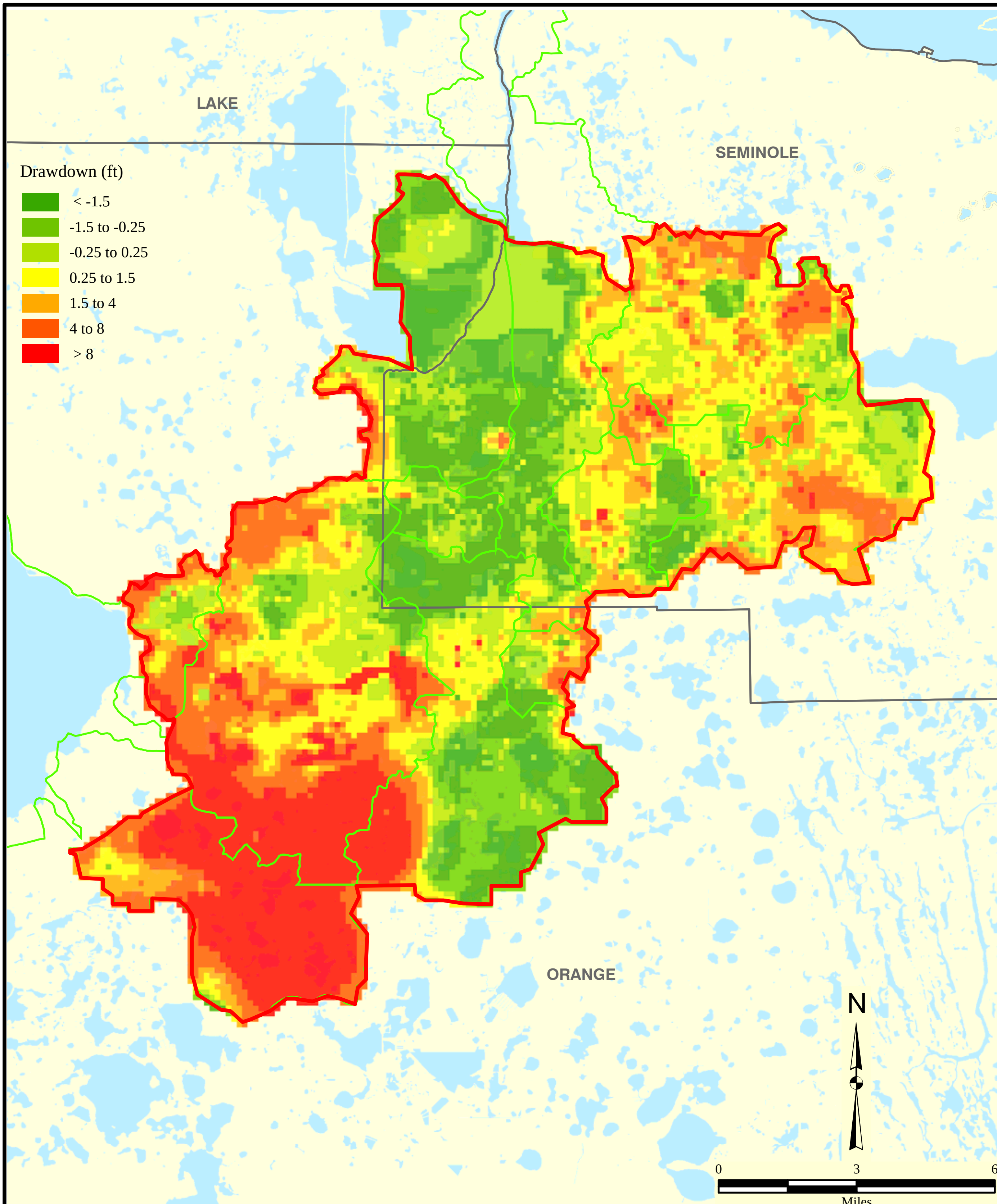

Source:
Filename: X:/SJR017/TO1/Maps/
Conceptual_model_report/Dd_SAS_May99-2025.mxd
Project: SJR017-001-99
Revised: 01/06/05 TB

Legend

- Model Boundary
- Surface Water Basin
- County Boundary
- Surface Water Bodies and Wetlands

Figure 11.9
Drawdown in the SAS from May 1999 to May 2025

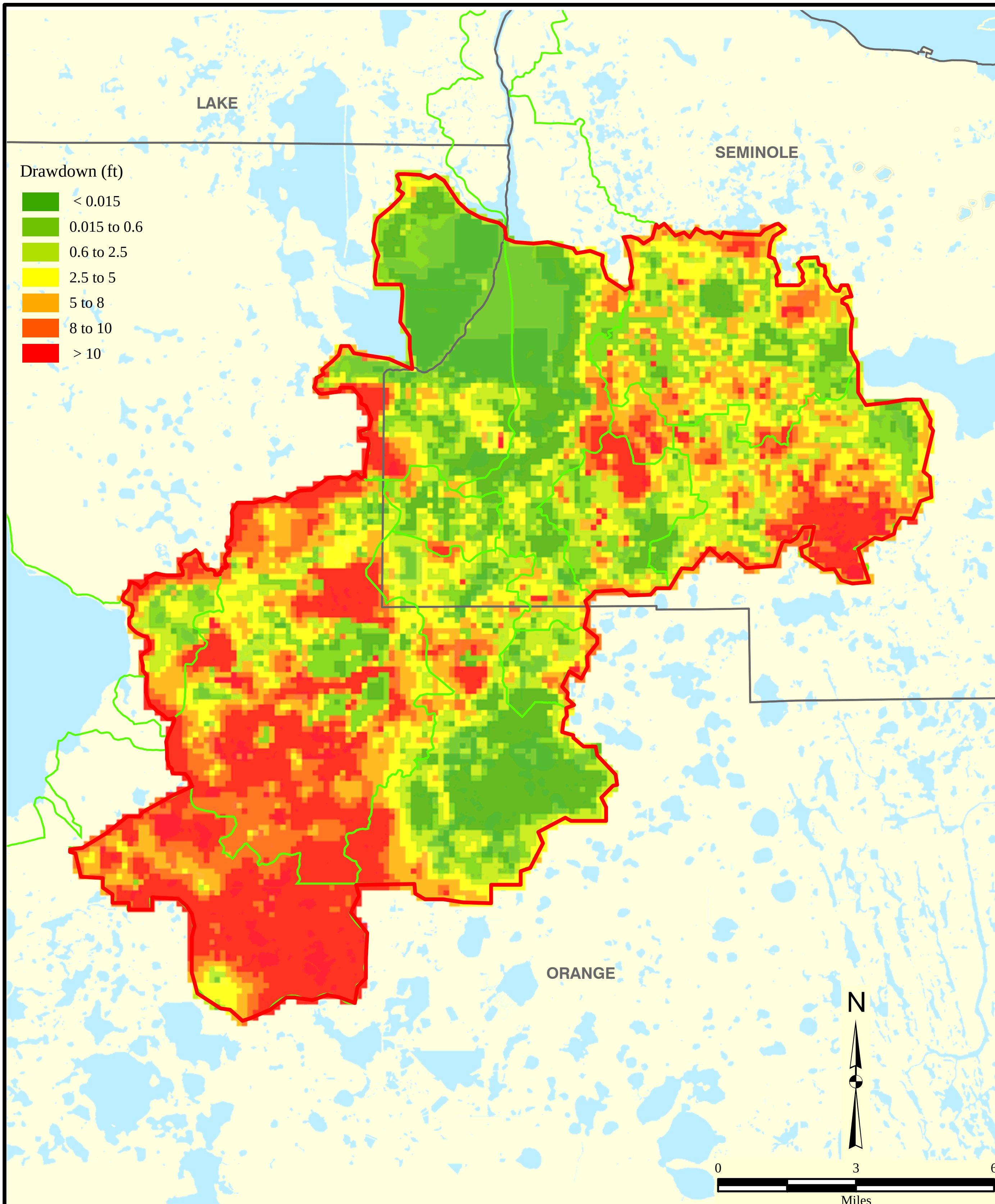

Source:
Filename: X:/SJR017/TO1/Maps/
Conceptual_model_report/Dd_SAS_Sept99-2025.mxd
Project: SJR017-001-99
Revised: 12/27/04 TB

Legend

Model Boundary
Surface Water Basin
County Boundary
Surface Water Bodies and Wetlands

Figure 11.10
Drawdown in the SAS from September 1999 to September 2025

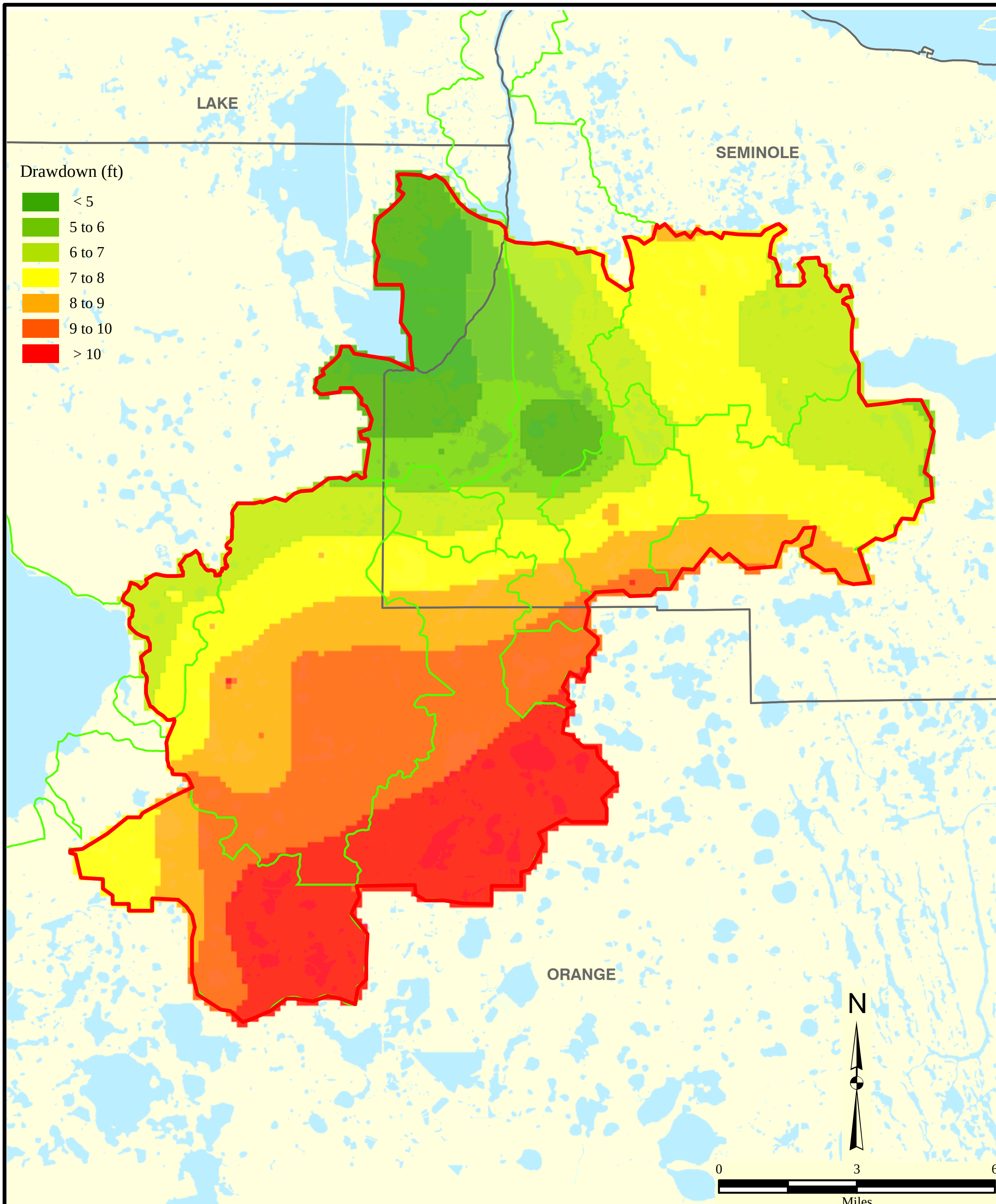

Source:
Filename: X:/SJR017/TO1/Maps/Conceptual_model_report/Dd_UFA_May99-2025.mxd
Project: SJR017-001-99
Revised: 12/27/04 TB

Legend

- Model Boundary
- Surface Water Basin
- County Boundary
- Surface Water Bodies and Wetlands

Figure 11.11
Drawdown in the UFA-UZ from May 1999 to May 2025

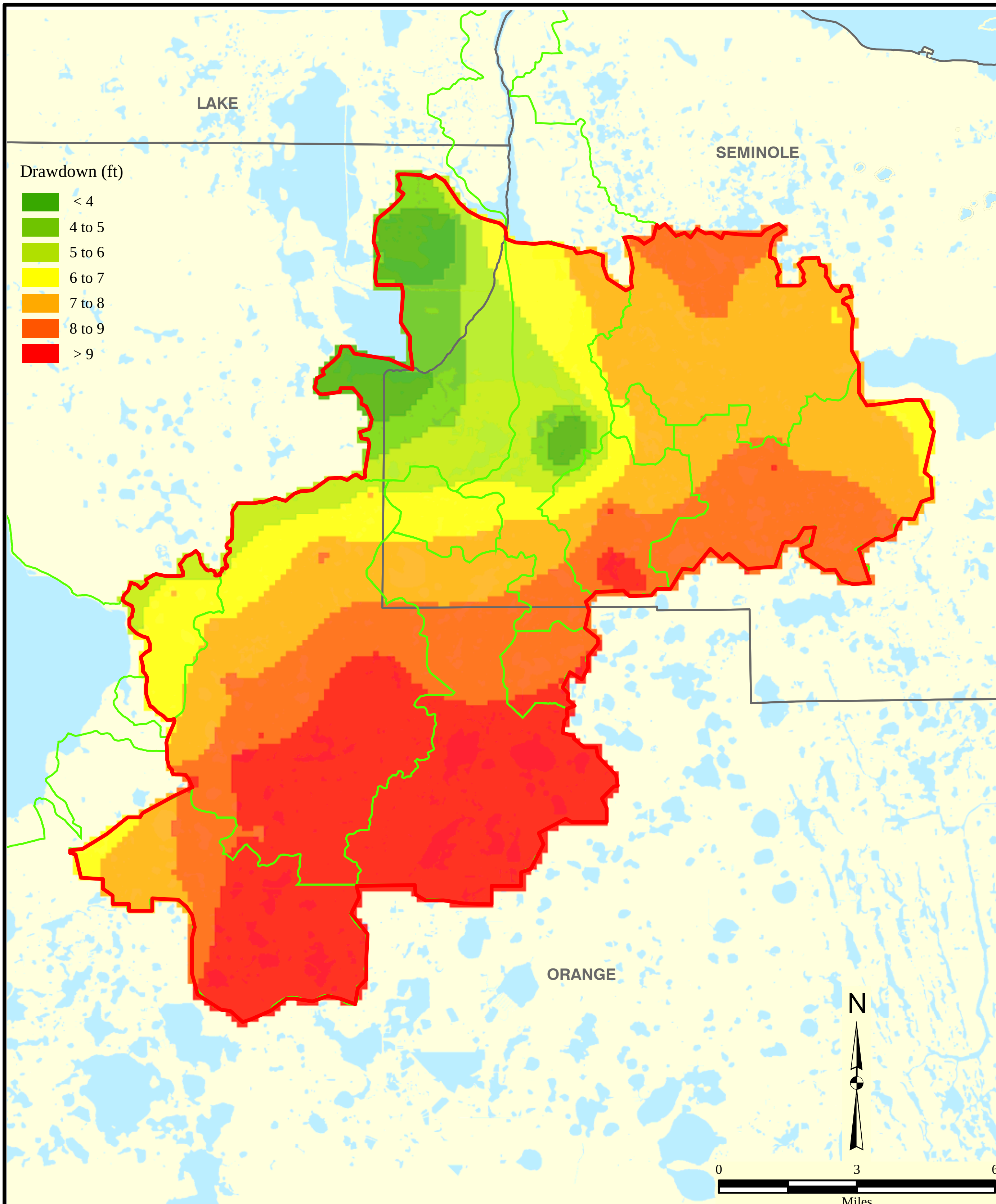

Source:
Filename: X:/SJR017/TO1/Maps/
Conceptual_model_report/Dd_UFA_Sept99-2025.mxd
Project: SJR017-001-99
Revised: 12/27/04 TB

Legend

Model Boundary
Surface Water Basin
County Boundary
Surface Water Bodies and Wetlands

Figure 11.12
Drawdown in the UFA-UZ from September 1999 to September 2025

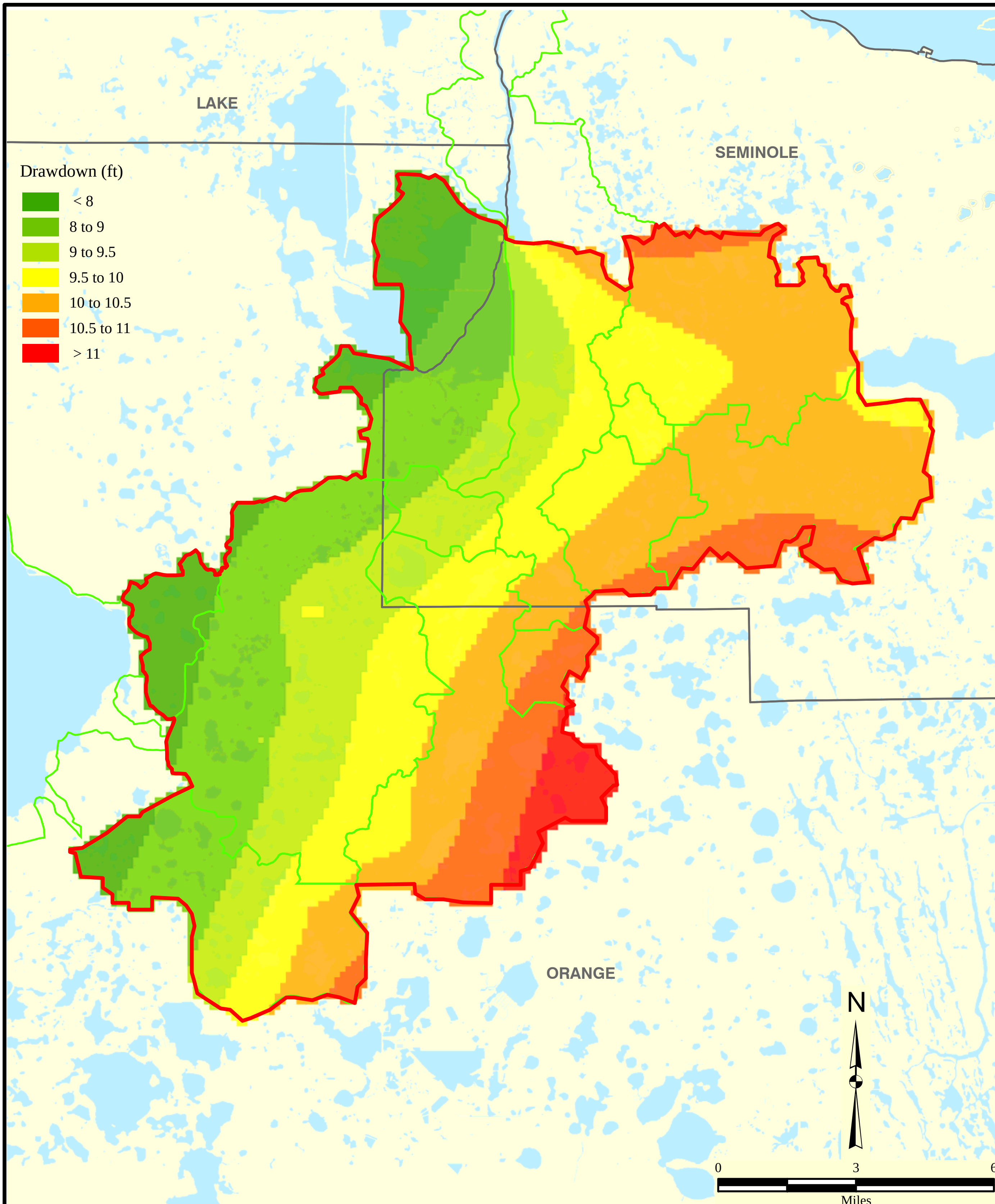

Source:
Filename: X:/SJR017/TO1/Maps/
Conceptual_model_report/Dd_LFA_May99-2025.mxd
Project: SJR017-001-99
Revised: 12/27/04 TB

Legend

- Model Boundary
- Surface Water Basin
- County Boundary
- Surface Water Bodies and Wetlands

Figure 11.13
Drawdown in the LFA from May 1999 to May 2025

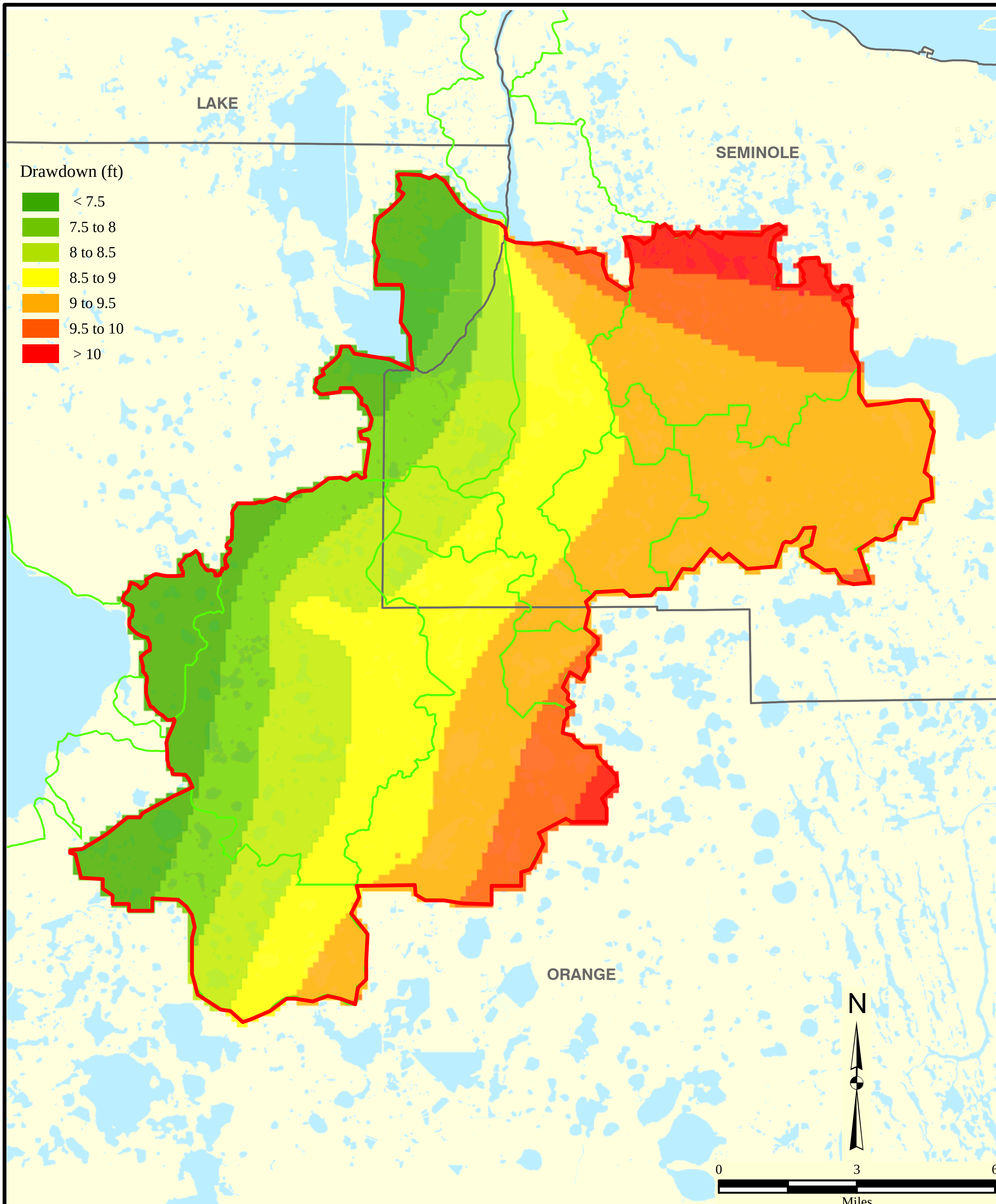

Source:
Filename: X:/SJR017/TO1/Maps/
Conceptual_model_report/Dd_LFA_Sept99-2025.mxd
Project: SJR017-001-99
Revised: 12/27/04 TB

Legend

- Model Boundary
- Surface Water Basin
- County Boundary
- Surface Water Bodies and Wetlands

Figure 11.14 Drawdown in the LFA from September 1999 to September 2025

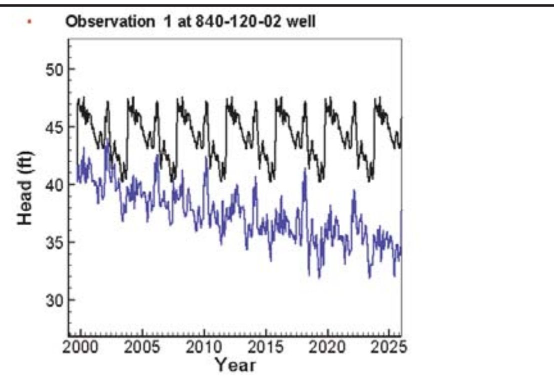

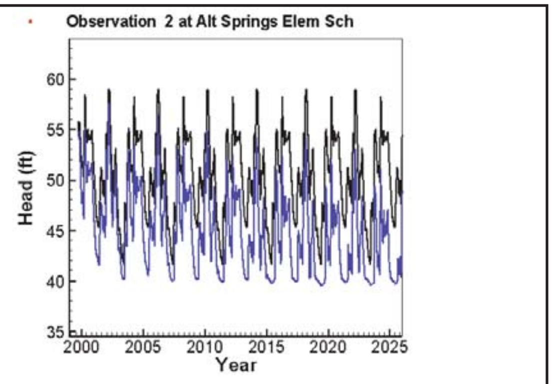

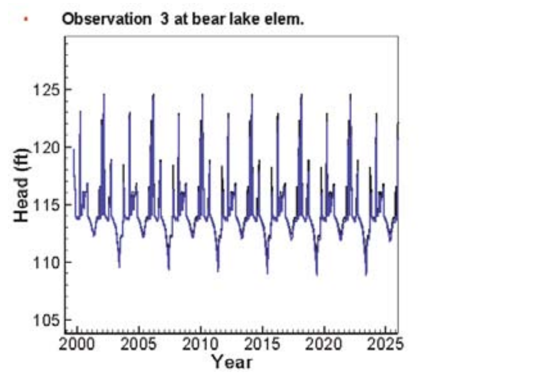

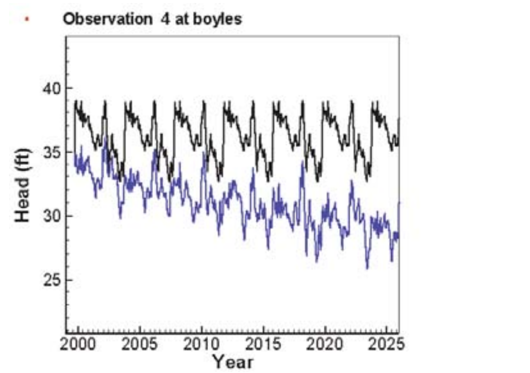

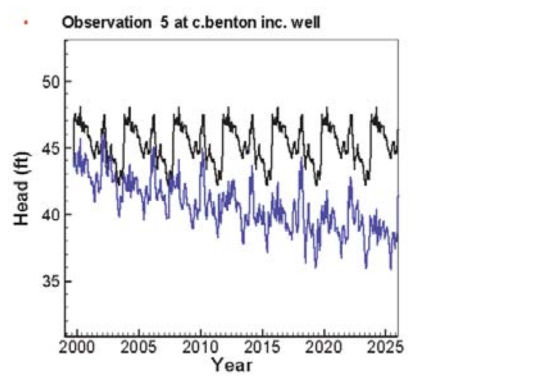

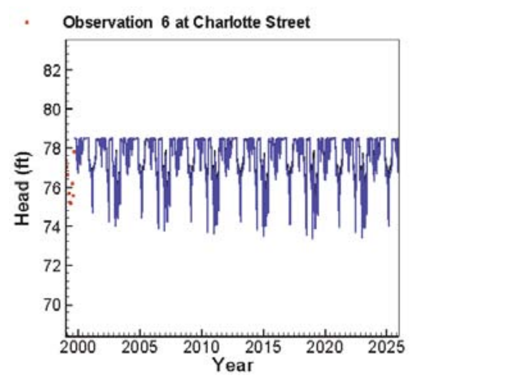

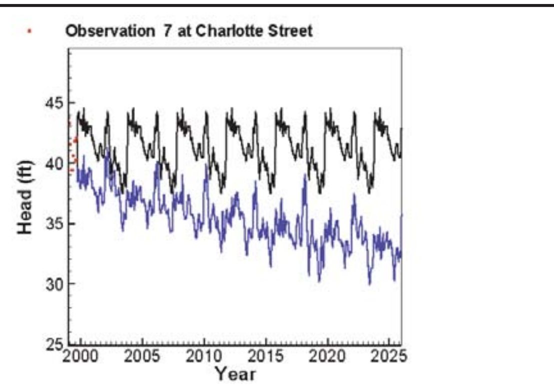

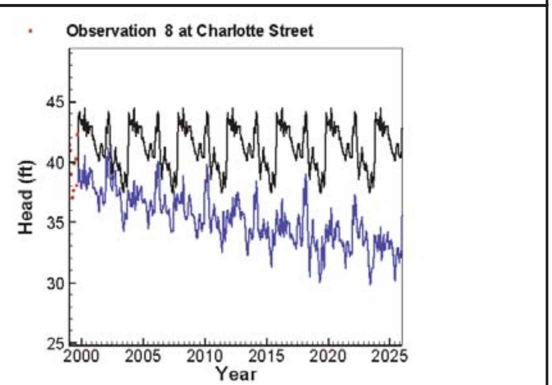

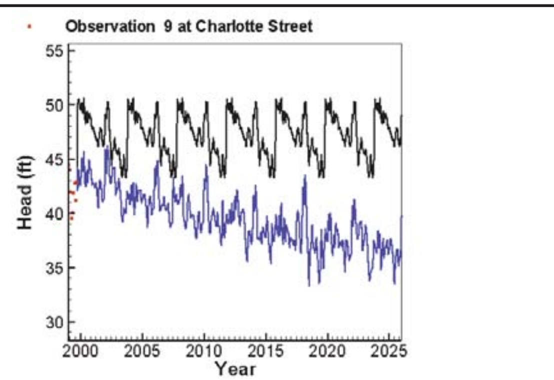

Figure 11.15 Transient Hydrographs at Observation Locations for Predictive Simulation of 1999 through 2025 Conditions. (Page 1 of 11)

Observed Data
Predictive Simulation with Recycled Data
Predictive Simulation with Projected Data

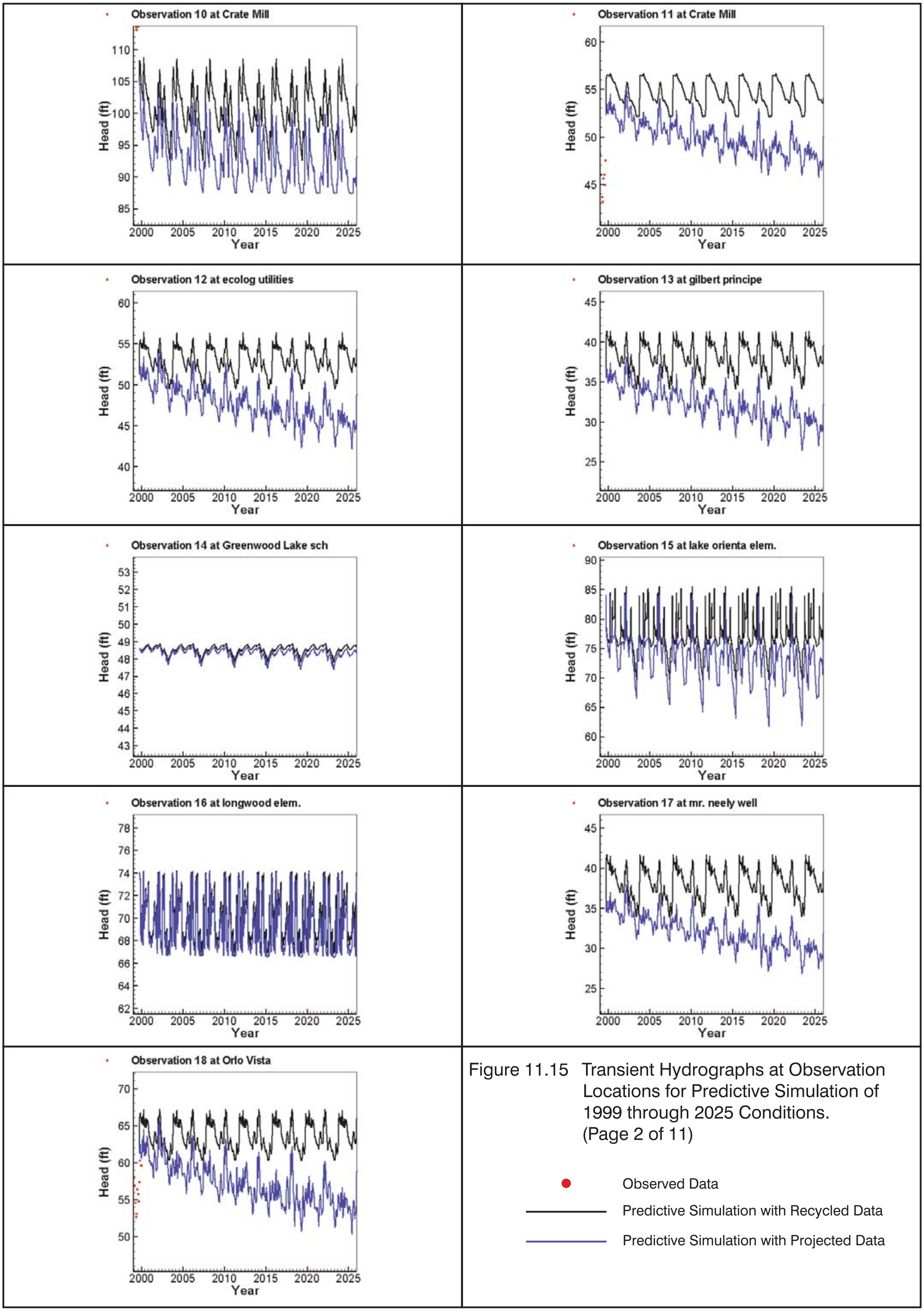

Figure 11.15 Transient Hydrographs at Observation Locations for Predictive Simulation of 1999 through 2025 Conditions. (Page 2 of 11)

X:\SJR017\TO1\Maps\Conceptual_Model_Report\predictive.cdr

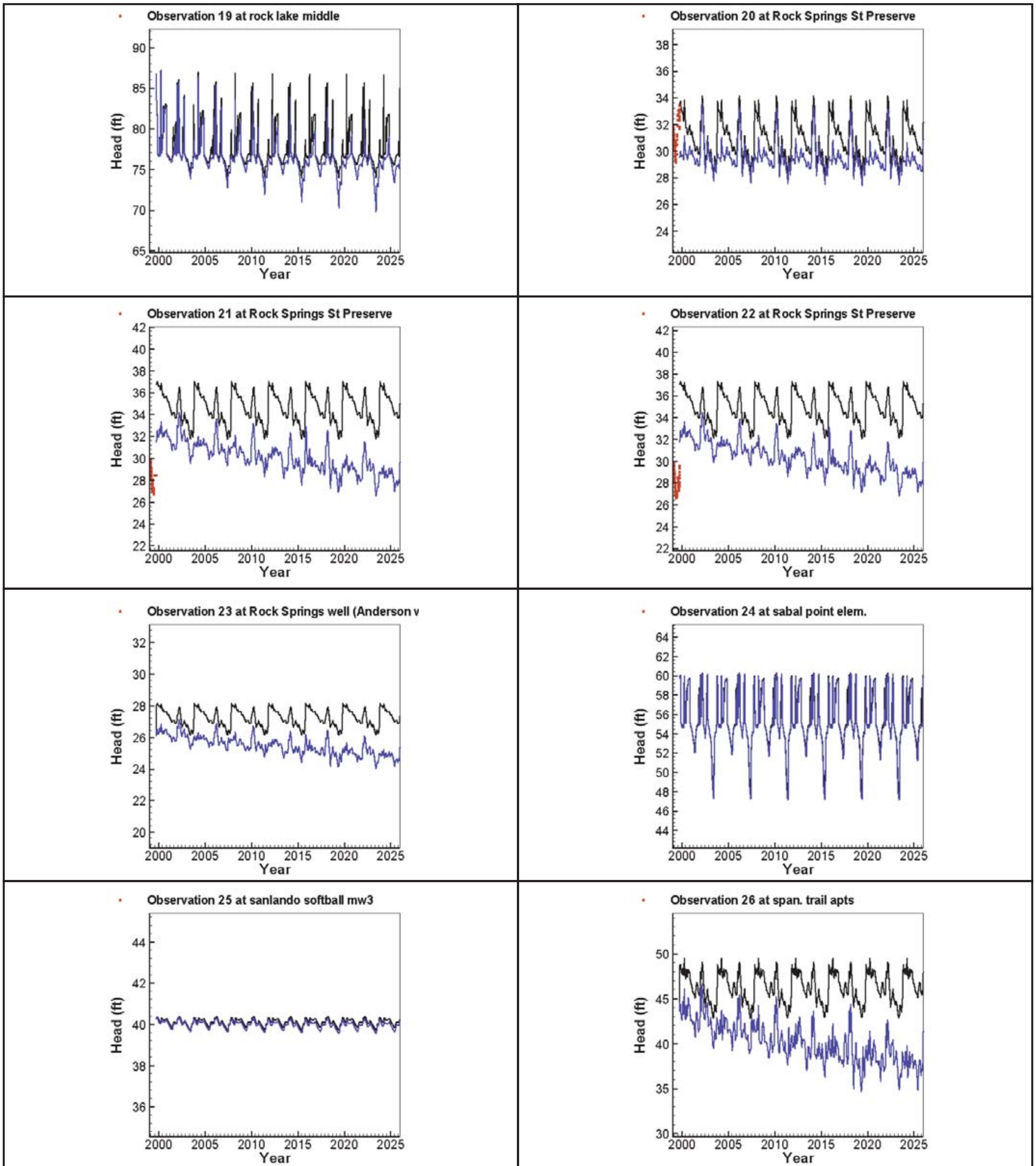

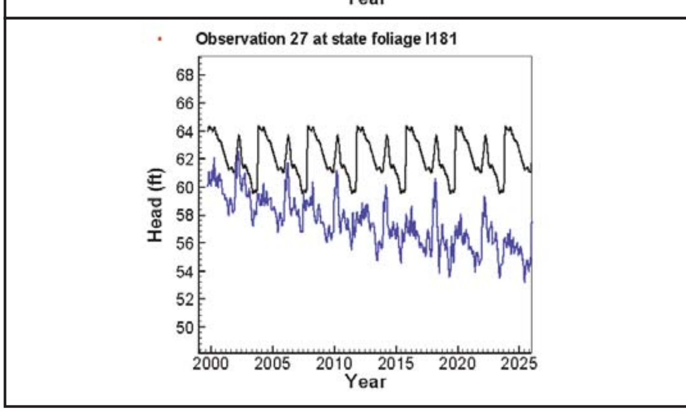

Figure 11.15 Transient Hydrographs at Observation Locations for Predictive Simulation of 1999 through 2025 Conditions. (Page 3 of 11)

Observed Data

Predictive Simulation with Recycled Data

Predictive Simulation with Projected Data

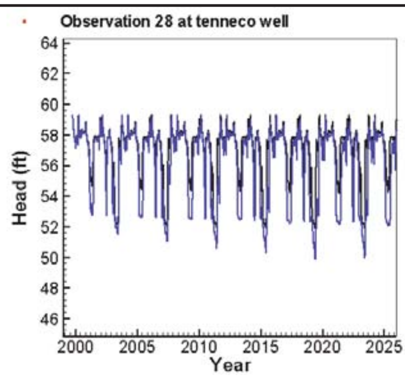

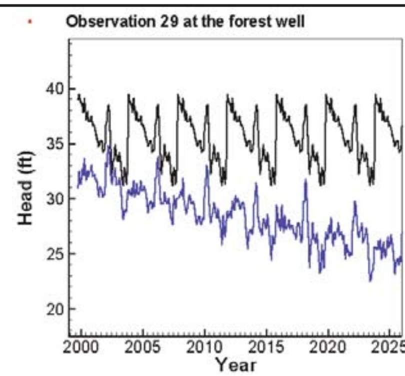

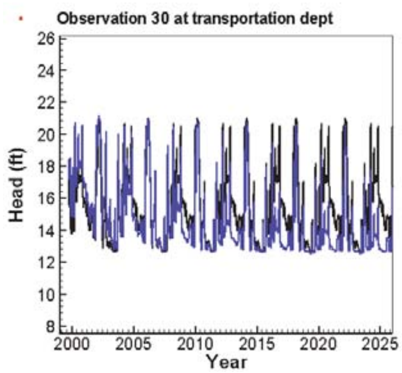

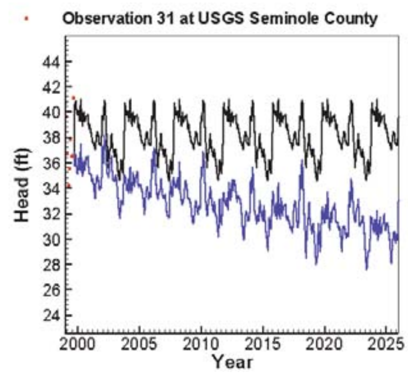

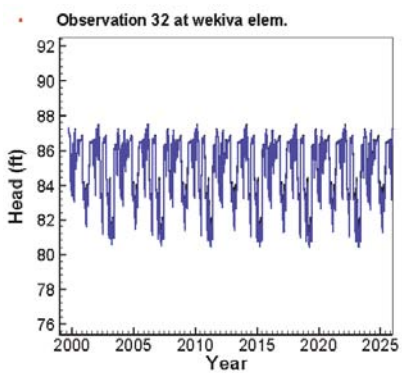

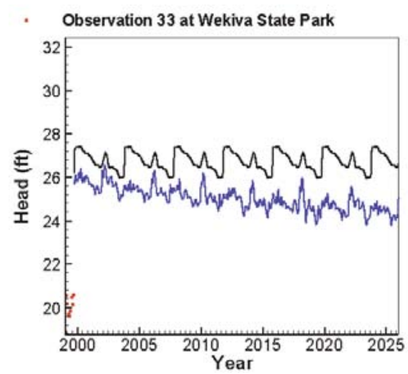

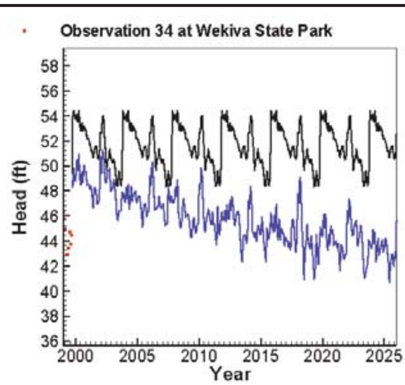

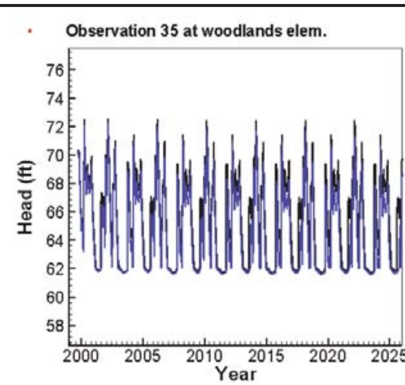

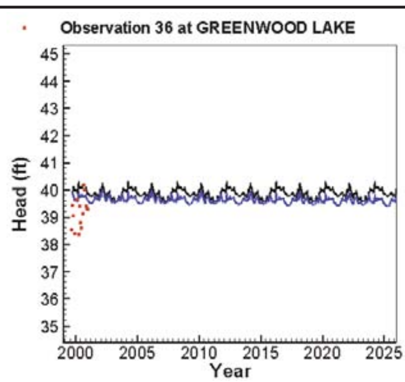

Figure 11.15 Transient Hydrographs at Observation Locations for Predictive Simulation of 1999 through 2025 Conditions. (Page 4 of 11)

● Observed Data

Predictive Simulation with Recycled Data

Predictive Simulation with Projected Data

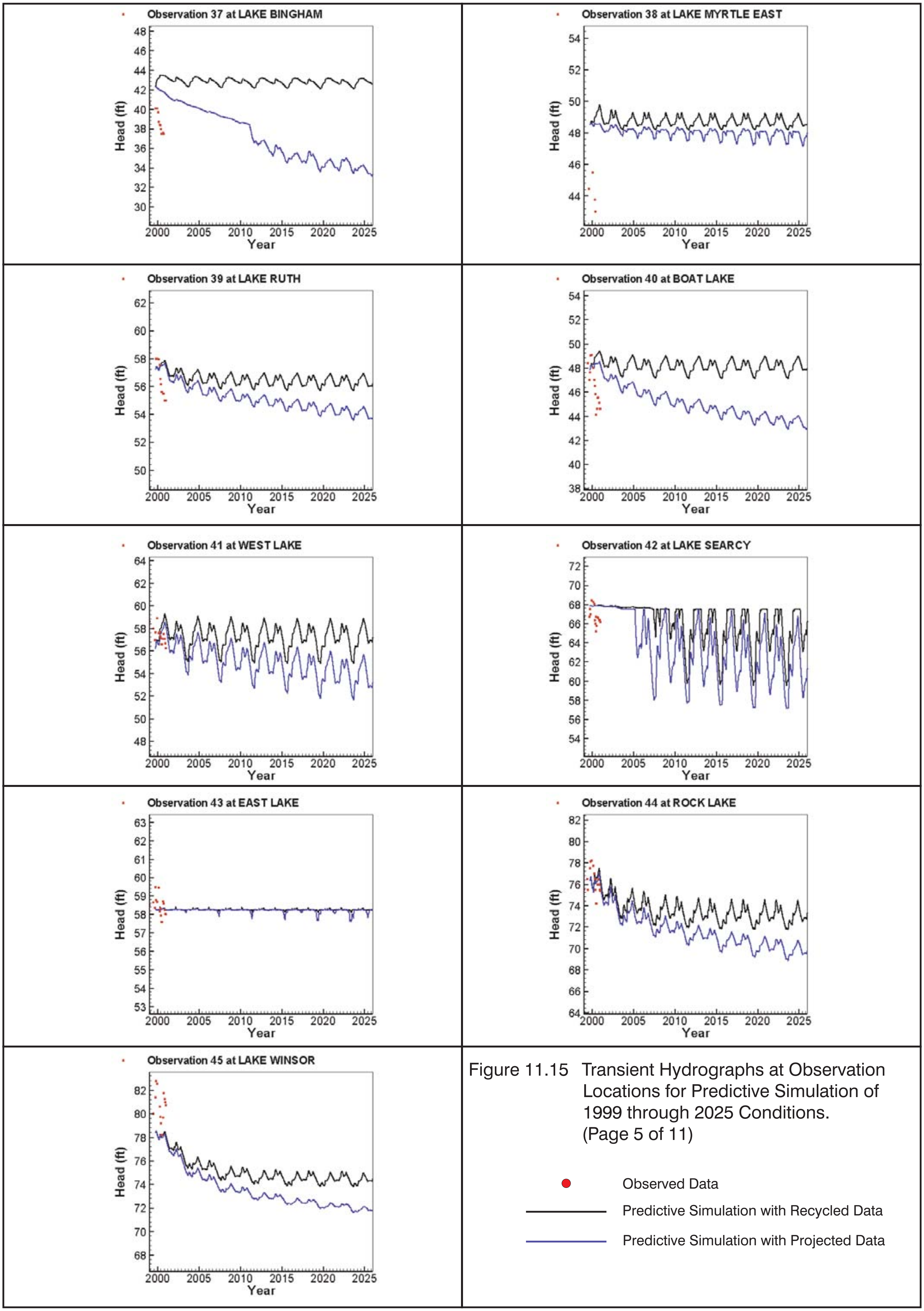

Figure 11.15 Transient Hydrographs at Observation Locations for Predictive Simulation of 1999 through 2025 Conditions. (Page 5 of 11)

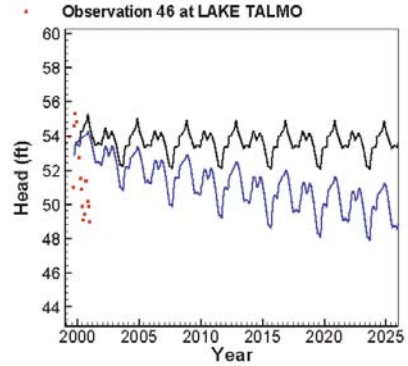

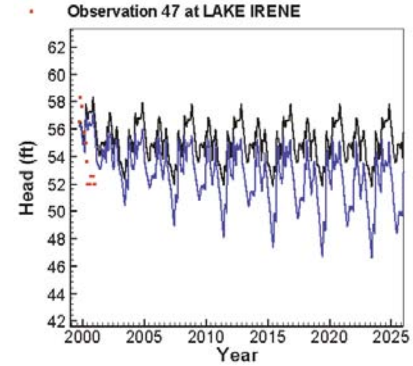

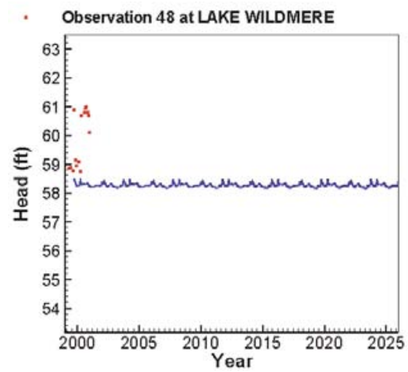

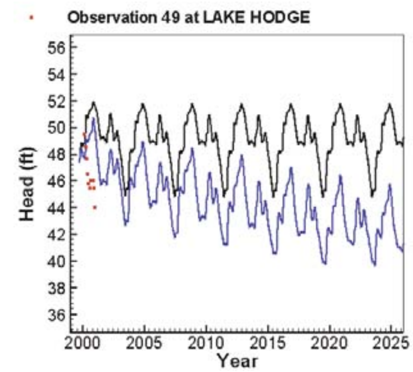

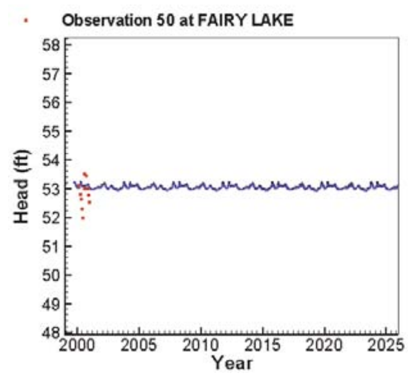

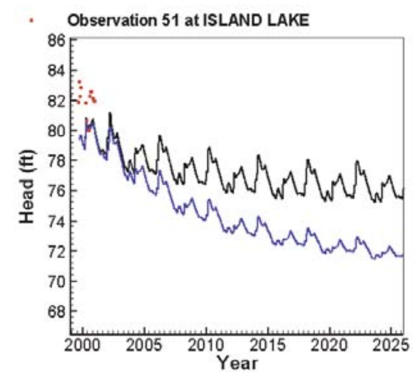

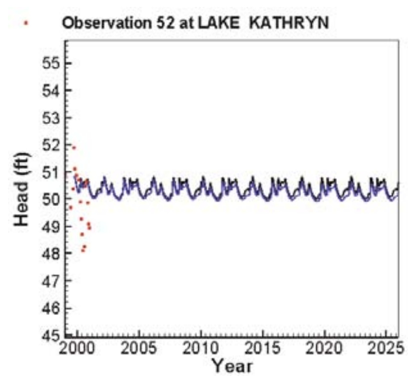

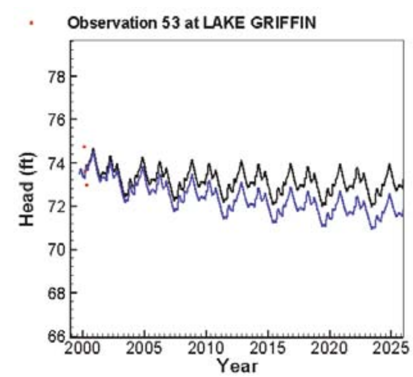

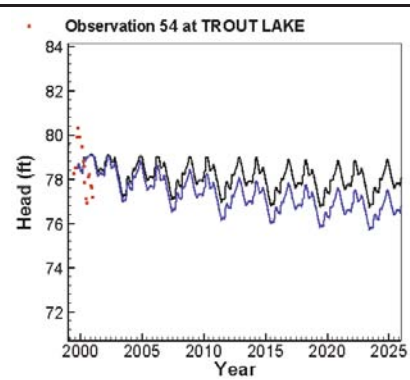

Figure 11.15 Transient Hydrographs at Observation Locations for Predictive Simulation of 1999 through 2025 Conditions. (Page 6 of 11)

Observed Data

Predictive Simulation with Recycled Data

Predictive Simulation with Projected Data

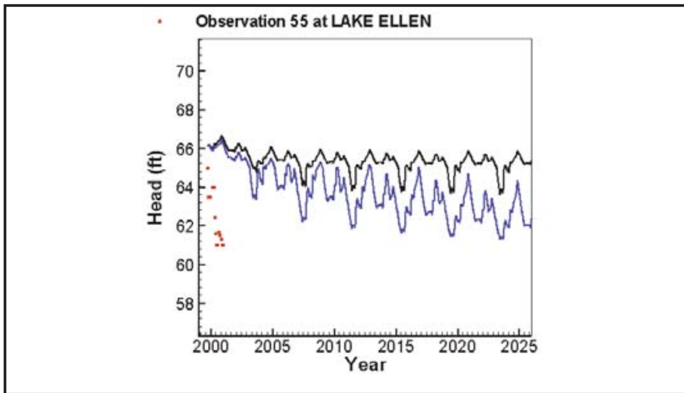

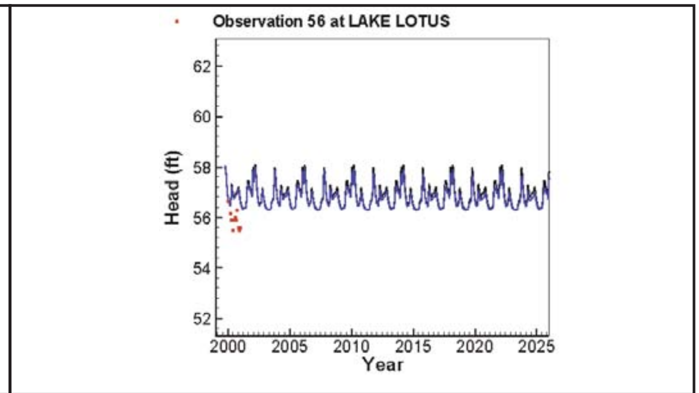

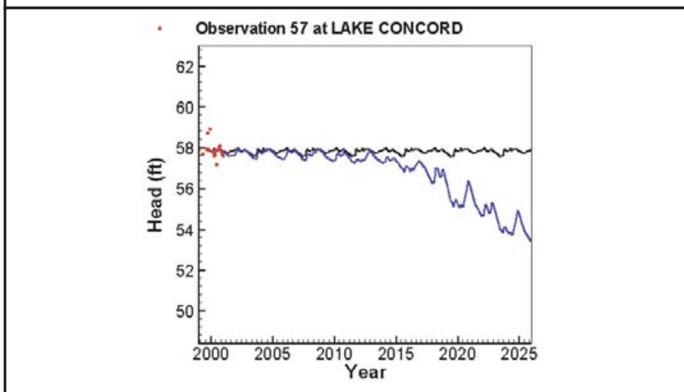

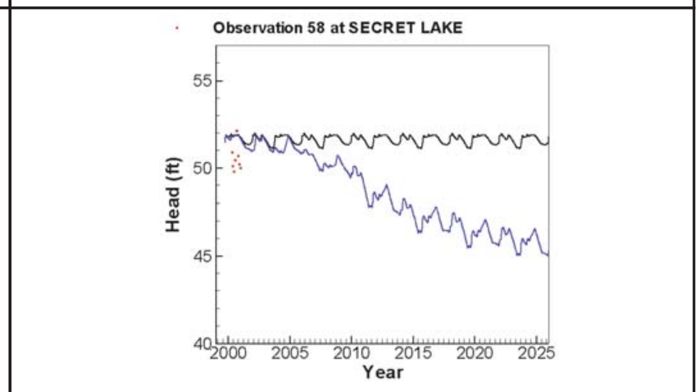

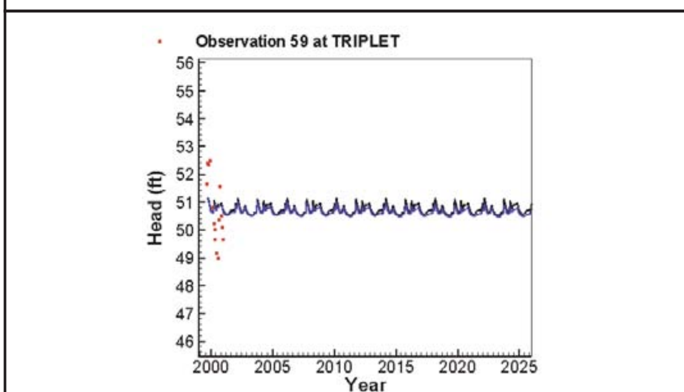

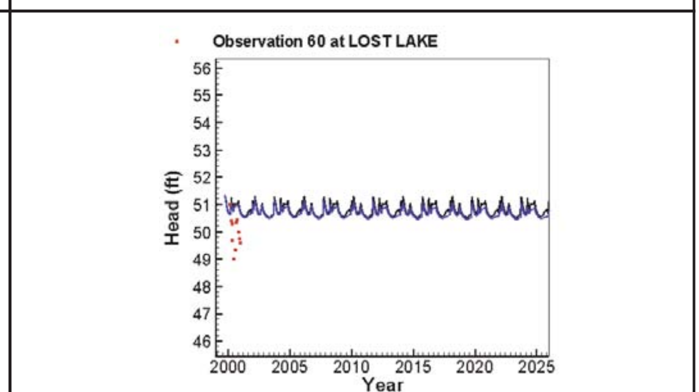

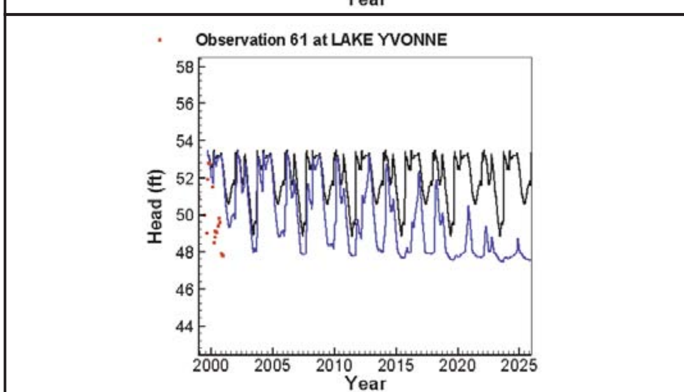

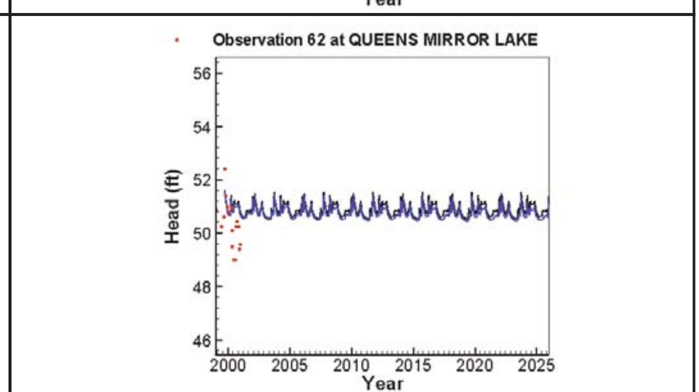

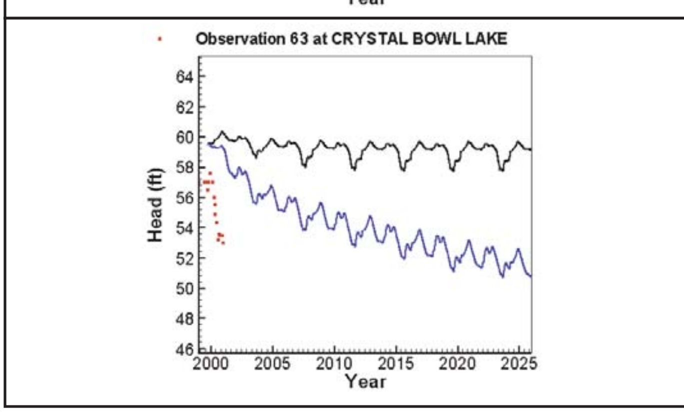

Figure 11.15 Transient Hydrographs at Observation Locations for Predictive Simulation of 1999 through 2025 Conditions. (Page 7 of 11)

- Observed Data
- Predictive Simulation with Recycled Data
- Predictive Simulation with Projected Data

X:\SJR017\TO1\Maps\Conceptual_Model_Report\predictive.cdr

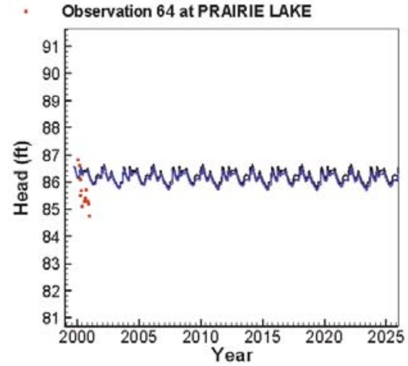

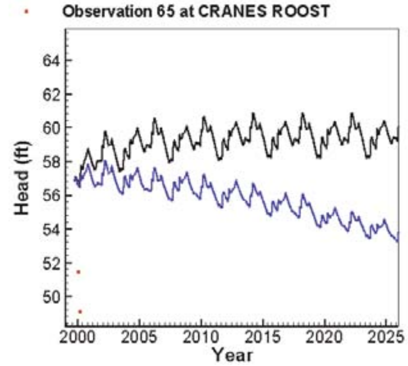

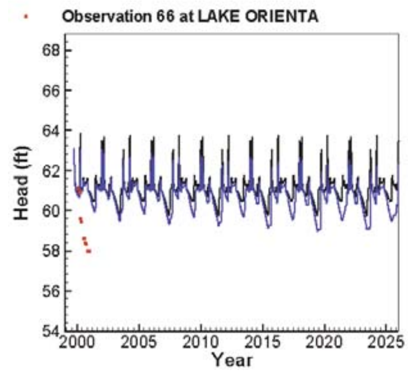

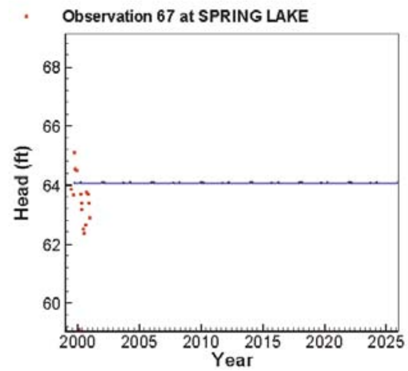

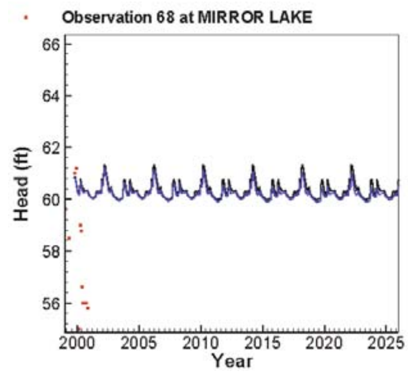

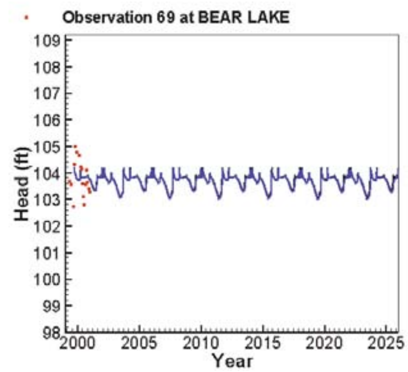

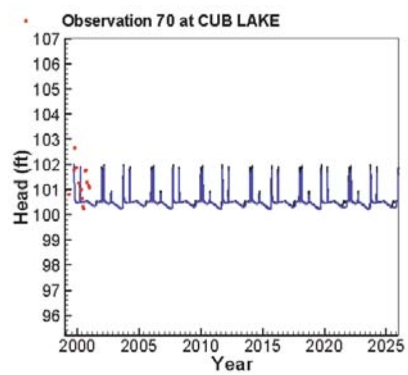

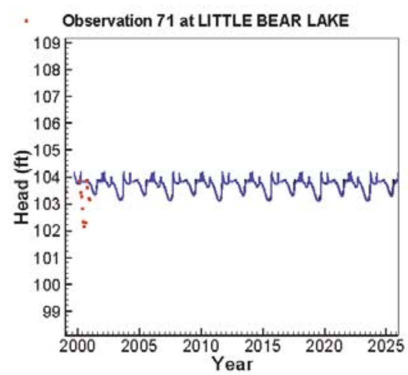

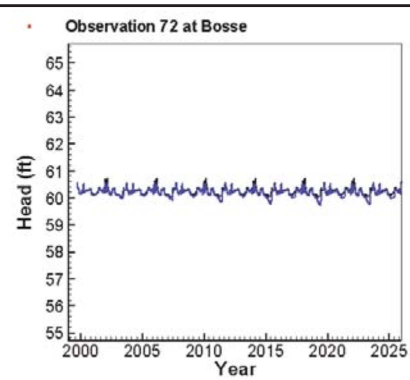

Figure 11.15 Transient Hydrographs at Observation Locations for Predictive Simulation of 1999 through 2025 Conditions. (Page 8 of 11)

- Observed Data
- Predictive Simulation with Recycled Data
- Predictive Simulation with Projected Data

X:\SJR017\TO1\Maps\Conceptual_Model_Report\predictive.cdr

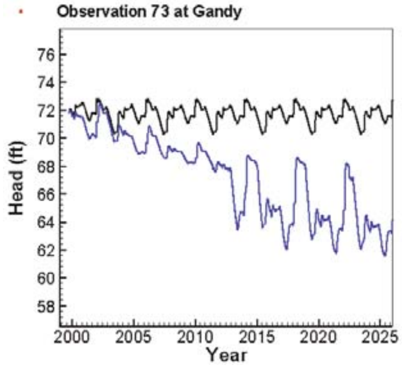

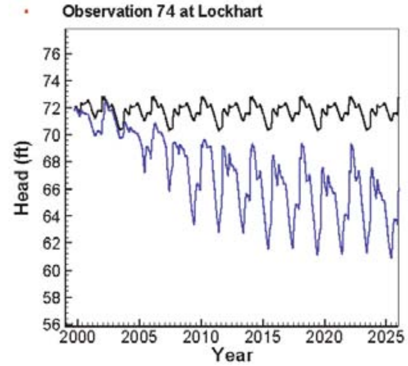

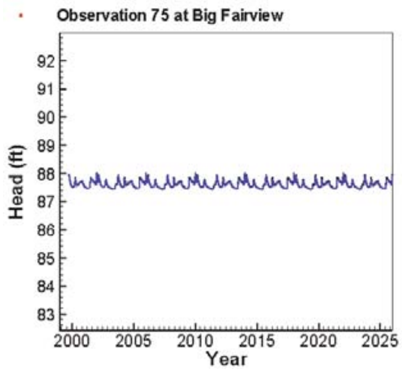

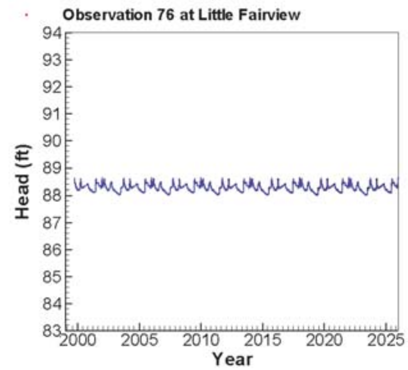

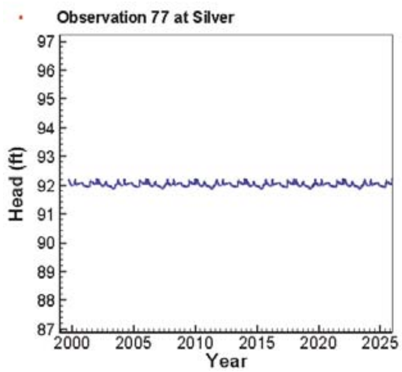

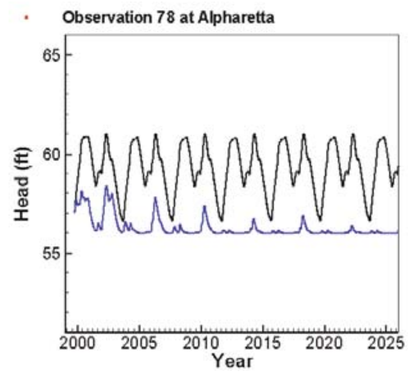

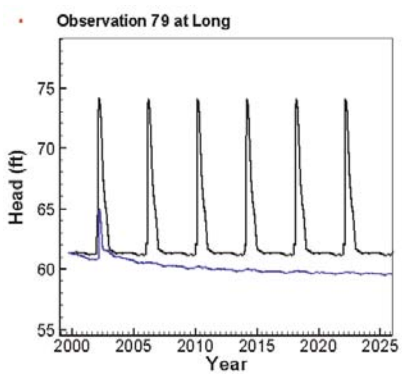

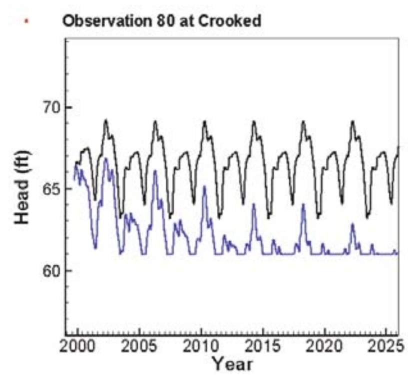

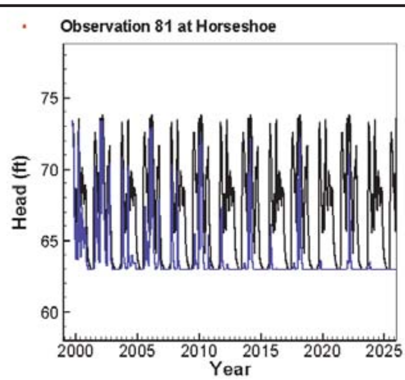

Figure 11.15 Transient Hydrographs at Observation Locations for Predictive Simulation of 1999 through 2025 Conditions. (Page 9 of 11)

Observed Data

Predictive Simulation with Recycled Data

Predictive Simulation with Projected Data

X:\SJR017\TO1\Maps\Conceptual_Model_Report\predictive.cdr

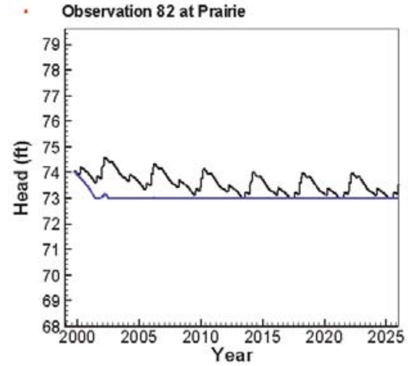

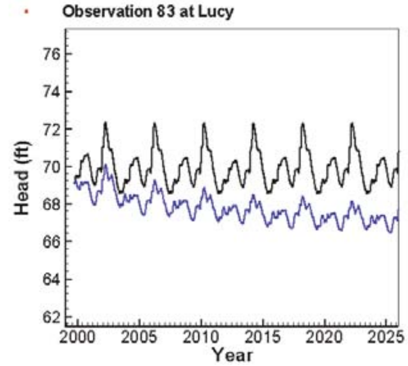

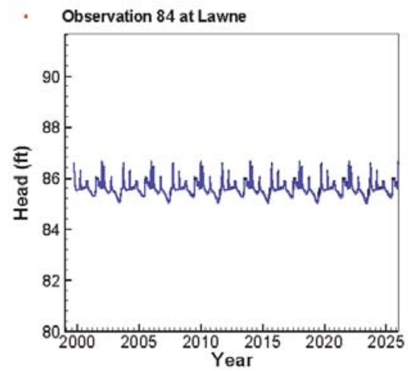

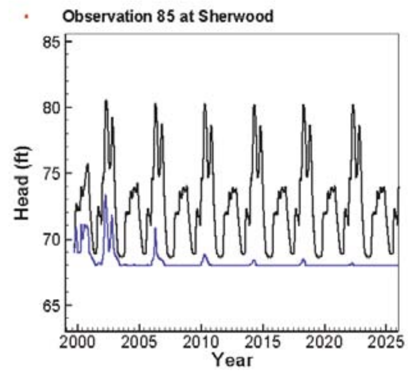

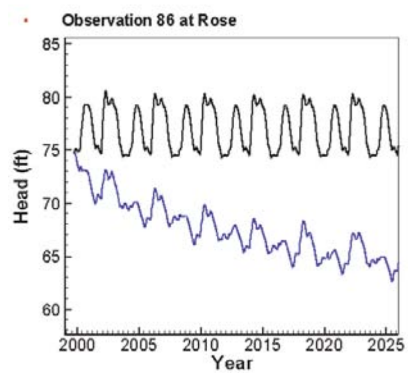

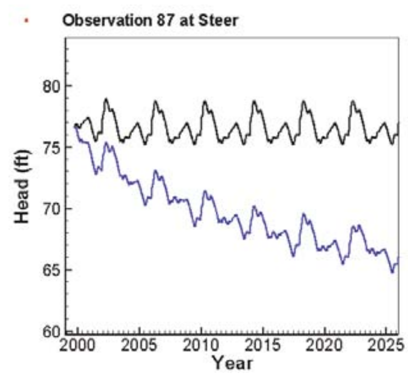

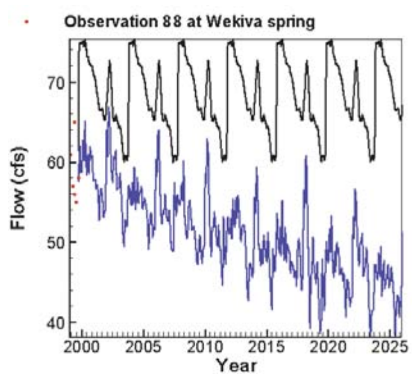

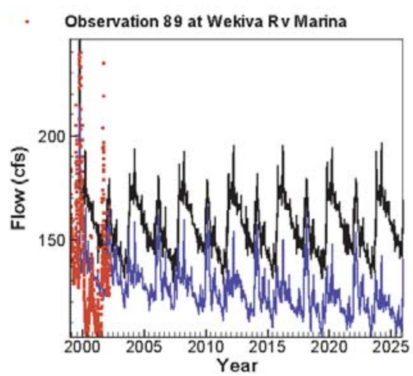

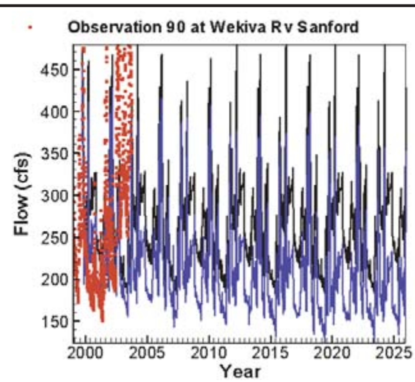

Figure 11.15 Transient Hydrographs at Observation Locations for Predictive Simulation of 1999 through 2025 Conditions. (Page 10 of 11)

Observed Data
Predictive Simulation with Recycled Data
Predictive Simulation with Projected Data

X:\SJR017\TO1\Maps\Conceptual_Model_Report\predictive.cdr

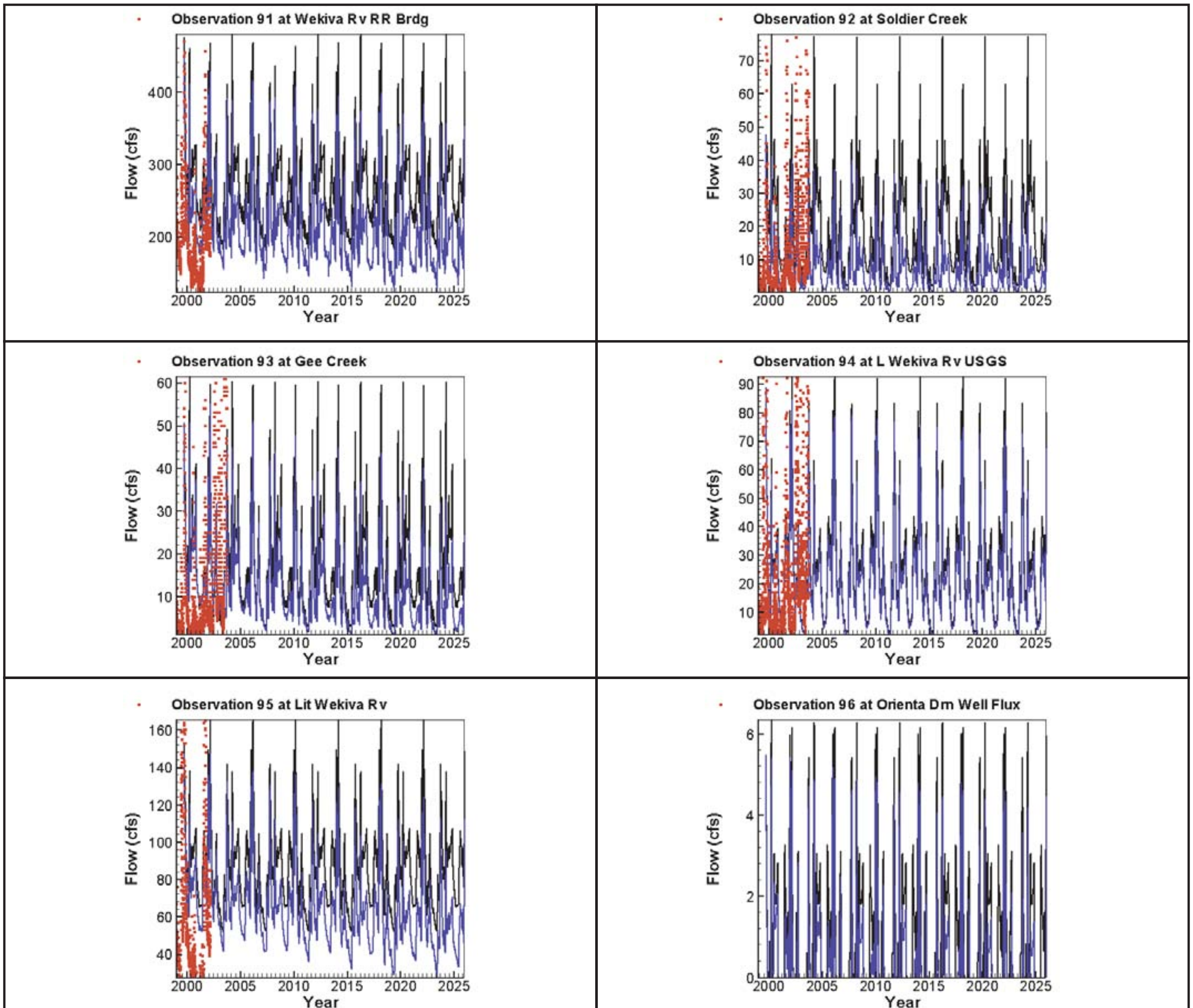

Figure 11.15 Transient Hydrographs at Observation Locations for Predictive Simulation of 1999 through 2025 Conditions. (Page 11 of 11)

Observed Data
Predictive Simulation with Recycled Data
Predictive Simulation with Projected Data

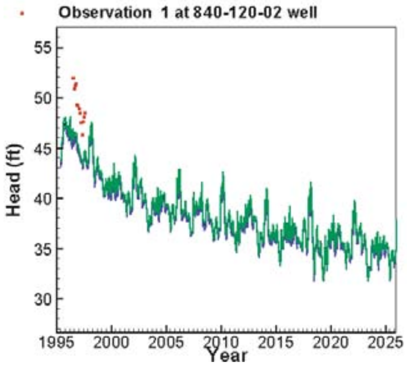

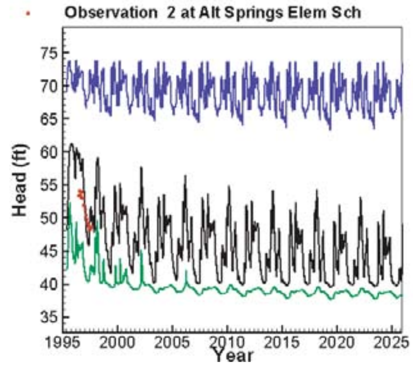

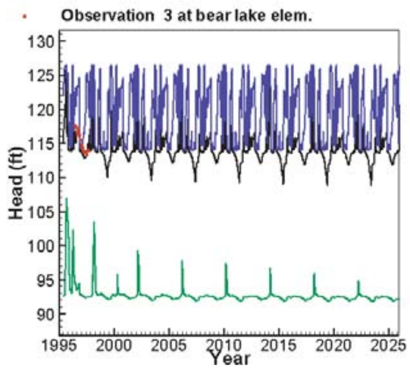

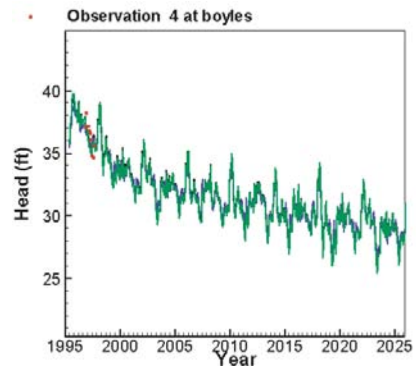

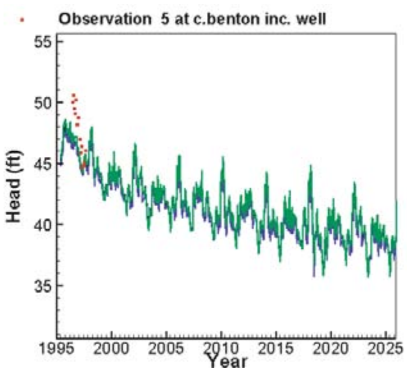

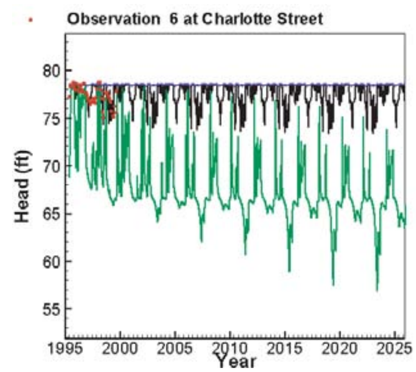

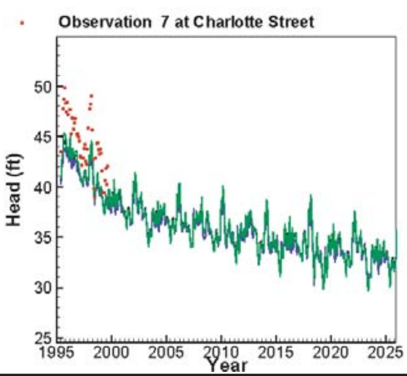

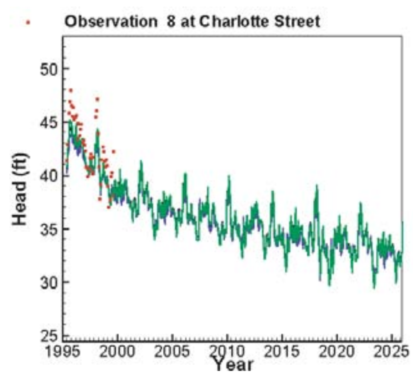

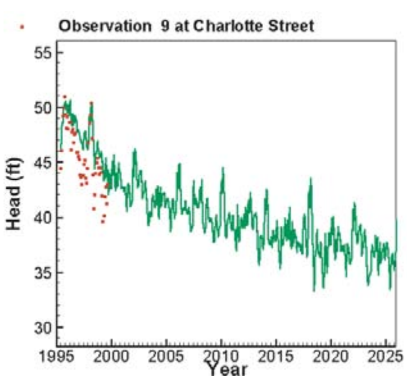

Figure 12.1 Transient Hydrographs at Observation Locations for Predictive Sensitivities of 1995 through 2025 Conditions. (Page 1 of 11)

Observed Data

Base Case Simulation

Simulation with Low ICU Leakance and Low Evapotranspiration

Simulation with High ICU Leakance and High Evapotranspiration

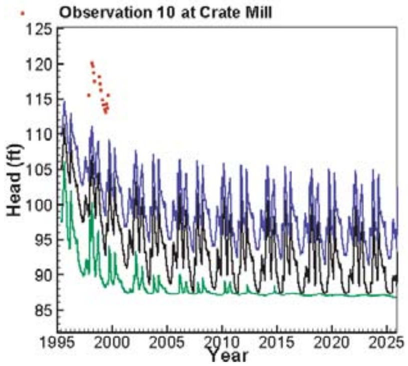

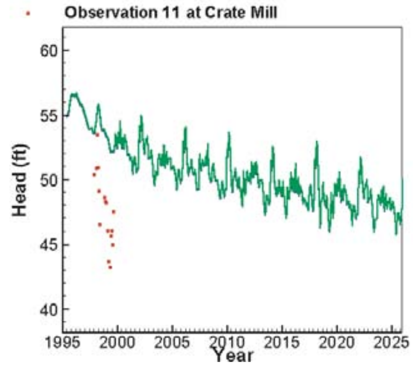

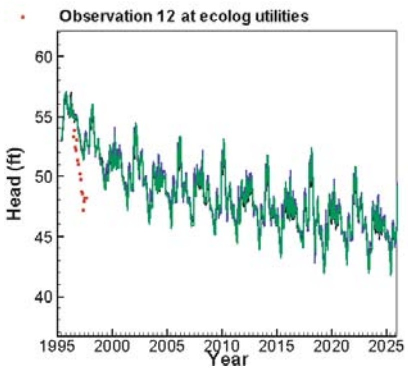

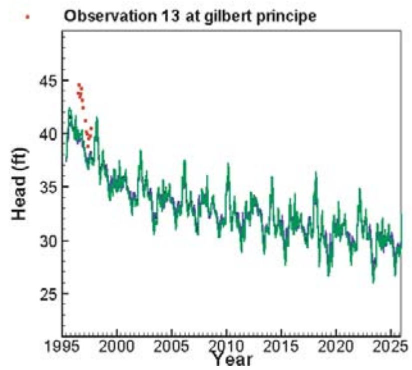

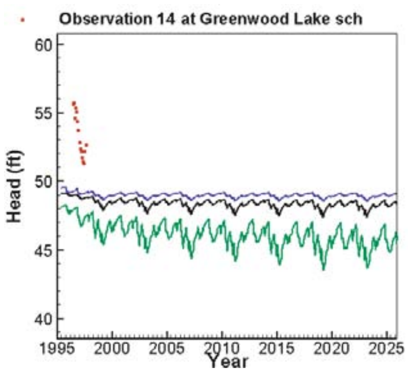

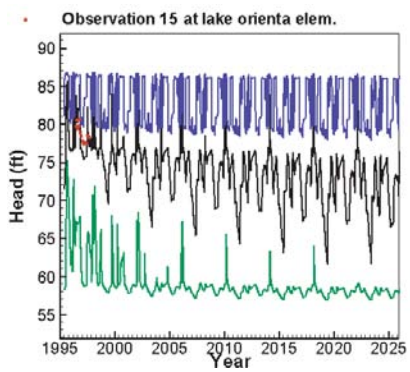

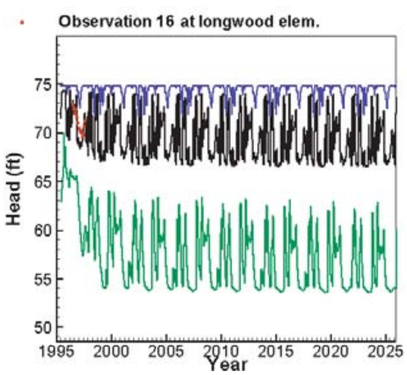

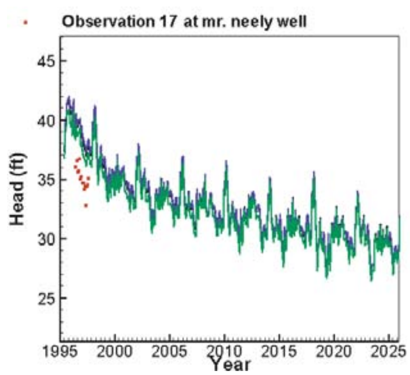

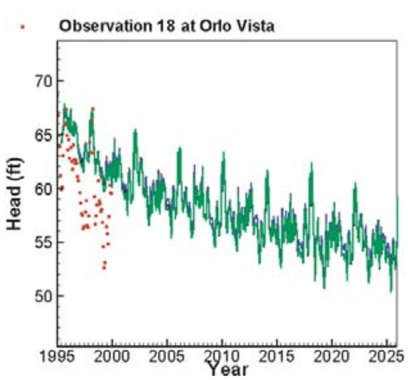

Figure 12.1 Transient Hydrographs at Observation Locations for Predictive Sensitivities of 1995 through 2025 Conditions. (Page 2 of 11)

Observed Data
Base Case Simulation
Simulation with Low ICU Leakance and Low Evapotranspiration
Simulation with High ICU Leakance and High Evapotranspiration

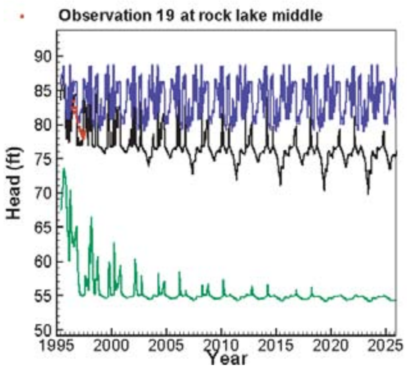

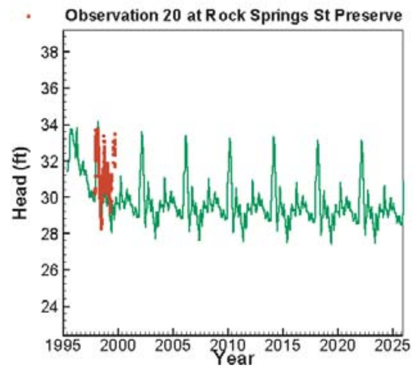

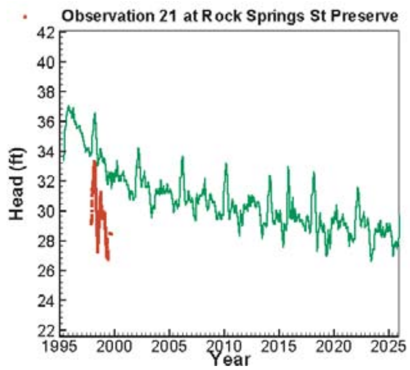

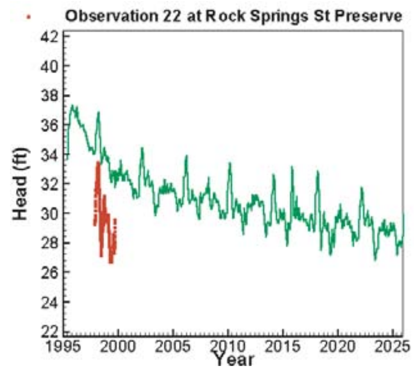

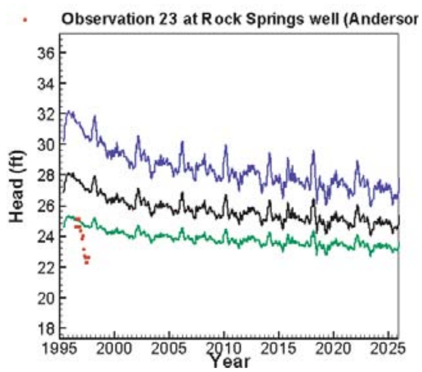

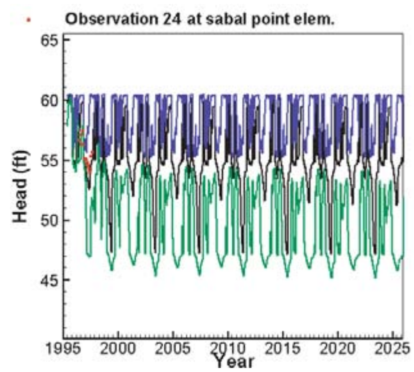

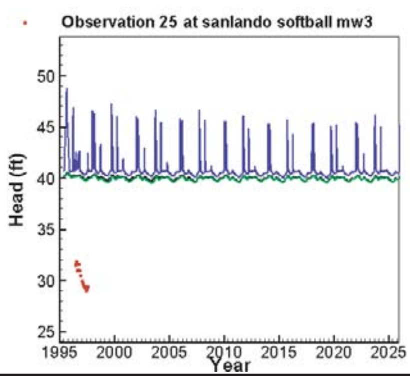

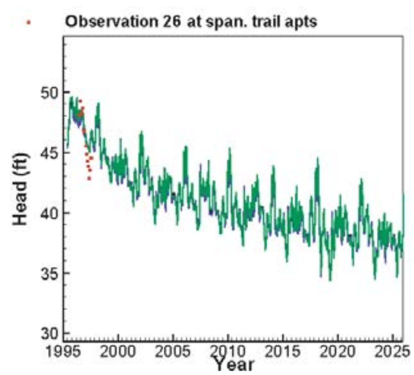

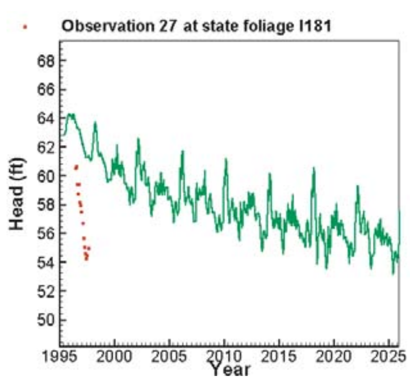

Figure 12.1 Transient Hydrographs at Observation Locations for Predictive Sensitivities of 1995 through 2025 Conditions. (Page 3 of 11)

Observed Data

Base Case Simulation

Simulation with Low ICU Leakance and Low Evapotranspiration

Simulation with High ICU Leakance and High Evapotranspiration

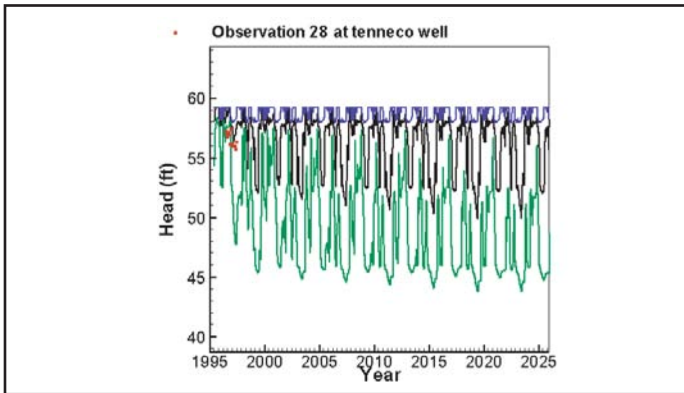

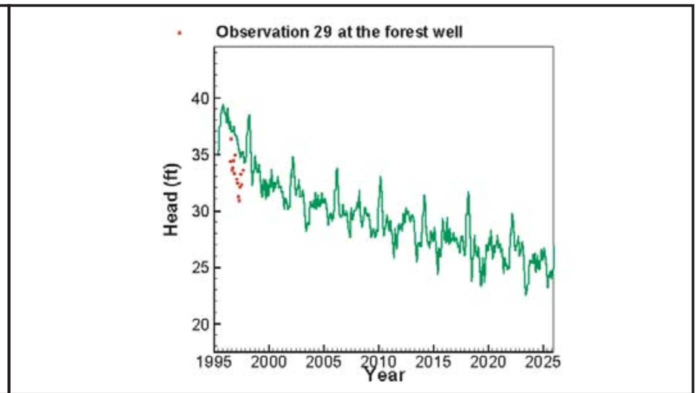

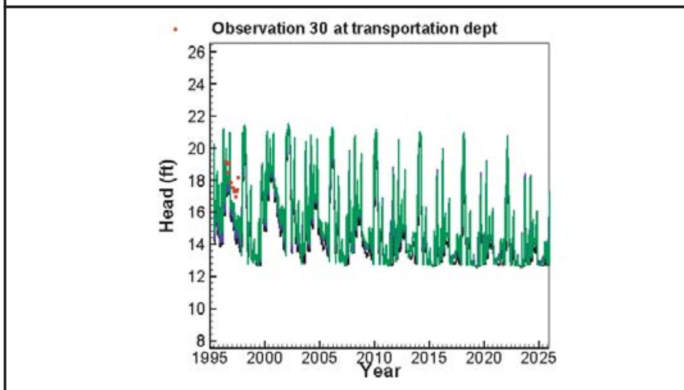

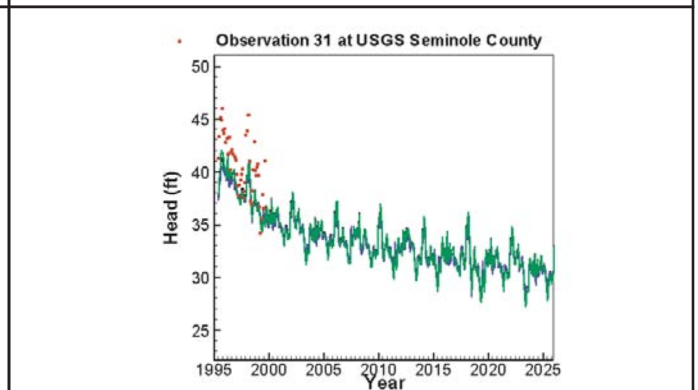

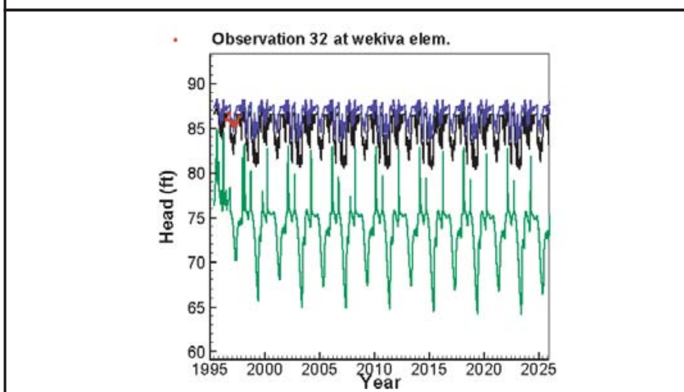

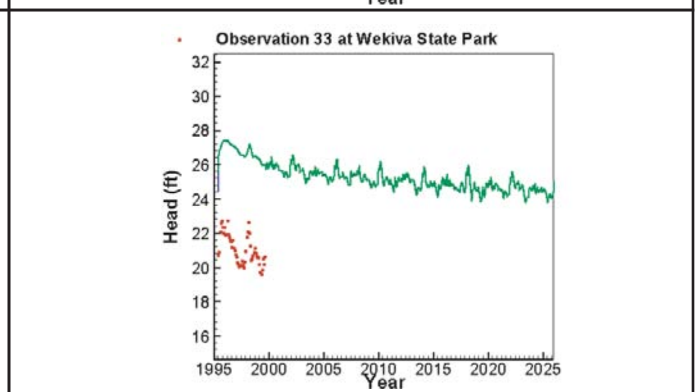

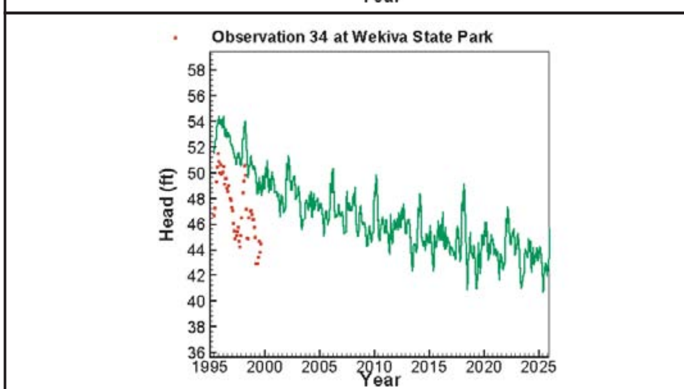

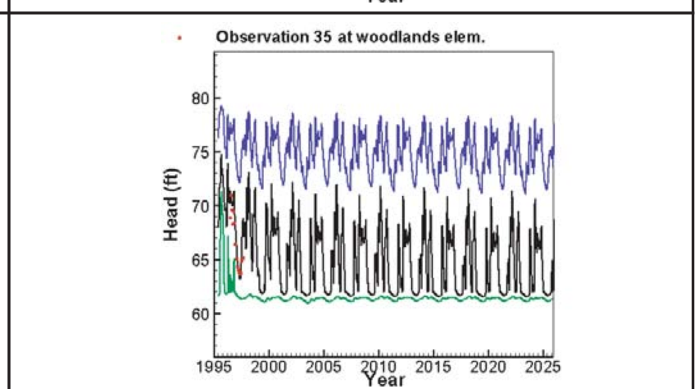

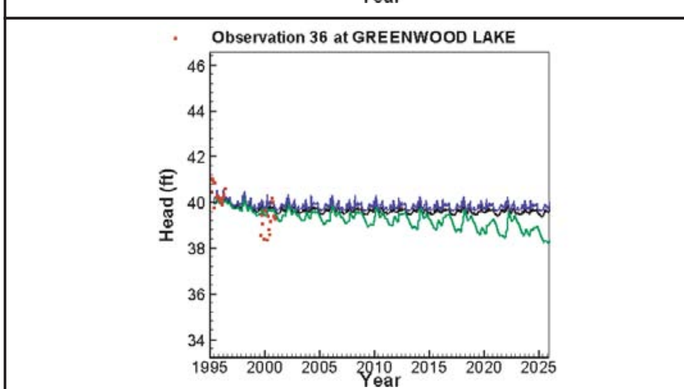

Figure 12.1 Transient Hydrographs at Observation Locations for Predictive Sensitivities of 1995 through 2025 Conditions. (Page 4 of 11)

Observed Data

Base Case Simulation

Simulation with Low ICU Leakance and Low Evapotranspiration

Simulation with High ICU Leakance and High Evapotranspiration

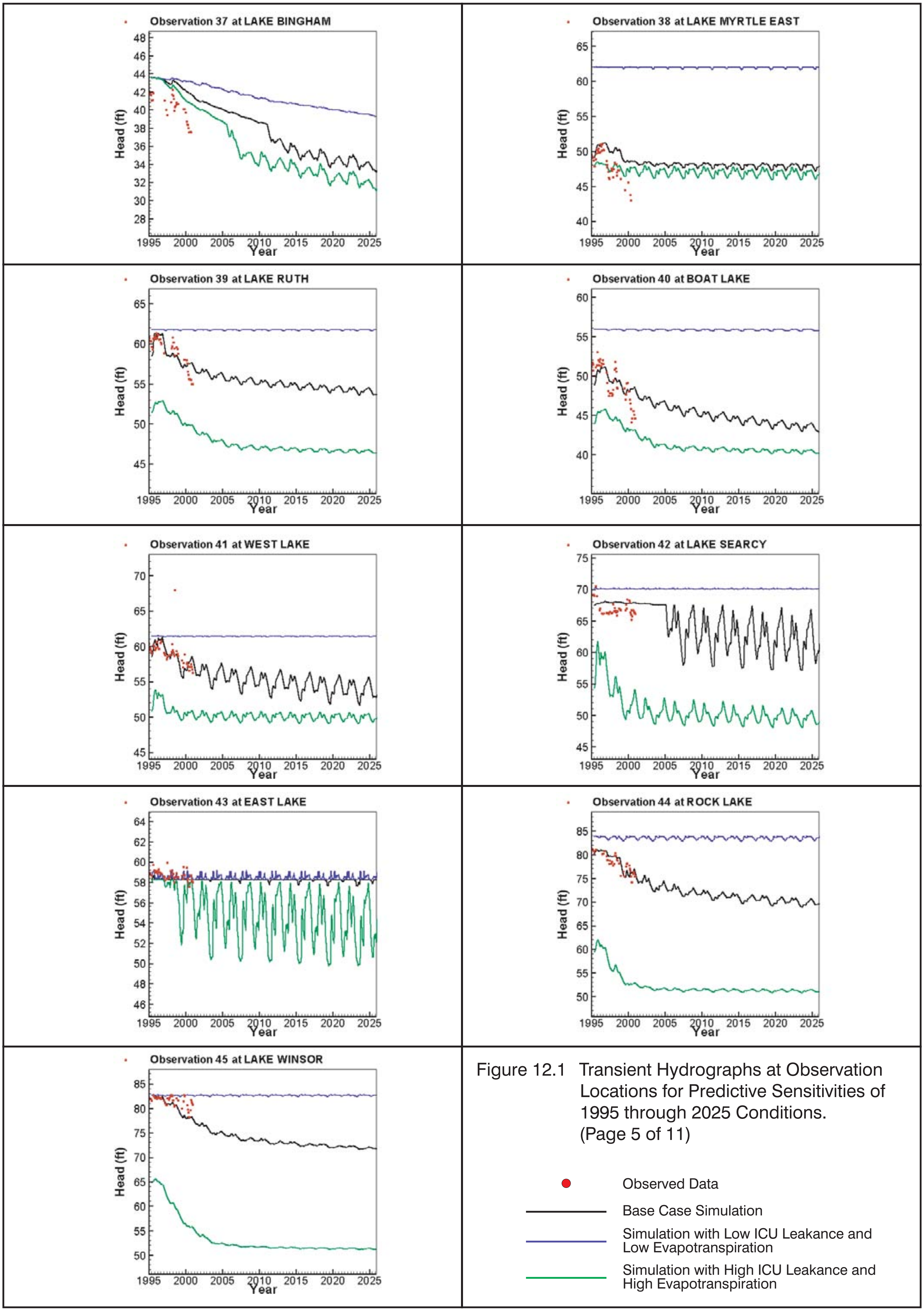

Figure 12.1 Transient Hydrographs at Observation Locations for Predictive Sensitivities of 1995 through 2025 Conditions. (Page 5 of 11)

X:\SJR017\TO1\Maps\Conceptual_Model_Report\graphs_evapotranspiration.cdr

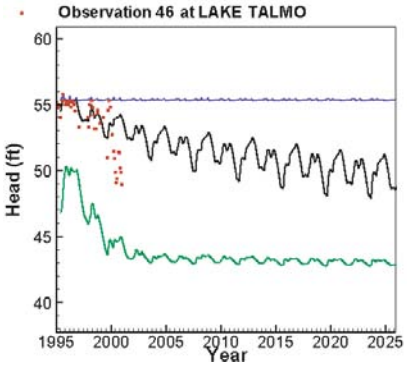

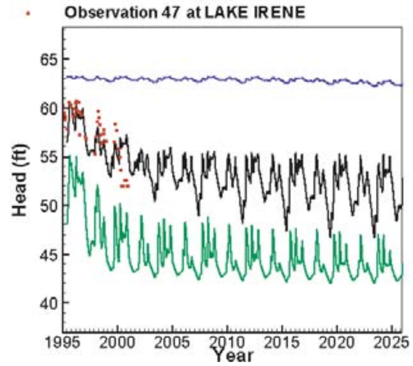

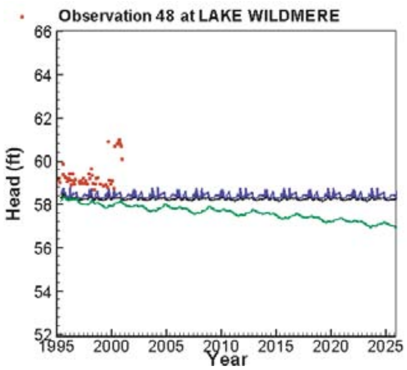

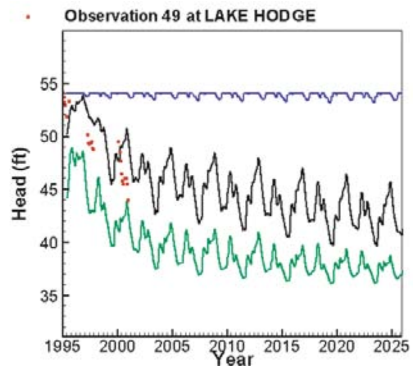

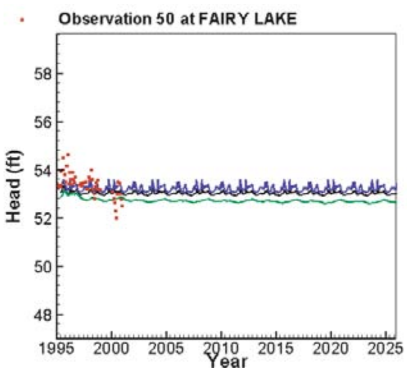

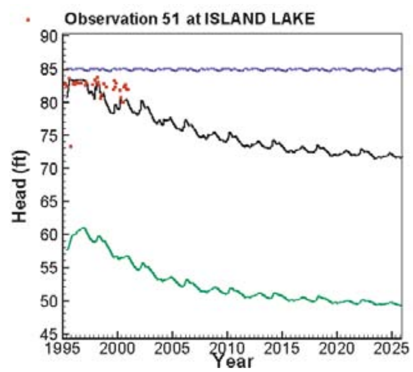

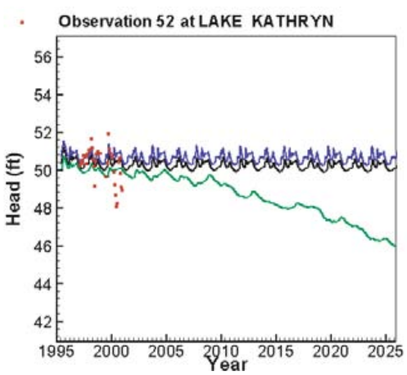

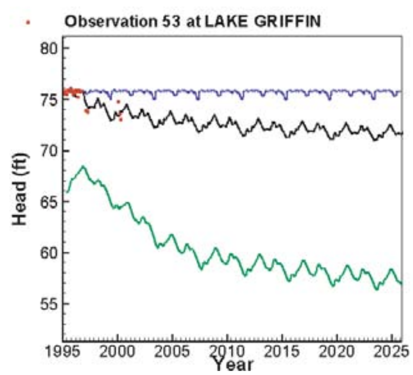

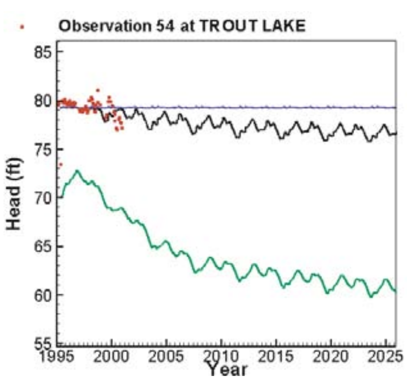

Figure 12.1 Transient Hydrographs at Observation Locations for Predictive Sensitivities of 1995 through 2025 Conditions. (Page 6 of 11)

Observed Data

Base Case Simulation

Simulation with Low ICU Leakance and Low Evapotranspiration

Simulation with High ICU Leakance and High Evapotranspiration

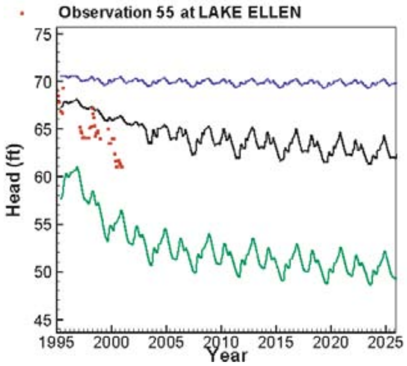

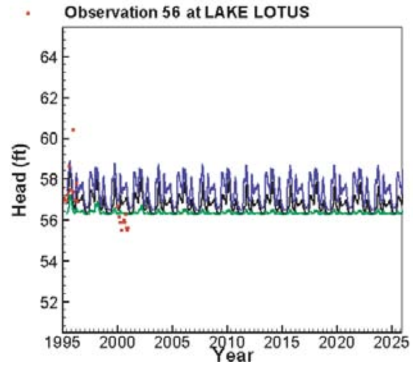

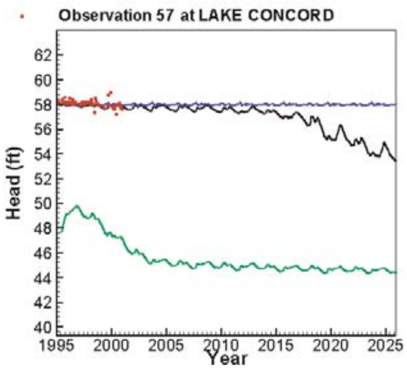

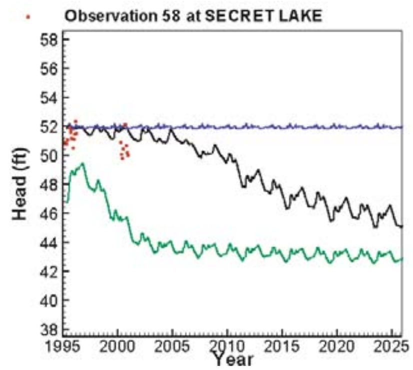

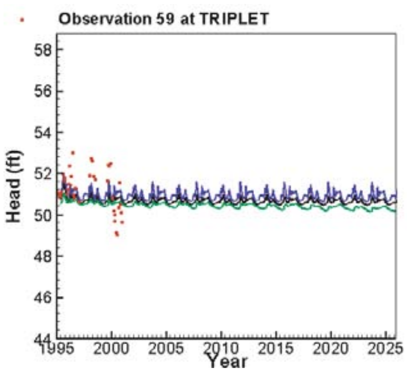

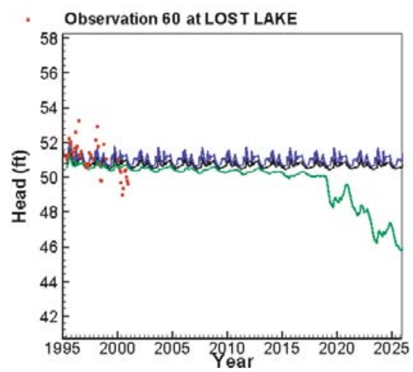

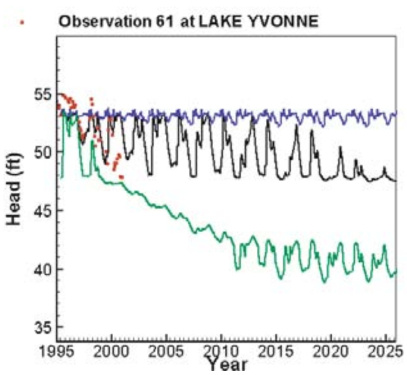

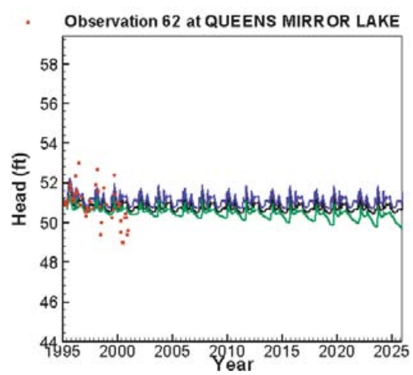

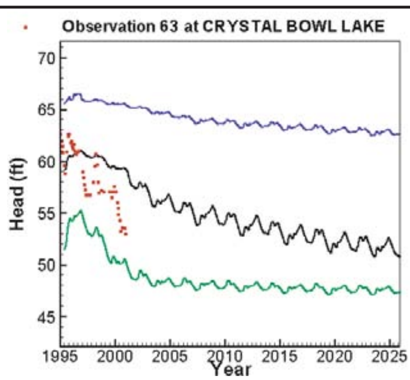

Figure 12.1 Transient Hydrographs at Observation Locations for Predictive Sensitivities of 1995 through 2025 Conditions. (Page 7 of 11)

Observed Data

Base Case Simulation

Simulation with Low ICU Leakance and Low Evapotranspiration

Simulation with High ICU Leakance and High Evapotranspiration

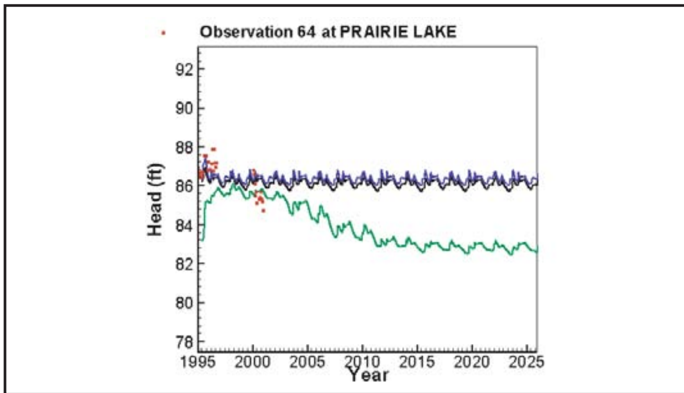

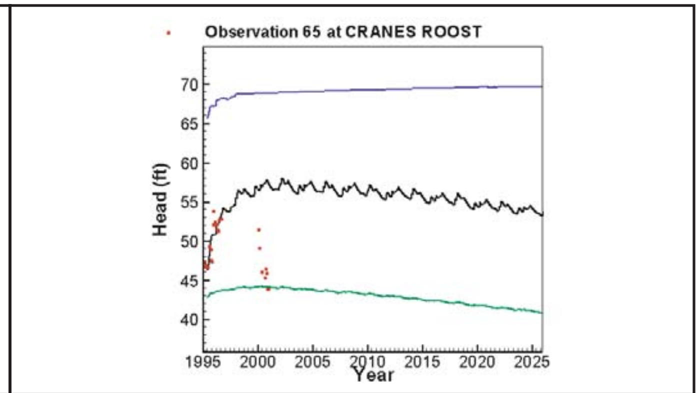

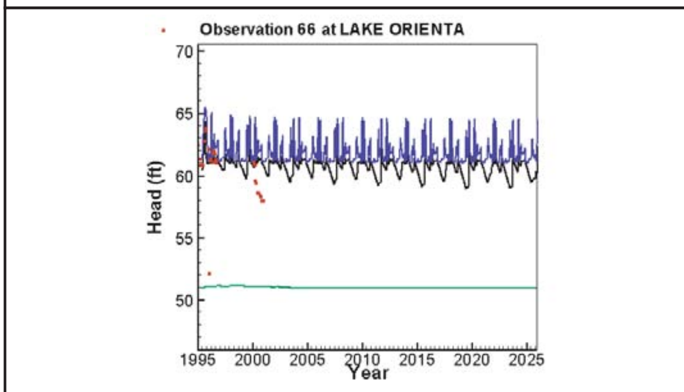

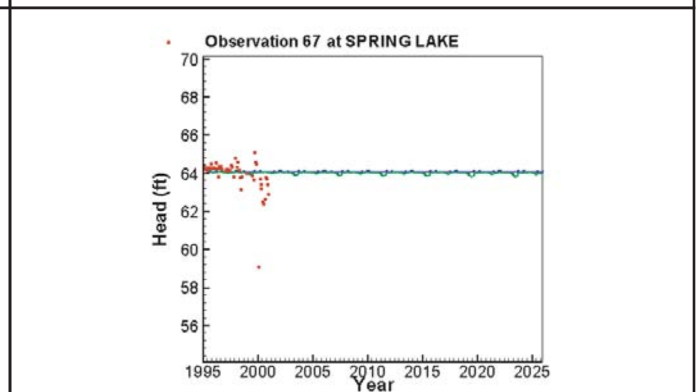

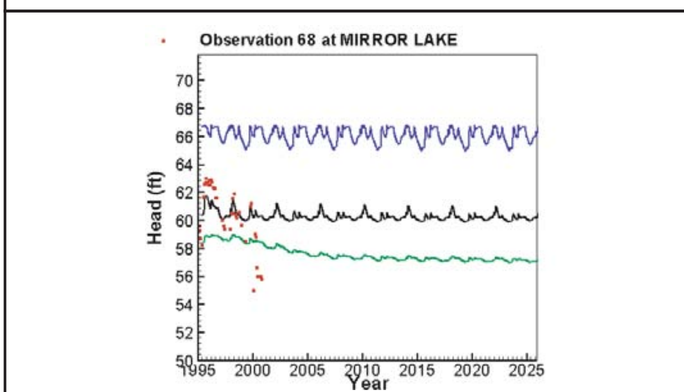

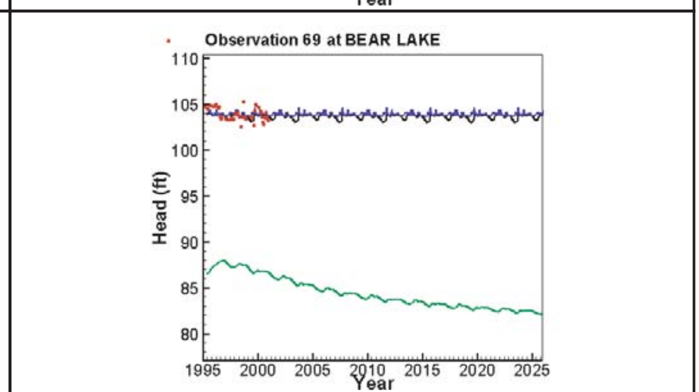

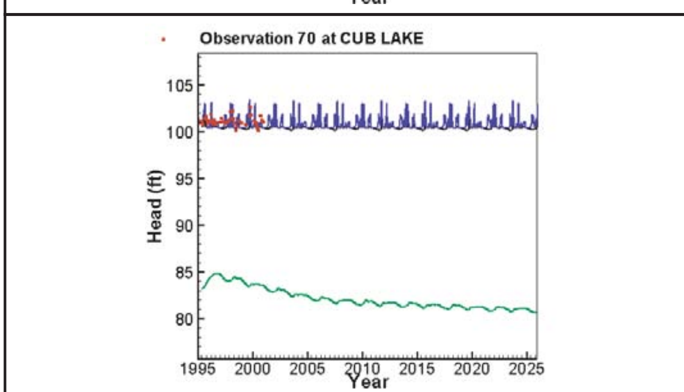

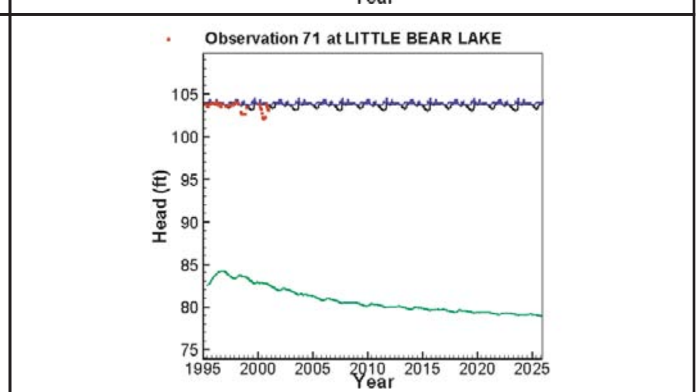

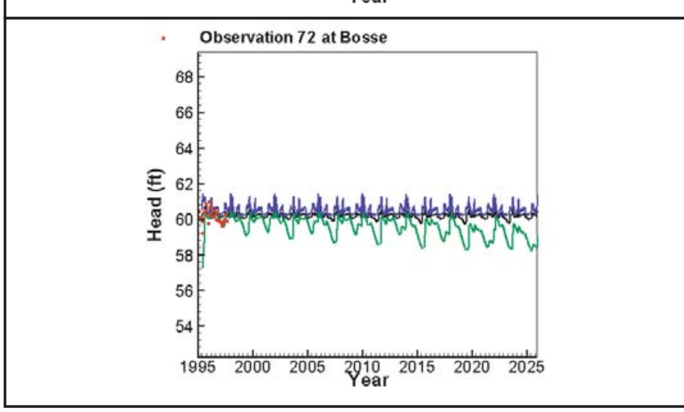

Figure 12.1 Transient Hydrographs at Observation Locations for Predictive Sensitivities of 1995 through 2025 Conditions. (Page 8 of 11)

Observed Data

Base Case Simulation

Simulation with Low ICU Leakance and Low Evapotranspiration

Simulation with High ICU Leakance and High Evapotranspiration

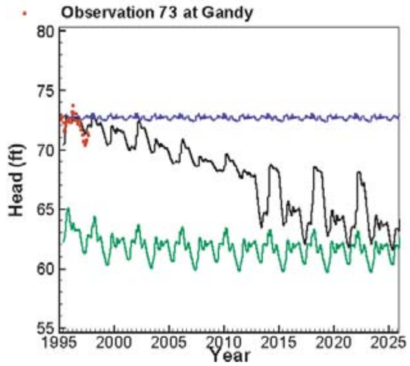

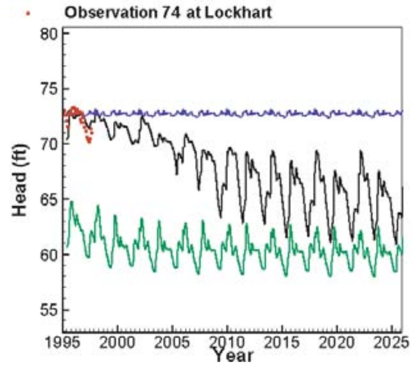

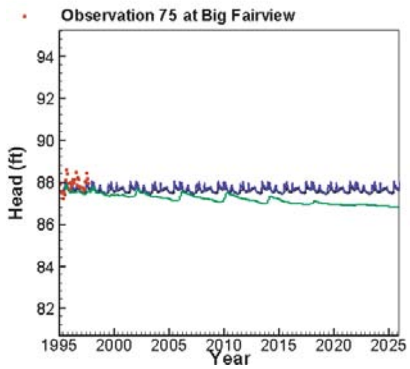

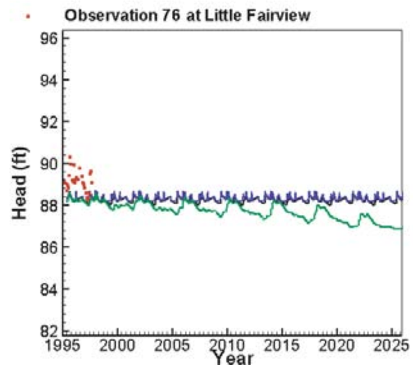

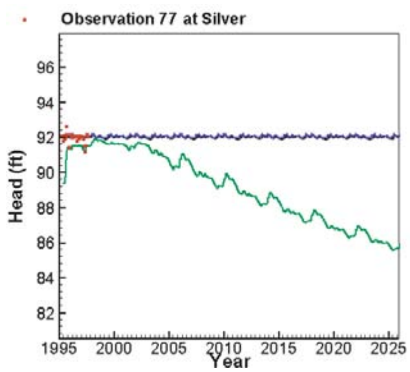

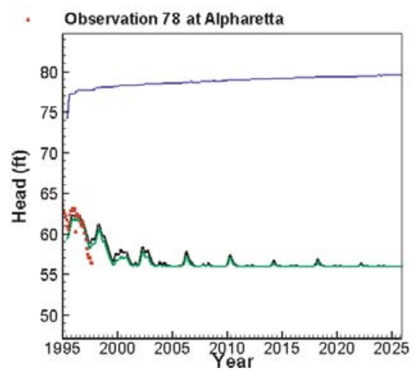

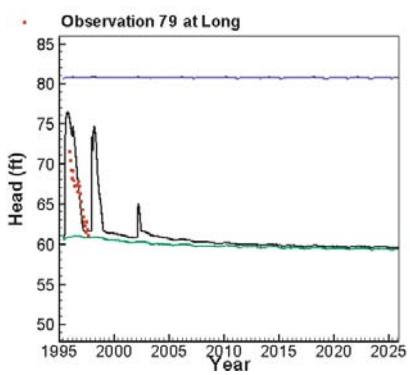

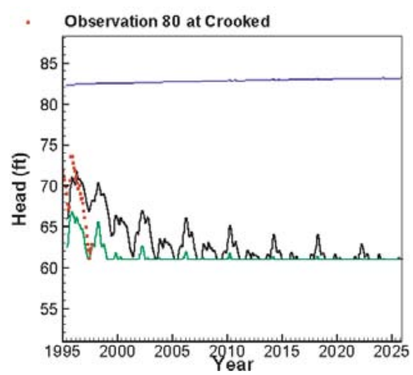

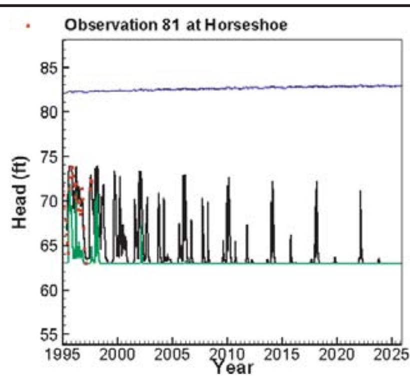

Figure 12.1 Transient Hydrographs at Observation Locations for Predictive Sensitivities of 1995 through 2025 Conditions. (Page 9 of 11)

Observed Data

Base Case Simulation

Simulation with Low ICU Leakance and Low Evapotranspiration

Simulation with High ICU Leakance and High Evapotranspiration

X:\SJR017\TO1\Maps\Conceptual_Model_Report\graphs_evapotranspiration.cdr

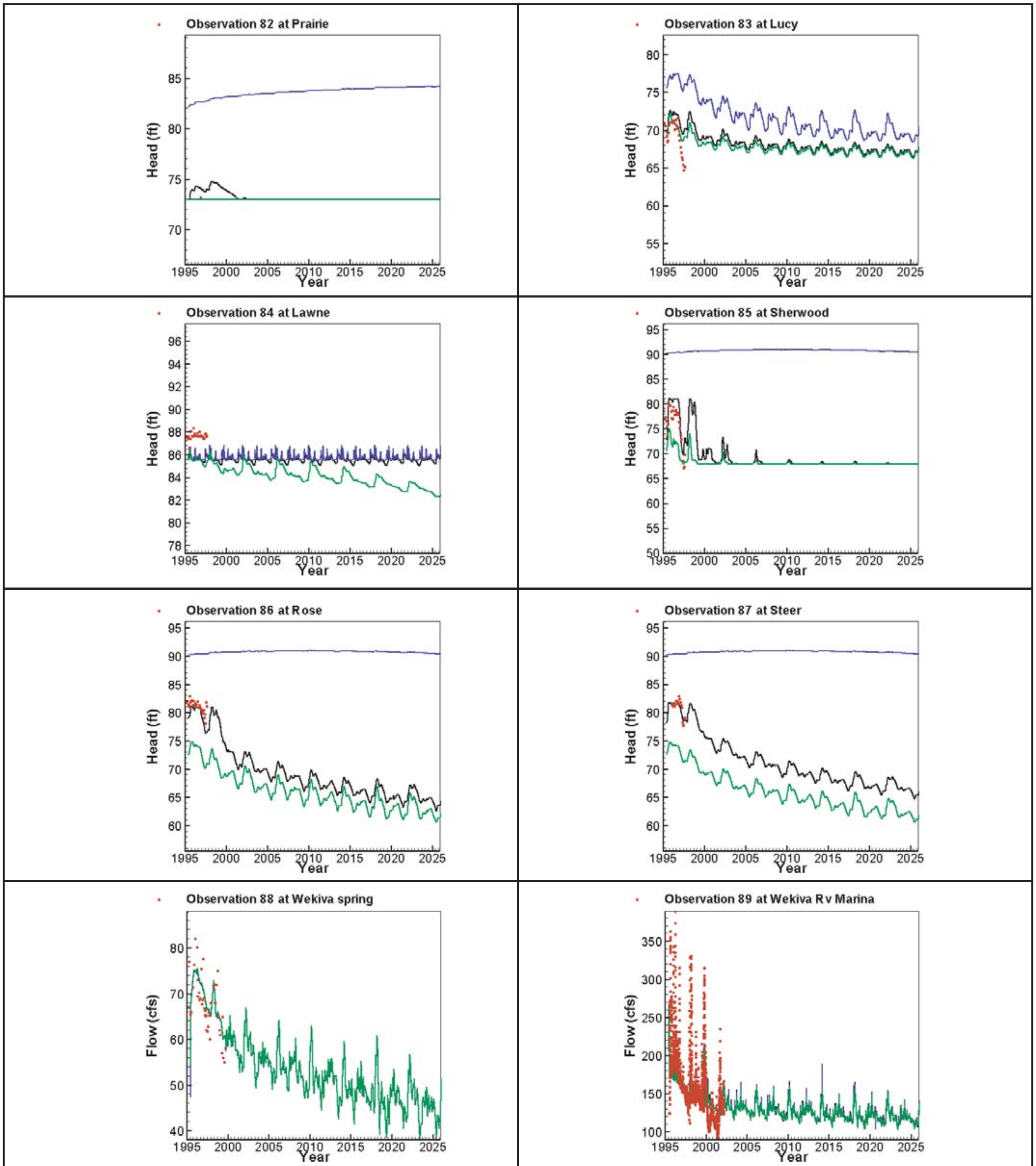

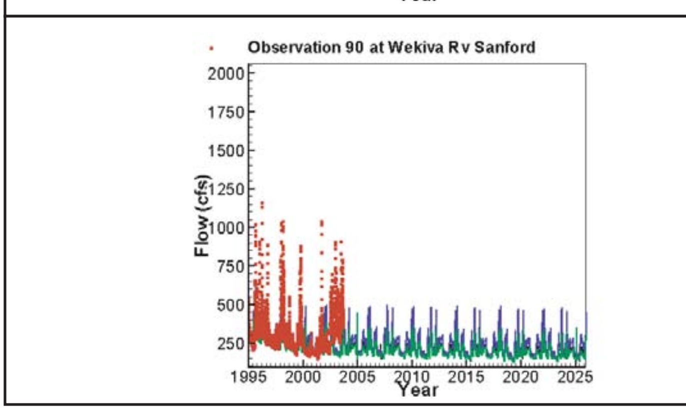

Figure 12.1 Transient Hydrographs at Observation Locations for Predictive Sensitivities of 1995 through 2025 Conditions. (Page 10 of 11)

- Observed Data
- Base Case Simulation
- Simulation with Low ICU Leakance and Low Evapotranspiration
- Simulation with High ICU Leakance and High Evapotranspiration

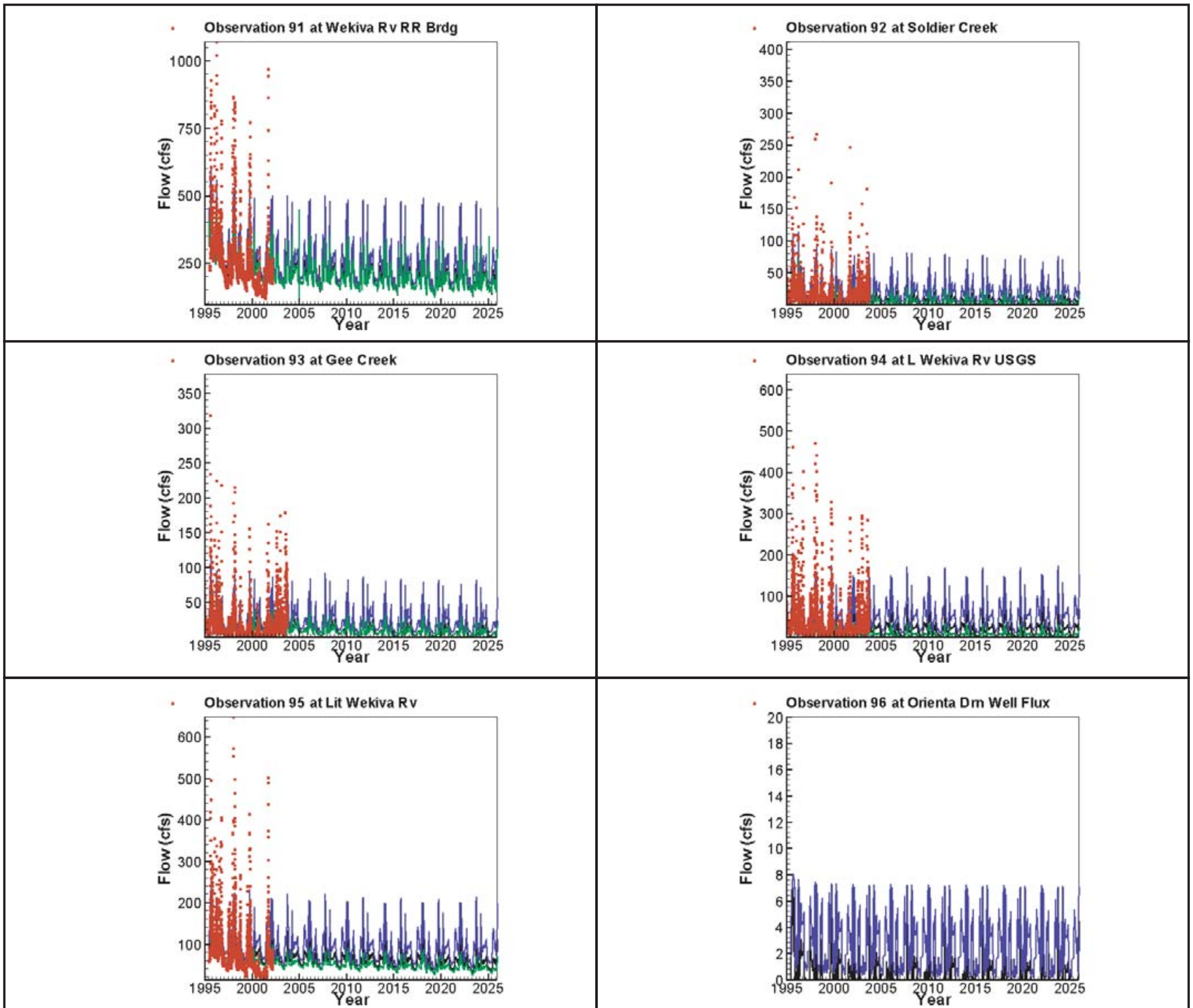

Figure 12.1 Transient Hydrographs at Observation Locations for Predictive Sensitivities of 1995 through 2025 Conditions. (Page 11 of 11)

Observed Data

Base Case Simulation

Simulation with Low ICU Leakance and Low Evapotranspiration

Simulation with High ICU Leakance and High Evapotranspiration